ELEVATED TEMPERATURE EFFECTS ON

INTERFACE SHEAR BEHAVIOR

A Dissertation
Presented to
The Academic Faculty

By

Tanay Karademir

In Partial Fulfillment
of the Requirements for the Degree
Doctor of Philosophy in the
School of Civil and Environmental Engineering

Georgia Institute of Technology
December 2011

ELEVATED TEMPERATURE EFFECTS ON

INTERFACE SHEAR BEHAVIOR

Approved by:

Dr. J. David Frost, Advisor
School of Civil & Environmental Eng.
Georgia Institute of Technology

Dr. J. Carlos Santamarina
School of Civil & Environmental Eng.
Georgia Institute of Technology

Dr. Susan E. Burns
School of Civil & Environmental Eng.
Georgia Institute of Technology

Dr. Robert Bachus
Geosyntec Consultants & Adjunct Professor,
School of Civil & Environmental Eng.
Georgia Institute of Technology

Dr. Arun M. Gokhale
School of Material Science & Eng.
Georgia Institute of Technology

Date Approved: August 19, 2011

To You My Dearest Mom and Dad

&

My Preciouses S and E

ACKNOWLEDGEMENTS

I would like to express my sincere gratitude to Dr. J. David Frost, who has provided me with the opportunity to pursue my PhD research study at Georgia Tech. I sincerely thank him for numerous guidance, encouragement and supervision not only about my academic pursuits but also about my life. Thank you for your hearty support and patience in allowing me to grow not only professionally, but also personally throughout this experience. It has been my pleasure to be one of his PhD students.

I would like to express my sincere gratitude to the committee members for offering support, guidance and suggestions to complete this thesis: Dr. J. Carlos Santamarina, Dr. Susan E. Burns, Dr. Robert Bachus and Dr. Arun M. Gokhale.

All the geotechnical society fellows and my friends at Georgia Tech are appreciated.

Finally, none of this would have been possible without the love and support of my family. I wish to express my sincere gratitude to the each member of my family for caring, sacrifice and prayers for me. This adventure could not have been achieved without your encouragement and motivation for which I will always be grateful.

To her, as approaching to the end of my academic journey in the States, I am so looking forward to the next chapter in our life together in Turkey. You definitely continue to impress and inspire me.

TABLE OF CONTENTS

LIST OF TABLES

LIST OF FIGURES

SUMMARY

Environmental conditions such as temperature inevitably impact the long term performance, strength and deformation characteristics of most materials in infrastructure applications. The mechanical and durability properties of geosynthetic materials are strongly temperature dependent. The interfaces between geotextiles and geomembranes as well as between granular materials such as sands and geomembranes in landfill applications are subject to temperature changes due to seasonal temperature variations as well as exothermic reactions occurring in the waste body. This can be a critical factor governing the stability of modern waste containment lining systems. Historically, most laboratory geosynthetic interface testing has been performed at room temperature. Information today is emerging that shows how temperatures in liner systems of landfills can be much higher.

An extensive research study was undertaken in an effort to investigate temperature effects on interface shear behavior between (a) NPNW polypropylene geotextiles and both smooth PVC as well as smooth and textured (co-extruded, structured) HDPE geomembranes and (b) sands (rounded, angular) and smooth PVC and HDPE geomembranes. A unique temperature controlled chamber (TCC) was designed and developed to be utilized to simulate the field conditions at elevated temperatures and evaluate shear displacement failure mechanisms at these higher temperatures. The physical laboratory testing program consisted of multiple series of interface shear tests between material combinations found in landfill applications under a range of normal stress levels from 10 to 400 kPa and at a range of test temperatures from 20 to 50 °C.

Complementary geotextile single filament tensile tests were performed at different temperatures using a dynamic thermo-mechanical analyzer (DMA) to evaluate tensile strength properties of geotextile single filaments at elevated temperatures. The single filament studies are important since the interface strength between geotextiles and geomembranes is controlled by the fabric global matrix properties as well as micro-scale characteristics of the geotextile such as filament strength and how it interacts with the geomembrane macro-topography.

It is known that the peak interface strength for sand-geomembrane as well as geotextile-geomembrane interfaces is mainly attributed to the geomembrane properties such as hardness and micro surface roughness. To this end, the surface hardness of smooth HDPE and PVC geomembrane samples was measured at different temperatures in the temperature controlled chamber to evaluate how temperature changes affect the interface shear behavior and strength of geomembranes in combination with granular materials and/or geotextiles. The aim of this portion of the experimental work was to examine: i) the change in geomembrane hardness with temperature; ii) develop empirical relationships to evaluate shear strength properties of sand – geomembrane interfaces as a function of temperature; and iii) compare the results of empirically predicted frictional shear strength properties with direct measurements from the interface shear tests performed at different temperatures.

CHAPTER I

1. INTRODUCTION

1.1. Introduction and Motivation for the Current Study

Geo-materials which are commonly utilized in geotechnical applications can be divided into three categories based on geometric terminology. These are fabrics, continua, and particulates. Under different load conditions, each category of material can lead to different responses and interactions. Composite installations are frequently preferred in diverse construction activities such as landfills, tunnels, dams and foundations (Giroud, 1984; Frobel, 1988; Girard et al., 1990). In such cases, the interface shear resistance between different materials may control the stability of the composite system. Examples may include flat or inclined surfaces and interfaces composed of particulates (soil) and fabrics/continua (geotextiles/geomembranes) in landfill, reservoir and canal applications. In these cases, failure often occurs by the cover soil sliding over a geomembrane, although sometimes the system fails due to the geomembrane sliding on an underlying lower friction surface or interface. Consequently, the contact behavior and interaction between these various materials is an important issue for geotechnical engineers. Due to their widespread application in civil engineering projects, it is also important to understand the behavior of these materials under varying environmental conditions such as temperature. The properties and behavior of polymeric geosynthetics are sensitive to temperature changes. In designing with geosynthetics, the interface strength between geosynthetic components is a critical factor, however, the temperature dependency of interface friction is generally not taken into consideration during design.

Polymeric geosynthetic materials including geotextiles and geomembranes have mechanical and durability properties that are strongly temperature dependent and have been widely used in practice due to their complimentary advantages in I) drainage, II) filtration, III) separation, IV) protection, and V) reinforcement applications such as landfills (Figure 1.1). The interaction between a geotextile and a geomembrane (i.e. fiber-texture interaction) as well as the contact behavior between a sand and a geomembrane (i.e. particulate-continua interface behavior) in landfill applications is subject to seasonal temperature variations. Moreover, in double layer lining systems which were legislated as the national specification for landfills in the United States in the mid 1980s, geosynthetics installed as a composite system at the base of landfills experience elevated temperatures as a result of exothermic reactions occurring in the waste body and the insulating effect of the waste itself (Figure 1.2). Limited understanding exists as to the effect of these temperature variations on the engineering behavior of these composite systems. In such applications, the functional engineering properties of geosynthetic interfaces should remain within acceptable limits during the required service life as it is a critical factor governing the integrity of the structure as well as the stability of these modern lining systems.

Figure 1.1 Photo of a landfill cell in construction stage (Kingcounty.gov)

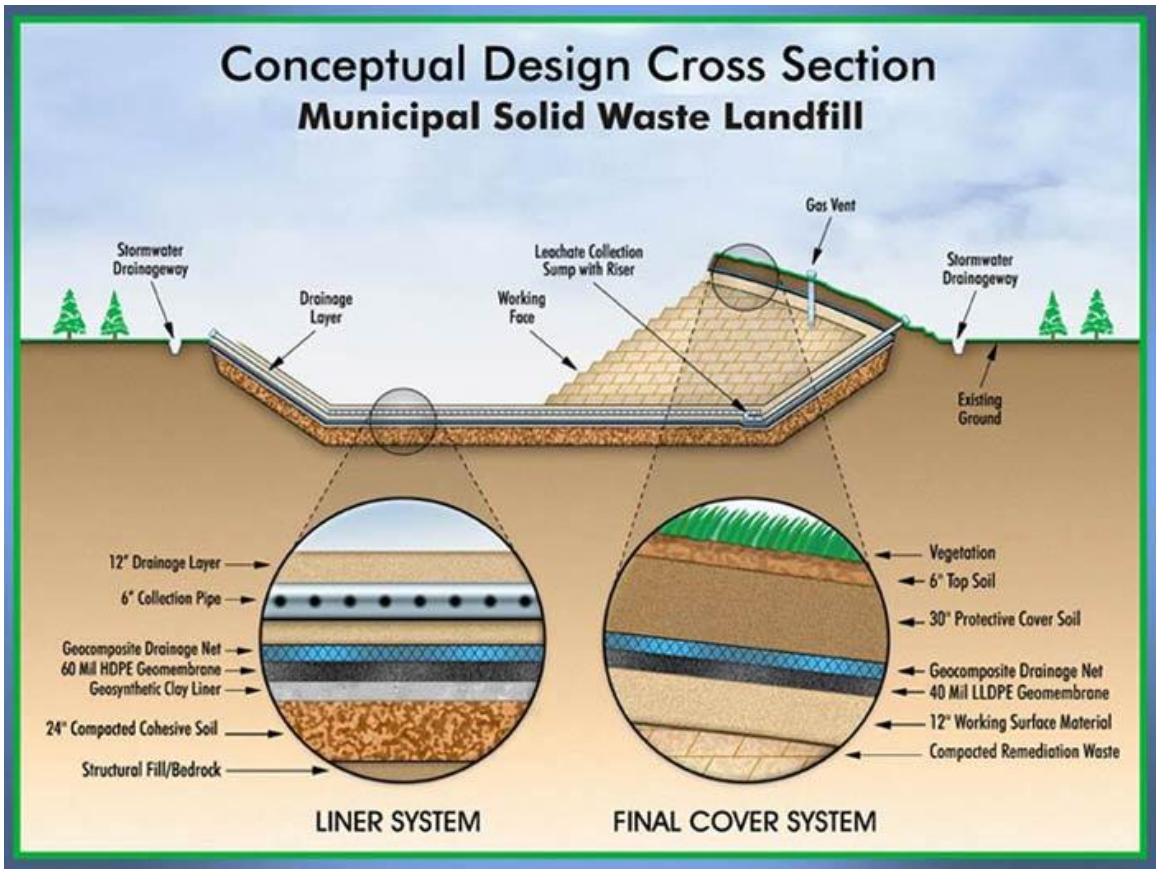

Figure 1.2 Schematic of Conceptual Landfill Design: Cross Section View (Eppersonwaste.com)

In response to these issues noted above, an extensive experimental research program was performed to investigate temperature effects on interface shear behavior between: (a) needle punched non-woven (NPNW) polypropylene geotextiles and either smooth polyvinylchloride (PVC) or smooth/textured high-density polyethylene (HDPE) geomembranes; or (b) sands (rounded or angular) and smooth PVC or HDPE geomembranes. The physical laboratory testing program consisted of a series of direct interface shear tests between combinations of these aforementioned geo-materials under different load conditions and at various temperatures. A unique temperature controlled chamber (TCC) was designed and developed to be utilized to simulate the field

conditions at higher temperatures and to replicate and evaluate triggered shear displacement-failure mechanisms under elevated temperature conditions. Complementary geotextile single filament tensile tests as well as geomembrane surface hardness and geomembrane surface roughness tests provided insight into the role of temperature in the observed behavior differences of the individual materials.

1.2. Scope of Thesis

This thesis presents the results and the findings of research studies into the influence of temperature on interface shear behavior between fabric-continuum as well as particulate-continuum interfaces with the goal of understanding the fundamental mechanisms responsible for the observed behavior differences. The scope of the thesis can be divided into five sections: (1) review of previous studies and the resultant current state of knowledge concerning interface behavior of geosynthetic systems (i.e. geotextile-geomembrane; sand-geomembrane) and temperature effects on mechanical and durability properties of polymeric materials (i.e. geosynthetics); (2) design and development of a unique temperature controlled chamber, description of test equipments and devices, application of experimental program and analysis techniques; (3) laboratory investigations and analysis of the micromechanical characteristics of single geotextile filaments under tensile loading and the hardness of geomembrane surfaces at different temperatures; (4) the macroscale study of behavior of geosynthetic interfaces using physical laboratory experiments; (5) analysis of micro and macro responses to enhance understanding of interface shear behavior of geosynthetic systems at elevated

temperatures. This thesis is organized into ten chapters including this introduction, with the content of each subsequent chapter summarized below:

Chapter 2: provides a historical perspective and background: a review of factors controlling the shear behavior of common interfaces; an overview of significant contributions to the current understanding of fabric-continua as well as particulate-continua interface shearing mechanisms and response; and presents a summary of fundamental concepts regarding temperature effects on mechanical and durability properties of polymeric materials (i.e. geotextiles, geomembranes); finally some information is provided on geotechnical examples which experience temperature variations such as landfill liner and cover systems.

Chapter 3: discusses the development and validation of the unique temperature controlled chamber test system as well as observations pertaining to system design criteria and the relevance to field conditions. The TCC was designed to simulate elevated field temperature conditions in the laboratory during physical laboratory shear tests (i.e. shear, tension, compression) to evaluate material functional engineering properties as well as operational performance such as triggered shear displacement-failure mechanisms at higher temperatures for interfaces between fabric-planar surfaces as well as particulate-planar surfaces.

Chapter 4: describes the extensive laboratory testing program undertaken to assess the influence of temperature on the properties of geosynthetic materials as well as

interaction of these materials at different temperatures. Physical properties of the selected materials are described, followed by a detailed description of all laboratory experimental devices/systems and equipment utilized throughout the research program. This chapter also presents the measurement procedures used to observe the macro-scale and micro-scale contact behavior of the test materials. The sample, test equipment preparation, characterization of tensile properties of geotextile single filaments and measurement of surface hardness of geomembranes are described.

Chapter 5: presents the results of geotextile single filament tensile tests conducted at different temperatures using a dynamic thermo mechanical analyzer to evaluate tensile strength properties of single filaments at elevated temperatures and to further understand and provide a basis for understanding the influence of temperature on the characteristics of the geotextile such as filament strength, and how it interacts with the geomembrane macro-topography.

Chapter 6: presents macro-scale results of experimental investigations from interface shear resistance tests at different temperatures and under several normal load conditions using a large displacement interface shear device enclosed by the temperature controlled chamber to show how interface shear behavior of geotextile versus *smooth* geomembrane interfaces changes with temperature. Failure envelopes at different temperatures and comparison of the results under different normal stress levels provide insight into the observed behavior differences. Analysis, discussion and comparison of test results for the

different geomembrane types obtained from several manufacturers produced using different *base polymers* (i.e. lining sheet core material type: HDPE or PVC) are essential to comprehending differences in the investigated interface shear behavior.

Chapter 7: presents macro-scale results of experimental investigations from interface shear resistance tests at different temperatures and under several normal load conditions using a large displacement interface direct shear device enclosed by the temperature controlled chamber to show how interface shear behavior of geotextile versus *textured* geomembrane interfaces changes with temperature. Failure envelopes at different temperatures and comparison of the results under different normal stress levels provide insight into the observed behavior differences. Analysis, discussion and comparison of test results for the different geomembrane types obtained from several manufacturers producing using different *texturing techniques* (i.e. coextrusion or structuring) are essential to comprehending differences in the investigated interface shear behavior.

Chapter 8: presents macro-scale results of experimental investigations from interface shear resistance tests at different temperatures and under several normal load conditions using a large displacement interface direct shear device enclosed by the temperature controlled chamber to show how interface shear behavior of sand versus geomembrane interfaces changes with temperature. Failure envelopes at different temperatures and comparison of the results under different normal stress levels provide insight into the observed behavior

differences. Analysis, discussion and comparison of test results for the different sands (i.e. rounded or angular) sheared against smooth HDPE or PVC geomembrane specimens are essential to comprehending differences in the investigated interface shear behavior.

Chapter 9: describes a practical analytical approach and addresses the results of the study for indirect assessment of temperature effects on particulate – continuum interfaces. The hardness of HDPE and PVC geomembranes at different temperatures are correlated to temperature change. Using the empirical correlation developed between hardness and temperature in this study and correlations between hardness and interface friction angle (δ) published by O'Rourke et al. (1990), a general model for interface friction properties of sand-geomembrane interfaces was developed in which interface friction angle (δ) is related to temperature and compared with direct measurements.

Chapter 10: provides a summary of the main conclusions and advancements made during the current research study. Additionally, recommendations for future work on the topic are provided.

References and appendices with supplementary information are presented at the end of the thesis.

CHAPTER II

2. BACKGROUND AND LITERATURE REVIEW

2.1. Introduction

An interface is the zone of interaction between different materials created by placement of materials having different properties adjacent to one another. Relative movement is likely to occur as a result of discontinuities at the interface which can make it the weakest point of the overall system in terms of shear strength compared to that of neighboring materials. Therefore, the shear strength of interfaces frequently controls the overall design and stability of systems consisting of more than one material.

The behavior of each interface is a combination of the interaction behavior between the counterface materials as well as the state of the interface. In addition to mechanical surface properties such as surface roughness, the relative hardness of the counterface materials impacts the interface shear response that develops. In addition, the interaction of a material surface with that of another is also influenced by physical and chemical properties of the surfaces themselves. Consequently, it is essential to thoroughly evaluate the characteristics of the materials at an interface to understand its behavior and to identify the factors controlling the shear stress-displacement response of common interfaces such as geotextile-geomembrane and granular soil-geomembrane (Dove, 1996).

One of the more common composite systems that has found widespread application in geotechnical engineering projects are those involving geotextiles and geomembranes or granular materials and geomembranes. They are generally used as

composite systems rather than as stand-alone solutions in practice due to their complimentary advantages. The interaction behavior between geotextiles and geomembranes as well as the contact behavior between granular materials such as sands and geomembranes are critical components in defining the interface strength governing the integrity of the overall structure as well as the stability of the constructed system. Over the past few decades, fiber-texture (i.e. geotextile-geomembrane) interaction has become a key issue in geotechnical engineering design. Non-woven geotextiles are porous and fibrous materials that consist of irregularly oriented long filaments which vary in terms of spatial distribution, curvature, orientation, size, and mass density. Geomembranes are continuum materials which depend on properties such as tensile strength, hardness, surface roughness, and chemical constitution. Both are made from polymeric material resins. Temperature has a significant effect on the physical and mechanical engineering properties of polymers such as tensile strength, modulus and hardness. While the importance of temperature on the functional engineering properties of polymeric materials such as textile fabrics (i.e. geotextiles) and continuous polymer sheets (i.e. geomembranes) have been studied separately, the effect of temperature on the interaction of these materials in contact as occurs at interfaces between geotextiles and geomembranes as well as sand and geomembranes has received limited attention. As noted by J.P. Giroud, (2005 Mercer Lecturer), the influence of temperature on shear strength of geosynthetic-geosynthetic and soil-geosynthetic interfaces is not known explicitly by the geosynthetics community. For this reason, there is urgent requirement for research to be carried out to investigate the temperature effects on geosynthetic interface systems.

2.2. Review of Factors Controlling the Shear Behavior of Fabric – Continua & Particulate – Continua Interfaces

An interface is created through incorporation of a geosynthetic material into another geosynthetic material or a soil. In other words, there occurs an interaction of man-made construction material with another geotechnical engineering related material or a natural material which becomes an integral part of a man-made system. The resultant interface generates a potential plane of weakness within the system or soil mass along which failure may occur (Koerner, 1998). The physical and mechanical properties of the materials at the interface define the shear behavior and the state of the interface as well as the interaction and contact behavior between the two materials (Dove, 1996). In order to prevent a failure from developing at the interface, it is essential to know the factors controlling shear strength-displacement behavior of that interface.

A review on factors controlling the interface shear behavior of geotextile-geomembrane as well as granular soil-geomembrane interfaces will be provided. Those factors are generally considered in evaluating the interface shear strength of these interfaces and must quantitatively be estimated to fully understand the mechanism of interface shear response and development of shear stress-displacement curve.

2.2.1. Surface Roughness/Topography – Texture

Surface roughness in general was defined in Ward (1982) as the irregularities in the surface texture which are inherent in the production process, but excluding waviness and errors in form for man-made materials. Surface roughness can be utilized as a quantitative measure to describe the surface topography of the geomembrane surfaces using one of several developed profiling methods by using different instruments listed in

Figure 2.1, depending on the research purpose and surface properties of the material being considered (Dove and Frost, 1996). Research studies (e.g. Dove, 1996; Lee, 1998) into the behavior of interfaces mentioned above have shown that the roughness of the geomembrane is one of the main factors in the development of interface strength. It has been established that geomembranes with textured surfaces show substantial increase in the strength of a geomembrane-geotextile interface (Williams and Houlihan, 1986; Stark et al., 1996; Frost and Lee, 2001) and a geomembrane-soil interface as well (Dove et al., 1997).

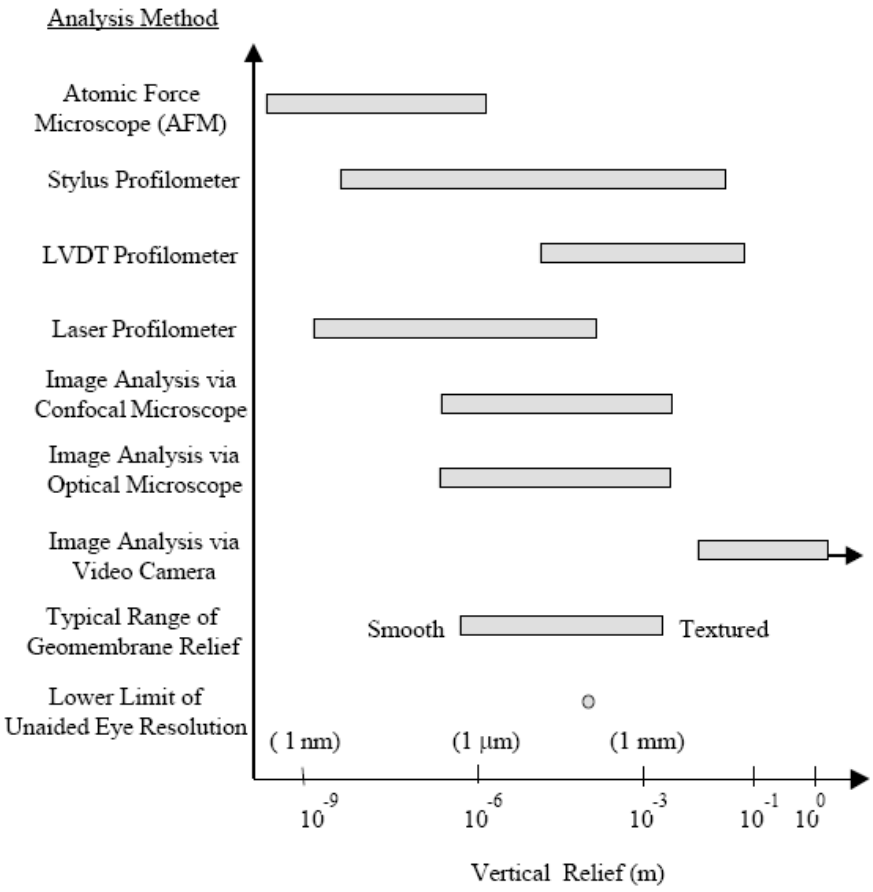

Figure 2.1 Approximate Profiling Equipment Operating Ranges (Dove, 1996)

The measurement of roughness for geomembrane surfaces are related to the surface topography that a geotextile filament (Frost and Lee, 2001) or a soil particle (Dove and Frost, 1999) will encounter when interacting with a geomembrane. The form of these interaction behaviors determines interface shearing mechanisms. For textured geomembranes, the manufactured texturing enhances interface shear properties of the material by improving its surface roughness primarily. Williams and Houlihan (1987) conducted tests on soil-geomembrane interfaces using a modified direct shear device. They found that the failure mechanism for smooth geomembranes was primarily sliding of the granular soil particles along the interface with limited particle rolling. However, the shearing surface for rough geomembranes was shifted into the adjacent soil resulting in higher interface friction angles. The surface roughness of a material can further be subdivided into the macro-topography and micro-topography features as defined in Dove and Frost (1996) and Dove (1996). The macro-topography features are the ones visible to human eye while the micro-topography features are visible only at the microscopic level with the aid of some instrument (Figure 2.1). The micro-topography features are much more localized variations and irregularities in the material surface compared with macro-topography features which can have a greater contribution to quantitative measurement of roughness (see Figure 2.2 for the Terminology used to describe Surface Topography).

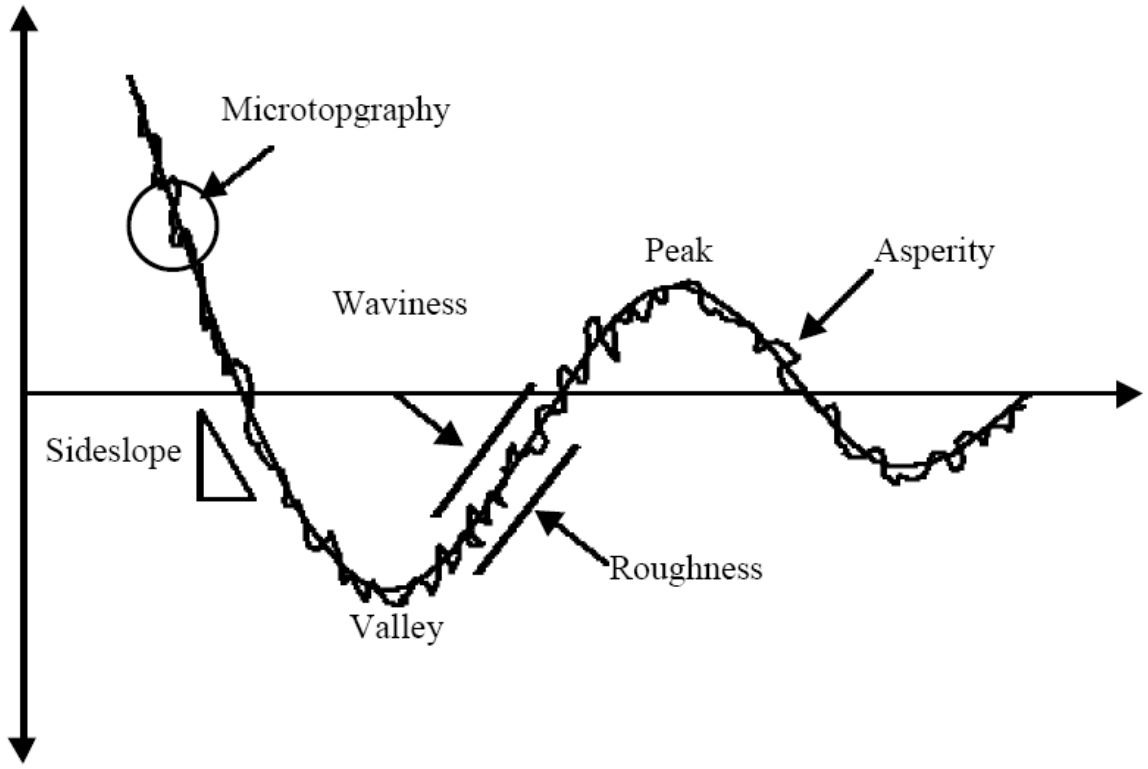

Figure 2.2 Terminology Used to Describe Surface Topography (Dove, 1996)

Williams and Houlihan (1986) indicated that the surface roughness of the geomembrane has a "significant" influence on the interface friction angle developed between geotextiles and geomembranes as a conclusion of the results of several tests performed between four types of geomembranes and seven types of woven or nonwoven geotextiles. Similarly, Stark et al. (1996) conducted a series of interface shear tests between nonwoven geotextiles and geomembranes (smooth or textured) using a torsional ring shear apparatus. Figure 2.3 presents a comparison of failure envelopes for smooth as well as textured geomembranes sheared against nonwoven geotextiles at normal stress levels ranging up to 400 kPa. They reported that the peak and residual interface strengths increased approximately 300 % and 200 %, respectively by the use of textured geomembranes instead of smooth geomembranes. These magnitudes of significant

strength (peak and residual) increases at geotextile – geomembrane interfaces due to geomembrane texture is important especially for geosynthetic composite system design on slopes. However, the post-peak strength loss is substantially greater with a textured geomembrane. The magnitude of post-peak strength losses at geotextile - textured geomembrane interfaces was also quantitatively evaluated by Frost and Lee (2001) as a function of surface roughness and will be discussed further below.

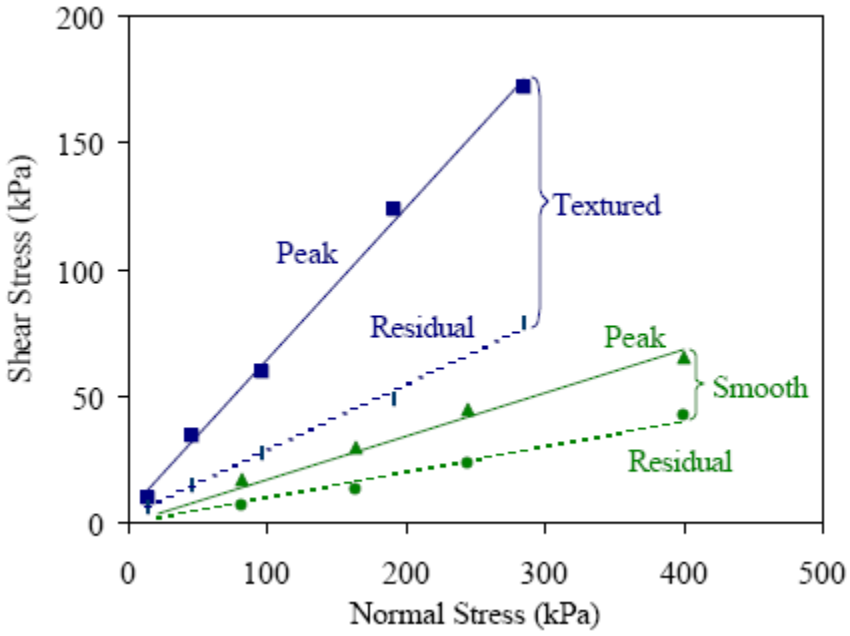

Figure 2.3 Failure Envelopes for Smooth and Textured Geomembrane-Geotextile Interfaces (Stark et al., 1996)

The surface roughness had not been quantified in the research work of Stark et al. (1996). Later, Frost and Lee (2001) in their study utilized a quantitative measure of surface roughness which is the three dimensional surface roughness parameter (Rs) to further investigate and quantify the influence of the use of textured geomembranes instead of smooth geomembranes in conjunction with geotextiles. Rs was originally

defined as the ratio of the actual area of the surface to the projected area of the surface and proposed to be used as a quantitative measure of surface roughness as well as the basis for a geomembrane texture/roughness classification scheme proposed by Dove and Frost (1996) based on the ranges of Rs values as tabulated in Table 2.1.

Table 2.1 Geomembrane Textural Classification (after Dove and Frost, 1996)

Textural Descriptor	**Rs Range**
Smooth	1.00 – 1.10
Slightly Textured	1.10 – 1.35
Moderately Textured	1.35 – 1.60
Heavily Textured	> 1.60

Similar interface shear test results to those of Stark et al. (1996) regarding the influence of geomembrane surface texture on geotextile – geomembrane interface shear resistance were obtained by Frost and Lee (2001) with the additional attribute that the geomembrane surface roughness was quantified. The relationship between surface roughness of the geomembranes and the peak as well as residual interface friction angles at normal stresses of 50 and 100 kPa for four different nonwoven geotextiles are shown in Figure 2.4. It was shown that the peak interface friction angle increased rapidly with small changes in roughness up to a "critical" Rs value, above which, the rate of increase of the peak interface friction angle became less (Figure 2.4a and 2.4b). As with the peak interface friction angles, it was reported that the residual interface friction angles also increased rapidly with small changes in roughness up to a "critical" Rs value, after which, the rate of increase became less (Figure 2.4c and 2.4d). Further, it was noted that even though the trends are the same for the peak and residual interface friction angles, the mechanism for the residual interface friction angle is different such that the "critical"

roughness values for residual behavior are lower than for peak behavior. This was attributed to the residual strength being primarily a function of macro-scale surface roughness and almost all the micro-texture being removed at displacements near the peak strength which means that, above a critical value of surface roughness, the residual strength is mainly governed by the pulling out and tearing of the filaments from the geotextile, and consequently, the strength is a function of the strength of the geotextile itself.

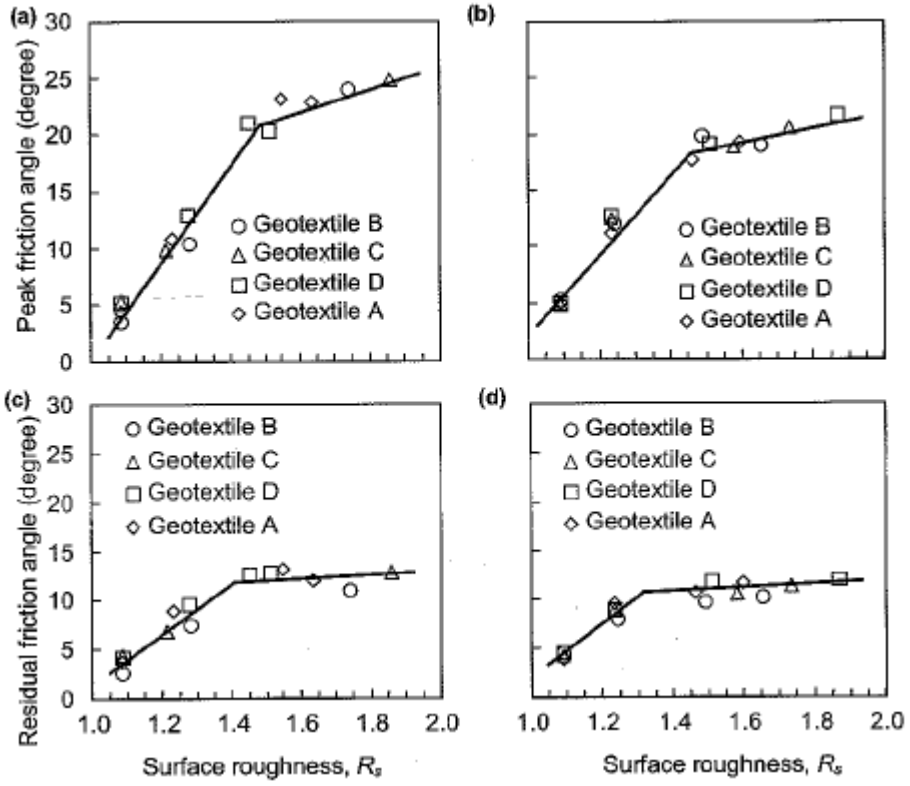

Figure 2.4 Peak and Residual Interface Friction Angles as a Function of Surface Roughness: (a) Peak at 50 kPa; (b) Peak at 100 kPa Normal Stress; (c) Residual at 50 kPa; (d) Residual at 100 kPa Normal Stress (Frost and Lee, 2001)
Note that: Geotextile A: Trevira Spunbond 011/550 continuous filament polyester NPNW (543 g/m2)
Geotextile B,C,D: Amoco #4506,#4510,#4516 staple filament polypropylene NPNW (203, 339, 543 g/m2)

Moreover, Frost and Lee (2001) defined a scalar parameter which is sensitivity ($\tau_{Peak}/\tau_{Residual}$) to numerically evaluate "post-peak strength loss" in geotextile – geomembrane interfaces, and additionally, related the sensitivity to the surface roughness of geomembrane (Figure 2.5) using Rs.

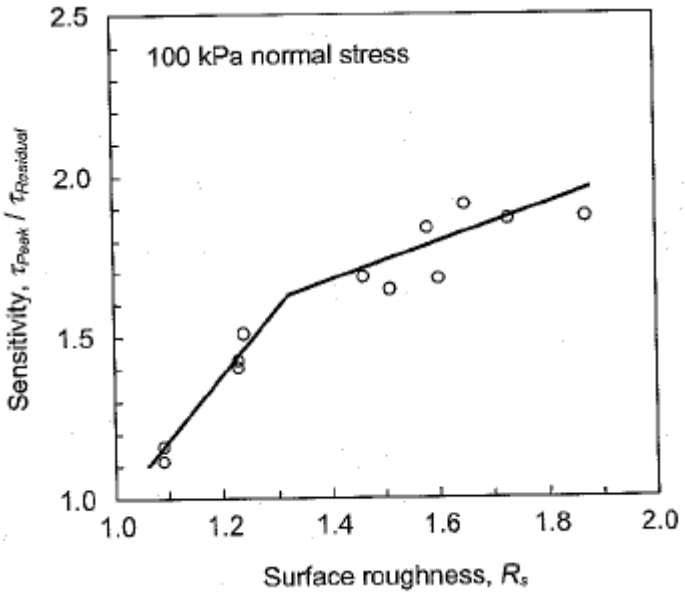

Figure 2.5 Geotextile – Geomembrane Interface Strength Sensitivity as a Function of Geomembrane Surface Roughness (Frost and Lee, 2001)

For the influence of surface roughness (i.e. geomembrane texture) on particulate – continuum materials interfaces, Dove (1996) reported important experimental results as a conclusion of a series of laboratory interface tests. A direct shear apparatus was utilized to investigate interface shear behavior of particulates against continuum materials and the mechanisms taking place during shearing with increasing surface roughness of continua. These findings were published in Dove et al. (1997) and quantitatively evaluated shear response of sand – geomembrane interfaces as the surface roughness changed using Rs [quantified by utilizing Optical Profile Microscopy (OPM) method, Dove and Frost

(1996)] as well as examined interface shearing mechanisms taking place at sand – geomembrane interfaces with increasing surface roughness. Four types of geomembranes based on textural classification scheme (see Table 2.1) and five different particulate materials (Ottawa 20-30, F-70, upper drain material, commercial blasting sand, and glass microbeads) to represent a broad range of geomembrane surface roughnesses in use and to provide insight for a variety of grain shapes and sizes. Their research showed that:

i. For smooth geomembranes, the grains at the surface were in a sliding mode of deformation and the shear zone was confined to the interface since the interface could not promote dilation.

ii. As surface roughness increased, the amount of dilatancy increased and the response became more consistent with classical soil mechanics principles.

iii. The peak and residual efficiency increased with small changes in roughness up to a certain Rs value, above which, the rate of increase with the change in roughness becomes less (similar to the behavior observed in geotextile – geomembrane interfaces by Frost and Lee (2001) with increasing roughness). This was attributed to the fact that the full soil internal friction was mobilized.

2.2.2. Texturing Technique/Method

Textured geomembranes are manufactured by several methods including structuring, coextrusion/blown coextrusion, impingement/spray on and lamination/ extrusion coating (Donaldson, 1995). The texturing technique has first order influence on the strength and durability of both the micro-topography (see Figure 2.2) and to a greater extent, the macro-topography (see Figure 2.2) created in the texturing process, as well as the bond strength between the features and the geomembrane core. As the bond strength

increases, the elongation abilities of the geomembrane are typically sacrificed. The texturing technique is known to influence the developed shear strength of fabric – continua as well as particulate – continua interfaces. According to the original work of Stark et al. (1996), the residual strengths for geotextiles sheared against textured geomembranes manufactured by the coextrusion method were higher than those measured on geomembranes manufactured by the lamination or impingement methods. The authors indicated that the applied shear stress can remove or damage some or all of the texturing at high normal stresses. The removal or damage of the texturing appears to be of greater concern for textured HDPE geomembranes created by the lamination and impingement techniques.

Hebeler (2005) carried out an experimental study to further observe the effect of texturing technique (coextruded textured versus structured textured) on interface shear response of geotextile – textured geomembrane systems. The stiff rounded macrotexture of the structured geomembrane was found to provide more frictional response and higher stiffness. The behavior of the two materials appeared to transition towards a convergent response at higher normal stress range (>100 kPa) where macro and base geomembrane texture begin to control the system behavior. Selection of the sensitivity ($\tau_{Peak}/\tau_{Residual}$) to be utilized as a function of normal stress level was a useful measure to highlight differences in the peak and pseudo-residual responses of the coextruded and structured geomembranes. The coextruded geomembrane-geotextile system exhibited higher sensitivity values at low normal stresses showing a measured maximum at the lowest normal stress tested. It was indicated that the global interaction mechanisms of the two systems (coextruded versus structured) show similar behaviors as a result of the

similarities in “macro” geomembrane surface texture, and the increasing contributions of matrix level geotextile – geomembrane texture interactions (Figure 2.6).

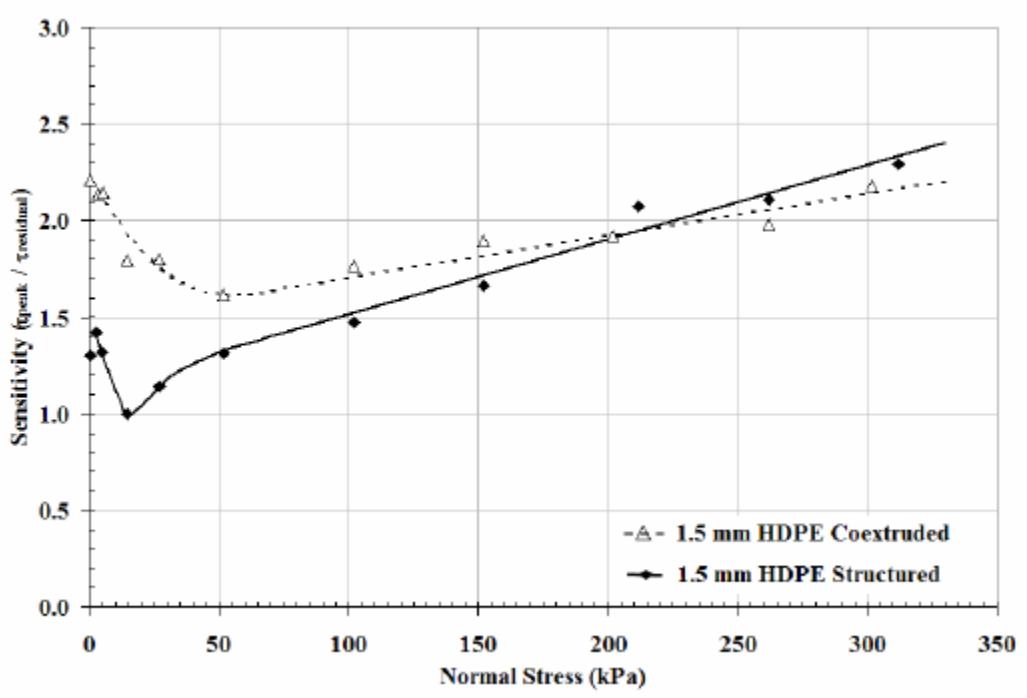

Figure 2.6 Comparison of the Sensitivity with Increasing Normal Stress Level for Coextruded or Structured Textured Geomembrane – NPNW-PP Geotextile (203 g/m^2) Interfaces (Hebeler, 2005)

2.2.3. Material Type/Base Polymer Composition

2.2.3.1. Geomembrane Core Material Polymer Composition

Geomembranes are produced from different base polymeric material compositions including high-density polyethylene (HDPE), linear low-density polyethylene (LLDPE), very flexible polyethylene (VFPE) and polyvinylchloride (PVC) amongst others, each of which has different interfacial shear as well as mechanical and durability properties. Therefore, it is crucial to understand their engineering behavior and to know the differences in the developed interface shear mechanisms as well as in the

observed tensile/compressive, puncture strength properties to ensure safe and stable design of geomembranes as a composite system in conjunction with geotextiles, sands or other geosynthetic materials. These important reasons have resulted in research efforts to investigate the influence of geomembrane base/core material polymer composition on the interface strength. Hillman and Stark (2001) carried out research work to observe the differences in the interface shear response and interface strength properties of HDPE, VFPE, and PVC geomembranes sheared against the same type of geotextiles in a torsional ring shear device. Shear tests were performed on both smooth and faille finish PVC geomembranes. The smooth side of the PVC geomembrane yielded higher peak and residual interface shear strengths than the faille side (Figure 2.7).

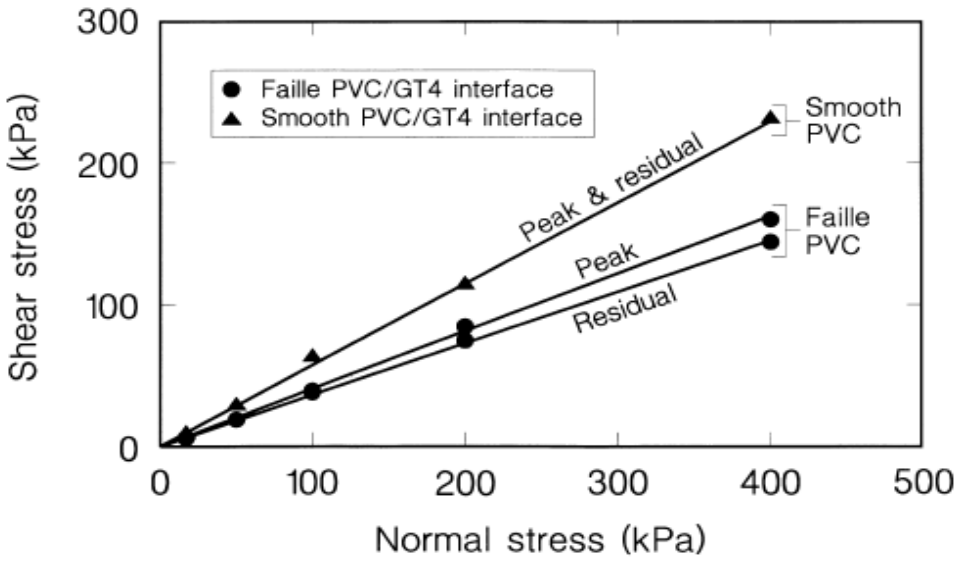

Figure 2.7 Comparison of Failure for Smooth and Faille PVC geomembrane – Nonwoven PP Geotextile (540 g/m^2) Interfaces (After Hillman and Stark, 2001)

The higher frictional strength of the smooth side of a PVC geomembrane was attributed to its higher surface pliability and more adaptable surface than the faille side

which possess surface depressions when in contact with the counterface material (i.e. geotextile) that result in a decrease in the interface contact area. Since the faille side of a PVC geomembrane renders a lower interface shear resistance than the smooth side, they deemed appropriate to report and focus on the shear strength of PVC geomembrane interfaces so that lower bounds for PVC geomembrane peak and residual interface shear strengths were established. The following results were attained at the end of their experimental study (Figure 2.8a and 2.8b):

i. The faille PVC and the textured HDPE geomembranes had similar peak failure envelopes. However, the peak strength of textured VFPE geomembrane interface was less than the other two geomembrane interfaces.

ii. The magnitude of post-peak strength losses experienced by the faille PVC and the textured VFPE was comparable; while, there was a significant post-peak strength loss occurred in textured HDPE geomembrane interface as reflected in the residual failure envelopes. This behavior observed was attributed to the geomembrane texturing being smoothed or polished as well as the fibers of the geotextile being torn and pulled out by the stiffer asperities of the texture HDPE geomembrane.

iii. The faille PVC geomembrane was found to have the best post-peak interfacial shear properties in conjunction with the geotextiles. Since the faille PVC geomembrane was able to tear or pull out only a small quantity of fibers from geotextile so that the geotextile can stay relatively intact and maintain the interface strength.

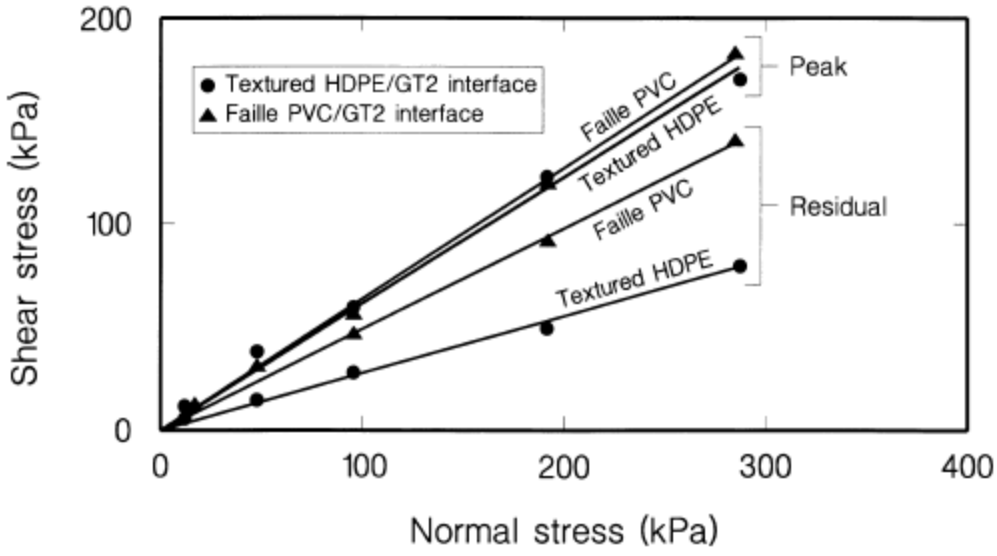

(a)

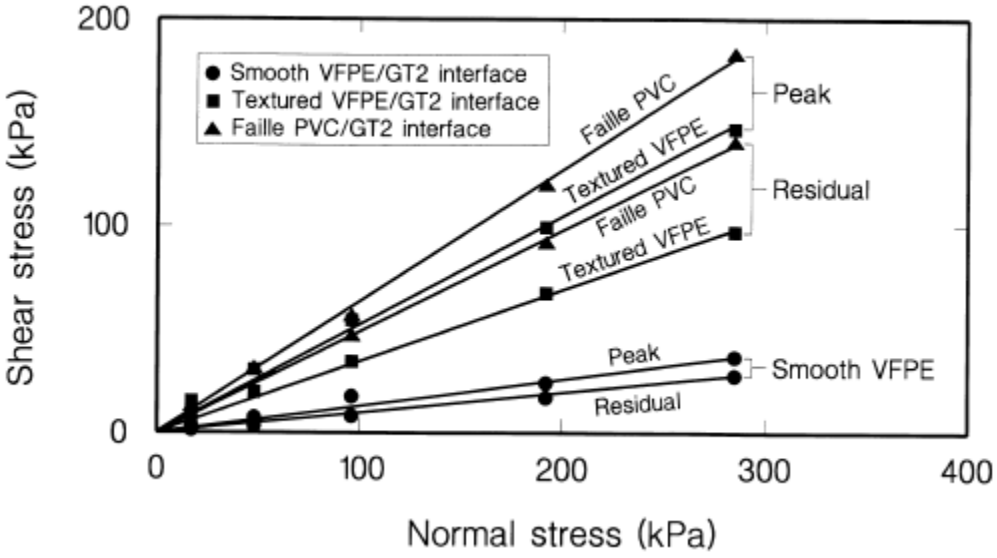

(b)

Figure 2.8 Comparison of Failure Envelopes: (a) Faille PVC and Textured HDPE Geomembrane – NPNW-PET (540 g/m^2) Geotextile Interfaces; (b) Faille PVC, Smooth VFPE, and Textured VFPE Geomembrane – NPNW-PET (540 g/m^2) Geotextile Interfaces (After Hillman and Stark, 2001)

2.2.3.2. Geotextile Filament Polymer Composition and Fiber Type

Several different polymeric materials are utilized to manufacture geotextile fibers such as polypropylene (PP), polyester (PET), polyethylene (PE), polyamide (PA) (nylon). These basic polymers are made into fibers by melting them, forcing them through a spinneret, and then hardening them by one of the three following methods: i) wet; ii) dry; or iii) melt (Koerner, 1998).

The friction coefficients between four types of flexible geomembranes and seven types of geotextiles made from "polypropylene" or "polyester" and produced from different fabric manufacturing methods (woven versus nonwoven) were evaluated in the extensive research work of Williams and Houlihan (1986). They found that woven geotextiles, which tended to have smaller contact areas, generally had lower interface friction angles than that of nonwoven geotextiles against relatively stiff geomembranes. Further, polyester geotextiles showed slightly higher frictional resistance than polypropylene geotextiles against geomembranes in sliding mode.

Similarly, in the comprehensive experimental study of Stark et al. (1996), five types of nonwoven geotextiles were utilized to understand the effects of geotextile polymer composition (polypropylene or polyester); fiber type (staple filament or continuous single filament) on geotextile – textured geomembrane interface shear resistance. The peak nonwoven geotextile – textured geomembrane interface shear resistance appeared to be influenced by both the polymer composition and fiber type. The residual interface shear resistance appeared to be dependent on polymer composition but independent on fiber type (Figure 2.9). This behavior was attributed to the continuous single fibers being longer and having more contact area with the geomembrane. The

greater contact area might have caused an increase in the shear force on the continuous fiber resulting in more tearing and pulling out. Once the continuous fiber is removed from the geotextile, it is oriented parallel to the shear direction resulting in a larger reduction in the post-peak strength due to the long nature of fiber (See the peak and post-peak strength envelopes of GT1 and GT4 in Figure 2.9). This behavior may not be "fully" observable and feasible especially for continuous single fiber geotextiles tested in the direct shear devices as opposed to "very large" displacement torsional ring shear apparatuses.

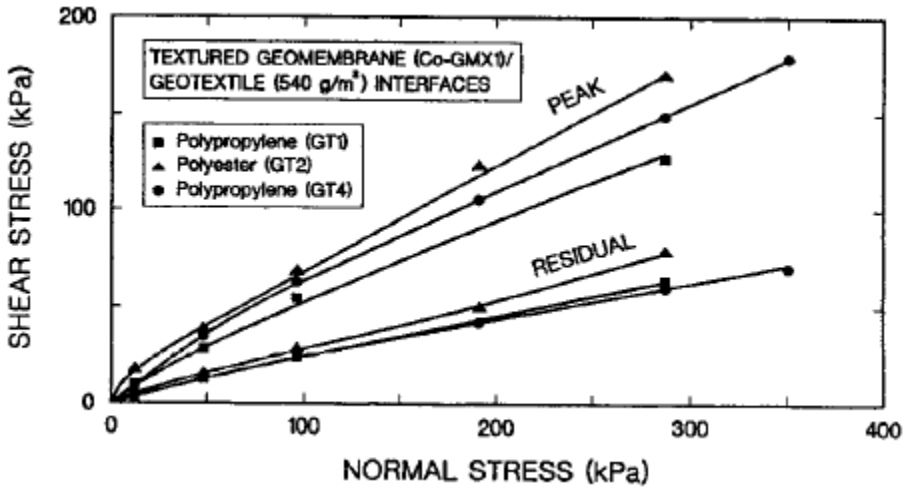

Figure 2.9 Effects of Nonwoven Geotextile Polymer Composition and Manufacturing on Interface Shear Resistance (Stark et al., 1996)
Note: GT1: Staple; GT2 & GT4: Continuous Single Filament

Similar results were obtained by Hillman and Stark (2001) such that the two most common geotextile type (NPNW continuous single fibers, 540 g/m^2) made from different base polymers PP and PET were sheared against a faille polyvinylchloride (PVC) geomembrane to further investigate the effect of geotextile fiber polymeric composition on interface shear strength. Again, the PET-based geotextile interface yielded higher peak

and residual frictional resistance/friction angles than the PP-based geotextile interface (Figure 2.10). This trend was attributed to the fibers having different polymeric compositional properties such that the filaments themselves do not possess the same "roughness" and "hardness" which is very important when temperature is being considered.

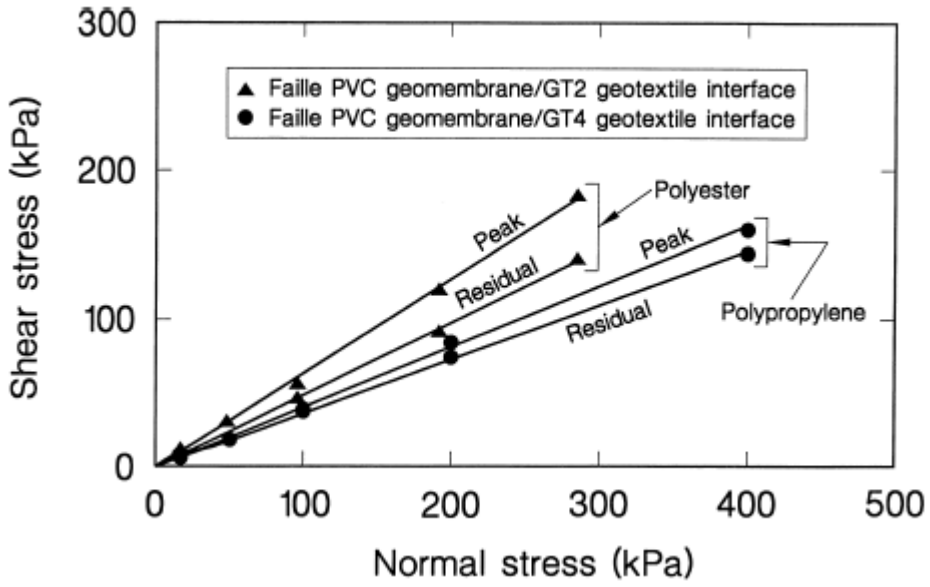

Figure 2.10 Effect of Nonwoven Geotextile Fiber Base Polymer on Interface Shear Strength (Hillman and Stark, 2001)

Additionally, two NPNW-PP (540 g/m^2) geotextiles were used in their study to determine the influence of geotextile fiber type (staple versus continuous) on the interface shear strength. As seen in the failure envelopes (Figure 2.11), the staple fiber geotextile yielded greater peak and residual interface strengths when sheared against a faille PVC geomembrane. Another important characteristic inferred from the failure envelopes is that the staple fiber geotextile did undergo a lesser amount of post-peak strength loss compared with the continuous single fiber geotextile. This behavior was attributed to the

staple fibers being too small or fine to embed into the PVC geomembrane to the same degree as the longer and larger diameter continuous single fibers. The geotextile specimens were observed at post-test stage and resulted in an explanation that fewer stable fibers were torn out during shear, which enabled the staple fiber geotextile to stay more "intact" than the continuous single fiber geotextile, and thus, prevented the interface from undergoing a large post-peak strength loss (Hillman and Stark, 2001).

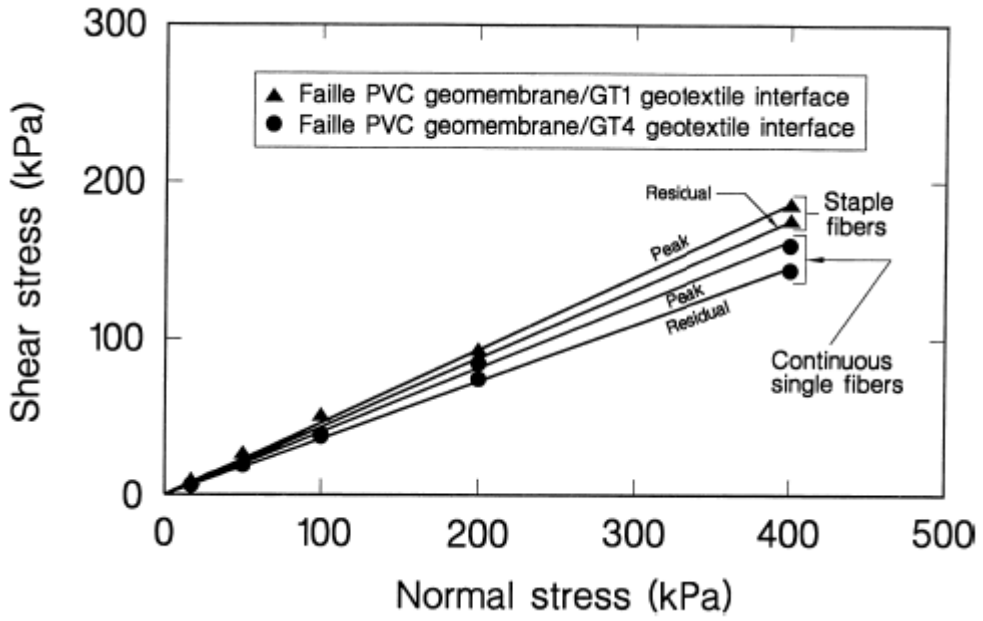

Figure 2.11 Effect of Nonwoven Geotextile Fiber Type on Interface Shear Strength (Hillman and Stark, 2001)

As a result, it is clearly seen that the mechanical properties of the fibers influence fabric – continua (geotextile – geomembrane) interface shear behavior.

2.2.4. Mass Density and Thickness

Depending on the purpose of use and manner of employment in the field, geotextiles are produced by manufacturers with different mass densities/thicknesses such

as 8 oz/yd^2 (270 g/m^2), 10 oz/yd^2 (338 g/m^2) and 12 oz/yd^2 (405 g/m^2). The thickness of geotextile influences the magnitude of peak as well as post-peak (pseudo residual) shear strength that develops at geotextile-geomembrane interfaces. Stark et al. (1996) performed several torsional ring shear tests on interfaces comprised of coextruded textured high-density polyethylene (HDPE)-nonwoven geotextiles having different mass densities (i.e. thickness, mass per unit area). It was found that there is negligible difference between peak as well as residual failure envelopes at normal stresses less than 100 kPa. Even, the thicker geotextile (mass per unit area: 540 g/m^2) exhibited very slightly higher shear strengths than that of thinner geotextile (mass per unit area: 270 g/m^2) (Figure 2.12). However, at normal stresses greater than 100 kPa, the thinner geotextile with lower mass density tends to yield a higher peak failure envelope than the thicker geotextile with larger mass density. It was anticipated that the larger mass per unit area or thickness resulted in some filaments being more easily pulled out or torn from the thick geotextile than the thin geotextile at large shear stresses. Consequently, it was suggested that a lower mass density may be more desirable for a liner system while the mass density does not appear to significantly influence the interface strength for cover systems. Additionally, the residual strengths obtained were comparable and there was almost no difference especially at very high stress levels greater than 250 kPa which was attributed to the fact that geotextile filaments were being pulled out and/or torn after the large shear displacement required to achieve a residual strength condition. Since a ring shear device allowing very large shear displacements compared to those achieved with a direct shear apparatus was used, the majority of geotextile filaments were oriented and combed parallel to the direction of shear at residual condition resulting in the residual

interface failure envelope appearing to be independent of the mass density or thickness of the nonwoven geotextile.

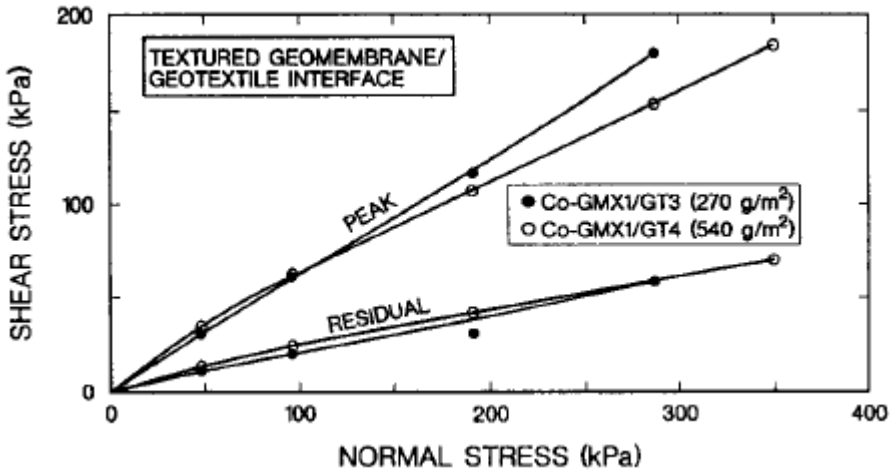

Figure 2.12 Effect of Nonwoven Geotextile Mass Density/Thickness on Interface Shear Resistance (Stark et al., 1996)

Frost and Lee (2001) reported the influence of nonwoven geotextile mass per unit area on textured geomembrane – nonwoven geotextile interface strength and required displacement to reach peak shear strength as shown in Figure 2.13. The trend for the geotextile with higher mass per unit area/mass density was in such a manner that it required more displacement to mobilize peak interface shear strength and exhibited higher peak interface shear strength between the geotextile and the geomembrane. The diameter of the filaments in each of the geotextiles was the same. They explained the different displacement behavior by the difference in geotextile thicknesses. It was observed that geotextiles with larger mass density were thicker even when subjected to the same normal stress. In addition, as the geomembrane was sheared against the geotextile, only the top of the thick geotextiles was displaced the same amount as the

geomembrane being sheared against it while the bottom of the geotextile is fixed to the geomembrane backing. They indicated that the magnitude of the relative displacement between the top and bottom surfaces of the geotextile is "proportional" to the thickness of the geotextile. They described that this might be called a "shear zone" within the geotextile.

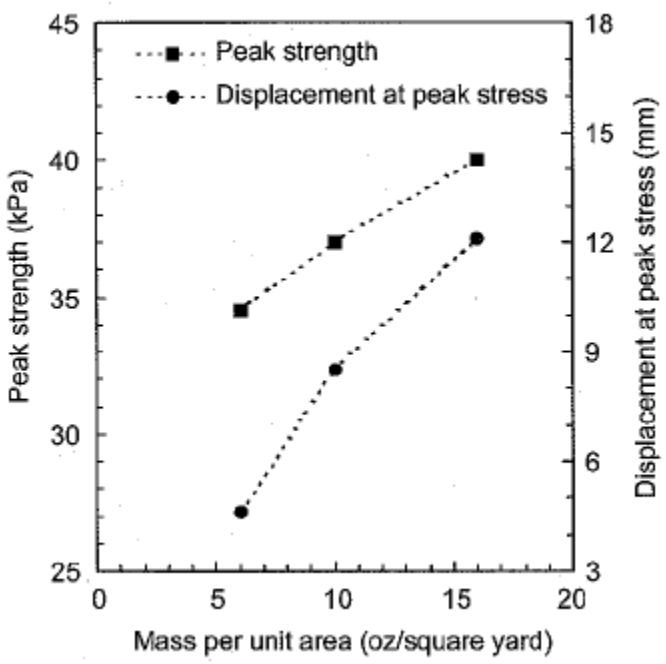

Figure 2.13 Effect of Mass per Unit Area of Geotextile on Peak Interface Shear Strength (Frost and Lee, 2001)

2.2.5. Hardness

Hardness which depends on stiffness and viscoelastic properties of the material is defined as the resistance of a plastic material to indentation (ASTM D 2240 – 05, 2005). An experimental research study was carried out by O'Rourke et al. (1990) who performed interface shear tests on sand-polymeric material (i.e. smooth geomembrane liner or pipe) interfaces with the focus being on the influence of hardness of the polymers

such as high-density polyethylene (HDPE), medium-density polyethylene (MDPE) and polyvinylchloride (PVC) on the developed interface friction angle relative to the direct shear friction angle of soil friction (Figure 2.14). Hardness of the polymers was determined by conducting Shore D Hardness measurements. A Scanning Electron Microscope (SEM) was utilized to take pictures of the surfaces at pre-shearing as well as post-shearing stages. The photographs of SEM showed that the surface hardness plays an important role in the mechanism of shear transfer, and consequently, in the development of interface strength. Relatively hard smooth polymer surfaces (i.e. HDPE liner) promoted sliding of sand grains, while relatively soft surfaces (i.e. PVC liner) induced sand particle rolling at the interface. They concluded that surface hardness is a good index for estimating the surface shear strength characteristics of polymeric materials (i.e. geomembrane). The interface friction angle relative to the direct shear friction angle of the soil was found to decrease with increasing Shore D Hardness of the polymers.

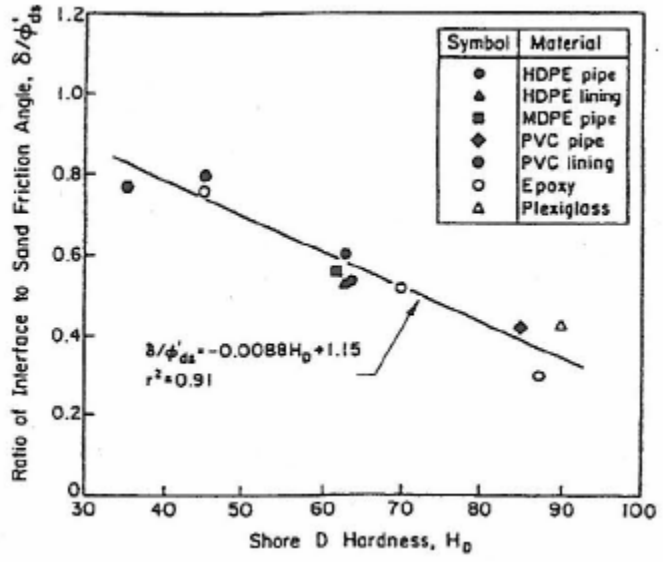

Figure 2.14 Ratio of Interface Angle of Shear Resistance to Direct Shear Angle of Soil Friction and Shore D Hardness (O'Rourke et al., 1990)

2.2.6. Particle Shape/Angularity

The shape of soil particles (i.e. rounded versus angular) in contact with a geomembrane is one of the other important factors in defining shear strength and further the interface shearing mechanism (i.e. sliding, rolling, plowing) developed at the interface during shearing. The behavior of granular soil and smooth or textured HDPE as well as PVC geomembrane interfaces was studied by Vaid and Rinne (1995) using a ring shear apparatus. It was concluded that the textured HDPE geomembrane-angular granular soil interfaces yielded interface friction angles close to sand internal friction angle. Besides, the authors observed for PVC geomembrane-angular granular soil interfaces that the failure surface was within the sand sample and not along the interface. For the smooth HDPE geomembrane case, scarring along the displacement path occurred. The grooves after shearing were deeper for the angular sands.

Frost et al. (1999) evaluated different sand structures adjacent to the interface during shearing with a direct shear apparatus. It was reported that the shear mechanisms for subrounded and angular uniform sands adjacent to geomembranes were directly influenced by the surface roughness of the geomembranes as follows:

i. The failure mechanism for smooth surfaces was sliding of the particles along the interface with minor changes in density up to a distance of two particle diameters ($2 * D_{50}$).
ii. The size of the affected zone within the soil sample increased to a distance of six particle diameters ($6 * D_{50}$) from the interface as the geomembrane surface becomes rougher.

Additionally, it was shown by Dove and Frost (1999) that the main component of the friction force was plowing at all normal stress levels for interface shear tests conducted with angular blasting sand as opposed to subrounded to rounded Ottawa 20-30 sand. They pointed out that the increased amount of wear/scar on geomembrane surface after shearing directly corresponds to increased force due to plowing, and consequently, increased shear stress at the interface. They concluded that the interface shear strength for granular soil-geomembrane interfaces are controlled by the mechanisms of friction acting during shearing such as slippage, rolling, or plowing which depends on sand particle angularity in addition to normal stress level at the interface and relative hardness of counterface materials.

Figure 2.15 presents strength envelopes from direct interface shear tests reported by Dove and Frost (1999) where the friction angles were determined from traditional linear regression of the data. The angular blasting sand resulted in the greatest friction coefficient and the spherical glass microbeads gave the lowest interface friction angle. Ottawa 20-30 sand had a friction coefficient intermediate between the blasting sand and the glass microbeads. All the particulate materials used in their study had similar mean grain size (D_{50}). The only difference was the shape/angularity of the particulate materials selected to be sheared against smooth geomembranes.

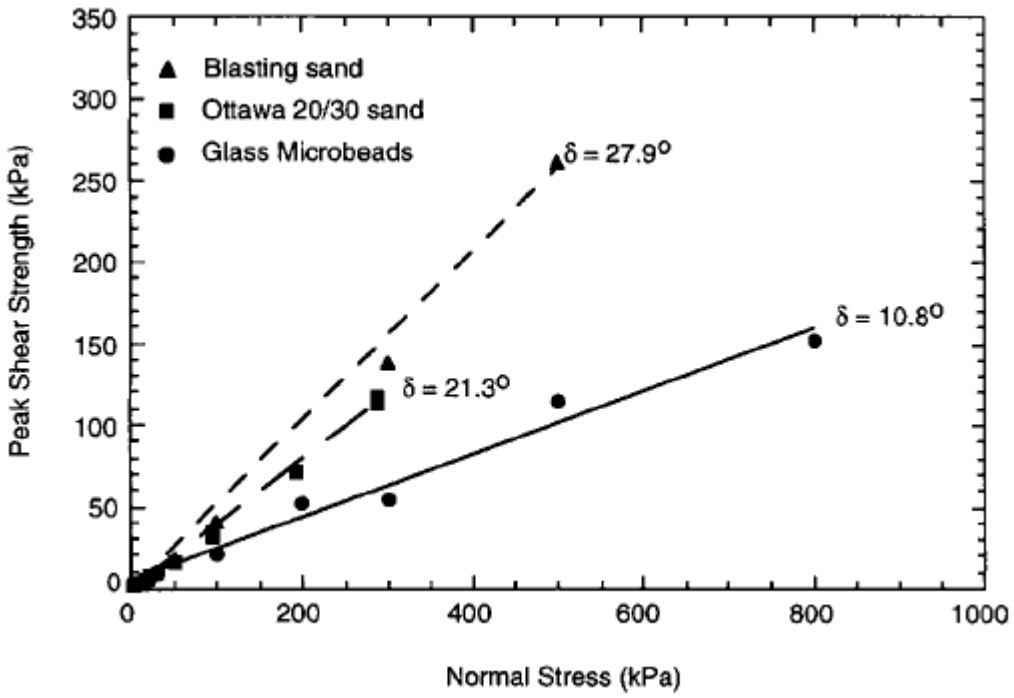

Figure 2.15 Effect of Particle Shape/Angularity on Peak Interface Shear Response between Particulate Materials and Smooth Geomembranes (Dove and Frost, 1999)

2.2.7. Mean Grain Size (D_{50})

Mean grain size of granular soil particles in contact with planar geomembrane surface influences the coefficient of friction of the interface. An experimental study by Williams and Houlihan (1987) using a modified direct shear apparatus for various geomembrane-soil interfaces showed that the magnitudes of interface friction parameters are dependent on mean grain size of granular soil in addition to surface roughness, confining stress and soil density. Furthermore, Vaid and Rinne (1995) reported that the grooves due to scarring/wear of smooth HDPE geomembranes by granular soil particles during shearing did not exceed 10 percent of the D_{50} of the sand.

The effect of the geometry of the surface roughness on interface shear strength of various geomembranes with Ottawa 20-30 sand was investigated by Dove and Harpring

(1999). The grain size (i.e. D_{50}) of soil particles and the texture of a geomembrane surface were related to interface performance using roughness parameters. They stated that in order to achieve full interface efficiency which was defined as the ratio of the peak interface friction angle to the peak soil friction angle, the followings must be satisfied:

i. The average spacing (S), which is the mean local peak to peak spacing between asperities, must be at least the D_{50} of the soil grains at the interface.
ii. The height of the asperities must be as large as the D_{50} of the soil grains at the interface.

Therefore, mean grain size (D_{50}) is one of the determining factors for full mobilization or relative mobilization of internal soil friction angle/resistance at granular soil-geomembrane interfaces.

Figure 2.16 shows the interface shear results from Frost and Han (1999) that the peak interface friction coefficient (symbolized as μ_P) between fiber – reinforced polymer (FRP) composite and sand decreases as the mean grain size (D_{50}) increases. It was indicated that this finding concurs with that of Rowe (1961) that large particles have a lower friction angle than small particles with the same mineralogy when a mass of the particles slides on identical rough surfaces. This conclusion was reinforced by the results of Frost and Han (1999) such that two data points of Ottawa 20-30 sand (OTW) falls within the range of the data for glass beads which is due to both Ottawa 20-30 and glass beads (GB) having the same mineralogy and round particle shape (Figure 2.16). Furthermore, it was expressed that Valdosta Blasting Sand (VBS) reasonably had a higher interface friction coefficient than that of Ottawa 20-30 and glass beads as it is an angular material.

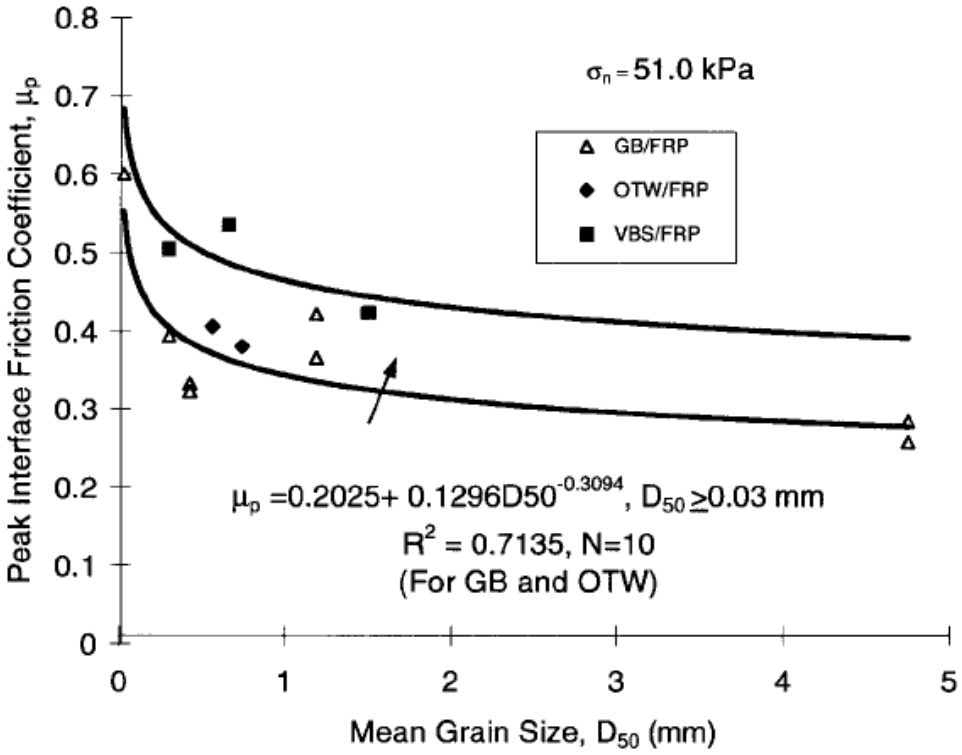

Figure 2.16 Influence of Mean Grain Size (D_{50}) of Particulate Material on Peak Interface Friction Coefficient (Frost and Han, 1999)

2.2.8. Density

The initial density or state of particulate materials influences the shear strength developing at the interfaces in addition to its significant effect on "internal" friction angle (φ) of the particulate material itself. Yoshimi and Kishida (1982) used a torsional ring shear apparatus to estimate the friction between dry sand and steel over wide ranges of sand densities. The soils selected for use in the tests were Toyoura, Tonegawa, and Niigata sands. The sand specimens were prepared by pluviating dry sand from a tube. They concluded based on the results of constant normal stress friction tests that the relative density (D_r) of the sand specimens does not have as much significant influence as that of the surface roughness of steel on the coefficient of friction.

Moreover, it was investigated by Dove (1996) and Dove et al. (1997) that:

i. An increase in the relative density produced an increase in peak interface shear strength for particulate material - textured geomembrane interfaces at 100 kPa normal stress level, whereas, an increase in the relative density resulted in a decrease in the peak interface strength for the smooth geomembranes.

ii. Varying the relative density did not appear to have an effect on the residual interface friction angles for the textured geomembranes; whereas, increasing the relative density caused a decrease in the residual interface friction angles for the smooth geomembranes.

Consequently, based on their results, it is evident that the influence of density of particulate material on the magnitude of peak as well as residual interface strengths developing at particulate material – continua interfaces depends on the surface roughness of continuum material adjacent to the interface.

Based on the experimental results obtained from interface shear tests of fiber – reinforced polymer (FRP) composite or steel and sands having different particle angularity, Frost and Han (1999) indicated that the peak friction angle for specimens in a loose state is closed to the friction angle at steady state, although the difference increases with an increase in relative density. This statement is also consistent with the steady-state theory revealed by Poulos (1971) and reevaluated by Vaid et al. (1990). The typical relationship between peak friction angle and relative density at a fixed normal stress with tests on angular Valdosta Blasting Sand (VBS) is shown in Figure 2.17. The friction angle increases with relative density; while, the friction angle at steady state remains constant.

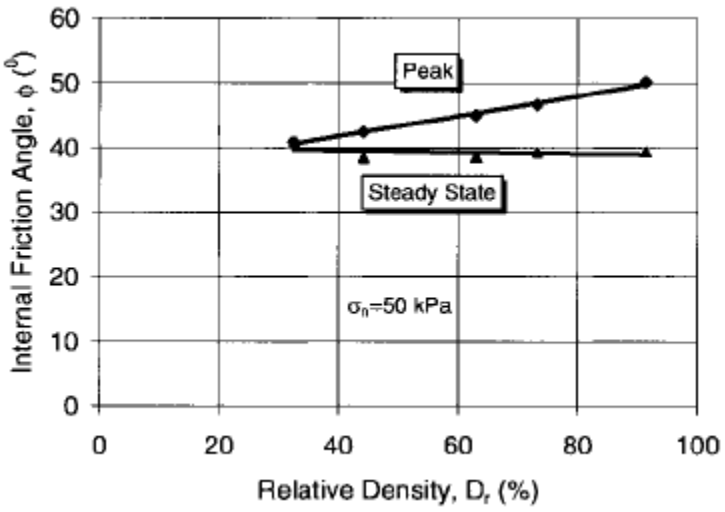

Figure 2.17 Relationship between "Internal" Friction Angle and Relative Density (Frost and Han, 1999)

The results of direct shear tests as illustrated in Figure 2.17 shows that the difference in the peak "internal" friction angle (φ) for an angular Valdosta Blasting Sand from a loose state to a dense state is about 10°. However, the peak "interface" friction angle (δ_P) is less influenced (only about 2° - 3°) by the initial density as observed from the results of interface tests between fiber reinforced polymer (FRP) composite or steel and Valdosta Blasting Sand (Frost and Han, 1999) (Figure 2.18). Besides, Lehane et al. (1993) had reported that the interface friction between steel and sand is dependent on the initial density of sand which concurs well with the findings noted above.

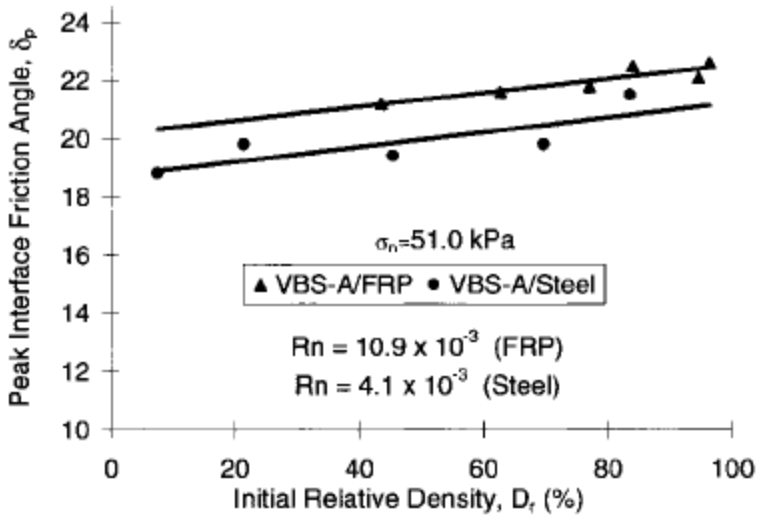

Figure 2.18 Relationship between "Peak Interface" Friction Angle and Relative Density (Frost and Han, 1999)

2.2.9. Normal Stress Level

Friction theory was first revealed by Leonardo da Vinci in the 15th century as a relationship governing the resistance between bodies in intimate contact. Amonton (1699) republished the basic theory of friction as: i) Friction force is proportional to normal load; ii) Friction force is independent of contact area (Bowden and Tabor, 1954; Bhushan, 1999).

The coefficient of friction (shear resistance normalized by normal force) is constant based on the fundamental rules of basic theory of friction. Most materials obey Amonton's Law. However, the interfaces comprised of polymeric materials do not obey these fundamental rules of friction. The friction force, (F) is governed by fundamental shear strength mechanisms as well as is being composed of one or more components as follows. For most continuous materials forming multi-asperity contacts, two components have been identified as: i) adhesion component; ii) "plowing" or plastic deformation component (Bowden and Tabor, 1954; Shooter and Tabor, 1952; Briscoe, 1992). For

interfaces comprised of polymers, as the normal load increases, the coefficient of friction (normalized friction: proportion of shear force to normal load) decreases with a constant slope or the magnitude of this reduction gets greater at very high normal stress levels. Primary findings regarding the influence of normal load on the normalized frictional resistance of polymeric material interfaces was published as a result of fundamental work of Archard (1957) (Figure 2.19).

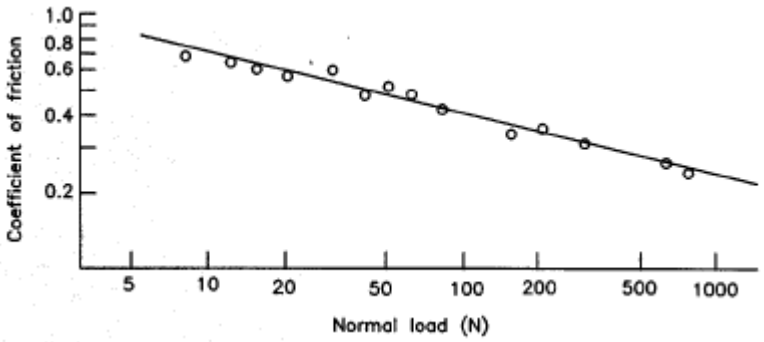

(a)

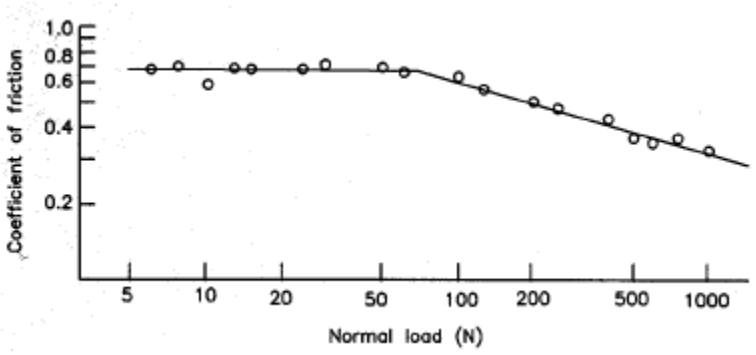

(b)

Figure 2.19 Inconstant Coefficient of Friction of Polymethylmethacrylate (PMMA): (a) Polished; (b) Lathe Turned (Archard, 1957)

The resulting linear peak and residual envelopes from direct interface shear tests between a range of geotextiles and geomembranes under different normal load conditions from Frost and Lee (2001) are shown in Figure 2.20. There is clearly some degree of

curvature especially for the peak failure envelope of moderately/heavily textured geomembrane and for the residual (post-peak) strength envelope of smooth as well as slightly textured geomembranes.

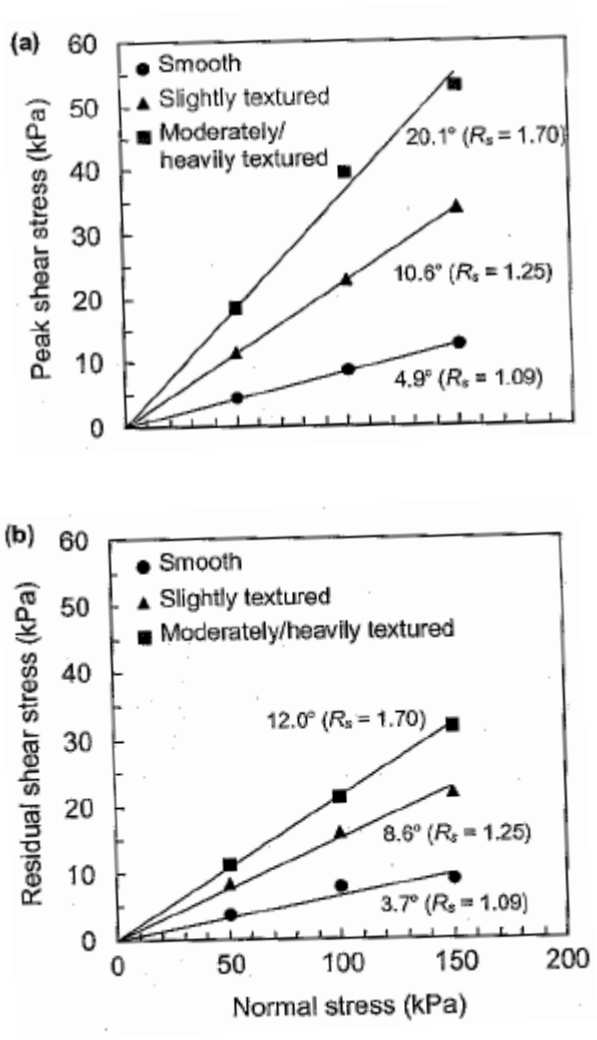

Figure 2.20 Peak and Residual Failure Envelopes for Geotextile - Geomembrane Interface: (a) Peak; (b) Post-Peak (Residual) (Frost and Lee, 2001)

Hebeler et al. (2005) reported the results of interface shear tests over a large range of normal stresses (0.4 kPa – 312 kPa) to capture variations in geotextile-geomembrane interface shear behavior as a function of normal stress level. Their results provided an

insight into textured geomembrane – geotextile interaction mechanisms and the development of interface shear response over a large range of normal stress levels. The structured geomembrane – NPNW geotextile composite system clearly exhibited a linear peak strength envelope over the entire range of normal stresses tested; whereas, the coextruded geomembrane – NPNW geotextile composite system showed a non-linear peak strength response at low normal stresses (< 15 kPa), later transitioned to a linearly increasing peak strength response over the remainder of the tested normal stresses (15 – 302 kPa) (Figure 2.21).

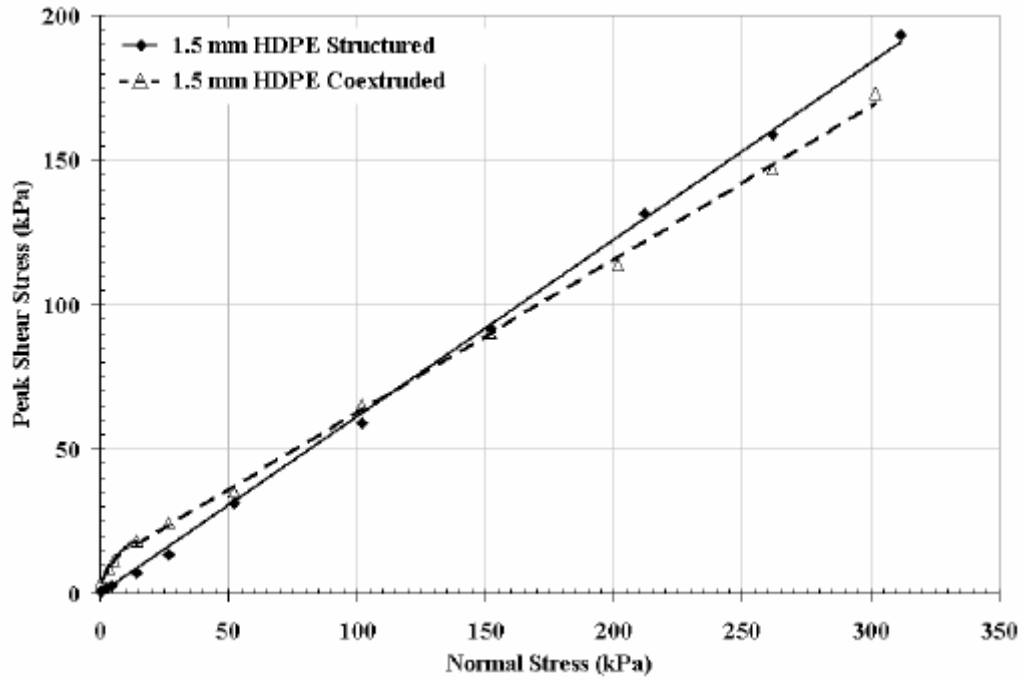

Figure 2.21 "Peak" Interface Shear Strength as a Function of Normal Stress Level for NPNW Geotextile – Textured Geomembrane (Hebeler et al., 2005)

On the other hand, the post-peak (pseudo-residual) interface shear strength (determined based on the shear stress values at 80 mm displacement) of both co-extruded

and structured textured geomembrane interfaces exhibited similar non-linear trends as a function of increasing normal stresses. The shape of pseudo-residual strength envelope is non-linear with a diminishing rise in the amount of increase in the post-peak shear strength as the normal stress increases (Figure 2.22).

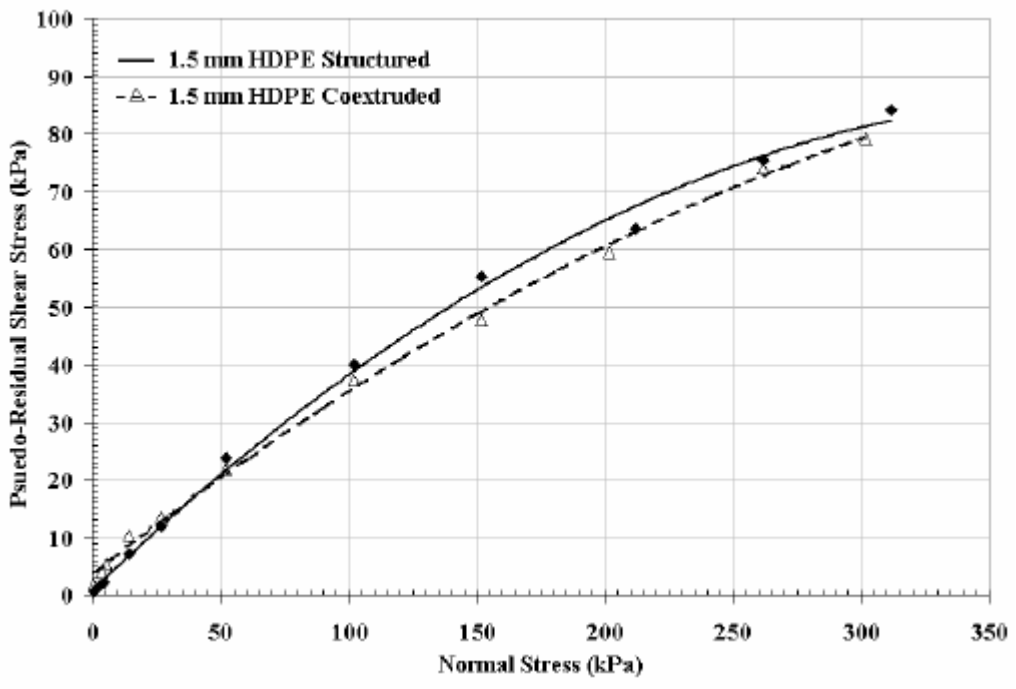

Figure 2.22 Pseudo-Residual Interface Shear Strength as a Function of Normal Stress Level for NPNW Geotextile – Textured Geomembrane (Hebeler et al., 2005)

The typical failure envelope for a soil – geomembrane interface is shown in Figure 2.23. Both the peak and the residual failure envelopes are generally curved. There is initially a significant increase in interface shear strength as the normal stress is increased, resulting in greater non-linearity in the failure envelopes. At higher normal stresses, the increase in interface shear strength is not as significant as at lower normal stresses, and therefore, the non-linearity of failure envelopes reduces at higher normal stresses. Without any significant loss of accuracy, a linear Coulomb-type failure envelope

can be drawn through the data points for a range of normal stresses expected in the field (Figure 2.23). This failure envelope is defined in terms of two interface shear strength parameters which are the interface friction angle (δ) representing its inclination in the shear stress-normal stress space, and adhesion (α) representing the intercept of the failure envelope with the shear stress axis. Stability of any slope containing a geomembrane can be assessed using these interface shear strength parameters (Fleming et al., 2006).

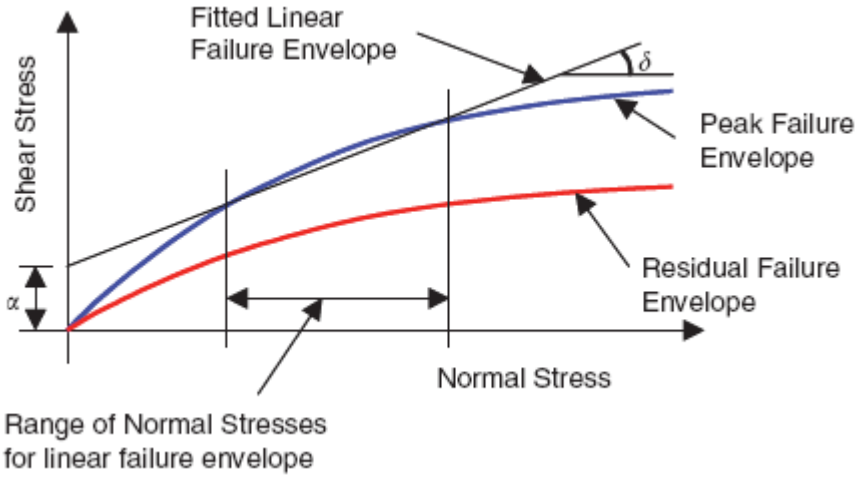

Figure 2.23 Typical Failure Envelopes for Soil - Geomembrane Interface (Fleming et al., 2006)

2.2.10. Material Combinations considering Overlying Material

The effects of overlying materials on geotextile (8 oz/yd^2 [270 g/m^2]; 12 oz/yd^2 [405 g/m^2]) - geomembrane (smooth or textured) interface shear resistance were studied by Kim (2006) using four different particulate materials. The selected particulate materials included Ottawa 20-30 sand, and Blasting sand (both had similar D_{50}) to observe the effects of particle shape (rounded versus angular) of overlying material on geotextile-geomembrane interface shear response as well as two different glass beads

having different mean grain sizes (D_{50}) to see the effects of particle size of overlying material on interface shear response: I) The 20-30 glass beads have a uniform size distribution similar to the selected sands; II) The large glass beads were 5 mm diameter. For both the light and the heavy geotextiles, the larger grain size (glass beads with 5 mm diameter) used as cover particles exhibited higher resistance than even the blasting sand sheared against smooth HDPE geomembrane (Figure 2.24).

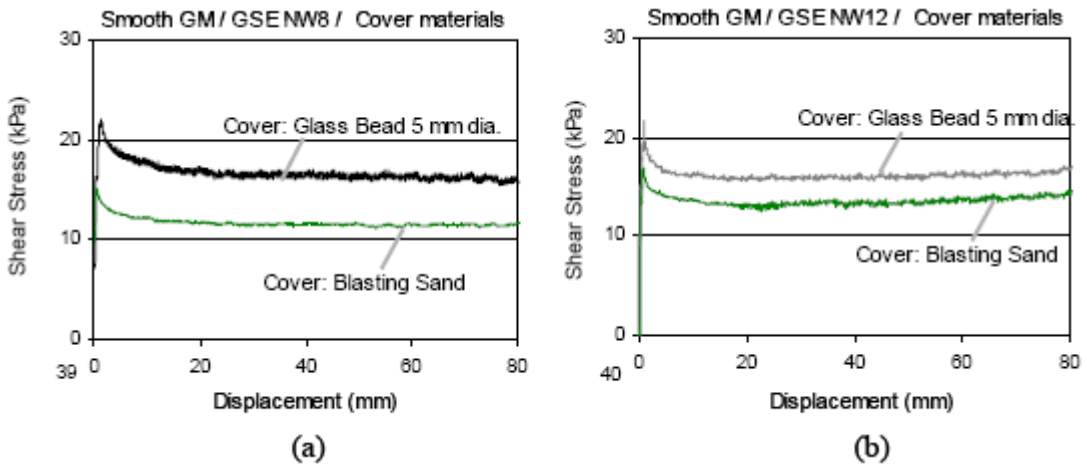

Figure 2.24 Different Material Combinations: Effects of Overlying Material on the developed Geotextile- "Smooth" Geomembrane Interface Shear Response (Kim, 2006)

For light weight or lower mass density geotextile, the shear stress-displacement response of geotextile - textured geomembrane interface with angular Blasting sand cover soil exhibited a lower displacement to peak, nearly the same interface shear strength for the peak, but lower interface shear resistance for the post-peak (pseudo-residual) than the Ottawa 20-30 sand configuration (Figure 2.25a). For heavy or thicker geotextile, the interface shear response of geotextile - textured geomembrane material combination underlying Blasting sand showed nearly the same displacement to peak, however higher

interface shear strength obtained for both peak and pseudo-residual conditions (Figure 2.25b).

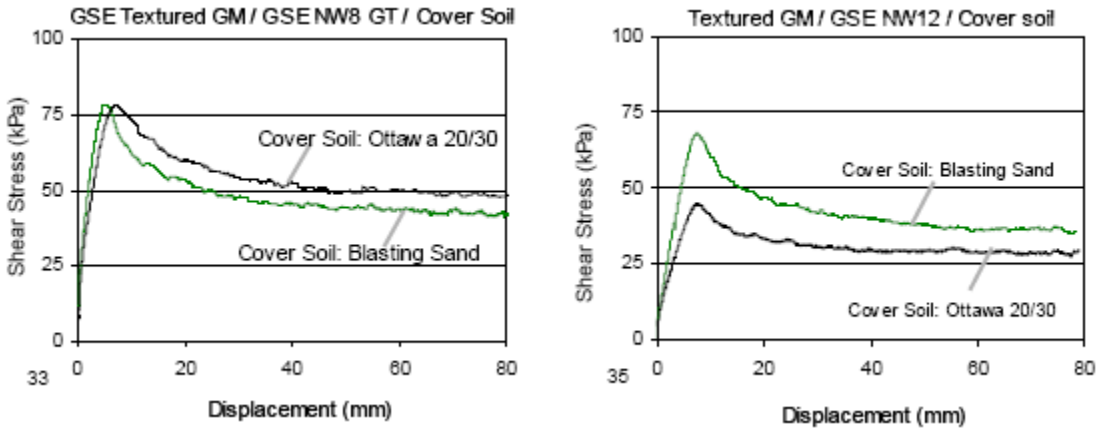

(a) (b)

Figure 2.25 Different Material Combinations: Effects of Overlying Material on the developed Geotextile – "Textured" Geomembrane Interface Shear Response (Kim, 2006)

Figure 2.26 shows the results of geotextile (thick and thin) versus textured geomembrane interface shear tests from Kim (2006) underlying large size borosilicate balls (glass beads with 5 mm diameter). The light geotextile (mass density: 270 g/m^2) exhibited a different shape of shear stress-displacement curve. The author has proposed that the first yield point on the curve resulted from the rearrangement of large borosilicate particles affected by geomembrane texture relief through the thin geotextile layer which was followed by the failure of geotextile-geomembrane interface. In addition, due to overlying uniformly graded large glass beads with 5 mm diameter, the stress concentrations through the thin geotextile layer onto the textured geomembrane surface resulted in higher interface resistance at large displacements. The heavy geotextile (mass density: 405 g/m^2) exhibited a typical shear stress – displacement curve without a local

failure in contrast to the case with the light geotextile. The displacement to peak was nearly the same as the displacement to local failure in the thin geotextile case due to rearrangement of the large size glass beads. The peak shear strength was comparable or very slightly lower than with the thin geotextile, but pseudo-residual shear response was lower than that of the light geotextile (Figure 2.26).

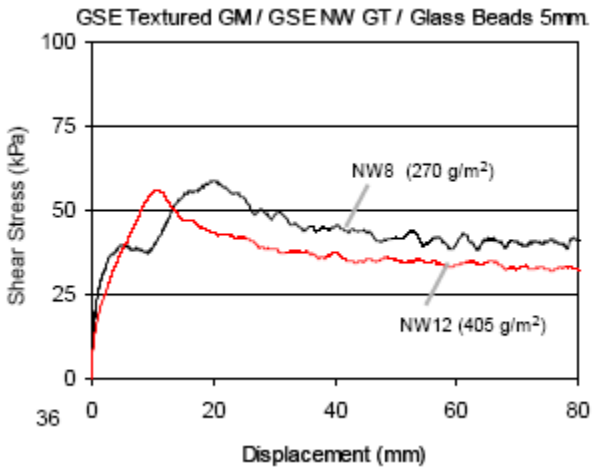

Figure 2.26 Interface Shear Response of "Textured" Geomembrane sheared against "Light" & "Heavy" Geotextiles covered by Borosilicate Spherical Glass Beads of 5 mm Diameter (Kim, 2006)

2.2.11. Shear Displacement Rate

The effect of shear rate on interface shear strength of composite geosynthetics system is insignificant in "dry conditions". Stark et al. (1996) reported that shear displacement rate does not significantly influence the measured peak as well as residual shear strengths developed at nonwoven geotextile - textured geomembrane interfaces (Figure 2.27). They performed the interface tests at shear displacement rates ranging from 0.029 mm/min to 36.7 mm/min (~1250 times of initial shearing rate). The peak and residual shear strengths vary slightly as the displacement rate changes. Consequently, as

was noted by Bove (1990), the interface shear strengths (peak and residual) in dry conditions are not sensitive to shearing rate.

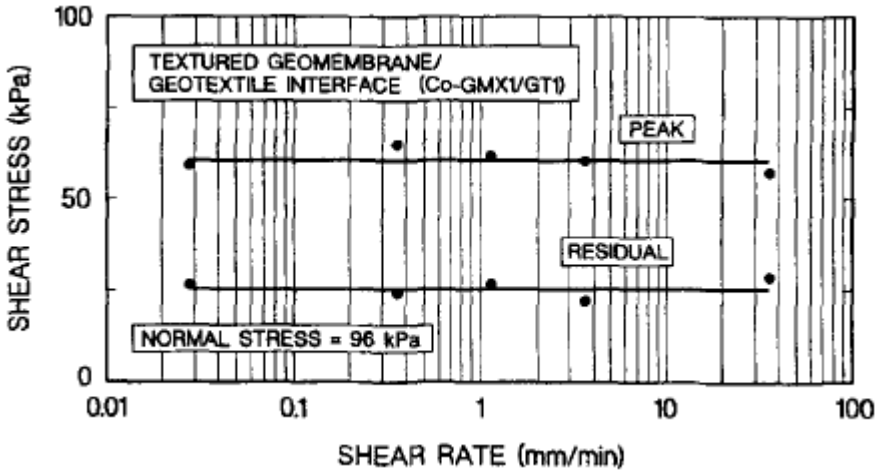

Figure 2.27 Effect of Shear Displacement Rate on Nonwoven Geotextile – Coextruded Textured Geomembrane Interface (Stark et al., 1996)

2.2.12. Summary

A qualitative assessment of several factors affecting the shear strength of particulate /continuum material interfaces is tabulated in Table 2.2. As shown in Table 2.2 and emphasized in this chapter as well, the surface hardness of geomembranes as well as the mechanical properties of geotextile filaments are significant factors influencing the resultant strength developed at the interface and the observed shear behavior/response of soil-geosynthetic as well as geosynthetic-geosynthetic interfaces. Consequently, changes in surface hardness of continuum materials and variations in physical or mechanical properties of fabric fibers will affect the interface strength. Additionally, particle shape/angularity, surface roughness, density, stress level, fibrous material mass density and continuum base material type have the most significant influence on the observed

drained stress-shear displacement response and the developed peak and post-peak interface shear strengths of particulate – continuum and fibrous – continuum material interfaces.

Table 2.2 Relative Importance of Factors Affecting Shear Behavior of Particulate – Continuum and Fibrous – Continuum Materials Interfaces At Room Temperature (21°C) (Adapted from Dove, 1996 and Lee, 1998)

		Qualitative Estimate of Effect		
Type	**Factor**	**Initial Modulus**	**Peak Stress**	**Residual Stress**
Particulate Material *(Soil)*	Angularity[1]	High	High	High
	Mean Grain Size (D_{50})	Medium	Medium	Medium
	Density	Medium	High	Low
	Coefficient of Uniformity (C_u)	Low	Low	Low
	Initial Soil Structure	Medium	Low	Low
	Particle Surface Roughness[2]	Low	Low	Low
Continuum Material *(Geomembrane)*	Surface Roughness	High	High	High
	Surface Hardness	High	High	High
	Type of Polymer/Core Material	High	High	High
Fibrous Material *(Geotextile)*	Mass Density/Thickness	Medium	Medium	Medium[5]
	Fabric Style	High	High	High
	Type of Polymer/Core Material	Low	Low	Low
	Type of Fiber	Low	Low	Low
	Fabric Opening	High	High	High
	Surface Roughness	High	High	High
Testing	Normal Stress[3]	High	High	High
	Test Method	High	High	High
	Strain Rate[4]	Negligible	Negligible	Negligible

Note: [1] Effect can be "low" for very rough geomembranes
[2] Effect can be "high" for smooth geomembrane
[3] Effect can be "low" for very rough geomembrane
[4] Tests in Dry/Drained Conditions
[5] Effect can be "low" at very high normal stress levels (i.e. > 250 kPa)

2.3. Temperature Effects on Polymeric Materials

To examine the influence of temperature on polymeric materials, it is essential to briefly explore the chemical structure of some common polymers whose resins are commonly used as a base material to manufacture geosynthetics that have found widespread applications in geotechnical engineering.

2.3.1. Chemical Structure of Common Polymers from which Geosynthetics Produced

2.3.1.1. Polyethylene (PE)

Polyethylene (PE) is a polymer consisting of long chains of the monomer ethylene. The ethylene molecule is chemically represented as C_2H_4 for which two CH_2 groups are connected by a double bond ($CH_2=CH_2$). The molecular chemical structure of ethylene which is the building stone of polyethylene is shown in Figure 2.28. It is generally used to produce geomembranes. Two types, which are high-density polyethylene and low-density polyethylene, commonly exist in the geosynthetic market. Low-density polyethylene is crystallizable up to 65% with linear chains and occasional branching, whereas, high-density polyethylene is crystallizable to 90% with linear chains. Both are thermoplastic (Daniels, 1989).

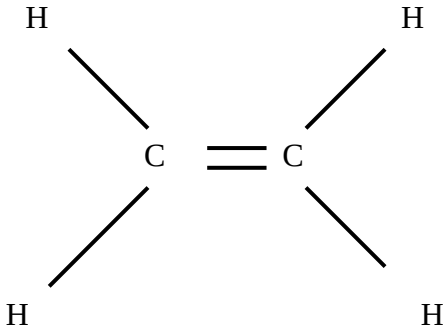

Figure 2.28 Chemical Structure of Ethylene Molecule
(Adapted from Painter and Coleman, 1997)

Polyethylene is created through polymerization of ethylene. It is produced through either radical polymerization, anionic addition polymerization, ion coordination polymerization or cationic addition polymerization (Osswald and Menges, 1995). The repeating unit of polymeric chain of polyethylene is illustrated in Figure 2.29.

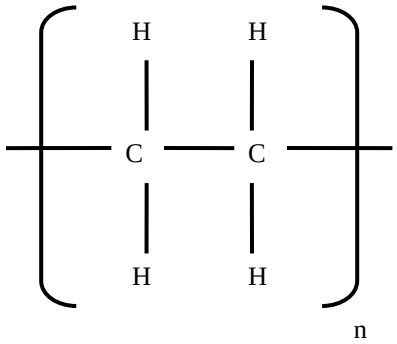

Figure 2.29 Schematic representation of the repeating unit of Polyethylene; C−H bond angles are not 90° as this diagram indicate, but are approximately 110°, as each carbon atom is tetrahedral (Adapted from Osswald and Menges, 1995)

2.3.1.2. Polyvinylchloride (PVC)

The only difference in the molecular chemical structure of polyvinylchloride (PVC) from that of polyethylene is that one of the H atoms in the ethylene monomer is replaced by a *Cl* atom. The molecular chemical structure of vinylchloride which is the building stone of polyvinylchloride is shown in Figure 2.30. In general, it is used to produce pipes and pipe fittings for construction purposes. However, with some recent advances in geosynthetics engineering, PVC geomembranes manufactured from polyvinylchloride resins has started to be utilized in geotechnical applications.

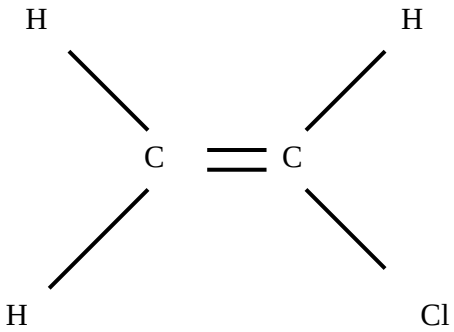

Figure 2.30 Chemical Structure of Vinylchloride Molecule
(Adapted from Painter and Coleman, 1997)

Polyvinylchloride is created through polymerization of vinylchloride. Its structure is thermoplastic and maximum crystallinity is 10% (Daniels, 1989). The repeating unit of polymeric chain of polyvinylchloride is illustrated in Figure 2.31.

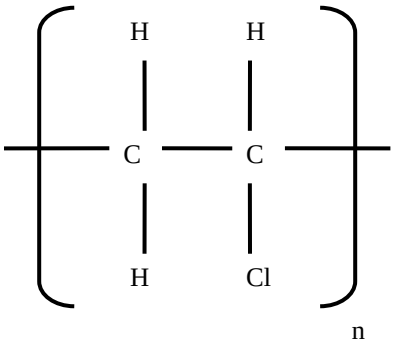

Figure 2.31 Schematic representation of the repeating unit of Polyvinylchloride;
C−H bond angles are not 90° as this diagram indicate, but are approximately 110°,
as each carbon atom is tetrahedral (Adapted from Osswald and Menges, 1995)

2.3.1.3. Polypropylene (PP)

Polypropylene (PP) which is a polymer consisting of long chains of the monomer propylene is used to manufacture geotextiles. The molecular chemical structure of ethylene which is the building stone of polypropylene is shown in Figure 2.32.

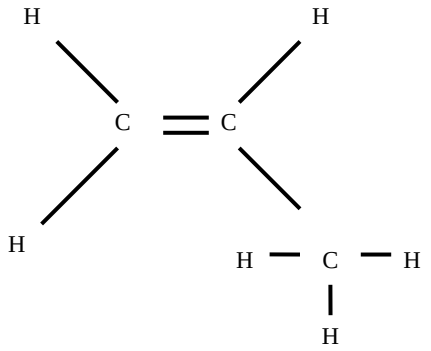

Figure 2.32 Chemical Structure of Propylene Molecule
(Adapted from Painter and Coleman, 1997)

Polypropylene is created through polymerization of propylene. It crystallizes up to 75% and its structure is thermoplastic (Daniels, 1989). The repeating unit of polymeric chain of polypropylene is illustrated in Figure 2.33.

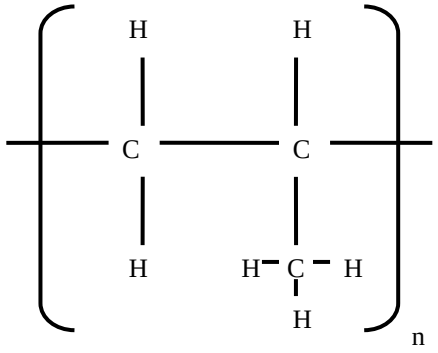

Figure 2.33 Schematic representation of the repeating unit of Polypropylene;
C−H bond angles are not 90° as this diagram indicate, but are approximately 110°,
as each carbon atom is tetrahedral (Adapted from Osswald and Menges, 1995)

All the polymers discussed above have good to excellent grade chemical stability and resistance to acids, bases, solvents, oils and fats (Painter and Coleman, 1997). Therefore, these polymer types have widely been preferred to produce geosynthetics.

2.3.2. Glass Transition Temperature and Melting Temperature

Polymeric materials such as high-density polyethylene (HDPE), polyvinylchloride (PVC), or polypropylene (PP) have different glass transition temperatures (Tg) and melting temperatures (Tm) at which they transform from a glassy state to rubbery state (i.e. phase change) and from rubbery state to melting state, respectively. The glass transition temperature, (Tg) is defined as the temperature which corresponds to mobility change in polymeric material. In glassy state, the thermal energy is not sufficient to permit polymer chains to move relative to one another. The rubbery state has a temperature range above the temperature range of the glassy state and is characterized by greater mobility (Nielsen and Landel, 1994).

The secondary bonds (i.e., hydrogen and van der Waals bonds) hold the molecular chains to one another at temperatures below the glass transition temperature of the polymer. For this reason, the polymer is able to respond only to bond stretching (Dowling, 2007). In the glassy state, the available space that allows the motion of molecules is substantially smaller than that of the rubbery state (Figure 2.34). The movement of the molecular groups is hindered and the polymer can only be strained a small amount before rupturing in a brittle manner (Roylance, 2001). In contrary, the secondary bonds at temperatures above Tg have less impact than those below Tg. The free volume also increases with temperature (Figure 2.34) (Li, 2000). Molecules will then have much more freedom of movement.

Physical properties such as density (ρ), glass transition temperature (Tg), melting temperature (Tm), and decomposition temperature (Td) of polymeric materials used in the "current study" are listed in Table 2.3.

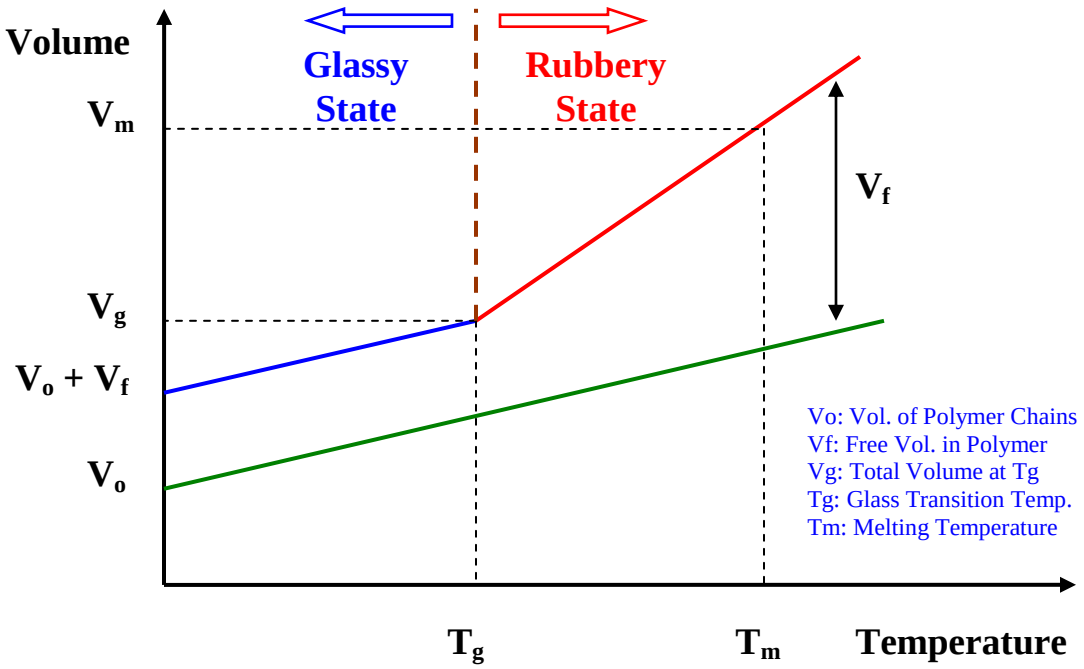

Figure 2.34 Volume Change of Polymer with Temperature Change:
V_o: Vol. of Polymer Chains, V_f: Free Vol. in Polymer, V_g: Tot. Vol. at T_g, V_m: Tot. Vol. at T_m, T_g = Glass Transition Temp., T_m = Melting Temp. (Adapted from Dowling, 2007)

Table 2.3 Physical Properties of Polymeric Materials used in the Current Study (Adapted from Dowling, 2007)

	ρ, Density (kg/m^3)	**Tg, Glass Transition Temperature (°C)**	**Tm, Melting Temperature (°C)**	**Td, Decomposition Temperature (°C)**
High-Density Polyethylene (HDPE)	940-960	-110	135	340-440
Low-Density Polyethylene (LDPE)	914-928	-90	115	340-440
Polyvinylchloride (PVC)	1380-1550	80	185	270-280
Polypropylene (PP)	900-907	-27	176	380-400

2.3.3. Stiffness (i.e. Modulus) and Temperature

The relationship of modulus with time and temperature is illustrated in Figure 2.35. The modulus at temperatures less than Tg is almost constant, whereas the modulus decreases significantly as temperature increases above Tg (Figure 2.35a). A rubbery stage can be observed after the melting temperature, (Tm) depending on the molecular weight of the polymer. The similar behavior is also detected between the modulus and time. Initially, the modulus is almost unchanged with time. Then, the modulus decreases dramatically, and follows a rubbery plateau for polymers with high molecular weights. The polymer initially behaves as solid-like in its properties, and then, changes to rubber elasticity. Finally, the modulus decreases sharply with increasing time with the result that the polymer can no longer hold its own shape, becoming a liquid-like material (Figure 2.35b) (Painter and Coleman, 1997).

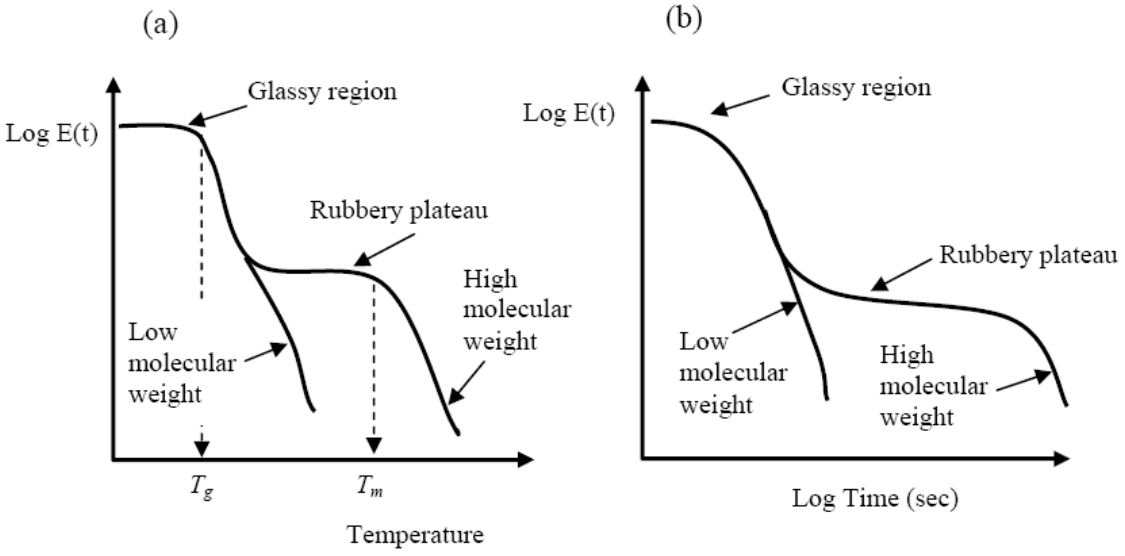

Figure 2.35 Schematic representation of the modulus as a function of (a) Temperature and (b) Time at T < Tg (Painter and Coleman, 1997)

2.3.4. Relaxation and Temperature

Stress relaxation is a time and temperature dependent behavior. It is defined as the time it takes for applied stresses to relax within a polymeric material. Relaxation time decreases exponentially with increasing temperature (Figure 2.36) (Osswald and Menges, 1995). Relaxation time can be from a few seconds to a few days, depending on the polymer. Long relaxation time means slow stress dissipation and higher internal energy. The primary effect of crystallinity in polymers is to lengthen relaxation time. Above Tg, in the rubbery state, polymer molecules are active enough to relieve stress concentrations rapidly and easily.

The relaxation time is long for all polymers at low temperatures. Glassy state polymers have long relaxation times and are not free enough to absorb the outside impact energy by chain slippage for a ductile failure. In other words, the failure occurring in glassy state polymers will be instantaneous brittle fracture (Osswald and Menges, 1995).

Another effect of temperature on the materials made from polymer resins is thermally induced relaxation. For example, fibers in polypropylene geotextiles lose their tensile strength due to thermally induced relaxation at higher temperatures (Tisinger et al., 1990).

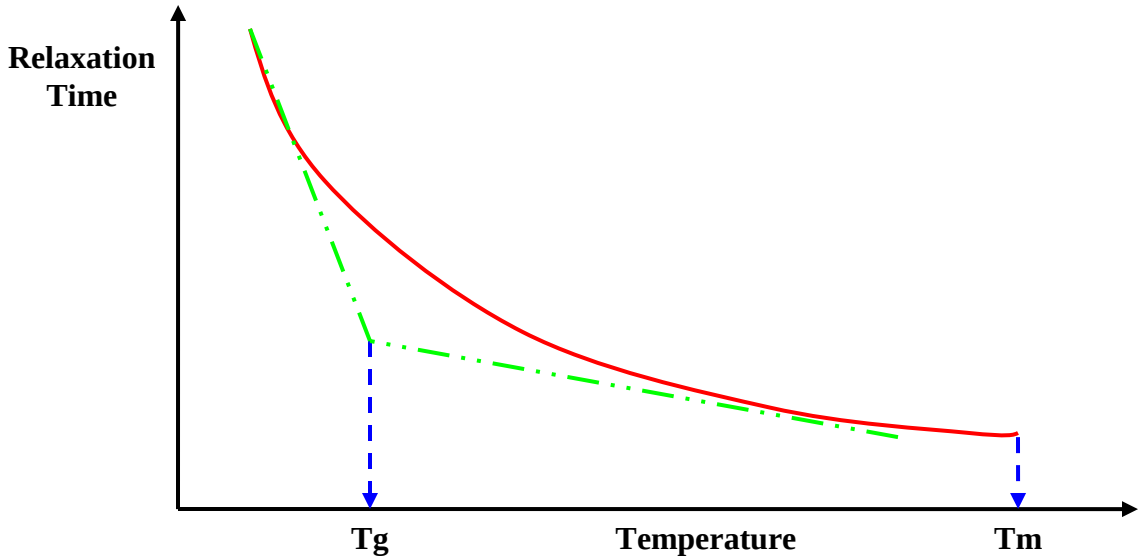

Figure 2.36 Relaxation Time in Polymeric Materials and Temperature
Tg: Glass Transition Temperature; Tm: Melting Temperature
(Adapted from Nielsen and Landel, 1994)

2.3.5. Coefficient of Friction and Temperature

An increase in internal temperature (i.e. energy) of a polymeric sample, or an increase in the temperature of the testing conditions will result in an increase in the coefficient of friction between polymers. The size and shape of a sample can alter the results of friction testing between polymeric specimens. In general, polymers exhibit both elastic and plastic deformation. The plastic deformation creates alignment of the chains relative to the applied force direction in the polymer structure. The plastic flow also tends to increase the contact area and higher surface pliability between the materials at the interface; thus, increase the measured coefficient of friction. The increased surface pliability results in a more ductile, malleable, or more adaptable polymeric material surface than that at low temperatures. The difference in the surface pliability of the polymeric material at high temperatures as compared to that at low temperatures can be

attributed to less flexible (i.e. rigid), more brittle polymer material properties at low temperature conditions which results in the polymeric material creating/possessing a less pliable and compliant polymer interface surface in conjunction with counterface material component. Additionally, the softer and flexible material properties of the polymer as well as the malleable and more pliable surface characteristics of the polymeric material at higher temperatures allows for a greater area of contact and interaction between it and the other counterface interface component because it does not possess the surface depressions of the polymer existing at lower temperatures due to inflexible and intractable material surface properties which decrease the contact area developing at the interface during the course of shearing. Furthermore, as shearing progresses, the higher surface pliability of the polymer at the interface allows it to embed into by the counterface material, resulting in the development of larger frictional shear resistance. Consequently, the higher polymer malleability and the larger surface pliability of the polymeric material at higher temperatures enables the shear strength increasing mechanisms discussed here to develop more readily that accounts for the greater friction mobilized at high temperatures. At low temperatures, heat generated at the interface due to shearing is less easily dissipated by the polymer than by other materials. However, as the temperature of the polymeric material increases, this generated heat due to friction testing can more easily be dissipated by the polymer resulting in higher interfacial frictional resistance existing between the interface materials; thus, obtaining higher coefficient of friction in the tests (Bely et al., 1982; Daniels, 1989).

For amorphous polymers such as HDPE and PP, at Tg or higher temperatures, polymer molecules are active enough to relieve stress concentrations (Nielsen and

Landel, 1994). Likewise, when the temperature increases, concentrated shear stresses are relieved, and more shear stress is required to overcome friction between these polymers. To sum up, an increase in temperature results in a decrease in hardness (Bilgin and Stewart, 2006); a reduction in relaxation time with applied stress (Nielsen and Landel, 1994; Osswald and Menges, 1995) so that stress concentrations at an interface can quickly be relieved and applied load will uniformly be distributed on the overall interface area; an increase in contact area, leading an increase in the coefficient of friction with easier and quicker dissipation of heat generated during shearing (Bely et al., 1982); and a decrease in stiffness (e.g. Young's Modulus) (Budiman, 1994; Lord et al., 1995).

2.4. Temperature Effects on Mechanical and Durability Properties of Polymers

Temperature has a significant effect on the mechanical properties of polymers, such as modulus, tensile strength, and hardness. Polymers soften and eventually flow as they are heated. Therefore, it is important to know the limiting temperatures at which polymer components can still be loaded with moderate deformations. Engineering mechanical and durability properties of polymeric materials can be examined in the following main topics: Creep; Fatigue; Mechanical Damping; Impact Strength; Friction; Fracture; and Tensile Properties.

2.4.1. Creep and Temperature

Creep behavior is defined as a time-dependent deformation process at a stress less than the strength of the material (Findley, 1960; Nielsen, 1974). A typical tensile creep behavior is illustrated in Figure 2.37 in which creep strain is represented by a solid line and creep strain rate by a dashed line. The creep behavior can be divided into three

stages: primary, secondary, and tertiary creep. In the primary (or transient) stage, after the instantaneous elastic response to the applied stress, the strain continuously increases with diminishing strain rate in time. During the secondary (or steady-state) stage, the strain (ε) increases linearly with time, resulting in a constant strain rate (έ) so that a plateau region is observed in strain rate versus strain (ε) or time graph. The tertiary stage is characterized by a rapid increase of strain (ε) as well as in the strain rate (έ) leading to creep rupture. Likewise, a compressive creep behavior exhibits the similar behavior to the tensile creep in the primary and secondary creep stages. However, in the tertiary stage (last stage), the creep strain rate (έ) decreases as opposed to an increase in creep strain (ε). In addition, the creep rupture does not occur in the compressive behavior as a consequence of the fact that the material behaves as an intact solid material in contrast to the tensile behavior (Dowling, 2007).

The creep mechanism of polymeric materials is fundamentally governed by load and temperature. Therefore, the influence of temperatures on the initiation and the speed of development of creep progress for the polymeric material are vital. Basically, the development of creep mechanism is described by the movement of molecules. When polymeric materials are subjected to higher temperatures for a long duration, or a static load for a long time, they deform via one or both of the fundamental atomistic mechanisms that are distortion of the lengths and angles of the chemical bonds connecting the atoms and secondly, rearrangements of the atoms (Findley, 1960; Roylance, 2001). These atomistic mechanisms under load cause changes of the molecular chains in the semicrystalline polymer such as uncoiling, straightening, and breaking in an amorphous region and slipping between the chains in a crystalline region. For example,

the molecular chains of polyethylene terephthalate (PET) under creep are changed by uncoiling followed by straightening, and lastly breaking of the chains in the amorphous region (Yeh and Young, 1998). In contrast, the creep strain of polyethylene (PE) which has a much simpler molecular structure proceeds with uncoiling followed by straightening of the chains in the amorphous region, then slipping between lamellar planes in the crystalline region, and lastly breaking of the chains in the amorphous region (Smeets et al., 2001).

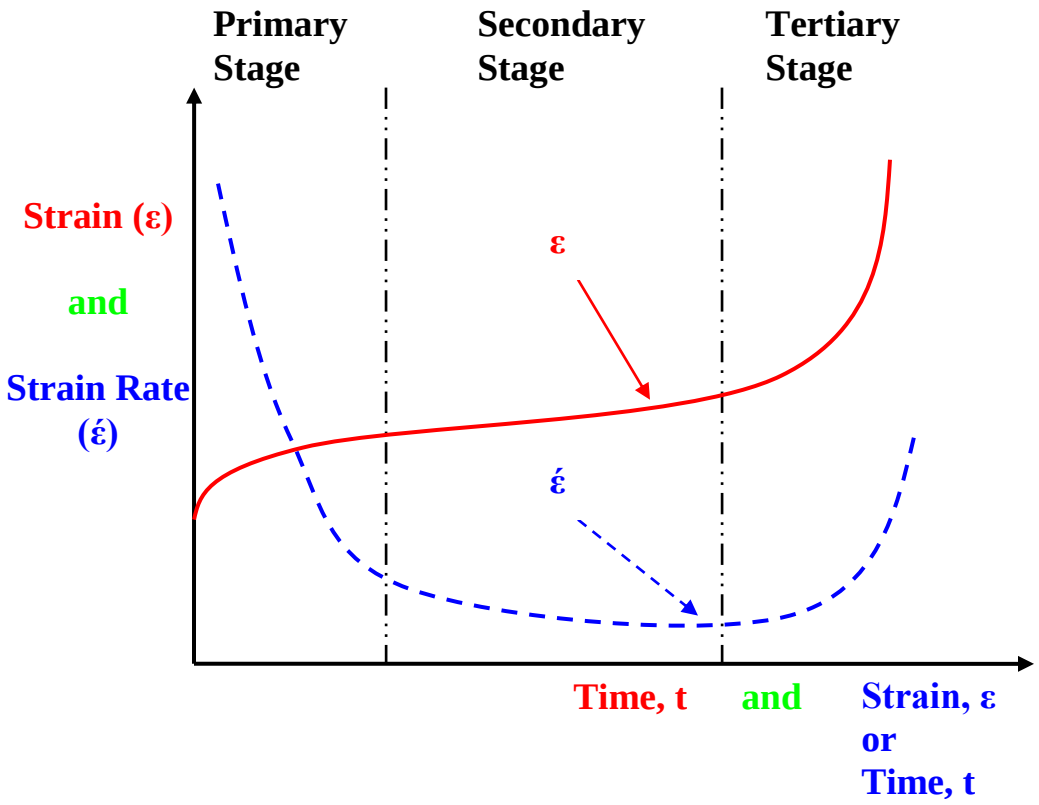

Figure 2.37 Typical Tensile Creep Behavior (Adapted from Dowling, 2007)

More creep strain occurs above Tg as molecules have much more freedom of movement with higher fraction of free volume (Vf) (Figure 2.34 and 2.36). As a result, the creep mechanism of polymeric materials is associated with motions of atoms, molecules, and vacancies in the polymeric material which are closely associated with temperature change. Increase in temperature and/or load results in an increase in instantaneous strain at the time of stress application, as well as an increase in the steady-state creep rate, and oppositely a decrease in the rupture lifetime (McCrum et al., 1997; Dowling, 2007). In fact, the creep behavior occurs as a result of a thermal activation process (Sinclair and Edgemond, 1969).

The rate of molecular mobility is used to examine the speed of creep mechanism with changing temperature. The rate is represented by the Arrhenius-type equation based on stress, temperature, and activation energy. (Equation 2.1) (Dowling, 2007):

$$\varepsilon'_{ss} = A.\left(\frac{\sigma}{\sigma_o}\right)^n.\exp\left(\frac{-Q}{RT}\right) \tag{2.1}$$

Where;

$\acute{\varepsilon}_{ss}$: Steady-state Creep Strain Rate (%/sec)

A: Pre-Exponential Factor (%/sec); *a.k.a*. Frequency Factor of the Thermally - Induced Process (i.e. Temperature-variance of creep rate)

σ: Applied Stress (kN/m^2)

σ_o: Initial Stress (kN/m^2)

n: Stress Exponent

Q: Activation Energy (J/mol)

R: Gas Constant = 8.314 J/mol.K°

T: Absolute Temperature (K°)

As seen in Equation 2.1, the creep strain rate increases with temperature and load. Therefore, higher temperature has a negative impact on the mechanical and durability properties of polymeric materials utilized in geotechnical applications as the speed of creep development in the materials increases dramatically at very high temperature conditions. For example, creep strain is much greater at temperatures above Tg than that below Tg (Roylance, 2001). Furthermore, an increase in the activation energy which is defined as an energy barrier that must be overcome for the occurrence of molecular motions, results in a decrease in the creep strain rate and subsequently less creep deformation (Lim et al., 2003). As shown in Equation 2.1, temperature has very significant influence on creep strain rate. For this reason, temperature dependence of creep behavior is used as a useful tool to experimentally characterize the creep process. For example, creep is predicted using elevated temperatures instead of long testing time (Painter and Coleman, 1997). The similarity between time and temperature with respect to material stiffness is illustrated in Figure 2.35. The modulus at temperatures less than Tg is almost constant, then, the modulus decreases significantly as temperature increases above Tg (Figure 2.35a). A rubbery stage could be observed after the melting temperature, (Tm) depending on the molecular weight of the polymer.

2.4.2. Fatigue and Temperature

The cyclic loading and unloading of a polymer induces a fatigue response. For example, the results of both tensile and compression testing are affected by the load applied, the speed of application of the load, the relative size of the sample, and more importantly the ambient temperature of the testing environment. In addition, the repetition of the loading is an important factor in fatigue occurrence as well. Figure 2.38 illustrates a fatigue curve for a typical polymer (Daniels, 1989).

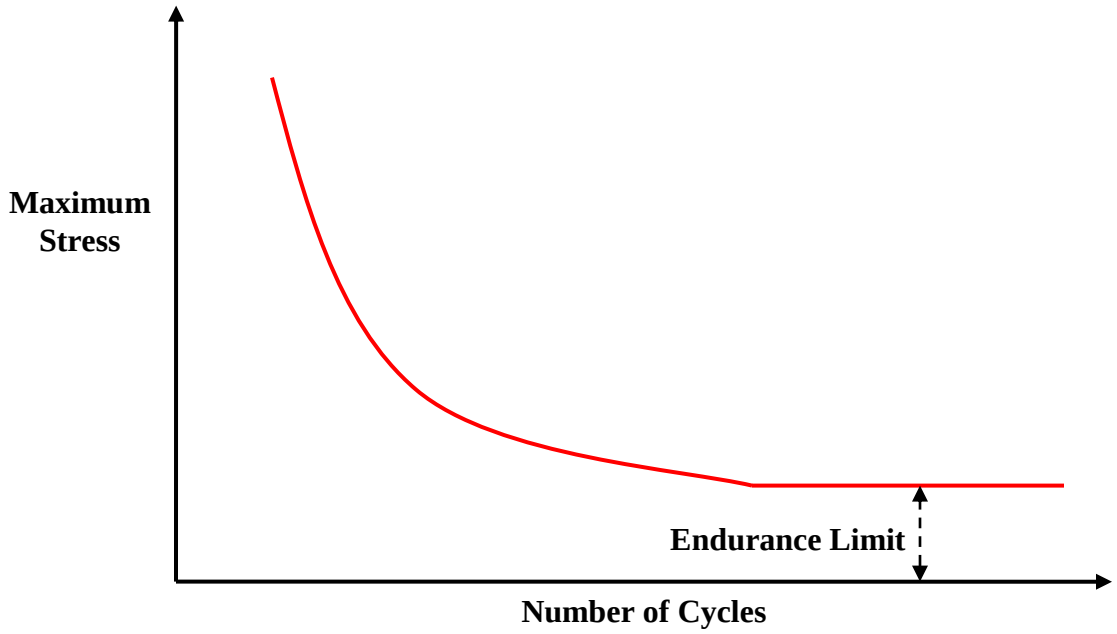

Figure 2.38 Fatigue Curve for a Typical Polymer
(Adapted from Nielsen and Landel, 1994)

Expected durability, lifetime of a polymeric material in fatigue is altered by the unloading extent and duration. If the polymer is completely unloaded between cycles and allowed to relax for the length of relaxation time at test conditions, then the polymer is

able to recover from the loading cycle which leads the segments/chains of the polymer to attain more favorable alignment for the next loading cycle, and thus; reduces the plastic flow the polymer will experience (Nielsen and Landel, 1994). Therefore, the plastic deformation per cycle will be less. In a very similar manner as expected in tensile tests, the fatigue life of the polymer will be prolonged by the reduced temperature, reduced maximum load, and reduced speed of loading. To sum up, the fatigue lifetime a polymeric material becomes shorter as the temperature increases meaning that temperature has an opposite impact on the overall extent of the continuation of fatigue progress.

2.4.3. Mechanical Damping and Temperature

Mechanical damping is the heat energy converted when a polymer is stressed. The remainder is put into a form of elastic and plastic deformation. The amount of damping a polymer displays is strongly related to the temperature of the polymeric material itself. For example, damping is low in the glassy state. The damping slightly increases as the polymer transforms into the rubber state. However, the damping experiences a peak during the transition from glassy state to rubbery state (Figure 2.39). High mechanical damping properties are desired in polymeric material applications so as to obtain a greater coefficient of friction and reduced amount of vibration (Dowling, 2007).

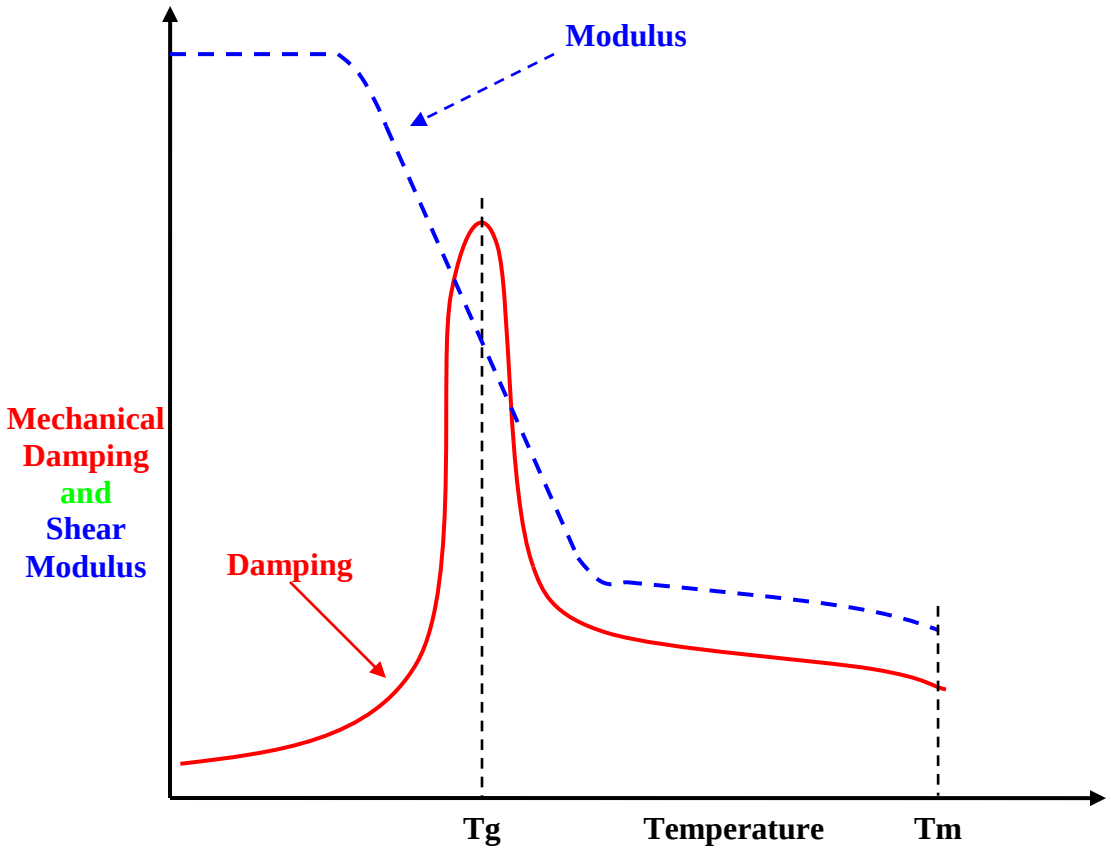

Figure 2.39 The General Mechanical Damping and Shear Modulus Behavior of a Polymer with respect to Temperature: Damping in Solid Line; Shear Modulus in Dashed Line (Adapted from Dowling, 2007)

2.4.4. Impact Strength and Temperature

The impact strength is dependent on the ability of the polymer to absorb energy very rapidly (Daniels, 1989). Therefore, a polymer structure which is freer to move will respond better to an impact and have greater impact strength. The impact capacity of a polymer is again strongly related to its temperature. A polymeric material in its rubbery state has higher impact strength than that in glassy state. The impact strength increases with increasing temperature.

2.4.5. Fracture and Temperature

Fracture is a combination of two different failure mechanisms likely to occur in a polymer structure that are slippage of the chains and chain scission. Therefore, it can be expressed that the normal mode of failure of a polymer under an applied tensile load is fracture. The amount of slippage the chains can support is a small part of the overall fracture damage, even in the condition that the loads are low and the time to fracture is long. The fracture progress takes place as follows (Daniels, 1989):

- Under tensile force, the slippage occurring increases the localized stress level and causes the initiation of chain scission.
- Chain scission progress during fracture begins when the stress on a small segment of the chain is greater than the bond strength sustained.
- Then, one or more primary polymer bonds break.
- Later, the initiation of fracture will take place at a flaw within the polymeric material.
- Crazing will start and become observable in the region around a flaw such as void which will not be able to sustain the applied force along with the unflawed regions of the polymeric material. Note that crazing is defined as the development of fine cracks (i.e. manifested by slight breaks in the material surface) on the surface of a polymeric material or plastic which may extend in a network on or under the surface of, throughout the body of the material. For precision evaluation, crazing is described as: i) microscopic crazing as observed with a stated magnification at minimum; ii) visible crazing as seen at close range with the naked eye (e.g. ~12 inches); iii) distant crazing as seen at ~3 feet with the

naked eye. When the underlying surface is visible, the break at the material surface is called a crack. This generally occurs as a result of differential thermal expansion and/or contraction of the material body.

- Once a craze begins to form at a flaw, the polymer chains in that region reorient in response to both the applied load and the reduced cross-sectional area, or; stress concentration at that point due to the flaw. That is, the chains align in the direction of the applied force to better carry the load.
- Cracking will happen and can be observed from outside.
- Once cracking has begun, it is only a matter of time until it propagates. At this stage, the influence of temperature on the time-span of fracture propagation is vital as the time can be quite slow and longer if the temperature of the polymeric material is high.
- Finally, fracture failure will occur in the polymeric material.

It is necessary to indicate that the energy required to produce failure for a polymer with an existing crack is less than that required for the polymer without any crack. Therefore, it requires more energy to form a crack in polymer than the propagation and growth of the crack causing fracture failure.

2.4.6. Tensile Strength Properties and Temperature

Tensile Stress-Strain (or: Tensile Force-Displacement) test is one of the common mechanical test types extensively used for polymers (Figure 2.40). The two test variables: rate of extension and sample size configuration (i.e. Length/Width Ratio, Shape of Cross Section) must be the same for all polymers tested to be able to make post-test comparison

on the experimental results. As indicated in Nielsen and Landel (1994) and Dowling (2007), the results can vary greatly for the same polymer depending on boundary conditions and sample configuration as a consequence of the diversity of chain and molecular structure found within the broad range of polymers. Similarly, the yield, tensile and break strength as well as yield and break strain are highly variable in the reported test results of the same polymer due to varying test conditions mentioned above. Furthermore, the compression properties of polymers (i.e. compression test results) are generally different than the tension properties. Temperature has a significant effect on tensile properties of polymers (Figure 2.41). Since polymers are anisotropic materials and highly sensitive to both temperature change and strain rate. As temperature increases in a polymeric material, a gradual expansion of the material occurs, resulting in more free volume (Figure 2.34) as well as weakening of the bonding forces which form the polymer structure and constitute the network of polymer chains holding the material together. For example, a reduction in van der Waals forces occurs between molecules resulting in less internal strength with increasing temperature which is reflected in a reduced maximum tensile strength. This is accompanied by an increase in the strain that the polymer can sustain without breaking. Figure 2.41 illustrates typical tensile test results of polymers in different states which were tested to failure with a moderate strain rate (Daniels, 1989).

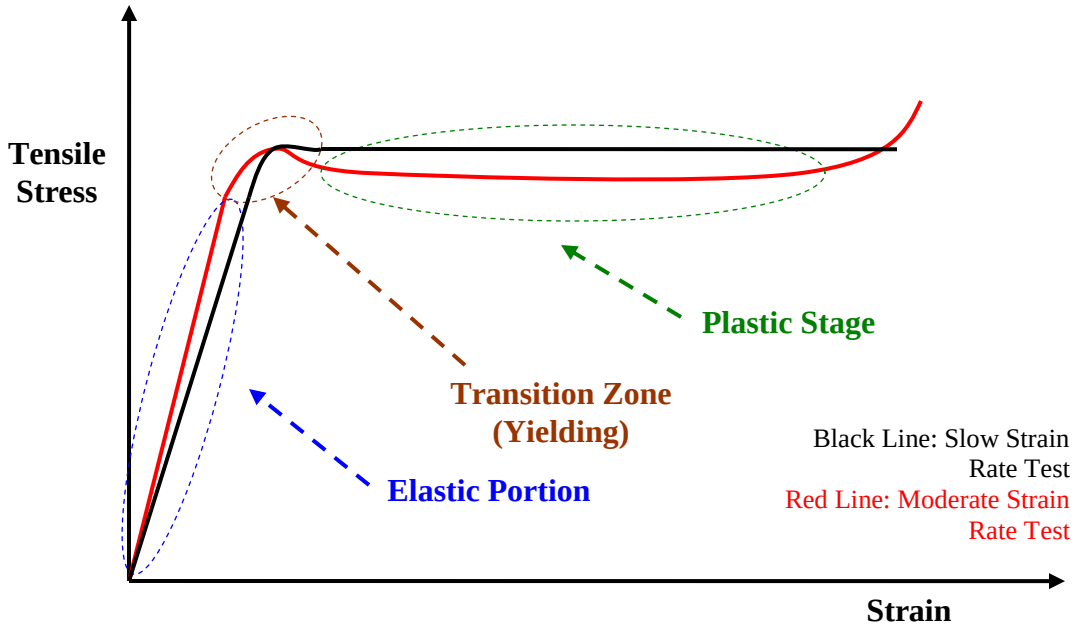

Figure 2.40 Tensile Test Graph for a Typical Partially Crystalline Polymer
(Adapted from Daniels, 1989)

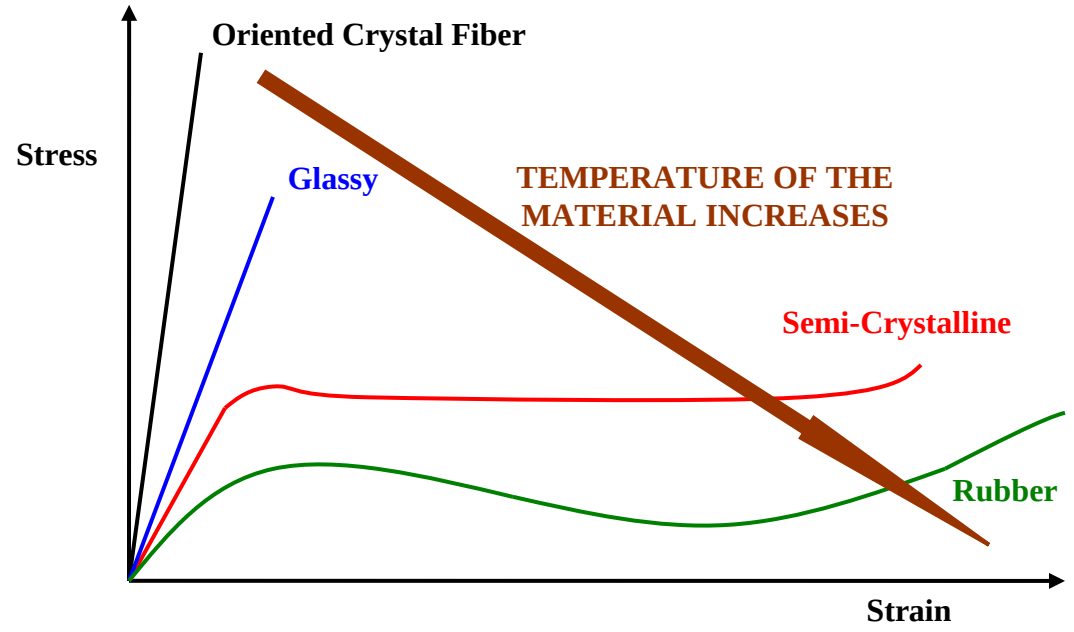

Figure 2.41 Typical Tensile Test Graphs of Four Different State Polymers tested to Failure: The State of Polymer is primarily related to its Temperature
(Adapted from Daniels, 1989)

As depicted in Figure 2.41, the tensile behavior of a polymer is strongly related to the state of the material which is dependent on its temperature. Polymers (i.e. Oriented Crystal Fiber, Glassy) are brittle at the lowest temperatures. As the temperature increases, they become more "tough", until they reach brittle-ductile transition above which polymers become sufficiently ductile so that they can exhibit necking behavior which is obviously seen in the yielding zone of the moderate strain rate test in Figure 2.40. Further increases in temperature leads to a rubber-like behavior as illustrated in Figure 2.41. Moreover, the type of behavior a polymeric material shows (i.e. brittle versus ductile) when tested depends on the strain rate of extension in tensile tests. For example, if extremely high strain rates are used, a polymer can exhibit brittle behavior at almost any temperature (Nielsen and Landel, 1994; Dowling 2007).

2.5. Temperature Effects on Geosynthetics used in Geotechnical Applications

Over the past few decades, the use of geosynthetics made from polymeric materials has been continuously increasing in a variety of geotechnical applications such as reinforced slopes, retaining walls, embankments, and waste containment systems. In many of these applications, geosynthetics are subjected to either tensile or compressive load throughout their service life. For example, geogrids (commonly made from highly oriented high density polyethylene: HDPE, or; polyethylene-terephthalate: PET) in reinforcement applications are subjected to tensile loading. In contrast, geonets (manufactured by extruding HDPE) are exposed to compressive loading in landfill liner and cover systems. In addition, geofoams (made from expanded polystyrene: EPS) experience compressive loading when serving as lightweight fill material. Temperature

has important influences on tensile strength properties of geosynthetics. The major impacts of temperature on tensile strength properties of geosynthetics in use for geotechnical applications are the decrease in ultimate tensile strength and reduction in stiffness (i.e. Modulus of Elasticity) that result in a loss of toughness. The degree of loss in tensile strength of a geosynthetic used in construction projects is strongly dependent on temperature variations (Koerner, 2005).

2.5.1. Tensile Creep Behavior of Geosynthetics

Geosynthetics exhibit viscoelastic properties similar to other polymeric materials. Under constant loading, geosynthetics exhibit creep strain which may potentially cause damage to the corresponding structural system. The extent of the creep strain depends on the temperature of the material itself and the magnitude of the loading as well as the type of polymer and manufacturing process of the geosynthetics.

Based on tensile creep properties of material obtained by various methods, the creep reduction factors are calculated to acquire the factor of safety (FS) for design applications under the tensile load (Koerner, 2005):

$$F.S = \frac{T_{allow}}{T_{required}} \tag{2.2}$$

$$T_{allow} = T_{ult}\left(\frac{1}{RF_{ID} \times RF_{CR} \times RF_{CD} \times RF_{BD}}\right) \tag{2.3}$$

Where;

F.S: Factor of Safety (To accommodate uncertainties in the design method)

T_{allow}: Allowable Tensile Strength (i.e. Tensile strength from laboratory testing)

T_{ult}: Ultimate Tensile Strength (From a Wide-Width Tensile Test) ($T_{allow} < T_{ult}$)

$T_{required}$: Required Tensile Strength (Obtained from design for particular field situation)

RF_{ID}: Reduction Factor for installation damage

RF_{CR}: Reduction Factor for creep to account for Long-Term Behavior

RF_{CD}: Reduction Factor for Chemical Degradation

RF_{BD}: Reduction Factor for Biological Degradation

The tensile creep reduction factor is determined by the Geosynthetic Research Institute (GRI) as shown in the following formula:

$$\mathbf{RF_{CR}} = \frac{\mathbf{T_{ST}}}{\mathbf{T_{LT}}} \tag{2.4}$$

Where;

RF_{CR}: Reduction Factor for Creep

T_{LT}: 10^5 (or 10^6) hour-design Life Strength of the Geosynthetics

T_{ST}: Short-Term Strength of the Geosynthetics in ASTM D 4595

T_{LT} can be obtained by extrapolation of a creep rupture curve (stress vs. creep rupture time) up to 10^5 or 10^6 hours (Figure 2.42).

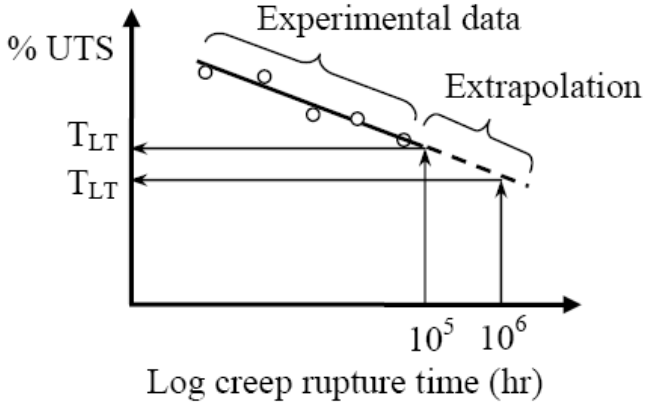

Figure 2.42 Method to determine Creep Reduction Factor using Creep Rupture Curve For a Tensile Creep Test (Koerner, 2005)

Creep reduction factors of several types of geotextile from Den Hoedt (1986), Lawson (1986), Task Force #27 (1991) and Koerner (2005) were compared and listed in Table 2.4. The variation of reduction factor is due to polymer type. Geotextiles, made from base polymer types such as HDPE and PP, have relatively large reduction factors, since they are in the rubbery state and exhibit the typical physical properties of rubbery polymer state (i.e. polymer chains readily undergo plastic flow under tensile stress at micro-level and the polymeric material exhibit plastic deformation/extension under tension force with ease) at typical ambient conditions (i.e. -10 °C < T < 50 °C) to which these geosynthetics are commonly exposed in most widespread geotechnical applications (Koerner, 2005).

Table 2.4 Creep Reduction Factors of Several Types of Geotextiles at 100 years (Adapted From Koerner, 2005)

Geotextile Fiber/ Yarn Type	**Den Hoedt (1986)**	**Lawson (1986)**	**Task Force #27 (1991)**	**Koerner (2005)**
Polypropylene (PP)	4.0	2.5 to 5.0	5.0	3.0 to 4.0
Polyethylene (PE)	4.0	2.5 to 5.0	5.0	3.0 to 4.0
Polyamide (PA)	2.5	1.5 to 2.5	2.9	2.0 to 2.5
Polyester (PET)	2.0	1.5 to 2.5	2.5	2.0 to 2.5

2.5.2. Previous Interface Shear Strength Tests on Geosynthetic Composite Systems at Various Temperatures

The results of experimental investigations on the influence of temperature on interface shear resistance of geosynthetics were published by Pasqualini et al. (1993) who conducted research to evaluate the interface shear strength between needle punched nonwoven (NPNW) polypropylene (PP) or polyester (PET) geotextiles and a smooth low-density polyethylene (LDPE) geomembrane at temperatures of 26 °C and 30 °C (Table 2.5). The interface friction angle was found to be 12.4° at 26 °C and 14.7° at 30 °C for NPNW-PP geotextile – LDPE geomembrane interfaces. Similarly, for NPNW-PET geotextile – LDPE geomembrane interfaces, the interface friction angle was reported as 13.8° and 15.9° at temperatures of 26 °C and 30 °C, respectively (Figure 2.44). In addition, it was shown that tests carried out in wet conditions gave shear resistances that were systematically 10% lower than those obtained in dry conditions.

Table 2.5 NPNW-PP or NPNW-PET Geotextile - Smooth LDPE Geomembrane Interface Friction Angles at Various Temperatures (Pasqualini et al., 1993)

	LDPE-PP		LDPE-PET	
	Temperature (26 °C)	Temperature (30 °C)	Temperature (26 °C)	Temperature (30 °C)
Friction Angle (Ø)	12.4	14.7	13.8	15.9

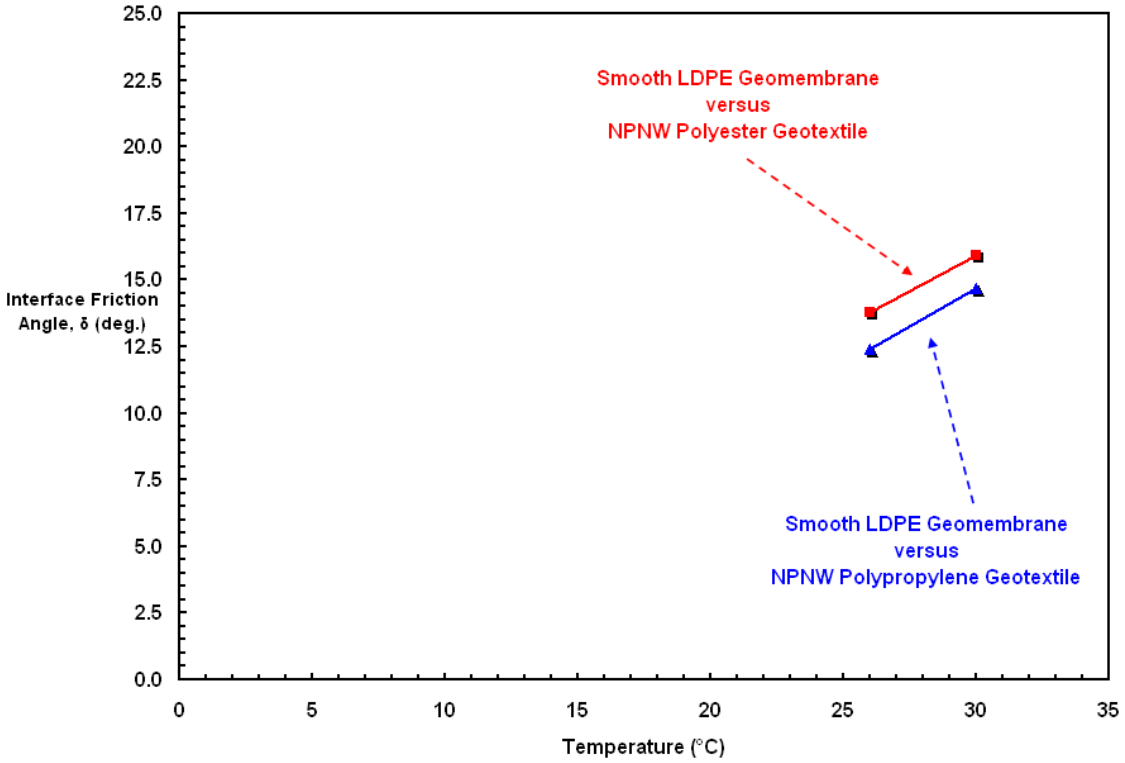

Figure 2.44 Variation of Friction Angle with Temperature for NPNW-PP or NPNW-PET Geotextile - Smooth LDPE Geomembrane Interfaces (Pasqualini et al., 1993)

2.6. Temperature Effects on Soils in General and Landfill Soil Covers & Clay Liners Specifically

There has been very little study on elevated temperature effects on performance of interfaces involving soils in general and almost none on granular soils. Nevertheless, for purposes of background, the effect of temperature on clay in general is reviewed below.

2.6.1. Crack Formation in Landfill Soil Covers

The ice fraction that develops in soils when frozen is controlled by the type of soil (i.e. fine versus coarse) and its water content. Frozen soil landfill covers and exposed soil

liners are subject to thermal contraction leading to increases in tensile stresses, and consequently causing potential crack formation in soil during periods of decreasing winter temperatures which occur annually in the northern states of U.S, and most of Alaska, as well as in Canada, Northern Europe and Asia. Potential cracking includes the full depth of freezing which can be larger than two meters in some of these locations. Soil has a thermal coefficient of contraction almost three times higher than that of steel and a small decrease in temperature quickly generates tensile stresses. Since frozen ground is relatively weak in tension, initial fracturing commences at the ground surface and penetrates into the cover soils to the depth needed to relieve the tensile stresses. The cracks are typically distributed over the cover surface in a pattern such that tensile stresses are reduced below the frozen-soil tensile strength. Thermal-contraction behavior and the tensile strengths of frozen cover soils depend on several variables including soil type, ice and mineral volume fractions, temperature and degree of ice saturation. The top-soil (loam) may be a combination of several soil types as indicated by Lutton, 1982 such as silty gravels, clayey gravels, silty sands, clayey sands, inorganic silts and inorganic clays. Above the water table, soils are only partially saturated with the degree of saturation related primarily to effective particle size (D_{10}) as described by Terzaghi (1952). An approximate relationship between effective grain size and degree of saturation for soils located above the water table in temperate zones with moderate rainfall is shown in Figure 2.45. The loam top soils, with degrees of saturation intermediate to sand and silt, have reduced tensile strengths. The clay barrier layer is close to or at full saturation with large unfrozen water contents (Andersland and Al-Moussawi, 1987).

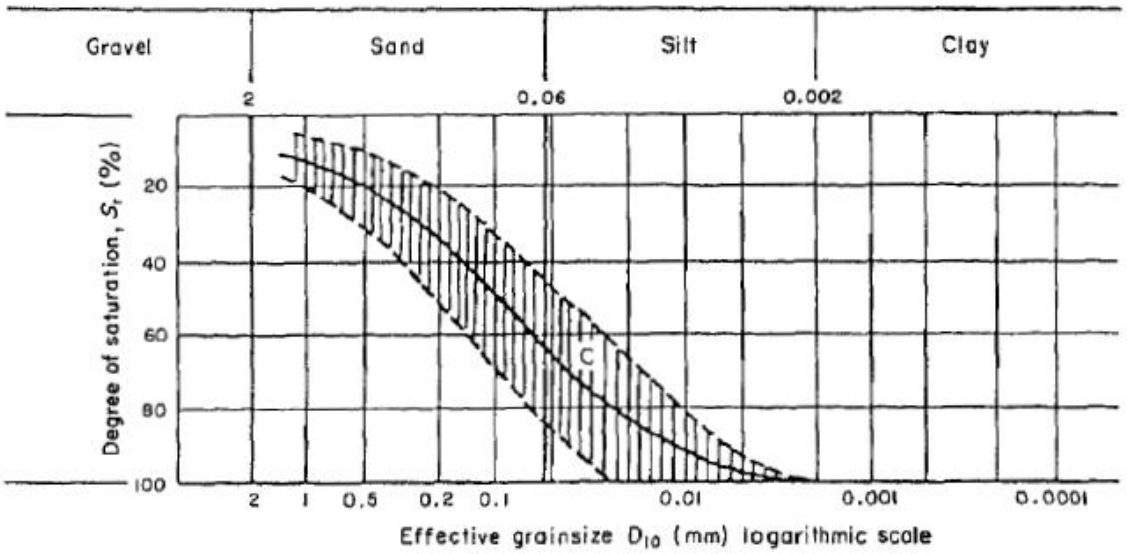

Figure 2.45 Approximate Relationships between Effective Grain Size (D_{10}) and Degree of Saturation in the Zone of Soil Moisture in Temperate Zones with Moderate Rainfall (After Terzaghi, 1952)

2.6.2. Thermal Contraction, Developed Tensile Stresses, and Soil Strength

As cooling occurs, the frozen soil-cover surface contracts unless constrained. Horizontal tensile stresses are generated with no observable horizontal strains. The horizontal "thermal strain" is given by the thermal contraction as follows (Andersland and Al-Moussawi, 1982):

$$\varepsilon_y = \varepsilon_z = \frac{\Delta L}{L_0} = \alpha.\Delta T \qquad (2.5)$$

Where;

α: The coefficient of linear contraction

L_0: The length at some reference temperature

ΔL: The change in length due to a temperature change (ΔT)

ΔT: Temperature Change

For example, experimental α value for saturated frozen dense sand is close to $2.8x10^{-5}$ per degree at -15 °C. If the cover soil is constrained and the frozen soil is assumed to behave "elastically", the "tensile stress" develops will be (Andersland and Al-Moussawi, 1982):

$$\sigma_y = \frac{E}{1-\mu}.\varepsilon_y = \frac{E}{1-\mu}.\alpha.\Delta T \qquad (2.6)$$

Where;

E: Young's modulus

μ: Poisson's ratio

2.6.3. Temperature Sensitivity of Clays (Atterberg Limits as Indicator)

Atterberg Limits have been repeatedly shown to be useful indicators of clay behavior. Temperature susceptibility of a clayey soil could be evaluated using Atterberg limits. This idea was first suggested by Tidfors and Sallfors (1989) and further developed by Jefferson and Rogers (1998). Atterberg limits were utilized by several researchers including Brandl (1992) to assess both consistency and chemical stability of clay soils, particularly employed in landfill liner construction.

As expressed by Jefferson and Rogers (1998), the evaluation of Atterberg limits at elevated temperatures could indicate how temperature affects key design parameters by utilization of the various correlations that exist. The Atterberg limits would, thus, provide a quick and simple means to indicate preliminary effects of temperature, including relative sensitivity. Among the studies conducted, the majority of researchers observed a

reduction in Liquid limit (w_L) of variety of clay soils with temperature (Youssef et al., 1961: Laguros, 1969; Ctori, 1989). It was considered by Mitchell, (1969) that these results were consistent with strength reductions observed in clays at elevated temperatures. Since the liquid limit is also an indirect measure of strength. Less consistency was observed with Plastic limit (w_P) in conjunction with temperature. Youssef et al. (1961) and Ctori (1989) observed a reduction in Plastic limit at elevated temperatures when testing between 15 and 35 °C and between 6 and 35 °C, respectively. On the other hand, Laguros (1969) observed an erratic trend overall when testing between 2 and 41°C.

Furthermore, Jefferson and Rogers (1998) assessed the effect of temperature on clays directly using Atterberg Limits (Figure 2.46). They obtained consistent results over a larger range of temperatures (i.e. 10 – 80 °C) than previously possible. Therefore, their work is potentially useful when assessing the behavior of clay soils which are likely to be exposed to elevated temperatures, such as landfill liners. They presented their results for kaolinite, smectite and mixtures of these clays of various percentages. Smectites are considerably more sensitive to temperature changes than kaolinites. The liquid limit increases with temperature for smectitic clay, whereas a very slight decrease occurs with kaolinite. The variation in liquid limit appears to be closely related to the specific surface area of the clay, and the resulting nature of inter-particle contacts (Jefferson and Rogers, 1998).

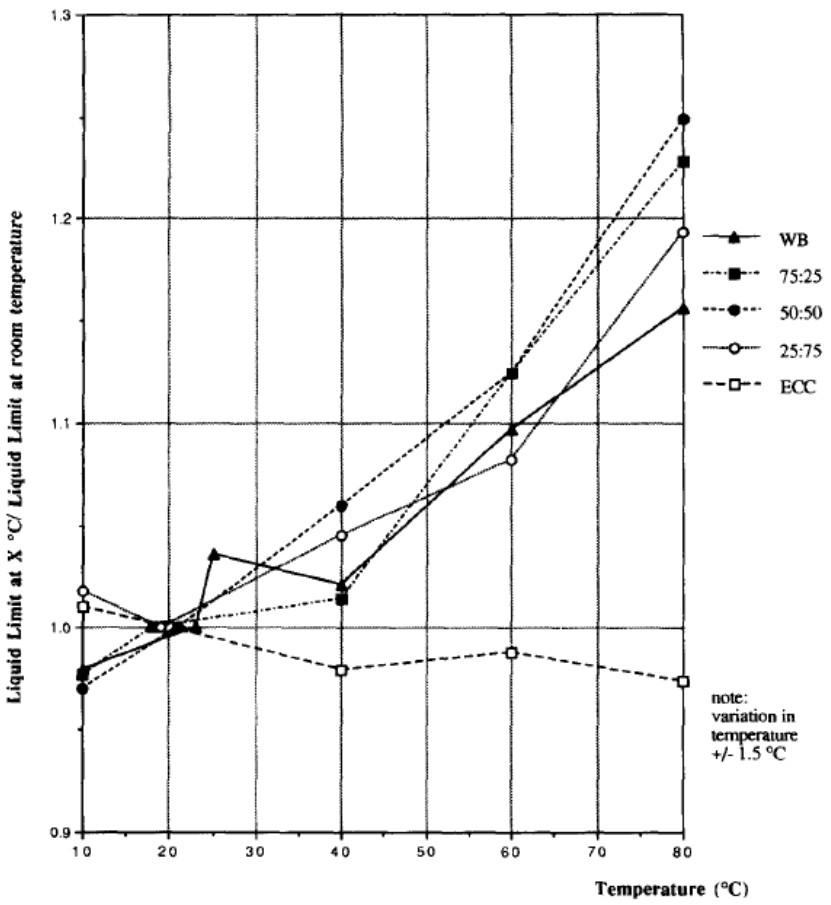

Figure 2.46 Proportion of Liquid Limit at Different Temperatures to the Liquid Limit at Room Temperature: (ECC: English China Clay; WB: Wyoming Bentonite; WB: ECC % Mixtures). (Jefferson and Rogers, 1998)

2.6.4. Desiccation of Landfill Clay Liners due to Heat Generation

Geosynthetic materials such as geomembranes and geosynthetic clay liners (GCLs) are frequently used as composite liners for municipal solid waste landfills. Heat that is generated within such facilities due to decomposition of organic material within the waste creating thermal gradients that have the potential to cause desiccation of the mineral component of GCLs, with potential impacts on long-term performance. The aerobic and anaerobic biological decomposition of organic matter in waste landfill involves exothermic reactions that causes heat generation; and consequently, increased

temperatures within the waste mass. Decomposition is likely to continue for as long as organic matter is present within the waste, resulting in elevated temperatures persisting likely for decades (Southen and Rowe, 2005).

One of the main reason of leachate collection system clogging is the increase of basal temperatures (Rowe et al. 1997), thus, the increase of diffusive and advective contaminant transport (Barone et al. 2000), leading to more rapid ageing of geosynthetic components (Hsuan and Koerner 1998; Rowe 1998; Sangam and Rowe 2002), consequently, the potential for desiccation of mineral layers. As indicated by Southen and Rowe (2005), the desiccation of clay liners arises due to the development of thermal gradients between the warmer liner and cooler groundwater table. A schematic of the conditions existing at the base of a landfill is shown in Figure 2.47.

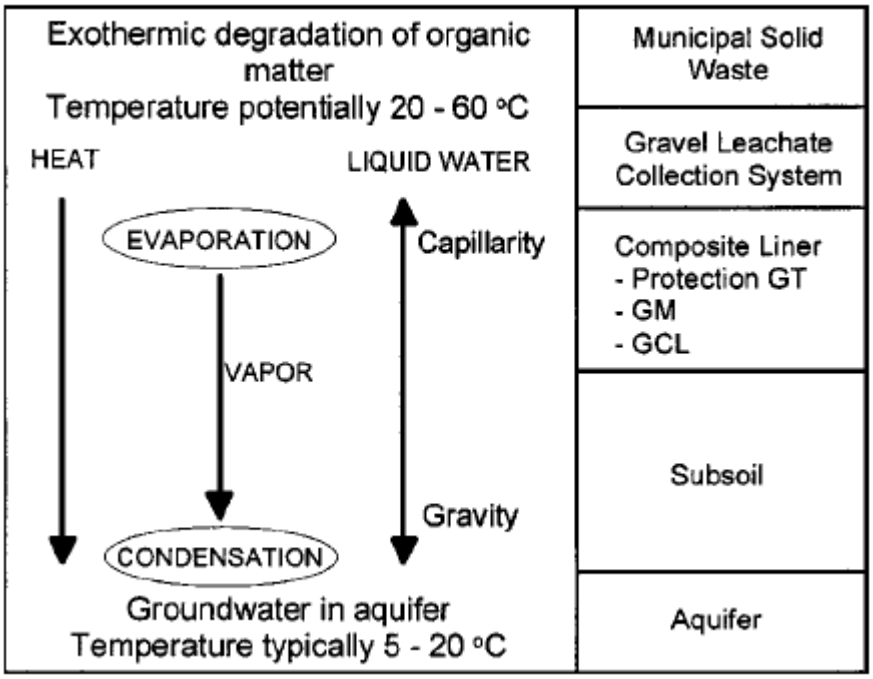

Figure 2.47 Vertical Profile through Geosynthetic Composite Liner and Its Subsurface with Typical Direction of Moisture Fluxes and Temperature Distribution (Southen and Rowe, 2005)

Water within the underlying subsoil will move downward to achieve hydrostatic equilibrium with the groundwater table due to the effects of the overburden stress and gravity. Water will also generally flow from the subsoil into the GCL, depending on water contents of the materials. When the temperature of the upper surface is increased by waste decomposition, heat flows downwards toward the cooler groundwater table. The temperature gradient thus established enhances the downward flux of moisture by inducing downward vapor diffusion due to the dependence of vapor density on temperature. The geomembrane which comprises the upper boundary of the system is practically impermeable to water, and thus the downward vapor flux must be balanced by the upward flux of liquid water under matric potential (suction) gradients. Especially when unsaturated hydraulic conductivity is low, this process has the potential to generate high matric potentials in the upper portion of the subsoil and GCL. These matric potentials and resulting low water contents may lead to shrinkage of the bentonite core of the GCL, with a corresponding risk of desiccation cracking. If the overburden stress and tensile strength of the GCL are not sufficient to prevent cracking of the GCL, clayey material will desiccate and shrink because of decreasing water pressure. As long as the overburden is large enough compared to the decreasing water pressure, mineral liner shrinks only vertically; if water pressure becomes too small, horizontal shrinkage occur leading cracking (Southen and Rowe, 2005).

2.7. Geotechnical Examples experience Temperature Variations

The diverse construction projects such as on-ground structures and infrastructures experience temperature variations due to several climate and human factors. Most of the construction materials that have found widespread application in civil engineering

projects are sensitive to temperature variations as their strength and deformation characteristics are influenced by varying environmental conditions. Consequently, it is important to understand the engineering behavior of these materials under different ambient conditions which are crucial to optimal designs. Several different geotechnical structures which experience temperature variations due to aforementioned reasons are identified and described in Table 2.6 which includes examples from all over the world.

Table 2.6 Geotechnical Examples on Temperature Variations

Construction Project/Natural Formation	**Example/Notes**
Thermal Islands (due to Pavement in Urban Areas)	e.g. Phoenix, AZ
Deep Mining (Temperature at Depth)	Global Warming; e.g. South Africa
Waste Landfills	Due to Exothermic Waste Reactions and Insulating Effect of Waste itself
Refrigeration Tanks	e.g. LNG (Liquid Natural Gas) Tanks
Transmission Lines	e.g. Trans-Alaskan Line
EOR (Enhanced Oil Recovery)	e.g. Middle East
Heat Exchangers	e.g. Piles
Building Insulations	Minimum Heating and Cooling Demand if constructed underground
Buried Transmission Lines	Cables (Overheating)
Nuclear Waste	e.g. k_T low ➔ T will increase a lot ➔ Clay Mineralogy changes
Thermally Induced Consolidation	e.g. Hot Climate Regions in the World
Frozen Ground	e.g. (Problem in Northeast America, Canada)
Volcano	Hawaii

2.8. Temperature Variations in Landfill Liner and Cover Systems

Historically, landfills have been the most common methods of organized waste disposal. Many landfills are also used for other waste management purposes such as temporary storage, consolidation and transfer, or processing of waste material (i.e. sorting, treatment, or recycling). Figure 2.48 illustrates modern landfill design, typical components of a landfill, waste disposal steps, subsurface geology, and leachate proximate existence to groundwater or aquifer in case not sealed properly. Techniques which are typically applied in non-hazardous waste landfills during the process of waste depositing into the landfill cells in order to meet predefined specifications are as follows: (1) Confine to as small area as possible; (2) Compact to reduce their volume; (3) Cover (i.e. daily) with layers of soil. A large number of adverse impacts may occur from landfill operations which can vary from fatal accidents, infrastructure damage and pollution of the local environment such as contamination of groundwater/aquifers by leakage, and off-gassing of methane generated by decaying organic wastes (Koerner, 2005).

A landfill, which is generally defined as a designated site by local authorities (i.e: State's Environmental Agencies) for the disposal of waste materials, can mainly be categorized as municipal waste landfills, industrial waste landfills, and toxic waste landfills. In United States, landfills are regulated by the State's Environmental Agencies who establish minimum guidelines none of which can fall below those set by the EPA (United States Environmental Protection Agency). The preservation of nuclear waste is a different phenomenon and is examined outside of the concept of regular waste landfills. Each category mentioned above requires different precautions to be taken in preservation of these wastes from less severe to more severe depending on the danger of the waste

material itself and the hazard it might cause in case not conserved in an appropriate manner to protect surrounding environment of the landfill.

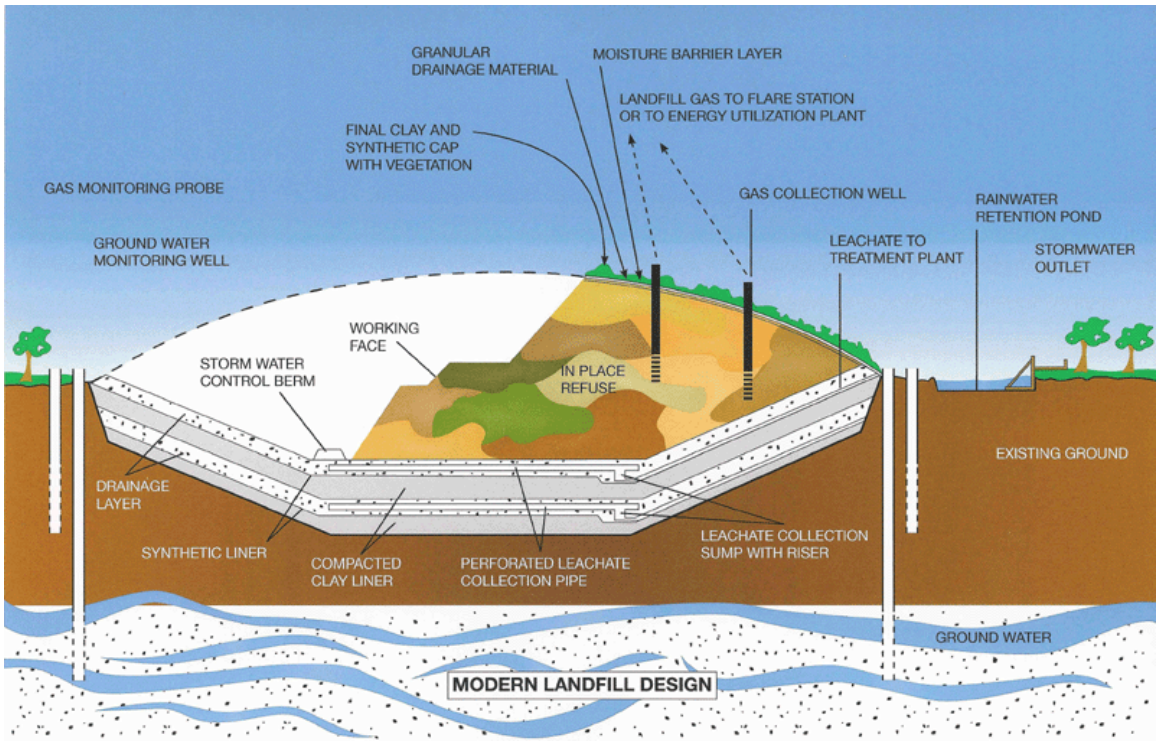

Figure 2.48 Modern Landfill Design and its Components
Showing Sub-Ground Geology as well (Runco Environmental, Inc)

After the waste is disposed and the landfill is closed, the ambient conditions inside the landfill changes. One of the important aspects of these changing conditions is temperature which is a very crucial factor impacting the mechanical and durability properties of the design materials (i.e. geosynthetics) used in the construction of landfill bases, side slopes and covers as well as their interaction with the other materials they are in contact with. The functional engineering properties of those utilized materials must remain within acceptable limits during the required service life for the sake of integrity of the structure as well as stability of the design. In spite of this fact, most geosynthetic

interface testing has been performed at room temperature. Information today is emerging that shows how temperatures in the bottom liners as well as in the cover systems of landfills can be much higher as summarized in Table 2.7.

Table 2.7 Summary of Temperature Measurements in Landfills

	Temperature monitored (°C)	**Measurement Location**	**Landfill Site**	**Notes**
Oweis et al. (1990)	As high as 55 °C	At the bottom of refuse in the base	Northern New Jersey, USA	Municipal Solid Waste Landfill
Collins (1993)	Between 30 °C to 40 °C	In refuse from top to the base	Germany	
Bleiker et al. (1995)	Highest at 59 °C	Above the base of refuse	Toronto, Canada	Measurements at the bottom of boreholes drilled to the base
Yoshida et al. (1997)	As high as 50 °C	In landfill base	Tokyo, Japan	
Barone et al. (2000)	Between 10 °C to 37 °C	At the base	Toronto, Canada	Municipal Solid Waste Landfill
Koerner and Koerner (2006)	From 18 °C to 40 °C	In bottom liner	Eastern Pennsylvania, USA	
Montgomery and Parsons (1990)	Between 7 °C and 27 °C	In final cover	Southern Wisconsin, USA	
Corser and Cranston (1991)	As high as 43 °C	In final cover	Southern California, USA	Measurements in a test section simulating a final cover
Khire et al. (1997)	From 1 °C to 30 °C	In final cover	Central Washington State, USA	
Koerner and Koerner (2006)	Between 0 °C and 30 °C	In final cover	Philadelphia, Pennsylvania, USA	

2.9. Summary and Conclusions

This chapter has provided comprehensive background information and a literature review showing historical research efforts on shear behavior of fabric-continua as well as particulate-continua interface systems and the impact of various material characteristics and state parameters on interface strength which complements the research to be presented in this thesis. Additionally, the physical, mechanical and durability properties of the materials at the interface defining the shear behavior and the state of the interface

as well as the interaction and contact behavior between two materials at varying environmental conditions such as temperature were examined extensively. The factors controlling shear strength-displacement behavior of the interface as well as their cooperative or counteracting effects on the magnitude of shear resistance and the development of overall shear response between the materials having different physical properties was highlighted since every interface creates a potential slip surface that may ultimately lead to a failure. Those factors are generally considered in evaluating interface shear strength (i.e. peak, post-peak). Their influences on the resultant behavior observed with the changing engineering properties of particulate, fibrous and continuum materials (i.e. geosynthetics which made from polymers) under different ambient conditions must quantitatively be estimated to fully understand the mechanism of interface shear response and development of shear stress-displacement curve. Some useful supporting figures and tables from previous research studies and important equations for analysis and design were included to provide both a qualitative estimate and a quantitative determination of several factors affecting the shear resistance of particulate-continuum and fibrous-continuum materials interfaces. The temperature of the ambient environment is a significant factor for the shear resistance of an interface and the shear response developing at that interface and consequently, changes in temperature can influence the overall shear behavior and the strength (both peak and post-peak). As such, the focus of this thesis is to investigate the effects of elevated temperature conditions on composite geosynthetic systems (geotextile-geomembrane; sand-geomembrane).

CHAPTER III

3. DESIGN AND DEVELOPMENT OF TEMPERATURE CONTROLLED CHAMBER

3.1. Introduction

To date, most geosynthetic interface testing has been performed at room temperature (21 °C) in the laboratory as specified by various standard organizations (e.g. ASTM), however information is emerging that shows how temperature in infrastructure applications of composite systems incorporating different material interfaces can be much higher. Therefore, there is emerging interest and indeed requirement to create elevated temperature conditions (>21°C and <50 °C) in the lab while performing physical laboratory tests involving the materials (i.e. geosynthetics). This can allow for their mechanical and durability properties which are affected by the change of ambient temperature to be evaluated and the influence of temperature change on their interfacial shear strength in combination with other material types to be fully assessed.

As part of this study, a unique temperature controlled chamber was designed and developed for the purpose of performing interface shear tests on geosynthetic materials to simulate the field conditions at higher temperatures as well as to evaluate shear displacement-failure mechanisms under elevated temperature conditions. The development and validation of the unique temperature controlled chamber test system (Figure 3.1) as well as observations pertaining to system design criteria and the relevance to field conditions will be discussed.

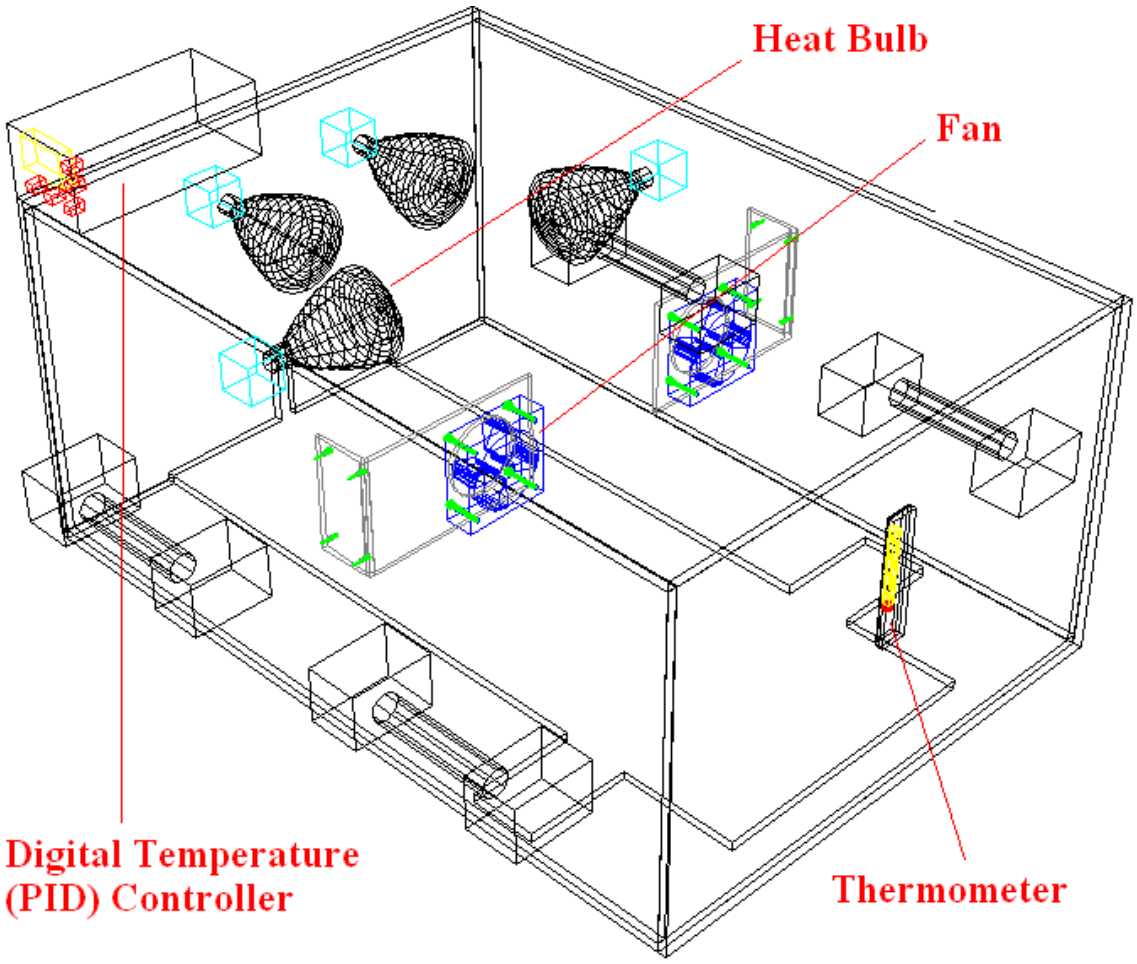

Figure 3.1 3D Drawing of Temperature Controlled Chamber
(Only 4 of 8 Heat Bulbs shown for clarity)

3.2. Design Criteria and Development of the System

To precisely simulate elevated temperature field conditions in the laboratory for the various physical laboratory tests (i.e. shear, tension, compression), a temperature controlled chamber (TCC) was designed and developed so that the behavior of materials under load and deformation at elevated temperatures could be accurately investigated. Performing tests in the TCC which encloses the large displacement direct interface shear device provides the opportunity of imitating triggered shear displacement-failure mechanisms at higher temperatures as well as observing temperature dependent interface

shear behavior between different interfaces such as fabric-planar as well as particulate-planar counterfaces. The temperature controlled chamber (Figure 3.2) consists of several components selected to fulfill different tasks for obtaining higher temperature conditions and maintaining the chamber environment without fluctuating from a preset target test temperature. The main selection criteria in the design for the parts/components were: I) functionality, II) size, III) efficiency and IV) long-lasting serviceability. Furthermore, the compatibility of the components especially for those employed in the electrical system for controlling temperature was a first order concern and considerations related to precision and accuracy of the units as well as reliability of performance during the tests (Figure 3.3) were of particular importance.

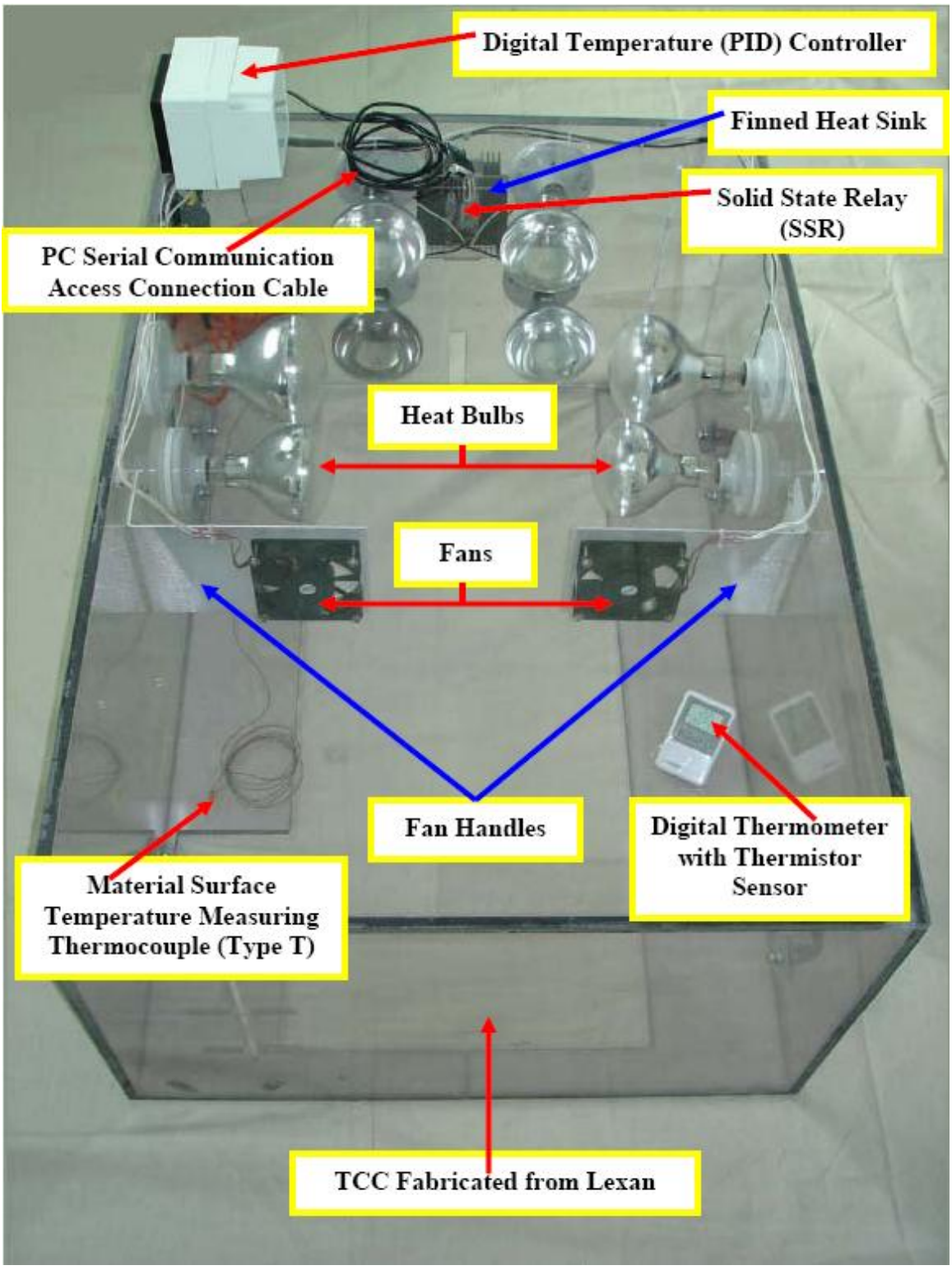

Figure 3.2 Picture of Temperature Controlled Chamber (TCC) (The Entire System)

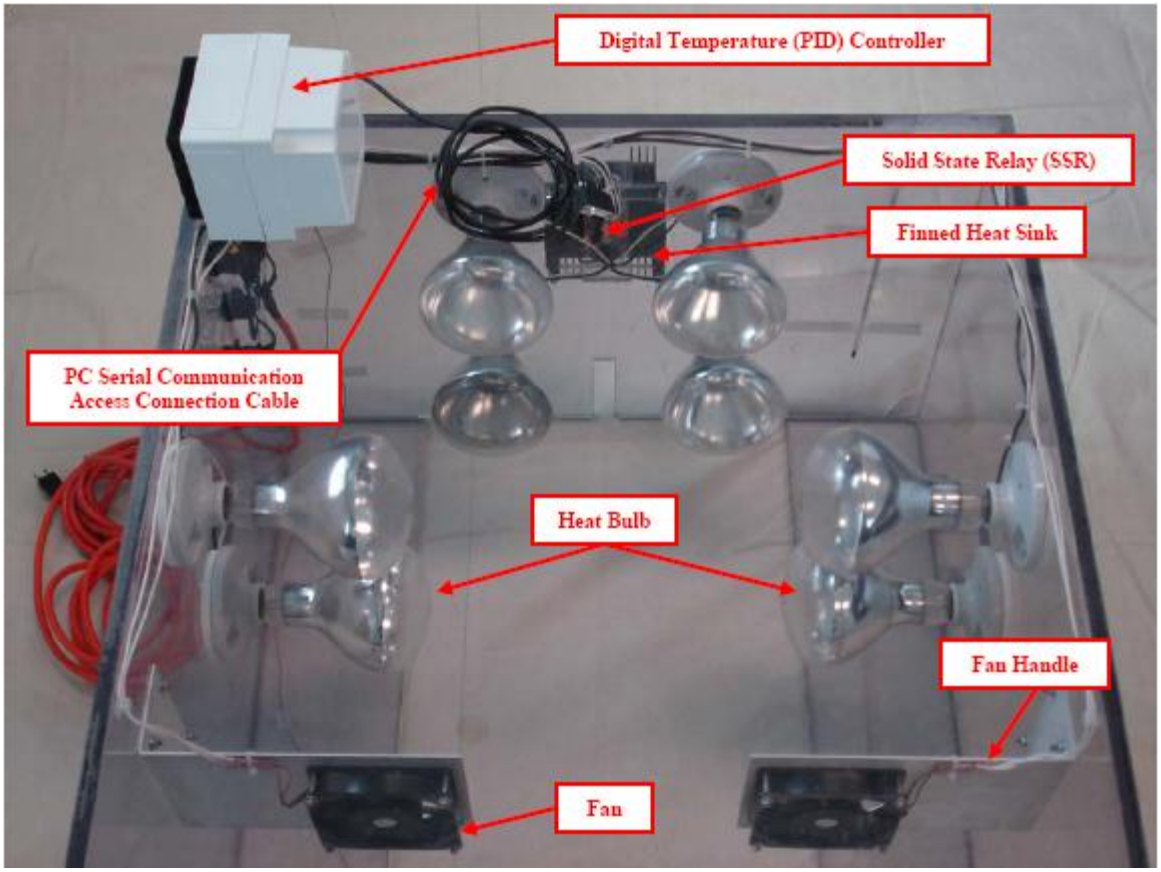

Figure 3.3 Picture of Temperature Controlled Chamber (Close-up View - showing Temperature Control, Heating and Heated Air Circulation Units)

3.3. General Description and Components of the Chamber

3.3.1. The material used to construct Temperature Controlled Chamber

The temperature controlled chamber has a size of 1100 mm in length, 760 mm in width and 510 mm in height (Figure 3.2). Lexan (polycarbonate sheet) (Figure 3.4) which is 30 times stronger than acrylic and 250 times stronger than glass was selected for construction of the chamber. It maintains its properties between -40 °C to 130 °C with a heat deflection temperature of 130 °C and a density of 1.2 g/cm^3. Moreover, lexan is a good choice in terms of heat conservation in the chamber environment. One of the concerns when designing the TCC was heat conduction through the walls of the chamber

due to the temperature gradient between the outside and the inside of the box. The thermal conductivity of lexan (k = 0.2 W/m$_*$°C) is low enough for heat conservation in the TCC as well as to reduce heat loss between the chamber and the surrounding environment. Therefore, energy loss due to temperature difference could easily be compensated by the heating source. In addition, the heat energy produced by the heat bulbs was sufficient to conveniently heat up the chamber environment and to reach test temperatures up to 65 °C in a reasonable amount of time.

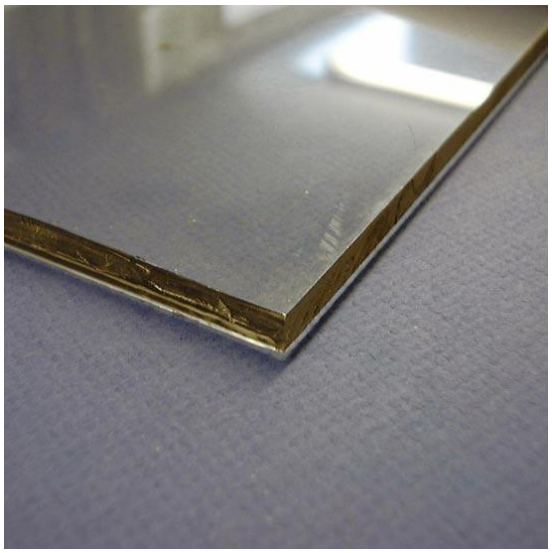

Figure 3.4 Clear Lexan (Polycarbonate) Sheet

3.3.2. Insulation Material (Radiant Barrier)

A flexible, lightweight radiant barrier insulation material (Figure 3.5) (Innovative Insulation Inc., Super R Supreme) which is a two sided reflective pure aluminum foil with reinforced scrim inside and designed to reflect 97% of radiant heat energy was used for its superior insulating qualities to cover the stainless steel table on which the interface

shear device is placed. This significantly reduced the heat loss through the lower surface and facilitated reaching desired temperatures in a shorter amount of time.

Figure 3.5 Radiant Barrier Insulation Material

3.3.3. Heating Unit

Temperatures above ambient conditions are obtained using heat bulbs (Figure 3.6) as a radiant energy heat source mounted on the walls (Figure 3.8) in the chamber. As their name indicates, 95% of total bulb energy is converted to heat; the rest is used for lighting. Heat bulbs (375 W) on each side wall are only used when heating the system up to target test temperature and are turned off once the preset test temperature has been reached in the chamber environment. These side heat bulbs are connected to DPST (Double Pole Single Throw) electrical switches which is a switch device that changes connections (i.e. opens, closes) in both conductors of the same circuit and at only one of the extreme positions of its actuator. Heat bulbs (250 W) at the rear wall of the chamber are connected to a digital temperature controller which is employed to maintain the chamber temperature at ±1 °C of the nominal testing temperature for the duration of the tests.

Figure 3.6 Heat Bulb used as heat source for reaching and maintaining Elevated Temperature Conditions in the TCC

3.3.4. Heated Air Circulation and Temperature Uniformity Unit

Fans which have square dimensions of 120 mm by 120 mm and a depth of 25 mm and are made with steel blades with an aluminum frame were selected to be utilized for circulating heated air within the chamber to ensure a uniform distribution of temperature inside the TCC. Fans are attached to aluminum handles (Figure 3.7) and located at approximately the center of the chamber (Figure 3.8). They are capable of blowing 80 cubic feet (2.27 m^3) of air per minute. Those fans which include a single phase motor can operate on alternative current (AC), at 50 Hz frequency and were connected to SPST (Single Pole Single Throw) electrical switches which is a switch device that opens, closes in a single conductor of an electrical circuit and at only one of the extreme positions of its actuator.

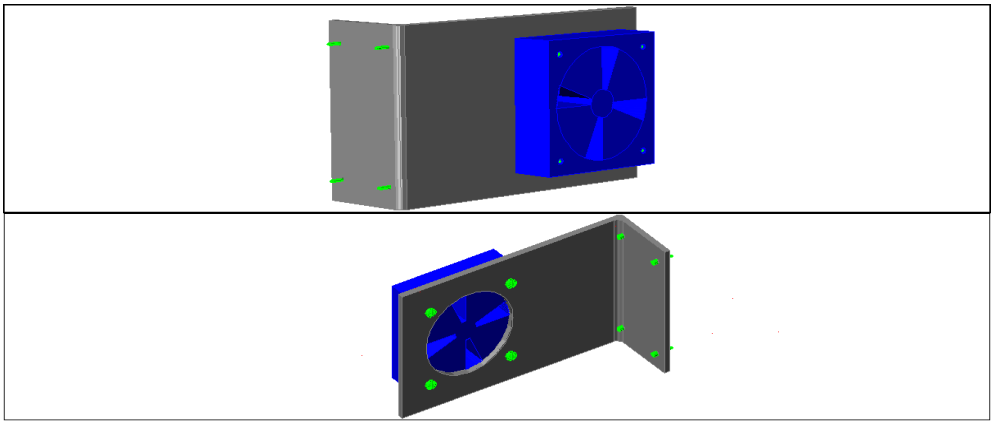

Figure 3.7 Fan attached to an aluminum bracket to locate at proximity of the center of the TCC for blowing air in longitudinal chamber direction for heated air circulation purposes

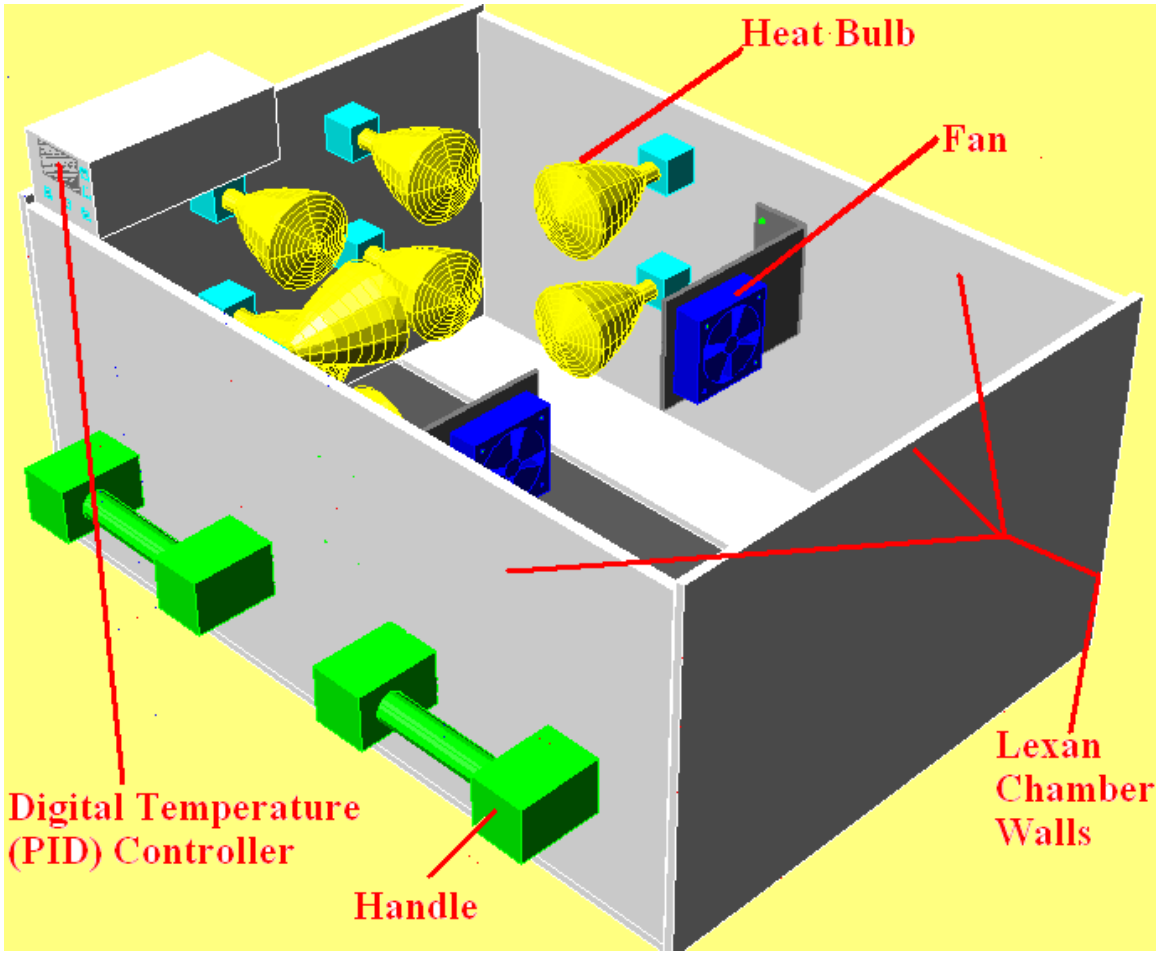

Figure 3.8 Solid Model Sketch of Temperature Controlled Chamber (TCC)
(Horizontal Placement Configuration)

3.3.5. Temperature Measurement Sensors

(Thermocouple, Thermometers, Radiation Pyrometers)

A surface-mount (measures surface temperature), fast-response (<0.15 sec.), self adhesive thermocouple (Type T; SA1XL-T; Omega Engineering Inc) (Figure 3.9a) is attached on the geomembrane surface to allow the exact temperature at geomembrane-geotextile as well as geomembrane-sand interfaces to be measured. The thermocouple which is a thermoelectric temperature sensor consists of two dissimilar metallic wires (i.e. one Copper, Cu and one Constantan, Cu-Ni for Type T) coupled at the probe tip or

measurement junction. The temperature of the material on which the thermocouple is adhered is detected by measuring the change in voltage and comparing the temperature difference between the probe tip and the electrically generated reference. The self-adhesive surface mounting thermocouple is ideal for targeted placement of the sensor element and measuring temperature of the surface on which it is attached. The main advantages of using a thermocouple as a temperature measurement sensor are its low cost, short response time, repeatability and accuracy, wide temperature range and robustness. Other than the thermocouple used for sensing counterface temperature, there were four more thermometers (Figure 3.9b) which were evenly distributed throughout the chamber to verify the uniform distribution of temperature inside the TCC. They were located in such a manner that each thermometer is on the center of each face of the chamber and is equally placed along the centerline of the interface shear device. These measurements indicated that the temperature variation within the chamber was ±1 °C of the preset test temperature. In addition, a laser/infrared (IR) thermometer (Radiation Pyrometers) (Figure 3.9c) capable of measuring temperature from a distance by detecting the amount of thermal electromagnetic radiation is utilized to verify chamber environment temperature from outside.

Figure 3.9 Temperature Measurement Sensors:
a) Thermocouple (Left); b) Thermometer (Middle); c) Radiation Pyrometers (Right)

3.3.6. Digital Temperature Controller and Electrical Wiring & Compliance Requirements

A digital temperature (PID) controller (CN 3251-DR-S2; Omega Engineering Inc) (Figure 3.10) with universal sensor inputs as well as relay and DC pulse outputs module was selected for controlling the chamber temperature and maintaining it at a constant value. Controller generated commands were sent to the heating unit to turn on/off heat bulbs depending on the thermocouple measurements of the current temperature relative to the preset value entered through the controller front panel interface by the operator. It has an accuracy of 0.2% for the process variable (preset target test temperature value) when a Type T thermocouple is used as an input to the controller to sense temperature (see Figure 3.11 for electrical wiring connections). This process controller is a cost effective, high-performance, single loop controller that can be utilized for temperature, flow and pressure control applications. The heat bulbs are connected to the digital temperature controller through a solid state relay (SSR; VDC Input-VAC Output) (Figure 3.12) which is preferred for controlling large resistance heaters (i.e. heat bulbs) in conjunction with temperature controllers. Basically, solid state relays (Turn On/Off Time: 20 msec.) are SPST (Single Pole Single Throw), normally open switching devices with no moving parts and capable of millions of cycles of operation. Since, switching takes place at the zero voltage crossover point of the alternating current cycle, no appreciable electrical noise is generated in the circuit. Heat develops in a solid state relay due to the nominal voltage drop across the switching device. To dissipate the heat, the SSR must be mounted on a finned heat sink and located on the outside face of the rear wall of the chamber where the ambient temperature is relatively low. It is essential that a properly rated, fast blowing I^2T

fuse be installed in the electrical circuit to protect from the condition of an overloaded circuit.

Figure 3.10 Digital Temperature (PID) Controller

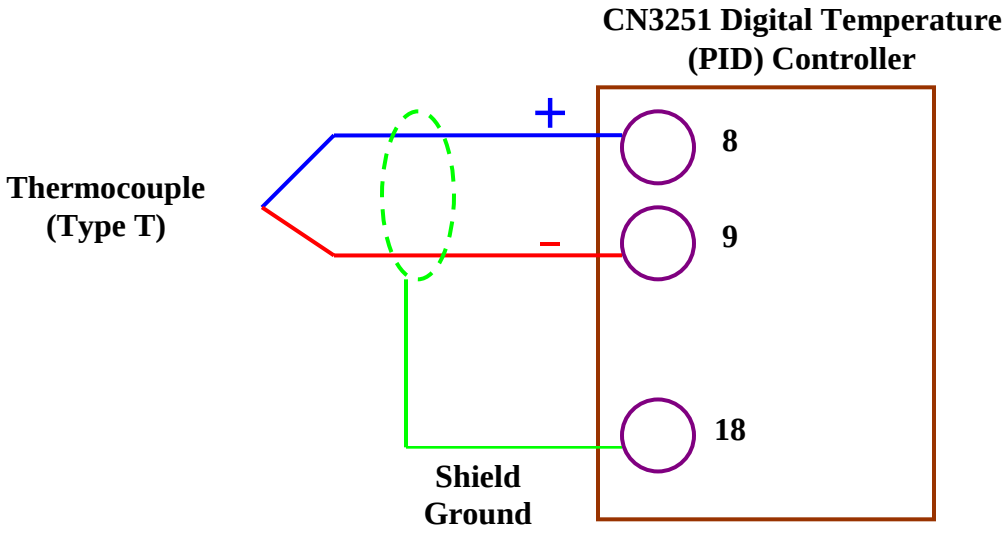

Figure 3.11 Thermocouple Sensor Input Connections

Figure 3.12 Solid State Relay mounted on Finned Heat Sink

3.4. Instrumentation and Data Logging/Acquisition

To monitor and record test duration temperature data into a computer, the digital temperature controller was connected to a PC serial port through RS232 digital communications board (included in the controller) by a serial connection (Figure 3.13). The software (CN3200-SOFT-WIN2) installed in PC for communications option gives the controller the ability to interface with the computer as well as to monitor and record the temperature measured via the thermocouple. Plots demonstrating the relationship between active set-point (current temperature) and process variable (preset value) can be generated for comparison purposes both in-test and post-test stages. Conversely, the temperature controller can be accessed and manipulated from the computer by means of the aforementioned special communication software. For example, for overnight tests or long duration experiments, test progress and temperature variation in the test system can be observed by remotely accessing the computer via internet connection so that the chamber environment temperature can be administrated from a distance (Figure 3.14).

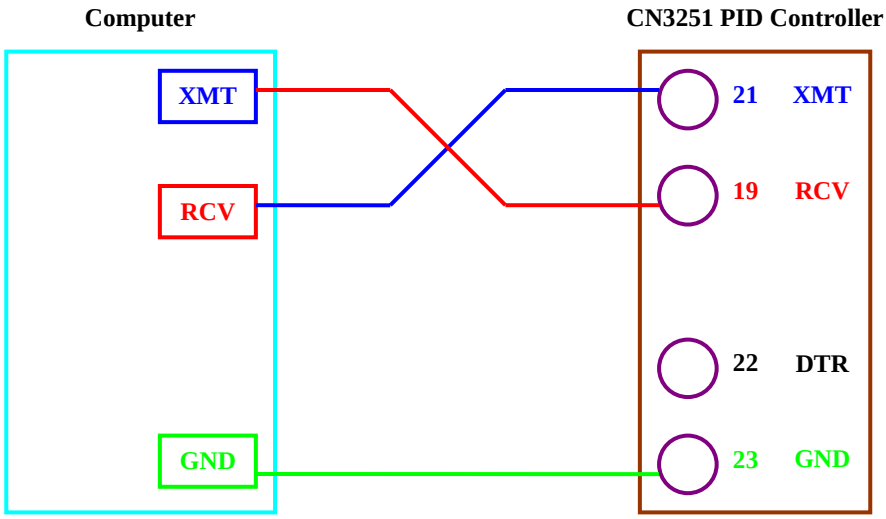

Figure 3.13 RS 232 Digital Communications Wiring Connections
Using Shielded Serial Interface Cable

Note: XMT: Transmit; RCV: Receive, GND: Ground; The DTR output is always enabled when the CN3251 PID Controller power is on.

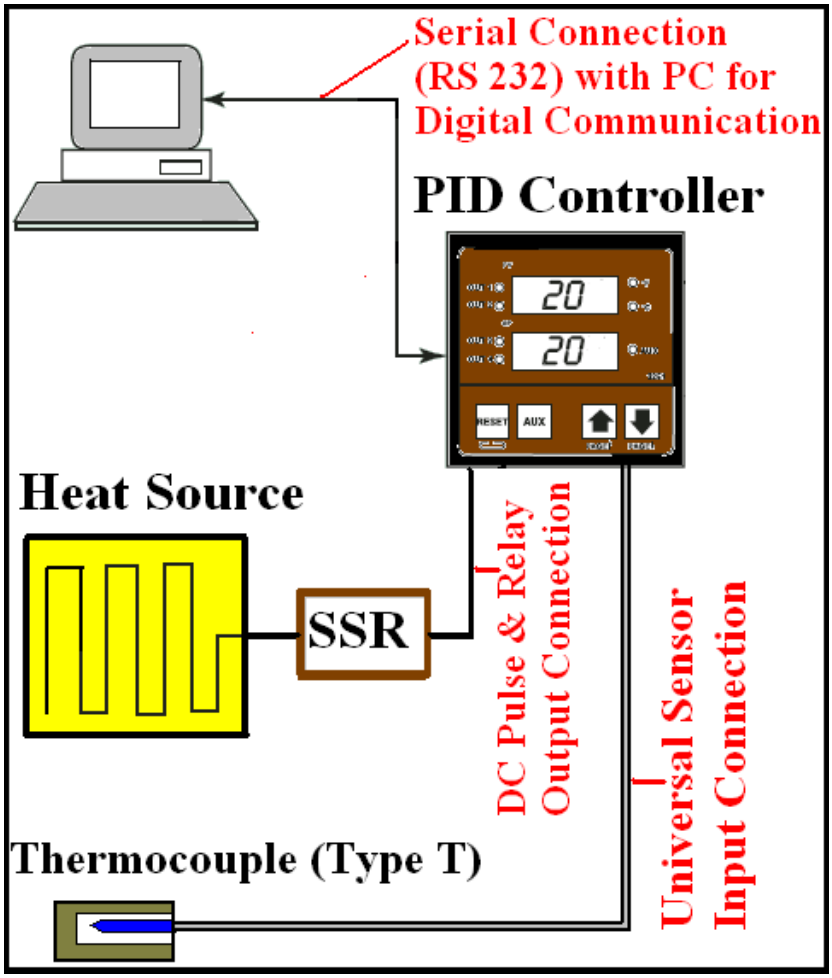

Figure 3.14 Instrumentation, Data Logging and Electrical Wiring Configuration

3.5. The TCC Heat-up and Stability Performance Evaluation

Test progress in the temperature controlled chamber testing system can principally be categorized in two fundamental stages: I) Heat-up Process and II) Test Duration at Constant Temperature Level. In addition, experiments can be performed at varying temperature conditions by programming the digital (PID) temperature controller based on the user needs and research purposes. The performance of the TCC test system was evaluated by considering several criteria in terms of different test progress durations depending on constant or changing temperature conditions to validate the repeatability and the consistency of the heat-up process as well as the stability of constant temperature conditions. It was observed that there were very minor temperature fluctuations from constant test temperature level during long test periods. In this manner, the reliability and robustness of operations in the TCC and the accuracy of measurements performed in the TCC environment were verified.

3.5.1. Repeatability and Consistency of System Heat-up Process

Temperature data were measured and logged several times during the period of heating-up of the TCC test system up to different elevated temperature levels (e.g. 30, 35, 40, 45, 50 °C) to observe the repeatability of the heat-up process. For demonstration purposes, an elevated temperature of 50 °C was selected here due to the fact that 50 °C is one of the highest temperature conditions that the construction materials experience in civil engineering applications such as landfills. Figure 3.15 shows temperature measurements performed for four different trials during the system heat-up and confirm that all the measurements coincide very well with each other which show the consistency

of the temperature increment process. The average time duration to reach 50 °C in the TCC environment was 145 minutes with a time variation of only ± 5 minutes from the average. This verifies appropriate insulation of the TCC test system, heat conservation in the chamber, and robust performance of the system heating unit in obtaining the same elevated temperature conditions for the same preset target test temperature at different experiment times in the TCC. Further, obtaining the higher temperature condition (50 °C) in the chamber with a time variation of only ± 5 minutes indicated that the fans used for heated air circulation and temperature uniformity performed their functions well.

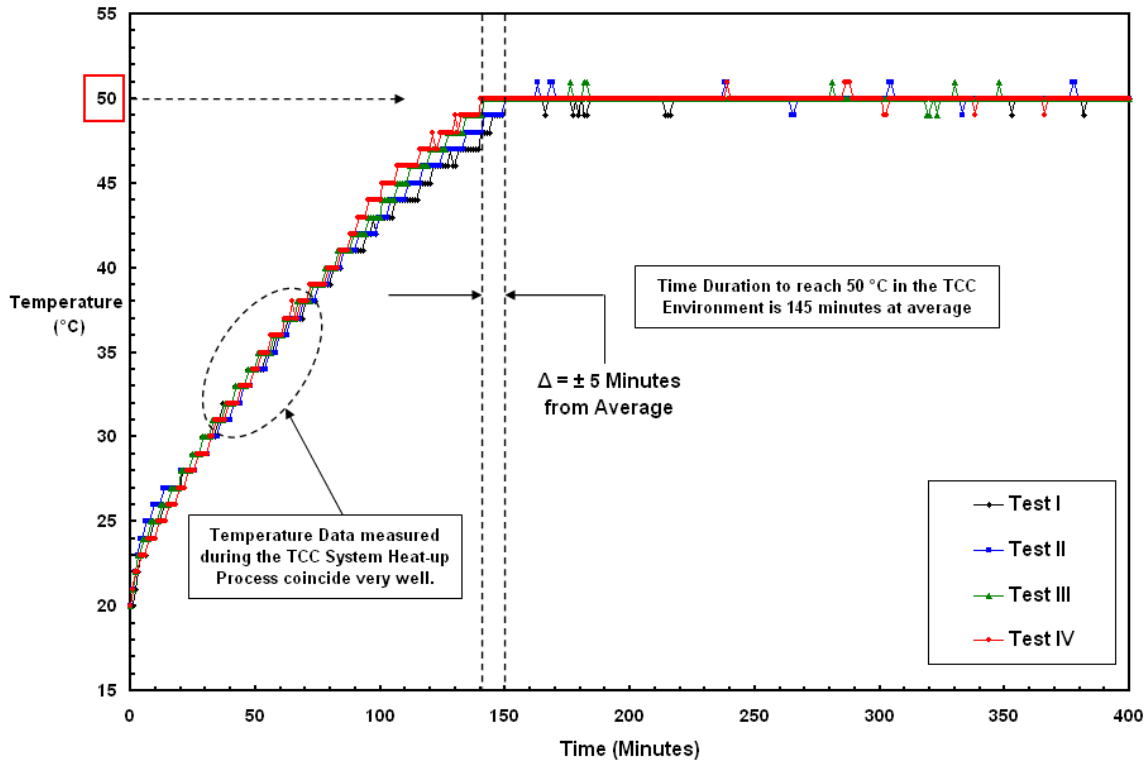

Figure 3.15 Temperature versus Time Data during Heat-up Process

3.5.2. Temperature Fluctuations from Preset Constant Test Temperature

The temperature controlled test system was heated up to 40 °C and kept at this elevated temperature level for 10 hours to show long term stability of the TCC test system by providing steady state experiment conditions in the chamber environment for the tests that would last for long durations with minor fluctuations from the constant preset test temperature (Figure 3.16). The maximum deviation from the preset target test temperature was only ± 1 °C at any elevated temperature level up to 65 °C. This verifies overall operational stability of the TCC test system at higher temperatures over long test durations as well as precise and accurate control of the digital temperature (PID) controller to maintain the chamber environment temperature at constant level without fluctuating significantly from the preset target test value. In addition, the robust operational performance of the developed heating system consisting of heat bulbs, PID controller, temperature sensor (i.e. thermocouple), SSR, and finned heat sink was validated by successfully maintaining the TCC environment at constant temperature level for such a long duration. Consequently, it is evident that the air heated by the heat bulbs circulates within the chamber environment in a desirable manner enabling uniform distribution of temperature inside the TCC. As shown in Figure 3.16, it only takes about 75 minutes to reach 40 °C temperature in the chamber environment with a heat-up time duration variation of ± <5 minutes.

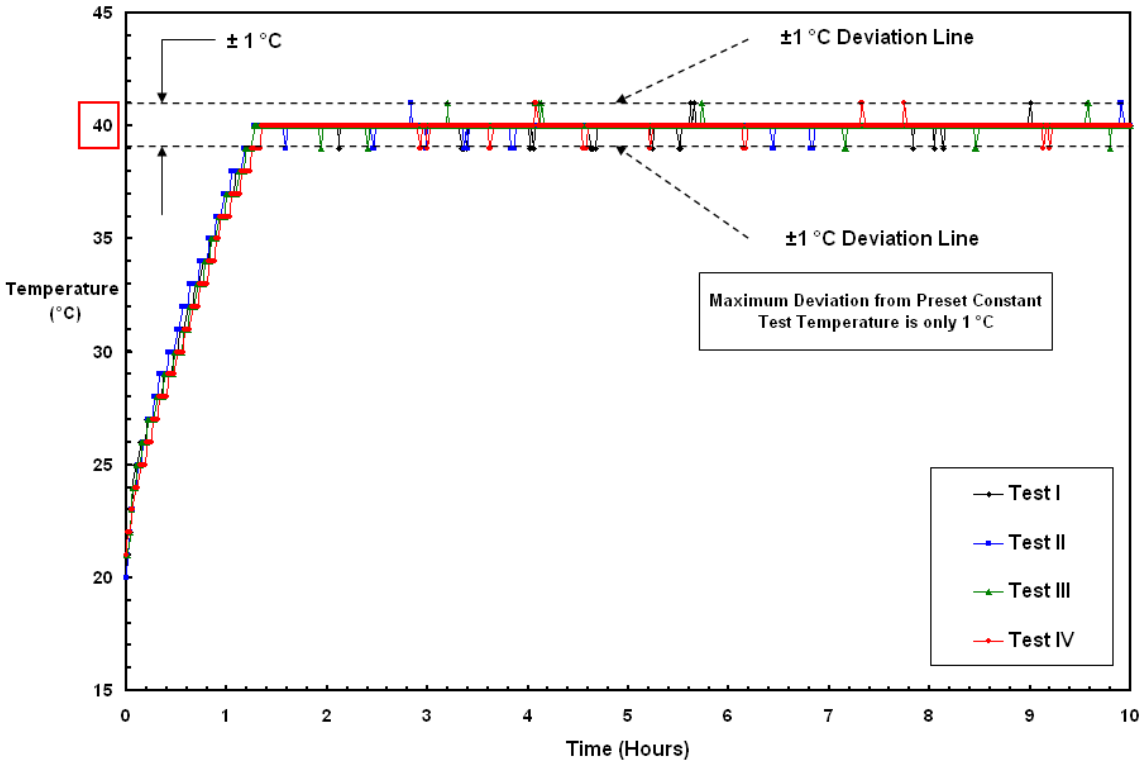

Figure 3.16 Temperature versus Time Data during a Long Test Period at Constant Temperature

3.6. Summary and Conclusions

The field conditions at elevated temperatures have to be precisely simulated in the laboratory in order for the interface shear tests conducted to evaluate the geosynthetic materials in-situ functional engineering properties and operational performance to be accurately determined. The designed and developed temperature controlled chamber (TCC) provided the ability to examine the temperature dependent interface shear behavior of geosynthetic-geosynthetic as well as sand-geosynthetic composite systems with a large displacement interface shear device enclosed by the TCC. Reliable operational performance of the TCC test system has been achieved by appropriate

selection of the parts following the main design criteria which were functionality, size, efficiency and long-lasting serviceability. The components employed in the electrical system for controlling temperature were a first order concern to ensure precise and accurate control of the TCC during the laboratory tests.

The overall performance of the TCC test system was evaluated by considering several criteria for the development and validation of the system as well as observations pertaining to system design criteria as follows:

- Repeatability and consistency of heat-up process
- Long time stability of the TCC test system to provide steady state experiment conditions in the chamber environment
- Reliability and robustness of operations in the TCC
- Accuracy of measurements performed in the chamber environment
- Stability of constant temperature conditions
- Appropriate insulation of the TCC test system and heat conservation in the chamber
- Robust performance of the system heating unit to obtain identical elevated temperature conditions at different experiment times in the TCC
- Precise and accurate control of the digital temperature (PID) controller
- Reliable operational performance of the developed heating system consisting of heat bulbs, PID controller, temperature sensor (i.e. thermocouple), SSR, and finned heat sink
- Circulation of heated air and uniform distribution of temperature inside the TCC

CHAPTER IV

4. EXPERIMENTAL METHODS

4.1. Introduction

This chapter describes the experimental program conducted to study the effects of elevated temperature on the behavior of geosynthetic interfaces including: I) Geotextiles-Geomembranes (fiber-texture interaction) and II) Sands-Geomembranes (particulate-continua interaction). The properties of the test specimens will be described and several different experimental systems utilized for the testing program along with further details on the scope of the extensive laboratory experimental program will be presented. Complementary geotextile single filament tensile tests, geomembrane surface hardness tests as well as geomembrane surface profile measurements which provide important insight into the role of temperature in the observed behavior differences will be summarized. These latter tests are critical for microscale analysis of elevated temperature effects on interface shear behavior.

4.2. Materials Tested

To investigate fiber-texture interaction at elevated temperatures, interface shear testing was conducted using a needle punched nonwoven polypropylene geotextile (NPNW) in combination with either a smooth polyvinylchloride (PVC) or a smooth, a co-extruded, or a structured micro-spike textured high density polyethylene (HDPE) geomembrane. Additionally, to investigate particulate-continua interaction at elevated

temperatures, interface shear tests were performed using either a rounded or an angular sand sheared against either smooth polyvinylchloride (PVC) or high density polyethylene (HDPE) geomembranes.

4.2.1. Fibrous Material Characteristics

The staple fiber polypropylene needle-punched nonwoven geotextile is one of the most widely used types because of its enhanced engineering properties generated through a fiber-fiber bonding process and the resulting spatial arrangement of filaments to fulfill the requirements for frictional resistance, tensile properties, permeability, soil stabilization, separation, drainage, gas transmission, cushion, filtration and liner protection applications. GSE needle punched nonwoven geotextiles are designed to meet or exceed GRI GT12 and AASHTO M288 specifications and functional properties (Table 4.1). Although GSE geotextiles have a highly porous structure, they have high strength, durability and flexibility properties. Geomembrane liners are sensitive to damage and puncture during construction activities as well as over the life of a project. Therefore, geomembranes must be protected from top and bottom. Needle punched nonwoven geotextiles are ideal for this purpose because of their cushioning ability. The geotextile selected to be used in this laboratory testing program has a mass per unit area of 270 g/m^2 (8 oz/yd^2) (per ASTM D 5261) and apparent opening size of 0.18 mm (per ASTM D 4751).

Table 4.1 Summary of Geotextile Properties

	GSE NPNW 8 oz./yd^2 Geotextile	**Test Method**
Material	Polypropylene	-
Fiber Type	Staple Fiber	-
Mass per Unit Area, g/m^2	270	ASTM D 5216
Grab Tensile Strength, N	975	ASTM D 4632
Grab Elongation, %	50	ASTM D 4632
Puncture Strength, N	525	ASTM D 4833
Trapezoidal Tear Strength, N	395	ASTM D 4632
Apparent Opening Size, mm	0.180	ASTM D 4751
Permittivity, sec^{-1}	1.30	ASTM D 4491
Permeability, cm/sec	0.30	ASTM D 4491
Water Flow Rate, 1/min/m^2	3865	ASTM D 4491

Note: Source – GSE Lining Technology Inc., Product Literature

4.2.2. Continuum Materials Characteristics

Geomembranes are manufactured from a variety of polymer resins with the most common types being high density polyethylene (HDPE), linear low density polyethylene (LLDPE), very flexible polyethylene (VFPE), polyvinylchloride (PVC) and polypropylene (PP). Geomembranes are used in a wide variety of waste containment related applications such as landfill liners (primary and secondary containment), landfill caps/closures, lagoon liners, agriculture pond liners, canal linings, raw water treatment reservoirs, potable water reservoirs, retention ponds, floating covers, and waste water treatment lagoons. High density polyethylene (HDPE) produced from formulated polyethylene resin is the most widely used geomembrane material due to its high tensile properties at low strain levels. On the other hand, polyvinylchloride (PVC) geomembranes are selected for use in infrastructure projects which require more flexibility in three dimensional performance as well as having less hardness of the

geomembrane itself which can lead to enhancement of interfacial properties for combined and layered applications consisting of different material types.

- EPI PVC Smooth Geomembrane: PVC liners manufactured by Environmental Protection Inc. are produced with polyvinylchloride as the principal polymer resin. All materials meet or exceed ASTM D 7176 specifications and functional requirements for the liner material itself. The benefits of PVC geomembranes are as follows: Flexibility for three dimensional performance, larger panels (up to 80% less field seams), long-term survivability (Figure 4.1a).
- GSE HDPE Smooth Geomembrane: GSE HDPE smooth geomembranes are the preferred products for lining projects requiring low permeability as well as chemical and ultraviolet resistant properties for applications such as landfill liners, municipal waste containment, power plants and aquaculture projects. This product is designed to meet all aspects of GRI GM 13 (HDPE) specifications. GSE HDPE smooth geomembrane which is made from high density polyethylene resin contains 97.5% polyethylene and 2.5% carbon black and is specifically designed to be employed for flexible geomembrane applications. Additionally, antioxidants and UV stabilizers are added in the resin to assure long-term performance and UV resistance. This product exhibits a large elongation of about 700% after yield before reaching break point compared with other products having similar thickness and tensile strength (Figure 4.1b).
- GSE HDPE Co-extruded Textured Geomembrane: Textured geomembrane has upper and lower textured surfaces with high shear strength and multi-axial performance produced through a coextrusion process to enhance the ability of the

material to improve geosynthetic profile stability which ultimately maximizes the available volume that can be contained by the geomembrane; the steeper the slope, the larger design capacity and the less overall cost. This product was designed to be utilized in projects with steep slopes where the interface strength between geosynthetic components is a critical factor for the integrity of the structure as well as the stability of modern lining systems (Figure 4.1c).

- Poly Flex HDPE Blown-Film Textured Geomembrane: Poly Flex HDPE textured geomembranes manufactured from polyethylene resin are produced to combine long-term durability with strength and flexibility as well as ultraviolet and chemical resistance in providing an impermeable barrier for a wide variety of applications. The blown-film texturing process provides an increased friction angle for higher stability on steep slope applications. This blown-film textured HDPE liner has smooth edges which result in more cost-effective, easier, more consistent, and better welding for the benefit of full prevention of leakage (Figure 4.1d).
- Agru HDPE Micro-Spike Textured Geomembrane: Agru HDPE micro-spike textured geomembrane is the only textured geomembrane type in industry manufactured through a flat die extrusion calendering production process that results in a structured profile consisting of a roughened surface and a regular series of small spikes completely integrated with the base liner material. It is designed to meet all the GRI GM 13 (HDPE) specifications and functional requirements. Micro-spike textured geomembranes also have smooth edges for thermal fusion welding between adjacent sheets. As with the coextrusion process,

there is no layered manufacturing process and the micro-spike texturing is an integral part of the liner itself. Additionally, the consistent structuring on the liner surface provides reproducible friction angle values with more importantly amongst the highest surface friction values. This material is principally designed for enhanced friction characteristics with sand, clay, geotextile and geocomposites where slope stability is an issue (Figure 4.1e).

Technical engineering properties of all the geomembranes used in the laboratory experimental program are summarized in Table 4.2.

Table 4.2 Summary of Geomembrane Properties

	EPI PVC Smooth	**GSE HDPE Smooth**	**GSE HDPE Textured**	**Poly Flex HDPE Textured**	**Agru HDPE MicroSpike**	**Test Method**
Density, g/cm^3	1.20*	0.94	0.94	0.94	0.94*	ASTM D 1505
Thickness, mm	1.0	1.0	1.0	1.0	1.0	ASTM D 5199
Carbon Black, %	-	2.0-3.0	2.0-3.0	2.0-3.0	2.0-3.0**	ASTM D 1603
Strength at Yield, kN/m-width	-	14	15	15	15.4	ASTM D 6693
Strength at Break, kN/m-width	17	26	13	11	15.4	ASTM D 6693
Elongation at Yield, %	-	13	12	12	13	ASTM D 6693
Elongation at Break, %	430	700	100	100	350	ASTM D 6693
Puncture Resistance, N	-	378	422	267	400	ASTM D 4833
Tear Resistance, N	44.5	124	142	125	133	ASTM D 1004

*ASTM D 792-Method B; **ASTM D 4218
Note: Source – Product Literature of Environmental Protection (EPI) Inc., GSE Lining Technology Inc., Poly-Flex Inc., Agru America Inc.

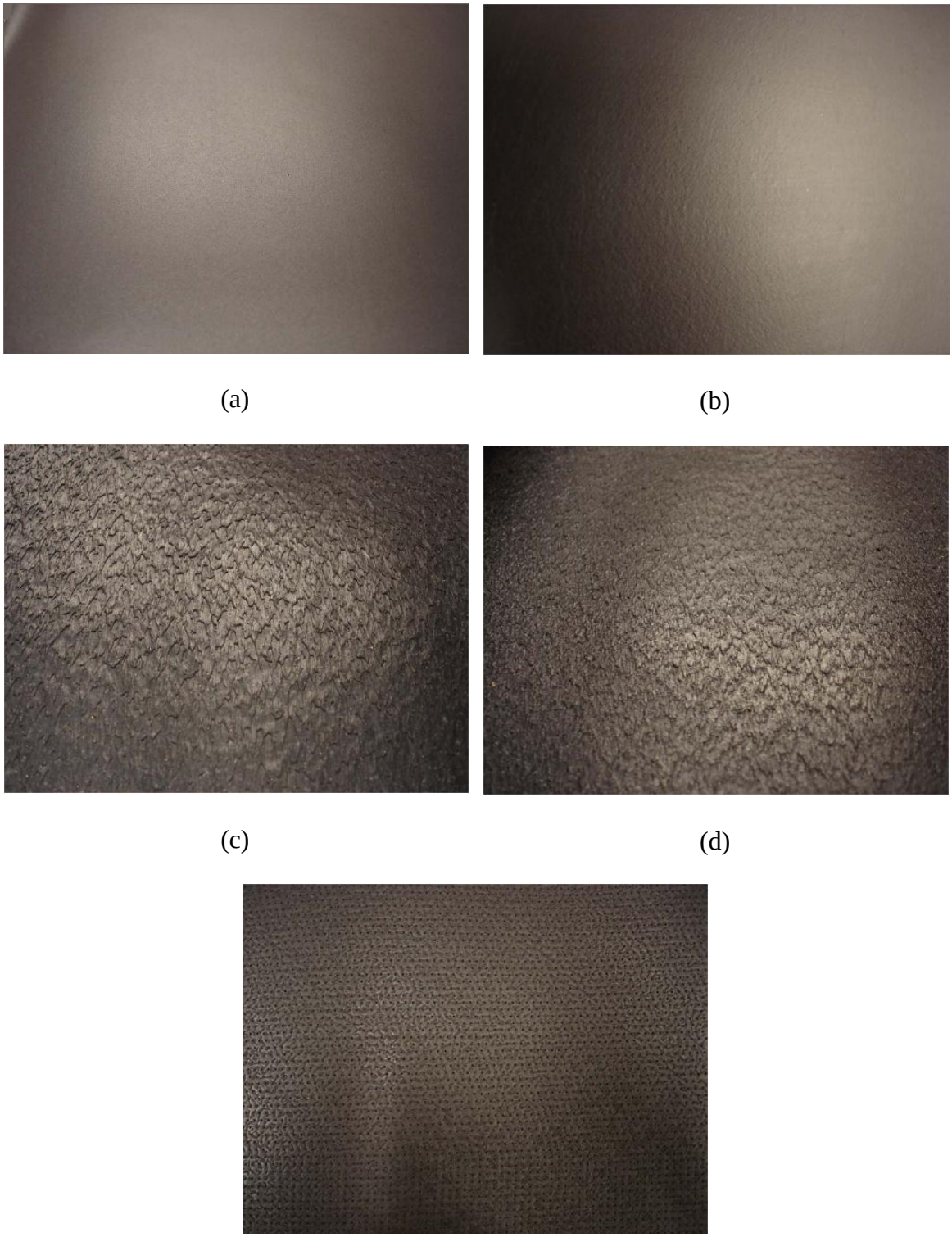

(a) (b)

(c) (d)

(e)

Figure 4.1 Pictures of Geomembrane Types used in Laboratory Experimental Program: (a) EPI PVC Smooth; (b) GSE HDPE Smooth; (c) GSE HDPE Co-extruded Textured; (d) Poly Flex HDPE Blown-Film Textured; (e) Agru HDPE Micro-Spike Textured

4.2.3. Particulate Materials Properties

Particulate materials including Ottawa 20-30 sand (US Silica Company, Ottawa, IL) and Blasting sand (Unimen Corporation, New Canaan, CT), were used to investigate particulate-continua contact behavior at elevated temperatures. The Ottawa 20-30 sand is poorly graded sand composed of rounded to sub-rounded quartz sand grains. The blasting sand is similarly a poorly graded sand, however, is composed of angular quartz sand particles. These two sand types which have a similar mean grain size (D_{50} = 0.72 mm) were selected to explore the role of particle shape and angularity on sand-geomembrane interface shear behavior at elevated temperatures.

The index properties of the particles are given in Table 4.3. Figure 4.2 illustrates the grain size distribution of the selected materials. Additionally, magnified microscopic images of individual sand particles are presented in Figure 4.3.

Table 4.3 Summary of Index Properties of the Tested Sands

	D_{50} (mm)	**C_u [a]**	**C_c [b]**	**G_s [c] (g/m^3)**	**e_{max} [d]**	**e_{min} [e]**
Ottawa 20/30	0.72	1.46	0.96	2.65	0.73	0.51
Blasting Sand	0.71	1.43	1.04	2.65	1.07	0.74

Note: [a]$C_u = D_{60}/D_{10}$; [b]$C_c = D_{30}^2/(D_{10}*D_{60})$; [c]AASHTO T133; [d]ASTM D4254-91, Method B; [e]ASTM D 4253-93, Method 2A

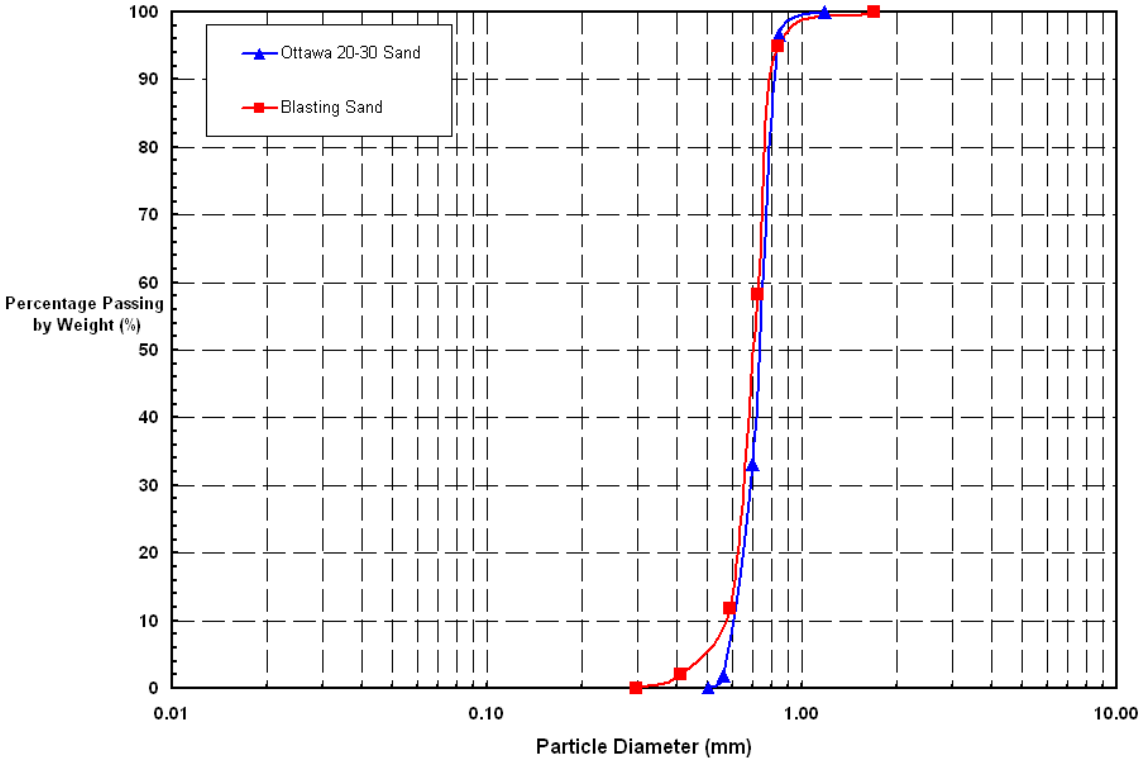

Figure 4.2 Grain Size Analysis of Tested Sands

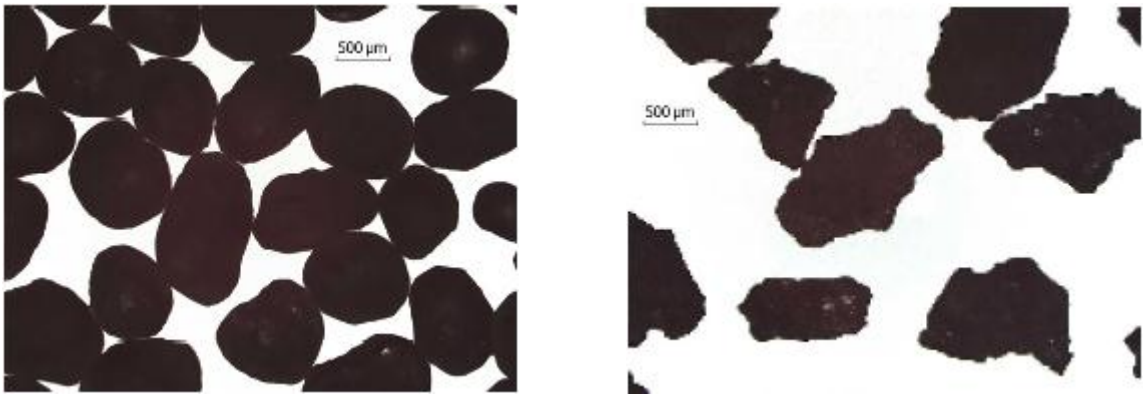

(a) (b)

Figure 4.3 Microscopic Images of Individual Sand Particles:
(a) Ottawa 20/30 Sand; (b) Blasting Sand (Adapted from McGillivray, 2009)

4.3. Interface Shear Test Equipment

The direct interface shear device (Figure 4.4) permits large displacements up to 60 mm such that pseudo-residual interface strength values can be obtained. Pseudo-residual shear strengths of the interface systems are defined as the shear strength measured at displacements sufficient to achieve an asymptotic approach of the shear stress to a constant value representative of the true residual strength (Stark et al., 1996). In the current study, pseudo-residual values were taken as the average (i.e. arithmetic mean) of the shear strength over a 2 mm range of shearing displacements from 57 to 59 mm.

4.3.1. Interface Shear Device

A mechanically driven system consisting of an ActionJac ball screw jack driven by a Bodine DC Motor (130 volt) controls the lateral movement of the shear box. Gear reducers exist in the system to enable the relatively slow displacement rates required for testing purposes to be achieved. An encoder (Dynapar Series H20) is available in the apparatus to achieve constant displacement rates during interface shear testing. The speed is digitally controlled through a speed control system (DART Company). There are two stopper switches located at forward and backward limit displacement locations to prevent the ball screw jack from displacing beyond its physical limits. A pneumatic cylinder is attached to the system beneath the interface shear device for the purpose of normal load application. The cylinder is located on a platform mounted on a set of linear rods with which the cylinder can traverse beneath the testing platform table (Figure 4.4).

4.3.1.1. Geosynthetic-Geosynthetic Interface Shear Testing Module

A geosynthetic-geosynthetic interface shear testing module enclosed by the temperature controlled chamber was used to perform interface shear tests at different temperatures. This module has some superior and improved properties in comparison to the conventional shear devices in terms of system errors associated with operation of conventional interface testing equipment during the experiments. For example, the geomembrane specimen is fastened on a platform which travels along a set of linear bearings (Thomson SPB-16 and ASB-16) that produce negligible system friction in the range of 0.1 – 0.2 % of the normal stress under the range of vertical test load of 680 kg (Kim, 2006). Additionally, the geotextile specimen can strain freely (unconstrained case) by being folded and pressure fastened around wedge-shaped plates suspended by the reaction wall on the leading edge of the module (Figure 4.4).

The lateral and vertical displacements are measured with a horizontally mounted LVDT and two vertically installed LVDTs on top of the acrylic block footing, respectively. The shear resistance and normal force are monitored with a horizontally mounted load cell and a vertical load cell, respectively, attached under the loading frame and placed on a steel ball to avoid moment and eccentric forces occurring in the system. All the LVDTs used in the experimental apparatus are DC to DC and have non-linearity less than 0.5 %. Both the normal load cell and shear load cell have a capacity of 1000 lb (SM Series, Interface Company). Furthermore, there is another higher capacity (2000 lb) normal load cell attached to the data acquisition system that is available for use in cases where the capacity of the regular normal load cell (1000 lb) is not sufficient. The entire experimental system is shown in Figure 4.4.

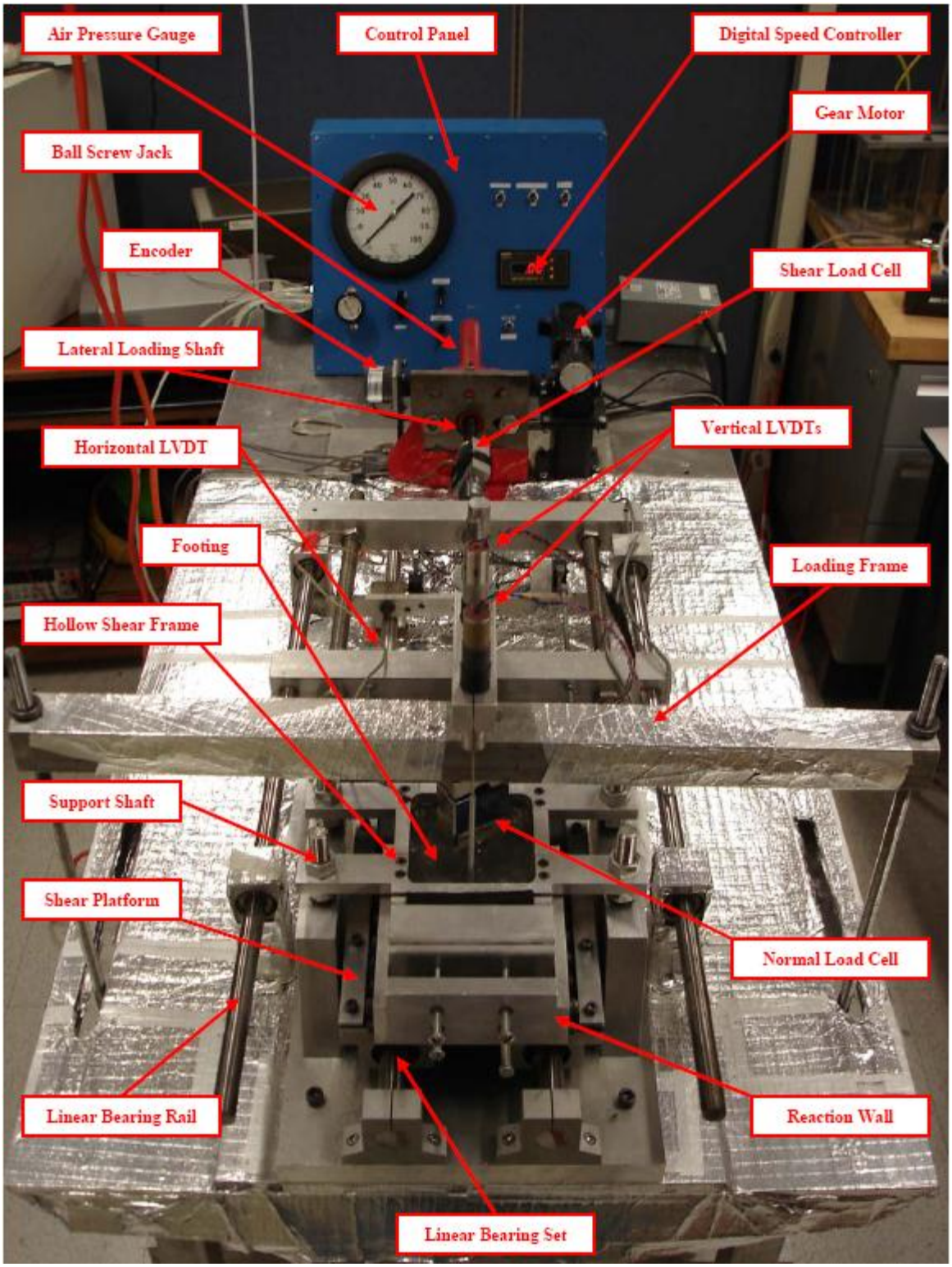

Figure 4.4 Picture of Entire Interface Shear Device Equipment on which Geosynthetic-Geosynthetic Module Mounted

The shear frame above the interface to be tested is suspended during specimen preparation and conditioning by four threaded shafts installed on the rigid walls mounted on either side of the sliding plate. Before initiating the tests, the position of the shear frame can be adjusted using the four-screw system in such a way that the shear frame becomes not only perfectly horizontal but also has no contact with the geomembrane to avoid over-estimating interface strength due to contact between the shear box and the geomembrane specimen. The shape of the shear frame is a hollow half-cube with dimensions of 100 mm in length, 100 mm in width, and 50 mm in height (Figure 4.5).

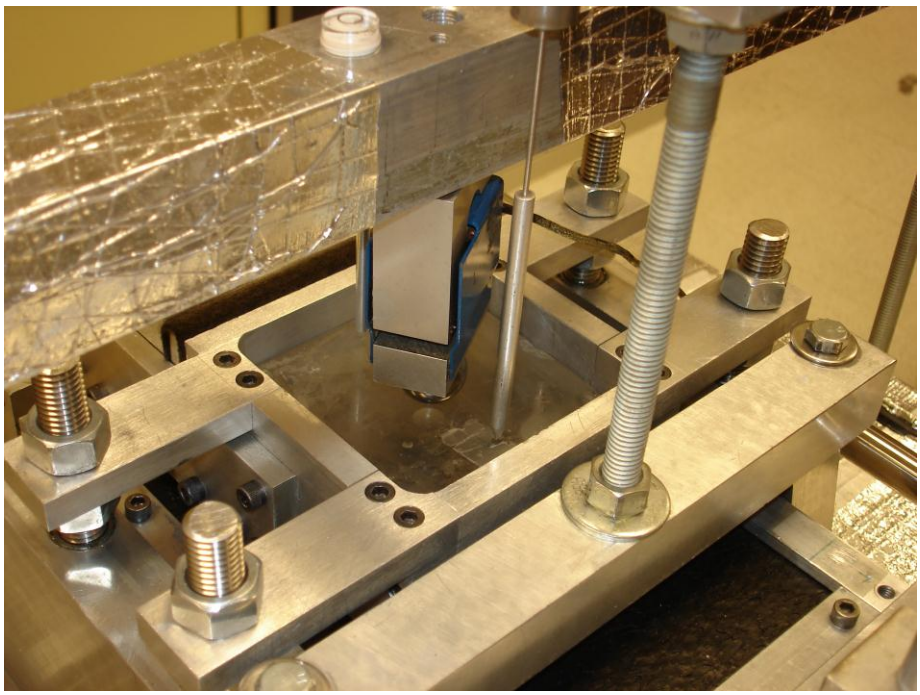

Figure 4.5 Close-up View of Geosynthetic-Geosynthetic Module

4.3.1.2. Sand-Geosynthetic Interface Shear Testing Module

The interface shear tests involving the particulate material (i.e. sand) and a continuum planar surface material (i.e. geomembrane) were performed by utilizing a Teflon shear box connected to the large displacement interface direct shear device. The box was laterally displaced on the upper surface of the geomembrane specimen that was fastened by clamping metal strips with bolts on a heavy metal block testing platform (Figure 4.6).

The normal load was applied on the sand specimen contained in the Teflon shear box through a metal cross beam by pressurizing the pneumatic cylinder. A metal round top cap was placed on top of the specimen and at the bottom of the load cell used to measure normal force. In addition, a steel ball was placed in between the normal load cell and the round top cap to prevent moment or eccentric forces from occurring during the test. Figure 4.6 shows this configuration in detail. Lateral and vertical displacements were measured by using a horizontally mounted LVDT attached on a moving metal frame connected to the lateral loading shaft and a vertically located LVDT on the round top cap over the sand specimen, respectively. The normal force and shear force were monitored by the normal load cell located under the loading cross beam and the shear load cell mounted on the lateral loading shaft that moved horizontally during the experiments. Both load cells have a capacity of 1000 lb (SM Series, Interface Company). The data for all transducers including both the load cells and the LVDTs were collected, recorded and real time displayed via the Agilent BenchLink Data Logger Software which digitally communicates with the data acquisition system. An image of the interface direct shear apparatus with the sand-geosynthetic module is shown in Figure 4.6.

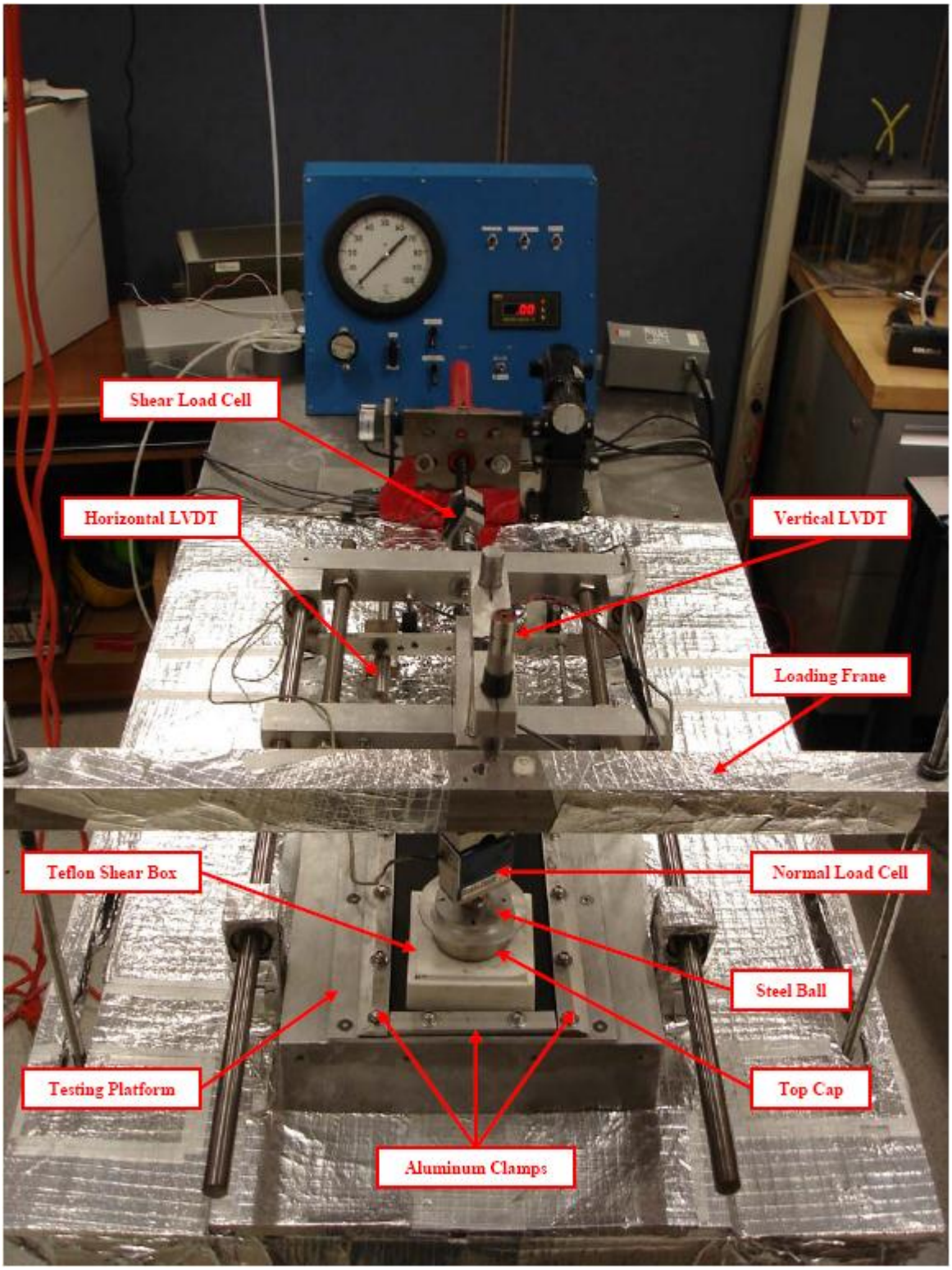

Figure 4.6 Picture of Entire Interface Shear Device Equipment on which Sand-Geosynthetic Module Mounted

The shear box is made from a Teflon block. A circular cross section cylindrical hole having dimensions of 62.5 mm in diameter and 37.5 mm in height to contain the sand specimen (Figure 4.7) is located at the center of the Teflon block. Teflon was originally selected by Dove (1996) for the shear box material because of its advantage of having a low friction coefficient so that the sand-geomembrane interface shear measurements are not affected and/or overestimated by the friction between the shear box and the upper surface of the geomembrane specimen which can result in obtaining incorrect and inaccurate interface shear results for sand-geomembrane tests. Additionally, plastic strips were placed under the edges of the Teflon shear box during sand specimen air pluviation and were removed prior to initiating the test to ensure that there was no contact in between the shear box and the geomembrane specimen.

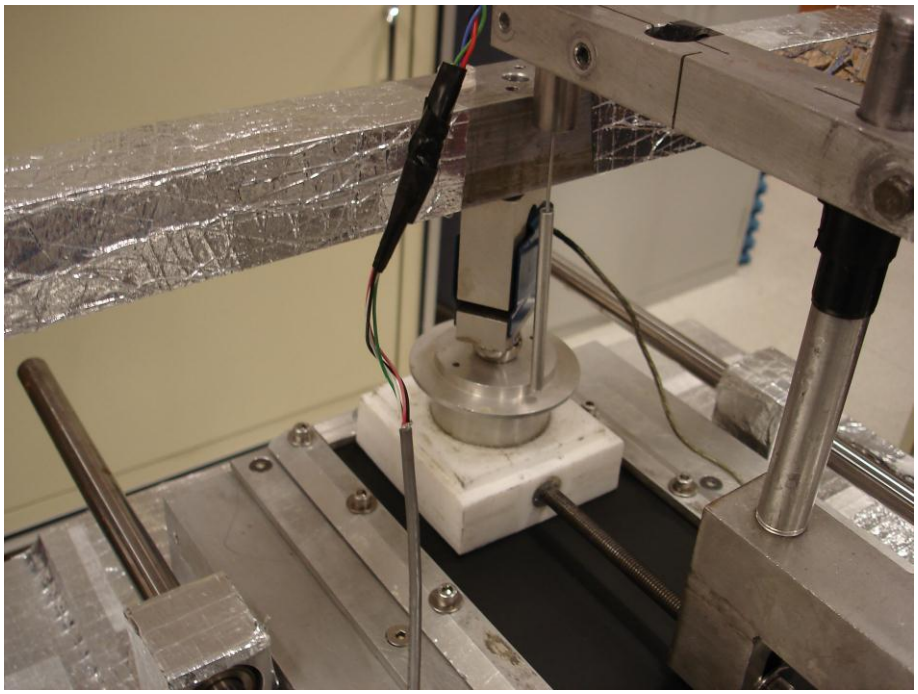

Figure 4.7 Close-up View of Sand-Geosynthetic Module

4.3.2. Instrumentation and Data Acquisition

A data acquisition system (Figure 4.8) (Agilent Module 34970A – Agilent Technology Company) was used to collect output signal readings of transducers (load cells and LVDTs) employed in the system to measure force and displacements during the tests. The data acquisition system consists of three different parts: i) Data Acquisition and Switch Unit, ii) High Speed Multiplexer Module (16 Channel), iii) Built in USB/GRIB and RS-232 Interfaces. This DAQ system provides performance measurements, universal inputs with built-in signal conditioning, and modular flexibility for different requirements and measurement purposes. It features 6½ digits (22 bits) of resolution, basic VDC accuracy of 0.004%, 50k reading nonvolatile memory with timestamp, and more importantly ultra-low reading noise. Scan rates are available up to 250 channels/sec to combine the aforementioned accuracies with high speed. A total of five channels (two for load cells, three for LVDTs) are used which means that it limits the maximum frequency of data gathering to 50 times per second from each of the five channels as the scanning rate overall capacity in the system is 250 channels per second. Agilent BenchLink Data Logger Software is used to collect sensor output data as well as to monitor and plot the real time data during test progress. Figure 4.9 shows the schematic diagram of wiring connections.

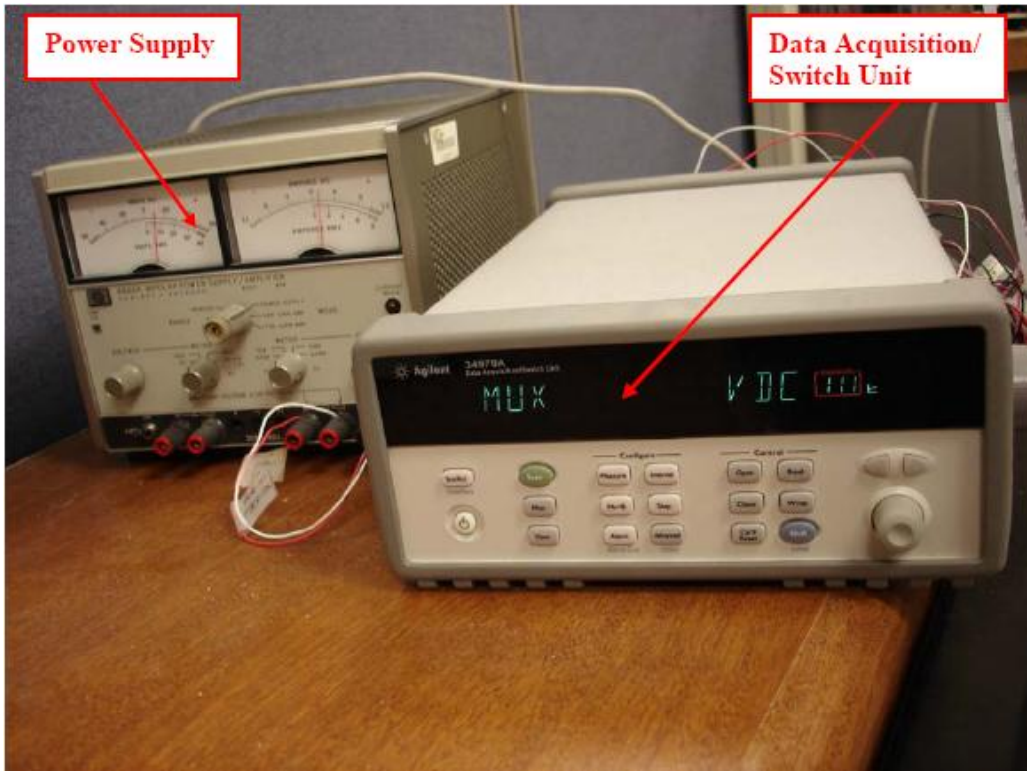

Figure 4.8 Picture of Data Acquisition System
(Left: Power Supply; Right: Data Acquisition/Switch Unit)

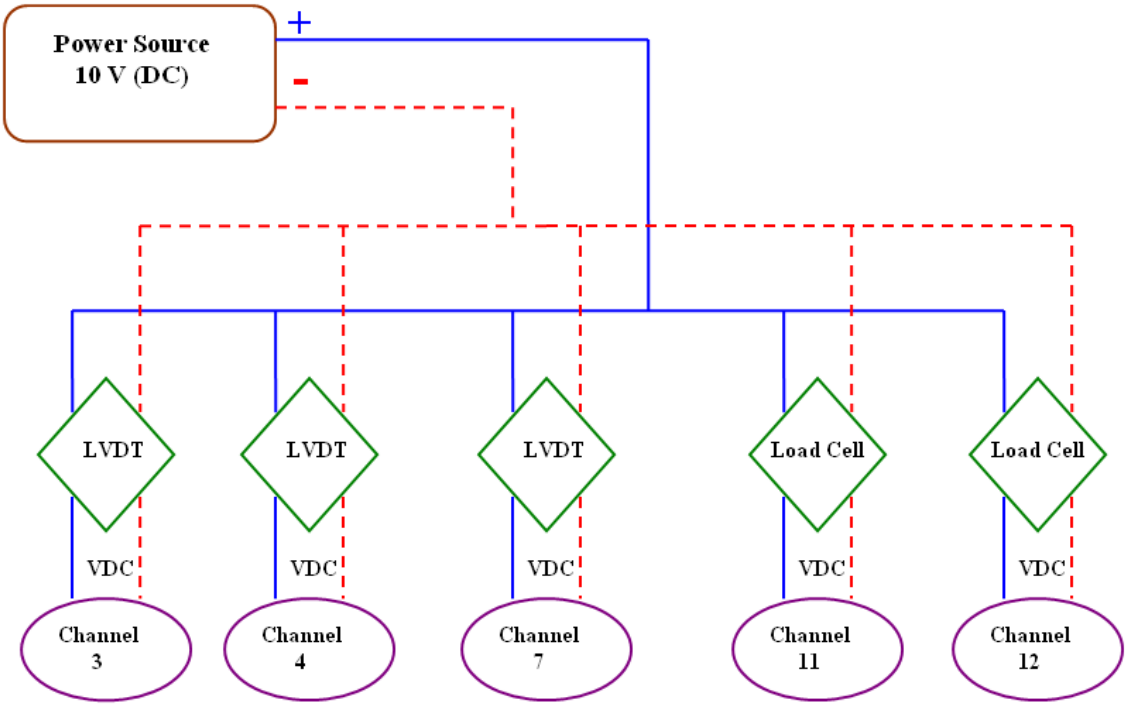

Figure 4.9 Schematic Diagram of DAQ System Wiring Configuration

4.4. Sample, Equipment Preparation and Test Procedure

4.4.1. Geotextile – Geomembrane Tests

The large displacement direct interface shear device enclosed by the TCC was utilized to measure the interface shear resistance between geotextiles and geomembranes at different temperatures (Figure 4.4). A geomembrane specimen 290 mm long and 200 mm wide was fastened by clamping using metal strips and bolts on a platform which travels along a set of linear bearings. The geotextile was folded around wedge-shaped blocks on the leading edge of the shear box and then, the geotextile specimen is secured by pressure fastening those wedges to a reaction wall using four screws. The remaining portion of the geotextile specimen was allowed to lay out freely on the upper surface of the geomembrane specimen to enable free strain of the geotextile during shearing against the geomembrane. Additionally, the upper frame suspending the geotextile was carefully lowered using four threaded bolts to assure that not only was it level but also that it was slightly (<2-3 mm) above the geomembrane surface to prevent contact of the shear box with the geomembrane. This also helped ensure that only the geotextile is in contact with the surface of the geomembrane for obtaining accurate and correct interface shear results for the geosynthetics tested. Use of this geosynthetic interface testing module enabled shear induced deformation and free straining of the geotextile against the geomembrane upper surface during shearing without the influence of gluing or screwing of the geotextile to a rigid element (Kim, 2006). After placing and conditioning the top and bottom specimens, the desired normal force was applied to the interface through a metal cross arm by applying air pressure to a bellofram piston located beneath the interface shear device. After test samples and the testing equipment had been prepared as

mentioned, the temperature controlled chamber was lifted down and placed on the stainless steel base table of the interface device to enclose the entire testing system. Later, the temperature of the testing environment was increased up to the target test temperature. In all cases, the test materials and the testing equipment were allowed to equilibrate at the testing temperature for 2 hours before the forces were applied and the shearing was initiated. In all tests, the specimens were sheared at a constant rate of displacement of 1 mm per minute over a displacement range of 60 mm. The lateral displacement of the shear apparatus was controlled by a ball screw jack driven by a DC motor. Load cells and LVDTs were employed to monitor loads and displacements in the normal and shear direction with test data acquired via a data acquisition unit. This device was used to permit large displacements and, hence, quasi-residual conditions to be achieved in the tests. Pseudo-residual shear strengths of the interface systems are defined as the shear strength measured at displacements sufficient to achieve an asymptotic approach of the shear stress to a constant value representative of the true residual strength (Stark et al., 1996). In the geotextile-geomembrane interface tests, pseudo-residual values were taken as the average (i.e. arithmetic mean) of the shear strength over 2 mm range of shearing at displacements from 57 to 59 mm.

4.4.2. Sand – Geomembrane Tests

The shear box consisting of a square Teflon block (Figure 4.6), with a circular specimen opening in the center was utilized for sand-geomembrane interface tests. The tests were performed using the same load frame enclosed in the temperature controlled chamber that was used for the geotextile-geomembrane interface module described earlier. A circular sand specimen having dimensions of 62.5 mm in diameter and 37.5

mm in height was prepared within the Teflon shear box connected to a platform which travels along a set of linear bearings to enable lateral shear displacement. This configuration of shearing device allows for the measurement of interface strength with shearing distance. Geomembrane specimens measuring 300 mm in length by 220 mm in width were fastened with metal strips and bolts to the testing platform as shown in Figure 4.6. The soil samples were prepared following the air pluviation method and using the apparatus developed by Frost (1989) (Figure 4.10). A target relative density of 80 (±2) percent was achieved for all specimens of each particulate material (i.e. rounded and angular) by varying the discs with a certain number and diameter of holes and controlling the fall height.

Figure 4.10 Picture of Air Pluviator used for Sand Specimen Preparation

After test samples and the testing equipment has been prepared as described, the temperature controlled chamber was lifted down and placed on the stainless steel table of the interface device to enclose the entire test system. The temperature of the testing environment was increased up to a target test temperature. In all cases, the test materials and the testing equipment were allowed to equilibrate at the test temperature for at least 2 hours before the stresses were applied and the shearing was initiated. In all tests, the specimens were sheared at a constant rate of displacement of 1 mm per minute over a displacement range of 60 mm.

4.5. Interface Shear Experimental Program

The contact behavior and interaction between various materials is an important issue in many engineering disciplines and understanding the shear mechanisms for interfaces is crucial to optimal designs. In geotechnical engineering, the interface shear resistance of geosynthetics has been measured using a variety of methods such as conventional direct shear and pullout resistance. Among all, the direct interface shear test method has been commonly preferred and used to measure the interface shear resistance between material combinations including planar surfaces (i.e. geomembranes), fibers (i.e. geotextiles), particulates (i.e. sands), and composite materials (i.e. FRP).

4.5.1. Direct Shear Tests and Counterface Material Combinations

In an effort to investigate temperature effects on the interface shear behavior of geosynthetic interfaces, a physical laboratory testing program consisting of direct

interface shear tests between (a) needle punched non-woven polypropylene geotextiles and either smooth polyvinylchloride (PVC), smooth, co-extruded or micro-spiked textured high density polyethylene (HDPE) geomembranes; and (b) sands (rounded, angular) and smooth PVC or HDPE geomembranes was conducted. A total of five series of interface shear tests involving over 140 configurations and including replicate tests as well as tests in which geomembrane specimens were cut in different orientations were performed. Figure 4.11 provides the details of the various test series conducted in this research study. In all tests, the specimens were sheared at a constant rate of displacement. All interface tests which consisted of an upper NPNW geotextile sheared against a lower geomembrane (smooth, textured); or upper sand specimen (rounded, angular) sheared against a lower geomembrane (smooth) were conducted on virgin material samples at test temperatures such as 21 °C, 26 °C, 30 °C, 35 °C, 40 °C and 50 °C and at different normal stress levels such as 10 kPa, 25 kPa, 100 kPa, and 400 kPa to incorporate the range of operational stresses typically encountered in geotechnical applications such as landfill covers, side slopes and liners. The very low normal stress level of 10 kPa which occurs in the initial placement of the geotextile on geomembrane in the field before overlying material layers are applied is selected to observe hook and loop interaction and initial interlocking of geotextile filaments within the interface of fabric-texture surfaces. The low normal stress level of 25 kPa corresponds to normal stresses between sands and geomembranes in applications such as landfill side slopes, landfill top cap and covers due to dead weight of overlying material either as cover soil to prevent freeze-thaw cycle or for vegetation for environmental protection. The higher stress level of 100 kPa was selected to imitate landfill liner conditions and geosynthetic material interfaces at base of

smaller landfills or larger ones during filling. The highest normal stress level of 400 kPa was used to check the linearity of stress-strain relationships under very high pressure at different temperatures and is reflective of conditions at or near the base of large landfills.

Series I was designed to investigate temperature effects on smooth geomembrane sheared against both NPNW geotextile and sands having different particle shape (i.e. rounded versus angular). Series II was intended to see the influence of elevated temperature conditions on a different material (PVC) other than HDPE. Series III and IV were modeled to observe the role of geomembrane surface roughness at elevated temperature conditions on interface shear strength change for which geomembrane roll samples were obtained from two major manufacturers producing textured geomembranes through a coextrusion process. Series V was conducted to compare the effect of texturing techniques of the geomembranes (i.e. coextrusion versus structuring) on interface strength at elevated temperature conditions.

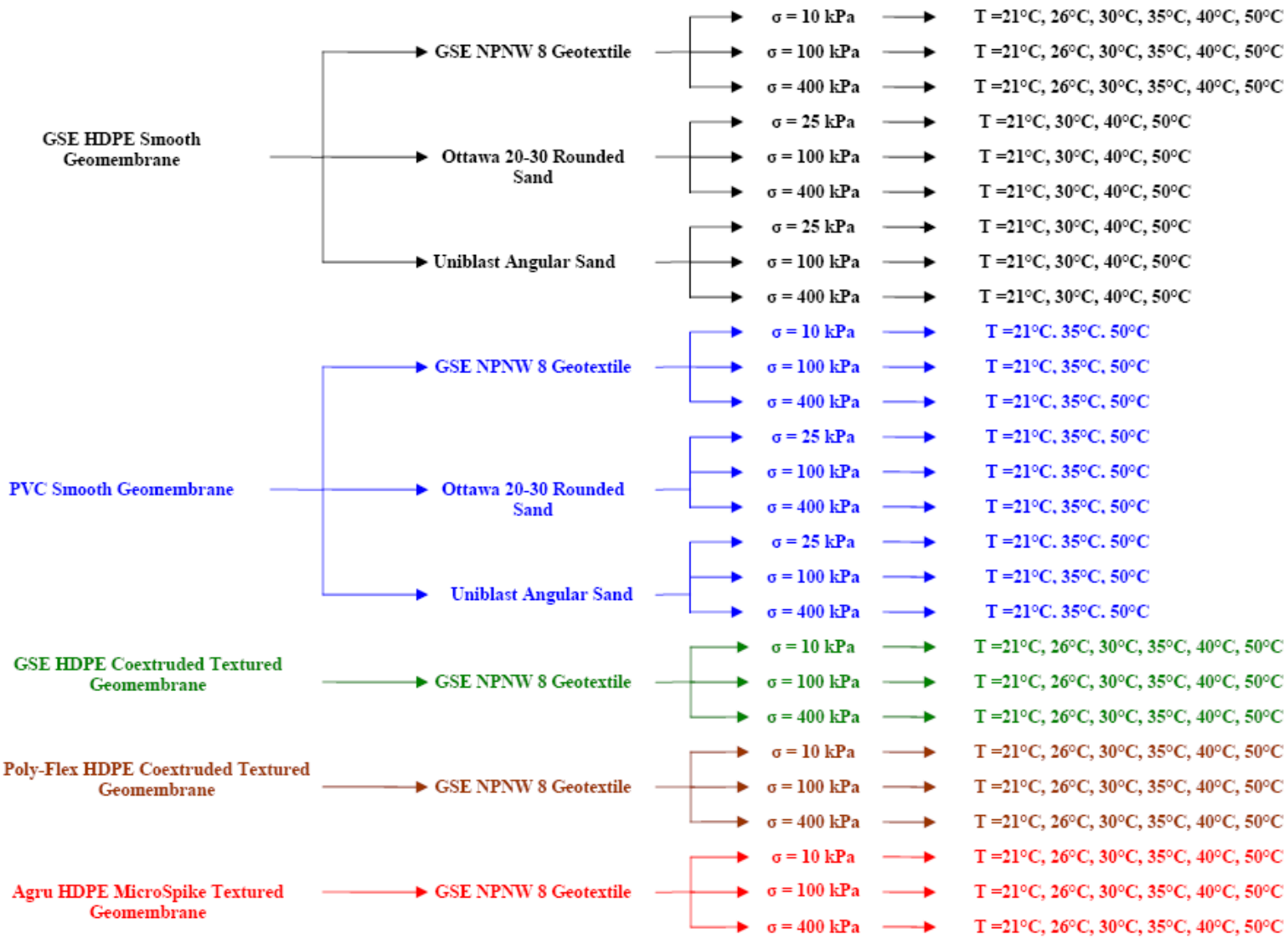

Figure 4.11 Interface Shear Laboratory Testing Program Summary

4.5.2. Geotextile and Geomembrane Specimen Orientation During Interface Testing

In general, geotextile and geomembrane specimens used in laboratory interface shear testing to determine appropriate values of interface friction to use in design are oriented such that the field anticipated direction of movement matches the test machine direction. For determining appropriate values for interfaces on slopes, this typically results in the machine direction from the geosynthetic manufacturing process being oriented in the test system shear direction while for interfaces that are on level surfaces and thus do not have a preferred orientation, this is less critical.

The present study was not focused on determining specific interface friction values for use in design and therefore material orientation was not as critical a factor. Instead, the emphasis was to determine relative changes in property values and behavior for various combinations of interface materials at different elevated temperatures. Similarly, for many geomembranes, the two surfaces are different and thus to avoid variations in measured interface strength, a consistent surface needs to be used in all tests. Given the availability of materials, the material orientations and surfaces utilized throughout the test program are summarized below.

– Geotextile Orientation: All interface shear tests were conducted with the geotextile oriented with the manufacturing machine direction in the interface shear device displacement direction.

– Geotextile Surface: All interface shear tests were conducted with the geotextile positioned with the bottom surface adjacent to the geomembrane surface. Note that no difference was observed between either geotextile surfaces.

– Geomembrane Orientation: All shear tests were performed with the geomembranes oriented with the manufacturing cross-machine direction in the interface shear device displacement direction.

– Geomembrane Surface: All shear tests for the various geomembranes were performed with the following surfaces adjacent to the geotextile or particulate material:

- EPI PVC – smooth surface
- GSE HDPE Smooth – top surface
- GSE HDPE Textured – top surface
- PolyFlex HDPE Textured – top surface
- Agru HDPE MicroSpike – top surface

To study the influence, if any, of selecting the cross-machine direction versus machine direction for the various tests involving geomembranes, a series of comparative tests were performed at room temperature under a normal stress of 100 kPa as follows:

- Test Series 1: GSE NPNW 8 Geotextile versus GSE HDPE Smooth Geomembrane (machine and cross-machine)
- Test Series 2: GSE NPNW 8 Geotextile versus GSE HDPE Textured Geomembrane (machine and cross-machine)
- Test Series 3: GSE NPNW 8 Geotextile versus Agru HDPE MicroSpike Textured Geomembrane (machine and cross-machine)

The results of the tests are listed and presented below in Table 4.4 and Figure 4.12, respectively. For the smooth and coextruded geomembranes, the mobilized peak and residual (i.e. post-peak) shear strength values are in good agreement. The resulting frictional resistances are similar with each other for the same interface material

combination regardless of the geomembrane specimen orientation during testing. The shear stress versus horizontal displacement failure curves of in-machine direction tests concur with those from cross-machine direction tests for the same interface system. The interface strengths for the structured geomembrane (peak and post-peak) are also similar for machine or cross-machine direction tests with the exception that the displacement to reach peak state is notably different (i.e. 9.5 mm and 14.5 mm for machine and cross-machine direction tests, respectively) due to unequal interval distance between two consecutive spikes in the machine and cross-machine directions. The separation distance between the spikes is greater in the cross-machine direction than that in the machine direction. The distance from peak of the spike to peak of the successive spike is ~8 mm and ~4 mm for cross-machine direction and for in-machine direction, respectively. It is noted that the difference between the displacements to peak is somewhat analogous to the variation existing on the structured geomembrane for the interspace gap between the spikes in the machine and cross-machine directions.

Table 4.4 The Mobilized Peak and Residual (i.e. Post-Peak) Interface Shear Strengths

	Peak Shear Stress (σ = 100 kPa) [kPa]	**Displacement to Peak [mm]**	**Residual Shear Stress (σ = 100 kPa) [kPa]**
GSE Smooth HDPE Geomembrane Versus GSE NPNW-8 PP Geotextile	22/22	1.5/1.5	16/16
GSE Textured HDPE Geomembrane Versus GSE NPNW-8 PP Geotextile	63/63	11/11	35/35
Agru Structured HDPE Geomembrane Versus GSE NPNW-8 PP Geotextile	76/74	9.5/14.5	44/44

Note: (x_1/x_2) = (Machine/CrossMachine) Direction

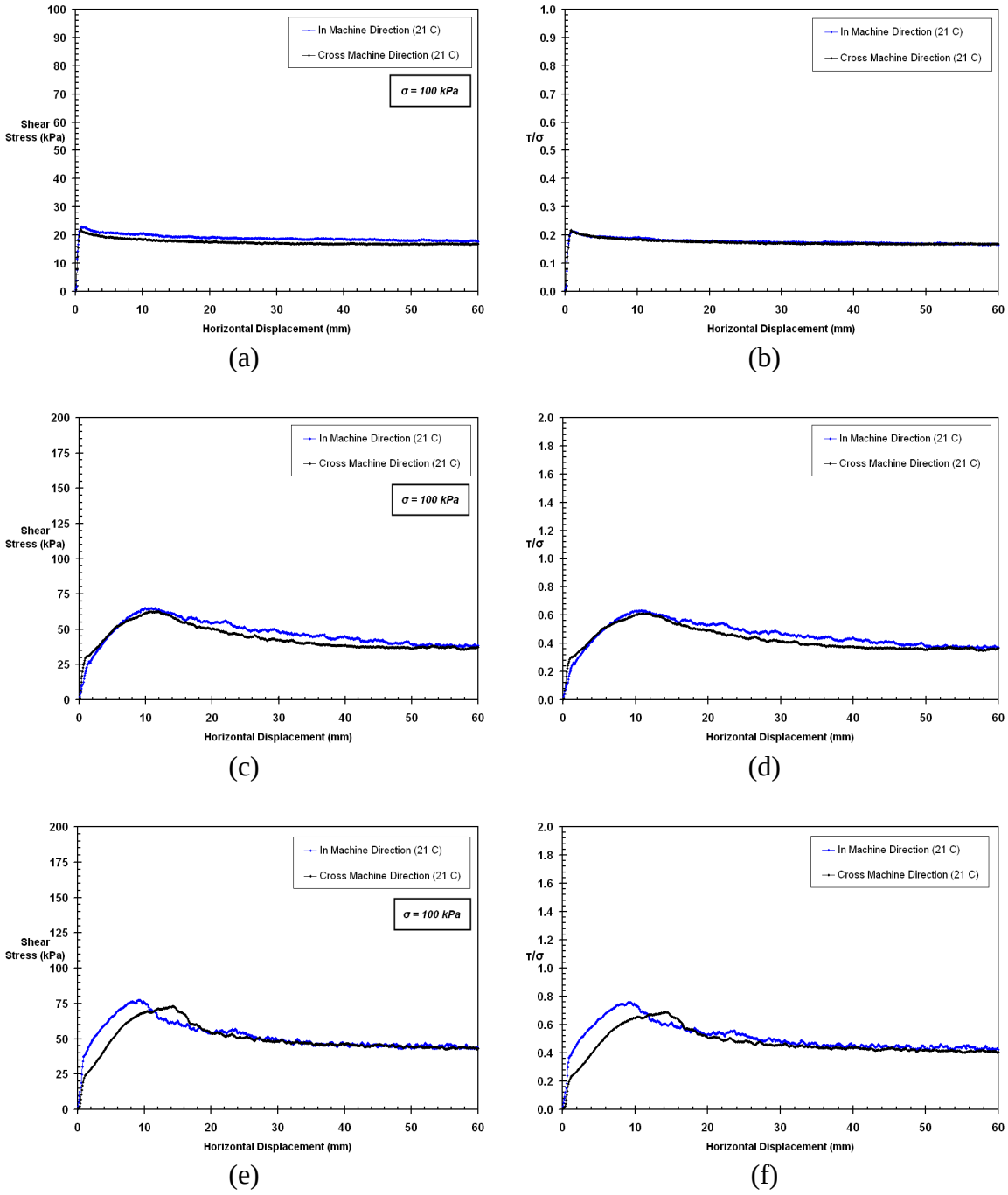

Figure 4.12 Shear Stress – Horizontal Displacement Failure Curves (Left Column); Normalized Shear Stress – Horizontal Displacement Curves (Right Column):
i) GSE Smooth HDPE Geomembrane vs. GSE NPNW-8 PP Geotextile **(a & b)**
ii) GSE Textured HDPE Geomembrane vs. GSE NPNW-8 PP Geotextile **(c & d)**
iii) Agru Structured HDPE Geomembrane vs. GSE NPNW-8 PP Geotextile **(e & f)**

4.5.3. Zero Load Shear Box Tests at Different Temperatures

To examine the friction between Teflon shear box and geomembrane (HDPE, PVC) at zero load as well as at the lowest and the highest test temperatures, the interface tests were performed at 21°C (room temperature) and at 50°C (the highest elevated test temperature). It was observed that a negligible friction occurs when Teflon shear box is sheared against HDPE or PVC geomembrane at zero normal load as well as at room temperature (21°C) and at the highest elevated test temperature level (50°C). The test results are presented below in Figure 4.13.

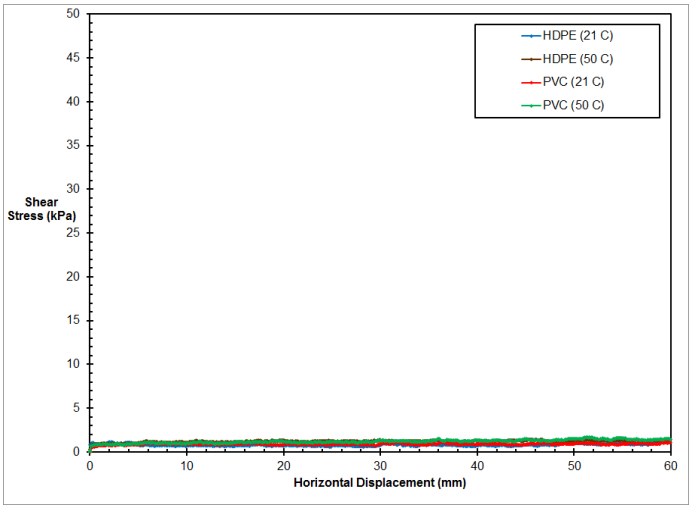

(a)

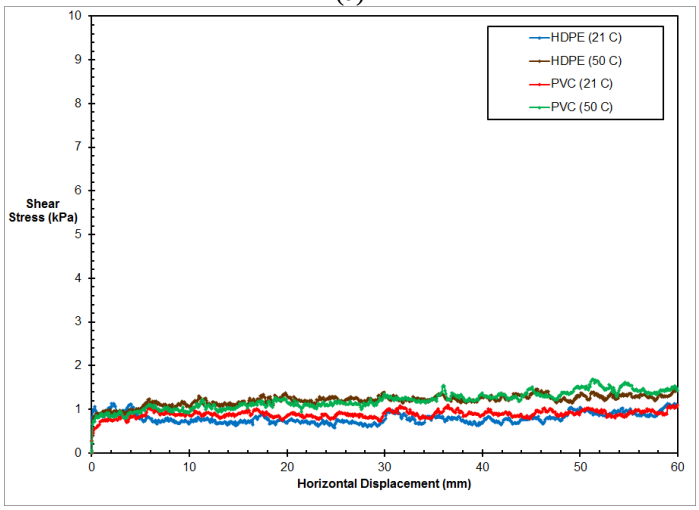

(b)

Figure 4.13 Zero Load Shear Box versus HDPE or PVC Geomembrane Interface Tests at Different Temperatures: (a) Normal Scale; (b) Enlarged Scale

4.6. Characterization of Tensile Properties of Geotextile Single Filaments

The residual interface strength is primarily attributed to the pulling out and tearing of the filaments from the geotextile and, consequently, is attributed to the characteristics of the geotextile such as filament entanglement, filament strength, and filament length/diameter and how it interacts with the geomembrane macro-topography (Hebeler et al., 2005). Therefore, tensile strength properties of geotextile filaments at elevated temperatures must be evaluated as well to further understand the influence of temperature on post-peak interface shear behavior and strength.

4.6.1. Experimental Device: Dynamic Thermo-Mechanical Analyzer

TA Instruments RSA III Dynamic Thermo-Mechanical Analyzer (Figure 4.14) was used to measure tensile strength properties of geotextile single filaments and provides a powerful platform for high performance, accurate, and consistent DMA measurements at different temperatures (Table 4.5). The RSA III uses an advanced direct drive linear motor to apply the strain and a force-rebalance transducer to measure force (Figure 4.15). Optimal sensitivity of measurements is provided by low friction air bearings. The RSA III is particularly well suited for high frequency, low stiffness measurements on fibers and filaments. The Gas Heating/Cooling Accessory (Figure 4.14) extends the operating range of the DMA from -150 °C up to 600 °C. Cold nitrogen gas is used for rapid heating/cooling capability of the system which is generated from controlled heating of liquid nitrogen.

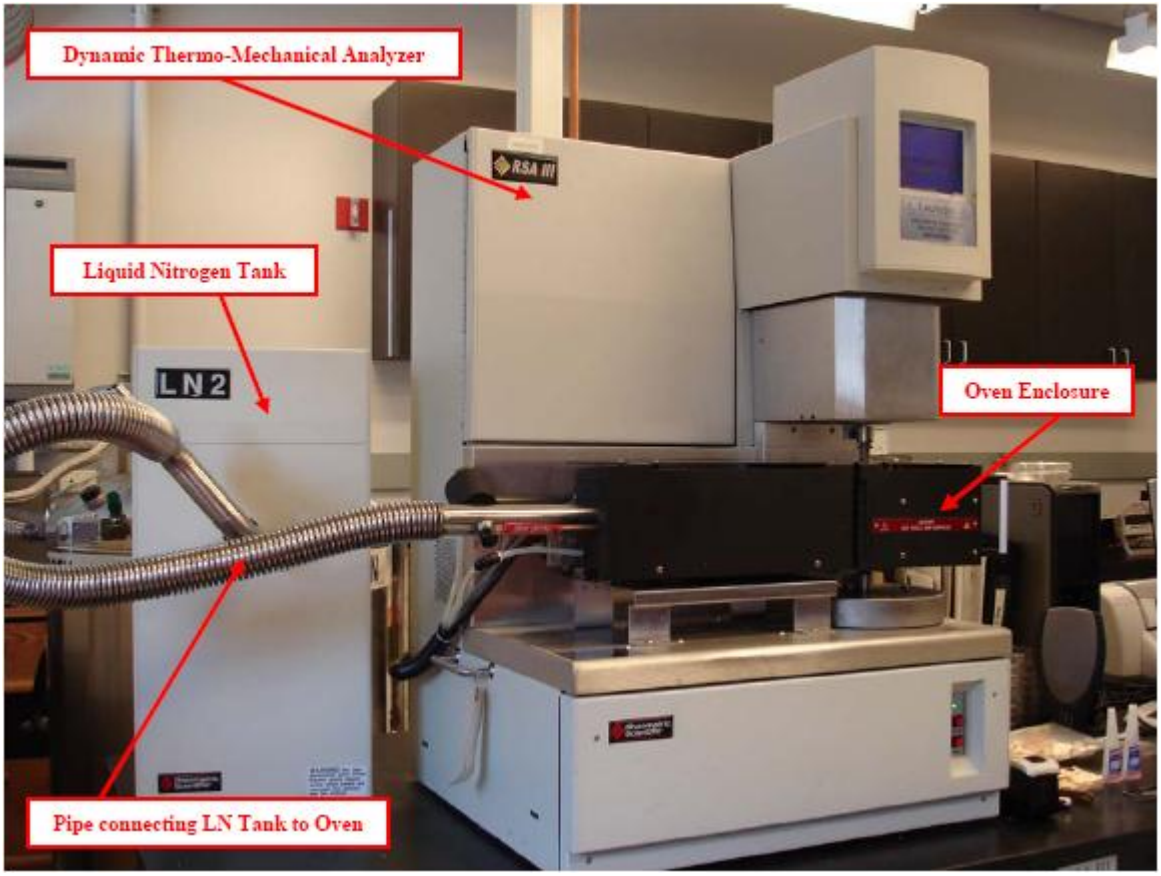

Figure 4.14 Picture of Dynamic Thermo-Mechanical Analyzer (Entire System)

Table 4.5 DMA Technical Specifications (Product Technical Specifications Manual)

Dynamic Thermo-Mechanical Analyzer RSA III Technical Specifications	
Maximum Force	*35 N*
Minimum Force	*0.001 N*
Force Resolution	*0.0001 N*
Strain Resolution	*1 nanometer*
Modulus Range	*10^{3} to 3x10^{12} Pa*
Modulus Precision	*± 1 %*
Tan δ Sensitivity	*0.0001*
Tan δ Resolution	*0.00001*
Frequency Range	*2x10^{5} to 80 Hz*
Dynamic Sample Deformation Range	*± 0.5 to 1500 μm*
Temperature Range	*-150 to 600 °C*
Heating Rate	*0.1 to 60 °C/min*
Cooling Rate	*0.1 to 60 °C/min*
Isothermal Stability	*± 0.1 °C*
Time/Temperature Superposition	*Yes*

Among several modes of operations (e.g. Multi-Frequency, Multi-Stress/Strain, Creep Stress/Relaxation, Isostrain) that the DMA RSA III provides, the Controlled Force/Strain Rate mode was used to measure tensile properties and to investigate the development of tensile force versus strain relationships of single geotextile filaments at different temperatures. In this mode of operation, stress or strain is ramped at a constant rate while the temperature is held constant (Figure 4.15). As a result, stress/strain plots are generated at several temperatures and Young's Modulus of each curve is obtained.

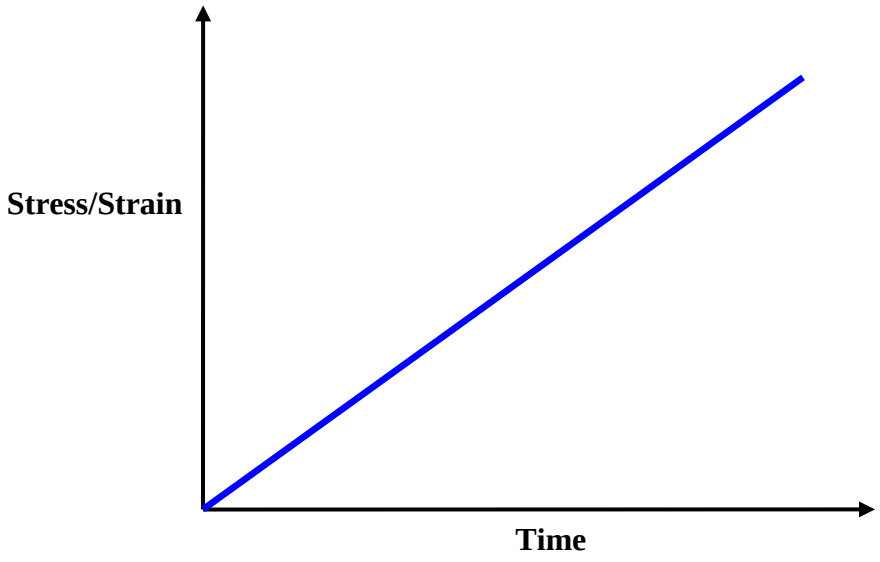

Figure 4.15 Controlled Force/Strain Rate Mode

4.6.2. Test Method, Sample Preparation and Experimental Procedures

Single geotextile filament specimens were tested to failure using a constant-rate-of extension (CRE) type tensile testing of a predetermined gage length and rate of extension at different temperatures. Using the force extension (elongation) curve (i.e. force-displacement, stress-strain), Tensile Strength, Young's Modulus (i.e. Modulus of Elasticity), Yield Point, Displacement Range of Yielding, Breaking Force, Elongation at Break and Elongation at Specified Force were determined.

Sample preparation and experimental procedures for measurements were conducted based on the procedures described in ASTM D 3822-07 providing specific test procedures and analysis methods for assessing shear – induced tension properties of single geotextile filaments. The distance between the clamps was adjusted to obtain the selected nominal gage length of 12.5 mm. This is one of the most common gage lengths used to measure tension properties of filaments. The tension smooth clamp fixture of the DMA RSA III (Figure 4.16a) with flat jaws for gripping the filament specimens are designed to minimize slippage in the clamps during the test. The sample is placed in tension between a fixed and moveable clamp. The clamps are suitable for both filaments and fibers. A paper tab is utilized with cementing techniques to centerline mount a single geotextile filament. An adhesive on a paper tab that has a slot at the center (Figure 4.16a) is used. The adhesive/cement (i.e. super glue) binds the paper tab to the filament without affecting the properties of the specimen (Figure 4.16b and 4.16c). The filament which is glued on the paper tab is gripped with a set of stationary jaws by removing slack without stretching the specimen and then, the axial alignment of the filament must be ensured by

carefully controlling the paper tab and the filament tension kit (Figure 4.16b and 4.16c). In other words, the specimen must be straight within the jaws so that the filament lies on the line of action between the force measuring device and the point where the fiber leaves the moving jaw face to prevent any misalignment that produces transverse motion of the clamps and jaws which will introduce errors in measurements of elongation and may contribute to premature filament failure. After moving the grips to ensure that the specimen is axially aligned straight, the paper tab is cut gently at the middle points of either side (Figure 4.16b and 4.16c). Before initiating the experiment to measure tensile properties and to investigate the development of tensile force versus elongation curve of single geotextile filaments at different temperatures, the oven is closed (Figure 4.16d) and the temperature is increased up to the target test temperature through the controller software of the system. The extension speed was set as a constant value of 0.125 mm/s to provide proper rate of elongation for the gage length (i.e. net measurement length of the filament) of 12.5 mm selected. Measurement data were collected every 0.15 seconds. After breaking the specimen, the tension clamp is returned to its original position (i.e. starting condition) and all remains of the failed specimen are removed from the clamp faces.

The area correction for the tested single geotextile specimens during the experiments are automatically performed by the controller software of the DMA based on the predefined and pre-test entered value of the Poisson's ratio for the tested material. For geotextile single filaments, the Poisson's ratio of 0.15 (Tisinger et al., 1990 and Koerner, 1998) was used in the tests. Figure 4.17 shows the details of geotextile single filament test specimen mounted in the DMA tension smooth clamp fixture.

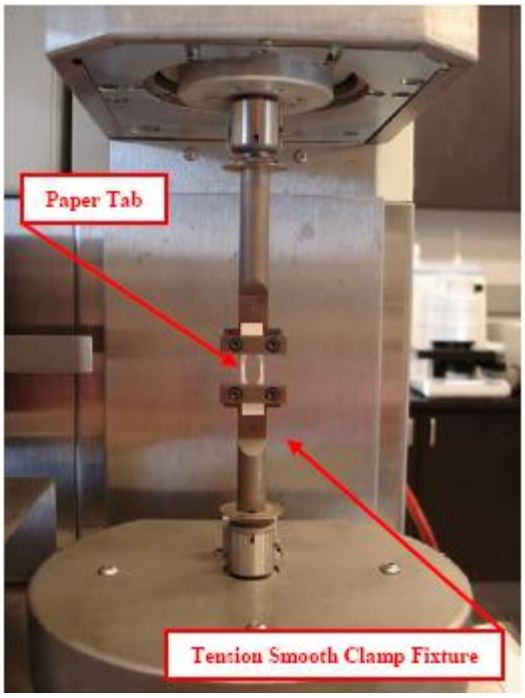

(a)

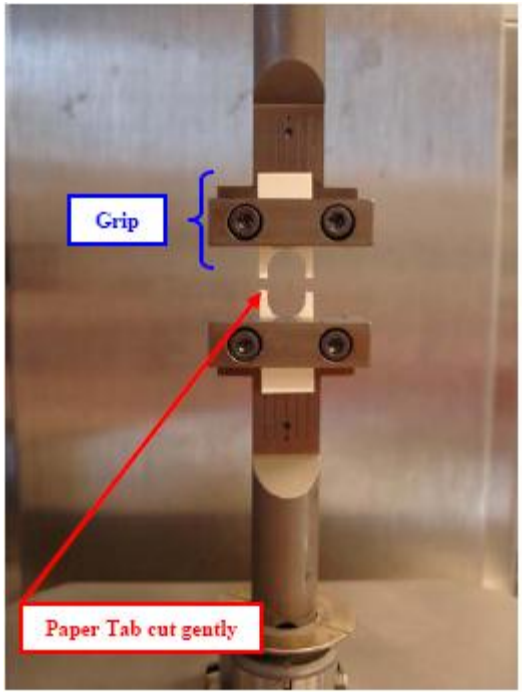

(b)

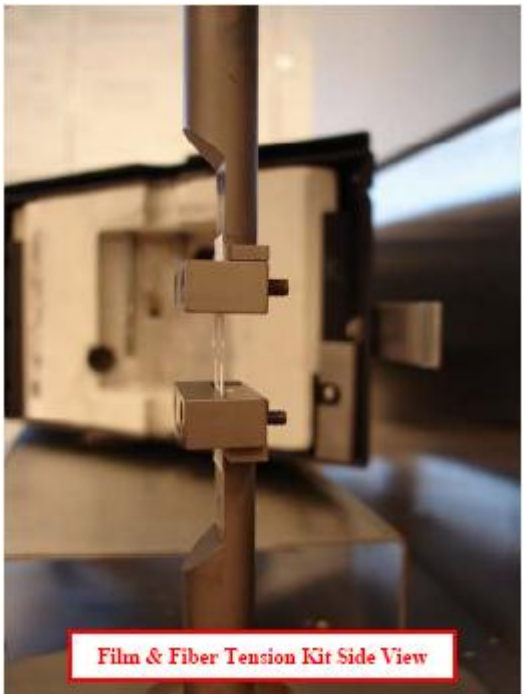

(c)

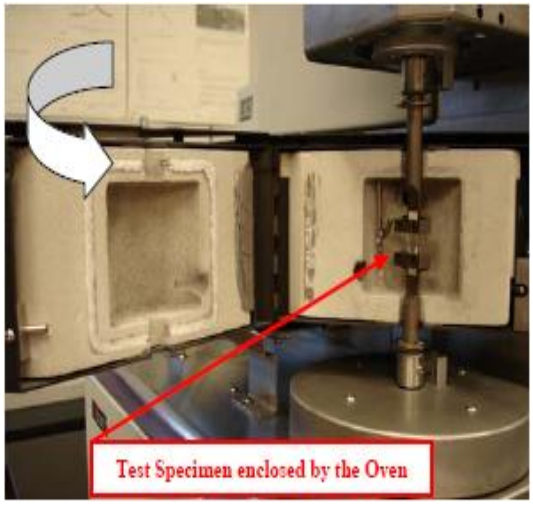

(d)

Figure 4.16 Geotextile Single Filament Test Specimen Preparation, Placement, & Conditioning

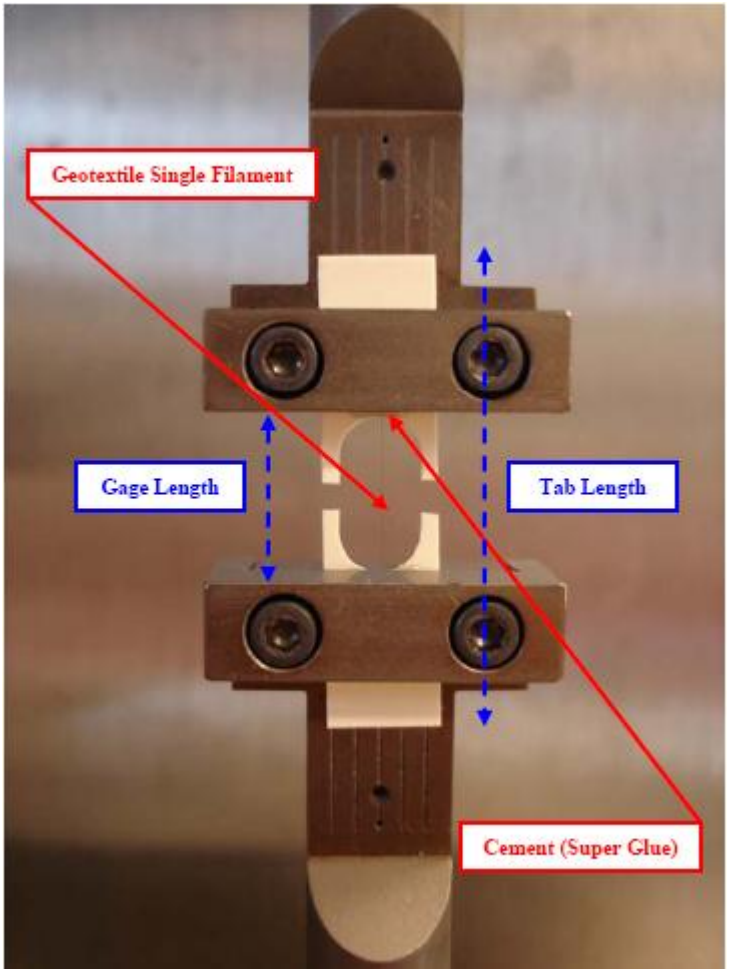

Figure 4.17 Details of Geotextile Single Filament Test Specimen on the DMA Tension Smooth Clamp Fixture (Close-up View)

4.7. Characterization of Surface Hardness of Geomembranes

The peak interface strength for geotextile-geomembrane as well as sand-geomembrane interfaces is mainly attributed to the geomembrane micro-texture and depends particularly on the geomembrane properties such as hardness and surface roughness. Measurements were performed to study the effect of temperature on surface hardness and interface friction of smooth high density polyethylene (HDPE) as well as smooth polyvinylchloride (PVC) geomembranes. Shore hardness measurement is a very

common method used to determine surface hardness of rubber and plastic materials (i.e. polymeric materials such as geomembranes). Two types of Shore Hardness Scale are used for rubber and plastics (i.e. Shore A and Shore D scales). The Shore A scale is preferred for relatively softer plastics whereas Shore D is used for relatively harder plastics and is an appropriate way of measuring surface hardness of geosynthetics (i.e. Smooth HDPE and Smooth PVC Geomembranes). Shore D Hardness (H_D) provides an index of the material surface hardness which can then be correlated to the interface friction characteristics of geosynthetic materials.

4.7.1. Test Equipment: Durometer with Constant Loader

A durometer is used to measure surface hardness of rubber and plastic materials. By pressing the indentor of the durometer into a surface, the material resistance force and the indentor spring force balance. The depth of the indentor is measured and provided a measure of the hardness of the material on a scale of 100 points. For example, when the indentor doesn't move into the body of the durometer, the measurement is zero. On the other hand, when the indentor moves all the way into the body of the durometer, the measurement is 100. Consequently, the results of the measurements change depending on the depth in which the indentor moves into the body of the durometer.

A durometer with a constant loader test stand composed of a flexible joint system and an air damper was utilized in this study to perform surface hardness measurements of geomembrane samples (Figure 4.18). This type of constant load stand maximizes repeatability of hardness tests by providing a variable speed control and a flexible joint on the load shaft to ensure complete contact with the sample material as well as to ensure

consistent measurements by applying a consistent force throughout all the measurements. Operational setup of the system and the procedure to be utilized is as follows. The test stand is placed on a flat surface. While holding the head, the height adjustment knob is loosened to move the head all the way up the support shaft and then, the knob is retightened. Later, the flexible joint is screwed onto the load shaft. After removing the cap of the durometer, it is screwed on the mounting adapter. Then, the durometer and the mounting adapter are installed to the flexible joint by turning the knurled section of the flexible joint so that the dial indicator of the durometer faces forward. Lastly, the weight is placed on top of the load shaft (Figure 4.18).

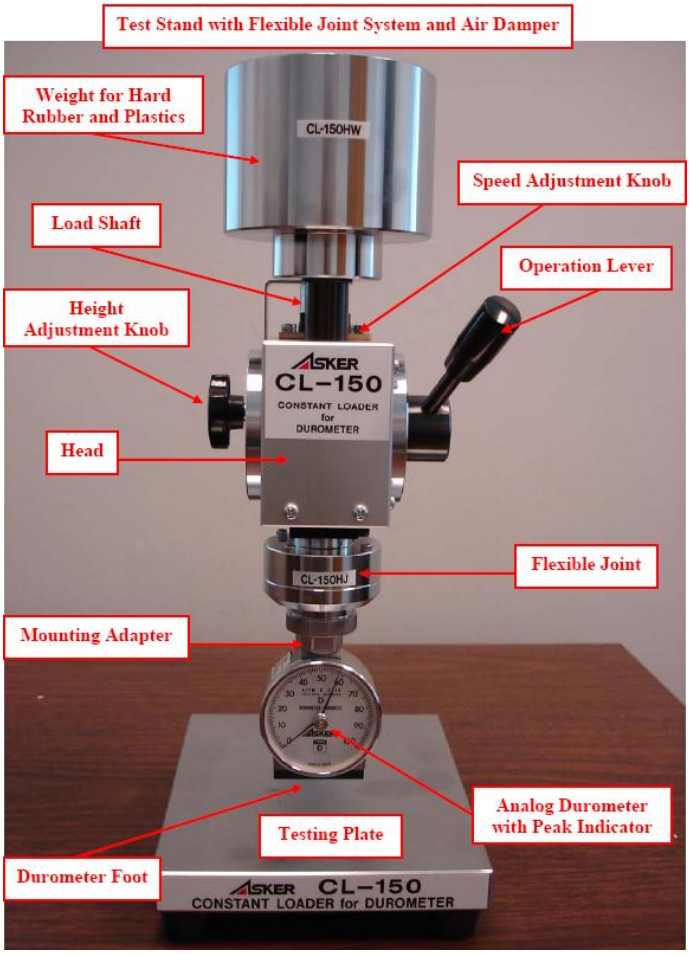

Figure 4.18 Durometer with Constant Loader Test Setup

To improve measurement accuracy with the durometer method, the material surface to be tested must be flat, clean and smooth. The maximum allowable surface roughness of the material for this method to be used to determine its hardness is ± 0.0254 mm. The size of the test piece must be at least 20 mm by 45 mm. It is recommended that each measurement should be performed at several different locations on the test specimen.

4.7.2. Test Procedure and Measurement

Shore D Hardness measurements were performed according to ASTM D 2240-05 (2005) at different temperatures to obtain an index value. To investigate the variation of this index value with changing temperature for smooth HDPE as well as smooth PVC geomembranes, the Durometer with the Constant Loader Test Stand were placed in the vertical configuration (Figure 4.19) of the Temperature Controlled Chamber (TCC). As previously noted, the TCC has precise temperature control from 21°C to 65°C. The digital temperature (PID) controller keeps the test temperature within 1 °C of the targeted temperature. The temperature controlled chamber has a size of 1100 mm in length, 760 mm in width and 510 mm in height. Temperatures above ambient conditions were obtained using heat bulbs as a radiant energy heat source mounted on the walls in the chamber as previously noted. Fans which have square dimensions of 120 mm by 120 mm and depth of 25 mm and made of steel blade, aluminum frame were selected to be utilized for circulating heated air within the chamber for uniform distribution of temperature inside the TCC. Fans are attached to aluminum handles and located at proximity of the center of the chamber. This temperature controlled system utilized for

geomembrane surface hardness measurements at different test temperatures was modified from the original temperature controlled chamber (TCC) (i.e. horizontal placement configuration) that had been used in the laboratory experimental program for geosynthetic-geosynthetic as well as sand-geosynthetic interface shear measurements at elevated temperatures enclosing the large displacement direct shear apparatus test system. To perform surface hardness measurements on smooth geomembrane samples at different temperatures by completely insulating the TCC environment from ambient conditions as well as to operate the durometer without temperature changing in the chamber, a lexan panel (length: 43.25 inches; width: 30 inches; depth: 0.5 inches) was constructed and assembled on the open bottom face of the original TCC and mounted using four-separate 24 inches (610 mm) long steel bar clamps. Additionally, an 8 inches (203 mm) round hole was cut in the lexan panel at a distance of 5.5 inches (140 mm) from bottom edge of the TCC vertical placement configuration as well as 11 inches equally distant to the right and left sides of the lexan box. A round PVC port (Renco Corporation) was affixed to this hole to accommodate an antistatic 32 inches (813 mm) long neoprene glove (i.e. hand) and sleeve (length:32 inches; thickness:15 mil = 0.6 mm) using silicone O-rings (8 inches = 203 mm). This configuration enabled instant access to the inside environment of the chamber at elevated test temperatures as well as allowed performing the durometer measurements at the target constant test temperature.

Hardness tests were performed at temperatures ranging from 21°C to 50°C. Smooth high density polyethylene (HDPE) geomembrane as well as smooth polyvinylchloride (PVC) geomembrane was tested in this study.

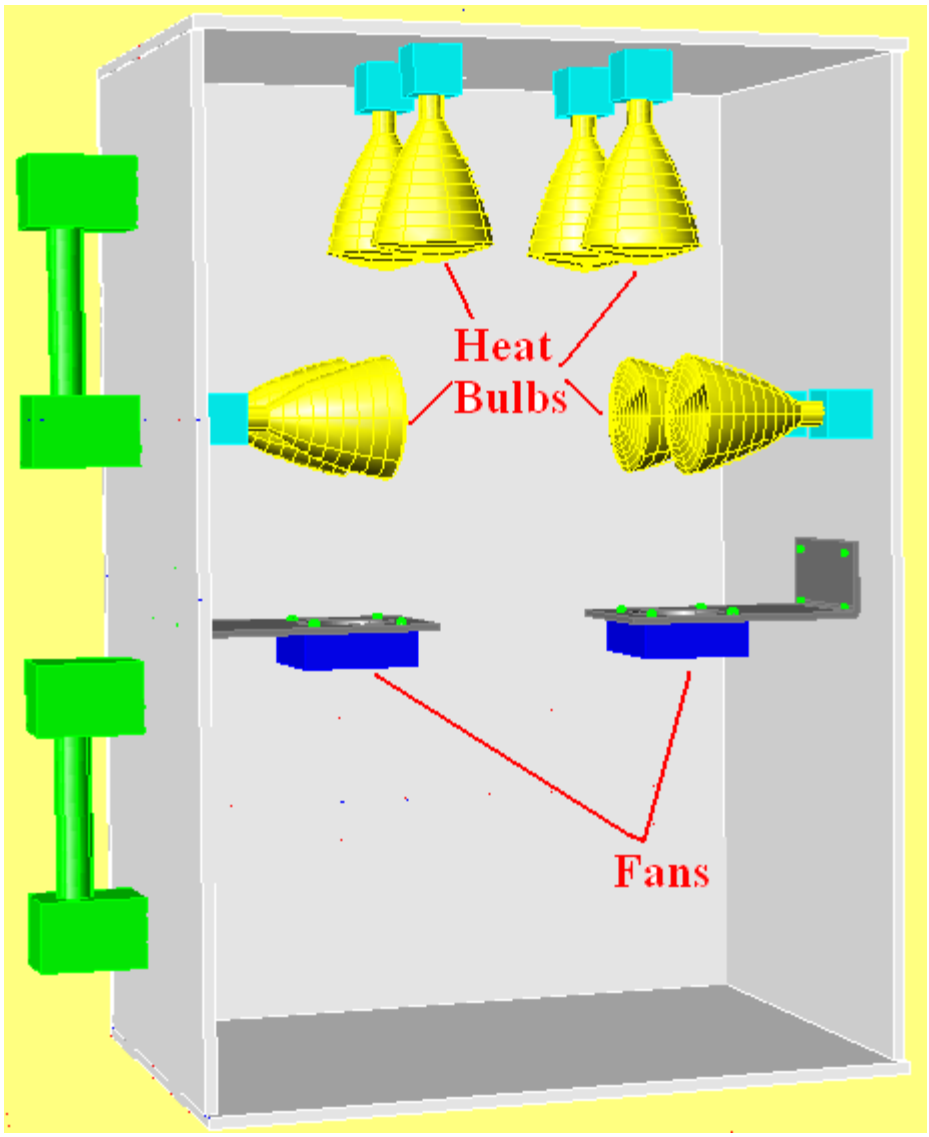

Figure 4.19 Solid Model Sketch of Temperature Controlled Chamber (TCC)
(Vertical Placement Configuration)

The geomembrane samples tested were neither corrugated nor textured and had smooth surfaces. Both HDPE and PVC geomembrane specimens were composed of plied pieces to obtain the minimum thickness of 3 mm as required by ASTM D 2240-05. The materials to be tested were placed in the temperature controlled chamber (TCC) and kept for 24-hours at each test temperature before the hardness measurements were taken. This was to ensure that the materials have uniform and stabilized temperatures at the time of

measurement. A surface-mount, fast-response (<0.15 sec.), self adhesive thermocouple (Type T; SA1XL-T; Omega Engineering Inc.) is attached on geomembrane material surface tested to be able to measure the exact temperature on geomembrane specimen. Hardness measurements were taken at various locations of each specimen to reduce error by allowing averaging and to investigate the homogeneity of readings throughout the sample in the following way (Figure 4.18). The operation lever of the constant load stand is moved to the rear (high) to bring the durometer to the up position. A piece of solid material approximately 1/4"-1/2" thick as a gauge is used and placed on top of the test material so that the foot of the durometer as well as the indentor of the durometer won't make contact with the test material surface. While holding the head, the height adjustment knob is loosened and lowered until the foot of the durometer makes contact with the gauge material on top of the test material, and then, the knob is retightened. It is necessary to make sure that the peak hold indicator is set to zero. Finally, the operation lever is forwarded slightly to initiate the downward movement of the load shaft. After the durometer foot has contacted the test material surface, the test result is read from the peak hold indicator. Before taking another reading, the peak hold indicator is reset to zero and the process mentioned above is repeated to obtain another measurement. According to the equipment specifications, the best test speeds are between 5 and 8 arranged on the speed adjustment knob (Figure 4.18). In order to maintain consistency in measurements and to obtain accurate test results, it is required to perform all the hardness measurements with the same speed for all the materials tested. A total of 240 measurements were taken on smooth HDPE and on smooth PVC geomembrane samples, with 30 readings at each test temperature. It is a recommended and good practice to take several readings and average

the results. Similar procedure was followed for both smooth HDPE and smooth PVC geomembrane samples. The measurements indicated that the scatter in measurements was uniform through all the samples tested. Figure 4.20 shows the modified TCC test system (i.e. vertical configuration) utilized for geomembrane surface hardness measurements using the durometer that is enclosed and completely insulated from laboratory ambient conditions.

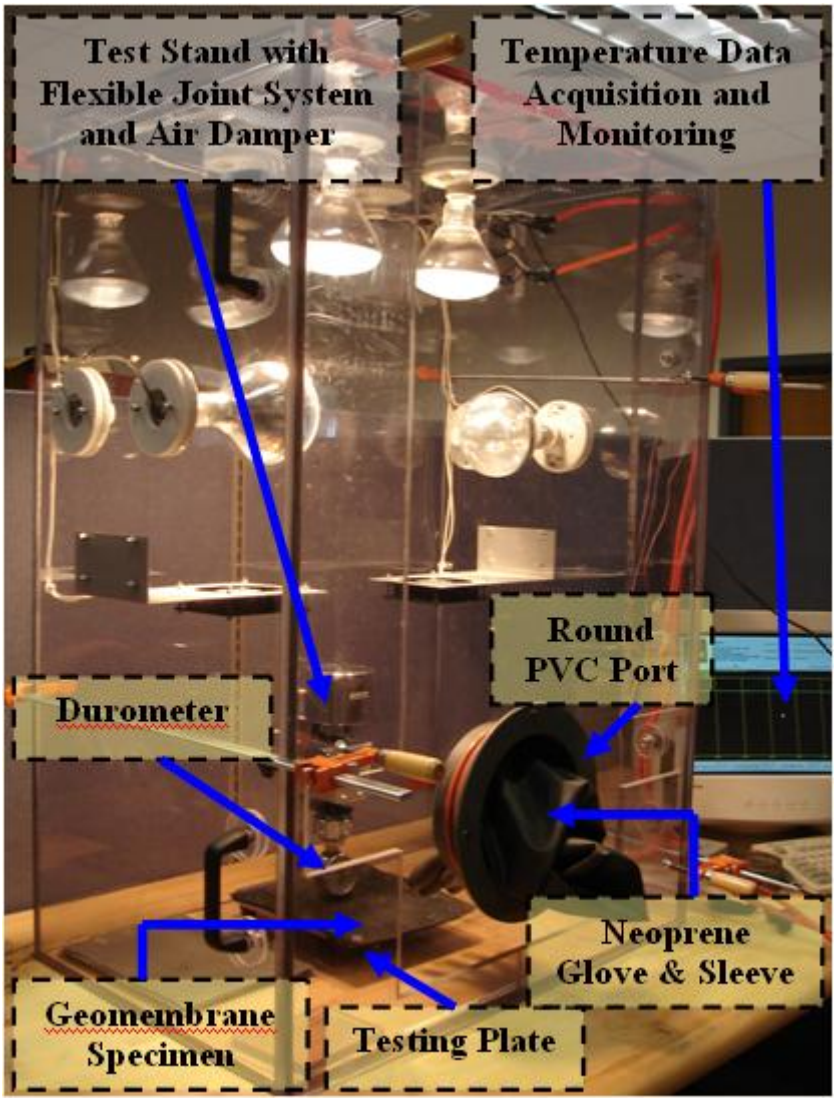

Figure 4.20 Durometer with Constant Loader Test Setup enclosed by the TCC (Vertical Placement Configuration)

4.8. Characterization of Surface Roughness

Pre-test as well as post-test surface roughness of geomembrane samples was measured to evaluate the magnitude of plowing and to quantify the wear induced on the geomembrane surface due to shearing with different particulate materials at different temperatures. The geomembrane surface experiences abrasive wear due to plowing of the sand particles (Williams, 1996). Abrasive wear on a geomembrane is quantified by Williams (1996) as the volume of material displaced as a result of the plowing action of the particles. Although the profilometer does not allow for the quantification of volume, it allows for a measure of surface damage and the magnitude of plowing of sand particles into the geomembrane surface to be made as a function of the hardness decrease of the geomembrane at elevated temperatures. The extent of surface damage is directly reflective of the amount of wear and plowing on the geomembrane surface. Consequently, the surface roughness profiles of post-test geomembrane samples at different temperatures illustrated in this study are a good indicator of plowing amount induced on the smooth geomembrane surface as a result of shearing with particulate materials.

4.8.1. Testing Apparatus and Instruments: Stylus Profilometer

The surface topographies of geomembrane samples were evaluated using a Taylor-Hobson Form Talysurf Series 2 (50 mm traverse unit) stylus profilometer. The profilometer is located on an isolation table to minimize the effect of disturbance and vibrations which might impact the results as the measurements are performed at micro-

level. A computer is connected to the profilometer for data acquisition purposes and to control test progress (Figure 4.21).

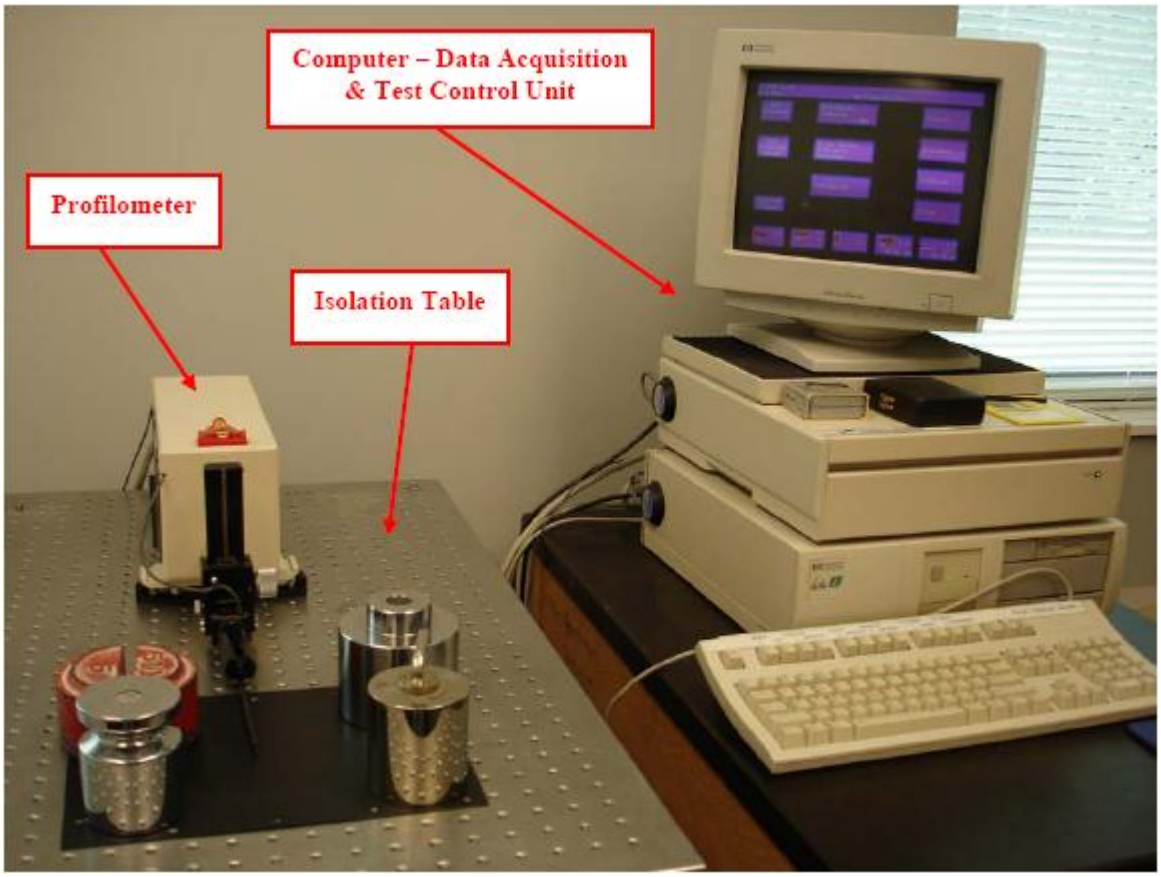

Figure 4.21 Picture of Stylus Profilometer (Entire System)

4.8.2. Measurement Procedure and Data Reduction

The profilometer measurements were performed perpendicular to the direction of shearing to record the amount of plowing occurring at different temperatures for different interface combinations including rounded sand versus smooth HDPE and smooth PVC geomembrane as well as angular sand versus smooth HDPE and smooth PVC geomembrane. The waviness component of the geomembranes was removed by placing weights on either side of the measurement line to ensure a flat geomembrane surface

(Figure 4.22). The gauge range for the relief was set at 2.5 mm and the data were acquired with a resolution of 32 nm in the vertical direction. In addition, the waviness component in the surface parameter calculations was minimized by applying a Gaussian roughness filter to the obtained profile. A 2.5 mm high pass cutoff, 8 mm low pass cutoff were used to remove the waviness component of surface profile of the geomembrane samples. In other words, this filter resulted in wavelengths greater than 2.5 mm and less than 8 mm being omitted from the surface profile.

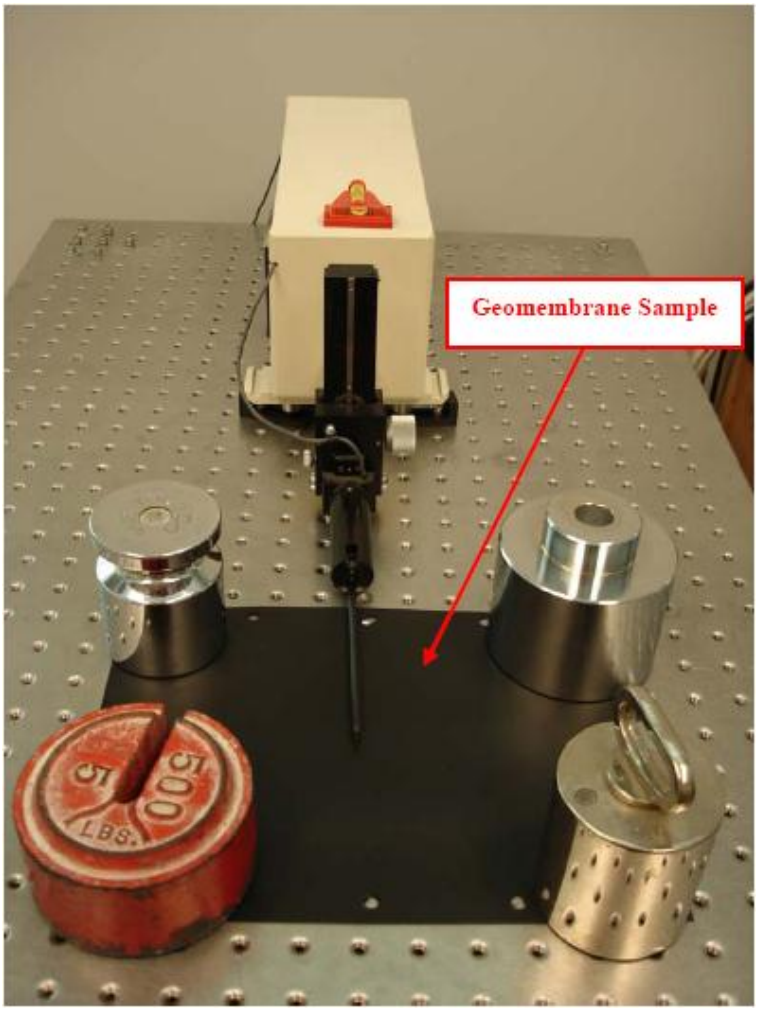

Figure 4.22 Close-up Test Setup

The horizontal movement of the stylus tip during profile relief measurements was at a speed of 0.5 mm/sec. The radius of this diamond stylus tip is 2 μm (Figure 4.23). Profile measurements were conducted across the midpoint of the shearing path between the initial and final specimen location. Since the midpoint experiences the full extent of shearing as the shear box traverses the geomembrane surface. The greatest degree of surficial damage and sand particle plowing into the geomembrane sample occurs at this location (Zettler et al., 2000).

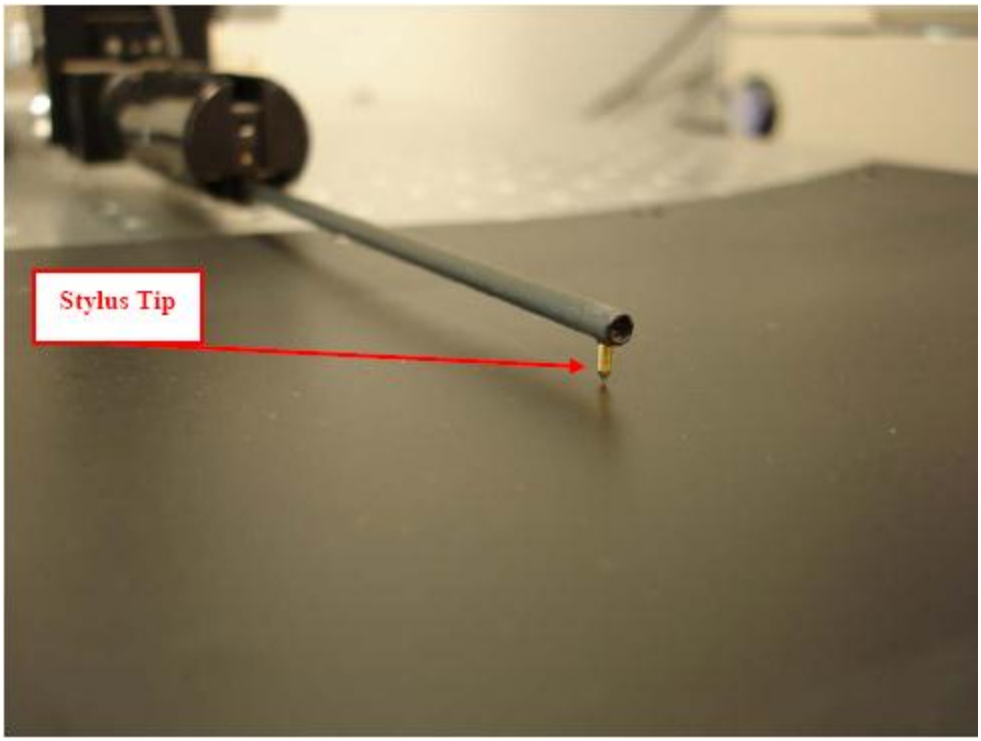

Figure 4.23 Diamond Stylus Tip on Geomembrane Surface

4.9. Summary

In this chapter, the details of the entire experimental program, including the tested materials and their properties, the advanced methods of sample and equipment preparation, the various test procedures followed, the instrumentation and data acquisition process as well as the advanced techniques used for characterization of tensile properties of geotextile single filaments, characterization of surface hardness of geomembranes and characterization of surface roughness of geomembranes were described. An interface shear device which allows the geotextile to strain during shearing against solid counterfaces was utilized and enclosed by the temperature controlled chamber to allow tests to be performed under elevated temperature conditions. Single filament tensile tests, geomembrane surface hardness measurements as well as geomembrane surface roughness measurements were described. These provide insight into the measured shear responses and the influence of temperature on the resultant interface shear behavior. The results and analysis of the entire experimental program will be discussed in Chapters 5 through 9.

CHAPTER V

5. TENSILE PROPERTIES OF GEOTEXTILE SINGLE FILAMENTS AT ELEVATED TEMPERATURES

5.1. Introduction

The tensile strength properties of geo-materials made from polymers is an important issue in geotechnical engineering design. For example, geosynthetics originally produced from several different varieties of polymer resins are widely used under load conditions in landfills, retaining walls, slopes, foundations and road subgrades in which they are subjected to tensile stresses throughout their service life (Koerner, 1998). Many design methods utilize long-term strength or a modulus value that incorporates a reduction factor to ensure the integrity of the structure and to limit deformation. Typically, the long-term strength values refer to a service life from 50 to 100 years depending on the type of the engineering structure. Thus, the influence of temperature variations on the tensile strength properties of geosynthetics such as geotextiles is especially crucial for long-term engineering design. The endurance properties of the geotextiles (i.e. mechanical and durability considerations for the material) must properly be evaluated at the "macro-scale" as well as at the "micro-scale" so that the appropriate factor of safety (FS) can be incorporated into the long-term design of structural systems as originally emphasized by Nielsen (1974). Additionally, there is an important aspect of fibrous materials (e.g. geotextiles) which must always be considered when fabrics are tested in tension mode. The geotextiles can exhibit different tensile stress-strain behavior

as well as show favorable versus adverse response to varied test conditions such as temperature and strain rate variations when tested at the "macro-scale" level versus when tested at the "micro-scale" level. This is due to the heterogeneous internal structural formation of the fibrous materials (geotextiles) such that the total deformation under extension or contraction loading is the cumulative result of filament/fiber deformation and internal structural rearrangement of the geotextile for which the initial elasto-plastic type deformation is strongly temperature and strain rate dependent, while the long-term rearrangement type deformation is not (Andrawes et al, 1984). Therefore, it is possible to observe a contradictory response of the geotextile when tested at the "micro-scale" level as opposed to the response inferred from tests at the "macro-scale" level resulting from the geotextiles having different "micro-structure" and "macro-structure" properties.

The needle-punched nonwoven (NPNW) type geotextile selected to be used throughout this study is the most widely preferred geotextile because of its enhanced engineering properties generated through the fiber-fiber bonding process and the resulting spatial arrangement of filaments to fulfill the requirements for frictional resistance, tensile property, permeability and filtration. NPNW geotextiles consist of spatially curved filaments that are often assumed to be randomly oriented and isotropically distributed. The influence of temperature on the observed tensile behavior and the observed tensile strength properties of the geotextile single filaments at a "micro-scale" level will be discussed in this chapter.

5.2. The Roles of Fabrics in Composite Layered Systems (Macro-Scale Mechanical Aspects and Endurance Properties)

The roles of fabrics (i.e. geotextiles) in composite lining systems were originally described by Martin et al. (1984) such that geotextiles and geomembranes in geotechnical field applications are generally installed adjacent to each other as a composite system due to their complementary properties and functions (Martin et al., 1984; Giroud, 1986):

i. Geotextiles protect geomembranes from ozone and ultraviolet attack before being covered with soil (e.g. landfill caps).
ii. Geotextiles cover geomembranes on slopes to improve the lining system performance.
iii. Geotextiles protect geomembranes from puncture and tear caused by angular materials.
iv. Geotextiles reduce tensile stresses transmitted to geomembranes from overburden materials through load spreading (e.g. landfill side slopes).
v. Geotextiles minimize the local burst failures of geomembranes brought by cavities, cracks, and local subsidence of ground beneath the geomembrane layer (e.g. landfill liner).
vi. Geotextiles act as lateral transmitters of water and gas, preventing excess tension in the geomembranes due to inefficient drainage.

5.2.1. Compressibility of Fabrics and Resulting Tension

The compressibility of a fabric is defined in Koerner (1998) as its thickness at varying applied normal stresses. The compressibility of a fibrous material indicates its resistance to the imposed external tensile loads and can be a measure of mobilized tensile stresses in the geotextile due to applied loads and/or installation conditions. In terms of Poisson's ratio (υ), $\left[\upsilon = -\frac{\varepsilon_{\perp}}{\varepsilon_{\parallel}}\right]$; (the negative sign reflects the fact that one strain is compressive while the other one is tensile (Santamarina et al., 2001)), the tensile strains (i.e. planar elongation) are perpendicular to the direction of loading and are related to the normal strains (i.e. compressibility) developed in the direction of loading. Therefore, larger compressibility will result in larger tensile elongation in the fabric and this must be properly evaluated as far as the design is concerned as most geotextile applications rely on its tensile property and the extra tension developing in the geotextile due to compression needs to be considered (Koerner, 1998). Compressibility is most important for needle-punched nonwoven geotextiles for which the compressibility is directly related to mass density (i.e. thickness; mass per unit area). In contrast, compressibility is relatively low for woven and heat-bonded nonwoven fabrics (Figure 5.1).

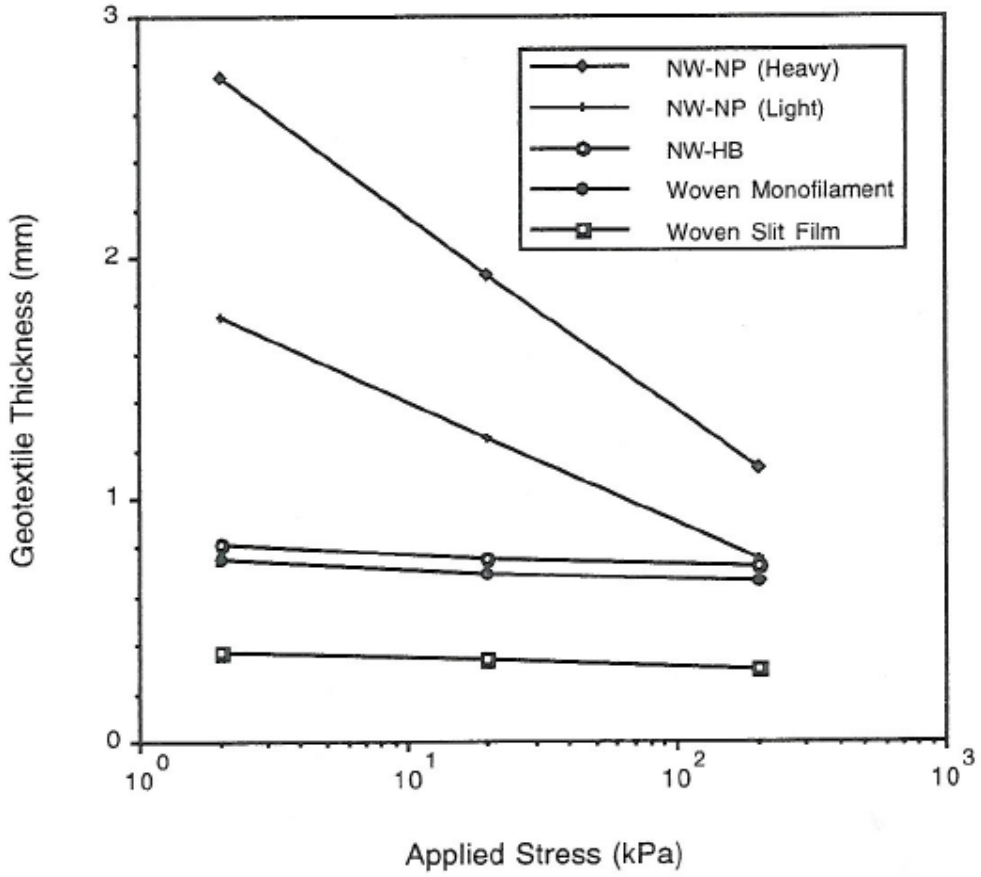

Figure 5.1 Compressibility of Different Types of Geotextiles – Manufactured through Different Processes (Koerner, 1998)
Note: i) NW-NP: Nonwoven Needle-Punched; ii) NW-HP: Nonwoven Heat-Bonded

5.2.2. Straining Behavior (i.e. Permanent Elongation)

Under constant load, fabrics (i.e. geotextiles) elongate, and thus, experience straining based on the direction of load application. The greatest sources of strain developing in fibrous materials is due to stress level, polymer type, and fiber processing (Figure 5.2a and 5.2b) as revealed by the classical work of Hoedt (1986). He observed the straining behavior of different fibrous materials over long durations and calculated the rates of elongation from the response curves. This information was then reported as a reduction factor for design purposes to avoid deformation of the fabric during use in various applications. The values of the rates were suggested to be adjusted for the

anticipated length of service life-time of the fibrous polymeric material. The influence of environmental conditions such as temperature giving rise to more rapid progression of the straining behavior (i.e. elongation) of fabrics must now be considered, and hence, the reduction factors may need to be revised.

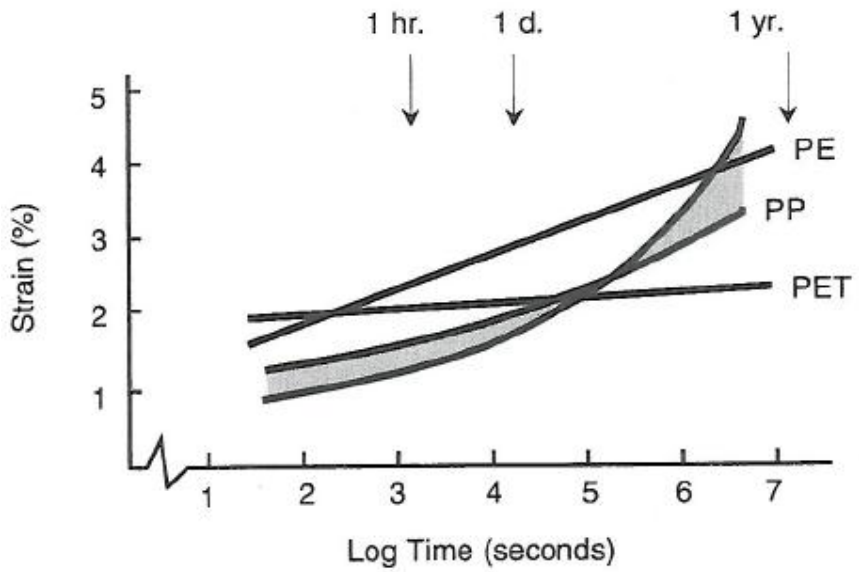

(a) Straining at 20% Load

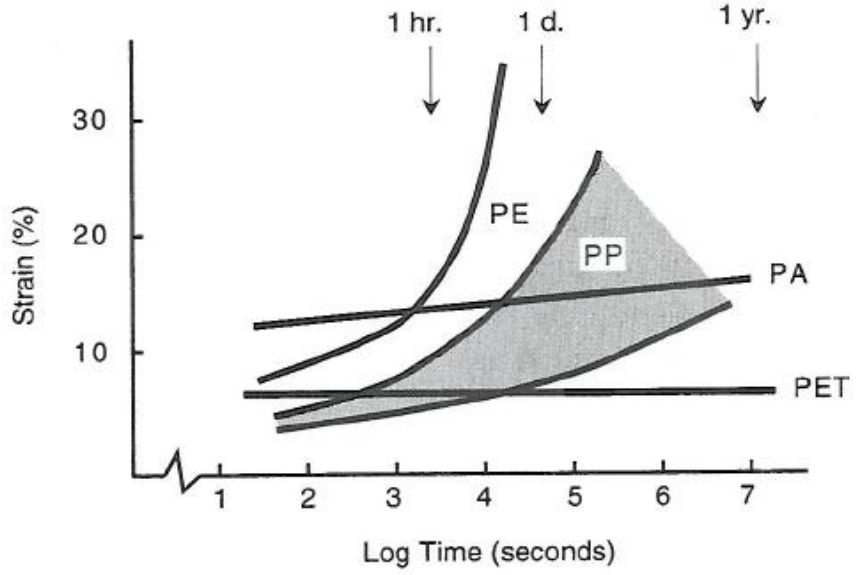

(b) Straining at 60% Load

Figure 5.2 Straining Behavior of Fabrics made from Different Polymers under Constant Load (Hoedt, 1986)

5.2.3. Reinforcement

One of the major functions of geotextiles utilized in geotechnical applications is reinforcement (i.e. enhancing tensile properties) to complement materials such as soils which are good in compression but weak in tension. In order to meet this requirement, geotextiles as a geosynthetic material have to possess necessary tensile strength. In the classical work of Broms (1977), the triaxial testing method was selected to evaluate the positive contribution of geotextile strength to the improvement of tensile properties of layered composite systems. The results of this experimental research study revealed the importance of location selection for the geotextile placement such that a significant amount of strength improvement could be realized when the fabric was properly placed. It was underscored by Broms (1977) that the geotextile interrupts potential shear planes and has beneficial influence on increasing the overall shear strength of the reinforced soil. Triaxial test results showing the effect of geotextiles placed at various locations within soil specimens at different confining pressures are given in Figure 5.3a and 5.3b. The base-line shear strength of the sand by itself is represented by Curve 1. The geotextiles were placed at non-acting dead zones of the conventional triaxial test in Curve 2. Therefore, the shear strength of the soil was not improved by a distinguishable amount. Clearly, the geotextile needs to be placed at appropriate locations to see their beneficial effect. The favorable effects of the geotextile are obvious in Curves 3 and 4. The double layers placed at the one-third points (Curve 4) made more contribution to the overall shear strength than a single layer placed at the center of the specimen which was attributed to more layers of the geotextile better interrupting the potential shear planes in the soil (Broms, 1977).

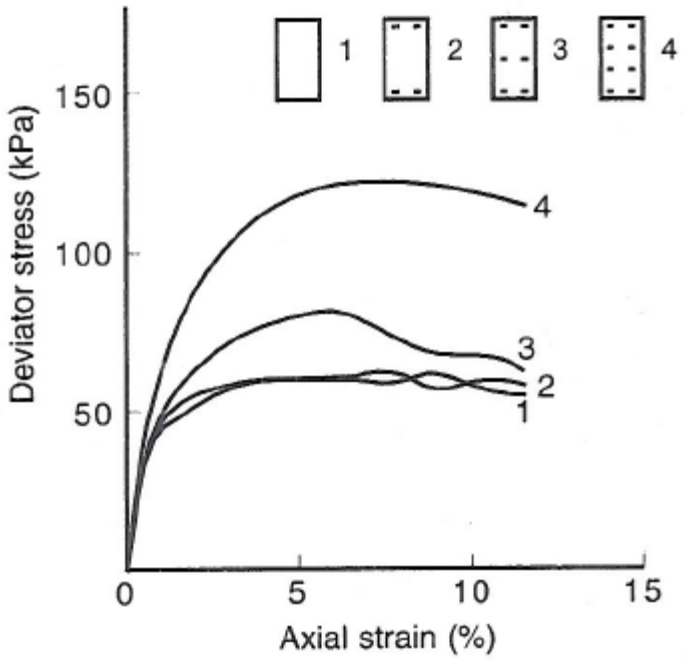

(a) Dense Sand at 21 kPa Confining Pressure

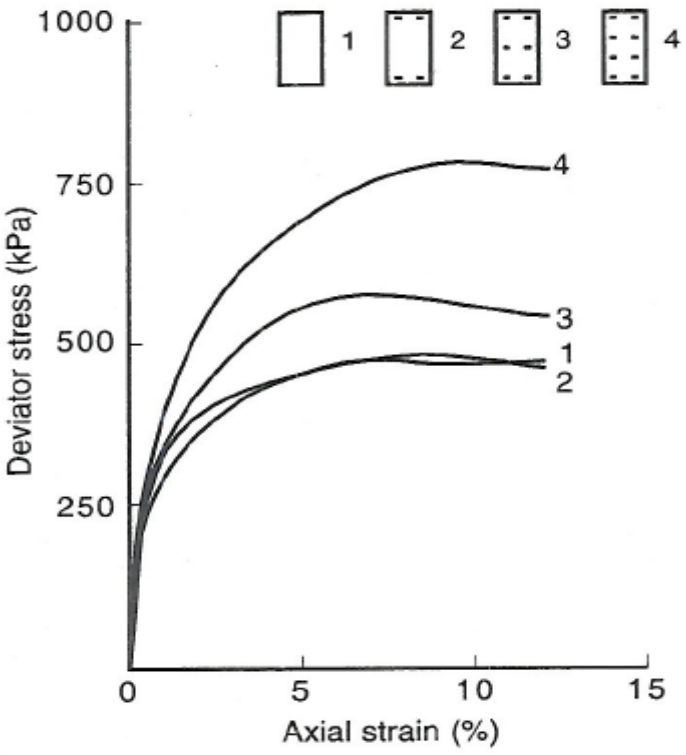

(b) Dense Sand at 210 kPa Confining Pressure

Figure 5.3 Triaxial Test Results showing Influence of Geotextiles placed at Various Locations within Soil Specimen (Broms, 1977)

There are three different reinforcement mechanisms that exist within the general function of geotextile reinforcement to enhance the tensile strength properties of the entire layered composite system.

5.2.3.1. Membrane Type

Membrane type reinforcement occurs when a vertical force is applied to a geotextile within a deformable soil body. Geotextile tensioning in the cross load direction develops and the amount of this tension depends on the distance from the load and its orientation. The in-plane tensioning stress of the geotextile due to out-of-plane compression (i.e. applied vertical downward force) can be evaluated as follows (Koerner, 1998):

$$\sigma_h = \frac{P}{2\pi z^2}\left[\left(3\sin^2\theta\right)\cos^3\theta - \frac{(1-2\mu)\cos^2\theta}{1+\cos\theta}\right] \tag{5.1}$$

Where;

σ_h: Horizontal Stress at Depth, z and Angle, θ

P: Applied Vertical Force

z: Depth beneath Surface where σ_h is being calculated

μ: Poisson's Ratio

θ: Angle from the Vertical beneath the Surface Load, P

Note that directly beneath the load, where $\theta = 0°$;

$$\sigma_h = -\frac{P}{\pi z^2}\left(\frac{1}{2} - \mu\right) \tag{5.2}$$

Since Poisson's ratio is less than 0.5, the horizontal stress developing in the geotextile will be negative indicating tension. As indicated previously, the geotextile is utilized to improve the soil tensile-strength and undertake/support some portion of the developed tension in the soil due to a vertical load placed at the ground. The amount of total tension which can be sustained by the geotextile depends on fiber bonding type used in manufacturing, the filament base polymer type and the geotextile size. Therefore, the total tensile capacity (i.e. strength) of the overall layered composite system at the macro-scale is determined through micro-scale properties of the fibrous material. Consequently, micro-scale integration and interaction of geotextile filaments drives macro-scale geotextile response.

5.2.3.2. Shear Type

Shear type reinforcement can be visualized by means of direct shear tests where; i) a geotextile is placed on a soil, ii) compressed in a normal direction, and then iii) the two materials are sheared at their interface. The resulting shear-strength parameters are obtained using an adapted form of the Mohr-Coulomb failure criterion as follows (Koerner, 1998):

$$\tau = c_a + \sigma'_n \times \tan\delta \qquad (5.3)$$

Where;

τ: Shear Strength between the Geotextile and Soil

σ'_n: Effective Normal Stress on the Shear Plane

c_a: Adhesion of the Geotextile to the Soil

δ: Friction Angle between the Geotextile and Soil

To check the efficiency of use of geotextile (i.e. beneficial contribution to tensile strength properties of complete system), the shear strength parameters c_a and δ of the composite system are compared to that of the soil by itself (i.e. direct shear resistance of soil) as recommended by Koerner (1998) in the following way:

$$\tau = c + \sigma'_n \times \tan\varphi \qquad (5.4)$$

Where;

c: Cohesion (soil to soil)

φ: Friction Angle (soil to soil)

As with membrane type reinforcement, the shearing process creates tension in the geotextile for which the overall tensile strength performance is controlled by micro-scale filament tensile properties and hence, base polymer type as well as fiber manufacturing bond type.

Furthermore;

$$E_c = \left(\frac{c_a}{c} \right) \times 100 \qquad (5.5a)$$

$$E_\varphi = \left(\frac{\tan\delta}{\tan\varphi} \right) \times 100 \qquad (5.5b)$$

Where;

Ec: Efficiency of Cohesion Mobilization

Eφ: Efficiency of Friction Angle Mobilization

The ratios, given in Equation 5.5a and 5.5b are generally called “efficiencies”, and have limiting values of zero and unity. While a value higher than unity is possible, such values can not be mobilized since the shear failure plane would simply move into the soil itself as highlighted by Koerner (1998).

5.2.3.3. Anchorage Type

Anchorage type reinforcement is similar to the shear type reinforcement with the distinction that, in this case, the soil acts on both sides of the geotextile and the developed tensile force tends to pull the geotextile out of the soil. The laboratory modeling of this type of mechanism is in such a way that soil is placed stationary in the upper and lower halves of the test device similar to a direct shear apparatus, and then, the geotextile extends out of the device at its center while normal compressive force acts on the soils and the geotextile within the test box setup. Therefore, the shear strength mobilized by the geotextile with the soil above and below are added up and the total shear strength is limited by the tensile strength of the geotextile (i.e. Wide-width tensile values). In other words, anchorage efficiencies greater than unity can occur; but are limited by the tensile strength of the geotextile itself (Koerner, 1998).

5.3. Fibrous Materials (Fabrics) Tensile Testing Perspectives

Tensile strength testing has been a widely used method to evaluate the engineering properties of various geosynthetics such as geotextiles. This is attributed to the fact that many geosynthetics are designed to complement the relatively low tensile capacity of soils (Mitchell and Seed, 1990; Koerner, 1998).

Over the decades, several researchers have conducted various types of tests on geotextiles following different methods and examined the influence of sample preparation, test conditioning, and test progress inputs as summarized below:

- Constant Rate of Loading (CRL) tests (Krais, 1928; de Meulemeester and Nicoloff, 1936)
- Constant Rate of Elongation (CRE) tests (Hindman, 1948)
- Gravimetric method (ASTM, 1954), Air Flow method (Lord, 1955), and Microscope method (Gonsalves, 1947)
- Fiber diameter or fineness (Morton and Hearle, 1962; 1993)
- Cumulative Creep tests (Morton and Hearle, 1993)
- Specific test procedures and analysis methods (ASTM D 3822 and ASTM D 3379)
- Effects of Sample Preparation and Test Conditioning on the test results (Myles and Carswell, 1986; Koerner, 1997; Jones, 2000; Mueller-Rochholz and Recker, 2000; Koerner, 2000)
- No universal relationship exists between specimen sizes and material properties (Koerner, 1998)

5.3.1. The Role of Fabric (i.e. Geotextile) Manufacturing Type (Strength Behavioral Performance Variations)

One of the focus areas of the current research study and also one of the most important property of a fabric (i.e. geotextile) is its tensile strength. Most geotextile applications have been developed by relying on this property (Koerner, 1998). The testing to attain the tensile parameters can be conducted in the laboratory as follows. The fabric is placed within a set of clamps or jaws in the loading frame of a mechanical testing machine, and then, the specimen is stretched in tension until failure occurs. During the extension process, the load and deformation are measured to be able to generate stress-strength-strain curve from which tensile strength properties (i.e. tensile strength, strain at failure, toughness, modulus of elasticity) of the tested fibrous material can be determined. Figure 5.4 shows the tensile responses of geotextiles produced with different manufacturing processes. Woven geotextiles exhibits brittle failure envelopes, while, nonwoven geotextiles shows more ductile responses compared to the woven types. Further, needle punching enhances the tensile strength of the geotextile, especially at higher strain levels. On the other hand, at low strain levels, heat-bonded type is more durable and able to support larger loads while exhibiting a lesser amount of strain (i.e. elongation) in comparison to the needle-punched type. Additionally, maximum elongation (i.e. strain at failure) of the fabric specimens is inversely related to maximum tensile stress (i.e. strength) which means that gaining ductility and flexibility in fibrous materials sacrifices tensile strength. As expected, the modulus of elasticity decreases with increasing ductility.

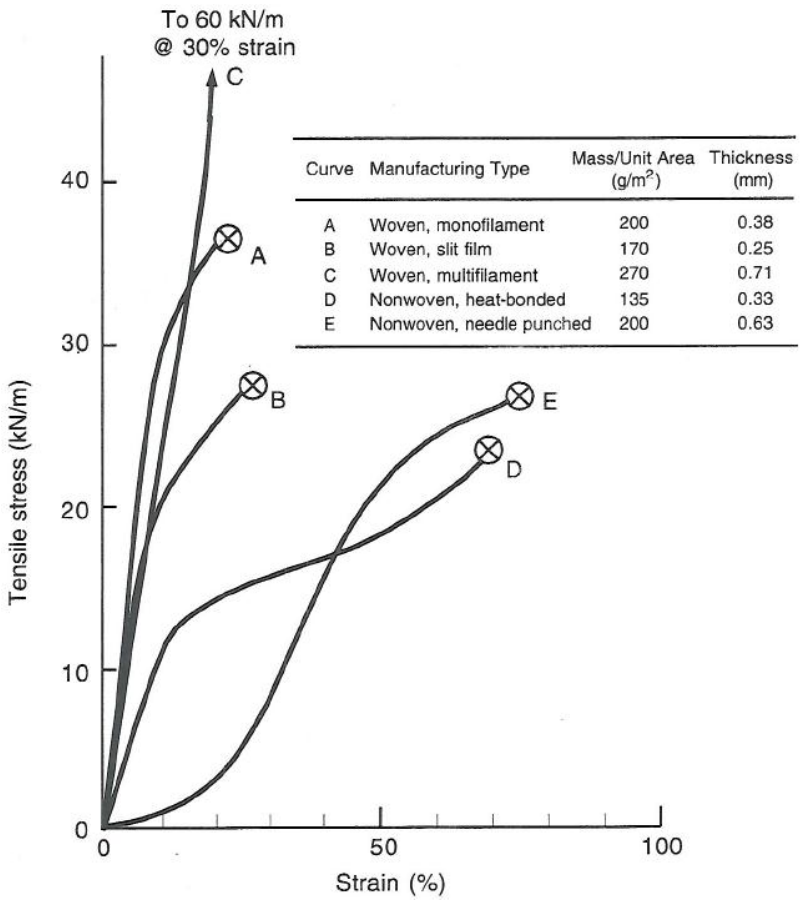

Curve	Manufacturing Type	Mass/Unit Area (g/m^2)	Thickness (mm)
A	Woven, monofilament	200	0.38
B	Woven, slit film	170	0.25
C	Woven, multifilament	270	0.71
D	Nonwoven, heat-bonded	135	0.33
E	Nonwoven, needle punched	200	0.63

Figure 5.4 Tensile Test Response of Various Geotextiles Manufactured by Different Processes: All are Polypropylene Fabrics; Initial Test Specimen: 200 mm wide and 100 mm high (Koerner, 1998)

5.3.2. Influence of Specimen Size (Width to Length Ratio) on Test Results

The results of tensile tests performed to measure tensile strength properties of the fabric materials are dependent on the size of sample tested. Fabric test specimen size can be evaluated by aspect ratio (length-to-width ratio) and several ASTM standards such as ASTM D1682, D751, D4632, and D4595 are available for tensile testing of fabrics in different sizes/shapes (Figure 5.5). The grab tensile test (ASTM D4632; Figure 5.5a) is a widely used and reported fabric tensile testing type used by manufacturers for documenting specifications, quality control or conformance testing of the fibrous

materials. For research and design studies, the wide-width test (ASTM D4595; Figure 5.5c) is necessary, especially for nonwovens (e.g. NPNW, HBNW) as they tend to have a severe Poisson's ratio effect under increasing stress when tensioned at high strains such that they experience rope-up and give artificially high values. Therefore, wide-width testing is commonly recommended for design-related measurements (Koerner, 1998).

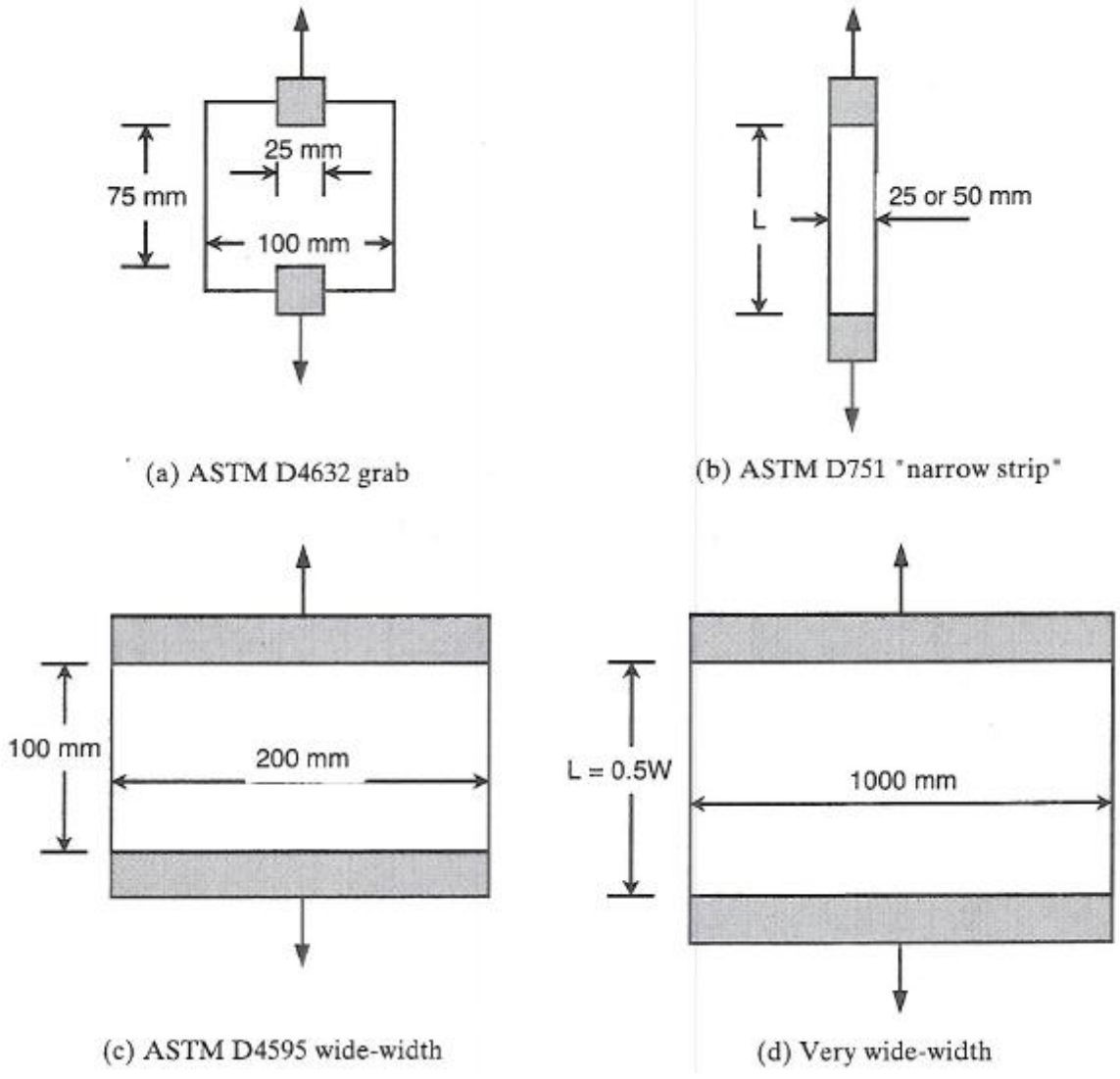

Figure 5.5 Various Tensile Test Specimen Sizes used to obtain Fabric Tensile Strength Properties (Koerner, 1998)

A universal relationship does not exist between the different test specimen sizes or shapes of the fabrics to allow correlation of the tensile strength obtained from one test type to another. Besides, the measured tensile strength properties of the fibrous materials depend on test specimen size and aspect ratio. Consequently, in the laboratory, it is possible to obtain different stress-strength-strain curves giving varied values of design parameters such as strength, modulus, and strain at failure for specimens of same type geotextile produced with the same polymer type, manufacturing process, and fiber type but having a different test specimen size/shape or aspect ratio. The specimen size and aspect ratio must properly be identified on the test data as underscored by several researchers including McGown (1982), Koerner (1998). In order to observe the influence of fabric test specimen geometry (i.e. size and aspect ratio), Andrawes et al. (1984) conducted an experimental study in which they examined the load carried by the geotextile at a given/predetermined strain level with respect to width-to-length (W/L) ratio (Figure 5.6). Their results are very significant in terms of showing the effect of specimen size/shape on fabric tensile strength. It was particularly underscored that the dimensions of the test specimen should be large enough to account for local structural variability of the geotextile and reduce the influence of heterogeneous fabric structure on the measured tensile strength properties. The test results from Andrawes et al. (1984) in Figure 5.6 indicated that the minimum value of the specimen width to length ratio should be two, at least up to 40 % strain, in order to provide reproducible test data for the purposes of design testing in these materials as well as highlighting the importance of the need to standardize sample sizes and geometry to allow comparison of material behaviors. In fact, as emphasized by Koerner (1998), needle-punched nonwoven

geotextiles are highly compressible and loosely structured (Figure 5.6), and are, therefore, more sensitive to geometry and width-to-length ratio of the sample in tensile tests.

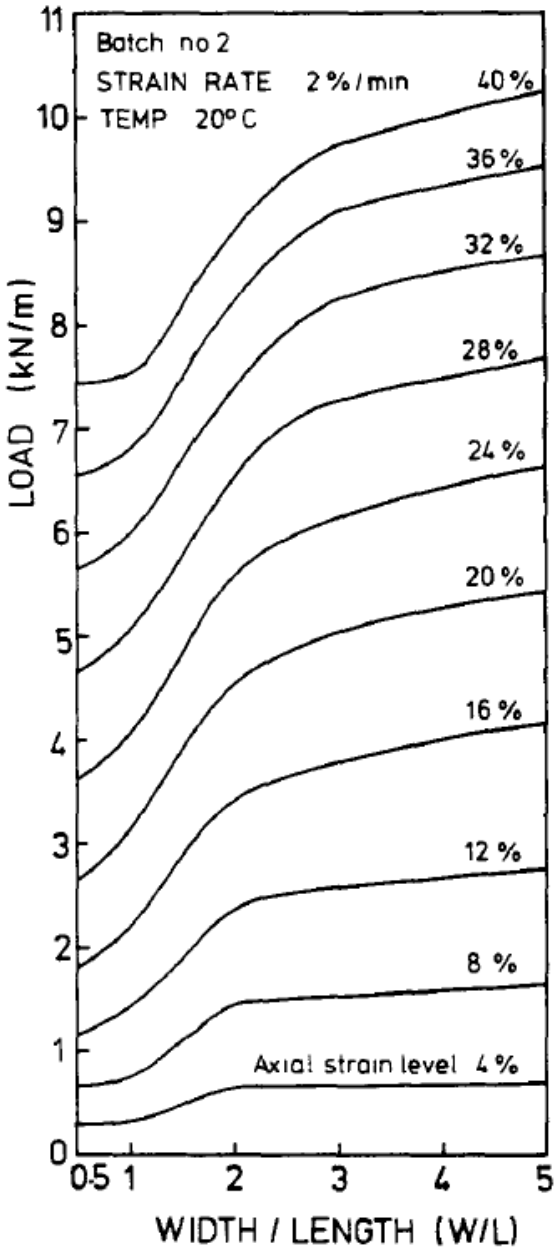

Figure 5.6 Effect of Specimen Geometry on the Load carried by a Continuous Filament Needle-Punched Polyester Geotextile at Given Strains (Andrawes et al., 1984)

5.3.3. Previous Macro-Scale Tensile Tests at Different Temperatures & Influence of Strain Rate on the Test Results

Since geotextiles are made from polymeric materials, it is well know that their behavior can be affected by test conditioning such as ambient temperature, and the rate of extension or contraction in tension or compression tests, respectively. The influence of temperature and strain rate on load-extension characteristics of geotextiles (100 mm long and 200 mm wide) were observed by Andrawes et al. (1984) as shown in Figure 5.7 and Figure 5.8, respectively. These results were attributed by the authors to the geotextile inner structure formation such that the total deformation is the summation of the deformations in the filaments and the deformations due to the rearrangement of the internal structure. Further, deformations due to the internal structural rearrangement are not sensitive to temperature and strain rate change, whereas, deformations of the polymeric geotextile filaments are sensitive to temperature. For example, the woven geotextiles with aligned filaments have virtually no structural deformation component; therefore, it is the filament polymer which controls the total deformation. Hence, the woven geotextile is significantly influenced by temperature and strain rate changes (Figure 5.7a and 5.8a), whereas, the filament polymer effect in the needle-punched nonwoven geotextiles are small compared to that of the structural changes, with the result that its deformation is almost virtually independent of the temperature and strain rate only at "macro-scale" level (Figure 5.7b and 5.8b) (Andrawes et al., 1984). However, as far as the tensile testing of the geotextile at "micro-scale" level is concerned, the effects of the rearrangement of internal structure of the geotextile on the test results attained are avoided (since only a single filament is being tested) and the tensile behavior developed

as well as the tensile strength parameters obtained are strongly dependent on the geotextile single filament polymeric properties. Therefore, temperature has a significant and crucial influence on tensile test results attained when the observation of tensile strength behavior of the fabrics at different temperatures is being considered at the "micro-scale" level. Consequently, the temperature effect on tensile strength behavior/properties of the fibrous materials (i.e. geotextile) at "micro-scale" is more pronounced in the tests and vital to the results than that at "macro-scale" levels.

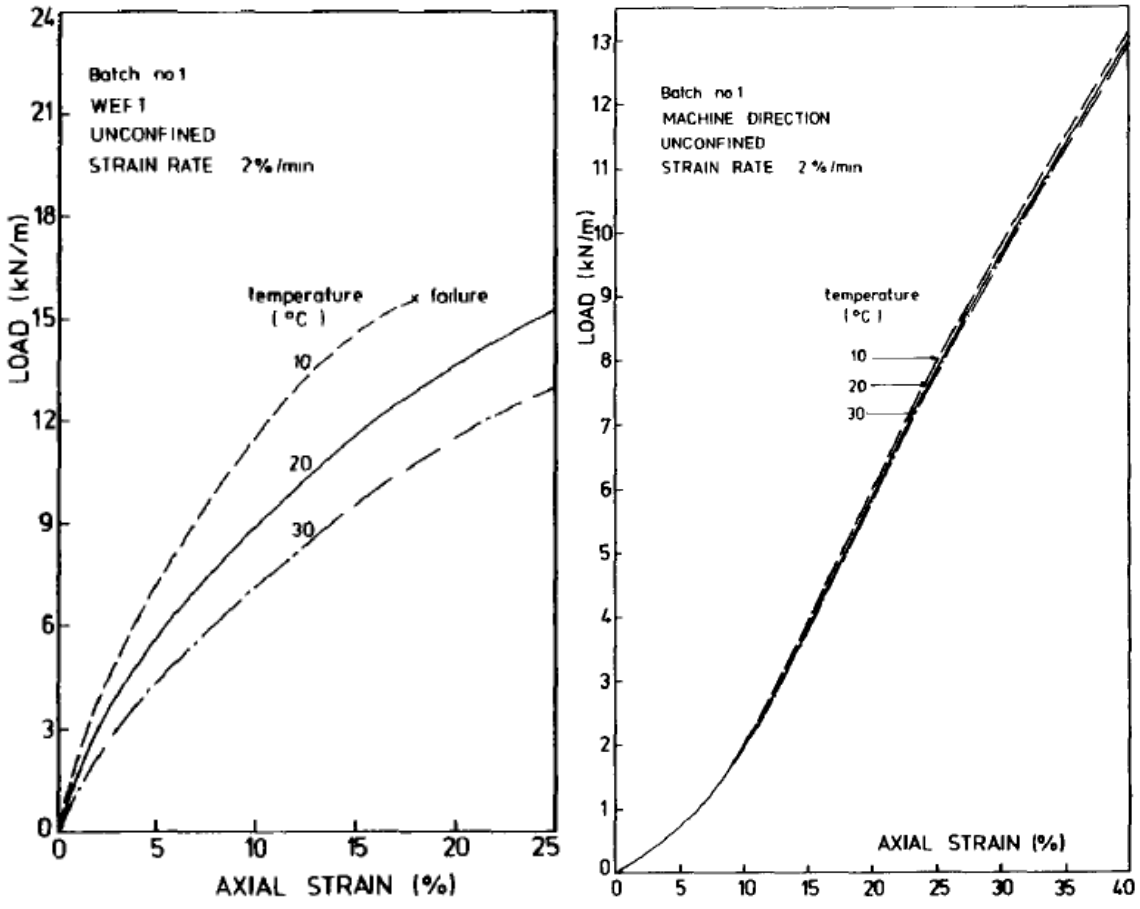

Figure 5.7 Effect of Temperature on Load versus Axial Strain Relationships for: (a) Woven Polypropylene Geotextile; (b) Nonwoven Polyester Geotextile (Andrawes et al., 1984)

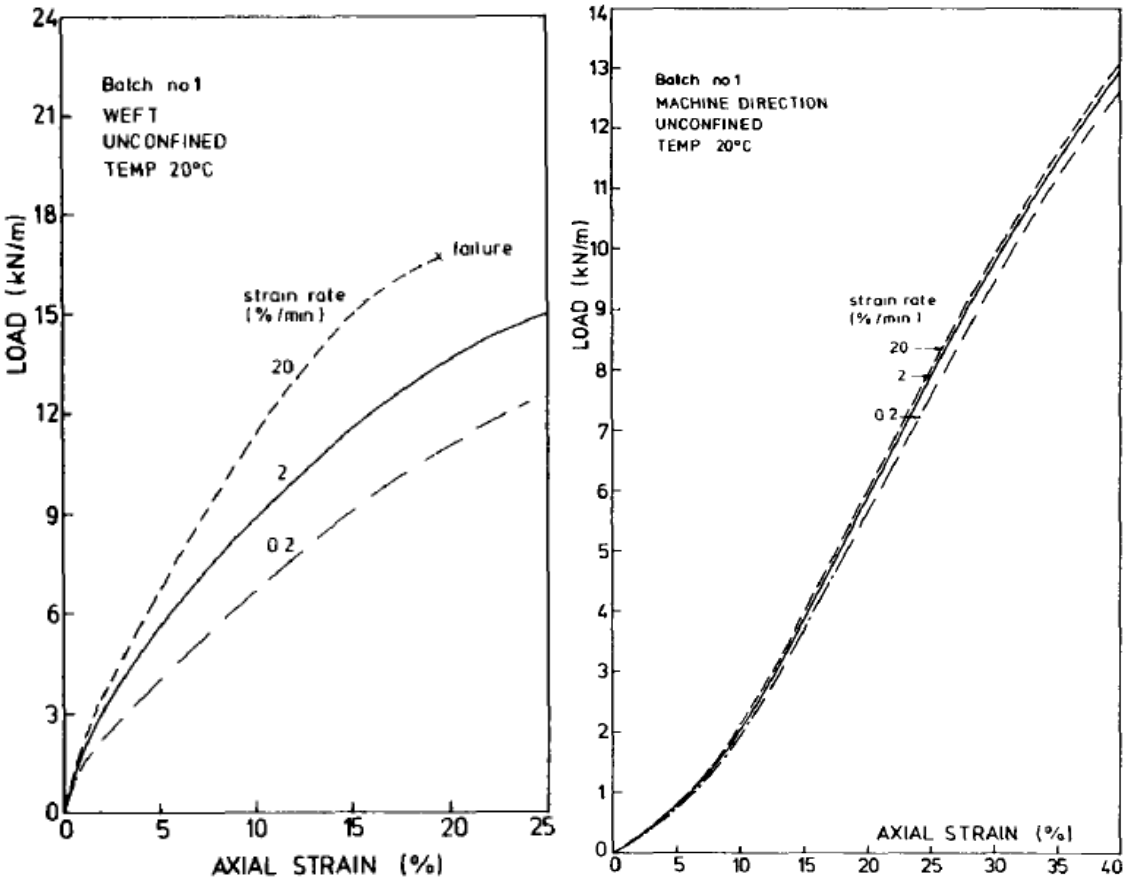

Figure 5.8 Effect of Strain Rate on Load versus Axial Strain Relationships for: (a) Woven Polypropylene Geotextile; (b) Nonwoven Polyester Geotextile (Andrawes et al., 1984)

As indicated by the authors, the data in Figures 5.7 and 5.8 also illustrate the effect of lowering the temperature is similar to increasing the strain rate and the effect of raising the temperature is similar to lowering the strain rate as far as the load-extension relationship for these geotextiles is concerned.

5.3.4. Effect of Confinement on Tensile Elongation Properties of Fabrics

McGown et al. (1982) conducted a research study to examine the effect of confinement on tensile elongation properties of fabrics. It was observed that soil confinement such as soil overlying and underlying the fabric in the field has a beneficial

influence on reducing the total amount of tensile elongation occurring in the fibrous materials (Figure 5.9a and 5.9b). Therefore, the total elongation of the geotextile obtained as a result of unconfined wide-width tensile test in the laboratory will yield an overestimation compared to the real behavior of the geotextile in the field with soil confinement. As seen in Figure 5.9, the major improvement with soil confinement is with need-punched nonwoven geotextiles which shows the importance of fiber type and manufacturing process on tensile properties of the fabrics.

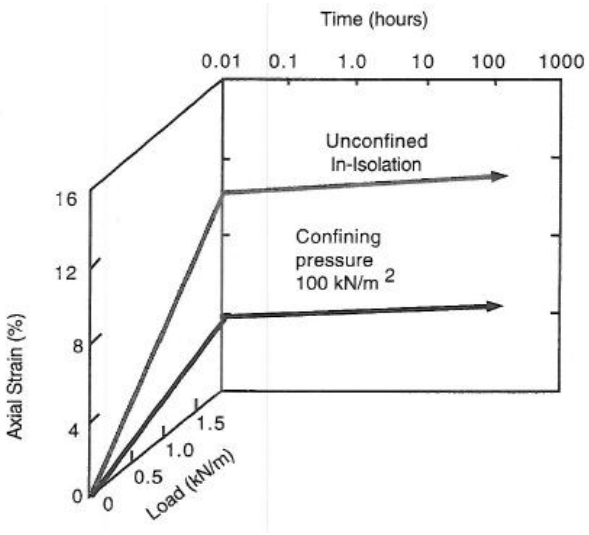

(a)

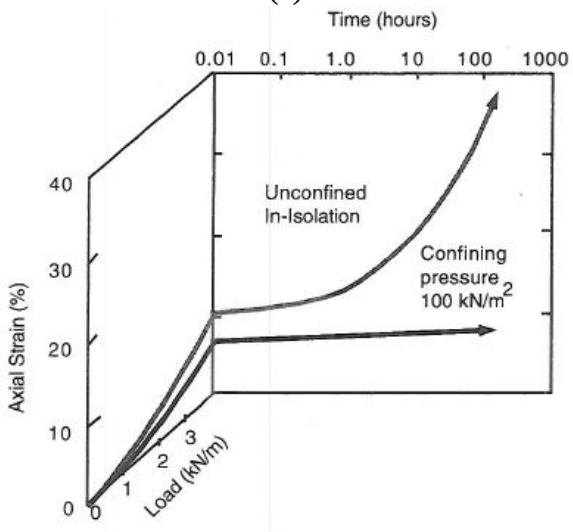

(b)

Figure 5.9 Influence of Confinement on Tensile Elongation Properties of Fabrics: (a) Needle-Punched Nonwoven; (b) Heat-Bonded Nonwoven (McGown et al., 1982)

5.4. Tensile Behavior of Geotextile Single Filaments at Different Temperatures (Micro-Scale Perspectives and Response)

5.4.1. Introduction and Scope

In order to investigate tensile behavior and the developed "micro-scale" stress-strain response of geotextile single filaments at different temperatures, laboratory tests were performed in this study by measuring filament thermo-mechanical properties using DMA in controlled force/strain rate mode. Detailed information on DMA test device, sample preparation and experimental procedures were provided in Section 4.6. Geotextile single filament specimens were stretched in tension and ruptured using a constant-rate-of extension (CRE) type tensile test at a gage length (i.e. initial sample length) of 12.5 mm, and rate of extension of 0.125 mm/sec at elevated temperatures for filament specimens having an average diameter of 0.035 mm (35 μm) (Figure 5.10). This strain rate was determined based on initial specimen length, L; $\left(\frac{d\varepsilon}{dt}=\frac{L}{100}\right)$ and intentionally used to observe the entire deformation behavior - consisting of i) elastic elongation; and ii) inelastic deformation of filament polymeric materials under tension until the rupture takes place. Using the resulting force-extension (elongation) curve (i.e. force-displacement; stress-strain), the tensile engineering properties of single geotextile filaments such as tensile strength (τ_{max}), modulus of elasticity (E), yielding strength, displacement range of yielding, breaking force, and elongation at specified force were determined and evaluated for elevated thermal conditions (i.e. 20 °C to 50 °C) likely to be experienced by geotextiles in field applications.

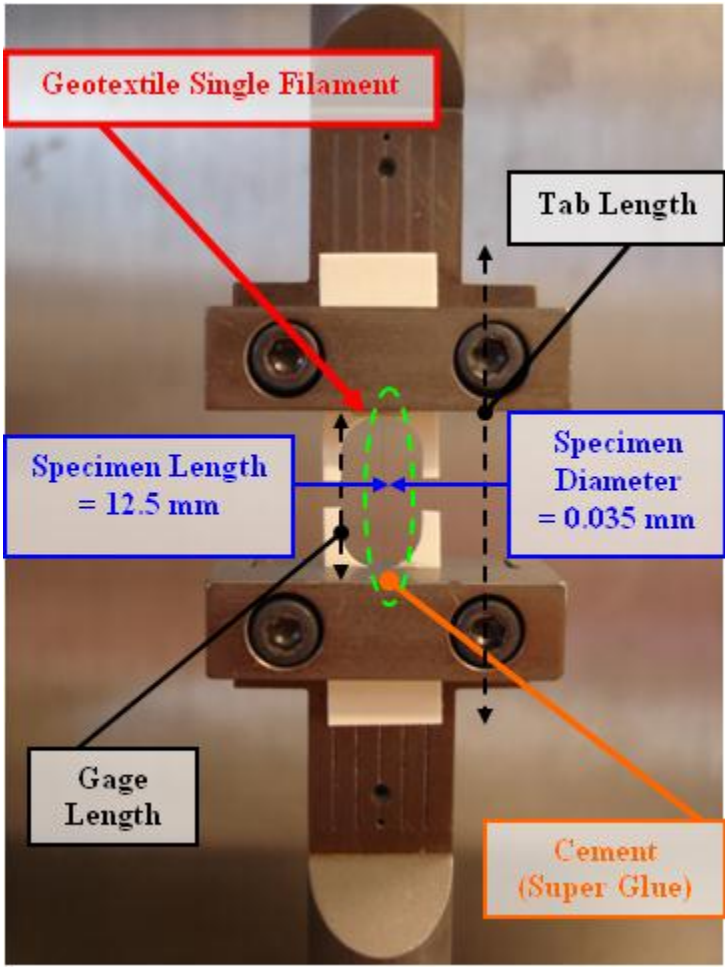

Figure 5.10 Picture Showing the Dimensions of Geotextile Single Filament Test Specimen

5.4.2. Influence of Physico-Mechanical Properties of Geotextile Polymeric Fibers on the Developed Temperature Dependent Tensile Response

When polypropylene (PP) (base polymer of the filament) is in the molten state, molecules flow past one another, and the polymer behaves as a viscous liquid. At melting temperature (Tm), crystallization zones develop at locations where the polymer molecules can pack into an ordered arrangement. Upon further cooling, the kinetic energy

of the molecules decreases, allowing secondary bond forces to develop between the polymer molecules. Secondary bond forces account for the increased "stiffness" of polypropylene filament at low temperatures. At the glass transition temperature (Tg), secondary bond forces overcome molecular kinetic energy, and molecular movement "ceases" within the amorphous zones. Below Tg, the polymer behaves as a glassy solid, and the filament will be "stiff", "hard", and somewhat "brittle". Since the operating temperature range in the field for PP geotextile is limited to temperatures much lower than Tm and higher than Tg, geotextile fibers manufactured from this polymeric material exhibit temperature dependent "stiffness" and "ductile elasto-plastic" tensile behavior (Painter and Coleman, 1997; Stein and Powers, 2006).

In light of the information provided regarding the influence of physico-mechanical properties of geotextile polymeric filaments on the observed temperature dependent stress-strain curve, the tensile behavior of single filaments were characterized by performing "micro-scale" thermo-mechanical tensile tests. The results were used to determine the elastic modulus, yield strength, yield strain, and ultimate strength for the single filament of NPNW-PP geotextile. Further, it is important to highlight that being a polymer, the filament mechanical behavior (i.e. tensile response) is highly dependent on the test conditions including strain rate and temperature, test specimen size/shape (i.e. aspect ratio) as previously indicated by Hoedt (1986), and Tisinger et al. (1990). Therefore, the test results provide an index of behavior at "micro-scale" level, but do not provide a comprehensive characterization for engineering design of the material under tension load at global or macro-scale. As already discussed in Section 5.3.3, the global ("macro-scale") tensile response of geotextiles is the summation of elastic elongations,

inelastic (plastic) deformations in the filaments as well as deformations due to the rearrangement of inherent internal structure including void space which is not sensitive to temperature change in contrast to the polymeric filaments elasto-plastic deformations under stress. Global mechanical response (i.e. tensile behavior) of geotextiles depends on the fiber process (needle-punched, heat-bonded etc.) and geotextile fabric manufacturing type (woven versus nonwoven) as well as filament polymer type. In this study, NPNW-PP geotextile was selected for study as it is most widely utilized in common geotechnical applications due to its enhanced advantageous properties in drainage, filtration etc.. Moreover, as discussed in Section 5.2.1., the mobilized tensile strain (i.e. tensioning behavior) and the capacity of the fabric to sustain tension is influenced by the geotextile compressibility properties, internal structure and fiber-fiber bonding process.

5.4.3. Micro-Mechanical Thermo-Tensile Tests on Geotextile Single Filaments

A total of 105 micro-mechanical thermo-tensile tests on single geotextile filaments were performed at temperatures ranging from 20 °C to 50 °C with 5 °C increments between different test temperatures and 15 tests at each test temperature to observe the repeatability of the developed tensile force-extension behavior as well as to see the reproducibility of filament tensile strength response at every test temperatures. Figure 5.11 presents these 105 tests in which the 15 replicate tests at each test temperature are shown in the same graph starting from the room temperature of 21 °C up to the elevated temperature of 50 °C.

As presented in Figure 5.11a through 5.11g, the shapes of force-displacement curves for all the tests performed on filament specimens at various temperatures were in good agreement and indicated that plastic elongation behavior occurs in polypropylene filaments under tension load prior to failure of the fibers. In the tests, the tensile force increases with increasing axial extensional displacement, then, it remains almost constant during inelastic deformation of the polymeric material after passing through yielding deformation. The inelastic portions of the stress-strain curves are essentially parallel.

Some specimens experienced larger strains prior to failure than others. Brittle tension rupture for the specimens was not observed for the temperature range tested. Brittle failure modes generally occur under glass transition temperature (Tg) of polymeric material as the nature of bonding between the molecules of polypropylene is based on ambient temperature. The filaments do not exhibit a particular trend for the strain at break. At every temperature tested, the filaments showed a similar mixture of extensibility. A few specimens break at low strain levels, whereas, the others possesses high level of extension. The filaments are highly ductile with the majority of the filaments experiencing a large amount of plastic deformation before rupture. For example, some of the filaments were able to extend up to a maximum strain of more than 120% which results in a high energy absorption level. This is favorable for interaction mechanism of geotextile filaments with geomembrane texture elements in developing interface shear strength, in particular during the post-peak stage of interface response. There is an apparent trend which can be observed in the series of graphs in Figure 5.11 of the tension force-displacement failure envelopes for polypropylene filament specimens diminishing as the temperature is increased. This variation in tension versus extension

behavior shows the influence of temperature on force-displacement response of geotextile single filaments at micro-level.

Based on observations made on post-test filament specimens after the experiments were completed, it was seen that the failure (i.e. rupture point) took place at different locations of the sample gauge length with some being close to the middle of the specimen, whereas, others were closer to either end (up or down) where the tension break rupture occurred in the upper or lower portion of the filament specimens gripped by the smooth clamp fixtures with flat jaws.

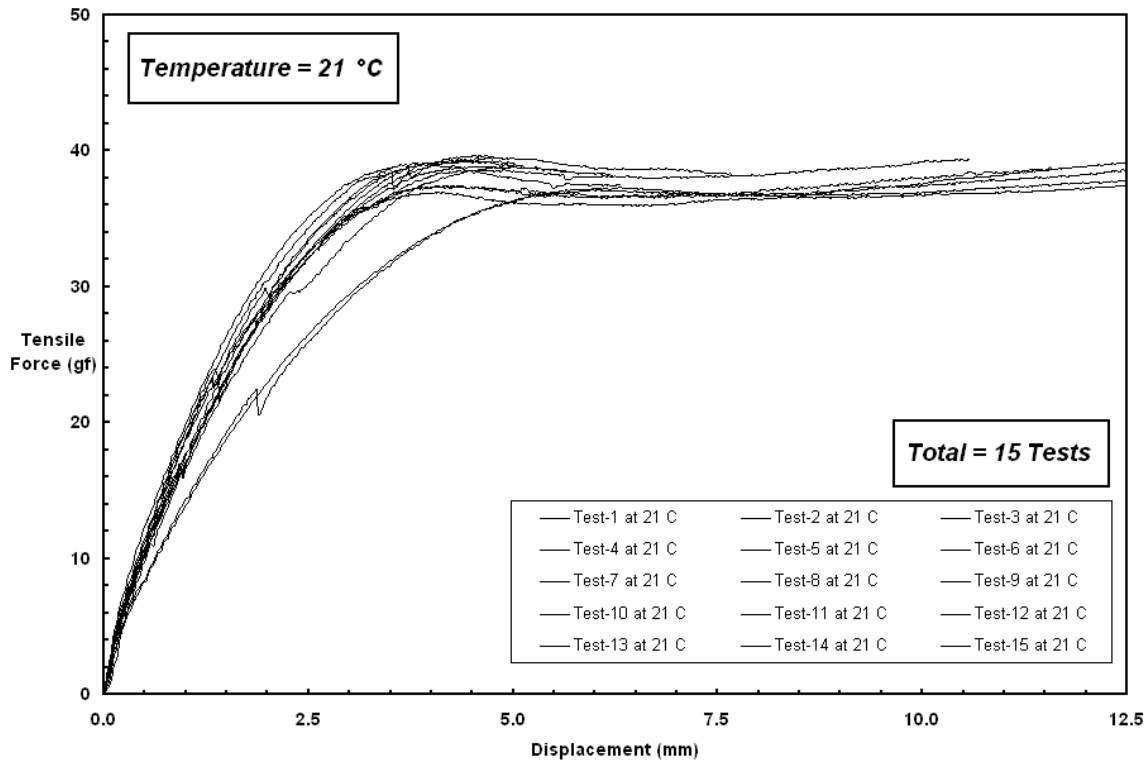

(a)

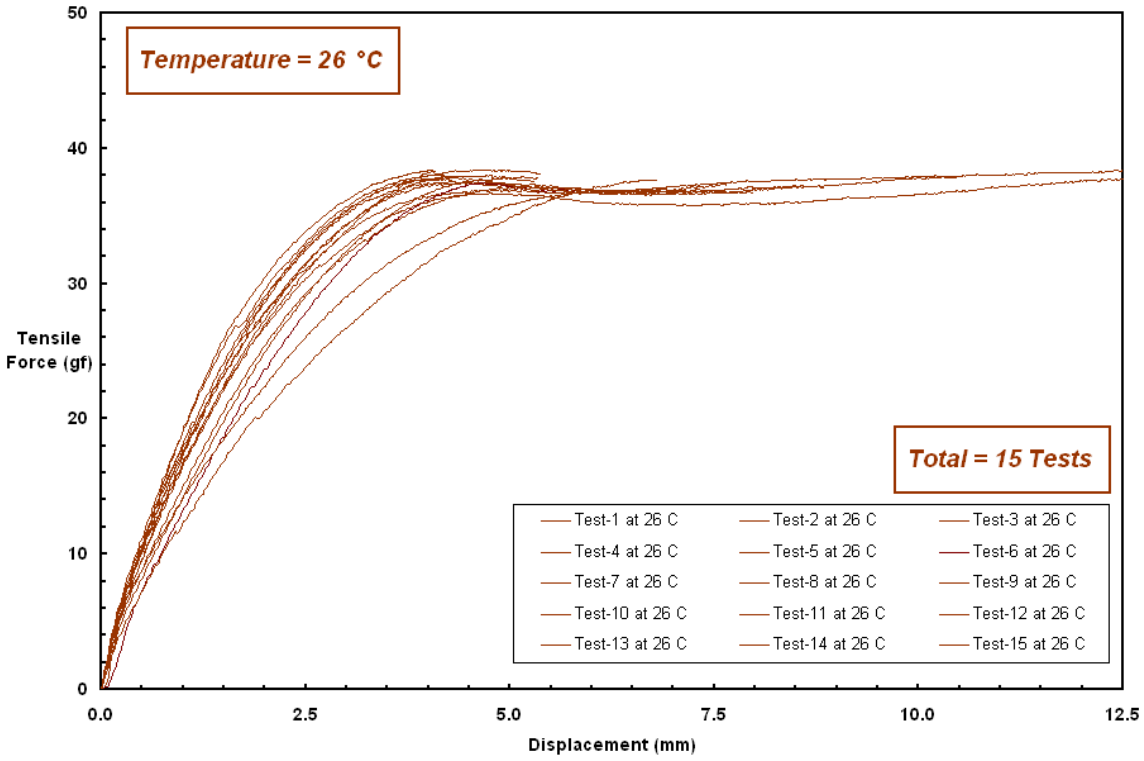
Temperature = 26 °C
Total = 15 Tests
Test-1 at 26 C
Test-2 at 26 C
Test-3 at 26 C
Test-4 at 26 C
Test-5 at 26 C
Test-6 at 26 C
Test-7 at 26 C
Test-8 at 26 C
Test-9 at 26 C
Test-10 at 26 C
Test-11 at 26 C
Test-12 at 26 C
Test-13 at 26 C
Test-14 at 26 C
Test-15 at 26 C
Tensile Force (gf)
Displacement (mm)
0
10
20
30
40
50
0.0
2.5
5.0
7.5
10.0
12.5

(b)

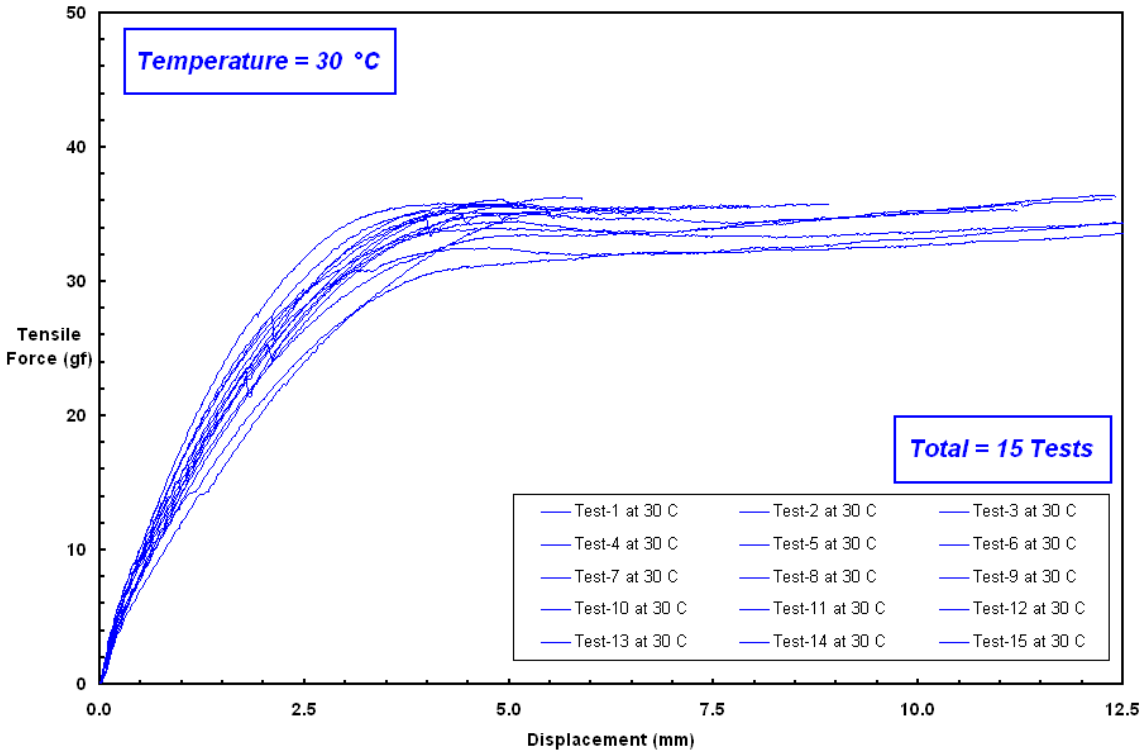
Temperature = 30 °C
Total = 15 Tests
Test-1 at 30 C
Test-2 at 30 C
Test-3 at 30 C
Test-4 at 30 C
Test-5 at 30 C
Test-6 at 30 C
Test-7 at 30 C
Test-8 at 30 C
Test-9 at 30 C
Test-10 at 30 C
Test-11 at 30 C
Test-12 at 30 C
Test-13 at 30 C
Test-14 at 30 C
Test-15 at 30 C
Tensile Force (gf)
Displacement (mm)
0
10
20
30
40
50
0.0
2.5
5.0
7.5
10.0
12.5

(c)

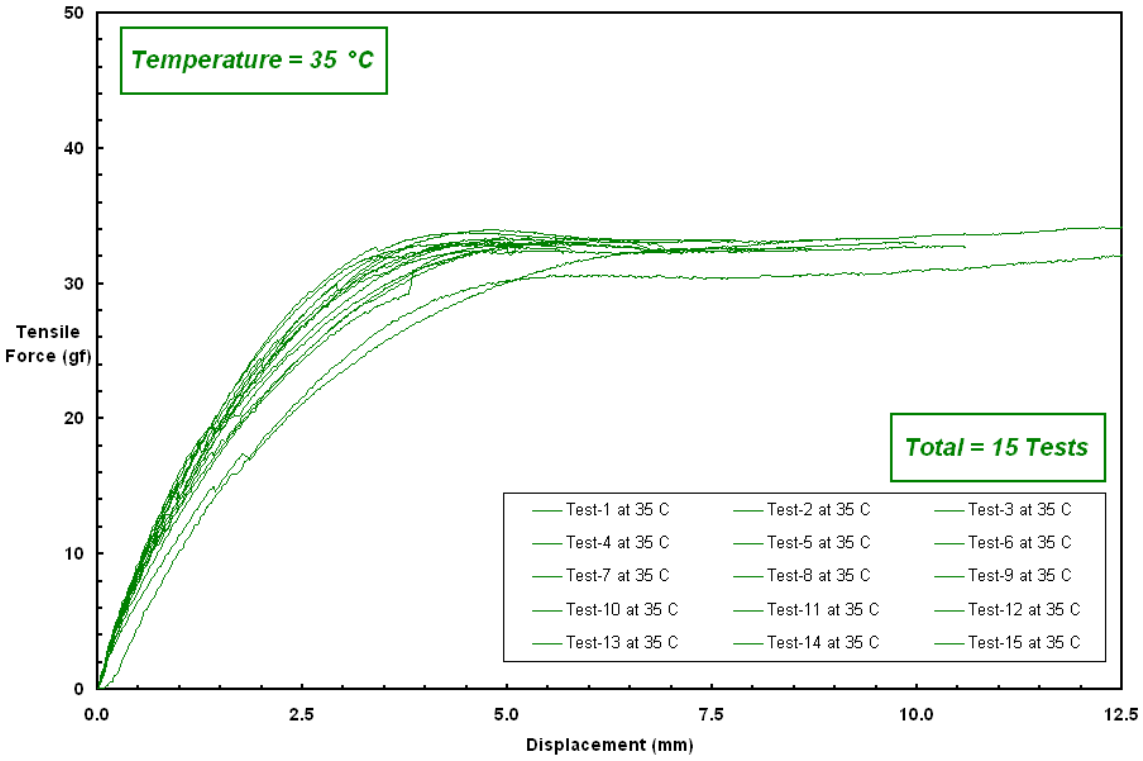
Temperature = 35 °C
Total = 15 Tests
Tensile Force (gf)
Displacement (mm)
0
10
20
30
40
50
0.0
2.5
5.0
7.5
10.0
12.5
Test-1 at 35 C
Test-2 at 35 C
Test-3 at 35 C
Test-4 at 35 C
Test-5 at 35 C
Test-6 at 35 C
Test-7 at 35 C
Test-8 at 35 C
Test-9 at 35 C
Test-10 at 35 C
Test-11 at 35 C
Test-12 at 35 C
Test-13 at 35 C
Test-14 at 35 C
Test-15 at 35 C

(d)

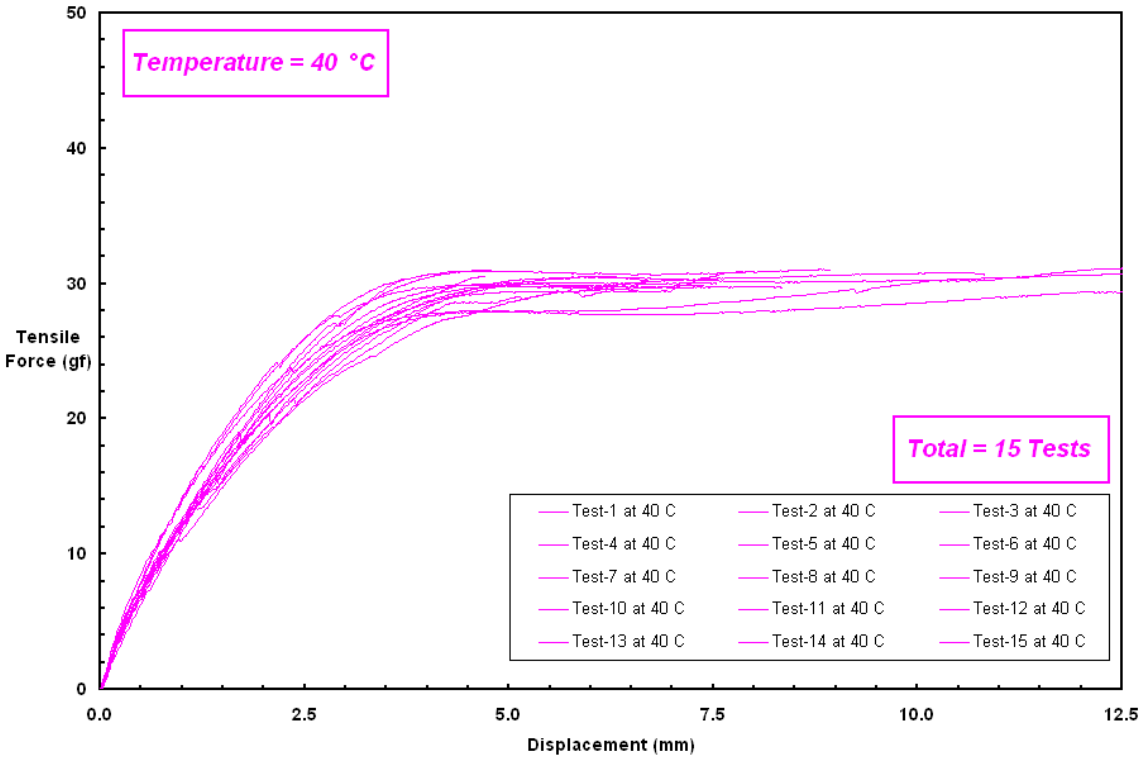
Temperature = 40 °C
Total = 15 Tests
Tensile Force (gf)
Displacement (mm)
0
10
20
30
40
50
0.0
2.5
5.0
7.5
10.0
12.5
Test-1 at 40 C
Test-2 at 40 C
Test-3 at 40 C
Test-4 at 40 C
Test-5 at 40 C
Test-6 at 40 C
Test-7 at 40 C
Test-8 at 40 C
Test-9 at 40 C
Test-10 at 40 C
Test-11 at 40 C
Test-12 at 40 C
Test-13 at 40 C
Test-14 at 40 C
Test-15 at 40 C

(e)

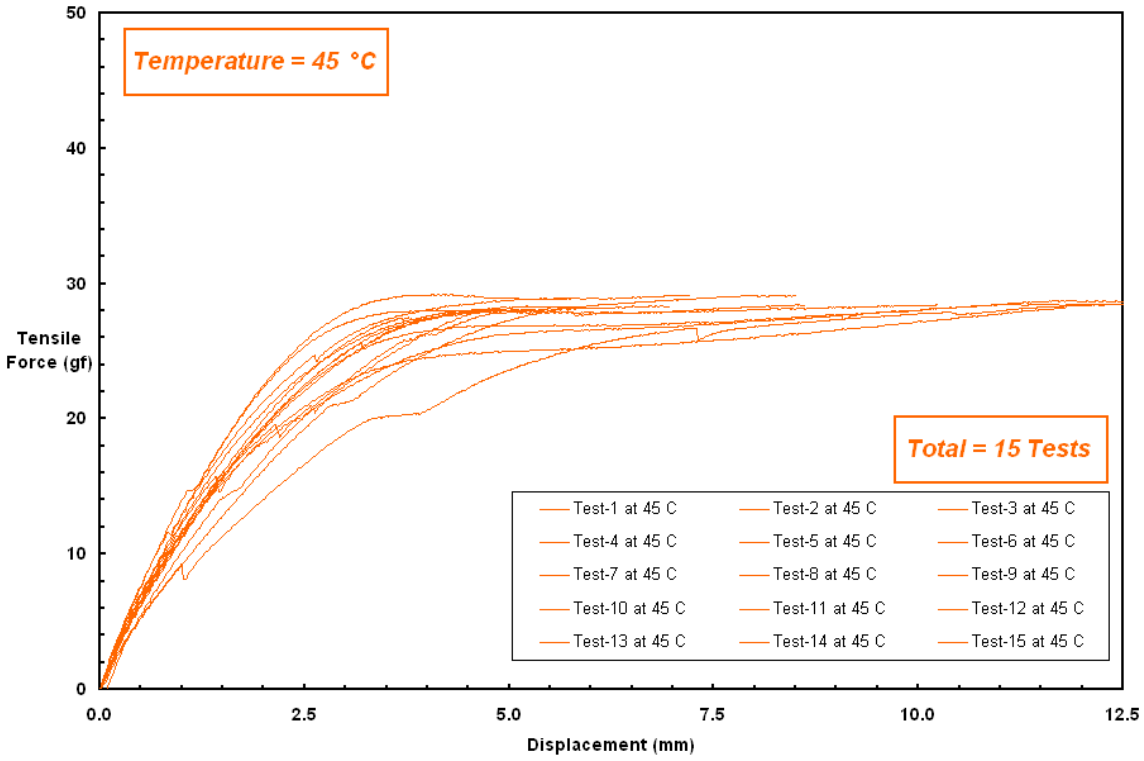

(f)

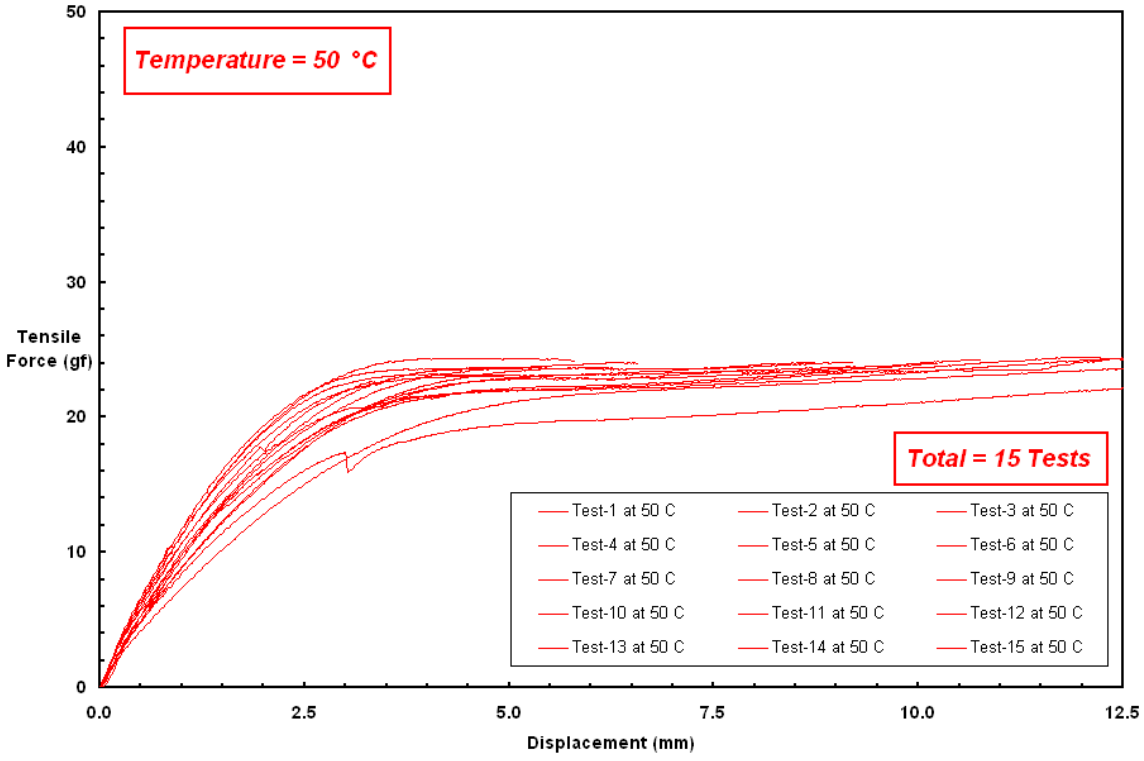

(g)

Figure 5.11 Force – Extension Curves: Overall of 105 Micro-Mechanical Thermo-Tensile Tests – Total of 15 Tests Performed per Each Test Temperature

In general, for polymeric materials such as geotextile filaments, higher temperatures cause a decrease in modulus and an increase in material ductility (Nielsen and Landel, 1994). The following example illustrates the influence of strain rate on polymers. For instance, when the temperature is held constant during mechanical testing, strain rate has a significant effect on material properties such that with a higher strain rate, molecular chains have less time to deform under load, leading to a stiffer response (Stein and Powers, 2006; Dowling, 2007). The influence of temperature and strain rate on the stress-strain response is *"interchangeable"* and a variation of one will produce the same response as a variation of the other (Andrawes et al., 1984). For example, the soft material response at high temperatures can be duplicated at a lower temperature by decreasing the strain rate. A decreased strain rate will allow the relatively rigid molecules at low temperatures to unwind and exhibit a relatively ductile behavior (Oswald and Menges, 1995). For instance, over the decades in polymer science, the equivalence between time and temperature has been utilized as a fundamental principle to facilitate analysis of very long-term response of the polymeric materials such as geotextiles in comparison to instantaneous tensile strength behavior (Dowling, 2007). The equivalence between temperature and time is explained based on alternating rate of molecular deformation in polymer with respect to load when the temperature is varied. At a low test temperature, the initial molecular deformation is relatively small compared to the relatively quick molecular deformation at a higher test temperature.

5.4.4. Shape and Development of Tensile Force – Displacement Curve

Figure 5.12 presents the mean force-displacement plots during extension loading as a function of the temperature at which they were obtained. Note that the colors of force-displacement curves used in Figure 5.11 for the replicate tests at each test temperature are consistent with the mean force-extension curves at different test temperatures in results presented in Figure 5.12 and subsequently. These mean curves are typical and descriptive in illustrating how the tensile behavior of single geotextile filaments at various test temperature conditions take form. The filaments from GSE NPNW-PP 8 oz/yd^2 geotextile resulted in a similar trend of tension load-elongation response at all test temperatures such that the tensile force-displacement curve has a nonlinear elasto-perfectly plastic form in terms of stress-strain relationship. The general pattern in force-elongation behavior of polypropylene filaments in tension tests can visually be portrayed in three segments: i) sharp increase to a local maximum; ii) steady rise at a reduced slope; then, iii) leveling off at higher strain levels. They exhibited nearly constant resistances after yielding until they reached rupture at elongations of between 70% and 120%. Before experiencing yield, the elastic portion of the curves develop with a relatively constant rate of change in tensile force with respect to displacement. As noted throughout this chapter, the observed micro-tensile straining behavior of single geotextile filaments plays a significant role in further understanding the interface shear response of geotextile-geomembrane layered systems.

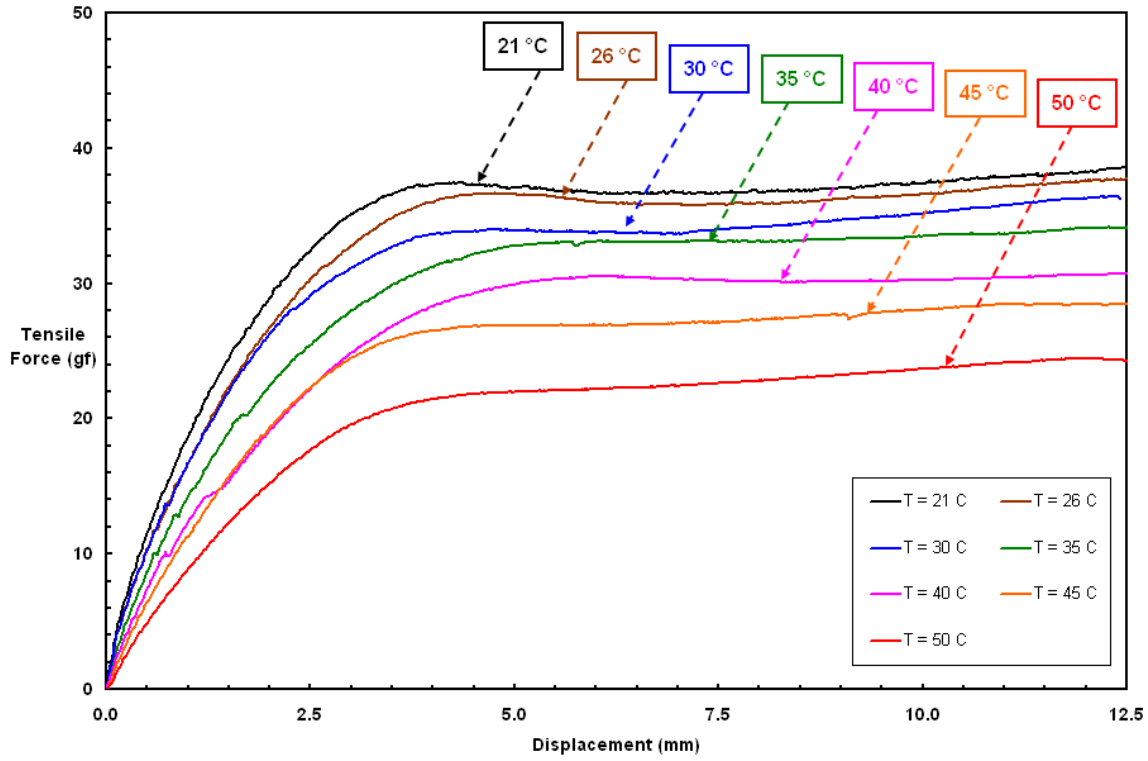

Figure 5.12 Mean Force – Displacement Curves of Single Geotextile Filaments made from Polypropylene at Different Temperatures

Moreover, the type of filament bonding and the generation of fiber networks in the geotextile have an important function and contribution to the elongation of the geotextile under tension such that the initial shape of the fiber networks is primarily determined by the degree of crimps of single filaments. Fabrics made from uncrimped fibers usually have a higher initial tearing strength and exhibit more stretching behavior at global-level. Under tension, the filaments constituting the geotextile are exposed to internal and external forces resulting in geotextile structure changes as well as single filaments strains. For example, the geotextile fibers are often connected in such a way that they present more volume and increased stiffness compared to their mass per unit volume (Lunenschloss and Albrecht, 1985).

To sum up, all filament specimens tested at different temperatures exhibited nonlinear elasto-perfectly plastic tension behavior under extension. The tensile strength was largest at room temperature and decreased with increasing temperature (Figure 5.12).

5.4.5. Stages of Force-Displacement Failure Envelope

Figure 5.13 illustrates the uniaxial force-elongation behavior for single filaments from a NPNW-PP geotextile under a "constant rate" of extension loading. The force-displacement curves underwent a relatively short elastic deformation stage compared with a longer plastic deformation phase. In other words, almost all filament specimens experienced larger strains prior to failure by progressing through all three main phases of elasto-plastic deformation. The tensile force increases rapidly within extensional displacement of 2.5 mm for the 12.5 mm long test specimens; then, it continues through the transition zone before reaching plastic deformation. It remains almost constant throughout plastic deformation until failure. In principle, the stress-strain behavior shown in Figure 5.13 can be divided into three separate zones, depending on the molecular response of the polymer to the level of applied strain (Stein and Powers, 2006; Dowling, 2007): i) Within Zone I, the response to load is instantaneous and elastic, since the deformations are recoverable upon load removal; ii) Deformations within Zone II are still recoverable, but not instantaneously. Time dependent response within Zone II usually is generally associated with visco-elastic behavior; iii) Within Zone III, the material exhibits an inelastic response in that the deformations are irrecoverable upon load removal and response within this region is related to visco-plastic behavior in which strains consist of visco-elastic as well as plastic components. In terms of physico-chemical considerations, the stretching of inter-atomic bonds occurs in Zone I when

going through elastic elongation. Throughout the transition zone (Zone II), polymer molecular chains get straightened. Lastly, the relative displacement of molecules in the polymer takes place in Zone III during plastic deformation.

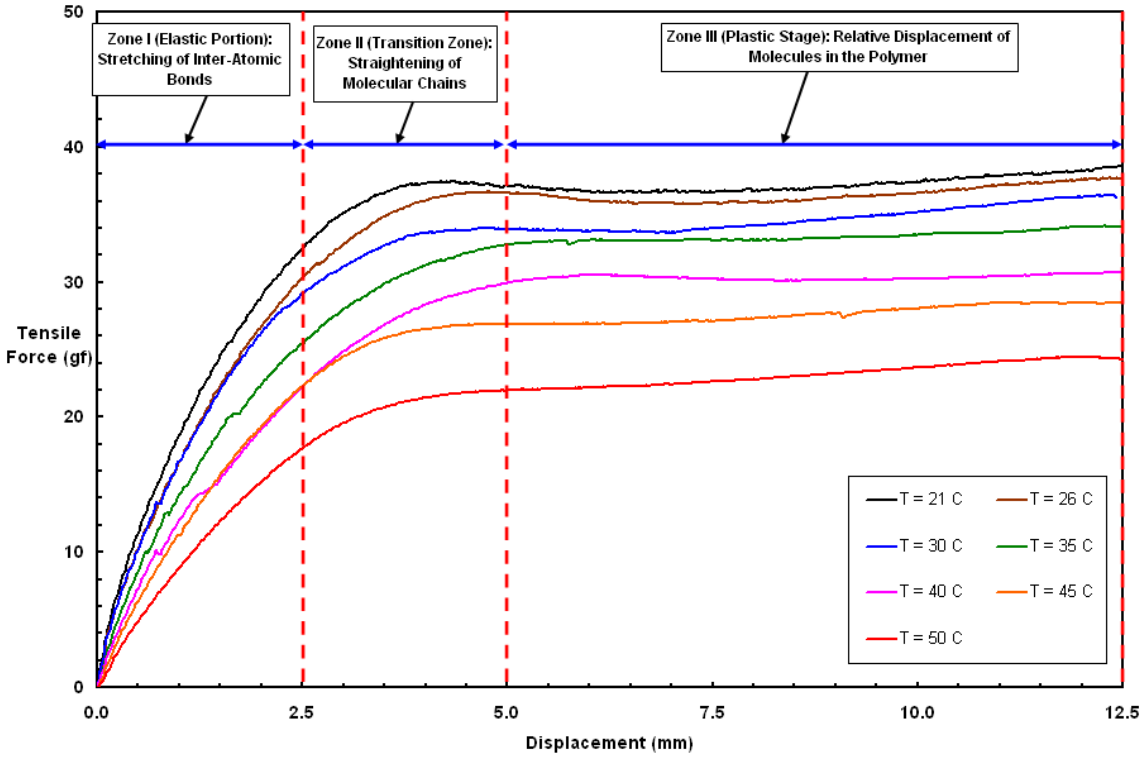

Figure 5.13 Complete Force-Extension Behavior of Single Filaments from NPNW-PP Geotextile Progressing through Different Deformation Zones

5.4.6. Modulus of Elasticity (i.e. Young's Modulus) and Temperature

It is very well known that polymeric materials typically exhibit nonlinear stress-strain behavior, since stress relaxation occurs throughout loading. The observed force-extension behavior of PP filament specimens indicated that the fibers become stronger and stiffer as temperature decreases under tensile load application. The elastic portion of

force-displacement curve rotates “clockwise” demonstrating the reduction in stiffness; hence, modulus with increasing temperature.

In order to compute elasticity modulus (Young’s modulus), the slope of initial linear portion of the force-displacement curves was used (which will later be visually illustrated in the chapter with some additional observations) as follows:

$$E = \frac{\sigma}{\varepsilon} \tag{5.6}$$

Where;

E: Young’s Modulus (Elasticity Modulus)

σ: Tensile Stress

ε: Tensile Strain

The mechanical properties of polypropylene fibers do not remain constant within the range of temperatures found in typical civil engineering applications. It was seen in the result of micro-scale thermo-tensile tests on single geotextile filaments that modulus of elasticity for polypropylene filaments decreased with increasing temperature. For the test temperatures evaluated in this study, the initial elastic modulus was the largest at room temperature. Figure 5.14 shows the change of elasticity modulus as a function of temperature. The data points were labeled according to test temperature beginning from room temperature rising up to an elevated temperature condition of 50 °C. The mean diameter of a single filament under zero tensile load is 35 μm (0.035 mm) which constitutes a cross sectional area of 9.62×10^{-10} m^2 (9.62×10^{-4} mm^2). When the measured

tensile forces on the order of 20 to 35 gram-force at various temperatures are divided by the small cross-sectional area of the filament; then, the resulting elasticity modulus values were in the order of tens of MPa. Geotextile filaments made from polymeric material were stiffer and firmer at lower temperatures and became relaxed and more flexible at higher temperatures. Therefore, temperature-induced changes in the modulus of polymeric filaments are important to consider in examining the variations in geotextile interface shear response with geomembranes, especially during the post-peak stage. Table 5.1 summarizes the statistical parameters for the modulus of elasticity for the single filament tensile tests at the various temperatures.

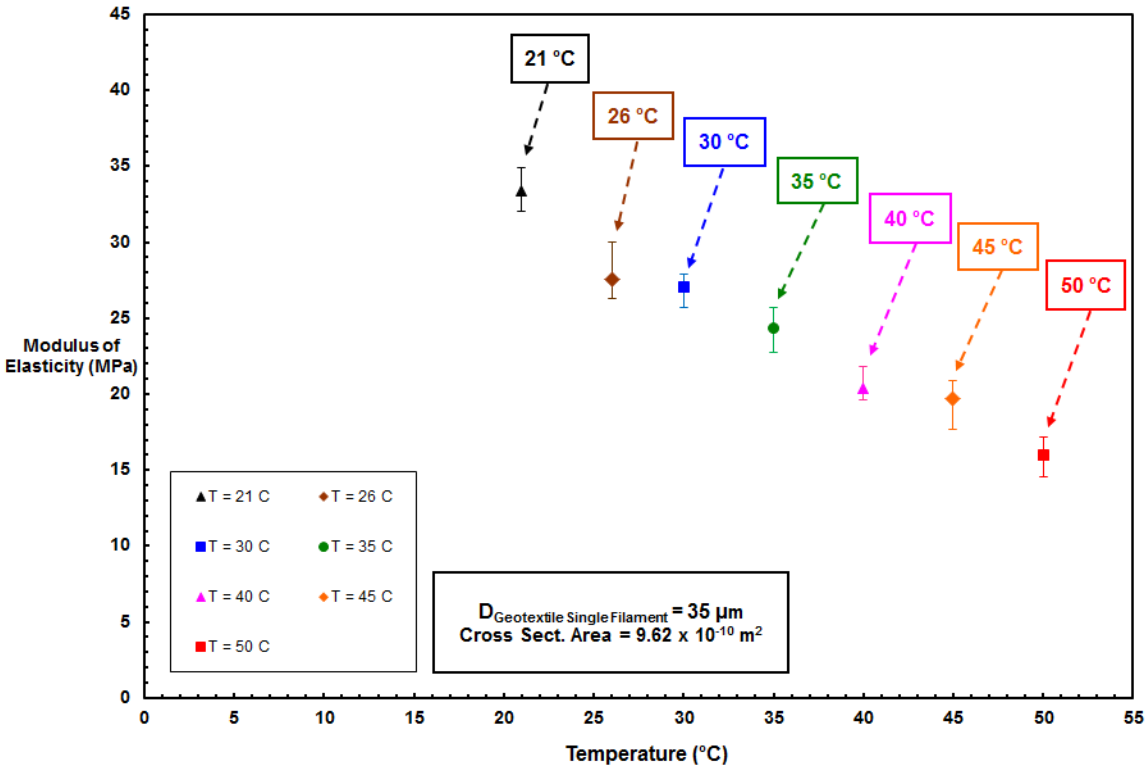

Figure 5.14 Modulus of Elasticity and Temperature for Polypropylene Single Filaments from NPNW Geotextile

Table 5.1 Statistical Parameters for the Modulus of Elasticity

Temperature (°C)	*Mean (MPa)*	*Std.Dev. (MPa)*	*Coeff. Of Variation*	*Range (MPa)*
21	33.40	0.97	0.029	2.89
26	27.52	0.59	0.021	3.73
30	27.09	0.42	0.016	2.25
35	24.33	0.71	0.029	2.91
40	20.40	0.48	0.024	2.23
45	19.71	0.92	0.047	3.16
50	15.97	0.41	0.026	2.63

An exponential regression analysis performed on the test data provided a good exponential decrease fit with a high "coefficient of determination" of 0.9722. The closeness of fit between the regression and test data indicates that there occurs a good correlation between the temperature and the modulus of the filaments (Figure 5.15).

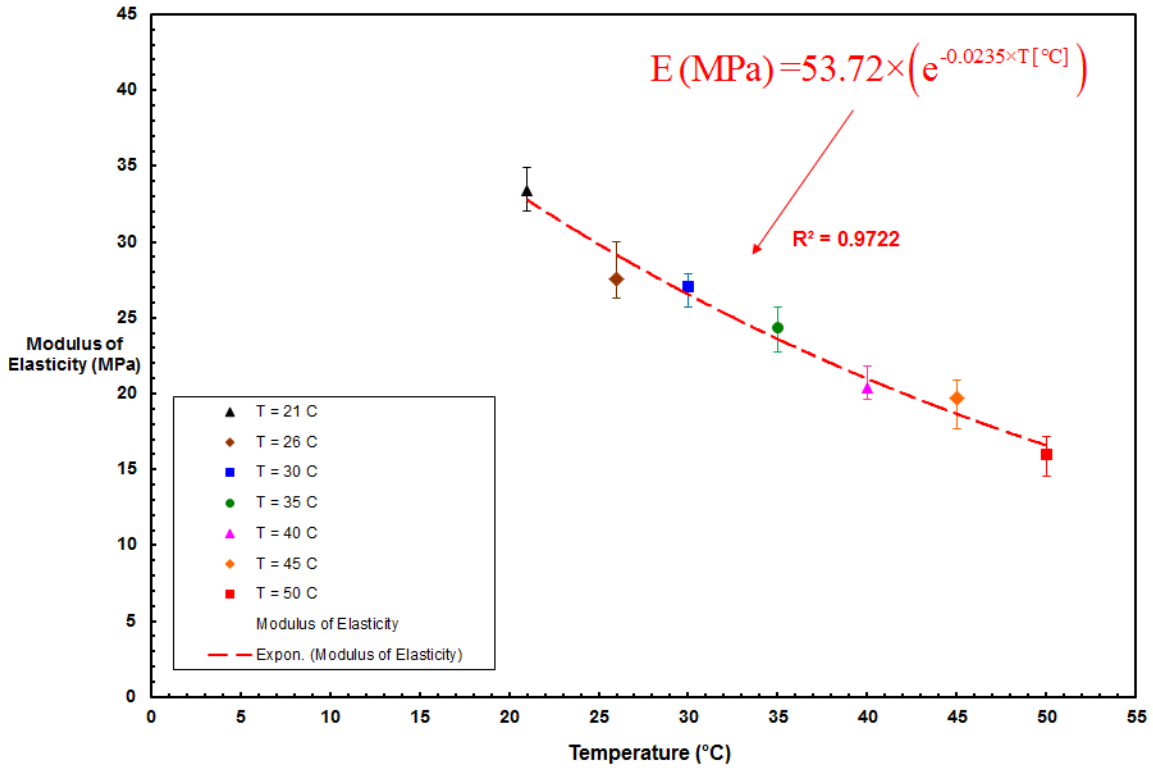

Figure 5.15 Exponential Correlation between Modulus of Elasticity and Temperature

The empirical relationship (Equation 5.7) between filament modulus and temperature was developed based on the results of micro-scale tensile tests at different temperatures and could be utilized as a mathematical equation to relate elasticity modulus to temperature change in which Young's modulus values follow an exponential pattern with increasing temperature for PP single filaments from NPNW geotextile.

$$E\,(\mathrm{MPa}) = 53.72 \times \left(e^{-0.0235 \times T[^{\circ}C]} \right) \tag{5.7}$$

Where;

E: Elasticity Modulus in MPa

T: Temperature in °C

5.4.7. Yielding & Elongation at Elastic to Plastic Transition and Temperature

Force-extension curves from the tension tests had a similar form with a sharp increase prior to arriving in the transition zone and ultimately experiencing plastic deformation at all temperatures. In light of this, the yield strength can be determined based on the concept of it being the point which has the largest curvature in the transition zone (i.e. elastic-to-plastic deformation) of force-displacement curve. Alternatively, the yielding strength could be identified at a point where the first departure from linearity occurs. In terms of physical considerations, the yield deformation is basically a transition zone from elastic to plastic straining (i.e. tensile elongation) wherein the deformations occurring are recoverable, but not instantaneously so as opposed to those developing in

the elastic stage which are instantaneously recoverable. The tensile response of polymers (i.e. PP geotextile filament) during yielding process is generally associated with visco-elastic behavior. The filament yield strength diminishes as temperature increases (Figure 5.16). Additionally, the mobilization of elastic to plastic deformation for polymeric filaments requires more elongation or displacement (i.e. straining) with increasing temperature as illustrated with blue arrow. The yield strength is largest at room temperature and shows a reduction at elevated temperatures. Further, as temperature rises, it requires less time to reach yield considering the tracks of quarter-circles in the force-extension curves in the graph (Figure 5.16).

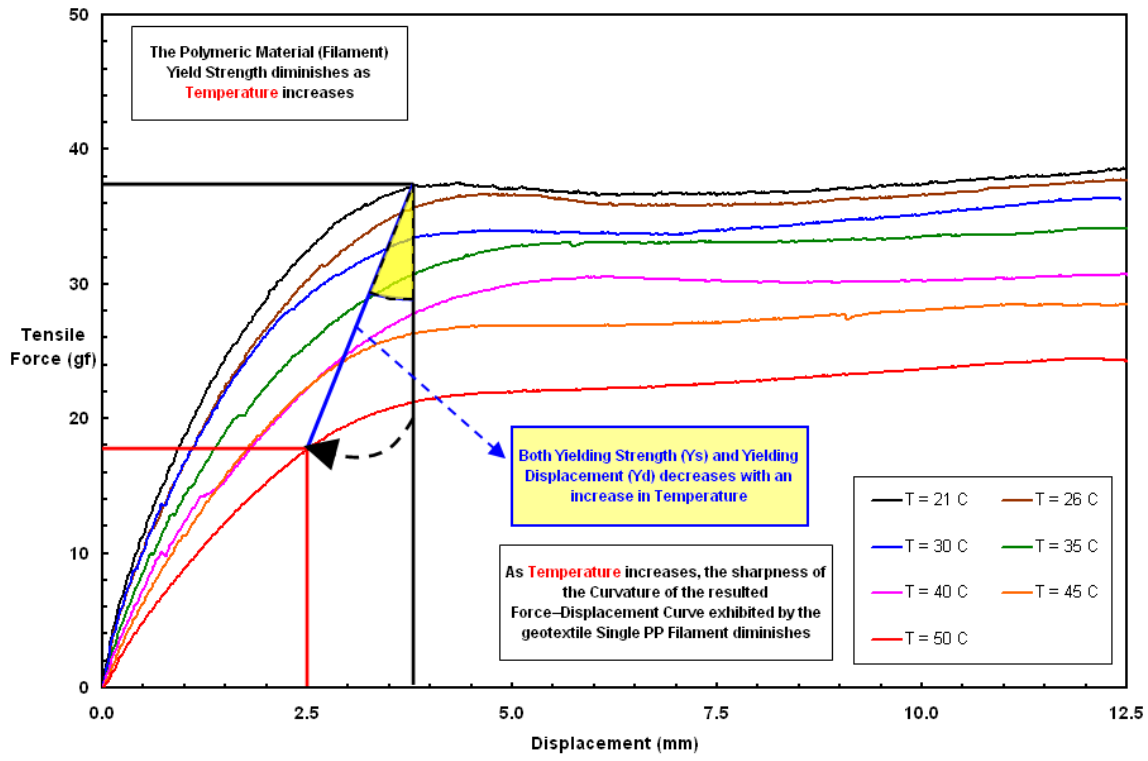

Figure 5.16 Alteration of Transition Behavior from Elastic to Plastic Elongation and The Change of Yield Strength with Temperature

The PP single filaments exhibited lower yield strengths and displayed smaller strains (i.e. extensional tensile displacements) prior to yielding at higher temperatures (Figure 5.17a and 5.17b, respectively). This is attributed to the loss of the polymer stiffness with increasing temperature. As such the polymeric material becomes softer and its endurance to sustain plastic deformation under tension and experiences permanent strains by encountering yield deformation stage at smaller tensile extensions. Tables 5.2 and 5.3 summarize the statistical parameters for the yield strength and yield displacement, respectively for the single filament tensile tests at the various temperatures.

Table 5.2 Statistical Parameters for the Yield Strength

Temperature (°C)	***Mean (MPa)***	***Std.Dev. (MPa)***	***Coeff. Of Variation***	***Range (MPa)***
21	380.09	1.53	0.004	14.36
26	362.21	2.96	0.008	15.28
30	333.23	3.35	0.010	14.82
35	295.35	4.07	0.014	17.37
40	250.89	3.82	0.015	20.84
45	245.72	3.11	0.013	31.36
50	181.08	3.78	0.021	19.25

Table 5.3 Statistical Parameters for the Yield Displacement

Temperature (°C)	***Mean (MPa)***	***Std.Dev. (MPa)***	***Coeff. Of Variation***	***Range (MPa)***
21	3.82	0.02	0.0052	0.12
26	3.75	0.02	0.0053	0.15
30	3.51	0.04	0.0114	0.11
35	3.26	0.04	0.0110	0.13
40	2.94	0.03	0.0102	0.15
45	2.88	0.02	0.0069	0.16
50	2.51	0.04	0.0159	0.17

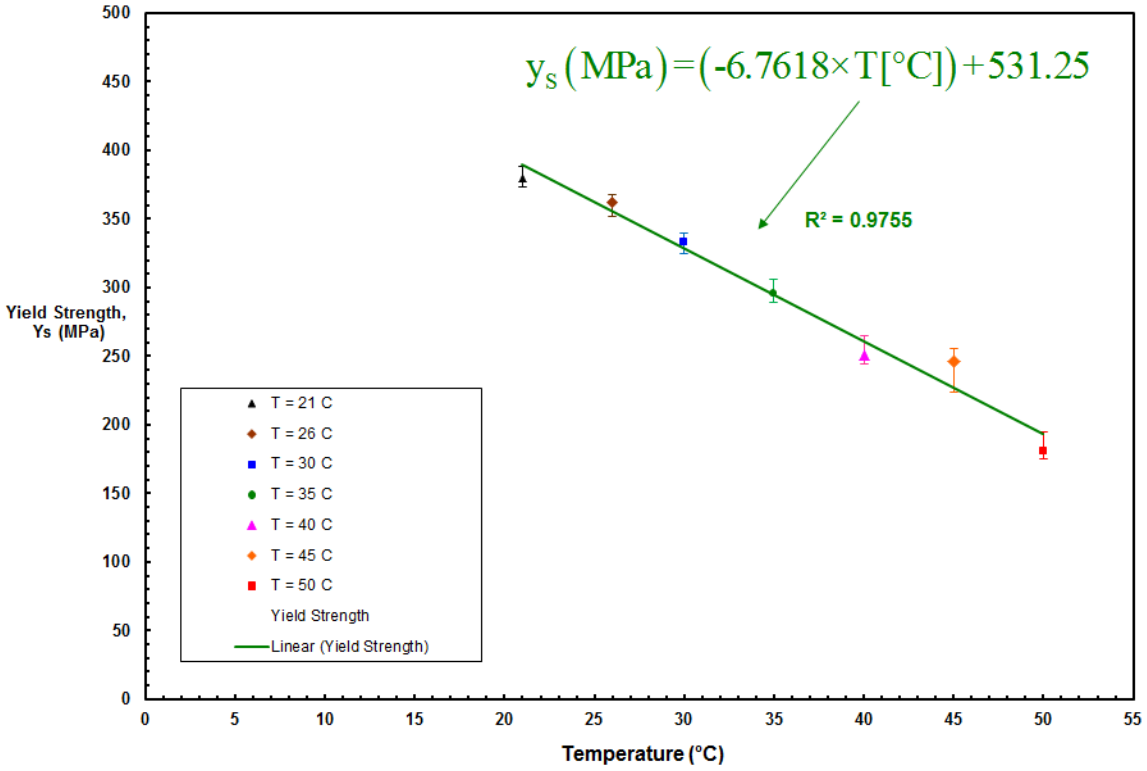

(a)

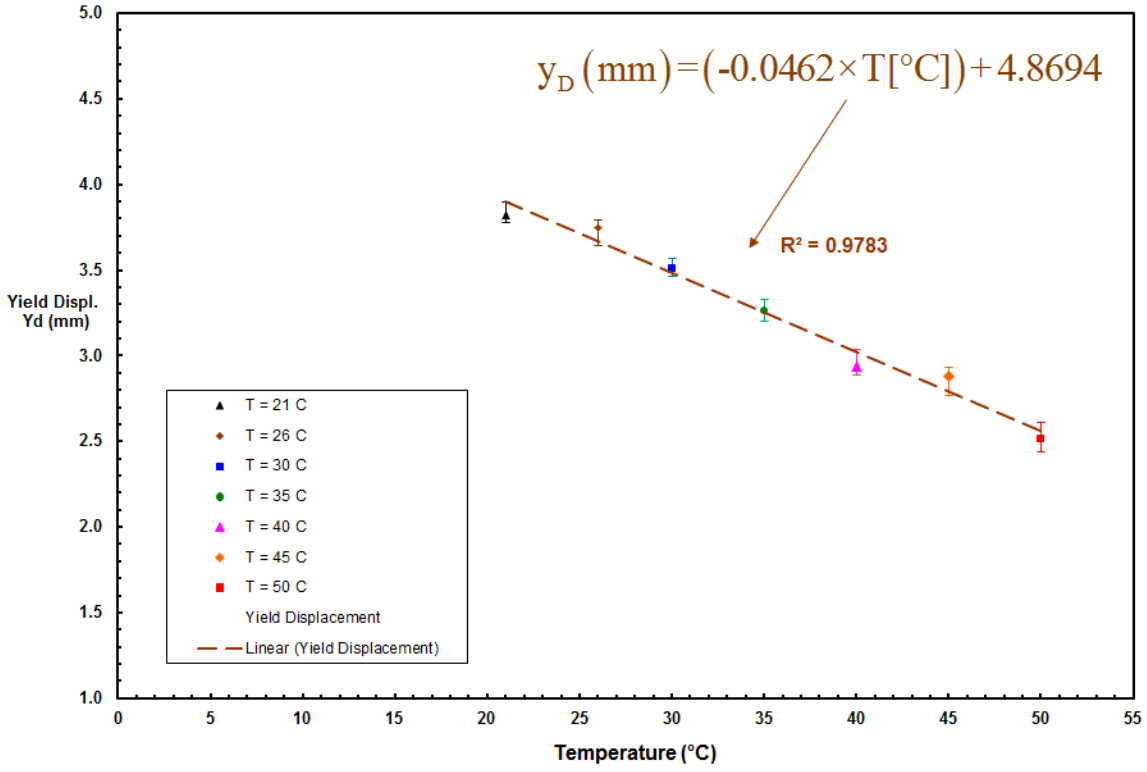

(b)

Figure 5.17 Change in Yield Strength (a) and Extensional Tensile Displacement exhibited to Yield (b) with an Increase in Temperature for NPNW-PP Geotextile Single Filaments

A linearly decreasing behavior was observed for both the yield strength and the tensile-extension displacement to yield as a function of temperature. The obtained empirical relationships (i.e. analytical equations) between yield strength and temperature as well as between yield displacement and temperature are given in Equation 5.8a (CoD = 0.9755) and 5.8b (CoD = 0.9783), respectively:

$$y_S\,(\mathrm{MPa}) = (-6.7618 \times T[^\circ C]) + 531.25 \quad (5.8a)$$

$$y_D\,(\mathrm{mm}) = (-0.0462 \times T[^\circ C]) + 4.8694 \quad (5.8b)$$

Where;

y_S: Yield Strength in MPa

y_D: Extensional Displacement to Yield in mm

T: Temperature in °C

5.4.8. Tensile Strength and Temperature

One of the most important mechanical properties of polymeric materials is its tensile strength under extension force that shows the toughness and indestructibility of the material employed in the field. Since a polymer type (i.e. PP) is used as a base material to produce geotextile fibers, they do not retain tensile strength and robustness properties with temperature change to which most geotechnical engineering applications are exposed. It was observed as a result of micro-scale thermo-tensile tests on geotextile

single filaments that tensile strength, (τ) for PP filaments decreased with increasing temperature with lower strength measured at higher elevated temperatures (Figure 5.18). In the experimental program temperature range (20 °C – 50 °C), the micro-tensile test at room temperature exhibited the largest toughness under extension and gave the largest tension strength value. Figure 5.18 shows the variation of the mean tensile strength as temperature changes. The data points were labeled according to test temperatures. The resulting computed tensile stress and strength were in the order of hundreds of MPa. Geotextile filaments at lower temperatures are more resistant but became weaker at higher temperatures. However, this is only micro-level response of single filaments extracted from a geotextile fabric. At global state, depending on fiber processing type and fabric manufacturing method, temperature has less significant influence on tensile properties of geotextile fibrous material sheet due to internal structural formation which is generated through fiber-fiber interlocking/bonding, nature of inner voids, and ability of filaments for rearrangement under external forces (See Section 5.3.3).

To sum up, there is an inverse proportion in between tensile strength of single filaments and temperature in which they possess higher strength values at lower temperatures due to more intact chemical composition and stronger bonding type of filament base polymer molecules (polypropylene) at cooler temperatures resulting from the material physico-chemical properties. An increasingly diminishing behavior in which the rate of decrease gets larger with increasing temperature was observed for the tensile strength and temperature relationship of the fibers. At the same time, no specific trend was observed for failure strain. Table 5.4 summarizes the statistical parameters for the tensile strength for the single filament tensile tests at the various temperatures.

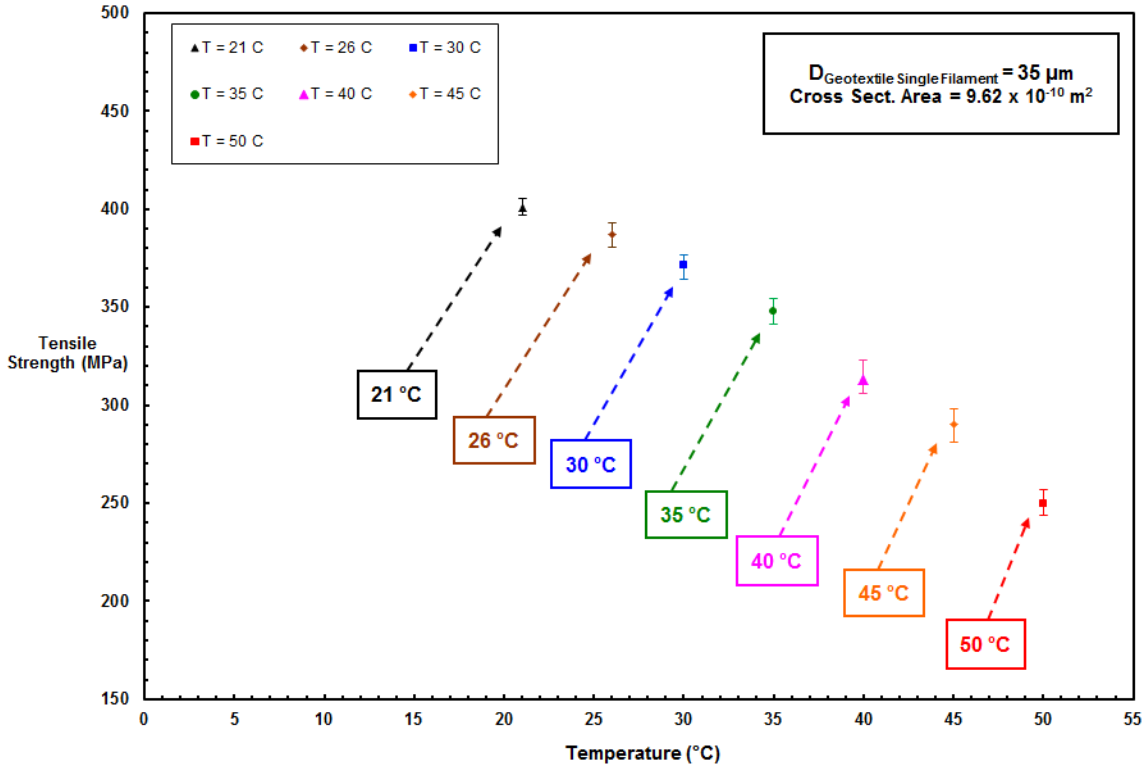

Figure 5.18 Tensile Strength and Temperature for Polypropylene Single Filaments from NPNW Geotextile

Table 5.4 Statistical Parameters for the Tensile Strength

Temperature (°C)	*Mean (MPa)*	*Std.Dev. (MPa)*	*Coeff. Of Variation*	*Range (MPa)*
21	401.05	2.13	0.005	8.18
26	387.27	2.71	0.007	12.18
30	371.16	2.47	0.007	12.54
35	348.03	2.89	0.008	13.50
40	313.06	2.92	0.009	17.34
45	290.35	3.74	0.013	17.03
50	249.47	2.35	0.009	12.78

Several different types of regression analyses such as linear, exponential, polynomial were performed on the micro-mechanical thermo-tensile test data. The 2nd

order polynomial regression provided the best correlation between tensile strength and temperature such that a very good fit between intermittent test data and continuous regression curve for which a higher coefficient of determination (CoD) of 0.9972 was obtained compared with that of linear or exponential regression methods which gave lower CoD values (Figure 5.19).

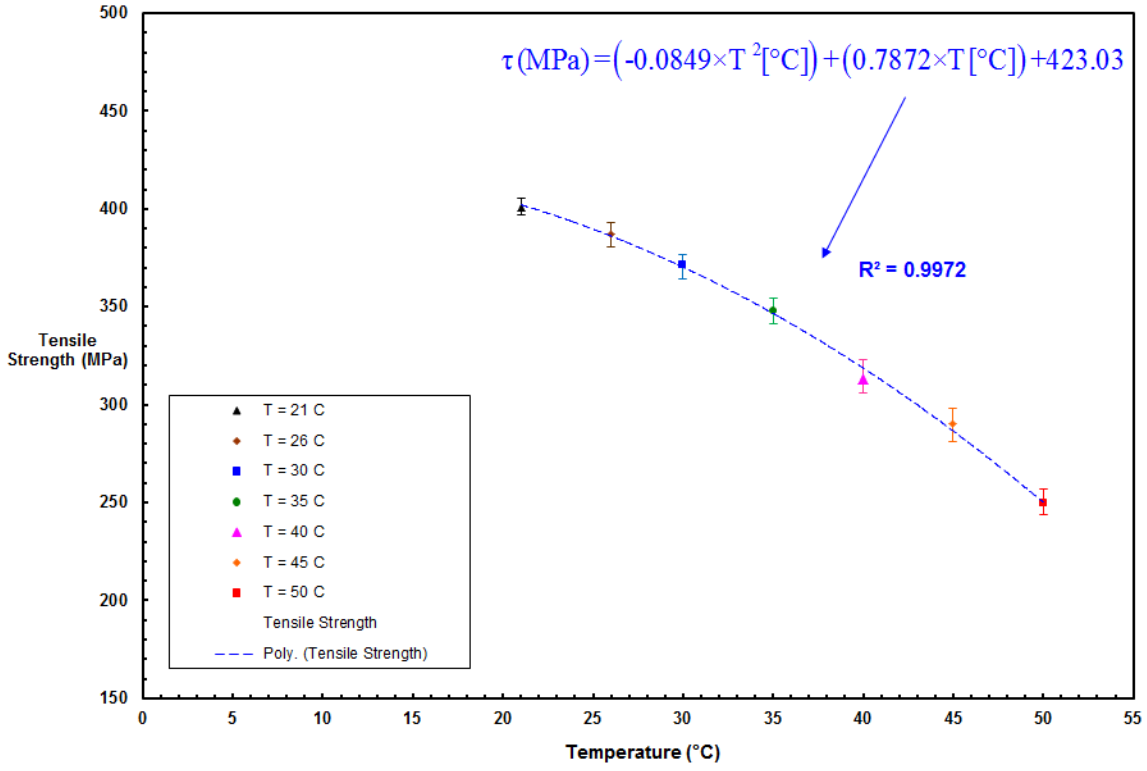

Figure 5.19 Second Order Polynomial Correlation between Tensile Strength and Temperature

For single filaments extracted from NPNW-PP geotextile and stretched under extension force at micro state at several temperatures, the equation relating tensile strength to temperature change is given as follows:

$$\tau(\text{MPa}) = \left(-0.0849 \times T^{2}[°C]\right) + \left(0.7872 \times T[°C]\right) + 423.03 \quad (5.9)$$

Where;

τ: Tensile Strength in MPa

T: Temperature in °C

This empirical relationship (Equation 5.9) developed through regression analysis of micro-tensile test data between strength and temperature can be utilized to relate the change in tensile strength to the variation in temperature.

5.4.9. Filament Base Polymer Type and Relative Importance of Tensile Properties of Geotextile Fibers (Perspectives in Different Design Purposes)

Fibers in geotextile fabrics lose their tensile strength due to thermally induced relaxation effects resulting from inherent physico-chemical properties of the material (Tisinger et al., 1990). Further, in addition to fiber-fiber processing and fabric manufacturing technique, the magnitude of tensile strength produced by fibers under load and the extent of durability in operation developed by filaments in geotextile are basically governed by the base polymer material from which the filaments are produced. For example, the sensitivity of geotextiles under tension increases in the order as polyester (PET) having the least, then polyamide (PA) and polypropylene (PP), and polyethylene (PE) possesses the most (Hoedt, 1986). For a quantitative comparison, under the same constant tension load, PET strains less than 2%; PA strains about 5%; PP strains 10-20%; PE strains more than 20% which is more than “10 times” the elongation that a PET

geotextile experiences. Therefore, it is recommended for geotextiles that are loaded for prolonged periods of time (i.e. 10-100 years), the permissible load for PET is of the order of 50% of the tensile strength; for PA of the order of 40% while for PP as well as PE geotextiles, a load below 25% is suggested (Hoedt, 1986). This highlights the importance of considering temperature in designs involving polymeric geotextiles in short-term versus long-term applications. For this reason, the results of micro-mechanical tensile tests at different temperatures on single filaments could be considered a useful measure for short-term design. Otherwise, polymeric geotextile endurance properties against outside factors impacting a long-duration application such as creep must be considered for the purpose of long-term construction in which a fabric will be subjected to tension in the application.

In this study, the influence of temperature on the tensile strength properties of filaments and in determining their interaction mechanisms with texture elements at the micro-scale in evaluating the developed interface behavior with changing temperature conditions was studied. However, it should be noted that geotextiles are used for a number of different civil engineering applications. The requirements the geotextiles have to fulfill depends largely on the type of application, and also, may differ widely depending on the geological and geometric boundary conditions when tensile strength properties of the geotextile are concerned (Hoedt, 1986):

i. In the case of geotextile separating layers, the fabric should be capable of separating soil layers and of keeping them separated; hence, the geotextile is allowed to gain tensile elongation and hardly contributes to reducing soil

deformations. ➔ The tensile force-elongation behavior of geotextile filaments/fibers is *"no criterion"* at all.

ii. The use of geotextiles as filter material requires that specific soil particles must be retained under all kinds of flowing conditions and that the permeability to water remains unchanged; hence, for the case of proper construction, the tensioning due to elongation are relatively low and moreover, the filter criteria are not so sensitive to an increase in geotextile tension, and consequently, to planar elongations only of the order of a few percent. ➔ The tensile force-elongation behavior of geotextile filaments/fibers is only *"a minor criterion"*.

iii. When geotextiles are used for drains, in particular, the water discharge capacity is decisive; hence, the tensioning of geotextile fabric, and consequently, the elongation of the fibrous material under the influence of soil pressures may show a slight importance. ➔ The tensile force-elongation behavior of geotextile filaments/fibers is a *"slightly important criterion"*.

iv. For reinforcing the soil, the geotextile itself must prevent or reduce soil deformations. The degree of elongation, and consequently, the created tension in the geotextile fabric is crucial to prevent instability and is vital for safety of the design. Therefore, the tensile properties of geotextile filaments, fiber bonding strength, fabric interlocking manufacturing process will become of importance in geotextile type selection to be utilized under tension loading. Since, too large an elongation inevitably leads to local or complete collapse of the construction. ➔ The tensile force-elongation behavior of geotextile filaments/fibers is a *"very important criterion"* which is crucial for the safety.

These conclusions previously highlighted by Hoedt (1986) were built on macro-level design perspectives and involved in global aspects of the strength and the frictional resistance properties of the fibrous geotextiles having heterogeneous structural characteristics. As such, the different macroscale design perspectives of the geotextiles were proposed and listed based on only the global-matrix behavior and the macro-response of the geotextile under load. However, it is noted that the magnitude of the tensile strength mobilized in the geotextile-structure as well as the resulting frictional resistance developed at its interface against another counterface component over the entire extent of the contact area are governed by and originated through the micro-scale filament interaction and interlocking mechanisms as well as the number of contacts between the fibers depending on boundary and stress conditions. The application of a load on the geotextile – geomembrane interface layered system results in the embedding of the roughness features (i.e. texture elements) of the geomembrane into the matrix of the geotextile containing void spaces (i.e. porosities) or the so-called holes designated and identified based on global-scale observations made on the fabric. Higher embedding/interbedding of the textural features of the counterface geomembrane corresponds to the geotextile possessing bigger holes (i.e. void spaces) (Hebeler et al., 2005; Bacas et al., 2011). As presented in Figure 5.20a – 5.20c showing SEM images for the structure (composed of i- fibers; and, ii- porosities) of different fabric types, a geotextile manufactured by needle-punching technique and made from staple-fibers (i.e. the geotextile type used in the laboratory testing program) possesses the largest void spaces in the fabric structure as compared to the geotextiles either made from mono-filaments or produced using a heat-bonding process.

Based on the primary research works of Barton (1973), Barton and Choubey (1977), Bandis et al. (1983), Barton et al. (1985), Stark et al. (1996) and Hebeler et al. (2005), an empirical relationship was developed by Bacas et al. (2011) to compute the value and to evaluate the magnitude of geomembrane texture elements embedding into the geotextile matrix under loading by defining a quantitative parameter called "interbedding factor" which depends on the type of the fabric. There are two different aspects of this phenomenon both of which favorably contribute to tensile strength properties of the fabrics mobilized in the course of shear displacement against a continua and the resulting tension of the geotextile developed under tensile forces. It was indicated that the *interbedding coefficient* increases with increasing normal stress as the geotextile is compressed and the interlocking mechanism between the textural features and the filaments increases. As per micro-scale perspectives, an external extensional force exerted on the geotextile matrix at global-level results in tension in the fabric that causes the fibers/filaments in the geotextile structure at micro-level to become stretched as well as exhibit elongation (i.e. axial strain) in the direction of the applied load. Therefore, transverse contraction and strain (i.e. thinning) occurs in the filament as it becomes thinner in the direction orthogonal to the loading (i.e. Poisson Effect). Since the filament is an elasto-plastic polymeric micro-scale material having a cross-sectional diameter on the order of the tens of micrometers (μm) and has a certain Poisson's ratio ranging from 0.1 to 0.2 depending on the base polymer type (e.g. PP, PET). Note that a PP polymer tape having a cross-sectional diameter on the order of tens of the millimeter can result in a Poisson's ratio up to 0.45 under extensional force which occurs largely at constant volume (Daniels, 1989; Dowling, 2007). As described in Stein and Powers (2006), the

Poisson's effect in the polymers is caused by slight movements between molecules on the molecular level and the stretching of molecular bonds within the material lattice to accommodate the stress. When the bonds elongate in the direction of the load, they shorten in the other directions. This behavior occurring at the molecular level is multiplied by an enormous number of repetitions and progresses throughout the material lattice driving the Poisson's phenomenon that results in extension in axial direction and accompanied by contraction in the transverse direction.

The transverse contraction due to the axial strain and extension occurred in the individual filaments results in a decrease in the contact area between the different fibers in the fabric structure. The decrease in the contact area is accompanied by an increase in the contact stress at the contact points between the separate filaments. Additionally, when the fibers becomes thinner and finer, the total number of contact points at a certain volume of the geotextile matrix increases which results in increased filament interaction (i.e. inter-contact) as well as increased interlocking (i.e. inter-connect) between the different fibers per unit area of the fabric. Consequently, this will enable the fibrous geotextile in sustaining (i.e. withstanding) greater tension under load, and additionally, facilitate the mobilization of larger frictional resistance (i.e. shear strength) in the course and during the mobilization of shear displacement against the geomembrane by allowing higher interaction and interlocking of the geotextile filaments with the counterface geomembrane roughness features.

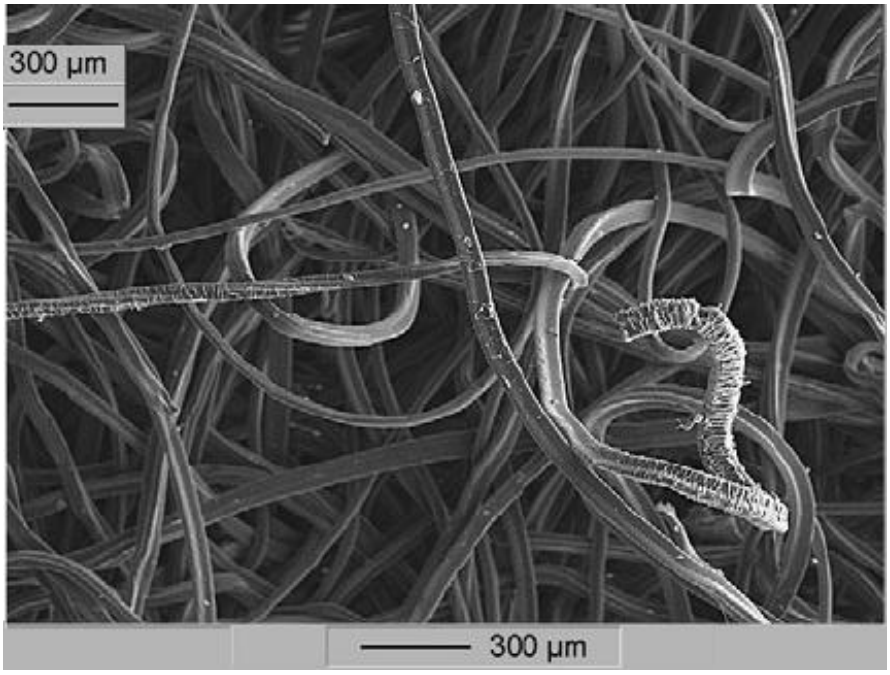

(a) ***NPNW-PP*** *Staple-Filament* Geotextile

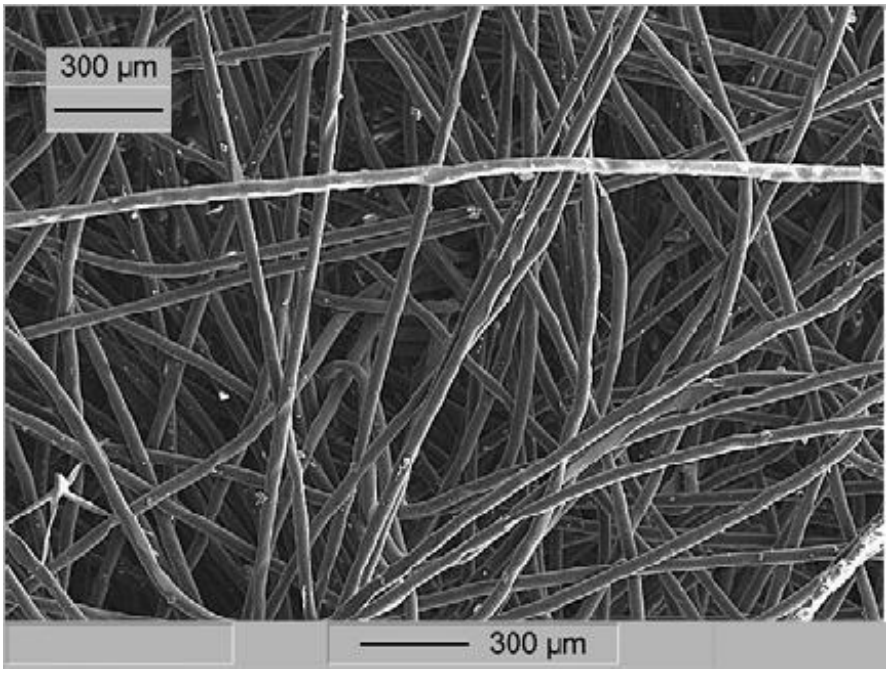

(b) ***NPNW-PP*** *Mono-Filament* Geotextile

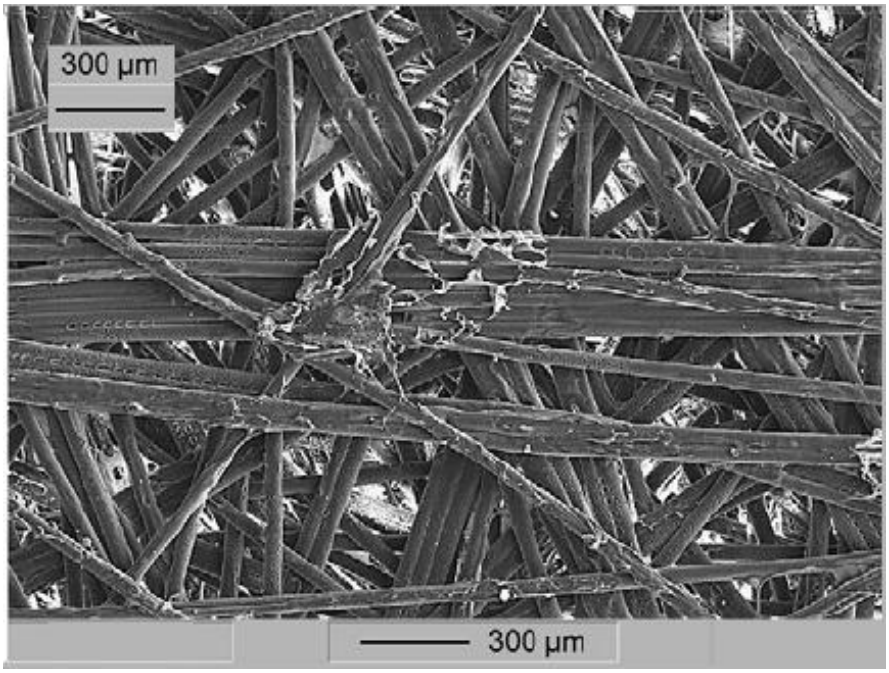

(c) ***HBNW-(70% PP & 30% PET)*** *Mono-Filament* Geotextile

Figure 5.20 SEM Images of Different Types of Geotextiles Showing *Micro-Scale* ***Filament Interactions*** (Inter-Contacts) and *Micro-Level* ***Fiber Interlockings*** (Inter-Connections) governing Macro-Scale (Global Level) Frictional Resistance Characteristics and Tensile Strength Properties (Bacas et al., 2011)

For a quantitative estimate of the resulting shear strength mobilized at geotextile – geomembrane interface based on geotextile compression under load application and embedding the roughness features (i.e. texture elements) of the geomembrane into the counterface geotextile fabric matrix produced using different manufacturing techniques (i.e. needle-punching, heat-bonding), Bacas et al. (2011) developed an empirical relationship by proposing a comparative index called the interbedding coefficient (I) which provides the relative interbedding of the texture elements into the different types of the geotextiles. It was noted that the shear strength mobilized at geotextile – geomembrane interface is primarily influenced by the amount of embedding/interbedding

and the degree of roughness. Equation 5.10 shows the peak strength criterion proposed by Bacas et al. (2011) for geosynthetic interfaces based on the results of direct shear tests on different geotextile – textured geomembrane interfaces:

$$\tau = \sigma_n \times \tan\left[HL \times I \times \log\left(\frac{GCS}{\sigma_n} \right) + \varphi_r \right] \quad (5.10)$$

Where;

τ: Peak Shear Strength

σ_n: Normal Stress

GCS: Geotextile Reference Compression Stress

HL: Hook and Loop Coefficient

I: Interbedding Coefficient

φ_r: Residual Friction Angle

It was indicated that, for practical purposes, the GCS can be found using Equation 5.11 as follows (Bacas et al., 2011):

$$GCS \approx \left[\frac{2 \times T_M}{\text{Geotextile Thickness}} \right] \quad (5.11)$$

Where;

GCS: Geotextile Reference Compression Stress

T_M: Maximum Tensile Strength of the Geotextile

This empirical relationship can be used to approximately assess the tendency for the compressibility of the geotextile due to applied tensile load in the planar areal extent of the fabric sheet. Similarly, the stronger interlocking interaction mechanisms produced between the individual fiber elements during shearing result from planar straining/tensioning of the fibrous geotextile.

To provide a comparative evaluation between different types of the geotextiles in facilitating or promoting the embedment of the counterface texture elements and thereby allowing for the mobilization of greater frictional resistance at the interface, the ratio of the interbedding factors,(I) for NPNW-StapleFilament, NPNW-MonoFilament geotextiles relative to that of HBNW-MonoFilament geotextile (i.e. defined as basis since it allows the least amount of embedment of the counterface textures) are 1.80 and 1.35, respectively. It is noted that these are not absolute "I values" which can be utilized for the aforementioned geotextile types for the calculation of the peak shear strength (Equation 5.10), but only relative values provided to make comparison between different geotextile types in terms of the relative amount of the embedment occurring at the interface in conjunction with the rough geomembranes. The larger openings (i.e. void spaces) available in the NPNW-StapleFiber, as shown in Figure 5.20a, expands the understanding (i.e. strengthens) and agrees with the occurrence of greater embedment of the texture elements into the geotextile and expands the understanding for the development of higher interaction, larger inter-contact and interlocking between the filaments and the macro-roughness features.

The analytical relationship developed through empirical results and presented in Equation 5.10 features three unique distinct parameters including GCS, HL and I. The physical implications of every parameter were described in Bacas et al. (2011) as follows:

- The geotextile compression stress (GCS) is defined as a reference value such that it is the normal stress on the geotextile which causes a normal strain of 0.8 in the geotextile. The geotextiles they tested showed an inflection point at 0.8. Beyond this point, the normal stress increased asymptotically. It was indicated that the GCS controls the interaction mechanisms between geotextiles and textured geomembranes.
- The hook and loop coefficient (HL) represents the engagement of the geotextile fibers (i.e. loop structure) with geomembrane roughness (i.e. hook material) proposed based on interpretation made on the previous primary research work of Hebeler et al. (2005) for the development of the mechanism of hook-loop interaction between the filaments and the texture elements.
- The interbedding coefficient (I) was characterized as the penetration of the roughness features of the geomembrane into the geotextile. It is noted that the interbedding factor depends on the type of geotextile. Higher interbedding corresponds to geotextiles with bigger porosity openings on the geotextile matrix as shown for the geotextile manufactured by needle-punching and using staple fibers. Additionally, it was indicated that the interbedding coefficient increases with increasing normal stress due to larger compression of the geotextile and the resulting tension and elongation in the geotextile planar extent that is perpendicular to the normal load application, and therefore, the interlocking between the filaments and the textures increases.

The total contact area involved during shearing of the geomembranes against geotextiles depends heavily on the development of tension in the fiber and the tendency of the filament to elongate such as occurs at high temperatures, or the higher amount of axial strain and the resulting larger transverse contraction exhibited by the individual filaments as encountered by the geotextile – geomembrane interface systems at elevated temperature conditions in the course of shear displacement. As such the frictional resistance mobilized at geotextile versus geomembrane interfaces is heavily governed by the magnitude of the interbedding of the roughness features into the fabric matrix. This facilitates stronger interlocking between the counterface materials resulting from the presence of larger contact stresses at contact points in the micro-level due to reduced contact area between the different individual filaments subjected to tensional elongation (i.e. axial strain) because of the existing tensile force developed on the geotextile structure under load application and during the course of shearing displacement.

5.5. Evaluation of Single Filament Test Results

5.5.1. Discussion on Elevated Temperature Effects on Geotextiles based on Single Filament Tensile Test Results at Different Temperatures

The field deterioration of geotextiles fundamentally results from damaging *"thermal effects"* and *"mechanical stresses"*. Therefore, it is very important to understand and hence, evaluate the influence of thermal effects on the micro as well as the global load-deformation response of geotextiles. The "thermally" induced relaxation effects on the fibers/filaments involves mechanisms which cause geotextile degradation

such that geotextile weight and thickness are subjected to deterioration resulting from mechanical breakage and loss of fibers. The resulting impact of this decay in geotextile fibers due to thermally induced relaxation is to yield a significant "reduction in tensile strength, ductility" and "loss of integrity" in fabric material. In addition, this degradation across the geotextile is nonuniform due to inhomogeneity in the manufacturing process producing regions of variable fiber orientation. Therefore, it is more crucial in terms of the fabric endurance properties at the global state (Tisinger et al., 1990).

In an attempt to further understand temperature effects on geotextile single filaments influencing particularly the post-peak interface behavior of geotextiles sheared against geomembranes, micro-scale tensile tests were performed on single filaments to characterize their thermal and mechanical response at elevated temperature conditions. Figure 5.21 provides an illustrative explanation regarding the general influence of temperature on the shape of the force-extension failure envelopes of single filaments tested at different temperatures. It was observed that all of the curves follow very similar pattern with an initial increase and thereafter a non-linear behavior however, the PP fiber tension failure envelopes diminish and the size of area under the curve shrinks as ambient test temperature increases (Figure 5.21). In other words, for the tested polymeric single filaments, the force-displacement curves from elevated temperature tests fall within the failure envelope of that defined by the room temperature test.

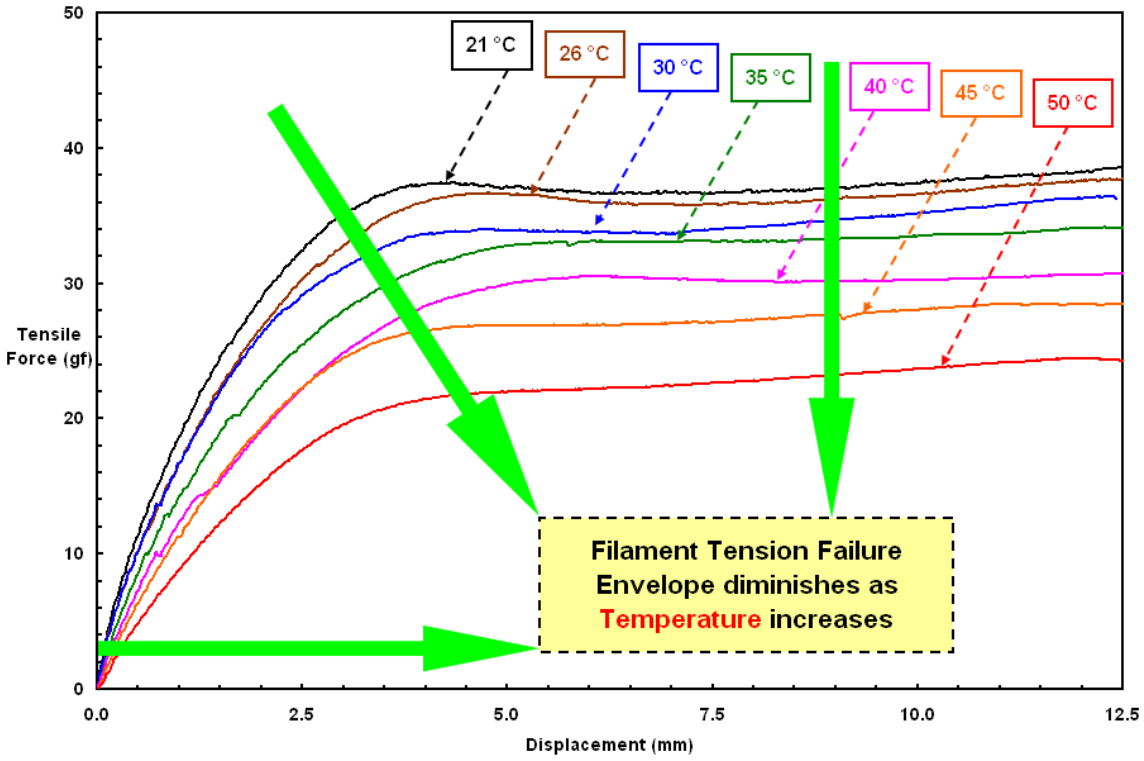

Figure 5.21 Modal Shape Alteration of Tensile Force-Extensional Displacement Failure Envelopes of Geotextile Single Filaments with Temperature Change

The tension curves are dominantly exhibiting a nonlinear pattern with a gradual decrease in inclination of initial linear slope as temperature increases indicating lower initial stiffness or modulus at elevated temperatures (Figure 5.22). In other words, the linear elastic portion of the curve rotates clockwise with increasing temperature demonstrating a reduction in the material stiffness. Therefore, it is evident that the filament modulus is inversely proportional to temperature. The maximum stiffness for all tests conducted in this study was obtained at the lowest temperature (i.e. room temperature). At higher temperatures, the filaments underwent larger deformation before proceeding to the occurrence of yielding or transition deformation from elastic to plastic elongation. The tensile strength values obtained at lower temperatures were higher than

those obtained at higher temperatures due to polymer physical properties varying with temperature and the bonding strength of polypropylene molecules (Figure 5.22).

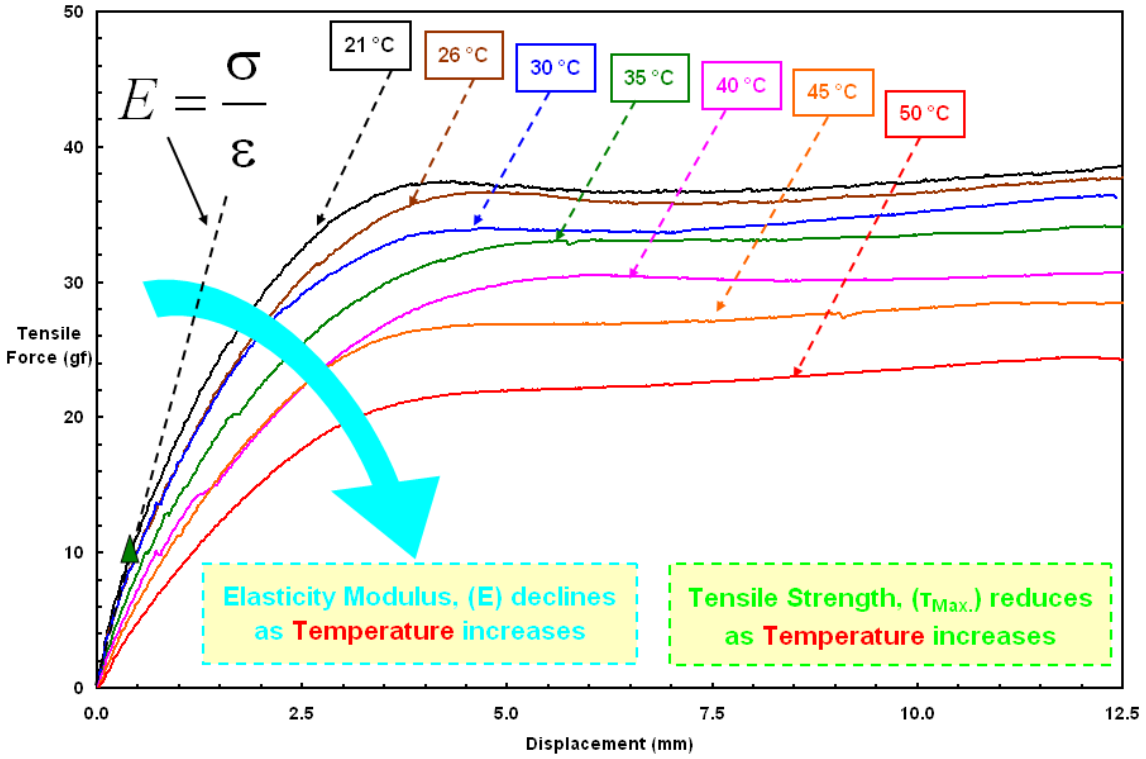

Figure 5.22 Clockwise Rotation of Initial Linear Elastic Portion of the Tension Curve and Reduction in Plastic Limit Strength

The ambient temperature change was found to be an important factor affecting the filament properties such as strength, ductility and elongation at yield. Fiber strength can be considered as the major factor controlling geotextile micro-scale, and consequently, macro-scale tensile strength properties. This is in confirmation with the findings of Andrawes et al. (1984) in terms of fabric tensile response at global state at elevated temperatures as well as with the observations of Tisinger et al. (1990) for the change of

mechanical and durability properties of fabrics as a result of thermally induced relaxation effects on the fibrous materials produced from polymers.

5.5.2. Efficiency/Contribution of Locally Developed Single Filament Tension to Globally Generated Tensioning of Geotextile Fabric

As indicated earlier, many geosynthetics such as geotextiles are designed to complement the relatively low tensile capacity of soils. Additionally, in the composite geosynthetic layered systems in which geotextiles and geomembranes are installed adjacent to each other and they create an interface, sliding failures are known to accompany tension of geotextiles (Mitchell and Seed, 1990). In this study, geomembranes with relatively high rigidities (i.e. HDPE) were selected to quantify the effects of geotextile strain on the shear behavior developed, thereby limiting the effect of geomembrane strains during the progression of stress-strength-strain response of geotextile – geomembrane interfaces. Consequently, it is worthwhile to examine the efficiency/contribution or the role of locally developed geotextile single filament tension at "micro-scale" level due to micro-mechanical interactions between fibers and textures at the interface to globally developed tension of a geotextile fabric sheet at macro-scale. This will provide an important insight and understanding in terms of linking up and relating single filament tensile behavior at "micro-scale" to geotextile tensile response at the "global-scale".

The wide-width tensile strength tests were performed by Kim (2006) following the procedure described in ASTM D 4595 on GSE needle-punched nonwoven (NPNW) geotextiles having mass density of 8 oz/yd^2 (270 g/m^2) to evaluate "macro-scale" tensile

stress-strain properties of a nonwoven geotextile widely used in geotechnical applications as well as to investigate the contribution of the developed tensile strength of single filaments to the overall wide-width tensile stress-strain properties of the geotextiles. Figure 5.23 shows the result of a wide-width tensile test on GSE NPNW 8 oz/yd^2 geotextile. In his study, 100 mm width by 200 mm height was chosen for the specimen size in order to satisfy the ASTM recommendation as well as to subject the specimen to boundary conditions similar to the specimens used for shear tests conducted on geotextile – geomembrane interfaces.

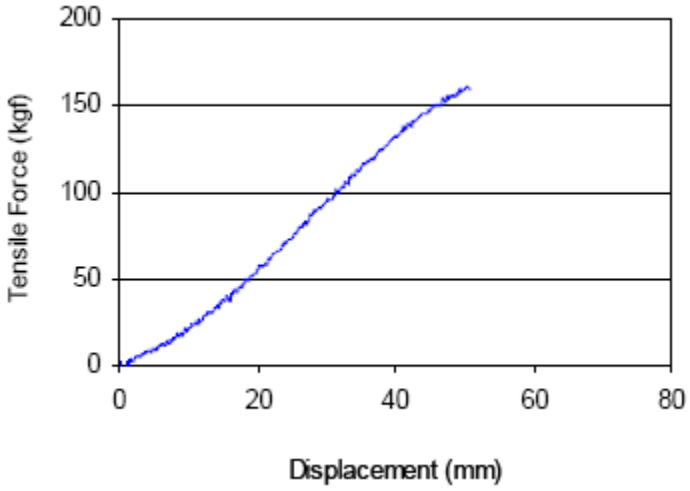

Figure 5.23 Result of Wide-Width Tensile Strength Test on GSE NPNW 8 oz/yd^2 (270 g/m^2) Geotextile (Kim, 2006)

It was reported by Kim (2006) as a result of wide-width tensile strength tests that GSE NPNW 8 oz/yd^2 had tensile modulus of about 3488 gf/mm for 10 cm width at an elongation measurement of 50 mm. The tensile strength corresponding to 12 mm elongation was about 41856 gf (Figure 5.23). A single filament from the same geotextile

had nominal yield strength of 33 gf. The average number of geotextile filament phases, he observed from the cross-section of a post-test wide-width geotextile specimen images, was approximately 18000 for a 10 cm width specimen. For 100 % efficiency of tension, where all the filaments contribute completely to generate their yield tensile strength, the total tensile capacity of "ideal" wide-width geotextile specimen (TC_{ideal}) computed was 594000 gf. As a result, it was noted that the geotextile has about 7.05 % $\left(= \left[\frac{41856}{594000} \right] \times 100\% \right)$ of its efficiency on tensile strength generation compared with the TC_{ideal} of the filaments.

This computational result comparing the total tensile capacity of a "real" wide-width geotextile specimen with total tensile capacity of "ideal" wide-width geotextile specimen by linking through 100% efficiency of tension where all the filaments contribute completely to generate their yield tensile strength is beneficial in further understanding as well as providing insight about geotextile inner structure formation such that the total deformation (extension or contraction) is the summation of the deformations in the filaments and the deformations due to the rearrangement of the internal structure as described by Andrawes et al. (1984).

5.6. Summary and Conclusions

Tensile strength is an important design parameter to be established properly when a composite layered system involving geotextile-geomembrane or geotextile-soil material interfaces are created or when a reinforcement inclusion is embedded in soil. The behavior of composite layered systems as well as reinforced soil structures are largely governed by interface interaction mechanisms that develop between fabric-texture and fabric-particulate materials originating through micro-scale fiber-texture interlocking that is closely related to the tensile strength properties of single geotextile filaments and fiber-particulate contact behavior. Therefore, the assessment of "micro-scale" mechanical and durability properties of single geotextile filaments in terms of tensile stress-strength-strain behavioral response is important to develop a safe geosynthetic composite system exposed to changing environmental conditions such as temperature. This study reports on the characterization of the tensile behavior of NPNW-PP single geotextile filaments at the "micro-scale" level to be taken into account in evaluating the interface shear behavior of fabrics (i.e. geotextiles) with continua (i.e. geomembranes) under varied temperatures. At the "micro-scale", the tensile failure takes place due to breakage of filaments whereas at the global scale, the slippage between filaments and the structural deformation due to inherent internal geotextile void space which is governed by fabric manufacturing and fiber processing type, dominates. Globally, full mobilization of tensile capacity of geotextile fabric is associated with full mobilization of filament tensile strength at micro-scale. Consequently, the development of force-elongation response of a fibrous material (i.e. geotextile) based on its characteristic tensile stress-strength-strain behavior is a

multi-scale phenomenon and this is very important to be considered in design and analysis of geosynthetic composite layered systems incorporating geotextiles. Since, as pointed out by Mitchell and Seed (1990), sliding failure mobilized at geotextile-geomembrane interfaces is known to accompany the tension of geotextiles.

The fiber processing type (needle punched, heat-bonded etc.) and the manufacturing technique (woven, nonwoven) are key parameters controlling geotextile mechanical strength properties (i.e. tensile strength) (Koerner, 1998). For example, the compressibility of the fabric in the loading direction and the induced tensioning in the orthogonal direction to the loading in the fibrous material sheet are basically governed by these key parameters. Additionally, the tensile strength of a geotextile is a complex phenomenon and strongly depends upon the fabric's dimensional and structural properties such that the total deformation (extension or contraction) under load is the summation of the deformations in the filaments and the deformations due to the rearrangement of the internal structure. It was previously noted by Andrawes et al. (1984) that the tensile strength properties of the nonwoven geotextiles are almost virtually independent of the temperature and strain rate for the fabric-matrix at macro-level. However, considering multi-scale aspects of the tensile strength response and the resulting global frictional resistance behavior of fibrous materials (i.e. geotextiles) having variable structural properties at micro-scale or heterogeneous fabric-matrix properties at macro-level, this interpretation inferred from global-level test results and laboratory observations noted by Andrawes et al. (1984) does not factor in micro-scale perspectives in terms of experimental evidence through micro-mechanical thermo-tensile strength tests. Since the mobilized global frictional shear response of the geotextile-matrix is

influenced by the degree of the interaction between the filaments as reflected by the magnitude of contact level stress and area as well as by the amount of the interlocking between the fibers as reflected by the total number of the contacts. As such the magnitude of the global tensile strength generated in the geotextile-structure as well as the resulting shear resistance mobilized at the geotextile interface against continuum geomembranes over the entire extent of the interface area are controlled by the mechanisms of the filament interaction (i.e. inter-contact) with the geomembrane roughness features at micro-level and driven by the degree of the interlocking (i.e. inter-connection) between the fibers at micro-scale.

In light of this phenomenon, the application of a load on the geotextile – geomembrane interface layered system results in the embedding of the roughness features (i.e. texture elements) of the geomembrane into the matrix of the geotextile containing void spaces (i.e. porosities). Higher embedding of the textural features of the counterface geomembrane corresponds to the geotextile possessing larger holes (i.e. void spaces) (Bacas et al., 2011). To this end, an external extensional force exerted on the geotextile matrix at the global-level due to shear displacement under load, results in tension developing in the fabric-matrix that causes the fibers/filaments in the geotextile structure at micro-level to become stretched as well as exhibit elongation (i.e. axial strain) in the direction of the applied load. This is accompanied by the transverse contraction and strain in the filament as it becomes thinner in the direction orthogonal to the loading. This transverse contraction due to the axial strain and extension occurring in the individual filaments results in a decrease in the contact area between the different fibers in the fabric structure. The decrease in the contact area results in an increase in the contact stress at the

contact points between the separate filaments. Additionally, when the fibers becomes thinner, the total number of contact points in a certain volume of the geotextile matrix increases and this results in increased filament interaction as well as the increased interlocking between the different fibers per unit area of the fabric. Consequently, this will enable the fibrous geotextile to withstand greater tension under load, and additionally, facilitate the mobilization of larger frictional resistance in the course and during the mobilization of shear displacement against the geomembrane by allowing higher interaction and interlocking of the geotextile filaments with the counterface geomembrane roughness features.

This chapter has described the mechanical and thermal properties as well as the developed tensile behavior under extension for single polypropylene filaments extracted from needle-punched nonwoven geotextiles. These filaments have been studied by performing an experimental program with thermo-micro-tensile tests using a computer automated dynamic thermo-mechanical system (DMA). Various test temperatures between 20 °C and 50 °C were chosen to simulate the elevated temperature range expected in the field for geotechnical applications such as landfill liners.

The following conclusions of this research study are drawn as a result of experimental findings based on micro-tensile test results obtained from polypropylene filaments at various temperatures:

- The major impacts of temperature on tensile strength properties of the polymeric filaments were the decrease in ultimate tensile strength and the reduction in stiffness which resulted in loss of toughness. The loss in tensile strength and stiffness of the fibrous material is basically a function of temperature variation.

- The filament specimens underwent the same failure mode that they followed "ductile" tension behavior under the application of tensile load as opposed to brittle failure generally exhibited in some other construction materials. PP filament specimens from NPNW geotextile experienced larger micro-strains (80% - 120%) prior to rupture or failure in the temperature range tested.
- The resulting force-displacement curves for lower temperature tests are located on the upper part of the load-extension space compared with force-displacement curves of higher temperature tests such that the tension failure envelopes for the tested filaments diminished as the ambient temperature increased.
- Temperature has also a significant effect on the modulus of PP filaments. The instantaneous temperature-dependent modulus for the range of elevated temperatures such as typical of landfilling practice decreased exponentially (i.e. follows an exponential pattern with a high coefficient of determination between the data and the regression curve). In short, PP filaments at cooler temperatures are stiffer than at higher temperatures.
- The tensile strength values obtained at lower temperature tests were higher than those obtained at higher temperature tests due to thermo-physical properties and molecular bonding strength of polymeric filaments at varied temperature conditions. A second order polynomial behavior was observed in tensile strength versus temperature relationship for the geotextile single filaments.

CHAPTER VI

6. ELEVATED TEMPERATURE EFFECTS ON GEOTEXTILE – *SMOOTH* GEOMEMBRANE INTERFACE SHEAR BEHAVIOR

6.1. Introduction

This chapter presents the results of a series of laboratory tests carried out to investigate the factors controlling the interface shear behavior and strength between geotextiles and smooth geomembranes as well as in particular to examine the role of temperature on geotextile – geomembrane interface performance and texture-filament interaction. The research study specifically involved smooth high density polyethylene (HDPE) as well as smooth polyvinylchloride (PVC) geomembranes in combination with needle punched nonwoven (NPNW) fabrics. However, the concepts presented herein may also be relevant to other geosynthetic systems manufactured by others from similar as well as different polymer resins. The effects of higher temperature conditions on geosynthetic interface performance were quantified through laboratory interface shear tests at elevated temperatures in the temperature controlled chamber (TCC), fibrous material single filament micro-mechanical tensile tests using a thermo-dynamic mechanical analyzer (DMA) (Chapter 5), and continuum material surface hardness measurements (Chapter 9). Large displacement interface shear testing was conducted over a large range of normal stresses (10 kPa – 400 kPa) to capture variations in behavior as a function of normal stress and ambient temperature.

6.2. Geotextile–Geomembrane Composite Multi-Layered Systems In Geotechnical Field

The usual design objective for waste containment facilities and impoundments is to maximize storage capacity. Therefore, two fundamental principles generally kept in consideration are: i) It is important to construct the side slopes as steeply as possible and ii) In order to reduce leakage of leachate, or stored water in reservoir, a liner system that incorporates an impermeable material is installed along with a fabric protective and strain compensating fabric material. For example, geomembranes are placed on a prepared subgrade, seamed and then covered with a backfill. The design principles of modern landfills have developed from the old dilute and disperse philosophy to state-of-the-art containment facilities (Koerner, 1998). Landfills are now designed on a fully contained basis to prevent the migration of leachate and uncontrolled escape of landfill gas. In order to meet the performance objectives for a landfill liner which comprises a combination of natural and geosynthetic materials, geomembranes are generally used either as a single liner, or form part of a composite lining system. There has been a movement away from the use of sand as a drainage and protection layer above the geomembrane due to concerns about clogging. Thick nonwoven geotextiles are increasingly being used to serve as a protective layer for the geomembranes with gravel layers forming the drainage layer.

As outlined by today's regulations for containment facilities design, construction, and post-closure management, domestic municipal and hazardous waste-containment

facilities are required to have a liner and cover system which consists of a compacted clay liner as well as geosynthetic materials. The geosynthetic components routinely include layers of geonet or drainage composite, geotextile cushions and/or filters and a geomembrane. An important slope stability characteristic is the shear resistance along the various component interfaces. A number of case histories suggest that the geomembrane can create a problematic interface due to low frictional resistance between it and another geosynthetic component or the compacted clay. The overall stability of such a composite system and the integrity of the geosynthetics are dependent on the shear strength at the interface between the various materials. There have been many examples worldwide of landfill slope failures associated with low shear strength interfaces such as The Kettleman Hills Failure which has been extensively reported with all aspects in consideration by Seed et al. (1988), Mitchell et al. (1990), and Byrne et al. (1992). This failure occurred primarily at the interface between the clay and smooth geomembrane of the secondary lining system, with sliding in the upper part of the sideslopes occurring along the primary geomembrane/secondary geotextile interface (Jones and Dixon, 1998).

The use of geotextiles which are fibrous pervious materials in conjunction with geomembranes which are impervious continuum materials has arise from operating landfill examinations carried out in the past (Brune et al., 1991). These demonstrated that the use of sand as a leachate drainage layer can lead to biological and chemical clogging, and the recommendation that a single sized gravel drainage blanket be used. However, gravel can easily damage, puncture, or tear the geomembrane lining material. For this reason, the use of a geotextile layer to protect the geomembrane from damage caused by the drainage layer has been adopted as the preferred solution. Although these composite

geosynthetic interfaces are routinely employed in landfill liners and are exposed to high elevated temperature conditions, there is very little information published in the literature to date on the influence of higher temperatures on interface shear behavior and strength characteristics of geotextiles in contact with geomembranes. This study aims to fill this gap in knowledge and to show how the developed shear mechanisms and interface resistance changes with elevated temperatures. This research study in particular focused on the most common geosynthetic materials used in current North American practice when placing geotextiles in combination with geomembranes. As such, two smooth geomembranes produced from different base polymers (GSE HDPE Smooth; EPI PVC Smooth) were tested in combination with a single staple type NPNW geotextile (GSE NPNW 8 oz/yd^2). Force-displacement failure mechanisms developing at geotextile-geomembrane interfaces at higher temperatures were determined by imitating elevated temperature field conditions in the insulated and temperature controlled environment of the TCC. The geomembrane liner samples were sheared against the geotextile fabric specimens at one of six temperatures (21°C, 26°C, 30°C, 35°C, 40°C, and 50°C).

6.3. Similarities in Between Interface Shear Response and Tensile Behavior of Geomembranes Lining Materials

6.3.1. Comparison of HDPE Geomembrane Individual Material Tensile Behavior to its Interface Response with Geotextile

Tensile strength testing has been a widely used method to evaluate the engineering properties of various geosynthetics. This is attributed to the fact that many geosynthetics are designed to complement the relatively low tensile capacity of soils. Figure 6.1a presents typical tensile test results for HDPE geomembranes. Rapid strain softening after peak stress is typical of HDPE liner materials. With this kind of behavior, as displayed in Figure 6.1a, the yield stress is in general interpreted as being the peak stress.

The typical interface response of smooth HDPE geomembranes when sheared against NPNW geotextiles is shown in Figure 6.1b. After a dramatic increase up to a sharp distinguished peak stress, a sharp transiton to a post-peak strain softening behavior occurs. This resemblance between the behavior is an indication of the influence of material physical and mechanical properties such as elasticity versus plasticity; ductility versus brittleness or flexibilty versus stiffness on the interface shear deformation characteristic as well as the tensile strength properties.

The effects of temperature on the tensile strength properties of HDPE geomembrane samples as shown in Figure 6.2 (Budiman, 1994) indicate a pattern where decreasing temperature results in an increasing stress level at yield and decreasing strain at yield. In addition, the ultimate strength is achieved at lower strains level indicating an increase in brittleness and a decreasing strain at rupture. In other words, the samples

tested at higher temperatures were weaker but more extensible than the samples tested at low temperatures. These geomembrane tensile behaviors observed at increasing temperature levels are in contrast to the influence of temperature on interfacial frictional characteristics of geomembranes as will be discussed in detail later in this chapter.

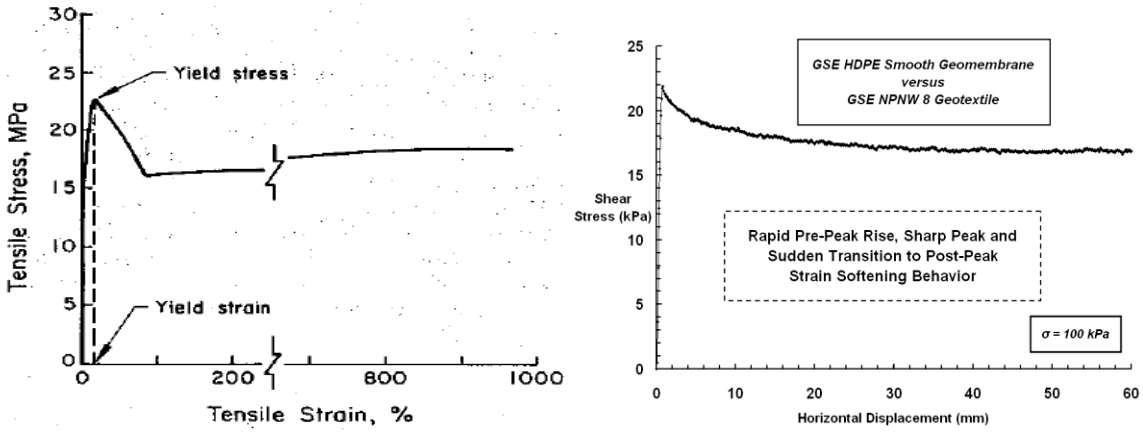

(a) (b)

Figure 6.1 (a) Typical Tensile Stress-Strain Data for Tensile Tests on HDPE Geomembrane (O'Rourke et al., 1990); (b) Interface Shear Response of HDPE Geomembrane Sheared Against NPNW Geotextile

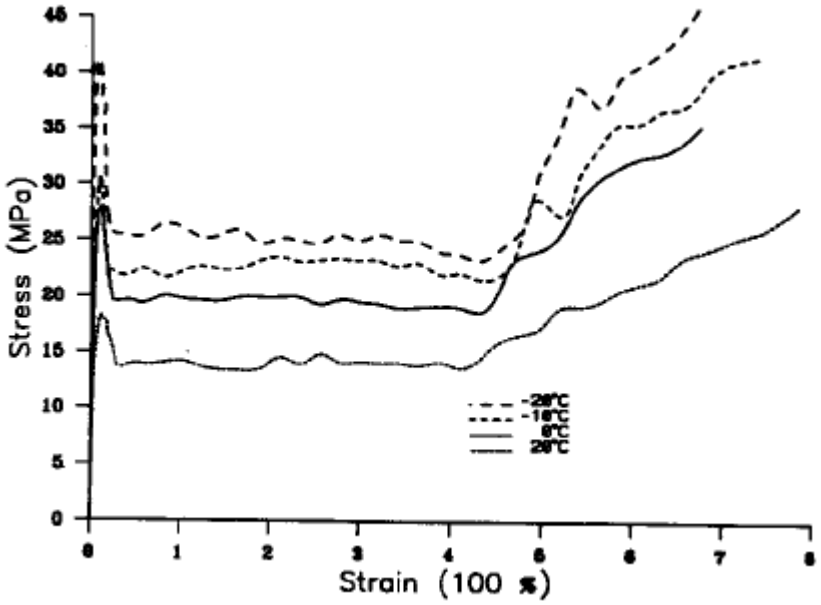

Figure 6.2 Tensile Stress-Strain Response for HDPE Specimens Tested at Different Temperatures (Adapted from Budiman, 1994)

6.3.2. Comparison of PVC Geomembrane Individual Material Tensile Behavior to its Interface Response with Geotextile

Figure 6.3a shows typical tensile test results for PVC geomembranes. Linear strain hardening after yield is typical of PVC lining specimens.

Similarly, laboratory interface shear tests for PVC geomembranes sheared against NPNW geotextiles show an elastic-perfectly plastic response in which shear stress rises after a small horizontal displacement range to peak stress and after passing a smooth peak, the curve develops an almost perfectly plastic manner (Figure 6.3b).

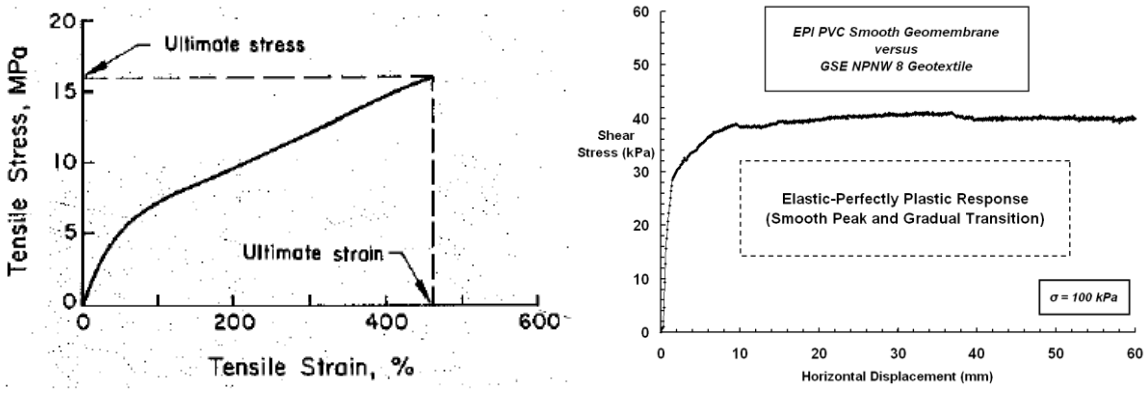

(a) (b)

Figure 6.3 (a) Typical Tensile Stress-Strain Data for Tensile Tests on PVC Geomembrane (O'Rourke et al., 1990); (b) Interface Shear Response of PVC Geomembrane Sheared Against NPNW Geotextile

6.4. Stress Relaxation Response and Thermally Induced Stress Behavior of Geomembrane Lining Materials

In geotechnical design, a geotextile and a geomembrane are often placed in direct contact with one another. In order to avoid the degradation of geomembranes due to puncturing, tearing, or excessive tension, highly flexible geomembranes have been developed (Koerner, 1998). The highly-flexible geomembranes however, may experience excessive strains due to changes in ambient conditions such as temperature which may result in low interface resistance as well as difficulties in handling in the field. For this reason, laboratory stress relaxation tests on the geomembrane specimens are performed by applying a constant value of strain over a certain period of time to observe the relaxation and straining behavior of geomembrane lining materials made from polymer resins (Koerner et al., 1993). In such experiments, the decrease in the magnitude of the initial stress is measured as a function of time. Figure 6.4 shows stress relaxation test results on a HDPE geomembrane test specimen (100 mm wide with a gage length of 50 mm) at various constant temperatures.

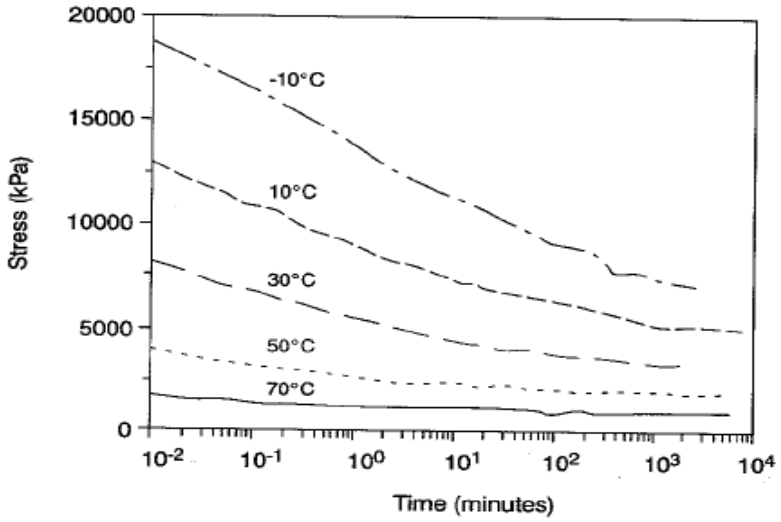

Figure 6.4 Stress Relaxation Behaviors of HDPE Geomembrane Specimens at Various Temperatures and at a Constant 3% Strain (Lord et al., 1995)

The amount of tensile stress arising in this polymeric material body can be determined as follows (Lord et al., 1995):

$$\frac{\Delta\sigma}{\Delta T} = \alpha \cdot E \tag{6.1}$$

Where;

$\Delta\sigma$: Change in Stress

ΔT: Change in Temperature

α: Coefficient of Linear Thermal Expansion

E: Elastic Modulus

For HDPE Geomembrane (Koerner, 1994):

$$\frac{\Delta\sigma}{\Delta T} = -70\,\text{kPa/°C} \tag{6.2}$$

In other words every one degree Celsius decrease in the ambient conditions will create 70 kPa tensile stress in the HDPE geomembrane liner material.

The results of laboratory experiments by Lord et al. (1995) are also shown in Figure 6.5 in which thermally induced stresses due to temperature decrease develops with time in HDPE geomembrane samples under an initially applied constant tensile strain. In other words, the lining specimen was basically subjected to a series of discrete

temperature drops at this small constant seating strain. This type of thermally-induced stress that builds up in the polymeric material is different than mechanically-developed stresses in terms of initiation, progression, and dispersion throughout the material.

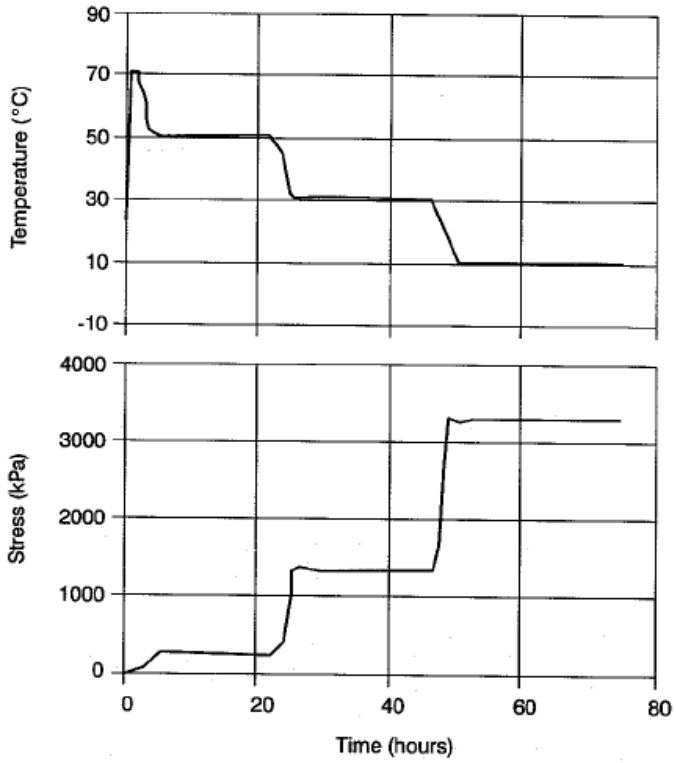

Figure 6.5 Thermally Induced Stress versus Time in a HDPE Geomembrane Specimen with a Very Small Constant Strain (Lord et al., 1995)

6.5. ***Smooth*** **Geomembrane – Geotextile Interfaces**

In this study, a geomembrane liner with relatively high rigidity (smooth HDPE) as well as the one with relatively low rigidity and high flexibility/softness (smooth PVC) were selected to quantify the effects of continuum material surface hardness on the shape of the shear-displacement curve and on the magnitude of interface strength attained in combination with fibrous materials (geotextiles).

6.5.1. HDPE Smooth Geomembrane/NPNW Geotextile

The typical behavior of HDPE smooth geomembranes when sheared against NPNW polypropylene (PP) geotextiles is brittle in nature with a sharp peak and rapid transition to post-peak behavior. The stress-displacement responses of HDPE smooth geomembranes, at all temperatures tested and at three different normal stresses representative of geotechnical field level stresses, were essentially an elastic-perfectly plastic response (Figure 6.6).

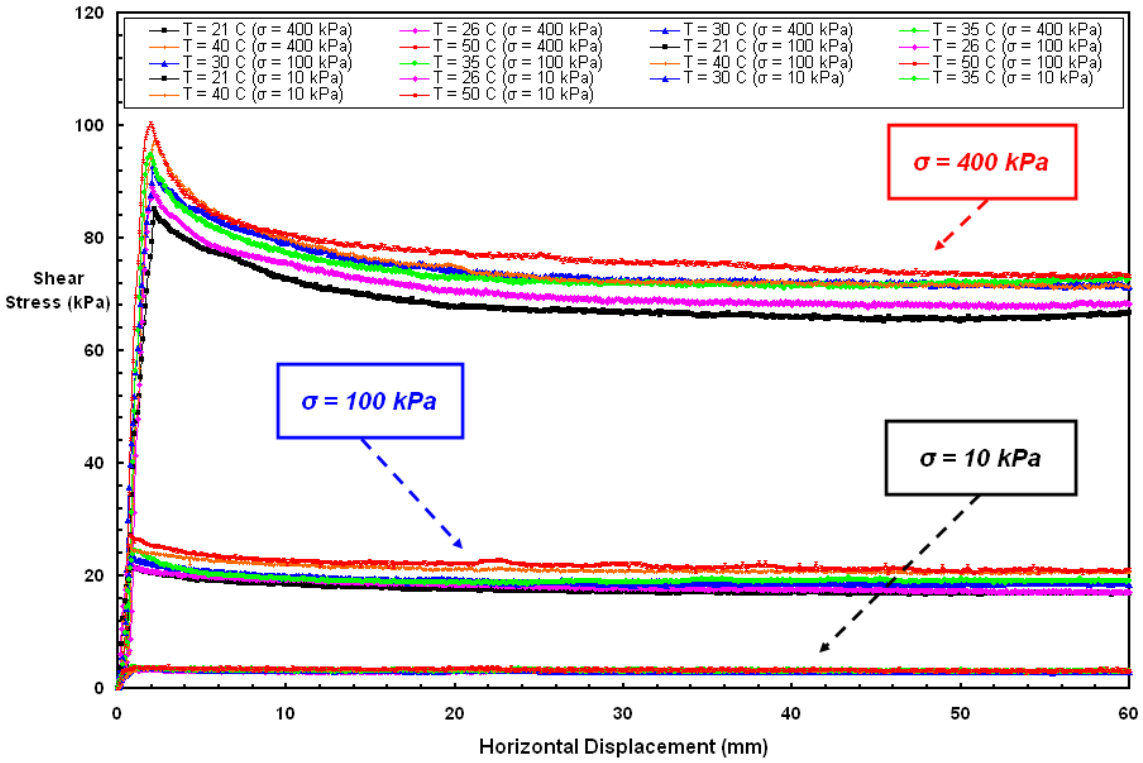

Figure 6.6 Shear Stress–Displacement Curves at Different Loading Conditions; & at Various Test Temperarures for GSE HDPE Smooth Geomembrane/NPNW Geotextile

Some post-peak softening was observed followed by a near constant large strain or residual shear stress value. The magnitude of this post-peak reduction in strength decreased with normal stress (i.e. largest at 400 kPa; insignificant at 10 kPa). The displacement required to mobilize the peak interface shear strength ranged from approximately 1 to 2 mm for the tests at temperatures ranging from 21 °C and 50 °C. Greater displacements were necessary to reach peak strength at higher normal stresses (Figures 6.7a, 6.7b, 6.7c). Horizontal displacements required to achieve pseudo-residual conditions were of the order of 10 to 14 millimeters in all cases and for each elevated test temperature. These differences in horizontal displacements to peak stress are the result of the different amounts of compression of the geotextile at the interface with the geomembrane before the shear stress is applied. The behaviour of smooth HDPE geomembrane versus PP geotextile interface can thus be described as an initial rapid increase in shear stress as soon as displacement starts followed by a peak shear stress at relatively low displacement of order of 1 to 2 mm. Additional shear displacement produced negligible to moderate reduction in shear stress. This strain softening behaviour was evident, in particular, at 100 kPa and 400 kPa normal stresses. Little additional decrease in shear stress occurred with further displacements (>20 mm). The post peak behaviour is slightly different at low normal stress level of 10 kPa with almost no reduction in shear stress and indeed, very minor strain hardening occurred. It is also noted that the HDPE smooth geomembrane rendered a substantially lower interface shear resistance than all the other geomembranes used in the study (smooth and textured).

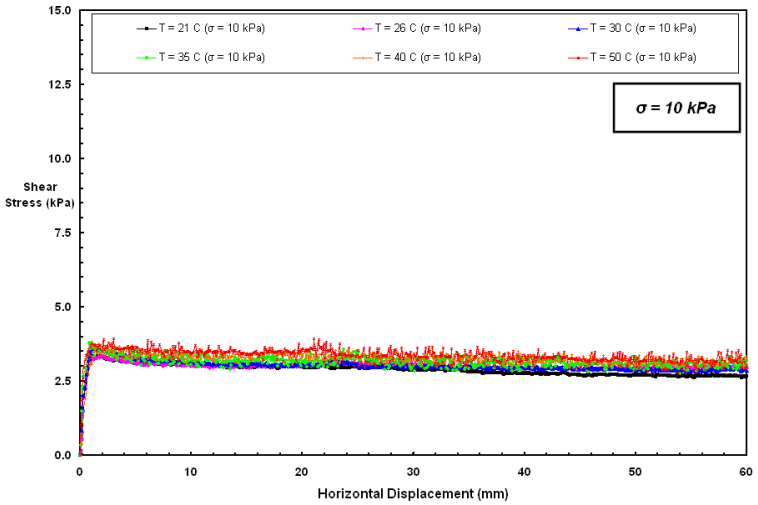

(a)

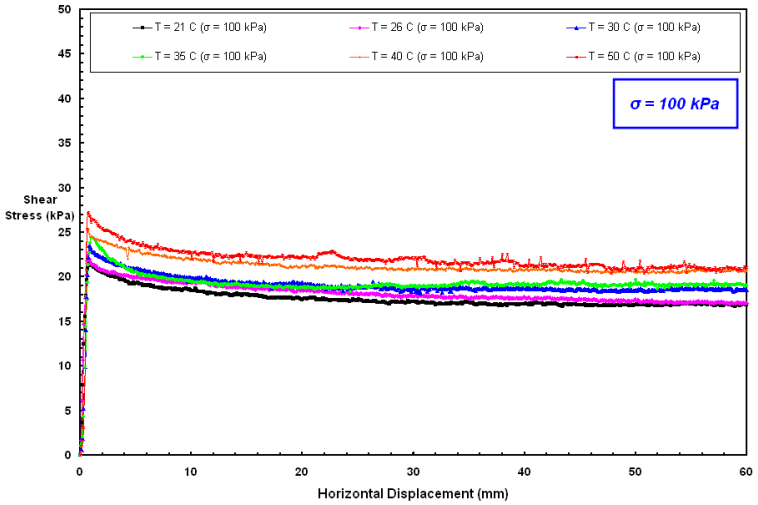

(b)

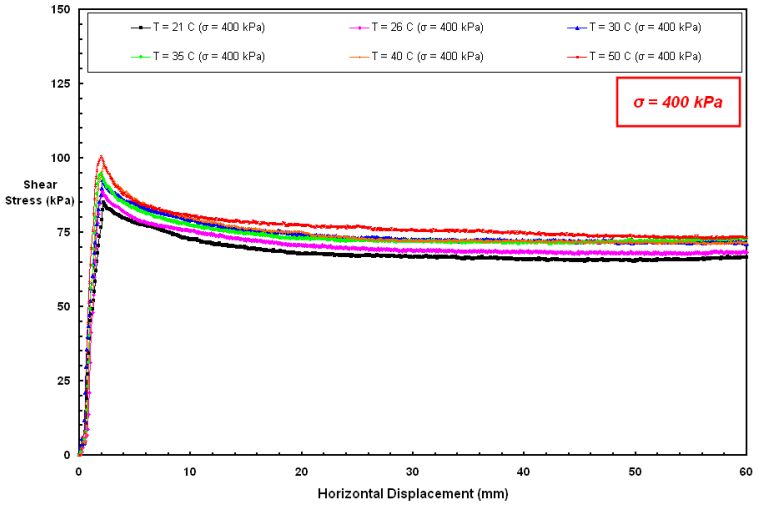

(c)

Figure 6.7 Shear Stress – Displacement Curves at Different Temperarures for GSE Smooth HDPE Geomembrane/NPNW Geotextile: (a) 10 kPa; (b) 100 kPa; (c) 400 kPa

The shear stress-displacement curves for the tests at a given stress level test at different temperatures were all similar in terms of shape. Therefore, one can conclude that the observed differences in the shear stress - displacement responses of the PP geotextile-HDPE smooth geomembrane interfaces are due to the temperature at which the interface tests were performed.

The variation in vertical displacement with horizontal displacement are shown in Figure 6.8a, 6.8b and 6.8c for tests at different normal stresses (10 kPa, 100 kPa and 400 kPa, respectively). The vertical displacement during shearing initially decreased to a near constant value as the horizontal displacement reached the residual state after which it maintained a constant degree of contraction with minor variations from the mean. The direct shear tests at higher temperatures exhibited an expansion in vertical direction which contributes to improvement/increment in shear strength and interface response. In summary, the interface experiences larger dilation as shearing progresses with increasing temperature which results in a shear resistance increase for this combination of materials.

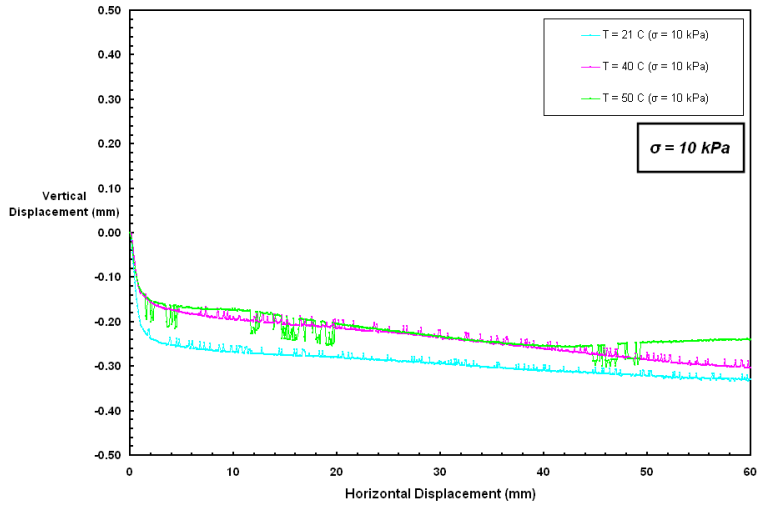

(a)

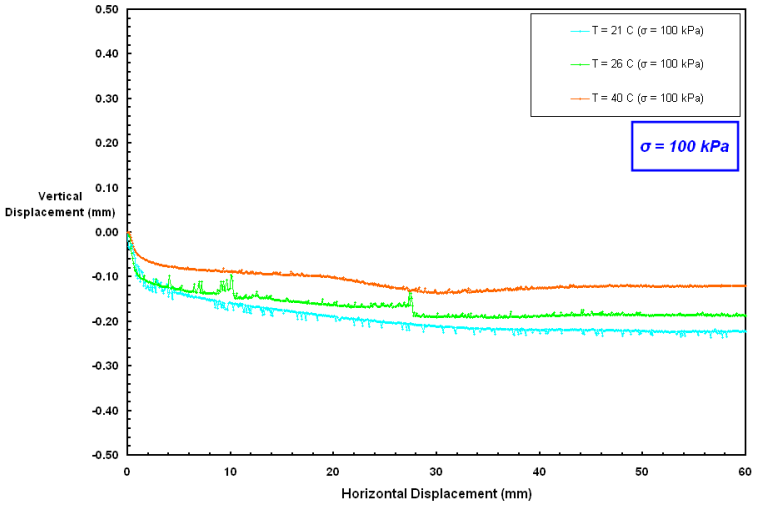

(b)

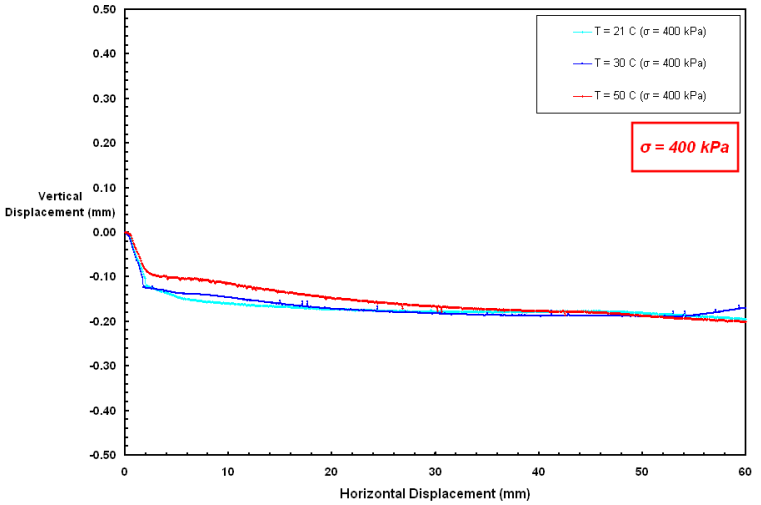

(c)

Figure 6.8 The Variation in Vertical Displacement against Horizontal Displacement at Different Temperatures for GSE HDPE Smooth Geomembrane/NPNW Geotextile

The peak and post-peak (i.e: pseudo-residual) interface strength values in terms of interface friction angle, (δ) as well as coefficient of friction, ($\tan(\delta)$) are presented in Figure 6.9 and 6.10, respectively, to display the trend with changing temperature. The post-peak strength values computed were based on shear stress values averaged over 2 mm range from 57 to 59 mm horizontal displacement. Both peak and pseudo-residual interface shear strength values increase with temperature.

This increase in the magnitude of δ, and $\tan(\delta)$ with temperature at the interface of polymeric materials during shear is consistent with observations made by the others including Bely et al., (1982); Daniels, (1989); Pasqualini et al., (1993); Nielsen and Landel, (1994). For geotechnical systems that experience temperature varitations, the interface friction angle or coefficient of friction selected to be used in the design needs to be defined as a function of temperature.

The coefficient of friction increases with temperature level while it decreases with normal stress. The magnitude of the coefficient of friction obtained at low normal stress levels (10 kPa) was the highest and its magnitude attained was the lowest at greatest stress level (400 kPa) (Figure 6.10).

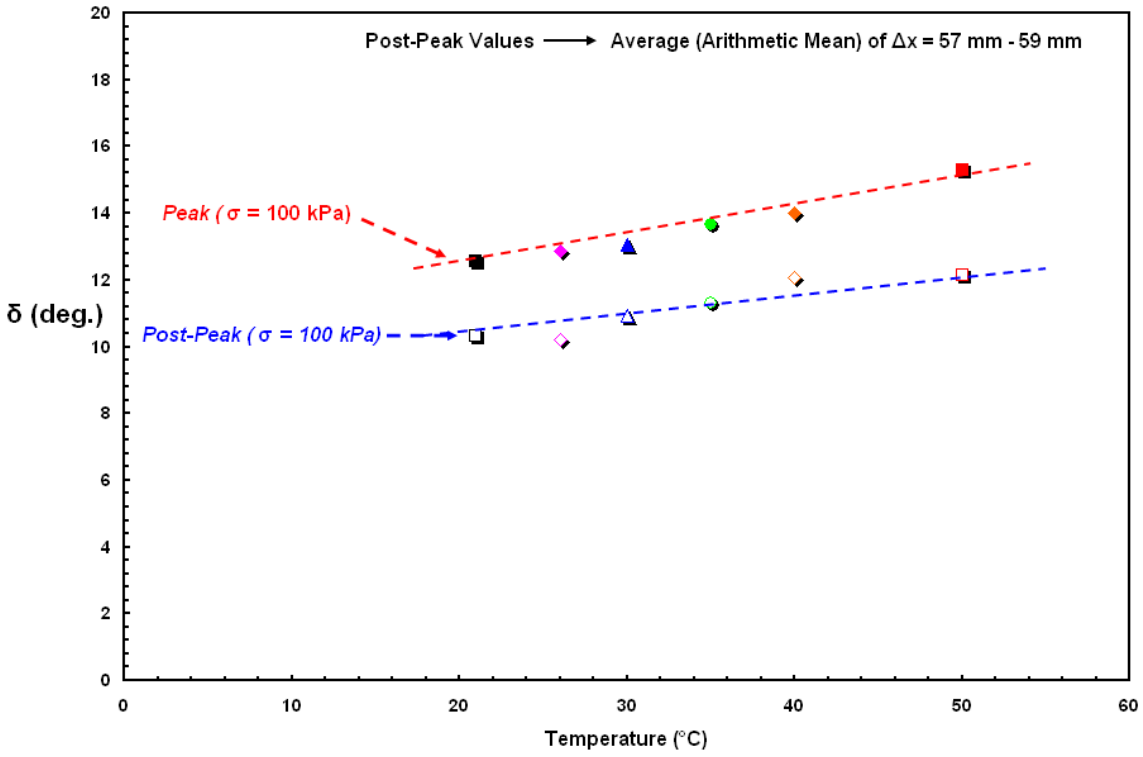

Figure 6.9 The Change of Interface Friction Angle, [δ] with Temperature for GSE Smooth HDPE Geomembrane/NPNW Geotextile Interfaces at 100 kPa Normal Stress

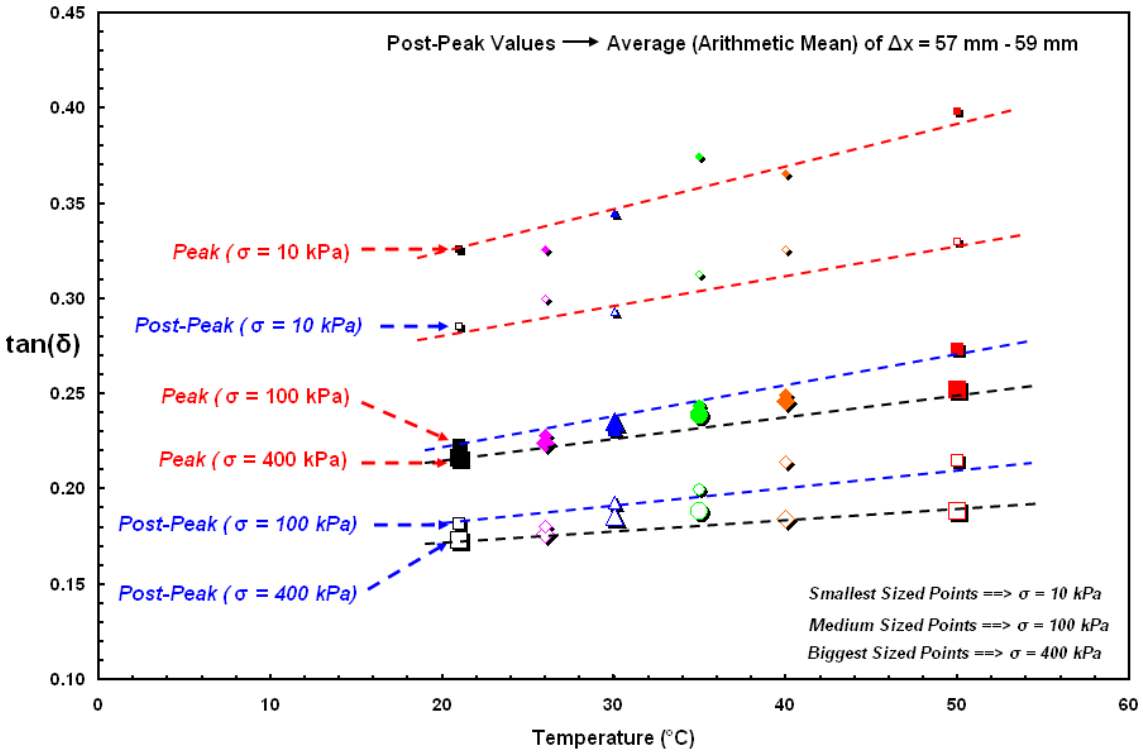

Figure 6.10 The Change of Coefficient of Friction, [tan(δ)] with Temperature at Different Loading Conditions for GSE Smooth HDPE Geomembrane/NPNW Geotextile Interfaces

The peak and pseudo-residual failure envelopes from the large displacement interface tests between NPNW PP geotextiles and HDPE smooth geomembranes under different normal load conditions ranging from 10 kPa to 400 kPa are shown in Figure 6.11. The interface shear test results reported herein over a large range of normal stresses and elevated temperature conditions are to capture variations in PP geotextile–HDPE smooth geomembrane interface shear behavior as a function of two variables (i.e. experimental and ambience conditional) altering such as σ (kPa), and T (°C). These results were intended to provide insight into HDPE smooth geomembrane – geotextile fabric interaction meachanisms at elevated temperature conditions in the field and the development of interface shear response over a large range of normal stress levels depending on geotechnical construction type. This smooth geomembrane – NPNW geotextile composite system clearly exhibited a linear peak strength envelope over the entire range of normal stresses tested and at all temperatures. The strength envelopes were replotted with both axes on a logarithmic scale (Figure 6.12) to highlight the behavior at low normal stress levels. It is possible to distinguish a difference in the shape of the peak as well as post-peak failure envelopes at low normal stresses. The strength envelopes (peak and residual) became curved (concave-up). However, the envelopes showed linearity at high stresses. Mohr-Coulomb failure envelopes were useful to see the behavioral differences at a range of different normal stress conditions. The slight curvature displayed at low normal stresses for higher temperatures demonstrates the favorable contribution of the adhesion component of the friction resulting from the polymeric geosynthetic counterface materials becoming more pliable at elevated temperatures.

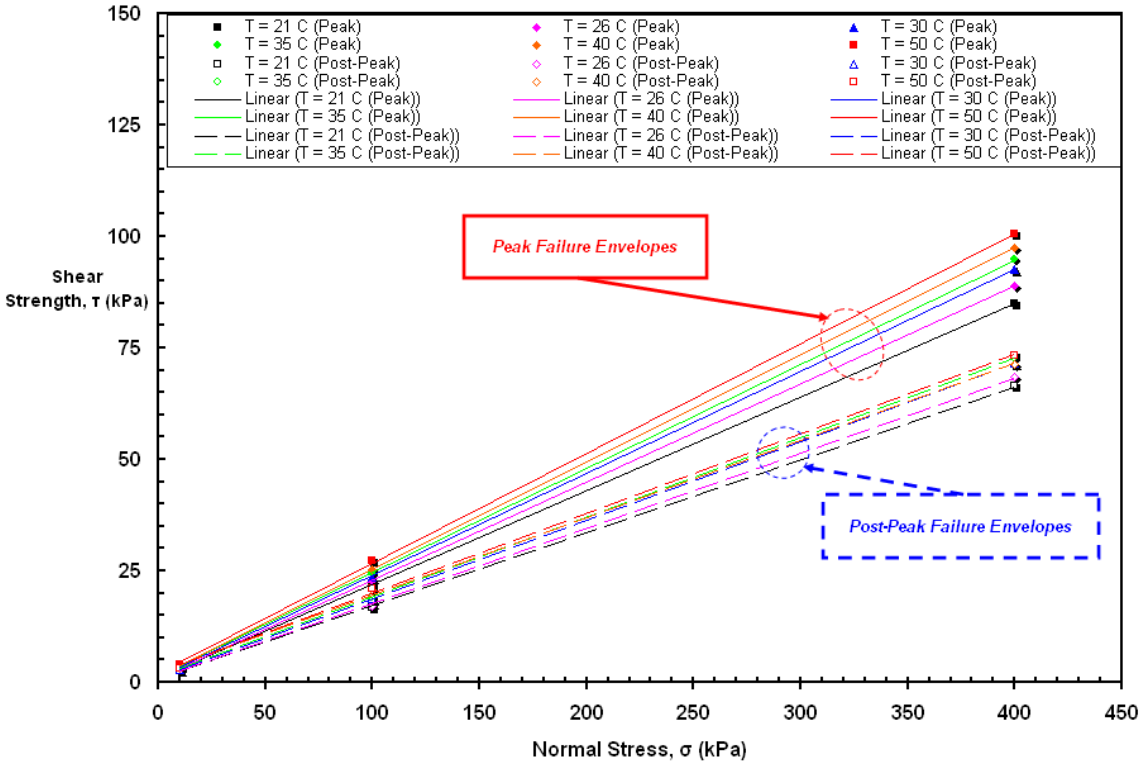

Figure 6.11 The Alteration of Peak and Residual Strength Envelopes with Increasing Temperature for GSE HDPE Smooth Geomembrane/NPNW Geotextile Interfaces

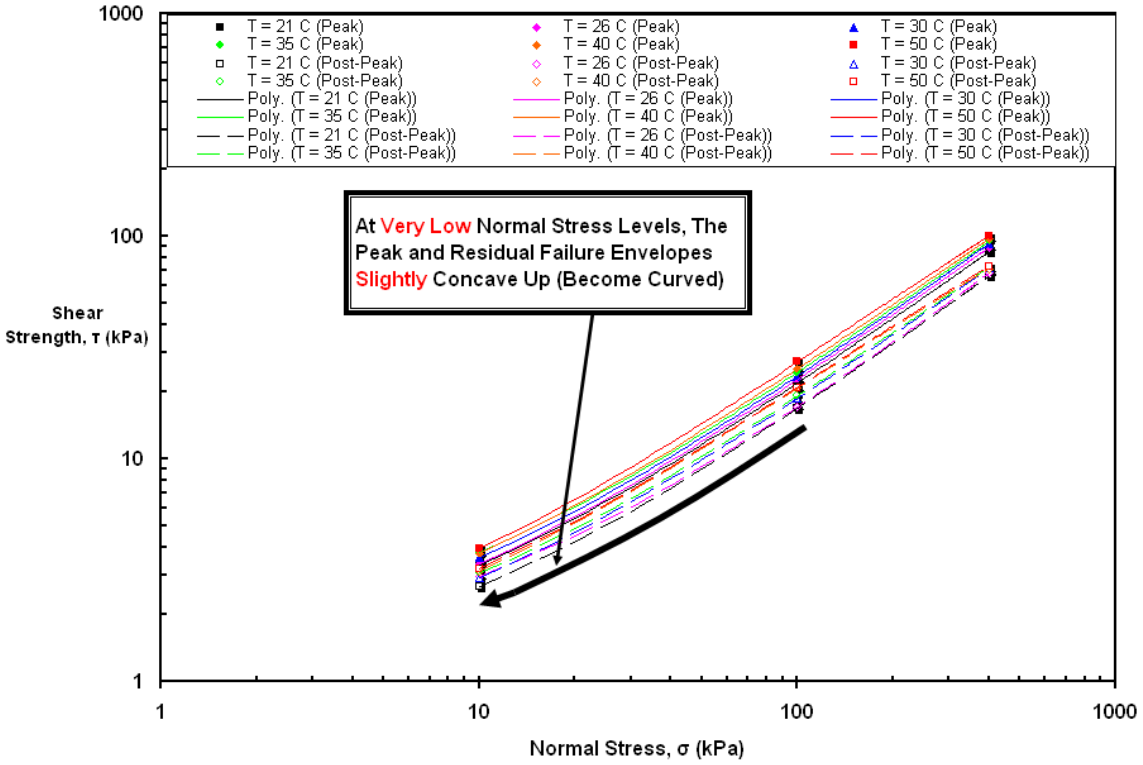

Figure 6.12 The Transformation in Failure Envelopes with Temperature at Different Loading Conditions for GSE HDPE Smooth Geomembrane/NPNW Geotextile Interfaces

To sum up, the effect of temperature is evident in the strength envelopes presented in Figure 6.11 and 6.12. At each normal stress, the interface strength increases as the temperature increases. The increase in interface strength with temperature is also apparent as shown in Figure 6.10. The temperature sensitivity of this NPNW PP geotextile – smooth HDPE geomembrane liner composite system is consistent with polymer softening (i.e. reduction in stiffness) as the temperature increases (Budiman, 1994; Lord et al., 1995), which results in greater pliability of the polymer under a given stress and an increase in contact area (Osswald and Menges, 1995). Finally, the results showed negligible (i.e: very close to origin) values of adhesion. This means the resistance of the smooth geomembrane is attributed to the sliding friction resulting in low coefficient of friction at relatively low normal stress. Similar behavior was observed for the residual failure envelopes.

6.5.2. PVC Smooth Geomembrane/NPNW Geotextile

PVC geomembranes in general offer higher deformation capabilities and increased interfacial strength and improved resistance to stress cracking as a result of their more plasticized and flexible nature. Figure 6.13 presents the stress-displacement responses between PVC smooth geomembrane and NPNW PP geotextiles under normal stresses ranging from 10 kPa to 400 kPa as well as ambient temperature conditions ranging from 21°C up to 50°C.

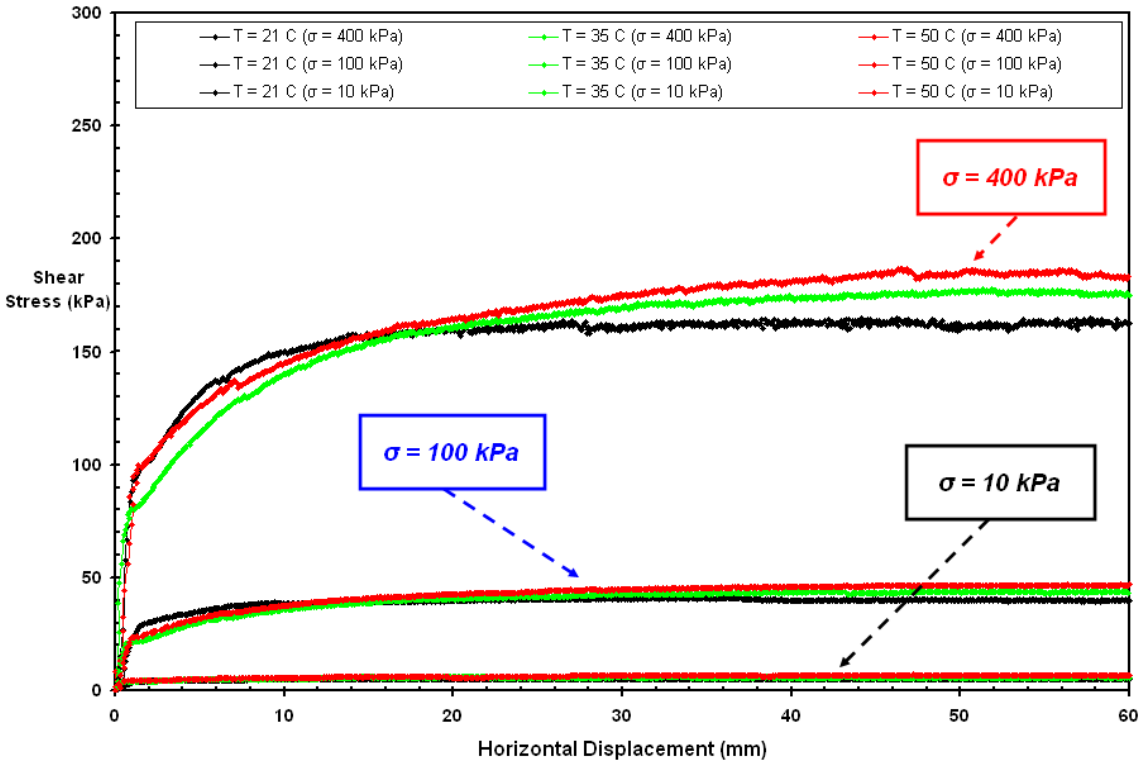

Figure 6.13 Shear Stress–Displacement Curves at Different Loading Conditions; & at Various Test Temperarures for EPI Smooth PVC Geomembrane/NPNW Geotextile

The interface tests carried out at elevated temperatures conditions showed similar responses in which shear displacement hardening behavior occurred after yielding in contrast to the behavior observed with smooth HDPE geomembranes where a post-peak strain softening response developed. The tendency of PVC smooth geomembrane – geotextile interfaces to behave in this fashion was completely dependent on the differing material properties compared with HDPE liners. Additionally, the hardness reduction contributed to some very minor increase in strength with increasing temperature level compared to HDPE. However, the smooth HDPE geomembrane showed a higher increase in strength with temperature for same normal stress level tested. The amount of horizontal displacement to peak increased with normal load. After a rapid increase in shear stress at very small displacement (1 – 2 mm), a yielding type pattern occurs with

displacement up to 8 mm to 10 mm displacement similar to that in terms of shape and progression observed in the polymeric material tensile tests. This stage of interface response could be described as follows. After a rapid rise at very small displacements of 1 mm – 2 mm for all test temperatures ranging from 21 °C to 50 °C, the rate of this rapid increase reduces, becomes gentle and lower during this stage with the interface response changing to plastic deformation. Later, the interface response becomes a perfectly plastic one in the horizontal displacement range of 60 mm at termination of the experiment. Hillman and Stark (2001) tested similar PVC smooth geomembrane interfaces against geotextiles over a very large horizontal shear displacement range of 1,000 mm using a ring shear device and showed no post-peak strength loss. As shearing progresses, the higher surface pliability of the PVC lining materials, possessed at all temperatures tested, allows it to get roughened by being embedded by the counterface geotextile owing to the malleable nature of the PVC liner and resulting in a larger shear resistance. The stiffer and harder nature of HDPE liners does not facilitate the counterface filament embedment into the geomembrane surface as much as the softer PVC liner. This also prevents the frictional resistance of the smooth HDPE from reaching that of the smooth PVC. In short, the higher surface pliability of the smooth PVC enables the strength-increasing mechanisms discussed above to develop more readily than for the smooth HDPE which accounts for the larger shear strength attained at test temperatures ranging from 21 °C to 50 °C. This also explains why no post peak strength loss was observed for the smooth PVC geomembrane-nonwoven geotextile interfaces. The strength-increasing mechanisms offset the strength-reducing effects including the damage given to the counterface due to imposed stresses during shear displacement, thereby preventing a loss of interface shear

resistance with increasing shear displacement. Similar discussions were provided by Hillman and Stark (2001) for the comparison of PVC geomembrane interface test results with those of HDPE liners. However, they only performed the experiments at room temperature. The influence of ambient temperature on these geosynthetic – geosynthetic layered systems has been examined herein to observe the behavioral differences as a function of varied temperature conditions. For the typical interface behavior of PVC geomembranes against NPNW geotextiles, it is not feasible to determine distinct peak strength from the stress-displacement curve. For this reason, in the analysis of the interface results at every test temperature and at each normal stress level, the shear stress values that correspond to the shear displacements of the mobilized peak strength values of the smooth HDPE geomembrane tested were selected for the determination of the peak interface strength. Similar to the analysis process performed on the smooth HDPE test results, post-peak strength values were taken as the average of the values at shear displacements from 57 mm to 59 mm. As the interface response of the smooth PVC is plastic at all normal stresses and at different ambient temperatures, the residual shear resistances mobilized at the interface are larger than the peak strength values and results from the slight strain-hardening shear behavior observed in the smooth PVC interfaces with NPNW geotextile. The shear stress – horizontal displacement curves for different ambient temperatures are presented in Figure 6.14a, 6.14b and 6.14c for tests at different normal stresses (10 kPa, 100 kPa and 400 kPa, respectively). The displacement required to mobilize peak interface strength ranges from 0.8 – 1 mm at 10 kPa; 1.1 – 1.5 mm at 100 kPa; and 2 – 2.4 mm at 400 kPa and show a higher shear deformation occurred at the interface due to the increasing normal load.

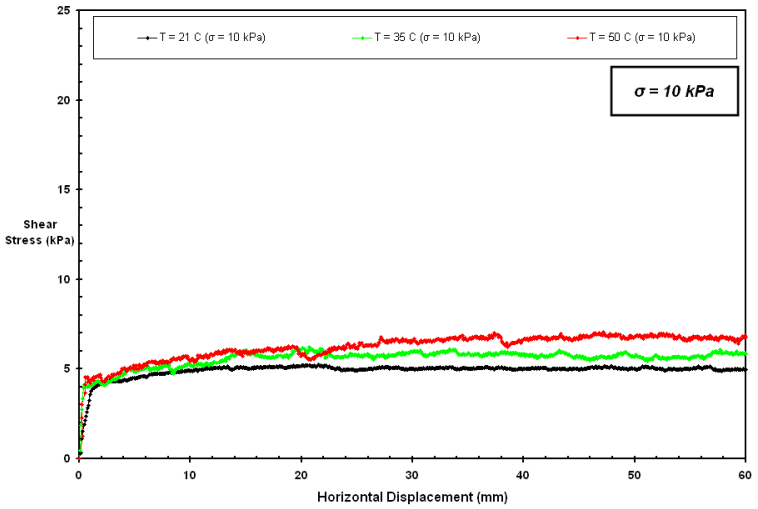

(a)

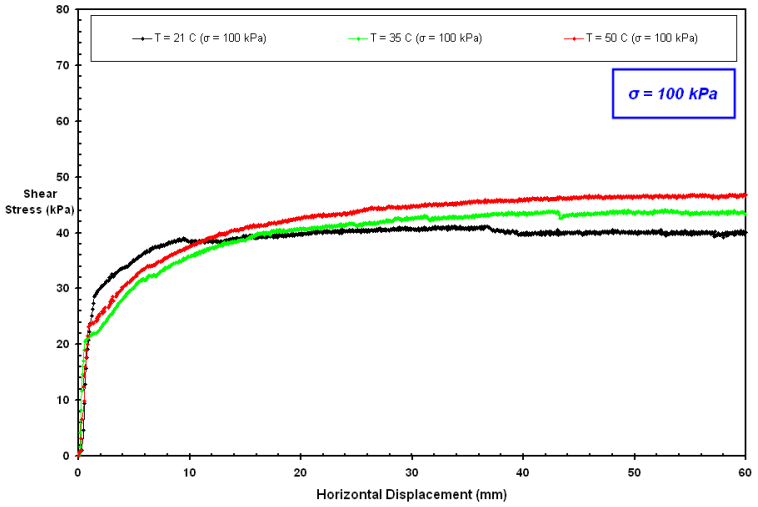

(b)

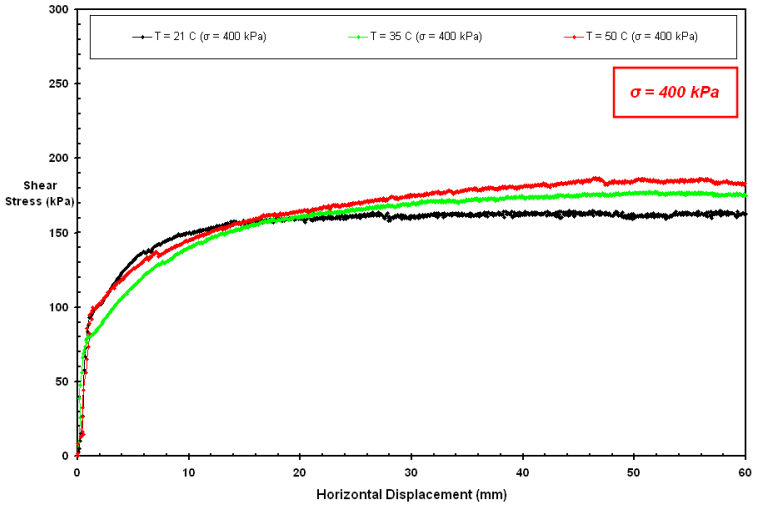

(c)

Figure 6.14 Shear Stress – Displacement Curves at Different Temperarures for EPI Smooth PVC Geomembrane/NPNW Geotextile: (a) 10 kPa; (b) 100 kPa; (c) 400 kPa

The variation in vertical displacement with horizontal shear displacement is shown in Figures 6.15a, 6.15b and 6.15c for tests at different normal stresses (10 kPa, 100 kPa and 400 kPa, respectively). The overall dilation/contraction response of the smooth PVC geomembrane – NPNW geotextile interface system is different than that of smooth HDPE geomembrane at all test temperatures and results from the different physical and mechanical properties of the smooth PVC geomembare. In contact with the same type of nonwoven geotextile, the softer geomembrane (PVC) showed higher adhesion as a result of its pliable and flexible (plasticized) nature and the amount of strength mobilized during shear displacement also depends on these physical properties. The higher adhesive property of the smooth PVC is also evident from the failure envelopes developed at different temperatures as will be discussed further when the peak and residual strength envelopes are presented. Further, the vertical displacement – horizontal displacement behavior in terms of the shape of the curve gives an impression as being symmetrical to the stress – displacement response of the interface with respect to the lateral x axis with an exception of the test results from low normal stress level (10 kPa). At higher normal stresses (100 kPa, 400 kPa), the relatively stiff PP geotextile was able to embed into the soft and pliable surface of the PVC liner. It is known that the interfaces comprised of relatively stiff counterface materials with rough surface features (e.g. textured HDPE geomembranes) tend to dilate as shearing occurs and is accompanied by an increase of the frictional resistance. The highly plasticized and malleable PVC liner surface allows embedment of the counterface geotextile which can reduce the amount of dilation occurring at the interface compared to the results of the stiffer HDPE geomembrane system. This behavior of the smooth PVC liners can be similar to the

behavior of other soft plastics. For example, when a point load is applied on a surface of a soft plastic material, the surface gets a bowl-alike shape to reduce the impact of the external force. In this way, the intensity of the load is allowed to dissipate. However, the surface of this type of materials tends to rebound to its original state after the removal of load. This response of the soft plastic materials can prevent or reduce the amount of dilation at their interfaces during shear displacement under a load and can result in a contraction at the interface. In contrast, at low loading condition (10 kPa), the interface is not highly constrained and thus more free to dilate. In addition, the counterface geotextile was not able to embed into the PVC liner as the magnitude of the load was not sufficient to exceed the PVC surface hardness threshold to allow indentation (i.e. penetration). The interface response of PVC geomembrane with nonwoven geotextiles can be described as ductile, elasto-plastic and strain-hardening stress-displacement behavior due to the pliable characteristics of the surface as well as the soft and flexible nature of the sheet material itself.

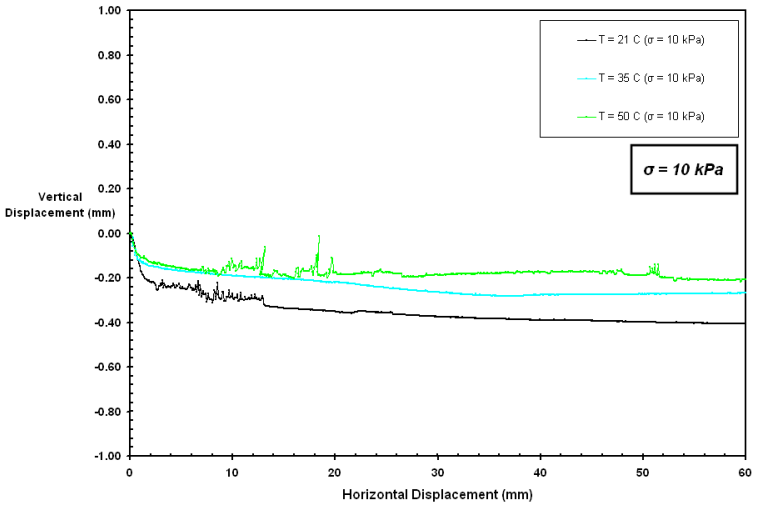

(a)

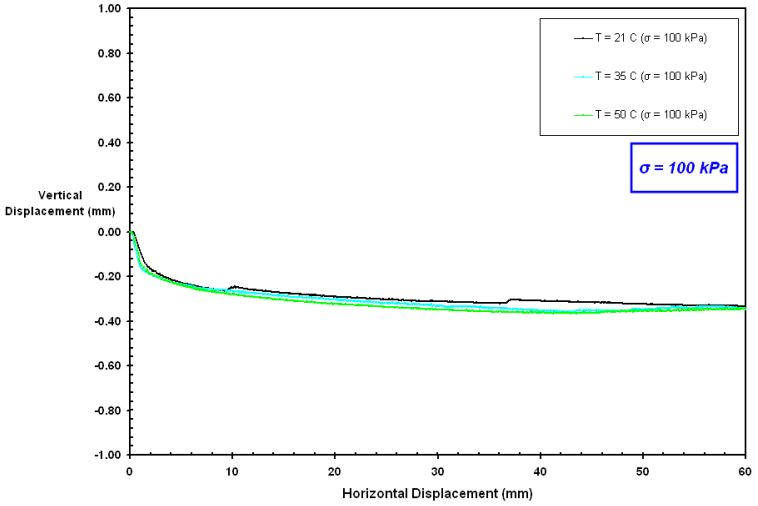

(b)

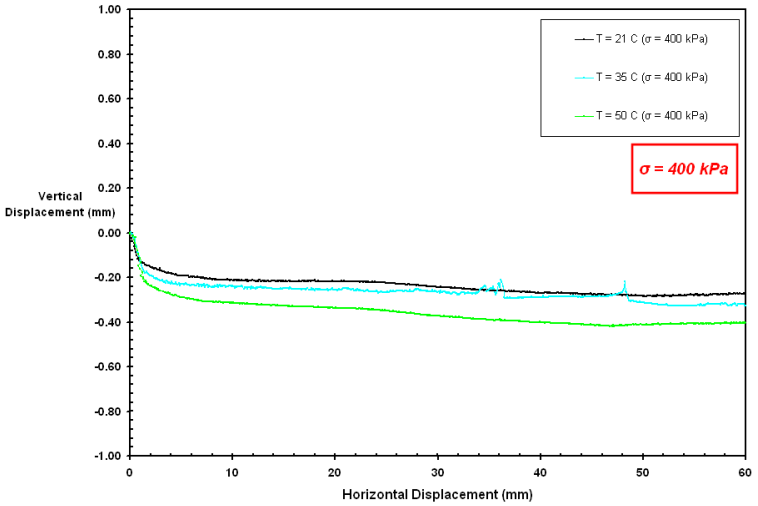

(c)

Figure 6.15 The Variation of Vertical Displacement with Horizontal Displacement at Different Temperatures for EPI PVC Smooth Geomembrane/NPNW Geotextile

The displacement hardening behavior can have important design implications in that PVC geomembranes can be well suited for applications in which low normal stresses are expected such as landfill top caps where a thin layer of soil is placed on top of the landfill for vegetation or landscaping purposes.

The higher frictional resistance and the larger interface shear response in terms of stress – displacement failure envelope is related to the physical properties of the geosynthetic layered systems including hardness, stiffness, and temperature dependency which tend to alter the shear strength mobilized at the interface. As shown in Figures 6.14 from the stress-displacement relationships for different ambient temperatures, the residual (post-peak) shear strengths of the PVC interface at all test temperatures were larger than the peak values. The peak frictional strengths were determined at small shear displacements (0.8 – 1 mm for 10 kPa; 1.1 – 1.5 mm for 100 kPa and 2 – 2.4 mm for 400 kPa normal stresses) to be consistent with the relatively small displacement range to peak values of the smooth HDPE system. In light of this, the resulting interface friction angles and coefficient of friction values as a function of temperature are presented in Figures 6.16 and 6.17, respectively. However, it should be underscored that the smooth PVC geomembrane interface under consideration exhibited approximately <5 % strength-gain with displacement for the plastic stage of the curves without any loss in shear resistance. As such if the peak strength of the interface is considered as the maximum mobilized frictional resistance of the interface, then it is appropriate to indicate that the smooth PVC system reaches peak-strength conditions at substantially larger shear displacements as compared to the peak displacement of the relatively stiff smooth HDPE interface.

The greater shear resistance of the smooth PVC is attributed to higher surface pliability enabling more interaction with the counterface geotextiles. Less surface indentations occur at the interface when the counterface materials are relatively stiff and less malleable. This can influence the extent of the contact area at the interface and the number of contacts developing between the counterfaces under the application of the load. As such when the surfaces of counterface polymeric materials show more adaptable and flexible characteristics under load application, this can facilitate a greater interaction developing at the interface between the counterfaces. Further, the increased surface pliability and soft material nature of the smooth PVC allows the geotextile to embed and establish more intimate interaction.

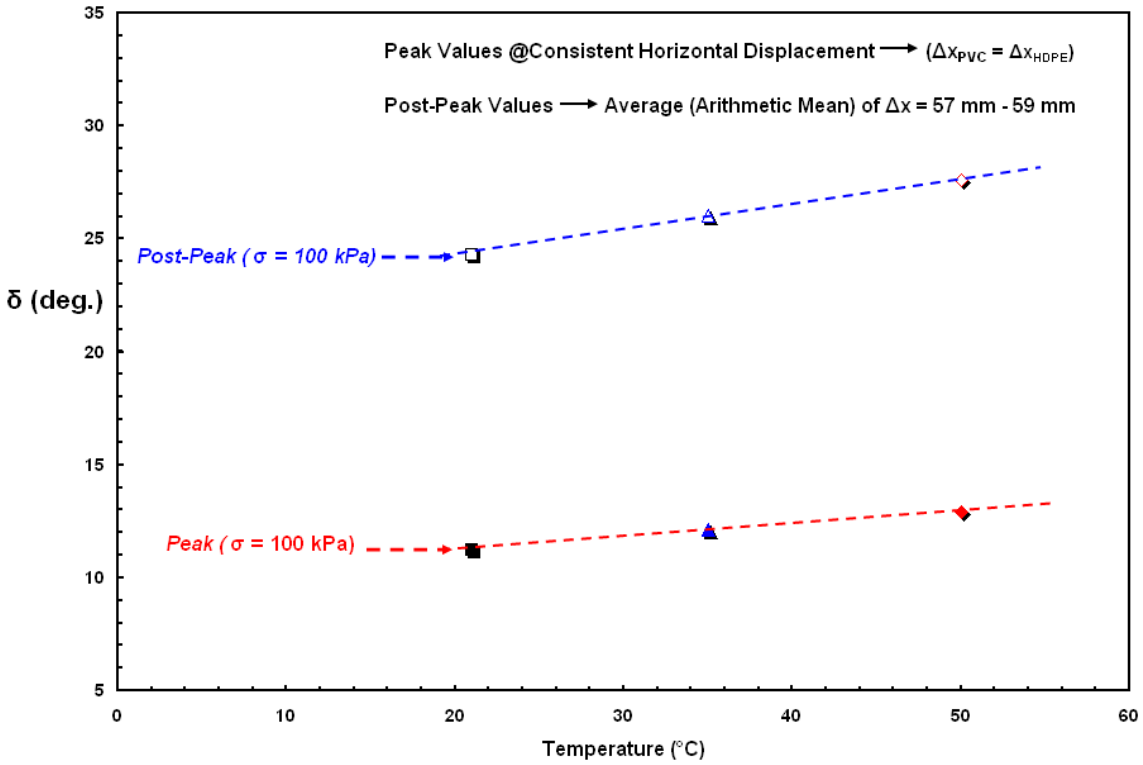

Figure 6.16 The Change of Interface Friction Angle, [δ] with Temperature for EPI Smooth PVC Geomembrane/NPNW Geotextile Interfaces at 100 kPa Normal Stress

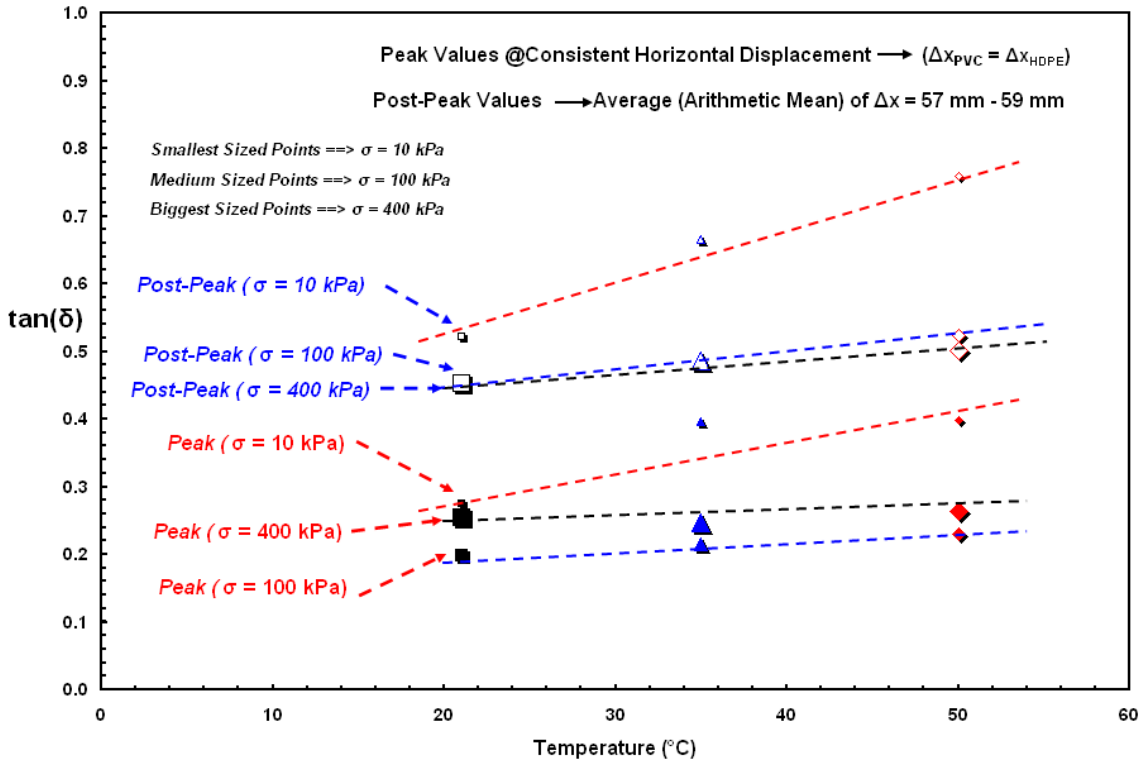

Figure 6.17 The Change of Coefficient of Friction, [tan(δ)] with Temperature at Different Loading Conditions for EPI PVC Smooth Geomembrane/NPNW Geotextile Interfaces

Figure 6.18 shows both the peak and the residual failure envelopes generated based on Mohr-Coulomb criterion at different temperatures. The slope of linear strength envelopes increases slightly with increasing ambient temperature. It is evident from a comparison of the strength envelopes of the smooth PVC with those of the smooth HDPE (Figure 6.18 and Figure 6.11, respectively) that the smooth PVC system yielded higher peak and residual (post-peak) shear strengths than the smooth HDPE system at all temperatures tested. Further, no post-peak strength loss (i.e reduction in frictional resistance) occurred at PVC interface due to higher surface pliability and material flexibility. As the shear stress – horizontal displacement behavior of the smooth PVC interfaces with NPNW geotextile at all temperatures tested is predominantly a plastic strain-hardening ductile response, the post-peak shear strength values mobilized at the interface were larger than the peak frictional resistances determined at small shear displacements determined at the peak-displacement values of the smooth HDPE tests. The Mohr-Coulomb failure envelopes plotted for different ambient temperatures using least squre fit method at a relatively large range of normal stresses from 10 kPa to 400 kPa for the PVC smooth geomembrane – NPNW geotextile interface provided a good straight line fit at all temperatures. In order to better capture the alteration in the interface behavior at low normal stresses, both the peak and residual strength envelopes were replotted on logarithmic scales (Figure 6.19) and it was observed that the failure enveloped showed some very slight curvature under low normal stresses, particularly at elevated temperatures.

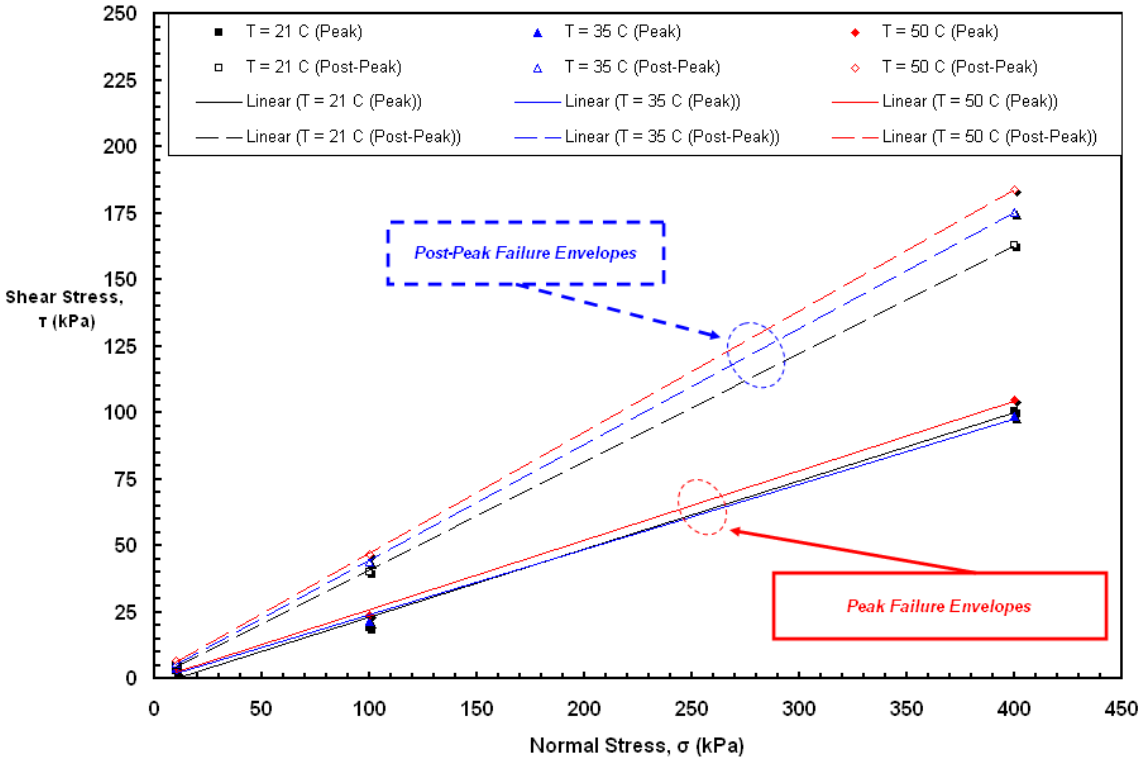

Figure 6.18 The Alteration of Peak and Residual Strength Envelopes with Increasing Temperature for EPI PVC Smooth Geomembrane/NPNW Geotextile Interfaces

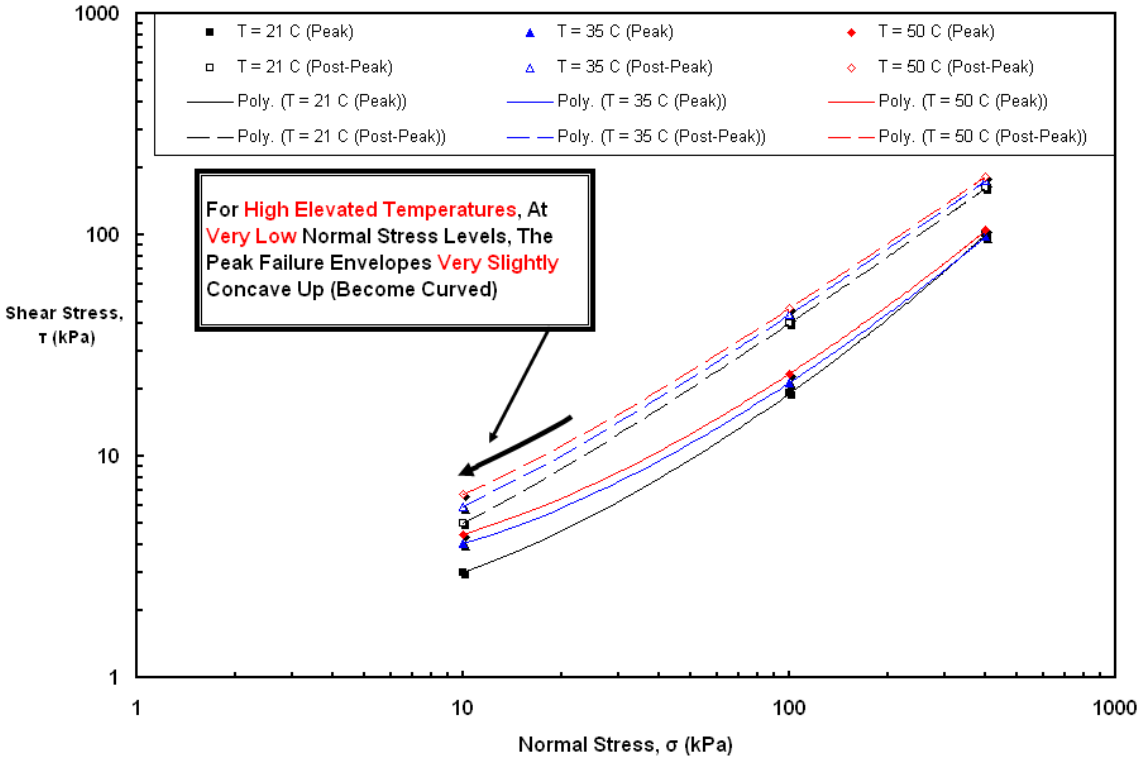

Figure 6.19 The Transformation in Failure Envelopes with Temperature at Different Loading Conditions for EPI PVC Smooth Geomembrane/NPNW Geotextile Interfaces

For the smooth geomembrane – nonwoven geotextile interfaces, sliding of the geotextile against the geomembrane at the interface is one of the primary mechanisms of the mobilized shear strength (Frost and Lee, 2001). Based on laboratory observations made on post-test geomembrane specimens, it was noted that the tested surface of the smooth HDPE geomembrane that had been sheared against the geotextile was polished particularly at higher normal stresses. The striations which had been created during the interface shear tests were parallel to each other and oriented in the shear direction. The surface of the smooth HDPE geomembranes are relatively stiff and firm, and therefore show less flexibility and malleability to the damaging impact of relatively stiff PP filaments of the counterface geotextile under load and the resulted shear stresses imposed due to shear displacement. The observed sensitivity of the smooth HDPE can be attributed to the polishing of this lining material with increased shear displacements. The post-peak strength loss exhibited by an interface can be quantified with a ratio (Interface Sensitivity, $S\tau$: Equation 6.3) between peak and residual shear strengths. The interface sensitivity increased slightly for smooth HDPE, while it remained constant for smooth PVC (with an exception of the highest normal stress level which showed a slight decrease) with increasing temperature (Figure 6.20).

$$S\tau = \left(\frac{\tau_{Peak}}{\tau_{Residual}} \right) \tag{6.3}$$

Where;

$S\tau$: Interface Sensitivity

τ_{Peak}: Peak Shear Strength mobilized at the Interface

$\tau_{Residual}$: Residual (Post-Peak) Shear Strength mobilized at the Interface

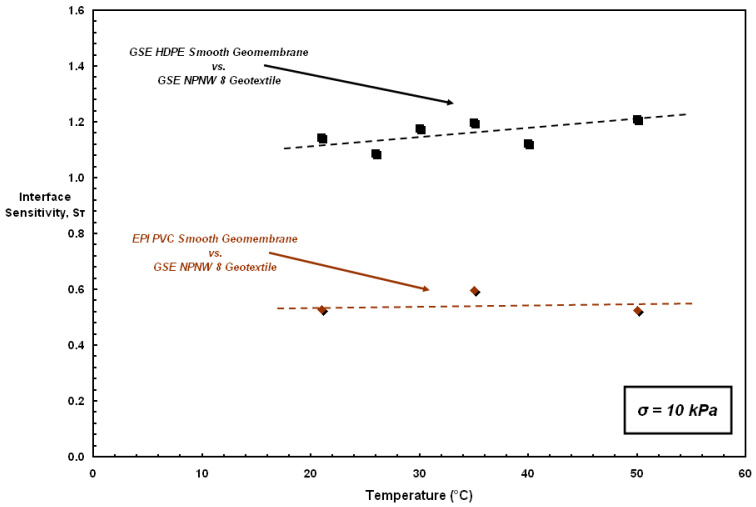

(a)

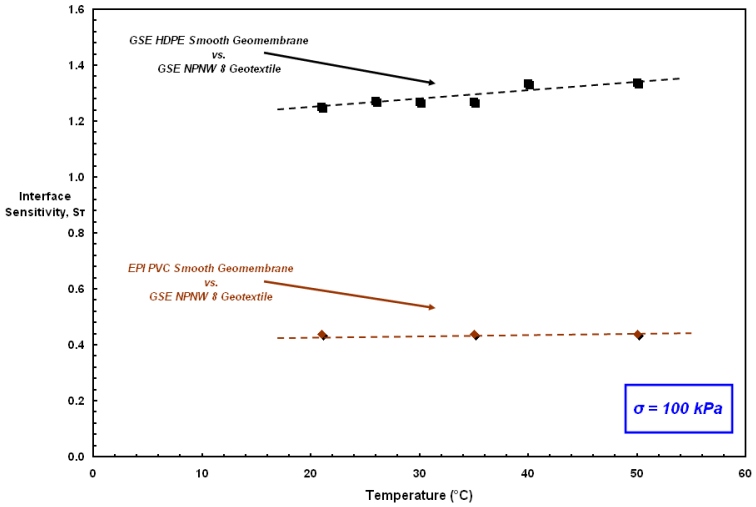

(b)

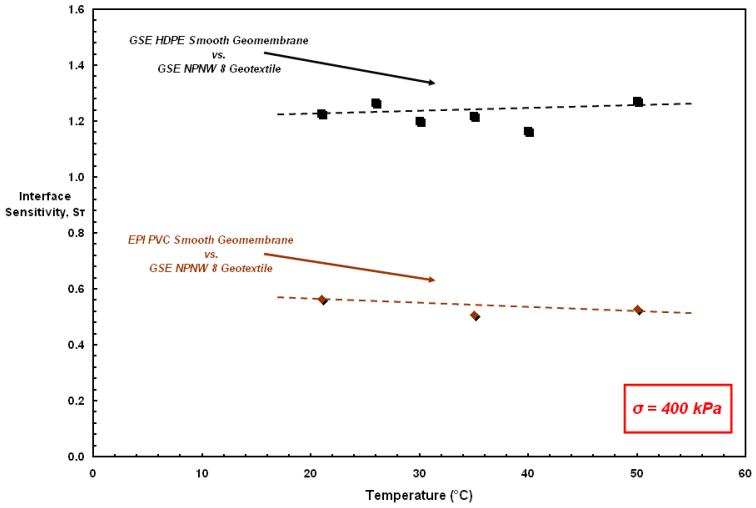

(c)

Figure 6.20 The Change of Sensitivity with Temperature for GSE Smooth HDPE or EPI Smooth PVC Geomembrane/NPNW Geotextile Interfaces: (a) 10; (b) 100; (c) 400 kPa

6.6. Relative Influence of Material Hardness on Interface Shear Behavior at Same Test Temperatures for HDPE and PVC Geomembranes

The smooth HDPE (GSE) and PVC (EPI) geomembranes tested against the same NPNW PP geotextile in the experimental program have analogous characteristics in terms of surface roughness, textural properties, and thickness, but are produced from different base polymer resins, and thus, have dissimilar surface hardnessess. Figures 6.21a, 6.21b and 6.21c show the results of interface tests at room temperature at three different normal stress levels of 10 kPa, 100 kPa and 400kPa, respectively, to examine the influence of load level on the shear response of the two materials. The subsequent plots (Figures 6.22a, 6.22b and 6.22c) present the interface shear test results at elevated test temperatures ranging from 21°C up to 50°C for normal stress levels of 10 kPa, 100 kPa and 400 kPa, respectively, to further investigate and to compare behavioral variations at elevated temperatures in the shear response of HDPE and PVC geomembranes. It is evident that there is a difference in the interface behavior as well as in the magnitude of the shear strength (peak and residual) mobilized at the interfaces. The differences in shear response as well as the peak and/or post-peak resistance even though both geomembranes possess similar surface roughness and other geometric properties results from the physical property of the polymeric materials including their hardness and surface pliability which are strongly temperature dependent. For example, an increase in temperature results in a decrease in surface hardness, and consequently leads to an increase in the amount of interface resistance/strength mobilized.

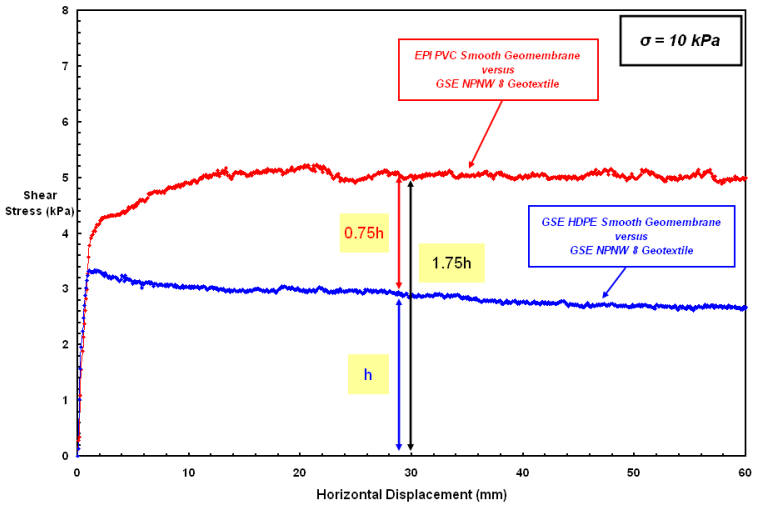

(a)

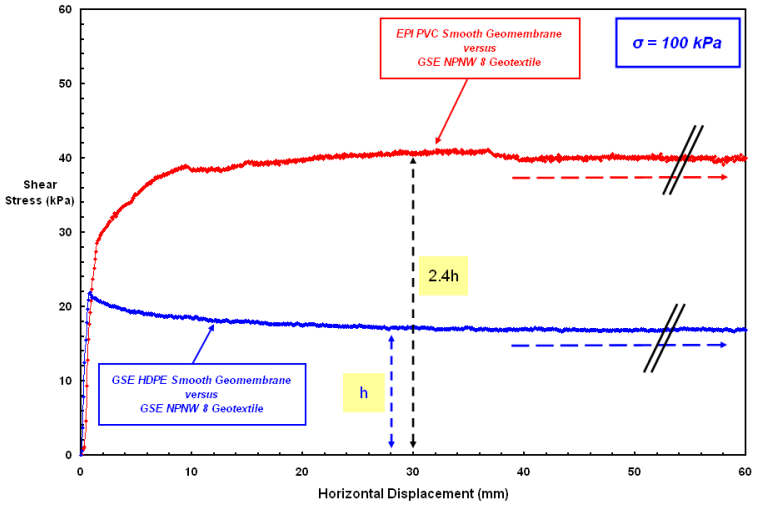

(b)

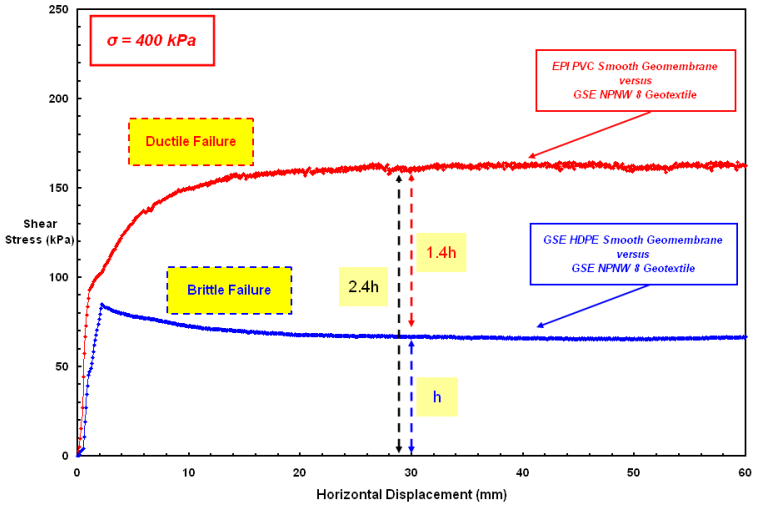

(c)

Figure 6.21 Comparison of Stress-Displacement Curves between GSE Smooth HDPE and EPI Smooth PVC Geomembrane/Geotextile Interfaces: (a) 10; (b) 100; (c) 400 kPa

The higher pliability nature of PVC geomembranes resulted in a ductile failure mode with shear deformation as opposed to the HDPE liner response which exhibited brittle interface failure (Figure 6.21). The PVC geomembrane interfaces reached peak strength conditions at larger displacements than the HDPE ones. Further, they did not experience a post-peak strength loss and displayed an elasto-plastic response in which no distinguished peak was observed. On the other hand, the HDPE interface peaked at lower shear displacements; progressed with a sharp peak in brittle failure mode; and finally involved a pronounced post-peak strain softening during the tests. The peak resistance attained from the PVC tests under same boundary conditions is approximately 1.75 times and 2.40 times at low (10 kPa) and at high (100, 400 kPa) normal stresses, respectively, that obtained from the HDPE tests. Further, it is likely that there is a direct correlation between the extent of contact area at the interface and the shear strength mobilized. Therefore, the PVC interface was estimated to have a contact surface area which is 30% to 40% larger than that of the HDPE because of its lower surface hardness.

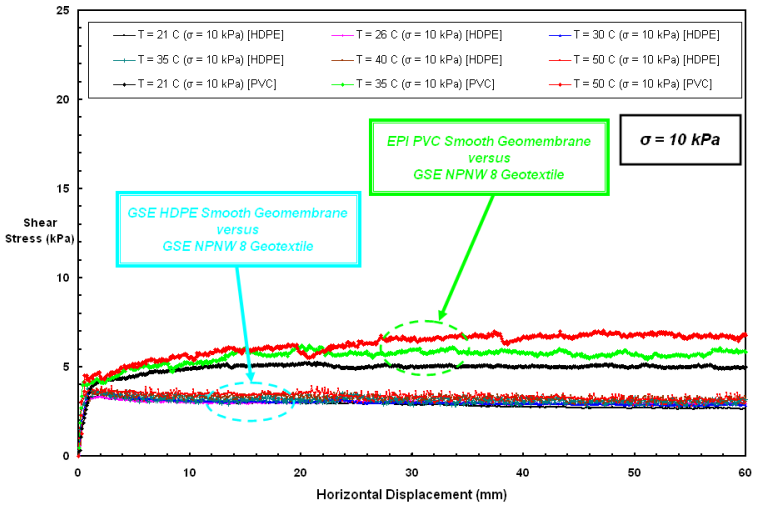

(a)

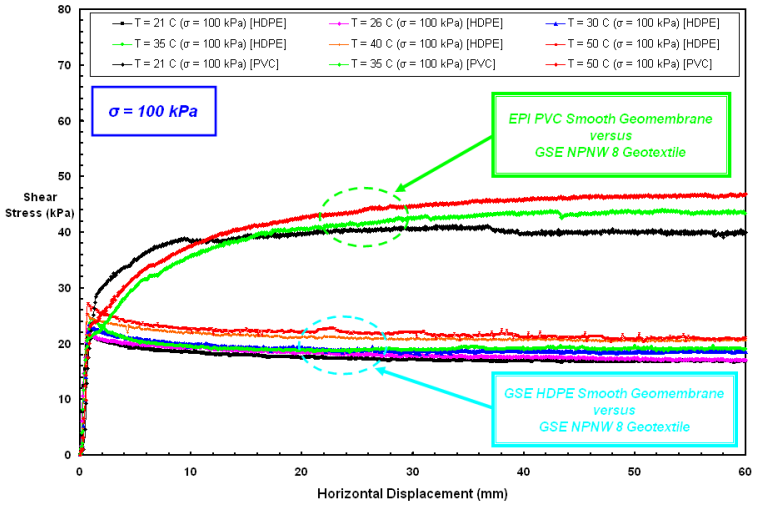

(b)

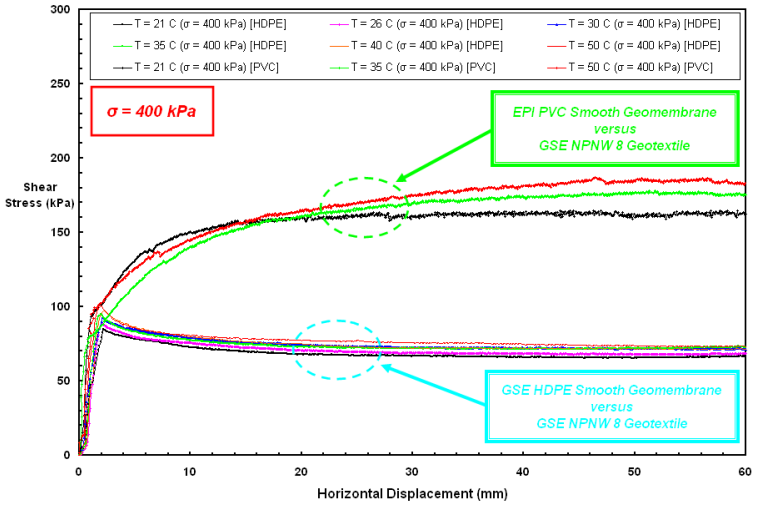

(c)

Figure 6.22 Comparison of Interface Test Results between GSE Smooth HDPE and EPI Smooth PVC Geomembrane/NPNW Geotextile: (a) 10 kPa; (b) 100 kPa; (c) 400 kPa

Visual observations of post-test geomembrane specimens showed that there are striations on the HDPE geomembrane samples after shearing at all test temperatures and normal stresses, particularly at 100 kPa and above. In contrast, the PVC specimens did not display any noteworthy striations after being sheared against geotextiles because of their flexible and elastic nature. It is considered that after the removal of the normal load applied during the shearing process, the highly plasticized PVC liner surface rebounds to its original state, similar to the behavior of other soft plastics. Consequently, this higher pliability of the PVC geoembrane accounts for the zero post-peak strength loss at all test temperatures ranging from 21 °C to 50 °C as shown Figure 6.22 as well as the larger shear resistances observed when located adjacent to nonwoven geotextiles in composite layered systems. The case for the shear tests with particulate materials is different and will be discussed in Chapter 8.

In contrast, the stiffer HDPE geomembrane did not allow the counterface geotextile to settle in completely. However, as the ambient temperature increases, the material hardness of the HDPE geomembrane decreases and becomes more pliable and consequently, the frictional resistance when sheared against geotextile gets larger. At the same time, it could not reach the strength of the PVC interface even at higher temperatures as the magnitude of surface hardness of HDPE at 50 °C (i.e. highest test temperature level) is substantially lower than that of the PVC regardless of the normal stress applied (Figure 6.22). In addition to the difference in surface hardness of these lining materials, the surface roughness of the untested PVC geomembrane is larger than that of the untested HDPE geomembrane ($R_{a\ PVC}$ = 0.17 μm > $R_{a\ HDPE}$ = 0.13 μm). The geomembrane surface roughness is one of the primary factors governing the resulted

frictional resistance mobilized at geotextile-geomembrane interfaces. In light of this, the differences observed in the mobilized shear strengths of the smooth HDPE and the smooth PVC geomembrane interfaces may also be influenced by minor differences in surface roughness of these lining materials.

The peak and residual (post-peak) coefficient of friction versus normal stress plotted on log-log scale are shown in Figures 6.23a and 6.23b, respectively for the lowest (21°C) as well as the highest (50°C) test temperatures. The coefficient of friction for both smooth HDPE geomembrane interface and smooth PVC geomembrane interface decreased with normal stress at low normal stress levels of up to ~100 that is consistent with Hertzian contact theory (Johnson 1982). Under high normal stresses, the coefficient became constant or increased with normal stress. This is related to the higher interbedding occurring between the counterfaces at larger normal load and is comparable to the plowing effect that is often found at a granular material/planar surface interface as previously noted by Dove and Frost (1999). In all cases, the effect of elevated temperature was to increase the peak and residual coefficient of friction at all normal stress levels.

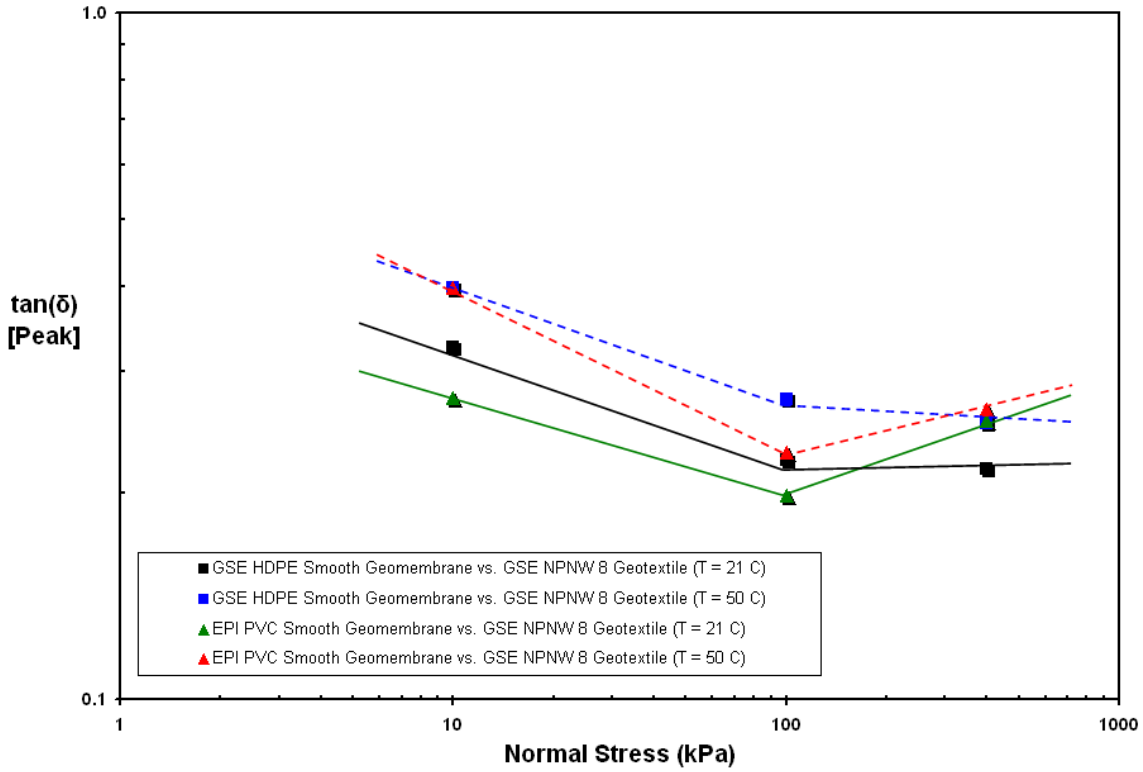

(a)

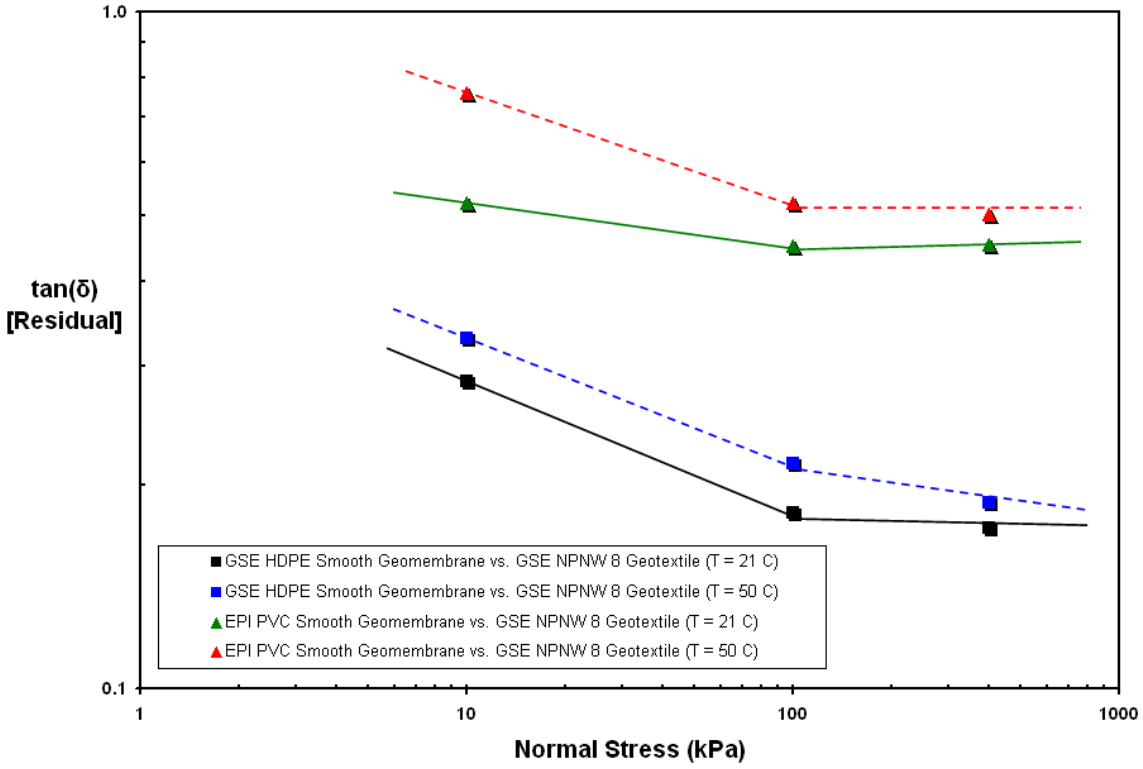

(b)

Figure 6.23 Log Coefficient of Friction [tan(δ)] versus Log Normal Stress [σ] Plots for the tested Smooh HDPE or PVC Geomembrane/NPNW Geotextile: (a) Peak; (b)Residual

Figures 6.24 and 6.25 show the surface hardness of both smooth HDPE and smooth PVC geomembranes measured at different temperatures and the change in their surface hardness with temperature, respectively. The hardness of PVC liners at all test temperatures is 0.4 – 0.5 times of the surface hardness of HDPE geomembranes; and this ratio continues in this range (0.4 – 0.5) even with increasing temperature as both the liner materials get softer and more malleable as their hardnessses are reduced. The PVC surface allows the counterface geotextile to interact more completely at all temperature levels tested. In addition, the softer nature of PVC assists the overlying/underlying interface component to embed into the geomembrane body by forming a more intimate interface interaction as shearing progresses at each elevated temperature. Finally, the geotextile fibers are interwoven and interconnected by means of a textile manufacturing method including bonding or needle-punching. If the PVC liners are more flexible and bendable, they are less likely to damage the overlying geosynthetic by pulling out and tearing delicate geotextile filaments from the fabric during the shearing process and allow the overlying material to remain intact with little damage. This can facilitate negligible or less post-peak strength loss (ie. reduction in frictional resistance) occurring at the interface of the geomembrane in conjunction with NPNW geotextiles.

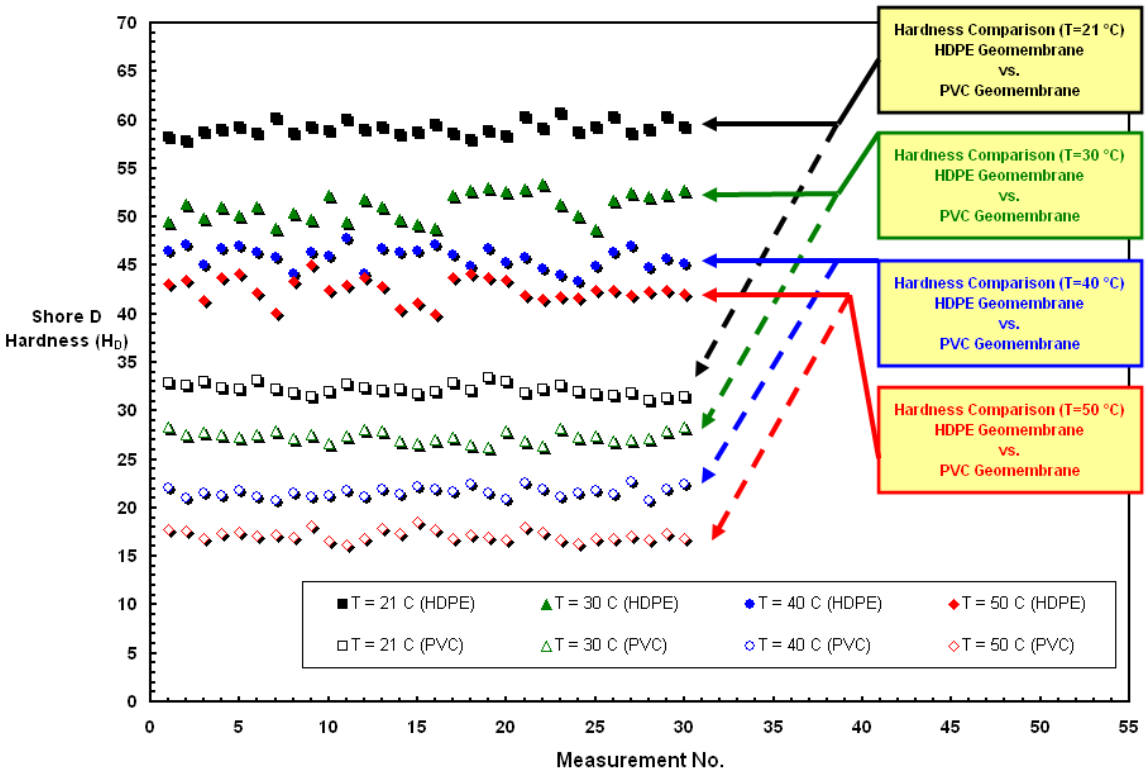

Figure 6.24 The Change in Surface Hardness of GSE Smooth HDPE Geomembrane and EPI Smooth PVC Liner with Temperature

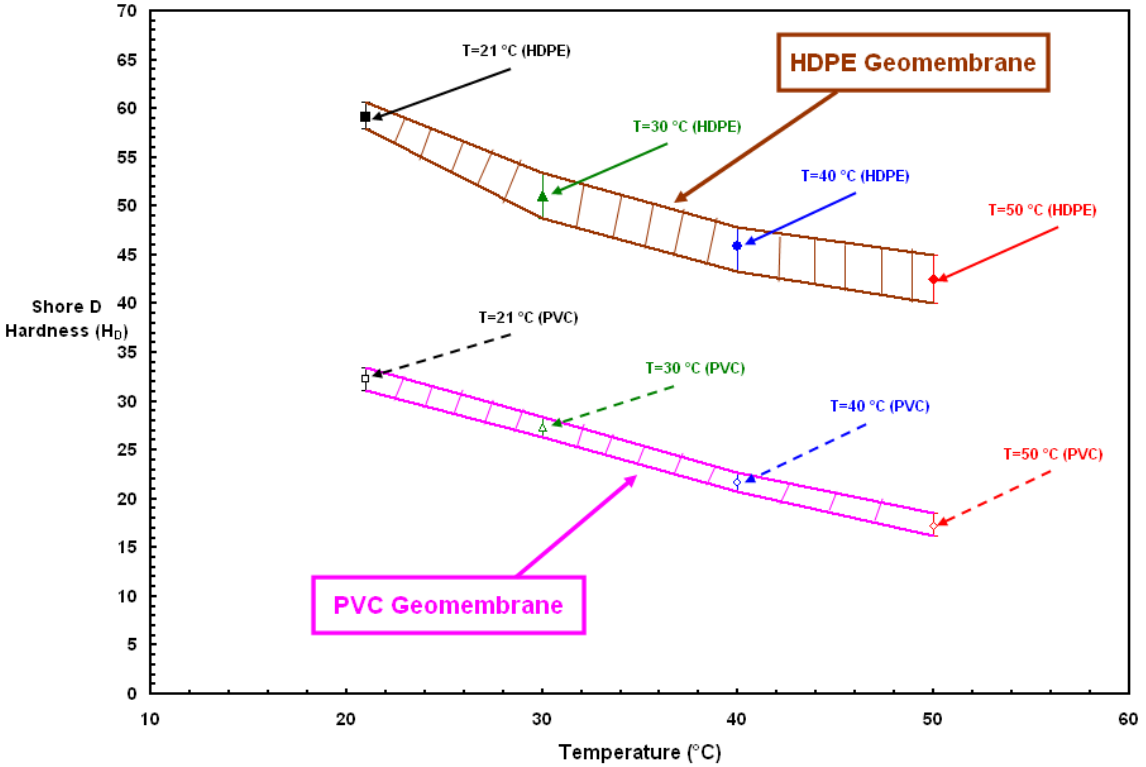

Figure 6.25 The Variation of Surface Hardness as a Function of Temperature for GSE Smooth HDPE Geomembrane and EPI Smooth PVC Liner

Comparing the peak coefficient of frictions, (tan(δ)) mobilized at smooth HDPE – NPNW geotextile interfaces and smooth PVC – NPNW geotextile interfaces over the entire range of test temperatures from 21°C up to 50°C, the interface frictional strength of the HDPE geomembrane is greater ([$\tau_{Peak\text{-}HDPE} \approx \{1.25 \text{ to } 1.35\} * \tau_{Peak\text{-}PVC}$]) (Figure 6.26). In addition, the rate of increase in the peak friction coefficient with temperature is slightly larger for smooth HDPE interface than that of smooth PVC interface. This can be an advantage of smooth HDPE interface layered systems at elevated temperatures in enabling higher small displacement shear resistances in conjunction with geotextiles as compared to smooth PVC.

The smooth HDPE interface exhibited a post-peak strength loss while the smooth PVC did not display any reduction in frictional resistance with displacement. PVC displayed a strength-gain shear response regardless of the temperature tested and/or the magnitude of load applied during the interface tests. The strength–increasing mechanisms are likely to offset the strength–reducing effects, and thereby, a loss in mobilized frictional resistance was prevented from occurring with continued shear displacement at all temperatures tested. The ductile shear behavior of PVC liner resulted from the pliable surface properties and the plasticized nature of the liner. For smooth HDPE, the interface exhibited a slight strength loss after peak resulting from strength-reduction factors including polishing of the geomembrane sheet surface by the relatively stiff PP filaments. The resulting shear stress – displacement behavior of smooth HDPE and geotextile interface shows in general a brittle response at all temperatures.

Figure 6.27 shows the change in the residual (post-peak) frictional resistance of both HDPE and PVC interfaces as a function of temperature (21°C< T <50°C). In

contrast to the rate of increase observed in the mobilized peak shear strengths with increasing ambient temperature, a higher rate of increase in the mobilized post-peak frictional resistances was observed for PVC interface. Additionally, owing to the strain-hardening response, the PVC interface displayed larger post-peak strengths at all temperatures tested, whereas, due to strain-softening behavior occurring at the interface, the HDPE exhibited lower post-peak strengths ($[\tau_{Residual\text{-}PVC} \approx \{2.3 \text{ to } 2.5\} * \tau_{Residual\text{-}HDPE}]$).

Under load application at the interface, the higher surface pliability (i.e: hardness related) of the polymeric geomembrane influences the development of surface depressions with the counterface material. This impacts the formation of larger contact and/or interaction point with the counterface. The response of a polymeric geomembrane is also related to its base sheet material physical properties including thermal relaxation and/or expansion with temperature.

Based on the change of the peak and the residual shear strengths with temperature (Figures 6.26 and 6.27, respectively), the PVC and HDPE shows similar susceptibility to ambient temperature change for both peak and post-peak strengths.

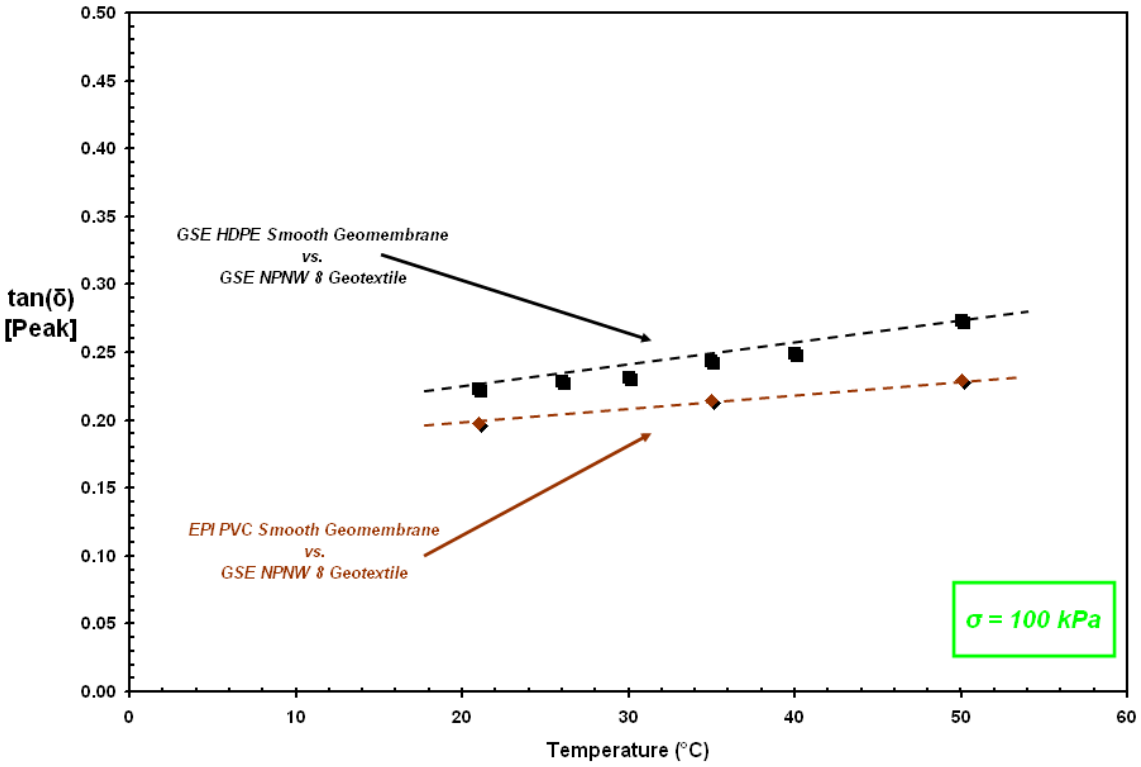

Figure 6.26 The Change of *Peak* Coefficient of Friction with Temperature for GSE Smooth HDPE or EPI Smooth PVC Geomembrane/NPNW Geotextile Interfaces

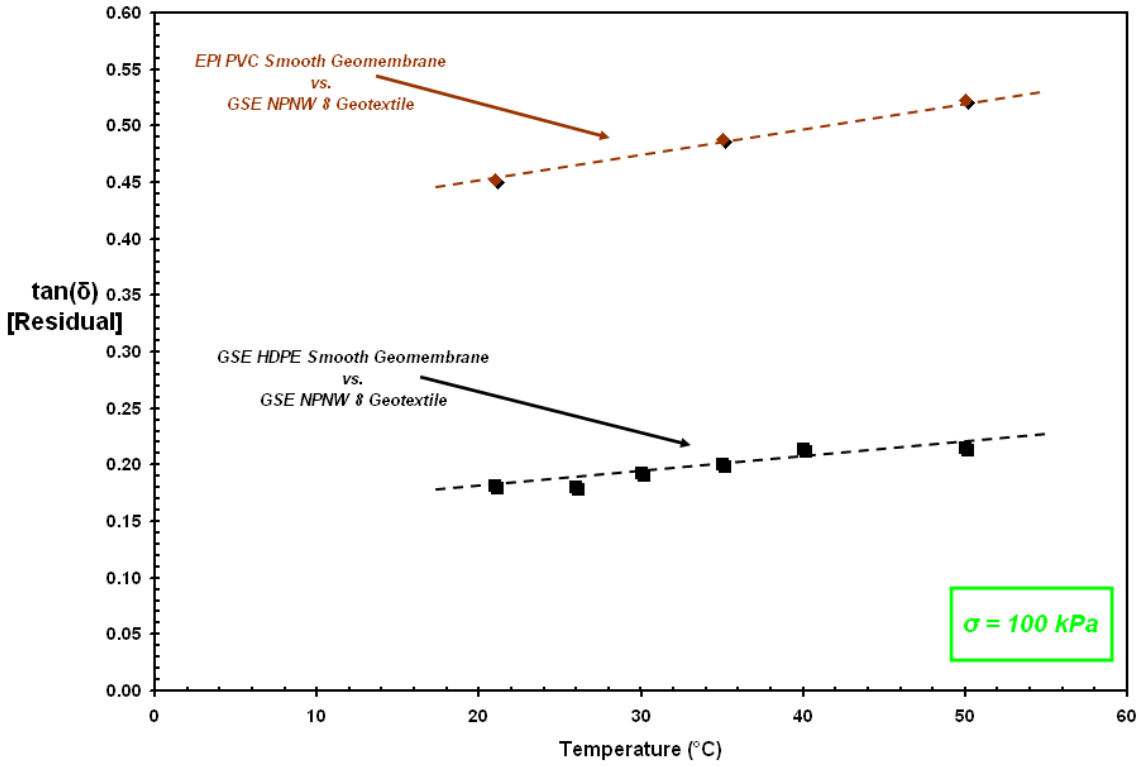

Figure 6.27 The Change of *Residual* Coefficient of Friction with Temperature for GSE Smooth HDPE or EPI Smooth PVC Geomembrane/NPNW Geotextile Interfaces

6.7. Replicate Interface Shear Tests at Various Test Temperatures

As a verification of the stability of the temperature controlled chamber during both heat-up as well as constant temperature stages, a number of replicate tests were conducted for different smooth geomembrane (HDPE, PVC) – geotextile combinations at different temperatures. The results are presented in Figures 6.28 – 6.30. Virgin geomembrane and geotextile specimens were used in each test. The results demonstrate a high level of repeatability achieved at different conditions involving various ambient test temperatures and various counterface materials.

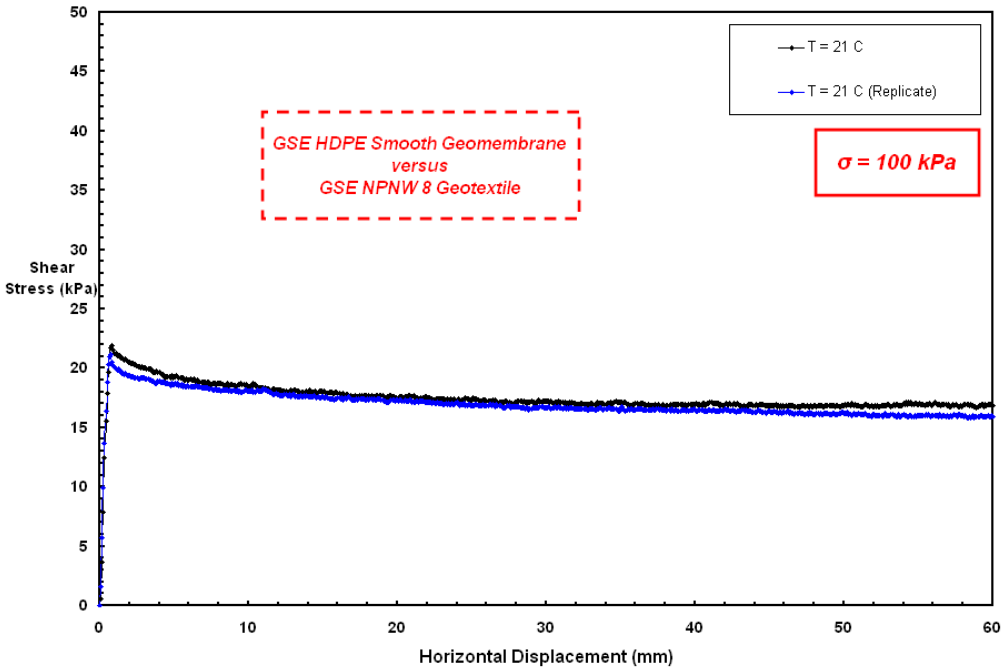

(a)

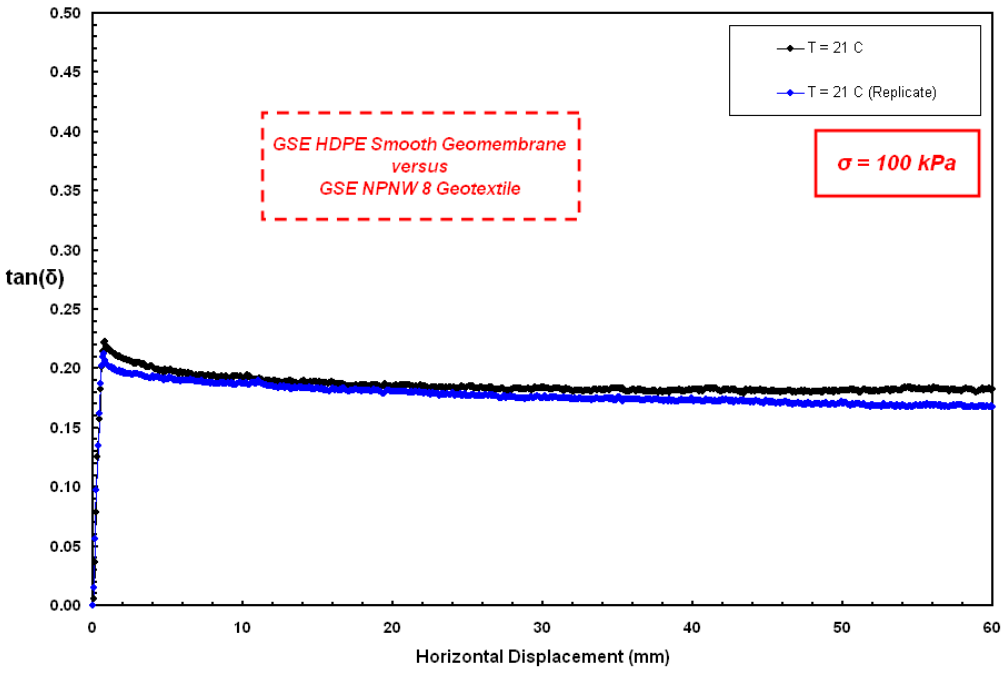

(b)

Figure 6.28 Replicate Interface Shear Tests on GSE HDPE Smooth Geomembrane versus GSE NPNW Geotextile Interfaces at Room Temperature (T = 21°C)

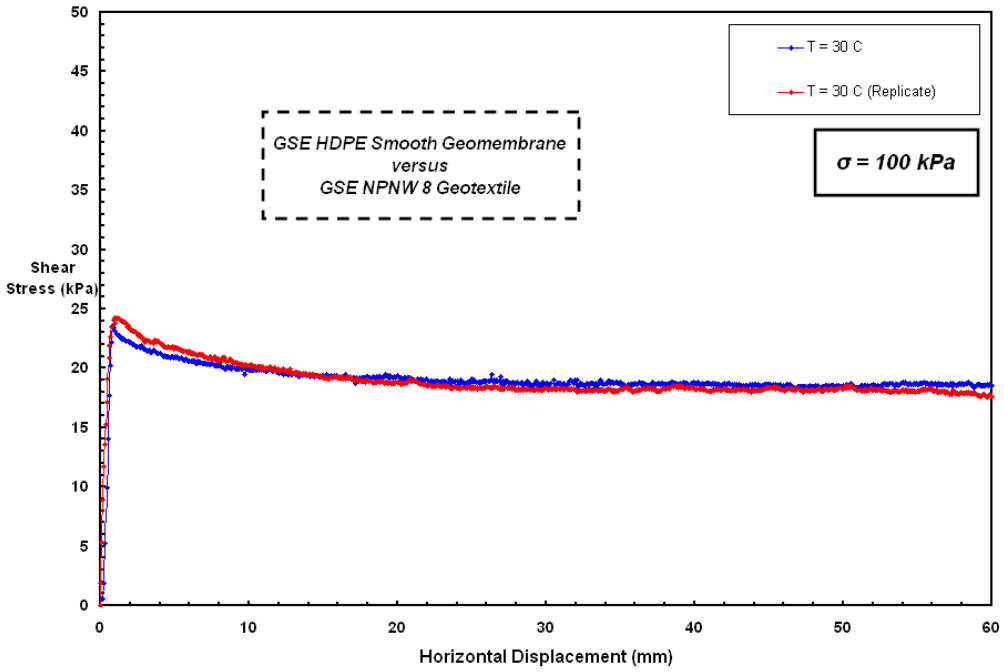

(a)

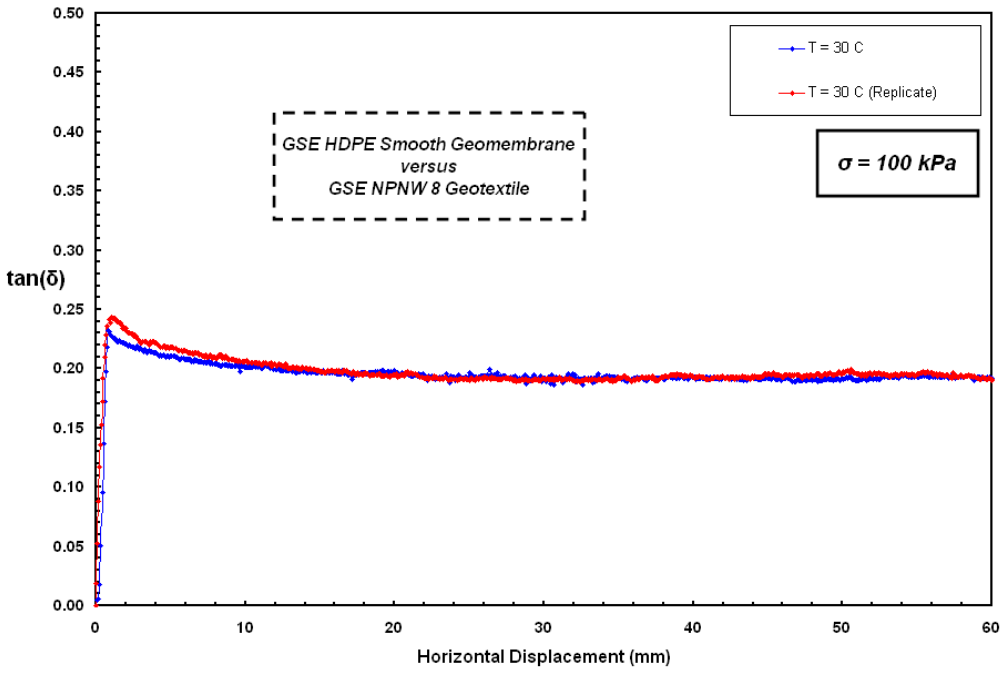

(b)

Figure 6.29 Replicate Interface Shear Tests on GSE HDPE Smooth Geomembrane versus GSE NPNW Geotextile Interfaces at Elevated Temperature (T = 30°C)

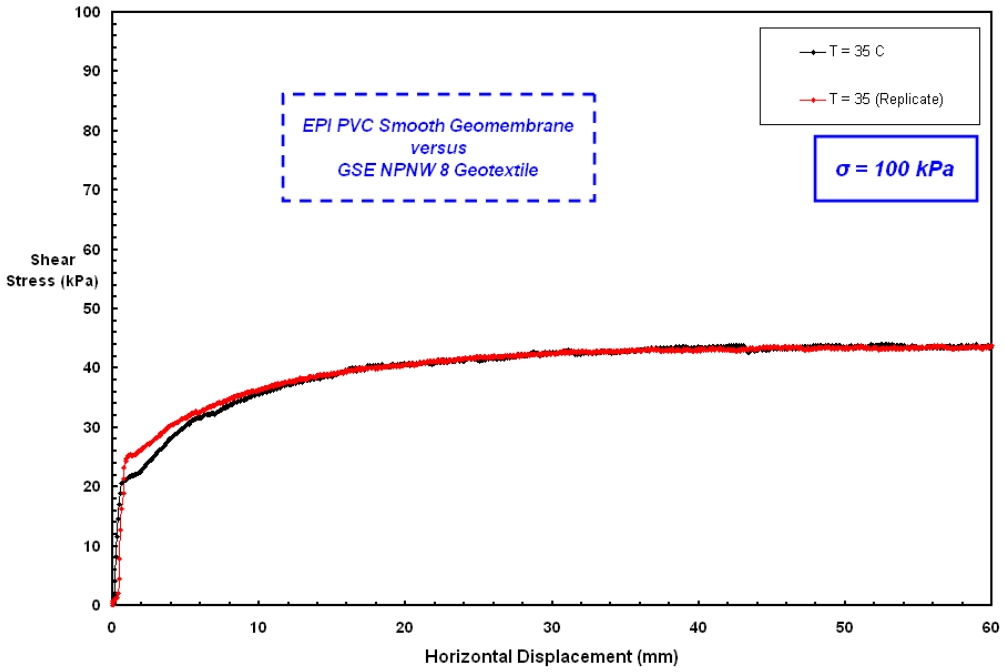

(a)

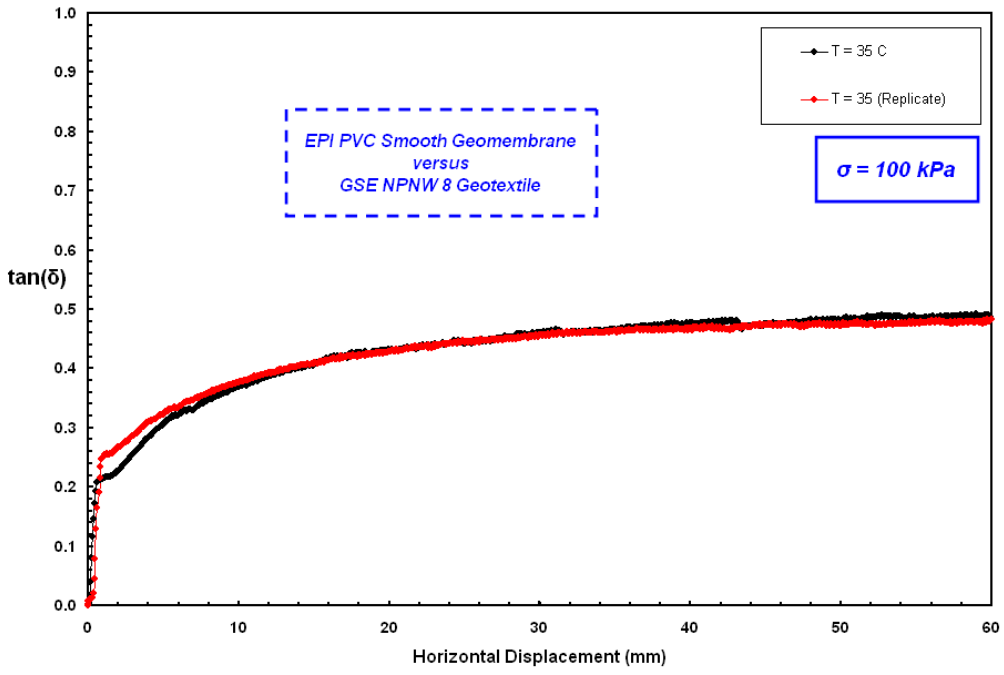

(b)

Figure 6.30 Replicate Interface Shear Tests on EPI PVC Smooth Geomembrane versus GSE NPNW Geotextile Interfaces at Elevated Temperature (T = 35 °C)

6.8. Summary and Conclusions

This chapter described the influence of elevated temperature on the interface shear behavior of relatively stiff and relatively softer smooth geomembranes and NPNW geotextile interfaces through a series of direct shear tests performed at different ambient temperatures in the TCC. The results of the interface shear tests conducted at different temperatures produced a database for the purpose of the comparison between the mobilized frictional resistances of the smooth HDPE geomembrane as well as smooth PVC liners with NPNW geotextiles at different ambient temperatures. The interface test results show the differences observed in the shear behavior of the tested materials.

The frictional resistance of geosynthetic interface layered systems is project-specific and product-dependent (Koerner, 1998). The presentation and discussion of the experimental results concentrated on the shear behavior and the changes in shear response due to change in temperature rather than providing specific shear-strength values for use in design applications. This experimental database can provide an insight into understanding the frictional shear performance of certain geosynthetic interfaces at elevated temperatures, as well as can provide guidance for selecting the appropriate geomembrane liner materials required for the design of composite layered systems comprising geotextiles in conjuntion with geomembranes to maximize the shear resistance mobilized at the interface in harsh environmental conditions at elevated temperatures. Additionally, it is noted that site-specific interface testing can be required to be conducted for the design of particular geotechnical applications exposed to varied temperature conditions.

The stress-displacement failure curves at the different normal stress levels, including low to high loading conditions were presented throughout the chapter with intention of enabling rigorous analysis of the various composite geosynthetic lining systems at different temperatures. The strain-softening/strain-hardening behavior of the interfaces at different ambient temperatures was quantified by a ratio between peak and residual strengths. The change in the interface sensitivity was plotted as a function of temperature. For interfaces with a relatively stiff HDPE geomembrane compared to those with a pliable PVC liner resulted in higher sensitivity values observed over the entire range of normal stresses and temperatures tested. Due to the differences in surface hardnesses of HDPE and PVC geomembranes, the smooth PVC exhibited higher shear stress – displacement failure curves than those of the smooth HDPE at all temperatures tested although both lining sheet material posssess similar and analogous surface roughness characteristics. In addition, there was no post-peak strength loss observed for the smooth PVC geomembrane interfaces when in contact with the NPNW geotextile. The greater frictional resistance of the smooth PVC geomembrane is attributed to its higher surface pliability and flexible sheet material nature. The high malleability and more plasticized nature of the PVC can also account for the marginal post-peak strength-gain (i.e: displacement-hardening behavior) observed with the counterface geotextile over the entire test temperatures ranging from 21 °C up to 50 °C. The counterface geotextile was able to embed into the softer surface of the smooth PVC geomembrane.

In short, the interface frictional resistance of both smooth HDPE or PVC geomembranes and NPNW geotextile interfaces increased with increasing ambient temperature owing to a decrease in material hardness, and hence, an increase in surface

pliability of the geomembranes. It is considered that the acceleration of the polymer relaxation at elevated temperatures resulted in quick dispersion of the concentrated stresses over the interface contact area after the application of load leading to more uniform stress distribution over the entire contact surface at the interface during shear displacement.

The temperature sensitivity of the smooth HDPE or PVC geomembrane and nonwoven geotextile interfaces is consistent with polymer intrinsic physical properties as being susceptible to ambient conditions (i.e. temperature). An increase in ambient temperature results in softening of the polymer and a reduction in stiffness as the temperature increases leading to greater flow of the polymeric material under a load application and greater interaction with the counterface. The peak and post-peak strength values as defined using the quantitative strength parameters including coefficient of friction, (tan(δ)) and friction angle, (δ) showed an increase with temperature. This is consistent with previous observations made by the others for the change of frictional resistance between polymers with increasing temperature. The change of tan(δ) and δ over the entire range of test temperatures ranging from 21°C up to 50°C pertains to the particular geosynthetic combinations utilized in this study.

CHAPTER VII

7. ELEVATED TEMPERATURE EFFECTS ON GEOTEXTILE – *TEXTURED* GEOMEMBRANE INTERFACE SHEAR BEHAVIOR

7.1. Introduction

In general, geomembranes used in combination with geotextiles are often textured to allow for better compliance and interaction between the synthetic materials. For example, past geosynthetic interface research has demonstrated that for layered systems involving textured geomembranes, the peak stress occurs at larger displacements (i.e: 5 mm to 10 mm) compared to that for smooth geomembranes; however, the textured geomembrane interfaces exhibit a significant decrease in shear stress after the peak stage as shearing displacement continues. Similar results and further discussions can be found from the primary studies on this issue including: Stark et al. (1996); Lee and Frost (1998); Hillman and Stark (2001); and Frost and Lee (2001).

In order to understand friction characteristics of fibrous materials such as geotextiles, an extensive range of methodologies have been utilized in the textile research and development industry to measure fiber friction and published in the textile engineering literature as follows:

i. One point contact of two single fibers (Mercer and Makinson, 1947; Olofsson and Gralen, 1947; Howell, 1951; Bartlett et al., 1953; and Pascoe and Taylor, 1955).

ii. Twist method using two single fibers (Lindberg and Gralen, 1948; Hood, 1953; and Van der Vegt and Schuringa, 1956).

iii. Interfiber friction (Adderley, 1922; Navcal and Turner, 1930; Wood, 1954; Lord, 1955; and duBois, 1956).

iv. Methods using a rotating cylinder and a stationary yarn (Saxl, 1936; Mercer, 1945; Schlien, 1953; and Roder, 1955).

This chapter presents the findings of an experimental program involving the results of multiple test series performed on geotextile versus coextruded as well as structured textured geomembrane systems to assess whether the temperature changes affect the interface shear behavior and strength between these geosynthetic counterfaces that are employed in multi-layered landfill liner systems. The temperature controlled chamber (TCC) previously described in this thesis for simulating elevated temperature field conditions was used with the large displacement interface shear apparatus. Variables in the various test series were temperature (21°C – 50°C), normal stress conditions (10 kPa – 400 kPa) (low, intermediate, high), and geomembrane texturing method (coextruded, structured).

7.2. Assessment of Texture Characteristics & Surface Profiles of Selected Virgin Continuum Materials Used in Laboratory Testing Program

Texturing technique has been shown to directly influence the strength and durability of both the microtexture and macrotexture created during the texturing process (Lee, 1998; Frost and Lee, 2001). The primary texturing processes currently used in North American geosynthetic practice are coextrusion and structuring, with impingement widely used as a third texturing process outside of North America (Hebeler et al., 2005). As shown in Figure 7.1, the coextrusion process generates random textures over a broad size range of features. The textured surfaces of coextruded geomembranes consisting of jagged macrotextures contain significant microtextures. Surface texture characteristics of virgin geomembrane sheets used in this laboratory experimental program were assessed through digital imagery at multible scales and orientations to yield representative views.

Another texturing method, "structuring", typically produces a more spatially uniform texture consisting of smoother macroscopic patterns, with micro and mesotexture existing on the base substrate (Figure 7.2). Microspike textured geomembrane is a relatively newer designed and produced product using a repeatable extrusion process resulting in it possessing textural uniformity on the liner material surfaces.

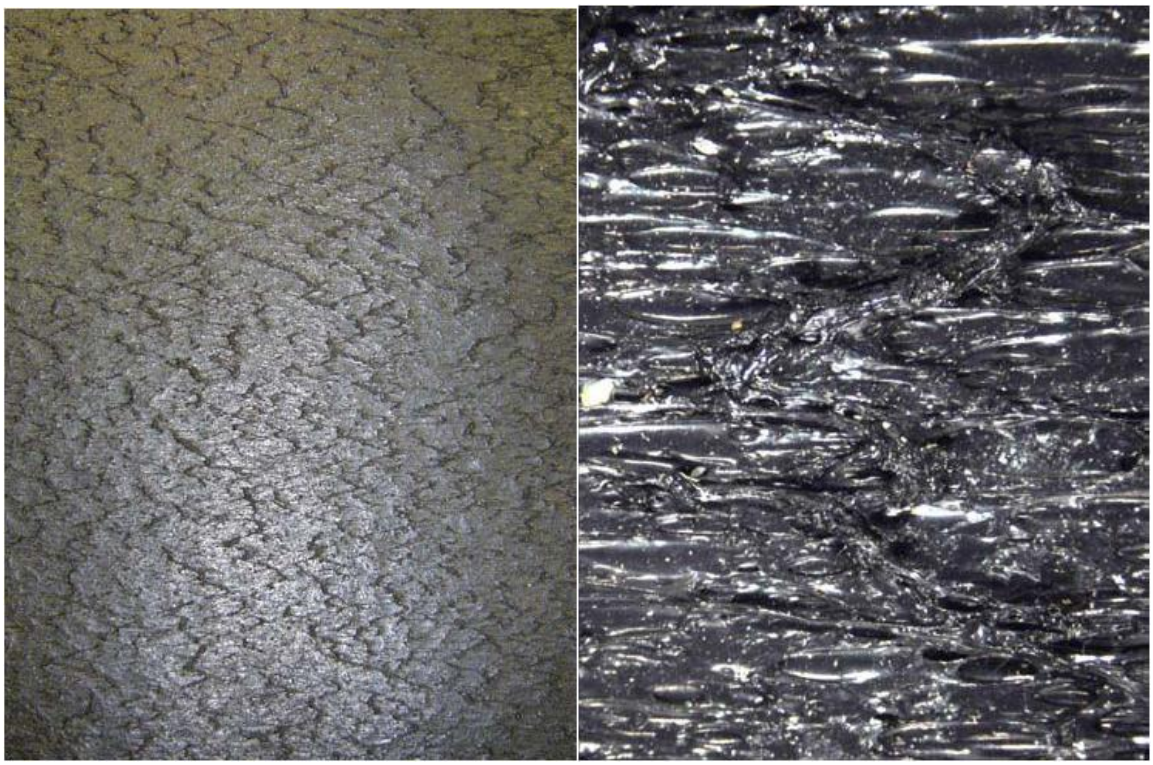

(a) (b)

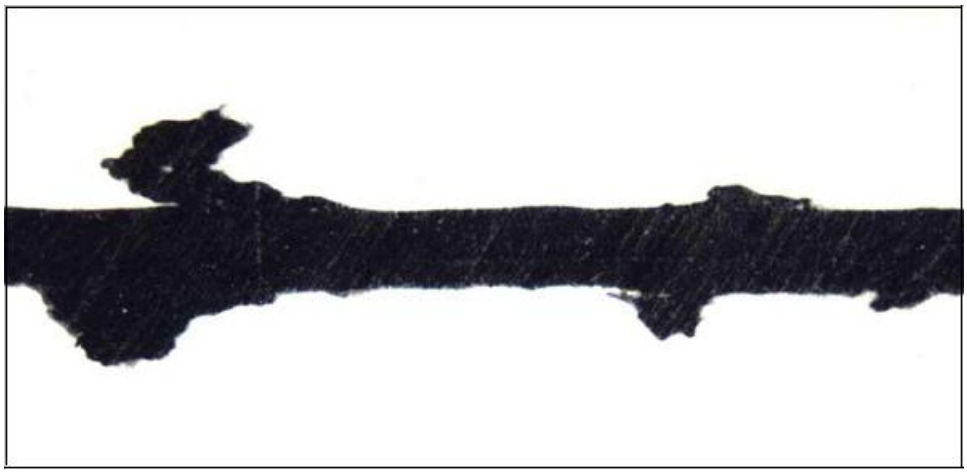

(c)

Figure 7.1 Images of Coextruded Geomembrane Used in the Test Program:
(a) Plan View - 115 mm x 150 mm; (b) Magnified Plan View - 9 mm x 13 mm; and
(c) Machine Direction Cross-Sectional View - 7.5 mm x 10 mm (Hebeler, 2005)

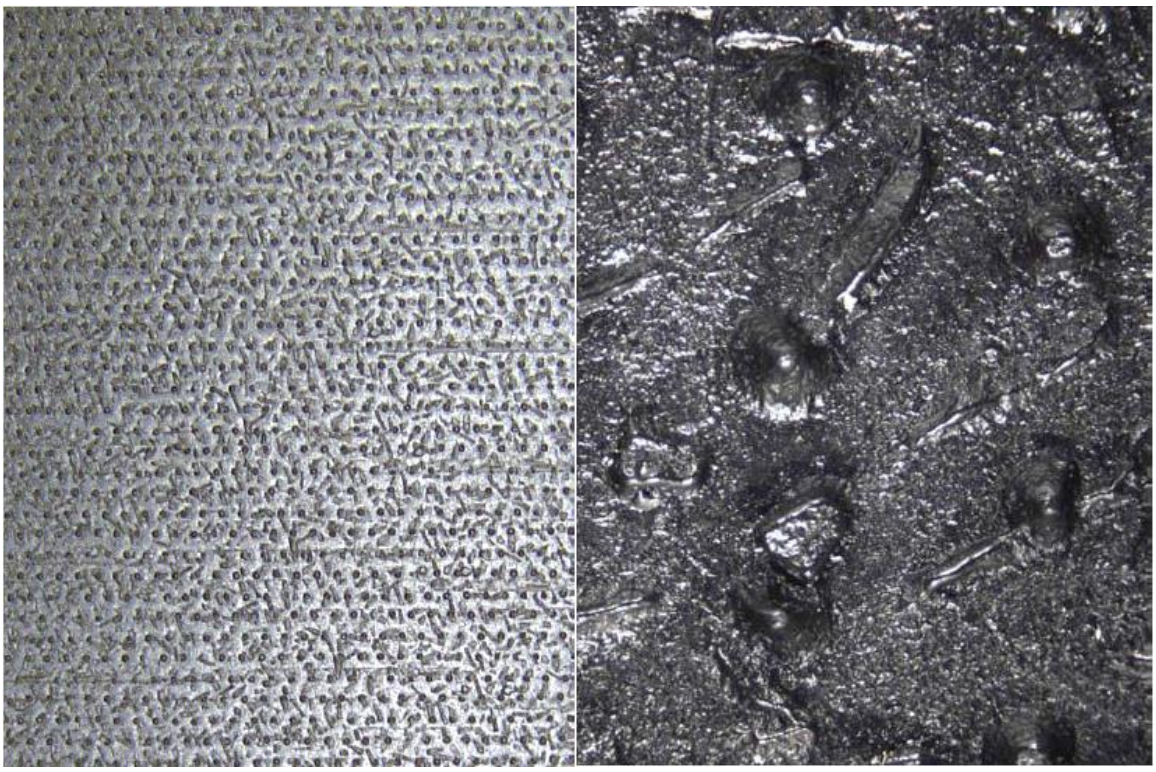

(a) (b)

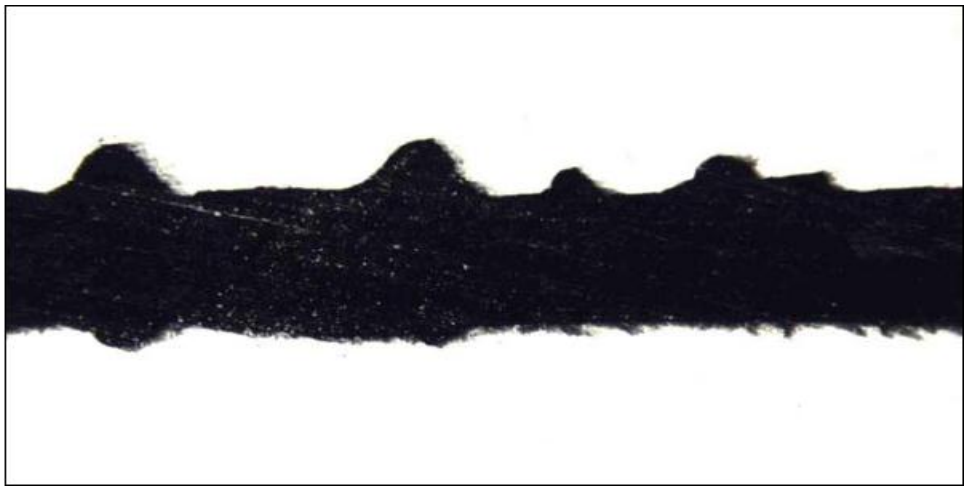

(c)

Figure 7.2 Images of Structured Geomembrane Used in the Test Program:
(a) Plan View - 115 mm x 150 mm; (b) Magnified Plan View - 9 mm x 13 mm; and
(c) Machine Direction Cross-Sectional View - 7.5 mm x 10 mm (Hebeler, 2005)

As will be discussed in Section 7.7 through 7.9, the structured texturing technique produces a more durable surface roughness as well as improved interface shear resistance when sheared against geotextiles. However, it also exhibits distinct peaks and troughs in the shear stress versus displacement relationship during the post-peak shearing stage.

Surface profiles of selected virgin geomembrane lining materials (Figure 7.3) were obtained using a stylus profilometer to capture an illustrative representation of geomembrane surfaces. Two independent profiles are presented for each of the materials. These profiles captured from virgin specimens provide a baseline against which wear during shear can be evaluated. The R_a values for the virgin (untested) liner specimens are 0.13 μm, 0.17 μm, 56.29 μm and 83.17 μm for GSE smooth HDPE, EPI smooth PVC, PolyFlex textured HDPE and GSE textured HDPE geomembranes, respectively.

7.3. Research on *Textured* Geomembrane – Geotextile Interfaces

Shear modes at geotextile – textured geomembrane interfaces will be discussed in this chapter by analyzing the results from interface shear tests at several different temperatures. Peak and residual shear resistances, shear stress reduction at residual states, variation in coefficient of friction and vertical displacement during shear will be evaluated for different ambient temperature conditions and confining stresses. Information regarding the influence of temperature in terms of factors such as the geotextile strain properties based on micro and global engineering scale considerations and the geomembrane surface hardness characteristics are analyzed elsewhere in the thesis.

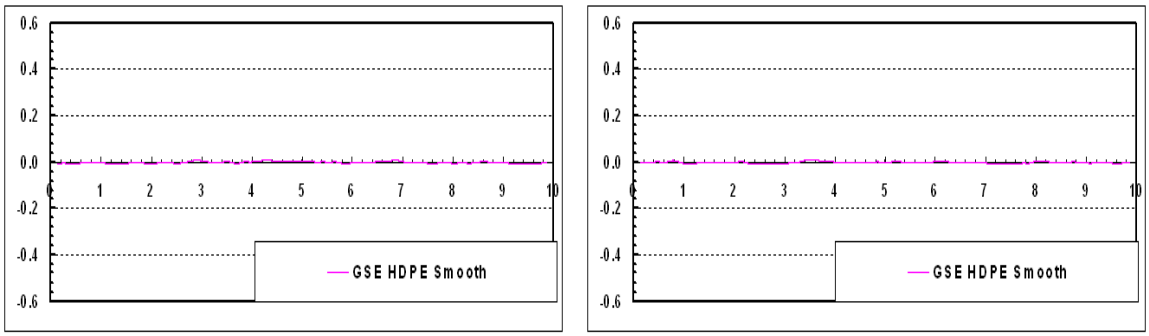

(a) ***GSE HDPE Smooth Geomembrane*** (b)

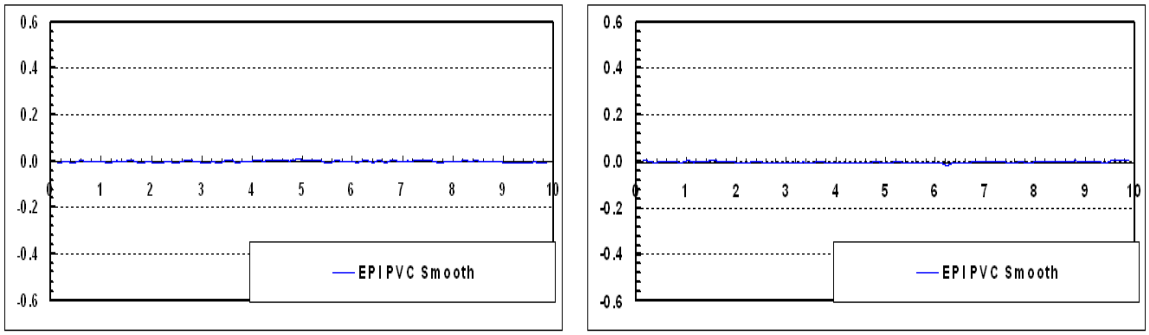

(c) ***EPI PVC Smooth Geomembrane*** (d)

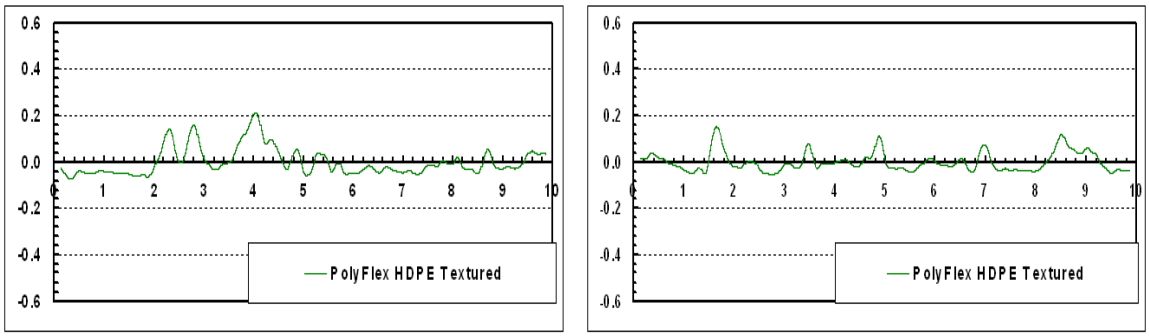

(e) ***PolyFlex HDPE Textured Geomembrane*** (f)

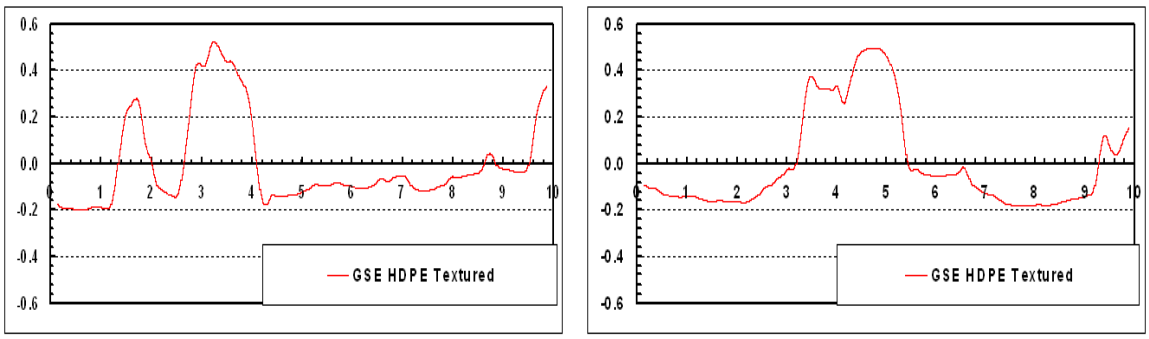

(g) ***GSE HDPE Textured Geomembrane*** (h)

Figure 7.3 Surface Profiles of Selected Virgin Continuum Materials
Used in the Laboratory Testing Program

Note: **y:** Profile Relief (Vertical Height) **[*mm*]**; **x:** Projected Profile Segment Length **[*mm*]**

7.3.1. Predominant Mechanism for Post-Peak Strength Reduction in Textured Geomembrane and Nonwoven Geotextile Interfaces

This section is intended to provide insight into the fundamental cause of post-peak strength reductions in textured geomembrane – nonwoven geotextile interfaces. In all interface tests performed in the laboratory utilizing the large displacement direct shear device enclosed in the temperature controlled chamber and previously described in Chapter 4, the geomembrane specimens were sheared against the geotextile specimens over a horizontal displacement of 60 mm. This is significantly larger than achieved in many laboratory systems. However, given that the average filament length of the staple NPNW geotextile tested is approximately 75-100 mm, this may influence phenomena such as filament pullout or other geotextile wear mechanisms. The loose filaments pulling out and/or tearing from the fabric matrix during virgin shearing can limit continued interactions at the contact surface and can detract from the frictional resistance of the interface at larger displacements ($\geq$ 75 mm). As a consequence, the geotextile wear mechanisms appear to mainly control the shear strength mobilized at the interface at larger shear displacements (e.g: the residual response in tests performed in ring shear device). For relatively smaller shear displacement range ($\leq$ 60 mm) as compared to the larger amounts of shearing displacements occur in ring shear devices, the texture elements of the geomembrane can engage the counterface geotextile globally (i.e. at fabric matrix level) under application of load at the interface. The macro-roughness features can substantially penetrate into the counterface fabric matrix, and thus, relatively stronger global frictional resistance of the interface can be achieved (Hebeler et al.,

2005). Similarly, Hebeler (2005) noted the isolation of geotextile wear over a shear displacement range up to 80 mm by showing the convergence of the sensitivity values after the repeated shearing of geomembrane specimens against virgin geotextile samples for interfaces comprised of coextruded or structured geomembranes. It was additionally noted that the majority of the geomembrane wear occurs within the initial tests of the wear sequence. The convergence in the sensitivity value for the two different textured surfaces represents the fact that the greater frictional strength losses that the geotextile – textured geomembrane systems exhibit when significantly larger shear displacements (~ 500 mm) occur at the interface during shear. The geotextile matrix is likely to lose its original intact structure due to the imposed larger displacements with the presence of interlocking between the counterfaces and interaction between the macro-texture features and the filaments.

Previous efforts in geosynthetic interface shear behavior have cited two possible sources of post-peak shear strength reduction. These are (i) polishing of and removal of asperities from the geomembrane liner sheet and (ii) breakage, pullout, and realignment of geotextile filaments. The former has widely been hypothesized to be a significant cause for large displacement strength loss occurring in the geotextile-textured geomembrane interfaces by the majority of the researchers with a few exceptions, most notably Stark et al. (1996); and Triplett and Fox (2001). However, their hypotheses were based only on the visual inspection of post-test specimens and not micro-level investigation and quantitative assessment.

An important research study was completed by Li and Gilbert, (2006) to investigate the predominant mechanism for the post-peak strength reduction at geotextile-

textured geomembrane interfaces by comparing the results of laboratory tests performed through one of two ways to provide precise direct evidence as to how each counterface material contributes to the post-peak reduction in shear strength. They performed a test program in a systematic method by repeating direct shear tests while replacing either the textured geomembrane specimen or the nonwoven geotextile with a fresh specimen after each increment of shear displacement to achieve accumulated shear displacement. For comparison purposes, direct shear tests with continuous displacement were also conducted using a double-interface shear device described in Gilbert et al. (1995) to identify the primary reason for the substantial post-peak interfacial strength loss as well as the relative contribution of the counterface component materials to the post-peak reduction in strength. At the end of the experimental program, it was observed that after replacing the geomembrane, the peak strength of the interface was recovered during subsequent displacements. However, it was noticed that after replacing the geotextile, the peak strength was *not* recovered. Figure 7.4 presents the direct interface test results from continuous as well as incremental shear displacements tests wherein the nonwoven geotextile specimens were replaced at the completion of every 23 mm increment of shear displacement. This indicates that the use of incremental shear displacements with new geotextile specimens is able to portray the post-peak strength reductions that occur at this interface with continuous shear displacement. In fact, this phenomenon had previously been noted by Li and Gilbert (1999) who attributed the post-peak strength loss in geotextile-textured geomembrane interfaces to the removal of the texturing on the geomembrane, but they had not quantifed the decrease in liner sheet surface roughness by comparing the continuous shear displacement test results with those of the accumulated

shear displacement in replacing geotextile specimen with a fresh sample after each increment.

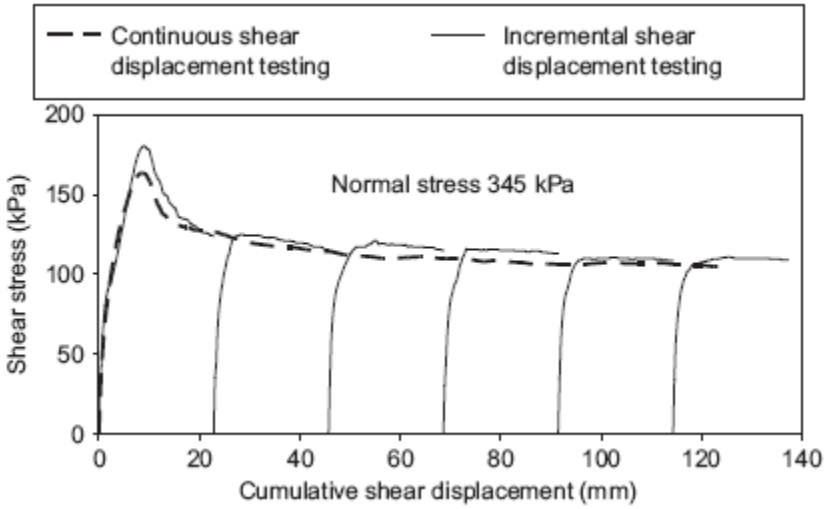

Figure 7.4 Comparison of Direct Shear Test Results for Continuous and Incremental Shear Displacements: The Nonwoven Geotextile Specimens Replaced after Each 23 mm Increment of Shear Displacement in the Incremental Tests (Li and Gilbert, 2006)

The results of the incremental shear displacement tests in Figure 7.4 suggests that the primary cause of the post-peak reduction in strength is not damage to the nonwoven geotextile (Li and Gilbert, 2006). Even though a fresh specimen of nonwoven geotextile is used after each shear increment, the peak shear strength, mobilized in a given increment, continuously decreased in successive increments with accumulated shear. In fact, a very insignificant amount of original shear strength was recovered as a result of the replacement of the nonwoven geotextile with a fresh specimen.

Additional test results from Li and Gilbert, (2006) are presented in Figure 7.5 which support this conclusion at normal stresses ranging from 16 kPa to 690 kPa and for various combinations of geomembrane type and geotextile type. Regardless of the

material type, the reduction in incremental peak shear strength is very significant with a fresh geotextile specimen which demonstrates that the relative contribution of the damage experienced by the geotextile to residual strength reduction at the interface is negligible. Therefore, the post-peak shear strength and interfacial behavior of geotextile–textured geomembrane interfaces depend essentially on the geomembrane properties itself such as hardness, surface roughness and stiffness. For this reason, the post-peak shear strength mobilized and the interface behavior developed at elevated temperature conditions in geotextile versus textured geomembrane interfaces needs to be evaluated with an emphasis on the change of the physical properties of polymeric continuum liners.

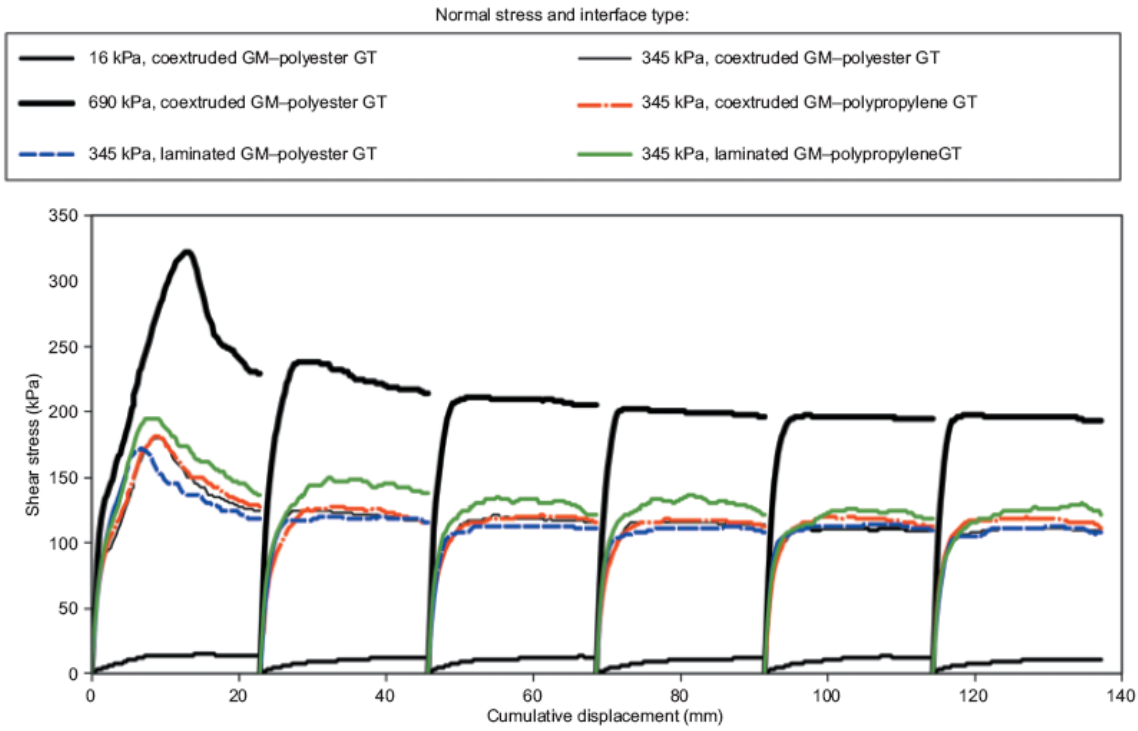

Figure 7.5 Direct Shear Test Results for Incremental Shear Displacement: The Nonwoven Geotextile Specimens Replaced after Each 23 mm Increment of Shear Displacement (Li and Gilbert, 2006)

While these test results indicated that the texturing is wearing down or becoming smoother, this damage to the textured surface apparently occurs at a microscopic scale and requires high resolution digital imaging to be seen as shown by Dove and Frost, (1996) whose findings clearly demonstrated that the post-peak shear strength reduction is primarily due to a small-scale wearing of the geomembrane texture as was reiterated by Li and Gilbert (2006) even though no discernible difference or visually detectable damage by sight was observed on the surface of the post-test textured geomembrane specimens after repeated incremental shear displacements.

A parallel series of direct shear tests with incremental shear displacements was conducted by Li and Gilbert (2006) where the textured geomembrane specimens were replaced with a fresh specimen after each increment of shear displacement to further confirm the primary cause of post-peak reduction in shear strength. As Figure 7.6 shows, most of the peak shear strength was recovered with a fresh textured geomembrane specimen, whereas much less was recovered with a fresh nonwoven geotextile specimen in each increment of shear displacement. In summary, the primary source of post-peak strength loss in geotextile-textured geomembrane interface systems is not damage to the nonwoven geotextile as previously assumed, but rather due to small-scale wearing of the geomembrane texture.

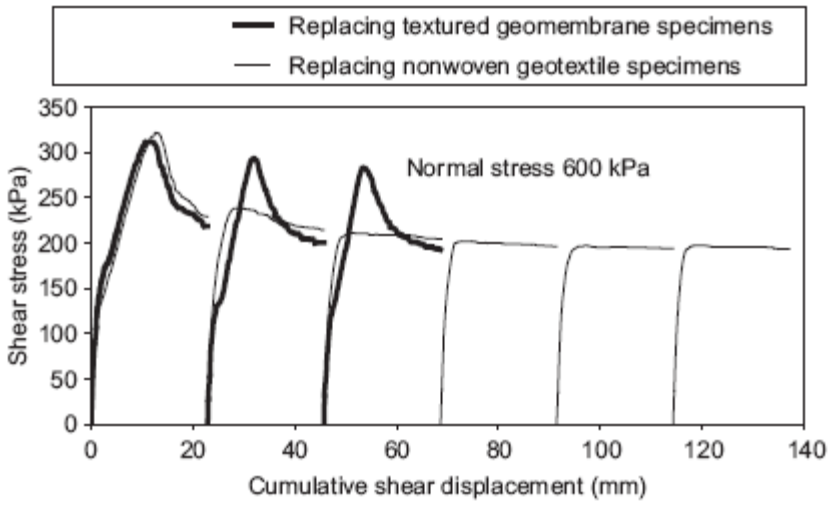

Figure 7.6 Comparison of Direct Shear Test Results for Incremental Shear Displacement: Nonwoven Geotextile Specimens; or, Textured Geomembrane Specimens Replaced After Each 23 mm Increment of Shear Displacement (Li and Gilbert, 2006)

7.4. GSE HDPE Coextruded Textured Geomembrane/NPNW Geotextile

Figure 7.7 shows the shear stress versus displacement relationship for GSE HDPE coextruded textured geomembrane versus nonwoven geotextile interface tests. A peak followed by a reduction to some lower residual shear stress condition was observed at all test temperatures ranging from 21 °C up to 50 °C and at three different normal stress levels of 10, 100 and 400 kPa. The horizontal shear displacements required to mobilize peak interface shear strength ranged from approximately 6-10 mm, 10-12 mm, and 14-18 mm for 10 kPa, 100 kPa, and 400 kPa normal stress levels, respectively (Figure 7.8a, 7.8b and 7.8c, respectively). Further, horizontal displacements to achieve post-peak (pseudo-residual) conditions at the test temperature range were of the order of 36 to 40 millimeters regardless of the normal stress applied.

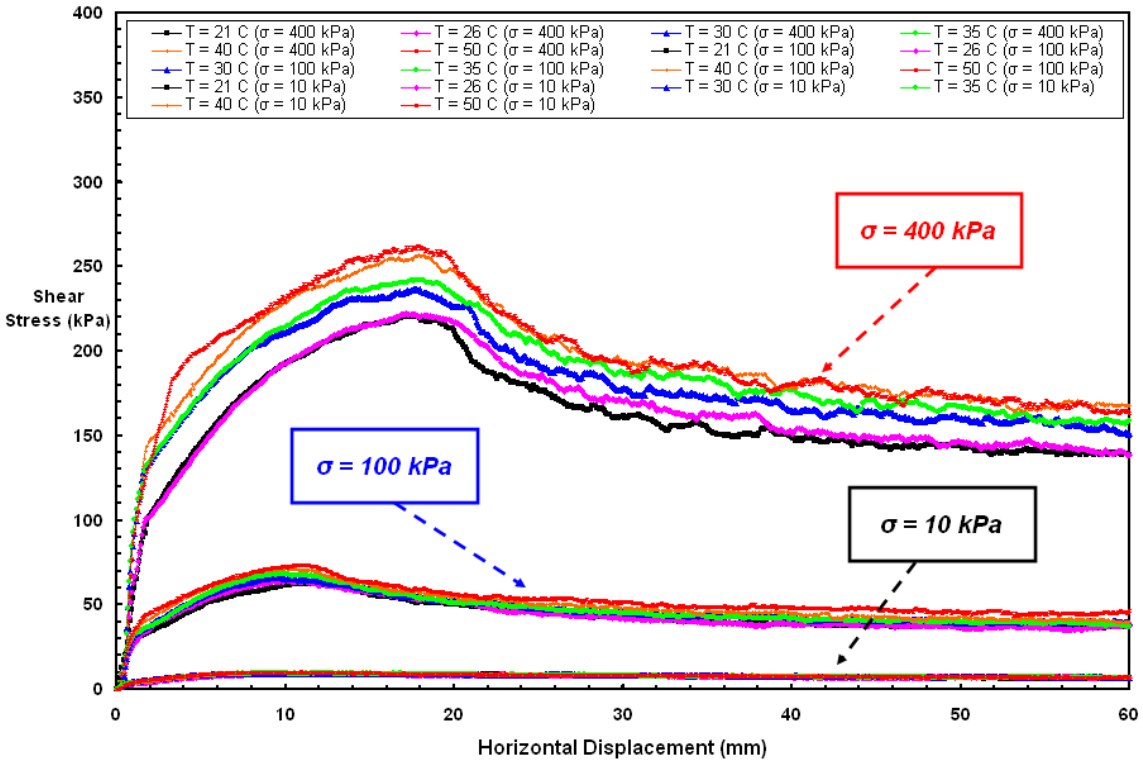

Figure 7.7 Shear Stress–Displacement Curves at Different Loading Conditions; & at Various Test Temperarures for GSE HDPE Textured Geomembrane/NPNW Geotextile

The significant post-peak softening at all test temperatures for the GSE textured geomembrane–geotextile interfaces represent a transition dominant mechanism in interface shear behavior. Additional shear displacement resulted in removing microtextural features from the geomembrane core. Therefore, the failure occurring at peak shear displacement can be considered to primarily be originated by the decrease in the micro-scale interlocking between continua micro-texture features and geotextile filaments due to geomembrane surface degradation at microscopic level because of shearing force and displacement. Such a failure mechanism results in a smooth peak and gradual transition of the stress-displacement curves. Increased normal stress level makes the geotextile filaments denser adjacent to the surface of the geomembrane which result

in deeper penetration of the geomembrane texture elements into the geotextile. This leads to higher resistance at the interface due to stronger opposition of the texture elements against shear motion through firmer interlocking of these two materials during compression and later in subsequent shearing. Previously, Lee et al., 1998 and Frost and Lee, 2001 had indicated that the true residual condition can only be achieved after all the weak micro-topographical asperities on the geomembrane surface are removed and only much stronger macro-texture features hold the geotextile filaments. Consequently, the residual strength is induced by the characteristics of the geomembrane itself (i.e. total amount of textural features; or proportion of micro-roughness to macro-topology). The stress-displacement curves generally begin to change slope at about 2 mm horizontal displacement and continues towards the peak value thereafter. After the peak, the stress-displacement relationship decreases towards the post-peak strength conditions. This phenomenon was found to be exhibited in a continuous manner/fashion throughout all the tests at different temperatures. In general, interface frictional resistance increases as the confining stress (i.e. normal load) increases for most materials. An exception to this is seen in the shear resistances between nonwoven fabrics and rough continuum surfaces which produce greater frictional strengths under low confining stress (Hebeler, 2005). Such a phenomenon is called the hook and loop effect (i.e. Velcro-type interlocking), and an evaluation method of this concept is available in ASTM standard (ASTM D 5169) to examine and measure this effect. In this study, such a phenomenon was observed in tests performed at 10 kPa normal stress that resulted in higher coefficient of friction values being attained compared to those at larger normal stress levels (Figure 7.8a).

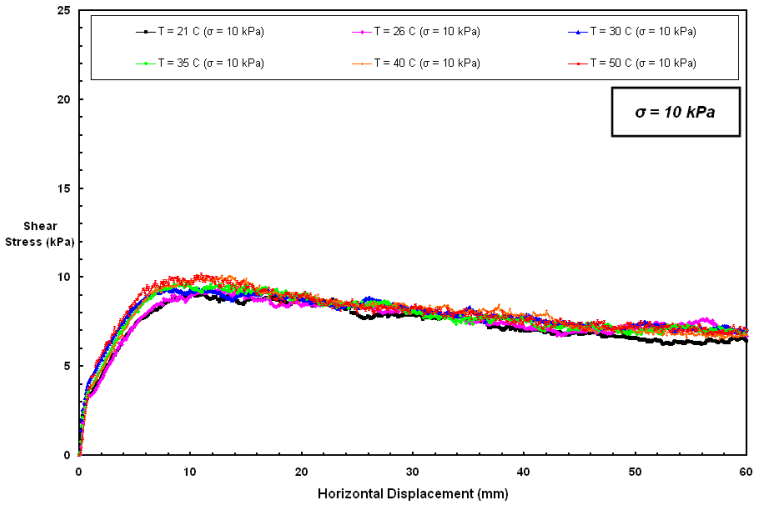

(a)

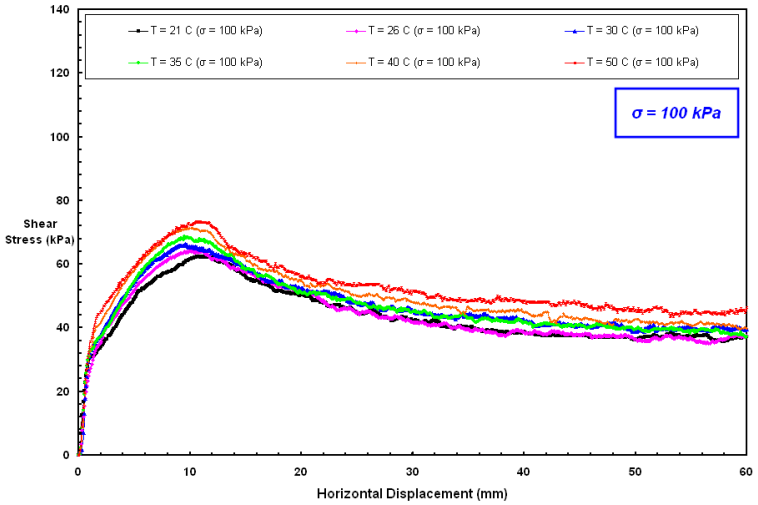

(b)

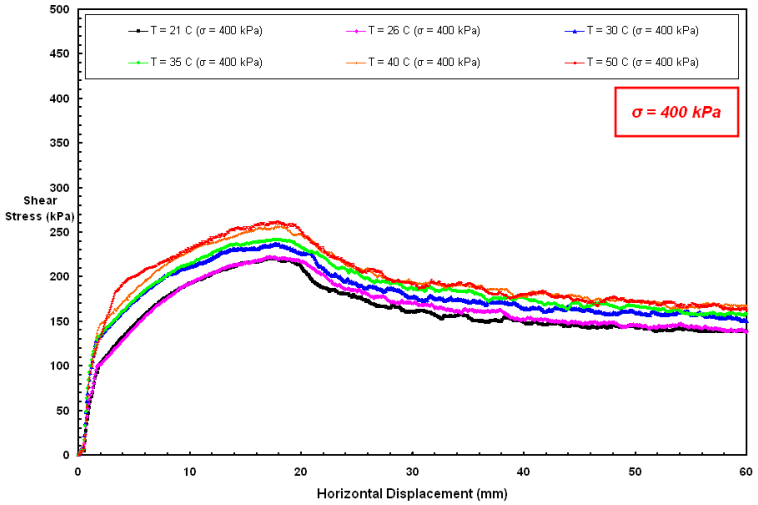

(c)

Figure 7.8 Shear Stress – Displacement Curves at Different Test Temperarures for GSE HDPE Textured Geomembrane/NPNW Geotextile: (a) 10, (b) 100 and (c) 400 kPa

The preceding plots show that a minor decrease in shear stress is seen to continue in the stress-horizontal displacement curves at post-peak stage (i.e. > 30 mm displacement) for the entire temperature range tested. This was previously demonstrated by Lee et al. (1998) and Frost and Lee (2001) in which they reused the geomembrane specimens to examine if the shape of the shear stress versus horizontal displacement curve would be affected. The direct shear tests performed using virgin textured geomembrane specimens resulted in a stress–displacement curve exhibiting a *distinct* peak followed by a decrease in shear strength; whereas the large displacement direct interface tests performed on the used geomembranes did not exhibit the same trend. Instead the shear stress–horizontal displacement curves more closely resembled those of smooth geomembranes, in which the shear strength rose to a peak value with little or no subsequent reduction in strength/resistance. Although changes in the *macro-scale* surface roughness of the reused geomembrane specimens were not evident through visual inspection, a change in the *micro-scale* texture could easily be detected both by touch after the first shear test, as well as visually. Their results revealed that micro–texture on virgin geomembrane specimens contributes significantly toward the peak strength of a textured geomembrane–nonwoven geotextile interface. More importantly, the micro-texture can be removed by a relatively small amount of displacement (≈8 mm to 12 mm), resulting in a substantial loss of strength at the interface. In summary, textured geomembrane–geotextile frictional interactions occur at much higher stiffness than smooth geomembrane–geotextile interactions for all test temperatures at which interface tests were conducted in this research study. However, the textured composite layered

systems in conjunction with the geotextiles were prone to undergo much more reduction in the magnitude of frictional resistance before reached the peak state.

Figures 7.9a, 7.9b and 7.9c show vertical displacement – horizontal displacement plots for GSE HDPE textured geomembrane – NPNW geotextile interfaces tested at normal stress levels of 10 kPa, 100 kPa and 400 kPa, respectively. The dilative response observed in the interface resulted from rough surface features on the GSE textured geomembrane. The amount of dilation exhibited in the interface increased with temperature. At low normal stress level (10 kPa), the interface is less confined and more free to dilate during shear displacement. As the normal stress applied to the interface increased to 100 kPa, the interface became more confined and the amount of the mobilized dilation during shear displacement observed in the nonwoven geotextile – coextruded textured geomembrane interface decreased. However, a larger dilation occurred at elevated temperatures compared to that exhibited at room temperature (21°C) for the 100 kPa normal stress level and was similar to that displayed at 10 kPa normal stress. At the highest normal stress level (400 kPa), the interface became more confined and restrained due to application of larger load in the interface during shear displacement. As the ambient test temperature increased, the amount of dilation exhibited during shear at the interface became more evident and larger even for this high normal stress condition of 400 kPa.

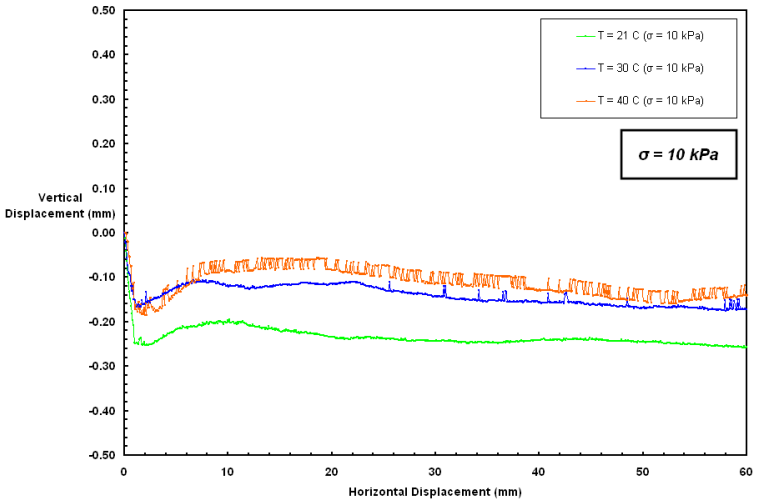

(a)

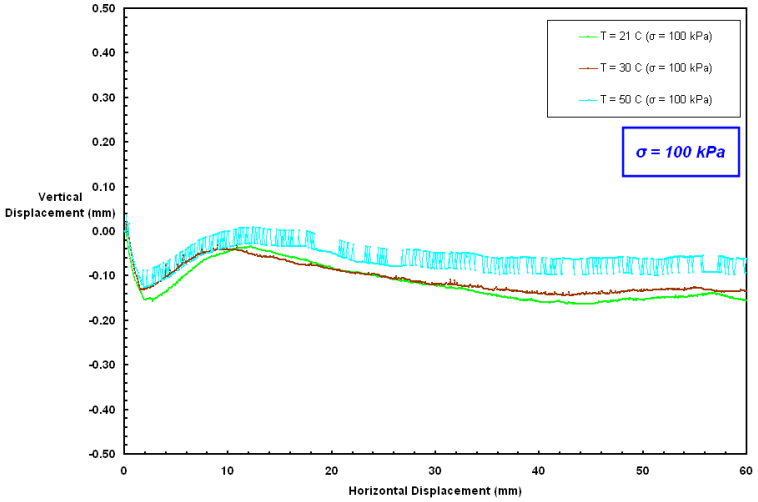

(b)

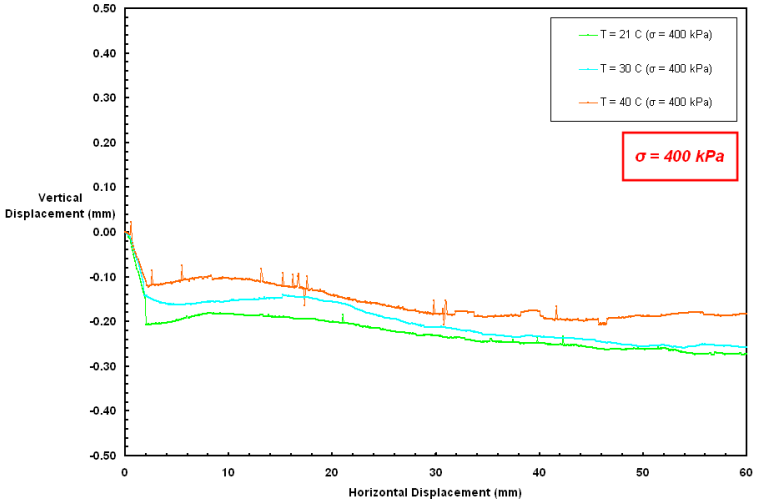

(c)

Figure 7.9 Vertical Displacement – Horizontal Displacement Behavior at Different Temperatures for GSE HDPE Textured Geomembrane/Geotextile: 10, 100, 400 kPa

At the different temperatures tested in this study, GSE coextruded textured geomembranes had interface friction angles about two times higher than their smooth counterparts. The peak and post-peak interface strength properties, including interface friction angle as well as coefficient of friction are presented in Figure 7.10 and 7.11, respectively. The pseudo-residual strength values determined and plotted against ambient temperature level were based on the evaluation of shear stress values obtained by averaging over 2 mm range from 57 to 59 mm horizontal displacement. Both peak and pseudo-residual interface shear strength values increase with a slightly larger increase in peak values in comparison to post-peak values for a similar rise in temperature. This increase in the magnitude of δ and $\tan(\delta)$ is consistent with previous findings of Bely et al. (1982) and Pasqualini et al. (1993). The more evident influence of temperature on peak interface shear behavior as indicated by the larger increase in the strength value with temperature (Figure 7.11) is due to the fact that the peak strength for textured geomembranes is mainly attributed to the geomembrane micro-texture; and thus, depends on the geomembrane properties such as hardness and surface roughness which have a first order influence on interface response and resistance. Further, PP fibers of nonwoven geotextile manufactured through needle punching process produce a strong filament composition and structure as well as more robust and better interlocked arrangement of fibers resulting in stable and tough fabric matrix constitution. As noted by Hebeler (2005), in the case of greater displacements (>75 mm; ring shear tests), the residual interface strength mobilized is also partially associated with the characteristics of the geotextile fabric such as filament entanglement, strength, filament length/diameter and how it interacts with the geomembrane macro-topography.

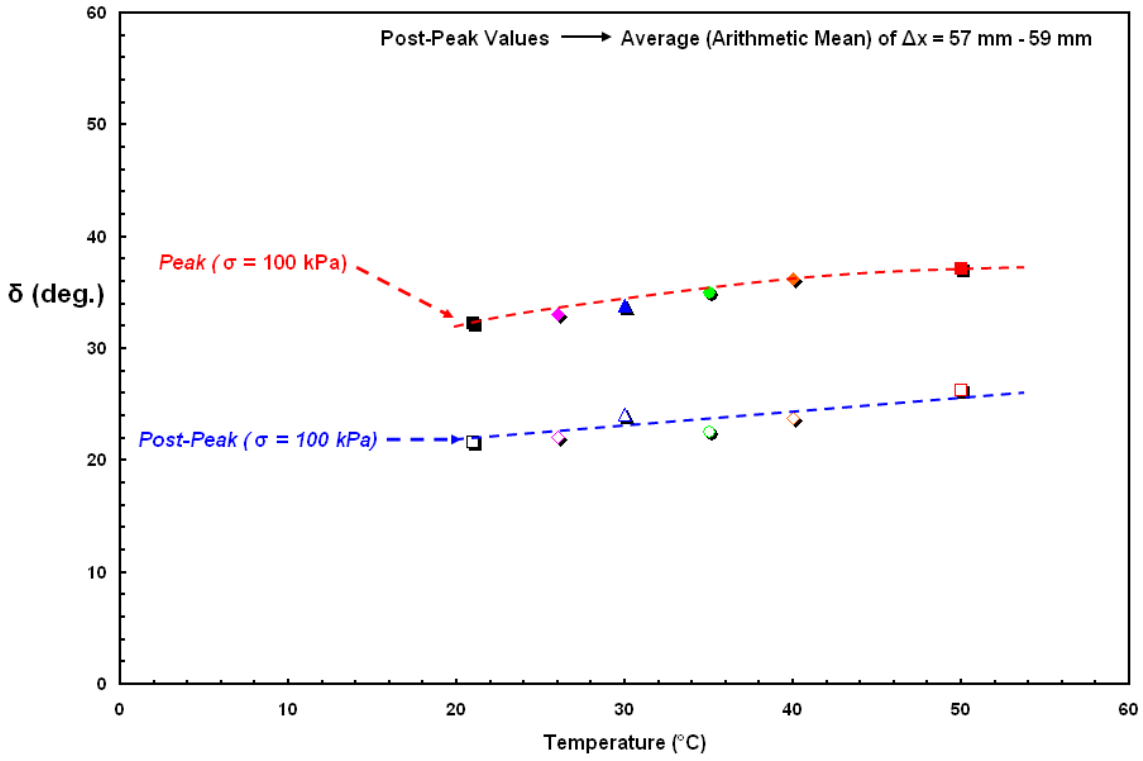

Figure 7.10 The Change in Interface Friction Angle, [δ] with Temperature for GSE HDPE Textured Geomembrane/NPNW Geotextile Interfaces

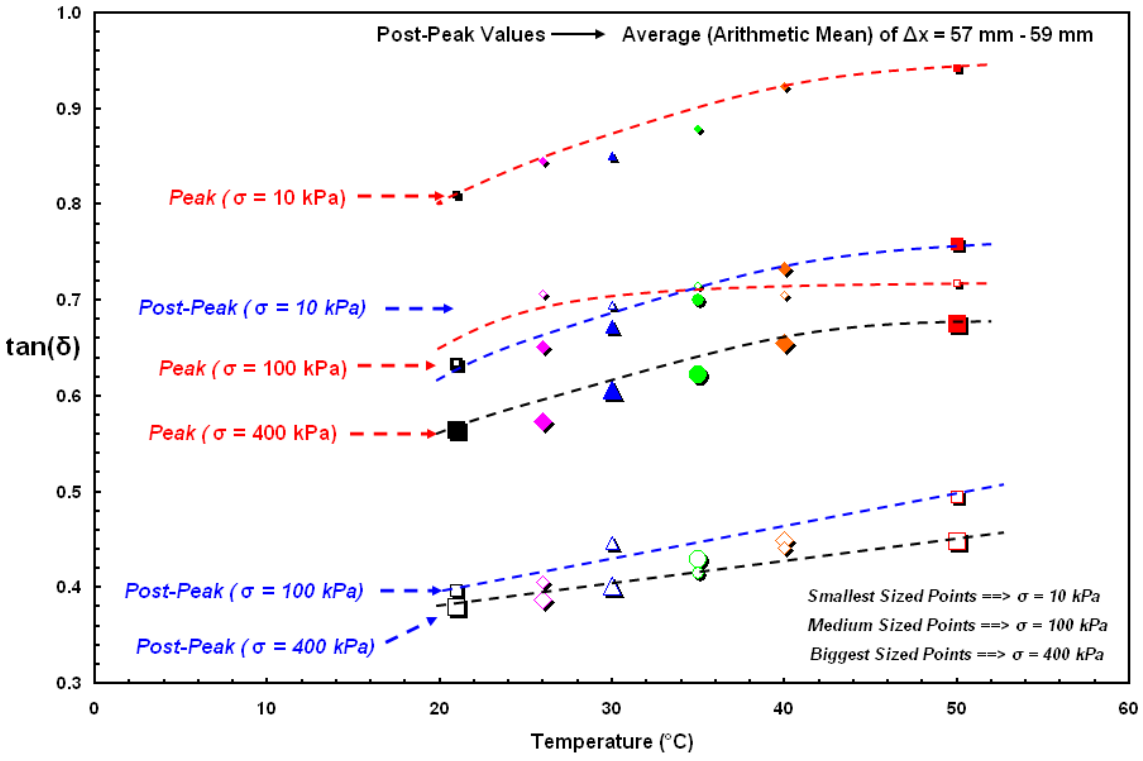

Figure 7.11 The Change in Coefficient of Friction, [tan(δ)] with Temperature at Different Loading Conditions for GSE HDPE Textured Geomembrane/NPNW Geotextile Interface

For the interface shear tests performed at higher elevated temperature conditions (i.e. comparing the test at 40 °C with 50 °C), the change in shear strength was not as pronounced as the change in shear strength for the tests at lower temperature conditions (i.e. comparing the test at 20 °C with 30 °C). Furthermore, the variation in coefficient of friction with temperature increases in contrast to the change with respect to normal stress level which decreases. The magnitude of the coefficient of friction obtained at low normal stress levels (10 kPa) was the highest; there was a decreasing trend with normal stress level for the corresponding test temperatures, and the magnitude attained was the lowest for the greatest stress level (400 kPa) (Figure 7.11). This behavioral trend in the magnitude of coefficient of friction (i.e. normalized strength) is consistent with the earlier findings regarding the interfaces comprised of "polymeric materials" (geotextile-geomembrane) which does not obey classical friction rules and shows a decreasing value of tan(δ) with increasing stress level. The friction force, (F) for the majority of the continuous materials forming multi-asperity contacts is governed by fundamental shear strength mechanisms as well as is composed of one or more components including adhesion component, and "plowing" or plastic deformation component (Bowden and Tabor, 1954; Shooter and Tabor, 1952; Briscoe, 1992).

For interfaces comprised of polymers, as the normal load increases, the coefficient of friction decreases with a constant slope or the magnitude of this reduction gets greater at higher normal stress levels. Primary findings regarding the influence of normal load on the normalized frictional resistance of polymeric material interfaces, in particular, was first published as a result of fundamental work of Archard (1957). Additionally, it should be emphasized that the favorable contribution of hook and loop

interactions developing in geotextile–textured geomembrane interfaces at low normal stresses contributes to the measured value of frictional resistance, in terms of either tan(δ), or δ, being greater than the expected. Further discussion on this issue can be found in Hebeler et al. (2005). Texturing method does not result in significant differences in microtextural properties (Hebeler, 2005). As such, the texture manufacturing technique on the base sheets of lining materials does not play an important role in the development of peak shear strength at the interfaces involving these different type of textured geomembranes (Li and Gilbert, 1999; Hebeler et al., 2005).

Strength envelopes corresponding to both peak and post-peak (pseudo-residual) conditions are presented in Figure 7.12 for GSE NPNW PP geotextile samples sheared against GSE coextruded geomembrane specimens at different ambient test temperatures ranging from 21 °C up to 50 °C. Regression analysis of shear strength with normal stress yielded the most appropriate fits, with high coefficients of determination (R^2).

The texture of coextruded geomembranes (GSE HDPE Textured), consisting of jagged macrotexture containing significant microtexture, results in a greater engagement of individual geotextile filaments with the rough topography of the liner sheet. As the applied normal stress increases, in addition to the ambient temperature increments, the geotextile becomes compressed and increasingly interbedded between the macrotextural features of the contacting geomembrane resulting in matrix level frictional interactions which basically give rise to frictional resistance improvement mobilized at the interface compared to the smooth counterparts as presented in Chapter 6.

Further, for geotextile–textured geomembrane interfaces, the prevailing mechanism controlling the shear behavior are these interbedded interactions between the

fabric matrix and the continua textural features due to load application as well as temperature increase that induce larger contact area built up at the contact surface of the materials as a result of relaxation at higher temperatures. The combination of surface texture and normal stress were sufficient to create larger interactions between the counterfaces particularly at higher loading conditions (≥ 100 kPa). The combination of sufficient amount of textures (roughness features: micro, meso and macro texture elements) to engage the geotextile fabric globally at matrix level instead of at individual filaments; and the application of normal stress to allow the geotextile fabric to further penetrate into the geomembrane texture allows a higher global strength of the NPNW geotextile to be realized for a particular normal stress level. In addition, the relaxation of the counterface materials at higher temperatures resulting in more effective placement, better deployment, and larger interaction (contact area) of the interface components in between leads the larger frictional response and resistance being realized at elevated temperature conditions compared to cooler ambient temperatures.

The pseudo-residual interface strength behavior of the tested nonwoven geotextile versus coextruded geomembrane interface system is primarily governed by the properties of the macrotextural features of the geomembrane as previously noted by Lee (1998); Frost and Lee (2001). The visual examination of the NPNW PP geotextile samples obtained from the manufacturer and employed in the direct shear tests revealed that the needle punching process establishes strong and robust interlocking between the geotextile fibers so they do not pull out from the fabric matrix. Further, the selection of polypropylene (PP) as a base polymeric material for the production of the filaments

yields a durable structure which prevents the filament from tearing or breaking from the fabric sheet.

Strength envelopes including both peak and post-peak states were replotted by converting shear stress as well as normal stress axes from linear to logarithmic scales in order to recognize and analyze diversities in interface shear failure behavior over full stress range, as well as to distinguish, in particular, the disparities at low normal stresses (<20 kPa) based on Mohr-Columb criterion (Figure 7.13). There is clearly some degree of curvature (i.e: from linear fashion becoming curved into a concave up manner) for the failure envelopes of moderately/heavily textured geomembrane at low normal stress levels for all test temperatures ranging from 21 °C up to 50 °C; while, the envelopes (both peak and residual) are almost linear regardless of ambient test temperature level. Therefore, these strength envelopes shown in Figure 7.13 depict that the coextruded textured HDPE geomembrane – NPNW PP geotextile composite system exhibited a non-linear strength responses at low normal stresses (<20 kPa). Linearly increasing peak and pseudo-residual strength responses were observed over the remainder of the tested normal stress range (20 – 400 kPa) and for entire test temperature range.

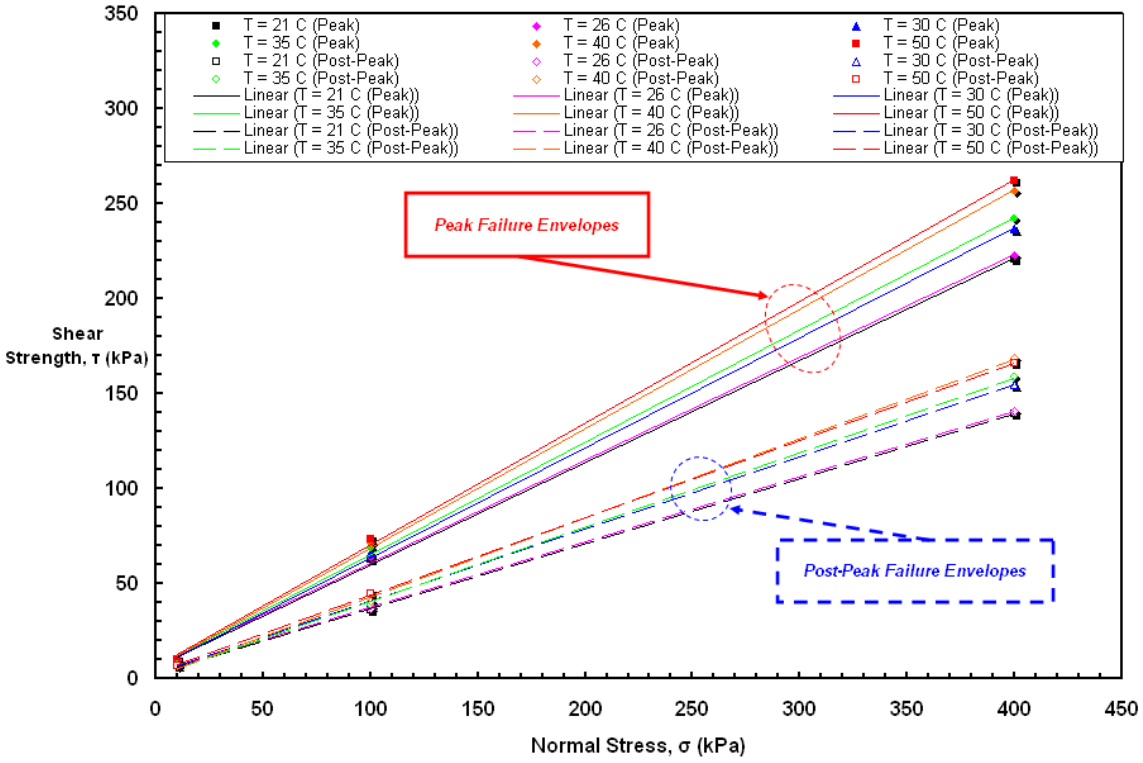

Figure 7.12 The Alteration of Peak and Residual Strength Envelopes with Increasing Temperature for GSE HDPE Textured Geomembrane/NPNW Geotextile Interfaces

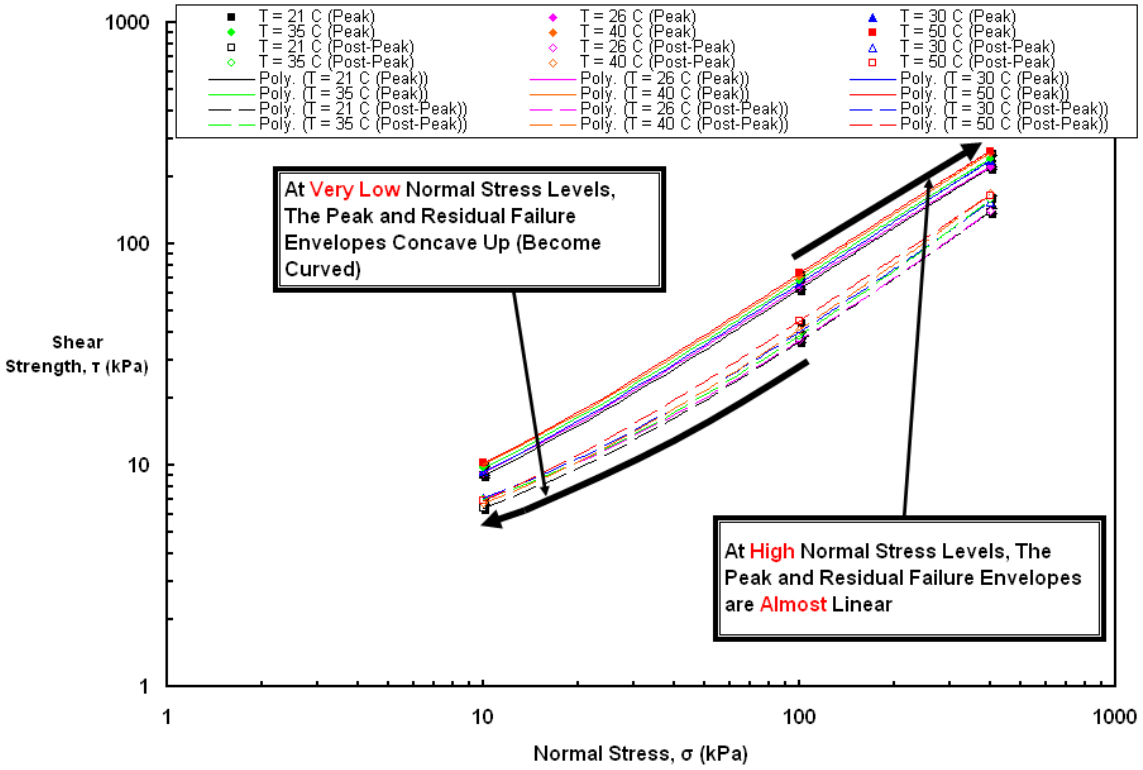

Figure 7.13 The Transformation in Failure Envelopes with Temperature at Different Loading Conditions for GSE HDPE Textured Geomembrane/NPNW Geotextile Interface

7.5. PolyFlex HDPE Coextruded Textured Geomembrane/NPNW Geotextile

Figure 7.14 shows the shear stress versus displacement relationship wherein the peak stress was followed by a significant post-peak softening for the coextruded PolyFlex HDPE textured geomembrane samples sheared against the NPNW geotextile. This response was typical for the entire series of interface shear tests at all elavated temperature conditions (21 °C< T <50 °C) regardless of the normal stresses applied with exception of low normal stress level of 10 kPa. The horizontal displacement to reach peak strength increased with the magnitude of normal stress applied during shearing such that the interface required in the range of 6-8 mm, 8-12 mm, and 12-16 mm shear displacements for 10 kPa, 100 kPa, and 400 kPa normal stresses, respectively for the temperature range tested to mobilize peak interface resistance (Figure 7.15a, 7.15b and 7.15c, respectively). It is noted that the displacements to peak for PolyFlex textured geomembrane interface tests were slightly smaller than for the GSE textured geomembrane. As will be described later, this difference could be due to the effect of the slight differences in the stiffness of the sheet materials along with adhered textural properties from the different manufacturers. It was found that as the core material of the continuum sheet becomes less ductile or less flexible, a more sharply peaked stress–displacement curve is likely to be observed. In addition, it is known that as continuum material roughness increases, the stress–displacement curves show greater post-peak strength loss/reduction. The horizontal displacements necessary to achieve pseudo-residual conditions were of the order of ~30 mm, ~35 mm, and ~40 mm at normal stresses of 10 kPa, 100 kPa, and 400 kPa, respectively for the entire test temperature range.

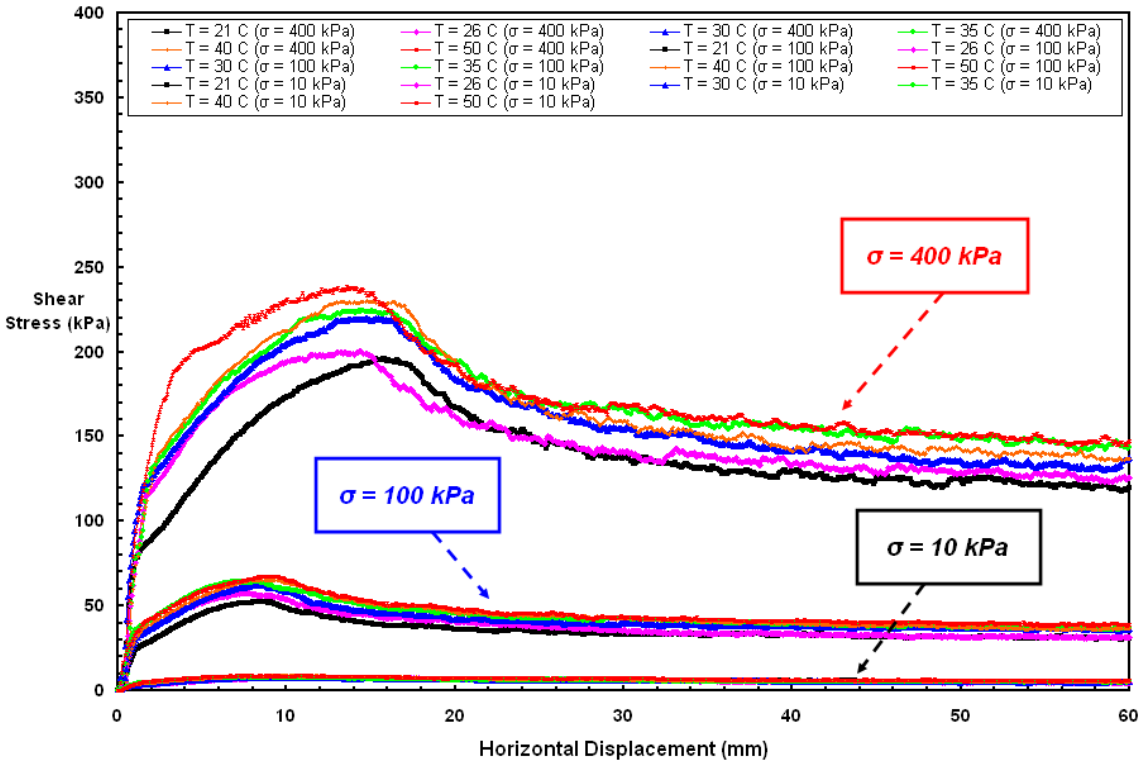

Figure 7.14 Shear Stress–Displacement Curves at Different Loading Conditions; & at Various Temperarures for PolyFlex HDPE Textured Geomembrane/NPNW Geotextile

Similarly to observations with GSE HDPE textured geomembrane, the PolyFlex HDPE textured geomembrane versus NPNW PP geotextile interfaces when compared with smooth HDPE geomembrane liner interfaces exhibited a smoother peak response throughout the test temperature range. This produces a shear–displacement curve consisting of multiple distinct stages including: i) initially, a sharp rise; ii) a reduction in the rate of this increase up to the peak point; iii) a decrease in resistance; and iv) finally, an interface response (i.e. remains essentially constant) which progresses in almost a fully plastic manner. Therefore, the stress-displacement failure envelopes (curves) demonstrate that a succession of mechanisms take place during a relatively short shear displacement range (<15 mm) regardless of normal stress level and ambient temperature condition. Further, it may be noted that a true steady state of shear (i.e. residual state) was not

achieved within the 60 mm of horizontal displacement applied in this study as the stress-displacement graphs for each test temperature level in Figure 7.15b and 7.15c, particularly for larger normal stress conditions (e.g. 100 kPa and 400 kPa, respectively), portray trajectories that are still very slightly decreasing regardless of ambient temperature level. This observation had already been confirmed by the experimental observations of Stark et al. (1996) in which the displacements ranging from 500 mm to 750 mm were reported as a minimal requirement to mobilize the true residual interface shear resistance using a torsional ring shear apparatus in geotextile-textured geomembrane interfaces.

Surface roughness and hardness properties of the PolyFlex liner were found to have first-order influence on interface shear behavior as well as the maximum resistance mobilized in combination with the fibrous materials (e.g. geotextiles) at different ambient temperatures and under various loading conditions. As previously discussed in Chapter 6, sliding of the geotextile was the main mechanism for the smooth HDPE geomembrane surfaces in combination with geotextiles. In contrast, the shearing/removal of micro-texture asperities from the PolyFlex textured HDPE geomembrane liner surface is the key failure mechanism for textured geomembrane interfaces. Based on laboratory inspections, the GSE coextruded-textured geomembrane liner is stiffer than the PolyFlex coextruded-textured liner which is a more ductile geomembrane liner sheet having more flexibility and less Velcro type attachment (i.e. hook and loop). To sum up, the more textured GSE geomembrane samples resulted in higher peak and post-peak strengths than the PolyFlex. Also, the displacements to achieve peak and pseudo-residual strengths were larger with GSE than PolyFlex textured geomembranes.

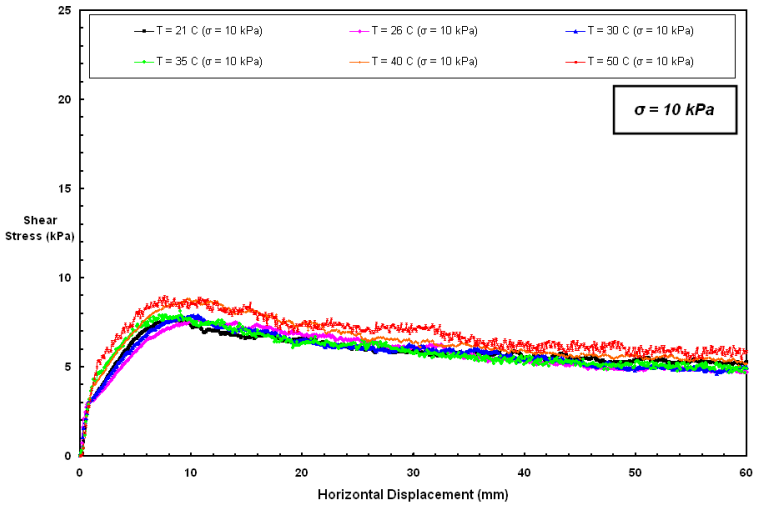

(a)

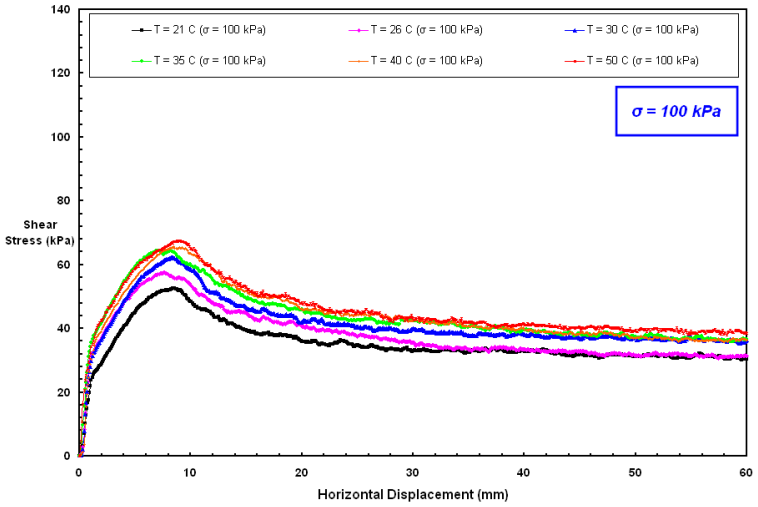

(b)

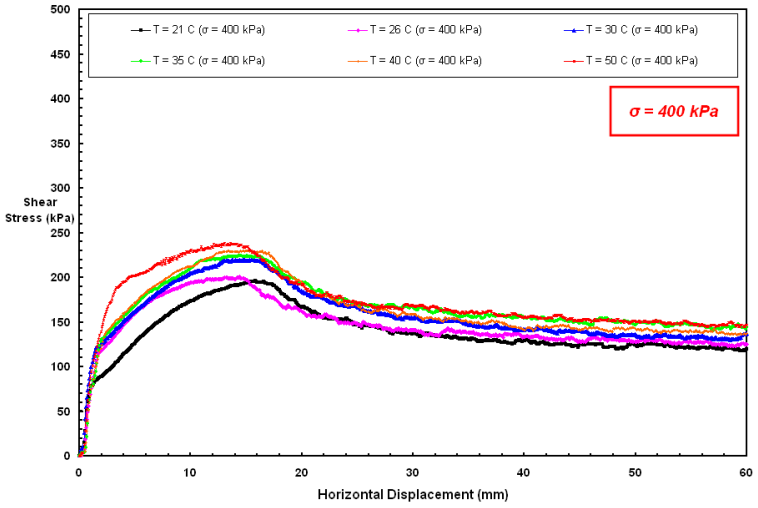

(c)

Figure 7.15 Shear Stress – Displacement Curves at Different Test Temperarures for PolyFlex HDPE Textured Geomembrane/NPNW Geotextile: 10, 100, 400 kPa

The ductility of PolyFlex textured geomembrane reflected in the preceding plots is due to surface roughness and loading level. The magnitude of the applied normal stress for similar surfaces promotes the retardation of peak and residual conditions being achieved in terms of shear displacement. Further, the dilative response developing during shear displacement of the textured geomembrane – geotextile interfaces is similar to the response (i.e. volumetric change: expansion/contraction) of dense soils for which dilation enables higher internal friction resistance being mobilized.

It is noted that the dilation observed in the textured geomembrane – geotextile interfaces results from the rough surface characteristics of the textured geomembrane liner sheet as it is known that the stress-displacement-volumetric change behavior of fibrous – continuum material interfaces is also dependent on surface roughness properties of the continua. As noted in Chapter 6, for smooth geomembranes, volume changes are small and contractive; however, during the shearing process, the interface exhibits some amount of expansion with increasing ambient test temperature level due to reduction in the stiffness of the counterface geosynthetic materials (geotextile-geomembrane). For the case of geotextile–textured geomembrane interfaces, as the roughness of the liner material increases, it results in dilative behavior at the interface during shear movement and this type of response becomes more consistent with classical soil mechanics principles.

The vertical displacement – horizontal displacement response of the PolyFlex geomembrane versus NPNW geotextile interface at different ambient temperatures for normal stress levels of 10 kPa, 100 kPa and 400 kPa are shown in Figures 7.16a, 7.16b and 7.16c, respectively. The volume change behavior up to peak state appears to be

typical of dense soil with an initial contraction followed by dilation. The peak occurs at the maximum rate of dilation. Residual conditions are achieved after steady-state deformation conditions are attained. Comparing the shear stress versus displacement curves with vertical displacement versus horizontal displacement responses, the post-peak stage of the both curves is similar in pattern. The magnitude of frictional resistance (shear stress) with horizontal displacement and/or the amount of volumetric change (vertical displacement) observed at the interface during residual-shear displacements remains relatively constant but with a slight decrease until the termination of shearing at 60 mm displacement.

The magnitude of vertical displacement changes throughout shearing for the geotextile – textured geomembrane interfaces in a comparable manner to that of dense soils wherein as normal stress increases, vertical displacement decreases. It can be argued that a geotextile is only a semi-continuous surface considering its unique structural properties containing distinct voids within a fibrous formation and compositional arrangement. It should be noted that the capability of rough polymer surfaces to stimulate dilatancy as well as the influence of temperature in increasing the magnitude of this dilative response at the interface which results in increased shear resistance along rough polymer surfaces depends on several factors such as size and orientation of interface asperities, polymer strength, hardness, stiffness and normal stress.

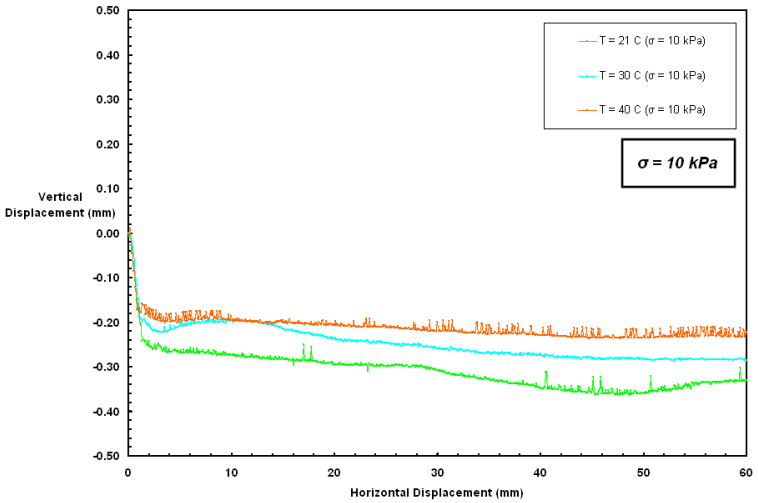

(a)

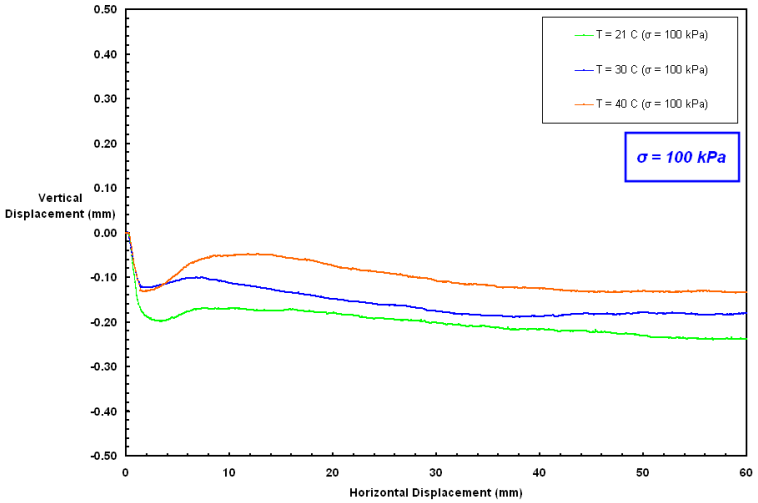

(b)

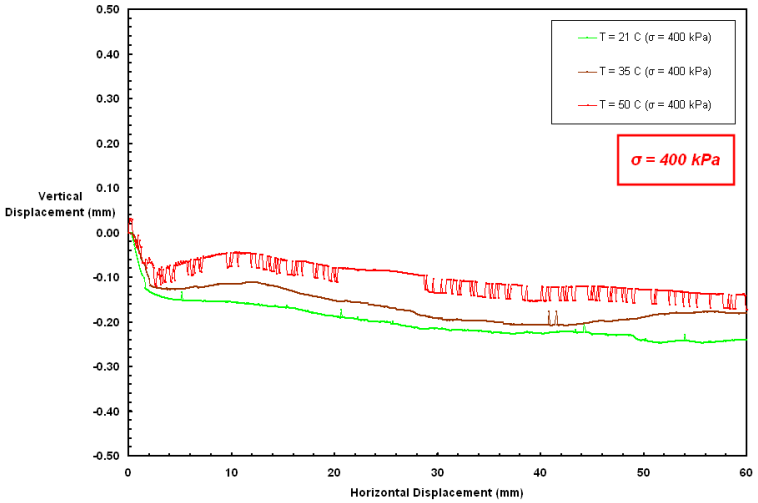

(c)

Figure 7.16 Vertical Displacement – Horizontal Displacement Behavior at Different Test Temperatures for PolyFlex HDPE Textured Geomembrane/NPNW Geotextile

The variation of frictional strength parameters as a result of the change in ambient temperature conditions are presented in Figure 7.17 and 7.18 in terms of interface friction angle, (δ) and coefficient of friction, ($\tan(\delta)$), respectively. The influence of temperature is greater on peak interface shear behavior. The peak interface strength for textured geomembranes is mainly attributed to the geomembrane micro-textural features while the residual interface strength is governed by the geomembrane macro-topographical characteristics.

This effect of temperature, in terms of change in interface shear behavior properties and strength is consistent with polymer softening (Bilgin and Stewart, 2006) which results in greater embedment and interaction of the polymeric materials under a given stress and an increase in the contact area (Lord et al., 1995; Osswald and Menges, 1995) at higher temperatures. Moreover, the peak and post-peak coefficient of friction values increased with temperature increase since concentrated shear stress was more easily and quickly distributed over the entire interface area; and thus, more shear stress is required to overcome resistant friction which is consistent with previous observations made by others (i.e. Daniels, 1989) for the variation of coefficient of friction between polymeric materials with temperature.

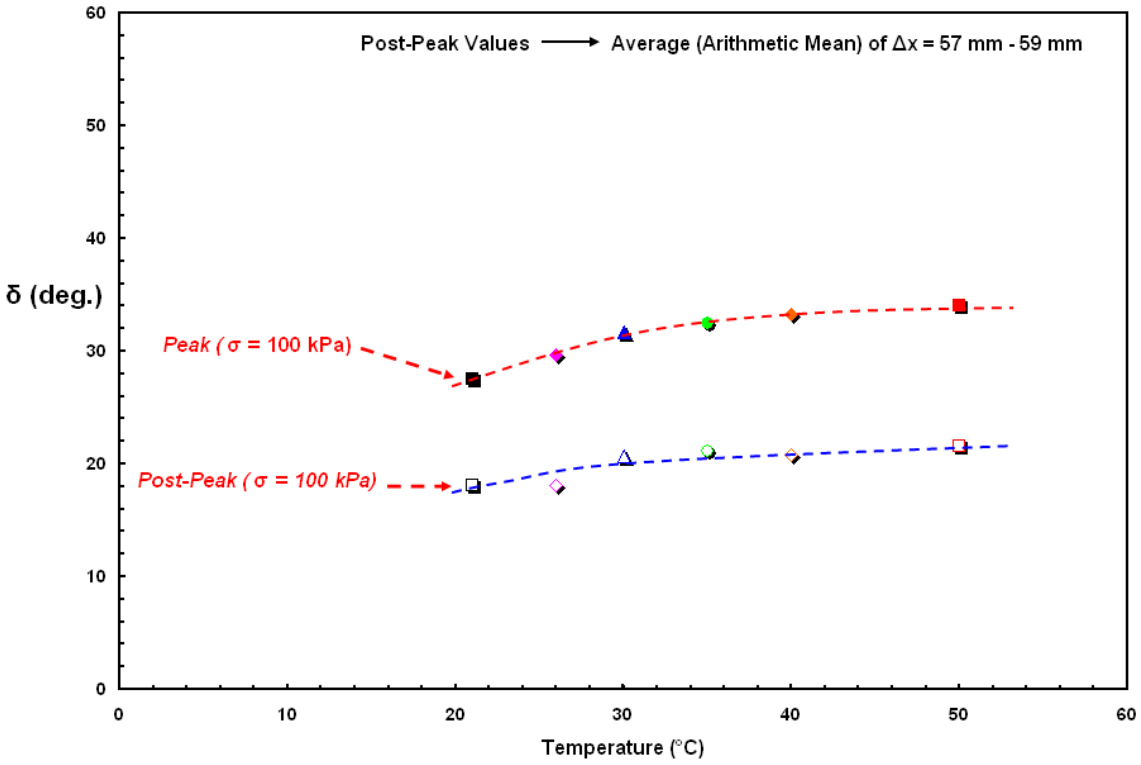

Figure 7.17 The Change in Interface Friction Angle, [δ] with Temperature for PolyFlex HDPE Textured Geomembrane/NPNW Geotextile Interfaces

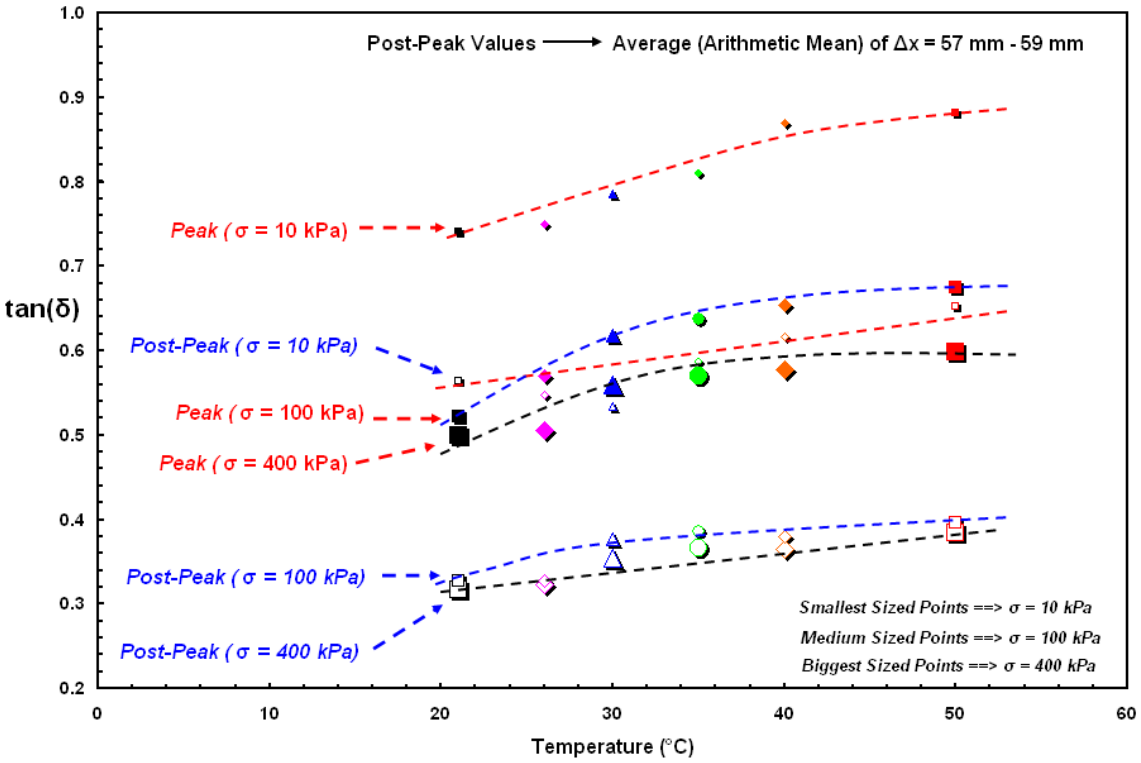

Figure 7.18 The Change in Coefficient of Friction, [tan(δ)] with Temperature at Different Loading Conditions for PolyFlex HDPE Textured Geomembrane/NPNW Geotextile

Strength envelopes corresponding to peak and post-peak conditions are shown in Figure 7.19 for NPNW PP geotextile–PolyFlex coextruded textured geomembrane interfaces at different temperatures (21 °C – 50 °C). Regression of shear strength data at various temperatures with normal stress yielded fits in which the peak and post-peak interface strengths of different temperature conditions can be represented by interface friction angle for the corresponding state.

The influence of temperature is evident in the strength envelopes as represented by differently colored plots in the chart. At each normal stress, the interface frictional strength increased with increasing ambient temperature. This temperature susceptibility of the nonwoven geotextile – PolyFlex textured HDPE geomembrane interface is consistent with polymer softening, reduction in surface hardness and material stiffness, surface pliability improvement leading an increase in contact area and additionally, greater relaxation (flow) of the polymer under a given stress resulting in a more uniform stress distribution over the entire areal extent of the interface by distributing concentrated stress peaks existing at the interface due to boundary conditions and instant load application as the temperature increases.

As Figure 7.19 illustrates, the difference between the peak and post-peak failure envelopes is more pronounced at all elevated temperatures compared to the results of smooth geomembrane interface tests (Figure 6.20). It is evident from the post-peak failure envelopes that the interface shear tests on PolyFlex coextruded textured geomembrane exhibited a range of higher strain/larger displacement interface strength values throughout the test temperature range. This improvement at greater displacement can be attributed to the increased interlocking between the geotextile filaments and the

macro-asperities existing on the surface of the liner sheet due to stretching of the geotextile as a result of normal load, shearing motion process, and better relaxation of counterface components onto each other.

In order to better evaluate variations in the behavior over the entire stress range and to recognize deviations at very high or very low normal stress levels, the peak and post-peak strength envelopes were regenerated as plots in which both x and y axes are in logarithmic scale (Figure 7.20). The failure envelopes become concave up at low normal stresses for higher test temperatures which resulted from the cooperative role of Velcro-type hook and loop interaction in terms of raising the magnitude of mobilized shear resistance at the interface as well as favorable contribution of elevated temperature conditions in terms of enhancing the adhesion properties (y intercept: c_a) of the polymeric geosynthetics due to increased surface adaptability and material malleability.

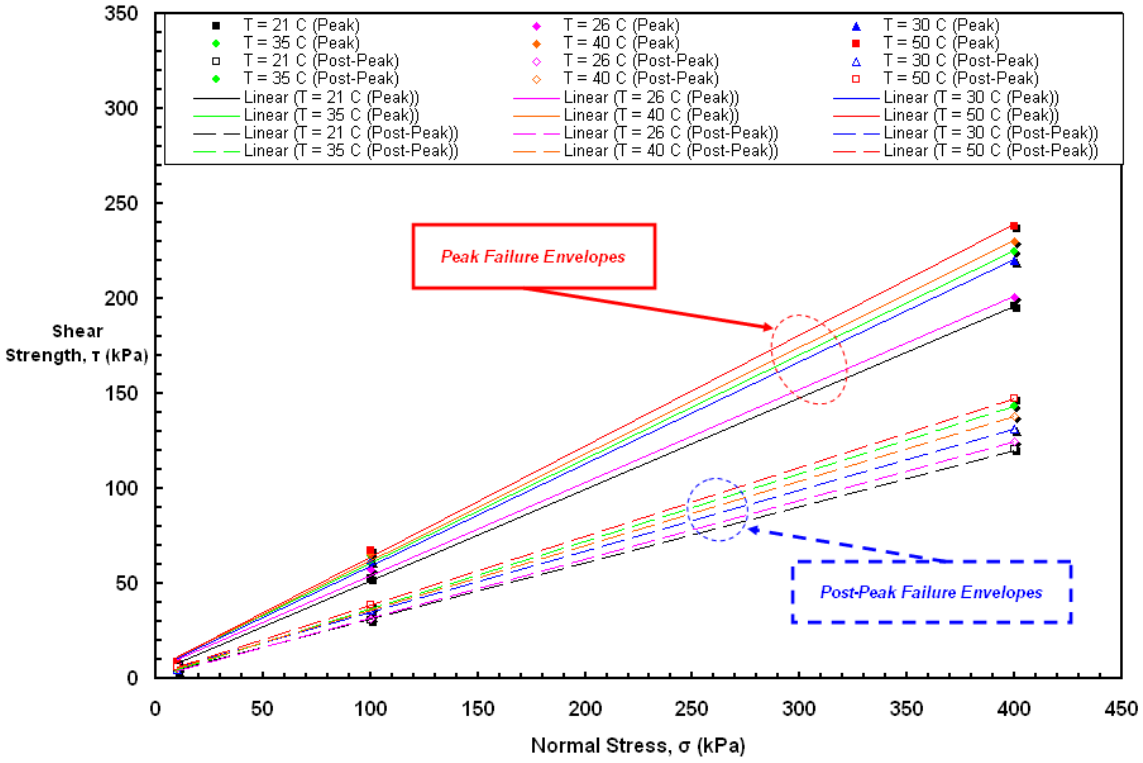

Figure 7.19 The Alteration of Peak and Residual Strength Envelopes with Increasing Temperature for PolyFlex HDPE Textured Geomembrane/NPNW Geotextile

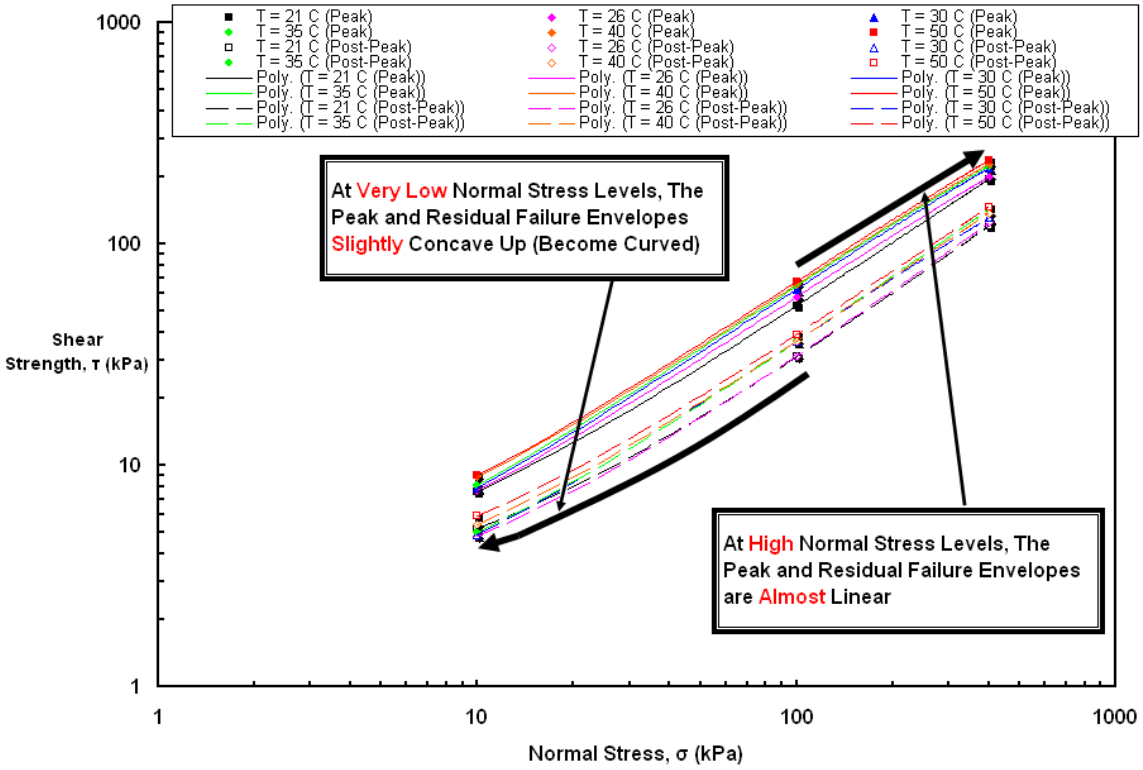

Figure 7.20 The Transformation in Failure Envelopes with Temperature at Different Loading Conditions for PolyFlex HDPE Textured Geomembrane/NPNW Geotextile

7.6. Agru HDPE Structured Textured Geomembrane/NPNW Geotextile

Structured textured (MicroSpiked) HDPE geomembrane liners were relatively recently introduced to the market by Agru Corporation. The macro-texture elements called microspikes are integrated on a base lining material surface forming homogeneous near isotropic pattern with a regular series of small spikes. This method creates a high-profile structured/roughened friction surface. Additionally, compared with heterogenous more anisotropic surface nature of textured liners manufactured using a coextrusion technique, the consistent (isotropic) structuring on the sheet surface has been argued to facilitate reproducible friction angle values along with the highest surface friction/interface resistance values in the industry.

Shear stress–horizontal displacement curves for microspiked textured Agru HDPE geomembrane specimens sheared against NPNW PP geotextile samples are shown in Figure 7.21 at test temperatures ranging from 21°C up to 50°C for three different normal stress levels (10, 100 and 400 kPa). Similar to smooth and coextruded textured geomembrane interfaces, the shear displacements/deformations necessary to attain peak and pseudo-residual states for this structured liner – fabric interface system increases with increasing test temperature as well as normal stress levels. It was found that nonwoven geotextile–structured geomembrane interface reached both peak and post-peak conditions at greater shear displacements than that of nonwoven geotextile – coextruded geomembrane interfaces (both GSE and PolyFlex). About 2 to 4 mm of additional displacement was required than for the cases with coextruded liners regardless of ambient test temperature and normal stress applied.

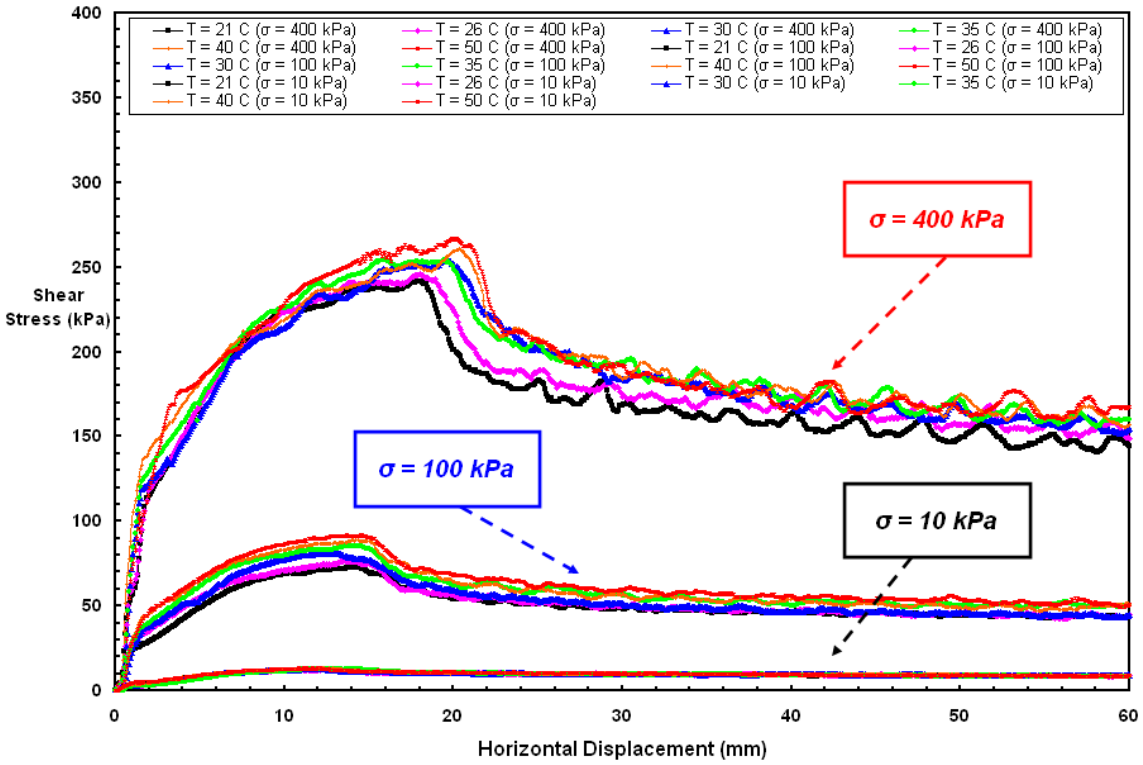

Figure 7.21 Shear Stress–Displacement Curves at Different Loading Conditions; & at Various Test Temperarures for Agru HDPE Structured Geomembrane/Geotextile

The Agru microspike interface required 10-13 mm, 13-15 mm, 16-18 mm of shear deformation to mobilize the peak strength at normal stresses of 10 kPa, 100 kPa and 400 kPa, respectively (Figure 7.22a, 7.22b and 7.22c, respectively). The shear displacements to peak for coextruded geomembrane interfaces had been on the order of about 6-8 mm, 8-12 mm, and 12-16 mm for normal stress levels of 10 kPa, 100 kPa, and 400 kPa, respectively, (for GSE and PolyFlex HDPE textured geomembranes as shown in Figures 7.8 and 7.15, respectively). The larger displacement required with the interface involving the microspiked liner can be attributed to the fact that as the liner sheet surface roughness increases, the displacement to reach peak state increases. The post-peak deformation required to achieve residual condition decreases as shown on Figure 7.22a through 7.22c

such that the nonwoeven geotextile – Agru textured geomembrane interface was able to reach post-peak conditions after about only 25 to 30 mm horizontal displacement. It is also noted that the denser geotextile structure under large normal stress (400 kPa versus 10 kPa) necessitated larger displacements to reach the peak resistance. This behavior is consistent with the smooth and the coextruded geomembrane cases where greater displacement was required under higher loading conditions to reach the peak resistance. The general shape of the stress-displacement curves at different temperatures shows an initial rapid rise in shear stress followed by a slower increase up to peak strength. A smoother transition through peak state is observed compared with the sharpness of the smooth HDPE geomembrane peak stage. A more dramatic reduction in interface shear resistance in comparison to that of coextruded geomembranes is seen. Finally, the shear stress remains relatively constant but with a slight decrease until the termination of shearing at 60 mm displacement. Therefore, it should be emphasized that Agru microspiked geomembrane interface evolved through three different stages of interface shear behavior during a relatively small displacement of less than ~30 mm. Subsequent to this, the shear stress – displacement curve progresses more or less constant with repeated peaks and troughs like a sinusoidal periodic motion. This unique behavior at larger displacement will be discussed in detail in Section 7.8. The overall appearance of the stress-displacement curve appears similar to that of the coextruded textured systems. Further, the less sharp peak stress phase followed by a significant post-peak softening for the structured geomembrane interface represents a transition dominant mechanism in shear behavior throughout the entire test temperature range. Similar with the other textured geomembrane interfaces, the strength loss after peak was the lowest at 10 kPa.

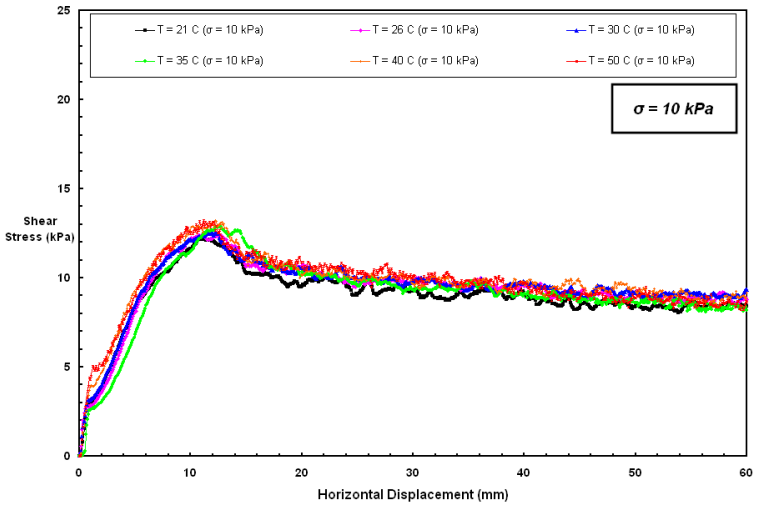

(a)

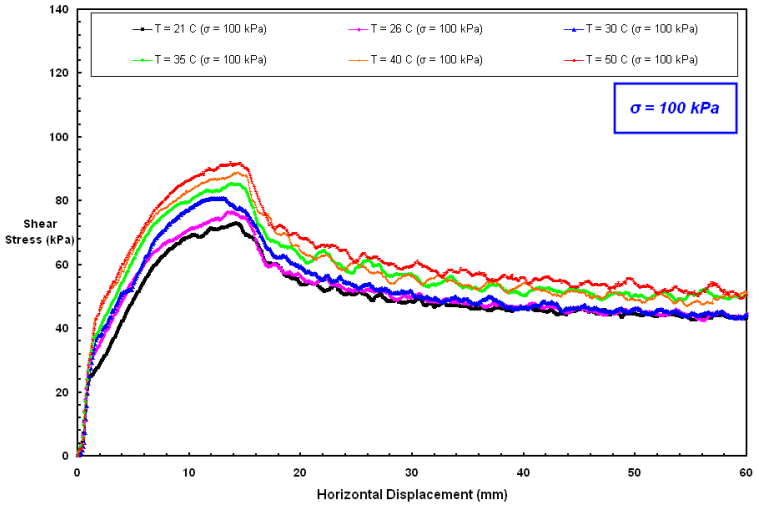

(b)

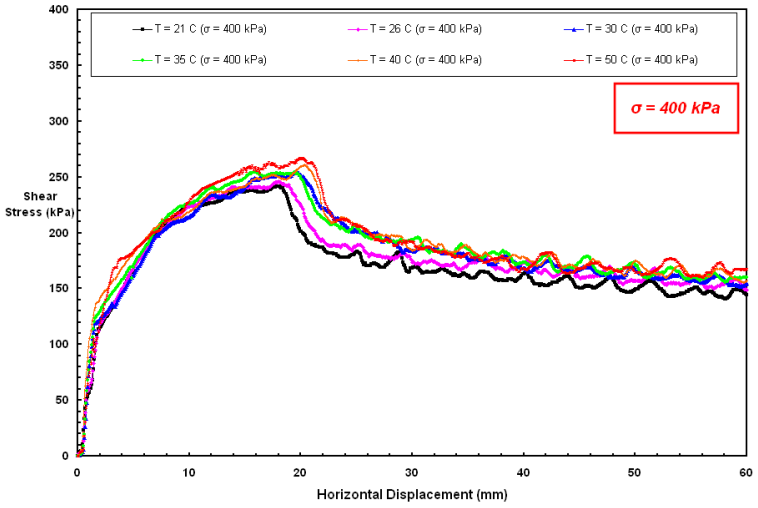

(c)

Figure 7.22 Shear Stress – Displacement Curves at Different Test Temperarures for Agru HDPE Structured Geomembrane/NPNW Geotextile: 10, 100 and 400 kPa

A detailed examination of the full shear stress–displacement behavior exhibited at different temperatures of the individual selected normal stress levels depicts an increase in displacement to peak stress with increasing ambient test temperature (from 21 °C up to 50 °C) which is indicative of greater geotextile filament engagement with the stronger rounded spikes as the surface pliability and the interaction capability of the continuum geomembrane liner increases. Consequently, the frictional interactions occur at greater depths into the geotextile matrix beyond interface contact surfaces with higher stiffness than the surficial shallow hook and loop interactions. The relatively comparable contribution of frictional hook and loop resistance could be observed from the trends of the stress-displacement envelopes/curves for the whole test temperature range at very low normal stress (10 kPa). This very low level normal stress interface shear behavior of textured geomembranes in combination with fibrous geotextiles is of importance. Since the characteristic textural features of the geomembranes (coextrusion asperities versus structured spikes) affect the amount of effort required in the field in handling these large lining sheets when locating and placing them. For example, as indicated by Hebeler et al. (2005), some contractors noted the benefit of additional interaction (i.e. hook and loop) between a geotextile and textured geomembrane during installation, as the system requires minimal or no supplemental restraints or temporary connections during placement and joining of the seams. On the contrary, other contractors noted the disadvantage of large interaction between the components of a geosynthetic composite system during installation as it greatly restricts realignment and minor adjustments of the geosynthetics after their initial placement.

Shear stress versus displacement curves for the entire test temperature range and at various normal stresses reveal some important aspects of the displacement to peak of the structured systems compared to coextruded systems at low normal stress levels. The initial interface stiffnesses of the two geomembrane systems are comparable, but diverge after the structured geomembrane system reaches peak strength, indicating that both textures provide comparable initial frictional stiffness. This was previously described by Hebeler et al. (2005) who noted that the added strength gained through hook and loop interaction is achieved at a much lower stiffness, due to the lower stiffness of individual NPNW filaments that are discretely involved in low normal stress hook and loop response mechanisms. As normal stress increases and similar interaction mechanisms begin to control the behavior of both geomembrane types, the stiffness characteristics of the two geotextile versus geomembrane systems are essentially equivalent. Further, they noted that the large displacements needed to mobilize the peak strength of both systems with different texturing techniques at operational normal stress levels should be noted when specifying the in-place strengths of these types of geosynthetic systems.

Figures 7.23a, 7.23b and 7.23c show the vertical displacement – horizontal displacement response of NPNW PP geotextile – Agru structured textured geomembrane interfaces at different test temperatures at normal stresses of 10 kPa, 100 kPa and 400 kPa, respectively. The volumetric expansion (dilation) developed at the interface between fabric and structured surface liner materials during shearing process contribute to the improved interface shear response in resisting the shear forces.

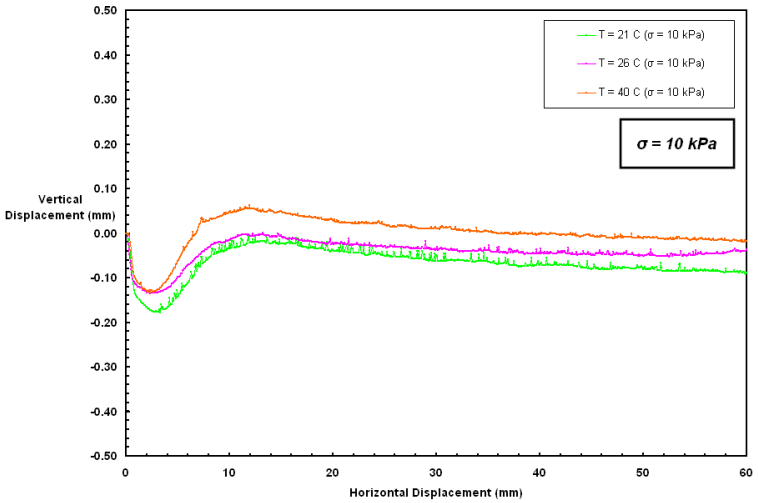

(a)

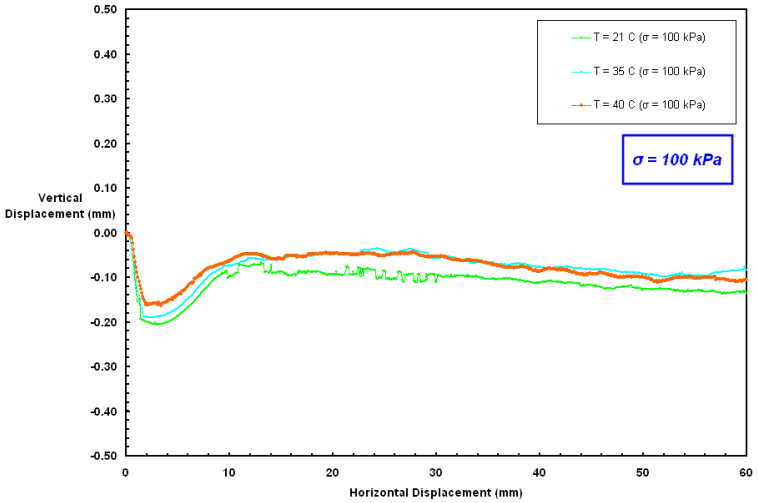

(b)

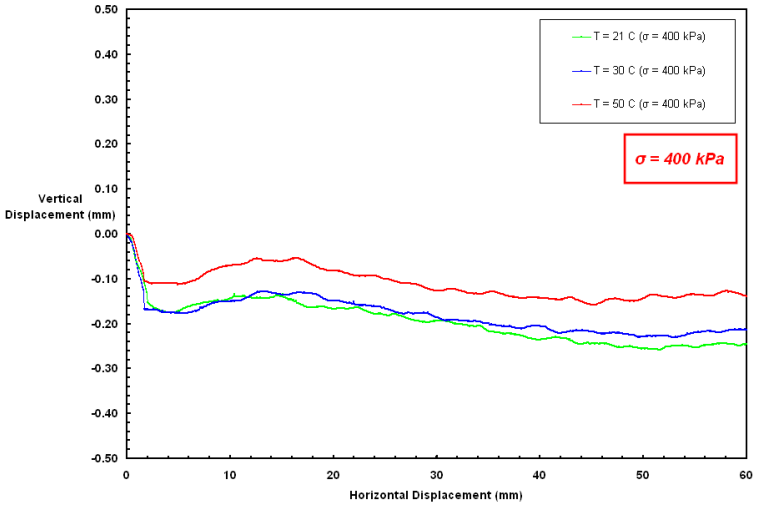

(c)

Figure 7.23 Vertical Displacement – Horizontal Displacement Behavior at Different Test Temperatures for Agru HDPE Structured Geomembrane/NPNW Geotextile Interface

The change in physical properties of the counterface geosynthetics promotes higher interaction and integration of the interface components due to greater adaptabilty of the counterface materials. In addition to the expansion of the counterface materials themselves due to ambient temperature increases, the unconstrained geotextile sample can freely adjust to the textural properties of the geomembrane, including the rounded, stiff spikes leading to dilative behavior at the interface during shearing. This type of response is consistent with classical soil mechanics principles in terms of frictional strength increase as a result of dilation in soil. The most significant benefit of this greater relaxation of the polymeric geosynthetics at elevated temperatures results from the dissipation of stress concentrations uniformly throughout the interface contact area. The displacements to peak resistance points and to maximum dilation points are very similar (Figure 7.22 and 7.23, respectively). The improved frictional response of lower strength and higher stiffness of Agru structured geomembranes in combination with geotextiles results from the stiff and rounded macrotextures called spikes which look like they are installed and situated to act as obstructing blocks against the movement of the fabric matrix under a driving shear force. The outward regions of the spikes engage geotextile fabric matrix as a result of fabric matrix compression amongst the macrotextural elements/features (i.e. greater interlocking depths).

In order to further comprehend and illustrate the influence of elevated temperatures on interface shear strength of Agru structured geomembranes, the variation in two important friction parameters (δ and $\tan(\delta)$), commonly utilized in layered systems engineering designs, were plotted as a function of temperature (Figure 7.24 and 7.25, respectively).

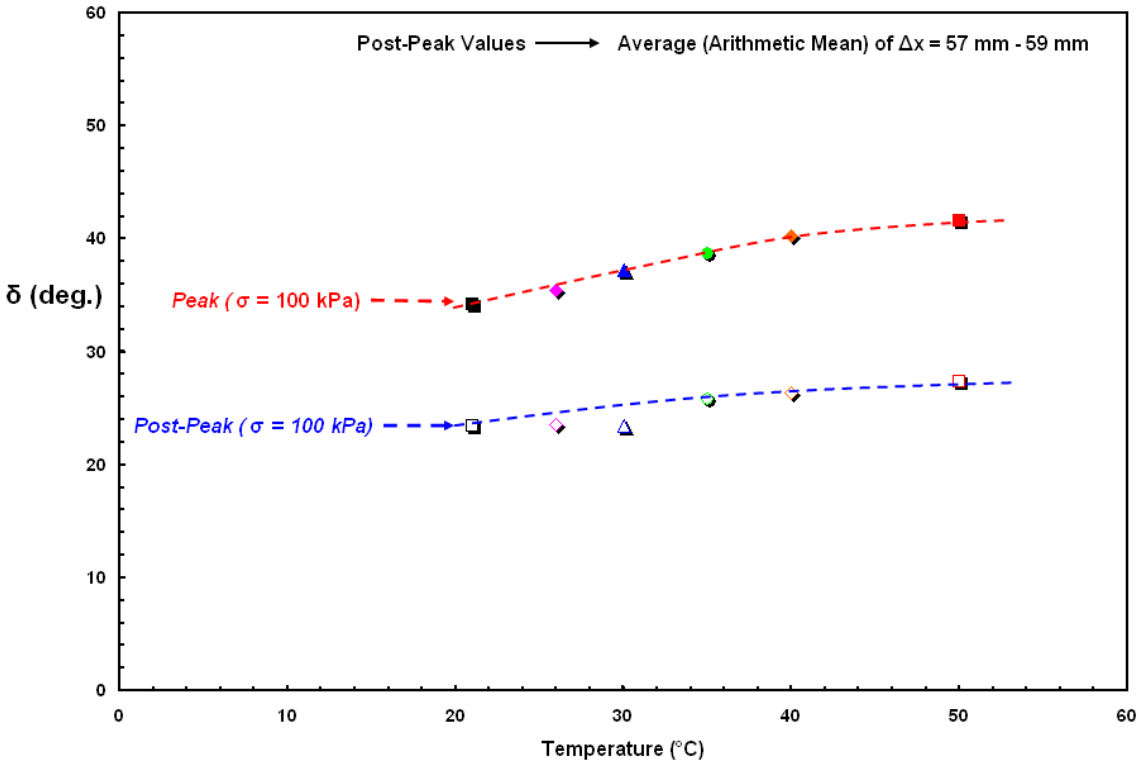

Figure 7.24 The Change in Interface Friction Angle, [δ] with Temperature for Agru HDPE Structured Geomembrane/NPNW Geotextile Interface Layered System

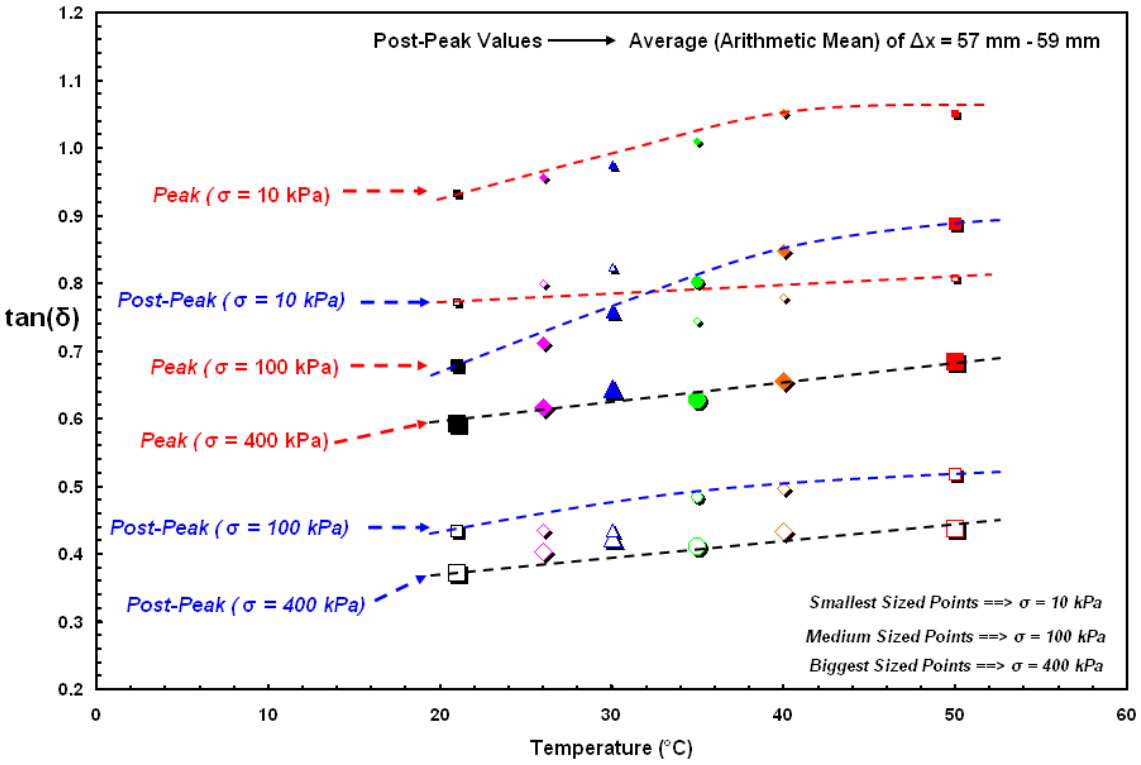

Figure 7.25 The Change in Coefficient of Friction, [tan(δ)] with Temperature at Different Loading Conditions for Agru HDPE Structured Geomembrane/NPNW Geotextile

Both peak and post-peak values of the frictional strength parameters increase with increasing temperature. The coefficient of friction decreased as the normal stress increased through a range of 10 kPa to 400 kPa which does not obey Amonton's first law. This is attributed to the characteristic frictional properties of polymer interfaces under the impact of loading and the resultant shear displacement. As shown in the preceding plots, the effect of temperature is greater on peak interface shear response with a larger increase in strength value as the peak interface resistance of textured geomembranes is associated with the geomembrane micro-roughness.

The differences in texturing technique (i.e. structured vs. coextruded) and roughness asperity pattern (i.e. quasi-isotropic vs. anisotropic) governs the depths of geotextile-geomembrane interlocking under different normal stress levels which in turn influences the shape of the failure envelopes. The variation in shear resistance with regard to normal stress for structured Agru HDPE geomembrane in contact with geotextile at different test temperature conditions is expressed in terms of Mohr-Coulomb relationship in Figure 7.26. There is clearly curvature, especially for the peak failure envelope of the structured Agru geomembrane at higher elevated temperature conditions at which some of the interface shear tests were performed. Second-order polynomial fit is appropriate for interpretation and formulation of this type behavior as previously proposed by Giroud et al. (1993) where a hyperbolic expression for geosynthetic–geosynthetic and geosynthetic–soil interface shear strength envelopes can be utilized when test results give a significantly non-linear shear stress versus normal stress relationship. For the residual (post-peak) strength envelope of Agru microspiked geomembrane, the degree of the resulting curvature at the highest test temperature level is

lower than that of the peak state. This observed curved trend is attributed to the performance of structured textured geomembranes consisting of the robust microspikes mobilizing larger resistances at medium to high stress levels (e.g. 100 kPa) for higher elevated temperatures (e.g. 40 °C – 50°C) compared to either coextruded textured liners (e.g. GSE or PolyFlex textured). Additionally, the interface resistance capacity of Agru microspiked geomembrane liners at 400 kPa high normal stress condition regardless of ambient test temperature is more pronounced than that of both coextruded lining materials from GSE and PolyFlex. In short, it can be emphasized that the structured geomembrane – NPNW geotextile composite system exhibited a linear peak as well as post-peak strength envelopes at room temperature conditions (21 °C) over the entire range of normal stresses tested. However, the failure envelopes have transitioned from linear trend to non-linear curved pattern as the ambient test temperature increases from 21°C up to 50°C. In other words, the shape of the envelope was altered due to the influence of the temperature.

The peak and post-peak strength responses of the structured geomembrane–NPNW geotextile composite system tested at different temperatures were replotted on log–log scale to further analyze the response in general and particularly for very low normal stress levels. Both of the strength envelopes (peak and post-peak) became curved (the transitions in the patterns are evident in the plots) at high as well as at low normal stresses in which the response depicted concave-up form and concave-down mode for high and low stress levels, respectively (Figure 7.27).

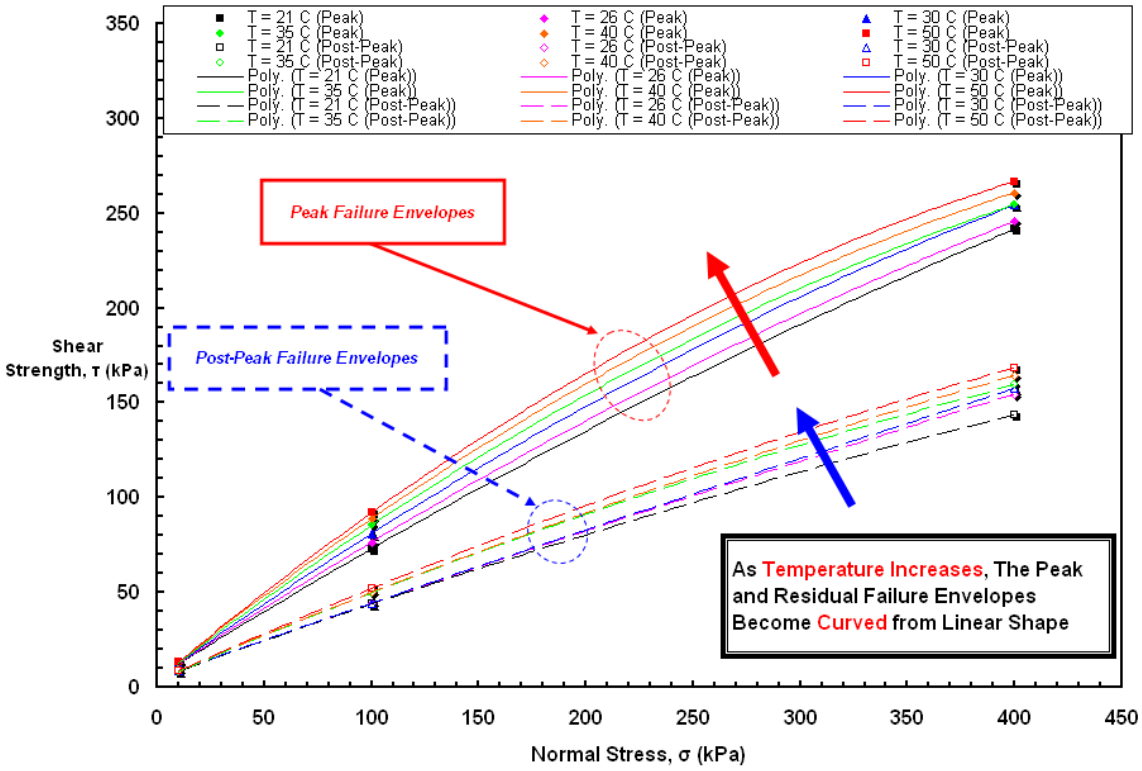

Figure 7.26 The Alteration of Peak and Residual Strength Envelopes with Increasing Temperature for Agru HDPE Structured Geomembrane/NPNW Geotextile

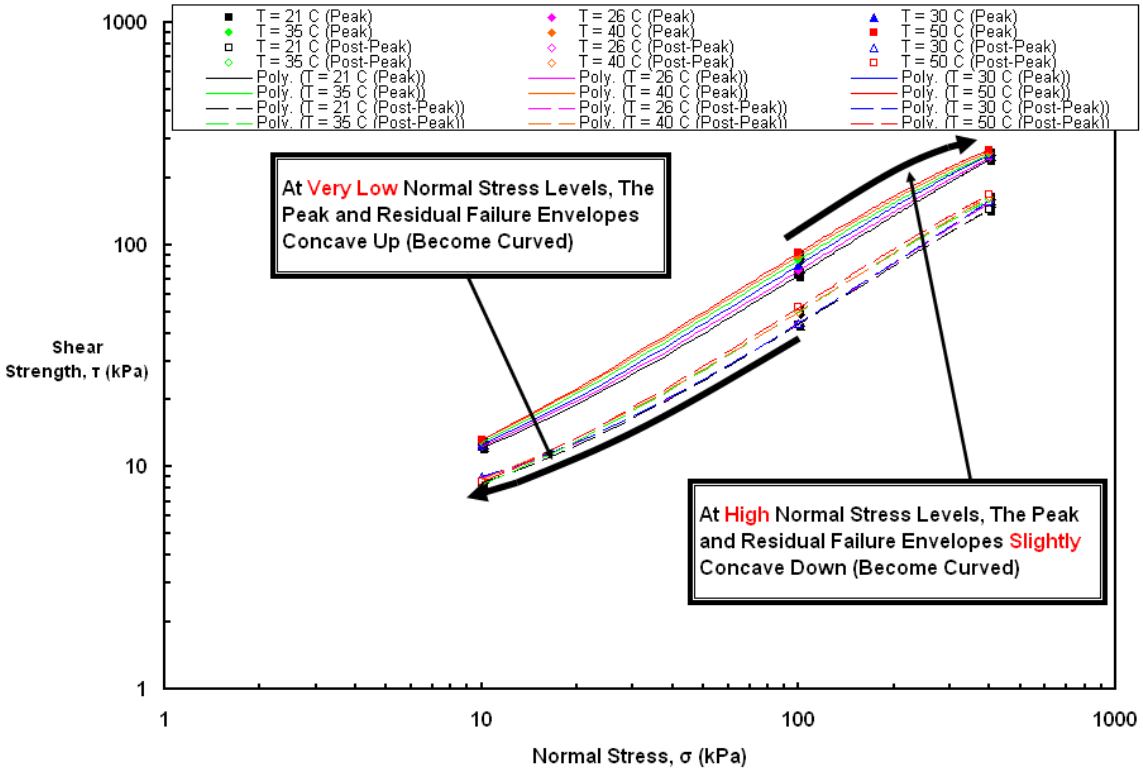

Figure 7.27 The Transformation in Failure Envelopes with Temperature at Different Loading Conditions for Agru HDPE Structured Geomembrane/NPNW Geotextile

To sum up, the deep-seated interaction and contact between stiff, rounded microspikes and the geotextile matix assist and further support the interface system in displaying greater resistance at larger shear displacements for the case of high normal loading conditions. Further, the trends of the peak interface shear stress results demonstrate that the structured system provide higher interface friction than the coextruded system at ambient temperatures ranging from 21 °C to 50 °C as well as within the normal stress range (construction – operational) tested, as represented in the conventional Mohr-Coulomb form. Additionally, the structured system exhibits marginally stronger residual response at operational stresses. Particularly for elevated temperature conditions, non-linear trends as a function of increasing normal stresses are typical of isotropically microspiked geomembrane and geotextile fabric composite layered systems. In other words, the strength envelopes are in the shape of second order polynomial curves at higher ambient temperature (>30 °C) such that there exists a decrease in the amount of increase in the shear strength envelopes with increasing normal stress.

7.7. Comparison and Assessment of Different Texture Characteristics for the Interface Strength of Geosynthetic Materials at Elevated Temperatures

The texturing process (coextrusion, impingement, lamination) used in textured geomembrane manufacturing was shown to be an insignificant factor as concerns microtexture removal during pre-peak and peak stages of shear displacement (Lee, 1998; Frost and Lee, 2001) with the exception of the more recently developed structured

texturing technique for liner sheets which was studied and reported by Hebeler (2005) and by Hebeler et al. (2005). Therefore, all former texturing methods create rough liner surfaces with similar microtexture features resulting in the peak strength not being dramatically affected by the texturing process. However, the texturing process impacts the residual strength as the integration of texture elements with the base liner material (i.e. core body of geomembrane sheet) depends on the type of texturing process used. For example, textured geomembranes manufactured with a secondary process (lamination or impingement) have much weaker adherence/bonds between the asperties and the core geomembrane. Therefore, removal of these asperities requires lower shear forces, and the residual strength of the interface will be typically weaker. For this reason, these two manufacturing methods have lost their popularity with the geosynthetics industry. Because of its superior endurance properties in possessing resilient asperities, the coextrusion technique has maintained its value in the market and has a large market share, particularly, in North-American industry. Further, geomembranes in which the texturing process is an integral part of the manufacturing process and thus, there is less potential for widespread separation under large load, will have relatively strong bonds between the asperities. Removal of the asperities will require higher shear forces; thereby a stronger interface resistance will be attained. The change in overall peak and pseudo-residual interface shear behavior (i.e. in terms of stress-displacement curve) of coextruded and structured textured geomembranes with increasing ambient temperature was already presented in Figures 7.8, 7.15 and 7.22, for GSE, PolyFlex and Agru, respectively (i.e: both liner produced from the same base material (HDPE) along with a discussion regarding the large displacement resistance of these two distinct interfaces,

primarily governed by the macrotextural properties of the geomembranes manufactured from different texturing techniques.

In general, three distinct size ranges have been utilized in order to quantify and classify the textural features existing on the geomembrane lining sheet materials as follows: i) Macrotexture refers to base structure, asperities, and or attached features >0.125 mm in out-of-plane dimension. ii) Microtexture refers to roughness present on the base sheet or macrotextural features of <0.05 mm. iii) Texture or roughness intermediate to those ranges are be described as mesotexture (Hebeler, 2005). Further, Frost et al. (2002) showed that texturing technique directly influences the strength and durability of both the microtexture, and to a greater extent, the macrotexture created during the texturing process. The durability of textural features is, in principle, defined as a measure of the strength loss at the geotextile–geomembrane interface from peak to residual values, and from virgin to repeated tests. In other words, the lower the strength loss, the greater the durability.

The differences in direct interface shear behavior over a large normal stress range (10 kPa – 400 kPa) at elevated temperature conditions from 21°C up to 50°C for the coextruded and the structured geomembranes were illustrated and the results were evaluated along with further discussion regarding the change/differentiation in the response as a result of temperature increase in the corresponding sections of this chapter for each liner material. All the textured geomembranes, including coextruded as well as structured lining materials, exhibited a bilinear pre-peak shear behavior consisting of an initial frictional response, followed by a secondary strength increase at a lower rate (i.e. stiffness) representative of supplemental filament – texture interaction. The peak stress

was followed by significant post-peak softening for the coextruded as well as structured samples over the entire test temperature range. The increment in displacement to peak stress with increasing normal stress represented a transition in dominant mechanism, from surficial velcro-type interactions to a more frictional response at higher normal stresses for all types of textured geomembranes. This incremental behavior in the mobilization of peak state was indicative of greater geotextile fabric matrix engagement by the asperities as the normal stress and the ambient temperature increased due to greater embedment, deeper insertion of the texture into matrix, and larger contact area resulting from the hardness decrease. As the geotextile becomes interbedded between the macrotexture of the geomembrane, the micro and mesotexture of the base substrate become involved in supplemental surface level filament-texture interactions resulting in further increase of the shear resistance. In other words, a transition in the interface shear mechanism controlled by surficial shallow interactions dominant within the geosynthetic system at low normal stress levels transforms, with increased normal stresses, into matrix level deep interactions controlling the shear behavior at higher normal stress levels when the effect of the geotextile matrix compression between the macrotextural features of the geomembranes was exceeded (Hebeler, 2005). At this stage, the height and size of the macro-asperities existing on the geomembrane become of importance. Moreover, the favorable contributing influence of higher temperature conditions, in terms of increased surface pliability as well as greater relaxation and flexibilty of the polymeric counterface geosynthetics, promotes an improved and complete settlement of one geosynthetic material into the other resulting in greater interaction and interlocking between interface

components. This results in the interface exhibiting larger shear responses at elevated temperature conditons for the same normal stress level.

As was seen in Figure 7.1 and 7.2, both the coextruded and the structured geomembranes contain micro and mesotexture across the base substrate providing for the significant surficial interactions observed at operational normal stresses. The presence of these micro and mesotexture features on the base of the tested geomembranes provided for the supplemental peak strength gains throughout the pre-peak stage of the shearing process before the removal of these features at later post-peak stages. As was previously revealed by Hebeler et al. (2005), the comparable global surface roughness measures of R_L=1.23 and 1.28 for the structured and coextruded geomembranes, respectively, are reflected in the similar stress–displacement behaviors observed in the operational normal stress range. In other words, the behavior of the two materials exhibited similar response in the operational stress range where macro and base geomembrane texture begin to control the system behavior. Additionally, the post-peak strength loss behavior with the change in temperature was quantified and presented in terms of the interface sensitivity further supported this statement.

To compare shear strength performance (i.e peak and post-peak) of the different textured systems with temperature change, from the interface direct shear data set, the peak shear stresses and the post-peak shear stresses were plotted against the corresponding test temperature levels for Agru, GSE, and PolyFlex textured geomembranes in Figure 7.28 and 7.29, respectively. The largest interface frictional resistances in contact with nonwoven geotextiles throughout all test temperature range (21°C – 50°C) were observed for the structured Agru lining material.

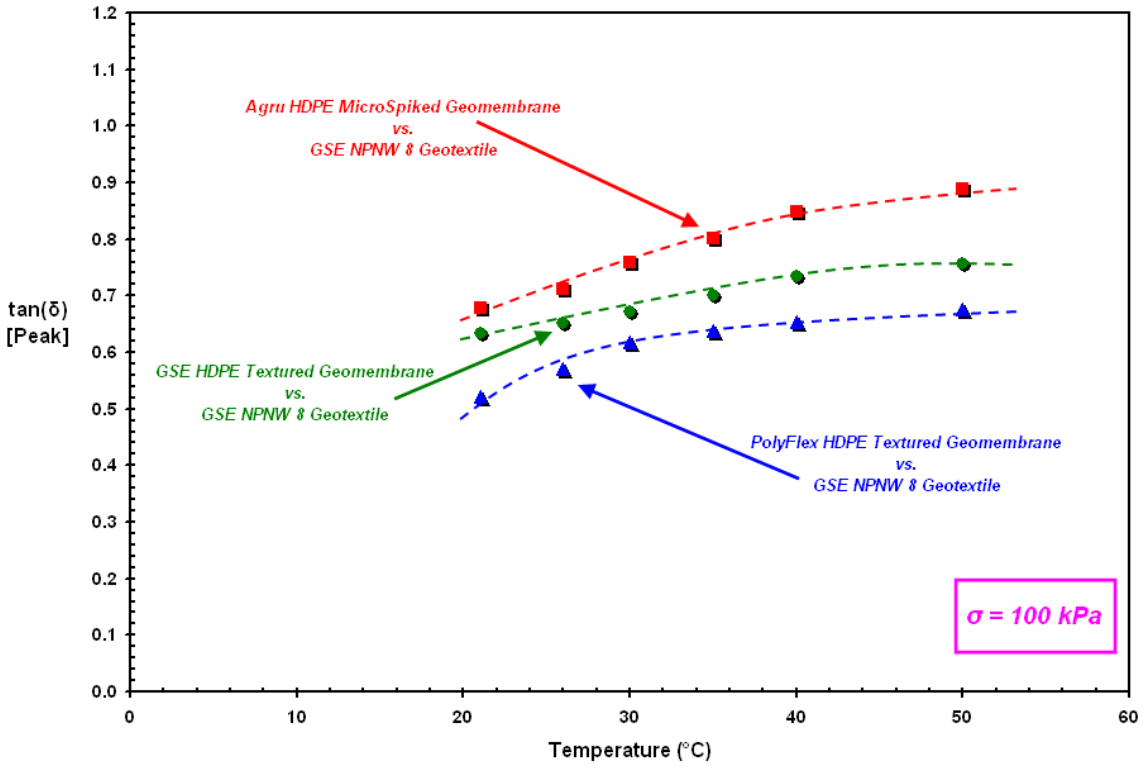

Figure 7.28 Comparative Analysis for the Variation in *Peak* Coefficient of Friction with Temperature for the Textured Systems, including: *GSE*, *PolyFlex*, and *Agru* Liners

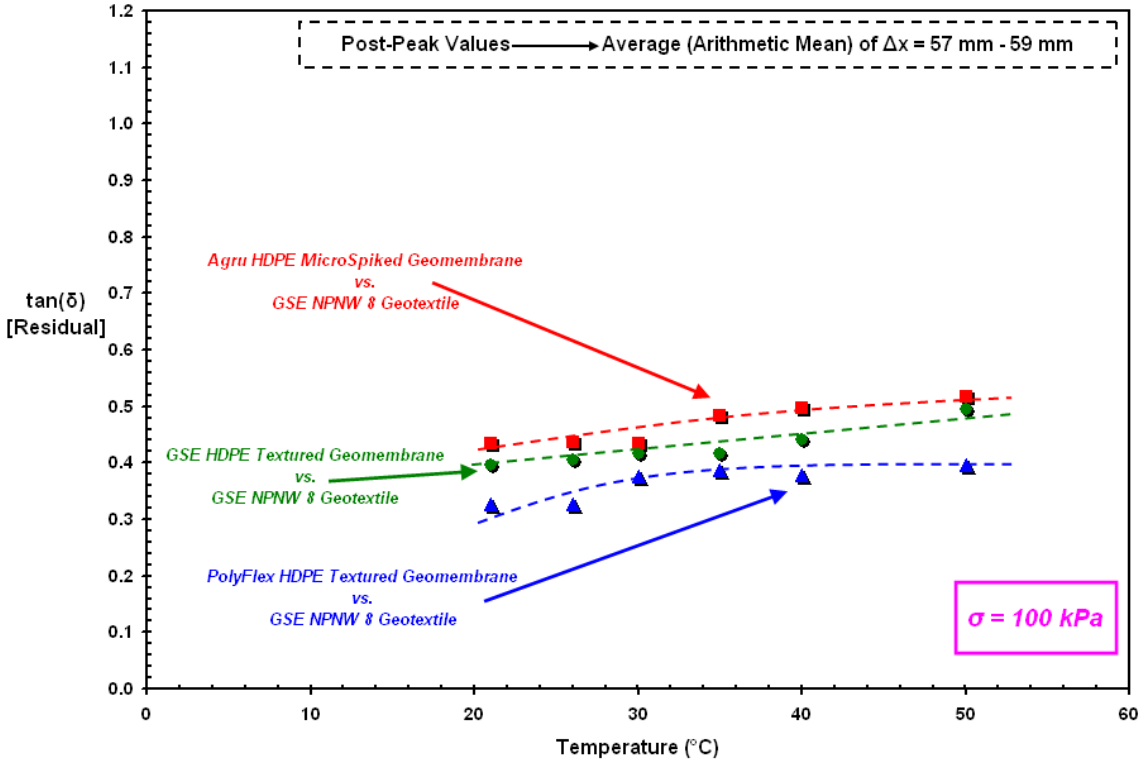

Figure 7.29 Comparative Analysis for the Variation in *Residual* Coefficient of Friction with Temperature for the Textured Systems, including: *GSE*, *PolyFlex*, and *Agru* Liners

As seen in Figures 7.28 and 7.29, Agru MicroSpike exhibited higher peak and post-peak friction than both GSE and Polyflex textured in combination with fibrous geotextiles over the entire test temperature range. This is attributed to the relatively strong texture spikes of Agru liner not allowing substantial tearing or deterioration in the asperities once the peak shear stress value had been surpassed. Consequently, it can be considered that MicroSpike is a more durable geomembrane in terms of showing better interface resistance performance at all elevated temperature condition (≤50°C) tested in this study. Therefore, the structured enhanced textural properties of Agru MicroSpike serves some practical advantage in applications where the interface in conjunction with geotextiles is likely to experience larger normal stresses and be exposed to higher temperatures. Throughout the entire laboratory experimental program, Agru MicroSpike functioned better than both GSE and Polyflex coextruded in terms of shear strength and overall response in addition to being a more durable and uniform product. Besides, the strength loss/resistance reduction from peak to pseudo-residual was considerably smaller for the microspiked than for the coextruded liners.

As a closing remark for providing a general synopsis on the complete interface shear behavior response observed for the coextruded systems as compared to the structured systems, the direct shear test results for the coextruded geomembrane systems exhibited a post-peak softening trend throughout the tested normal stress range (10 kPa – 400 kPa) at all temperatures tested. In comparison, the results of the structured geomembrane system displayed higher stiffness, lower strength, and limited strain softening at low (10 kPa) normal stresses, with post peak softening and mobilized strengths becoming comparable to the coextruded system as normal stress increases up to

the level of intermediate to high stresses (100 kPa to 400 kPa) over the entire test temperature range from 21°C to 50°C.

7.8. Assessment of the Influence of Geomembrane Macro-Texture Uniformity and Recurrence Characteristics on the Developed Post-Peak Behavior

The discussions provided in this section are intended to demonstrate some additional aspects of the observed post-peak response of the MicroSpike liners. The initial stiffness characteristics as well as the pre-peak and peak behaviors are equivalent and analogous to those of coextruded systems. Since both the structured and the coextruded geomembranes contain micro and meso texture across the base substrate, this results in similar behavior being mobilized and comparable pre-peak and peak response being observed.

As opposed to the coextrusion process which generates random textures over a broad size range of features, structuring typically produces more uniform surface textures consisting of macro-spike configuration organized in multiple sequential arrays of spikes recurring at distinct intervals (Figures 7.30a and 7.30b), with micro and meso texture existing on the base substrate only. Further, the structured geomembrane sheet can be visibly seen to be composed of two distinct surface textural schemes in terms of roughness properties such that the micro and meso texture region is seen as an elemental part of the liner sheet whereas, the microspikes appear as more external features.

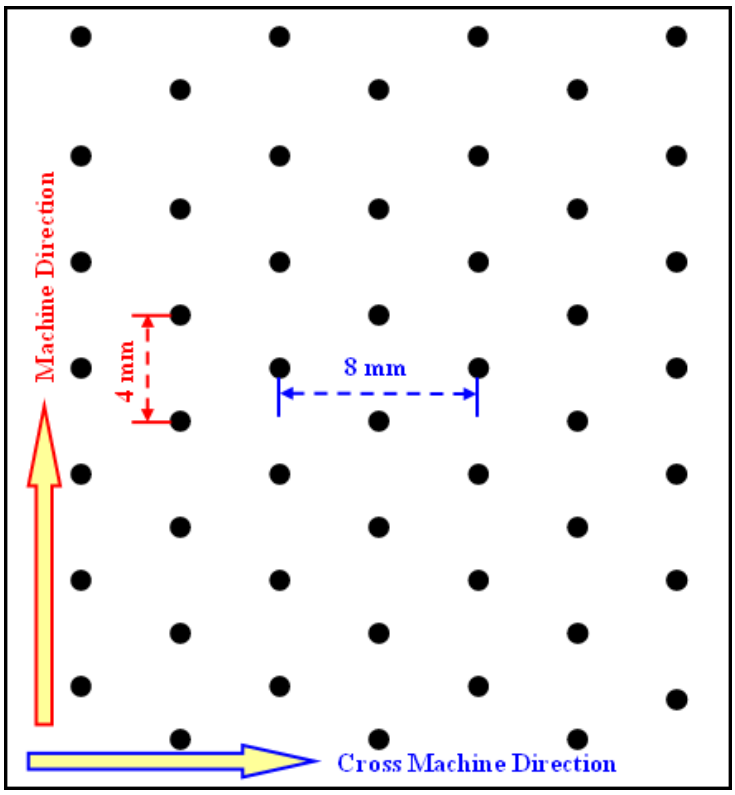

(a) *[Not to Scale]*

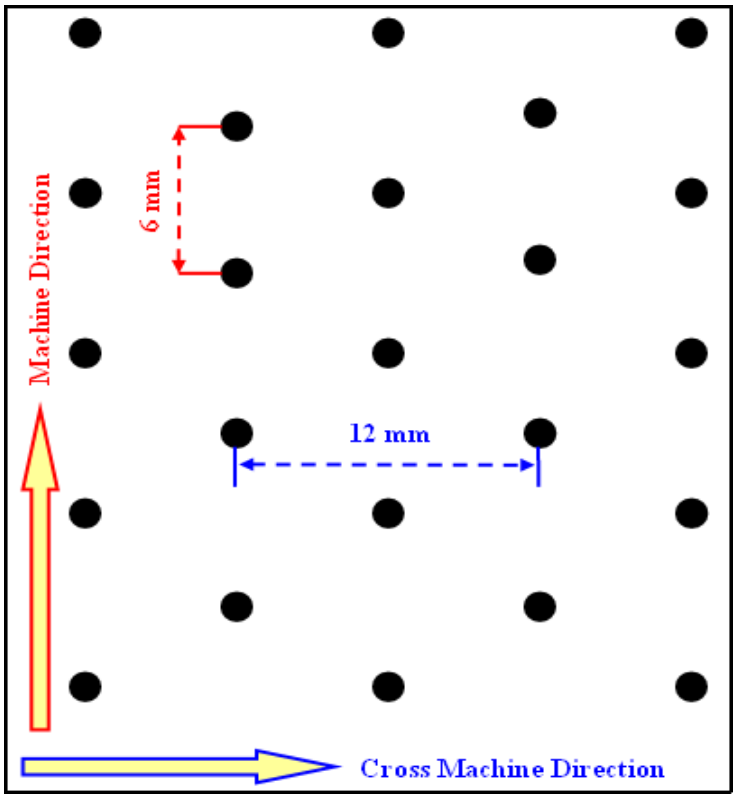

(b) *[Not to Scale]*

Figure 7.30 Sketch of the Spikes in Agru HDPE MicroSpike Structured Geomembrane
(a) Inside Face [Liner Sheet Top Face]; (b) Outside Face [Liner Sheet Bottom Face]

Figures 7.31 and 7.32 show results from interface tests performed to evaluate the influence of the microspike patterns of Agru structured geomembranes on the observed shear resistance. After the selected normal stress (400 kPa) is applied but before the shearing process is initiated, the geotextile becomes compressed and progressively interbedded between the macrotextural features (spikes) of the contacting structured geomembrane resulting in matrix level frictional interactions and interlockings. At the same time, the micro and meso texture of the base substrate become involved in supplemental interlocking interactions. Once the shearing is initiated, the micro and mesotexture present on the base of the tested geomembranes result in a counterface that provides for the supplemental interactions and interlocking in mobilizing higher peak strength gains and attaining the larger frictional resistance of peak level which is similar with that of the coextruded liners in terms of the shape of the curve.

No fluctuations were observed during pre-peak and peak stages of shear response as seen in Figure 7.31. On the other hand, the repetitive surface texture configuration of consecutive series of the spikes causes the development of oscillating post-peak interface behavior (Figure 7.31) when sheared against fibrous geotextile specimens under larger confinement which is not seen in the post-peak response of the coextruded systems.

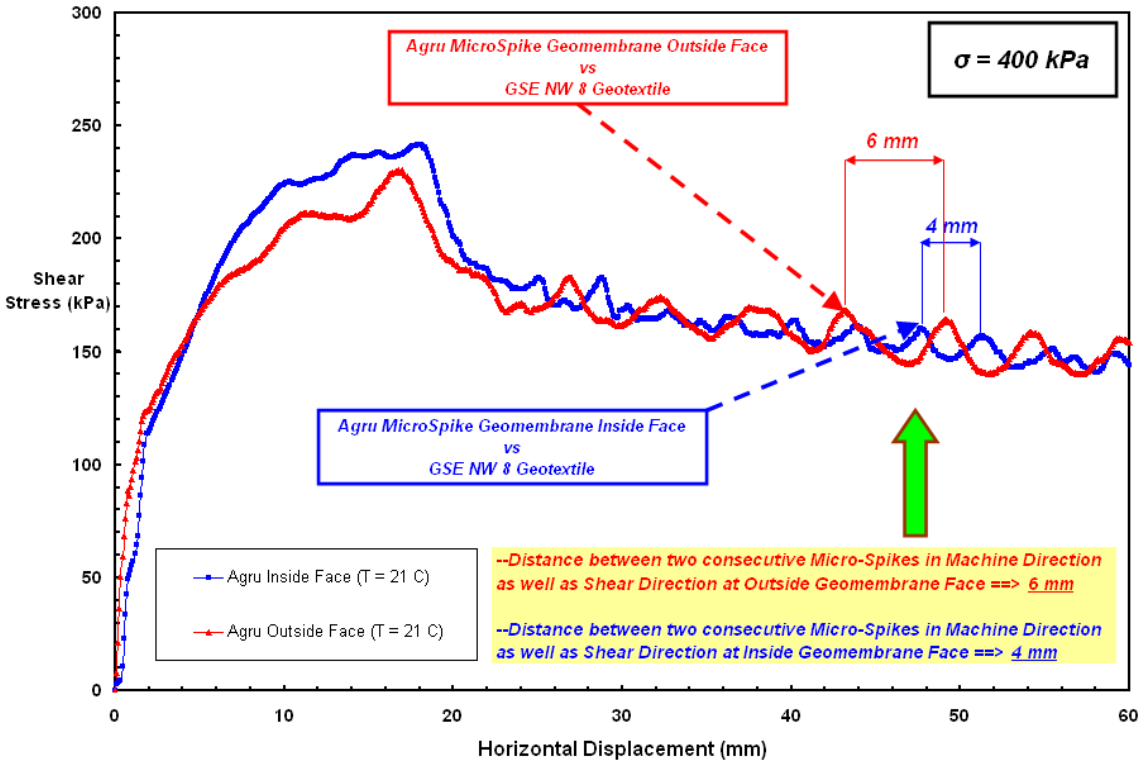

(a)

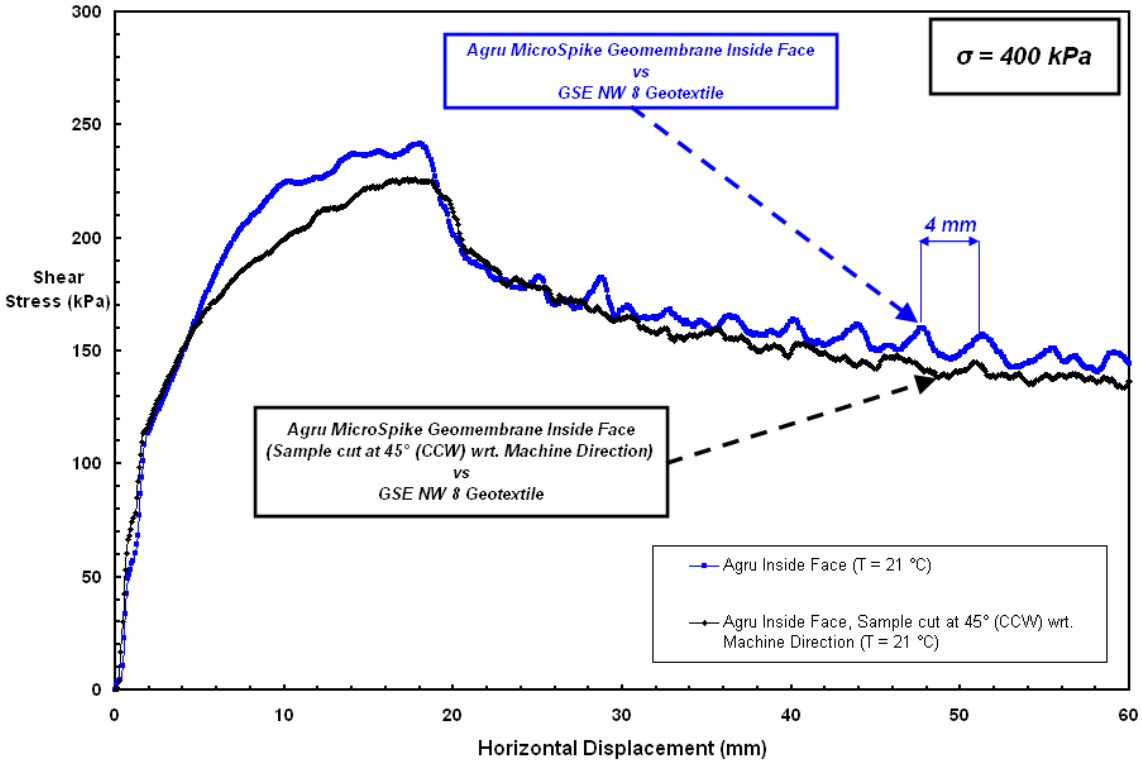

(b)

Figure 7.31 Comparison of the Interface Shear Behavior for Agru HDPE Structured Geomembrane: (a) Inside vs. Outside Face; (b) Specimens cut at Different Orientations

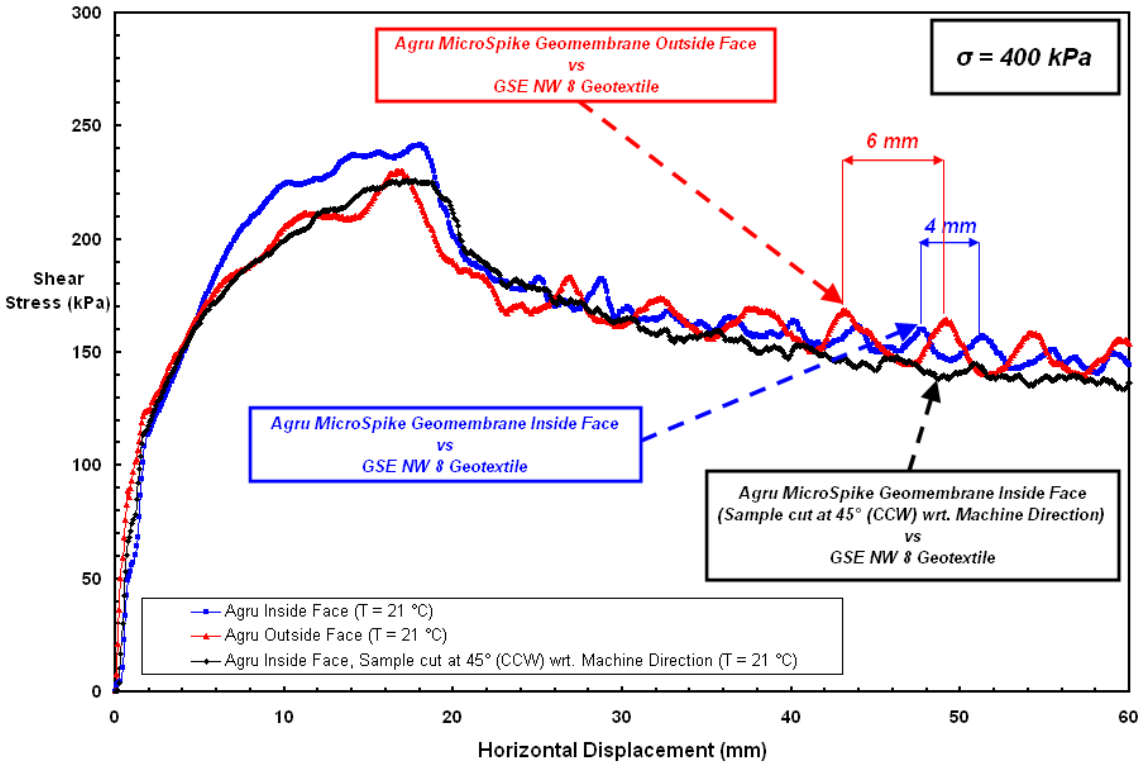

Figure 7.32 Assessment of Liner Sheet Macro-Texture Isotropy & Recurrence Properties for the Developed Response (Specimen: *Inside*; *Outside*; *Cut at Angled Orientation*)

The structured geomembrane in combination with the NPNW geotextile exhibited a continually altering (i.e. rising and falling) pseudo-sinusoidal pattern in the stress-displacement curve throughout the post-peak state. This results from the uniform surface texture scheme comprised of an ordered configuration of macro-spikes arranged in multiple consecutive rows at various spacing. Between these rows of spikes, there exist a zone of recurring micro and meso textural area on the base substrate. As Figure 7.31a presents, substantial peaks and troughs, with a period of about 6 mm, developed in the interface tests of geomembrane specimens where the *outside* face was sheared against geotextile samples. The 6 mm spacing is also the interval between two consecutive micro-spike sequences when spike elements are placed in the machine direction of

outside face of the lining sheet as shown in Figure 7.30b. Moreover, it was noted from the interface tests on the *inside* face of the liner that peaks and troughs (i.e. ups and downs) observed during the large displacement post-peak stage occurred at 4 mm which is again the size of the spacing between successive serial spike rows in the machine direction of the inside geomembrane face. On the other hand, negligible peaks and troughs (rise and fall) were observed during the pseudo-residual interface shear response of the geomembrane specimens (Figure 7.31b) which are from the *inside* face of the structured lining material oriented at 45° counter-clock-wise (CCW) with respect to shear direction. The amplitude of the oscillating patterns (i.e: fluctuations) is based on the the asperity height of spike elements integrated on the surface of the structured lining material sheet as the size of the rounded bolt-like spikes in terms of height and diameter is bigger on the *outside* face of the geomembrane compared to the *inside* face. Accordingly, as evident in the stress-displacement curves at pseudo-residual stage, the amplitude of both the peaks and the troughs generated are larger for the case of Agru *outside* surface interface shear tests in conjunction with geotextile sample in comparison to that of *inside* surface. Moreover, the results given below will implicitly demonstrate and supplement the generally accepted hypothesis that as normal stress increases from the construction to the operational stress range, the controlling behavioral mechanisms transfer from surficial to interbedded interactions and the surface topology of the textured geomembrane onsets to control the generated response model of the stress-displacement failure curve at post-peak. Further, these results aid in quantifying behavioral differences observed between geomembranes textured using different manufacturing processes

(structuring versus coextrusion), and provide macroscale mechanical insight into textured geomembrane-geotextile interaction mechanisms under higher stress levels.

To conclude, it is noted that the governing components of the evolution of the pseudo-residual shear behavior for geotextile and textured geomembrane interfaces are macro-texture isotropy, uniformity, and recurrence properties. The isotropical/ anisotropical configuration of macro-texture asperities influences the interface fricitional characteristics of the corresponding geosynthetic lining material in terms of exhibited interface shear response, in particular, during the residual state of the stress-displacement failure curves. The configuration of the spike elements on the structured geomembrane liner sheet resulted in recurrently rising and falling shear stress during the larger displacement post-peak stage.

7.9. Further Analysis and Comparison of Overall Geotextile – Geomembrane Test Results at Elevated Temperature Conditions

The strain softening properties of many geosynthetic interfaces – with an exception of smooth PVC geomembrane – NPNW geotextile as discussed earlier – means that the understanding of large strain shear strength performance is of particular importance. As indicated previously, the large strain or residual shear strength of geosyntehtic – geosynthetic interfaces are generally obtained using direct shear or ring shear device with an important distinction in between these two methods that the residual strength values attained may be different due to differences in the total horizontal displacement at which shear stress measuments are determined. In general, ring shear equipment measurements provide lower friction angle values as a result of higher disturbance of the geosynthetic specimens because of the amount of shear displacement compared to tests with direct shear devices. Therefore, the value of interface strength reduction (τ_{Peak} versus $\tau_{Residual}$) reported as a result of ring shear tests in the laboratory may be overconservative for some design purposes. The very large strains experienced during a ring shear test are likely to destroy textural features at larger amount of shear displacements.

Texturing liner material surfaces increases the interface sensitivity (Figure 7.33) compared to that obtained for smooth geomembrane liners (Figure 6.20) as a result of geomembrane surface with asperities which develops interlocking with the fibrous material filaments. Additionally, the increased interactions between texture elements and filaments were found to be the one of the dominant sources of higher shear resistances

mobilized at geotextile – coextruded textured geomembrane interfaces. The post-peak strength loss exhibited by relatively stiff HDPE textured geomembrane and NPNW geotextile interfaces at all test temperatures was fundamentally due to removal of micro-textures from geomembrane core sheet. The sensitivity (Equation 7.1) of the direct interface shear results is a useful measure to highlight the differences in the peak and psuedo-residual responses. For textured HDPE geomembrane – NPNW geotextile interfaces, the interface sensitivity, ($S\tau$) increased minimally as ambient temperature increased from 21 °C and 50 °C (Figure 7.33).

$$S\tau = \left(\frac{\tau_{Peak}}{\tau_{Residual}} \right) \tag{7.1}$$

Where;

$S\tau$: Interface Sensitivity

τ_{Peak}: Mobilized Peak Shear Strength at the Interface

$\tau_{Residual}$: Developed Residual (Post-Peak) Shear Strength at the Interface

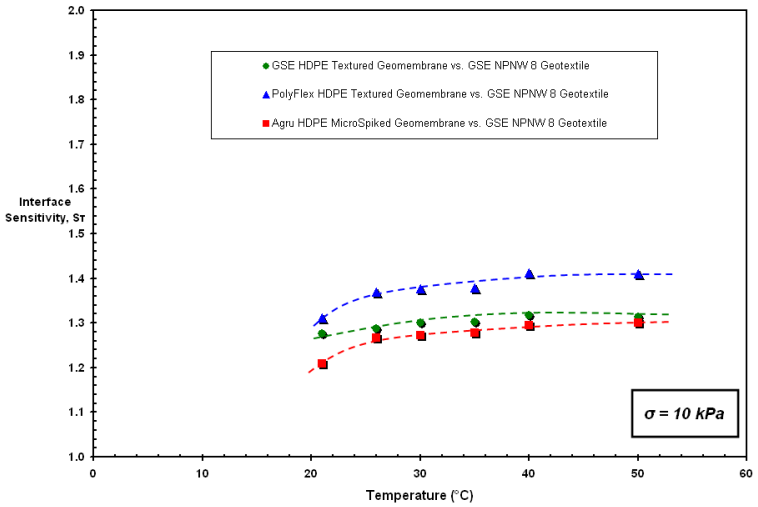

(a)

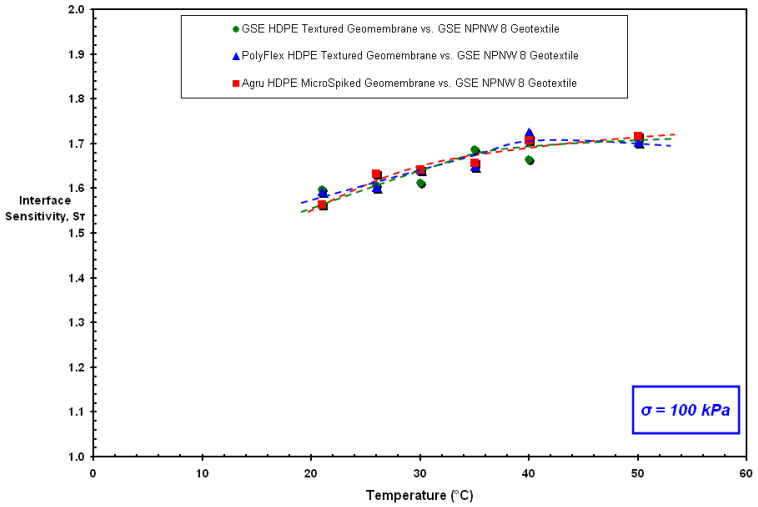

(b)

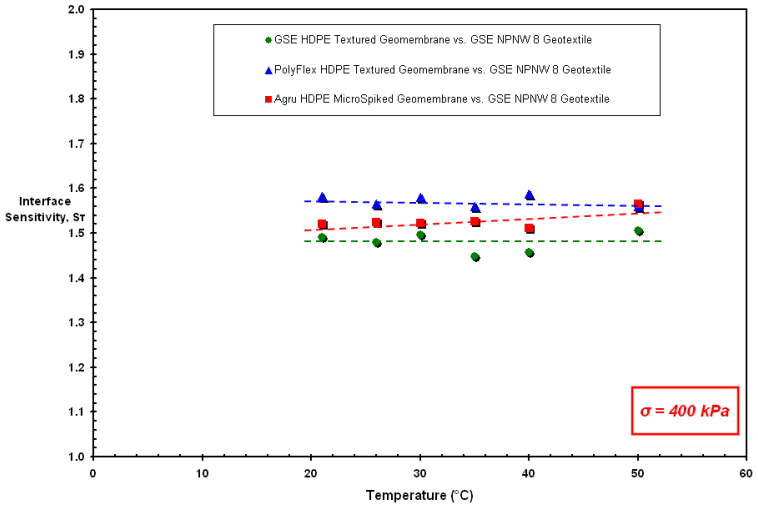

(c)

Figure 7.33 The Change in Interface Sensitivity, [Sτ] with Temperature and the Trend of the Variation for Coextruded or Structured Textured Geomembrane/NPNW Geotextile

PolyFlex HDPE coextruded textured geomembrane interface showed slightly higher interface sensitivity values than those from the interfaces of GSE coextruded and Agru structured textured geomembrane at all test temperatures ranging from 21°C to 50°C particularly for normal stress levels of 10 kPa and 400 kPa. However at 100 kPa normal stress, all the textured systems exhibited similar sensitivity values and displayed similar increases in the magnitude with temperature increase. For normal stresses of 10 kPa and 100 kPa in range of 21°C to 50°C, the value of sensitivity increased slightly with temperature from about 1.2 to 1.3 (for GSE and Agru); from 1.3 to 1.4 (for PolyFlex) and from about 1.6 to 1.7 (for all the interfaces), respectively. On the other hand, at high normal stress level (400 kPa), all the textured interfaces displayed no (for the coextruded systems, $S\tau$ values stay constant) or marginal increase (for the structured system) in the value with an increase in the temperature. The value of sensitivy was almost constant at 1.6 for PolyFlex and approximately 1.5 for GSE and Agru in ambient temperature range of 21°C to 50°C. The invariability in the resulting values of the sensitivity at 400 kPa normal stress level can be attributed to the higher confinement of the counterface materials due to greater magnitude of normal load applied on the interface during shear. In summary, with an exception of PolyFelx tested at 10 kPa normal stress, both the textured layered systems comprised of coextruded or structured geomembranes displayed similar measured maximum values of $S\tau$ at 50 °C which was the highest temperature level tested.

The magnitude of the increase in the sensitivity is more pronounced throughout test temperature range from 21°C to 50°C for the textured (coextruded or structured) geomembrane – NPNW geotextile interfaces compared to that of smooth counterparts.

This is attributed to the different shearing mechanisms mobilized at the interface during shear displacement. As such, the lesser increase in the magnitude of the interface sensitivity for the smooth counterface systems (GSE HDPE Smooth and EPI PVC Smooth), as discussed in Chapter 6, is due to the fact that the main frictional strength generating mechanism is sliding arising at the contact surface of the smooth liner – fibrous geotextile interface. Further, the global interaction mechanisms of the two distinct systems (smooth versus textured) displayed diverse interface shear behaviors (e.g. shape and progression of the stress-displacement curve) as a result of the distinctive characteristics and differences in the surface roughness properties.

The stress-displacement curves for the three textured systems (GSE, PolyFlex and Agru) at low normal stress level (10 kPa) displayed a smoother appearance (i.e. a less sharp peak stress phase). Once the peak resistance is reached, the interfaces of all the textured geomembranes experienced a lesser amount of strain softening or shear strength loss (i.e: smaller reduction in frictional resistance). The curves were generally portrayed an elastic-relatively plastic response. This is confirmed with the smaller magnitude of the interface sensitivities exhibited at low normal stress (10 kPa) compared to those at higher normal stresses (100 and 400 kPa) (Figure 7.33) throughout test temperature range (21°C to 50°C).

In order to quantify the interface strength loss occurring at different test temperature levels, a normalized quantitative parameter ($S_{[T°C/21°C]}$ = the normalized interface sensitivity) (Equation 7.2) was defined that is the ratio of peak shear stress (τ_{Peak}) to pseudo-residual stress ($\tau_{Residual}$) at an elevated temperature (26 °C – 50°C) relative to that at room temperature (21 °C). It was intended to compare the frictional

performance of the interfaces (peak strength versus residual resistance) at elevated temperatures in terms of a relative quantity for the different textured geomembranes produced through either of one of texturing methods (coextruded or structured).

$$S_{T°C/21°C} = \left(\frac{S\tau_{@°C}}{S\tau_{@21°C}} \right) \tag{7.2}$$

Where;

$S_{T°C/21°C}$: Normalized Interface Sensitivity w.r.t. Room Temperature (21 °C)

$S\tau_{@°C}$: Interface Sensitivity at T °C

$S\tau_{@21°C}$: Interface Sensitivity at 21 °C

The variations in the normalized sensitivity values as a function of temperature for all the textured systems at different normal stress levels of 10, 100 and 400 kPa are shown in Figures 7.34a, 7.34b and 7.34c, respectively.

At low normal stress level (10 kPa), the resulted values at same ambient test temperatures were comparable and the variational trend is similar for both PolyFlex coextruded and Agru structured textured geomembrane interfaces. Additionally, the normalized sensitivity increased from 1.00 to 1.08 with increasing temperature from 21°C up to 50°C. However, GSE coextruded textured geomembrane interface displayed lesser amount of increase (i.e. lowest variability) in the value from 1.00 to 1.03 with a smaller rate per unit temperature increment in the resultant normalized value. In the case of 100 kPa normal stress level, all the textured systems exhibited an increase in the

normalized sensitivity. It is notable that PolyFlex coextruded (from 1.00 to 1.07) and Agru microspiked (from 1.00 to 1.10) geomembrane interfaces showed a linear increase in the value for the normalized sensitivity up to the elevated temperature of 40°C whereas these values stayed constant beyond 40°C until the highest test temperature level (50°C). On the other hand, GSE textured system displayed the least variation in the normalized values of the sensitivity and depicted a consistent linear increasing trend from room temperature (21°C) up to the highest elevated temperature level (50°C). For all the textured interfaces, similar normalized sensitivity trends were observed for high normal stress level of 400 kPa and the normalized sensitivity stayed almost constant at around the value of 1.00 in temperature range from 21°C to 50°C with an exception that only Agru structured geomembrane showed a marginal change (slight increase) in the normalized value. Consequently, it is noted that at high normal stress level (400 kPa), all the textured geomembranes irrespective of texturing method (coextruded or structured) displayed similar degrees of change with elevated temperatures (≤ 50°C) in the magnitude of the sensitivity as normalized with respect to room temperature (21°C). This shows that a similar strain softening response occurred at the interface of the three textured geomembranes when sheared in conjunction with NPNW-PP geotextiles at 400 kPa high normal stress.

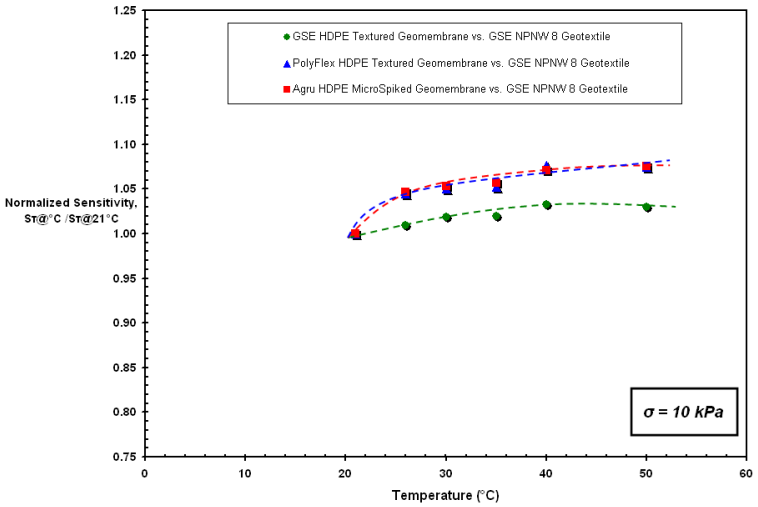

(a)

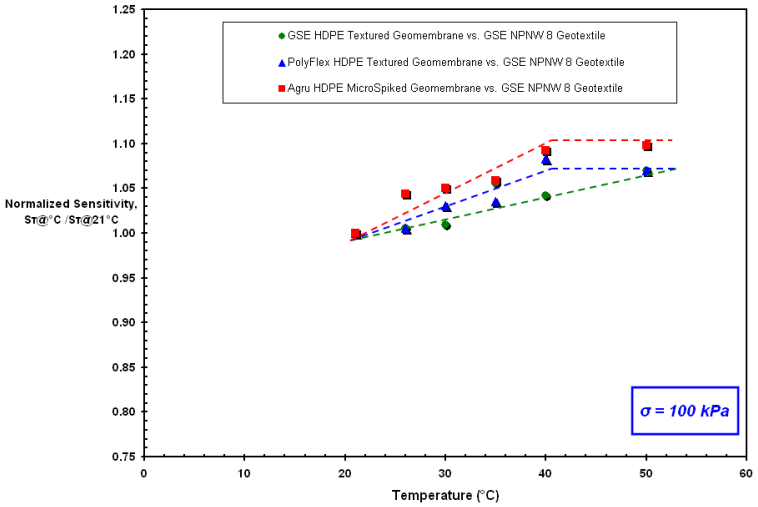

(b)

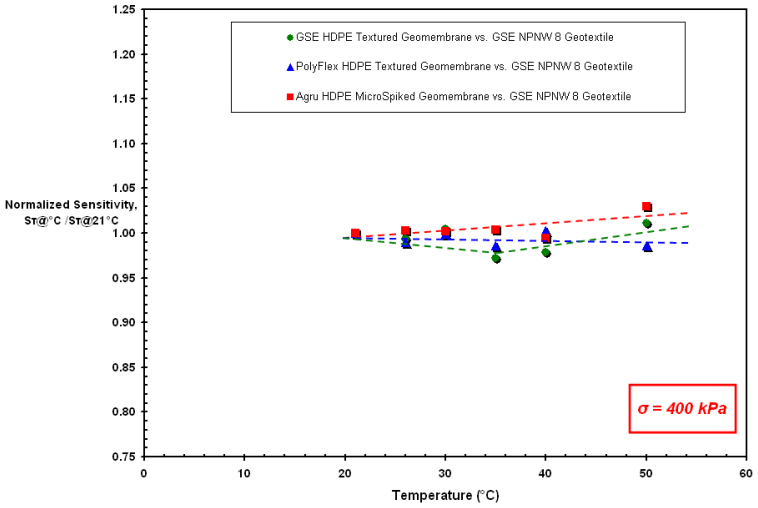

(c)

Figure 7.34 Normalized Interface Sensitivity versus Temperature for Coextruded or Structured Textured Geomembrane/NPNW Geotextile Interfaces: 10, 100 and 400 kPa

Comparing the two textured systems (coextruded and structured), a slight difference in the sensitivity values computed for different test temperatures as well as a very minor difference in the slope of the trend as a function of temperature resulted from differences in the peak behavior since the pseudo-residual behaviors were similar due to their dependence on the same geotextile and macro roughness properties. It follows logically that the increase in sensitivity with ambient temperature level between 21 and 50 °C at different normal stresses for the structured material system generally exceeded that of the coextruded system as noted above by the peak strength behavior differences.

7.10. Replicate Interface Shear Tests at Various Test Temperatures

Figures 7.35 and 7.36 show typical replicate interface direct shear tests performed on textured geomembrane–geotextile interfaces at two different temperatures. Virgin geomembrane and geotextile specimens were used in each test of the primary testing sequence. The normal stress was applied pneumatically and the same shear displacement rate was used throughout the entire series of the testing program. Further, the test specimen preparation and placement procedures as well as conditioning on the test apparatus, the force and shearing displacement application were all consistent.

To conclude, the attained results demonstrated a good repeatability achieved at different conditions involving various ambient test temperature level and various counterface material combinations.

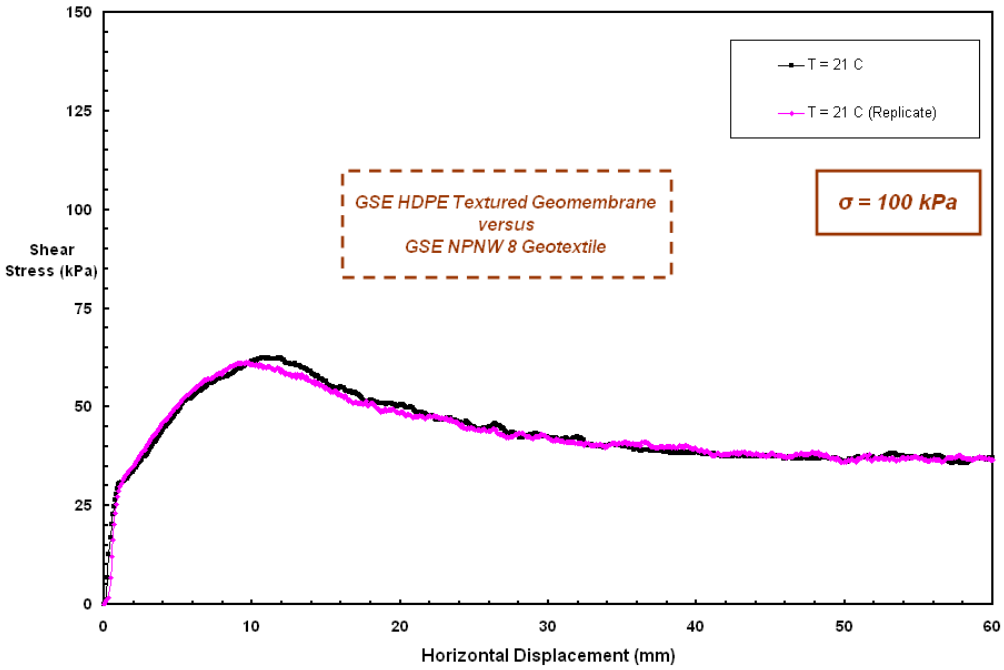

(a)

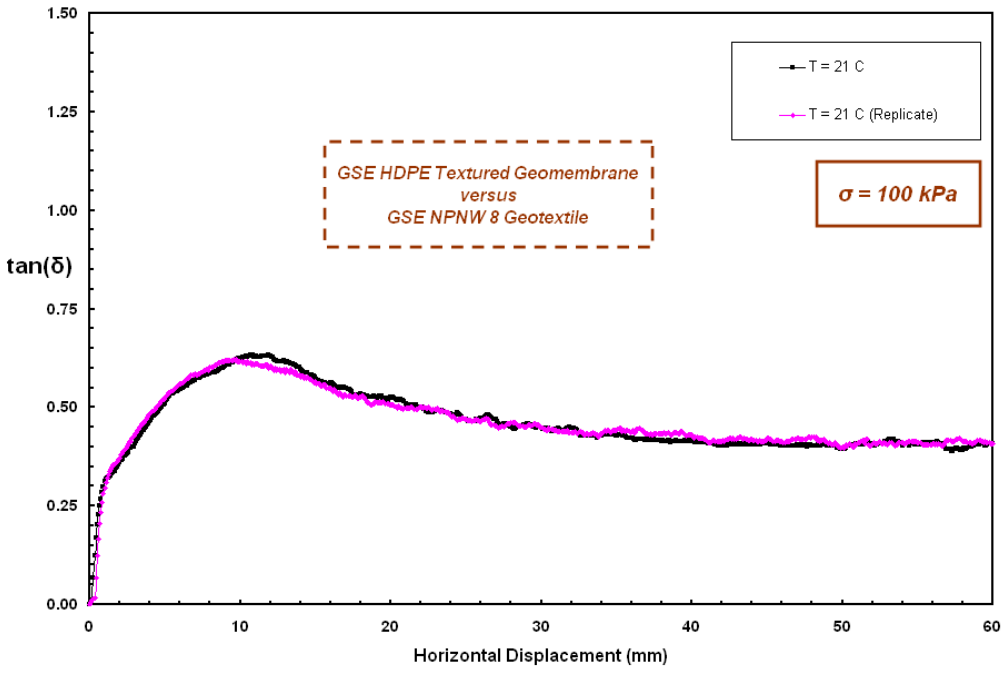

(b)

Figure 7.35 Replicate Interface Shear Tests on GSE HDPE Textured Geomembrane versus GSE NPNW Geotextile Interface at Room Temperature (T = 21 °C)

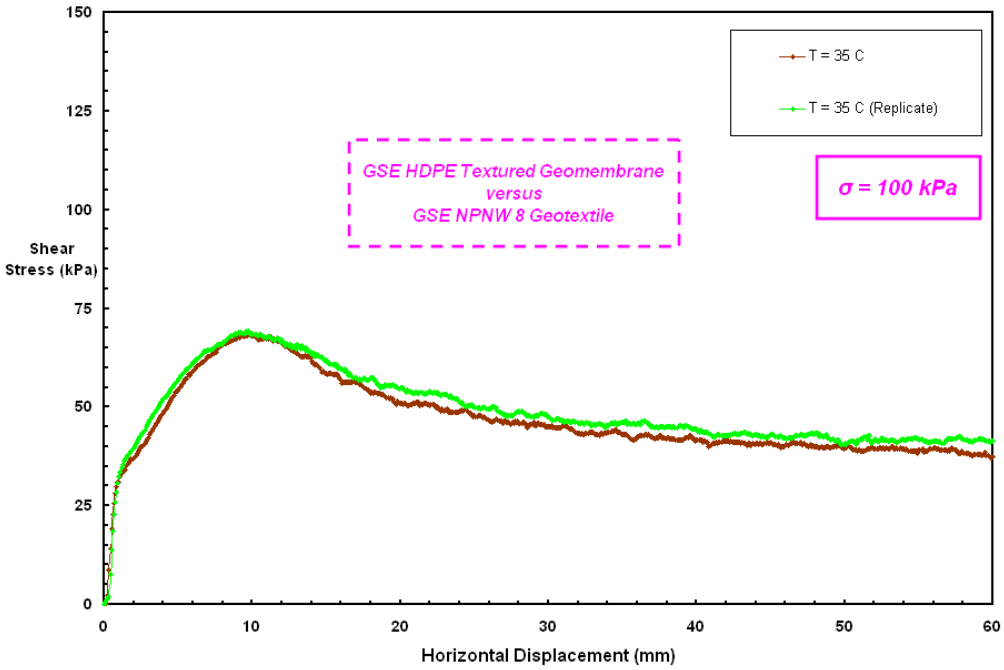

(a)

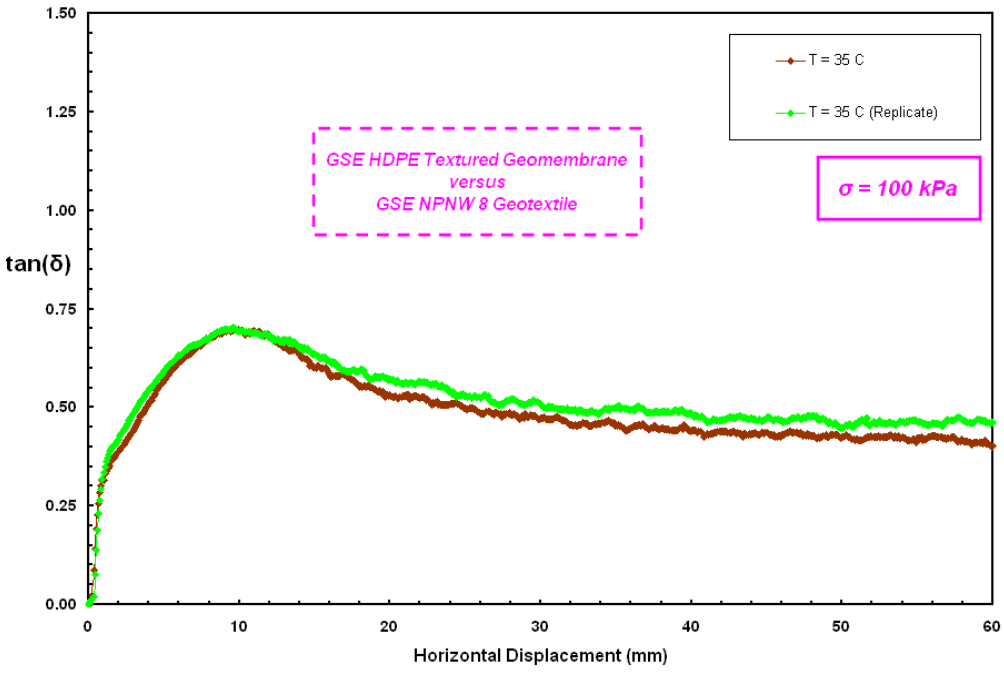

(b)

Figure 7.36 Replicate Interface Shear Tests on GSE HDPE Textured Geomembrane versus GSE NPNW Geotextile Interface at an Elevated Temperature (T = 35 °C)

7.11. Summary and Conclusions

This chapter presented the findings of multiple series of interface shear shear tests performed on textured (coextruded and structured) geomembrane – nonwoven geotextile interfaces at various test temperatures to examine and quantitatively illustrate the influence of elevated temperatures on the different geosynthetic material combinations having dissimilar lining sheet surface characteristics (i.e. the impact of roughness and texturing method) and possessing different sheet base material properties. Moreover, further evaluations of these experimental findings were presented by providing derived quantitative shear strength parameters and their variation with an increase in temperature. The observed changes in the shear strength properties with temperature as well as the assessment of test results at elevated temperatures with compared to those measured values at room temperature demonstrate how interface shear behavior of geotextile – textured geomembrane interfaces changes with temperature.

Variations in the experimental program were temperature (21°C, 26°C, 30°C, 35°C, 40°C and 50°C) and geomembrane texturing method (coextrusion, structuring). It should be noted that, to date, since most geosynthetic interface testing has been performed at room temperature (21 °C) in the laboratory environment, elevated temperatures up to 50°C with 5°C increments between each test temperature level were found appropriate for implementing multiple test series to evaluate frictional resistance and response of the different textured systems through direct shear tests. As the same geotextile type (NPNW) were used throughout the testing program, the observed behavioral differences can be attributed to the differences in the surface roughness features of the tested geomembranes.

CHAPTER VIII

8. ELEVATED TEMPERATURE EFFECTS ON SAND – *SMOOTH* GEOMEMBRANE INTERFACE SHEAR BEHAVIOR

8.1. Introduction

The design and development of geotechnical systems (i.e: composite structural systems) where soil (i.e. sand) is in contact with construction materials such as concrete, steel, or polymer (i.e. geosynthetics) is widespread. As such, particulate versus continuum interfaces (e.g. soil-geomembrane, soil-geotextile, soil-concrete, and soil-steel) governs the behavior of many geotechnical structures including deep foundations, synthetic impervious liners, trenchless technologies, and an assortment of earth retaining structures. The resisting forces at soil versus these construction material interfaces are mobilized due to relative movements between counterface materials (Dove, 1996).

Numerous man-made *polymer-based* construction materials such as geomembranes are being routinely used in conjunction with soils in various geotechnical applications and the demand for such composite soil–synthetic material systems is continuously increasing. The placement of these dis-similar materials adjacent to one another creates interfaces which can lead to relatively weak shear strengths compared to the frictional strength of the soil mass itself. One issue which has not been extensively studied to date is how increases in temperature effect interface behavior between granular materials and geomembranes. To this end, an experimental research study including multiple series of laboratory interface tests at various temperatures ranging from 21 °C up to 50 °C between different particulate materials (rounded, angular sands) and smooth

geomembranes produced from different base polymer resins (HDPE, PVC) was performed. This chapter will present the findings of this study along with a broad comparison between the test results of diverse composite layered systems involving the effect of elevated temperature, sand grain shape (i.e. particle angularity), and geomembrane base material type in terms of lining material surface hardness on the developed interface shear behavior and strength. Further, the interface direct shear test results will be examined in context of surface roughness changes on the post-test geomembrane specimens tested at different ambient temperatures as well as continuum material hardness measurements at the corresponding test temperatures measured using a durometer.

8.2. Temperature Effects on *Rounded* Particulate – Smooth *HDPE* Continuum Material Layered Systems

8.2.1. Ottawa 20-30 Rounded Sand/HDPE Smooth Geomembrane Interfaces

Shear stress-horizontal displacement plots at various temperatures and loading conditions for Ottawa 20/30 sand sheared against smooth geomembranes are presented in Figure 8.1. Interface shear tests were performed at normal stress levels of 25 kPa, 100 kPa and 400 kPa. The stress – displacement curves over test a temperature range from 21 °C up to 50 °C resulted in an initial rise in strength that is followed by a moderate decrease to an essentially constant value once the peak strength is mobilized in an elastic-perfectly plastic response. This experimental evidence demonstrates and supports the

earlier theoretical analyses that the shear mechanisms for rounded granular material–smooth geomembrane interfaces are elastic-plastic sliding.

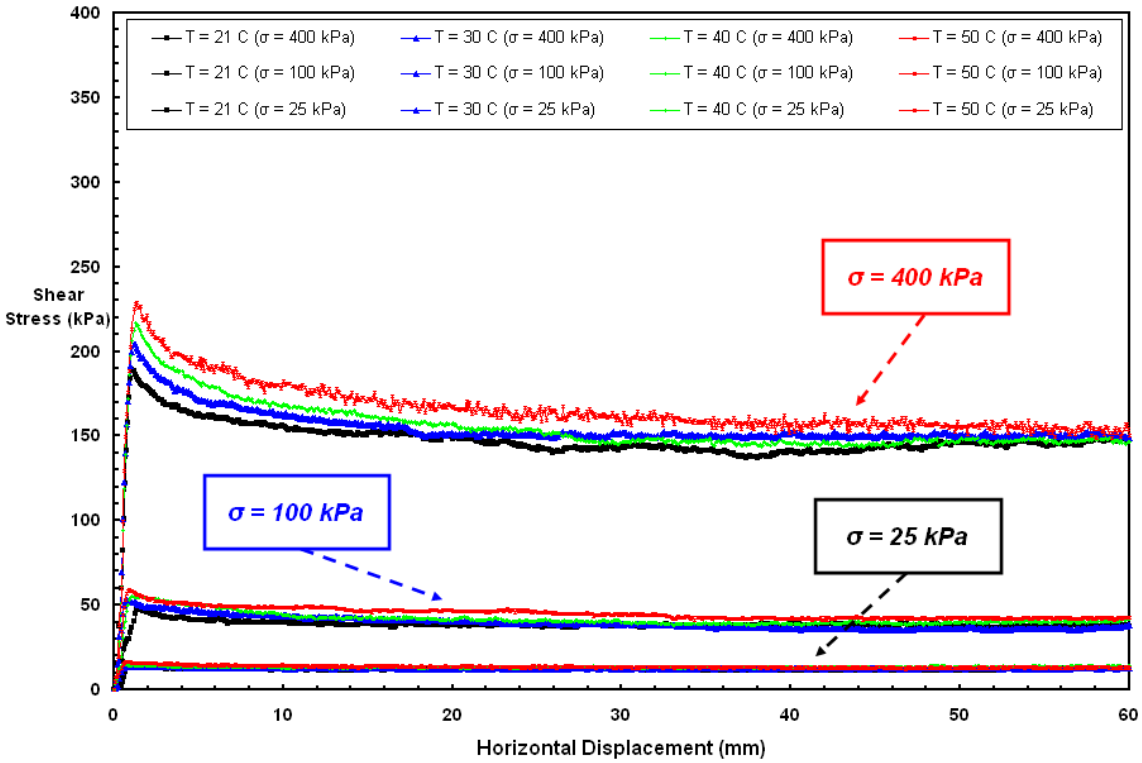

Figure 8.1 Shear Stress–Displacement Curves at Different Loading Conditions; & at Various Test Temperatures for Ottawa 20-30 Sand/GSE Smooth HDPE Geomembrane

The tests at higher normal stress levels (100 kPa, 400 kPa) resulted in much more ductile stress versus displacement curves where the peak occurs at larger horizontal displacements than that observed at low normal loading condition (25 kPa). The Ottawa 20/30 sand and smooth HDPE geomembrane interface system reached peak strength conditions after approximately 0.5 mm, 1 mm, and 2 mm of displacement at 25 kPa, 100 kPa, and 400 kPa (Figures 8.2a, 8.2b and 8.2c) normal stresses, respectively. Most post-peak strength loss preceeded continuous plastic deformation at relatively constant pseudo-residual frictional resistance until the test was terminated at 60 mm displacement.

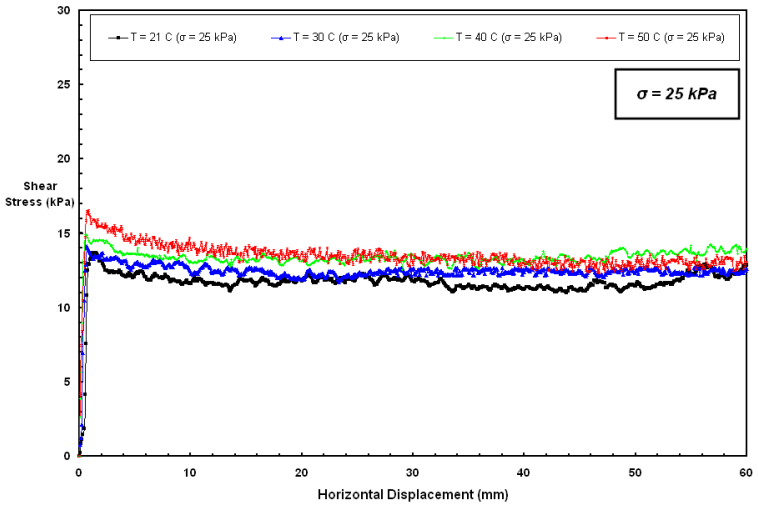

(a)

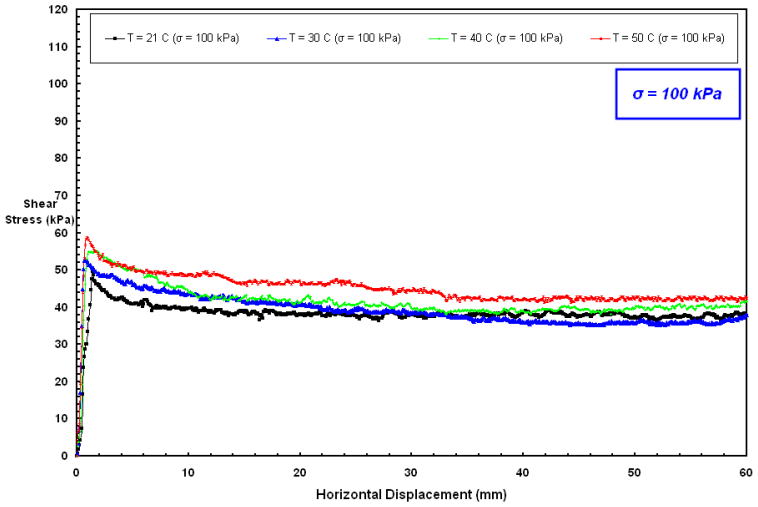

(b)

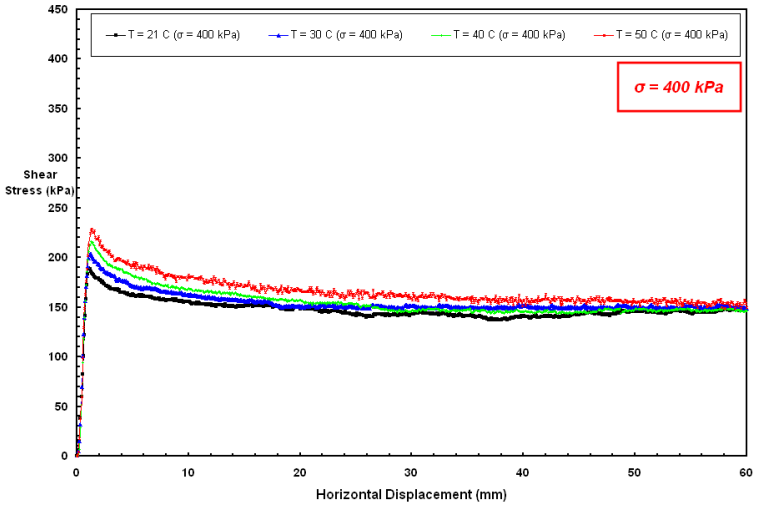

(c)

Figure 8.2 Shear Stress – Displacement Curves at Different Temperatures for Ottawa 20-30 Sand/GSE Smooth HDPE Geomembrane: 25, 100 and 400 kPa

In summary, the shear stress-displacement curves for the tests at different temperatures were all similar in terms of the developed shape of the shear stress–displacement failure envelopes. Therefore, it can be concluded that the only factor which matters in terms of force – deformation behavior of the Ottawa 20/30 rounded sand and smooth HDPE geomembrane interfaces is the temperature at which the interface tests were performed.

The surface topography of the manmade surface was quantitatively linked by Dove and Frost (1999) to the stress and volume change behavior of the interface systems for the development of insightful interface behavior models in which the two general end-member conditions for the behavior of interfaces between soil and a man-made construction material were defined. The first condition was when the size of soil grains was large with respect to the asperity height and spacing on the construction material surface (e.g. a sand grain contacting a smooth geomembrane). Experimental results for dense sand specimens against smooth geomembranes from Dove and Frost (1999) indicated that soil volume changes were small and the soil above the interface did not participate in the shear process. These interface systems were referred to as nondilative. Further, it was showed that peak strength of nondilative interface systems was controlled by particle contact conditions which, in turn, are principally controlled by *material hardness* and *surface roughness* of the bodies at the scale of the contact. This steady-state behavior is controlled by an abrasion mechanism (i.e. plowing). Moreover, in Dove and Frost (1999), the second end member condition was defined as the situation in which the particle sizes are small with respect to the surface asperities on the manmade material (e.g. textured geomembrane). In the case of sand grains against a rough geomembrane,

there occurs significant volume changes and interface strength can reach frictional resistance levels as great as, or greater than the soil internal shear strength. These interface systems were referred to as dilative. Additionally, it is evident that it is possible to observe the occurrence of an infinite number of states between the nondilative and dilative conditions at particulate – continua contact surfaces. In light of the discussion provided herein, the variation in vertical displacement at the interface is plotted against horizontal displacement for normal stress levels of 25, 100 and 400 kPa (Figure 8.3a, 8.3b and 8.3c, respectively) and shows that the rounded particulate – continua interface exhibited less contraction as shearing progresses with increasing ambient temperature due to the mobilization of increased frictional shear strength at the interface. This is due to the larger resistance of the counterface material against the sand particles during the course of shearing in the tests at higher temperature with a greater contribution of the plowing effect (i.e. sand grains in the interface penetrate deeper into the surface of the softened geomembrane at higher temperatures) to the mobilized mechanism at the interface during shear. The sand specimen experienced a relative volumetric expansion compared to that at lower test temperature levels to overcome the greater shear resistance of the counterface geomembrane liner at elevated temperatures due to occurrence of deeper plowing of the grains during shear displacement. In addition, a relative volumetric contraction compared to that at low normal stresses is exhibited at higher normal stress levels as a result of the higher confinement of the interface.

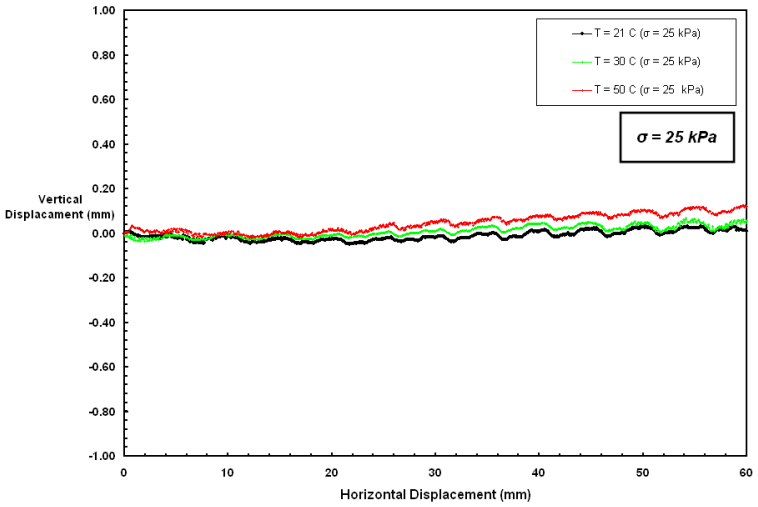

(a)

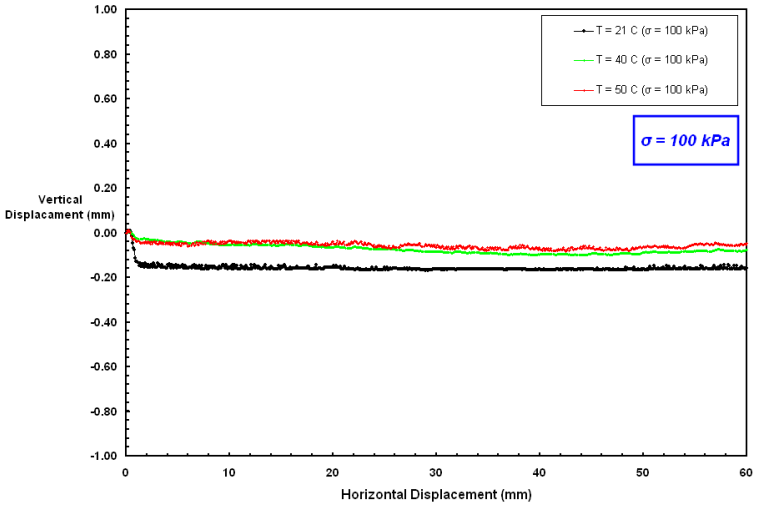

(b)

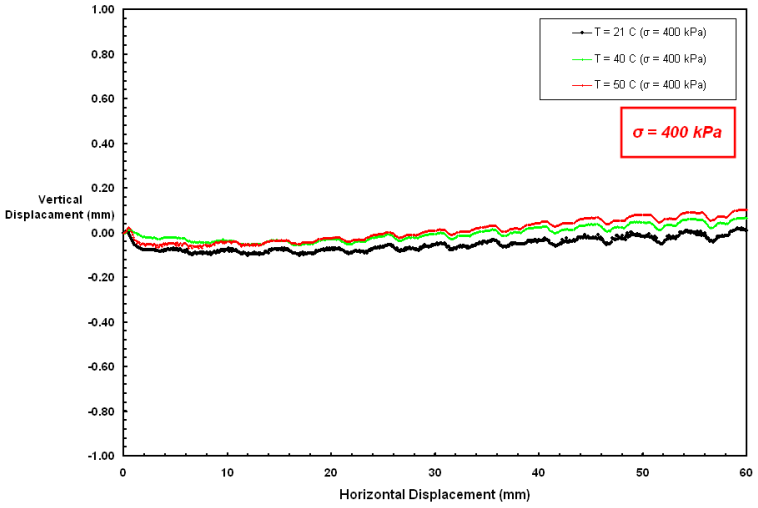

(c)

Figure 8.3 Vertical Displacement – Horizontal Displacement Behavior at Different Temperatures for Ottawa 20-30 Sand/Smooth HDPE Geomembrane: 25, 100 and 400 kPa

The resulting vertical displacement during shearing initially decreased slightly to a near constant value as the horizontal displacement reached the residual state, and later, maintained a relatively constant volumetric contraction with minor variations particularly for higher normal stresses (100 and 400 kPa). The direct shear tests at higher temperatures exhibited a lesser amount of contraction. Two compensating effects occur simultaneously during shear displacement. The sand specimen tends to dilate in order to generate a larger internal frictional strength due to the increased shear resistance mobilized at the interface resulting from the deeper sand particle penetration. At the same time, the sand specimen is subject to volumetric contraction due to increased confinement effect of loading.

The variation in δ and tan(δ) with respect to increase in temperature are shown in Figures 8.4 and 8.5, respectively. The values of these engineering properties increased over the temperature range (21 °C – 50 °C) at which the interface direct shear tests were performed. The polymeric geomembrane liner sheet becomes softer and shows less surface resistance. The sand grains can penetrate into and plow along the geomembrane surface during the course of shearing displacement with less energy than at cooler temperature conditions. At higher normal stress levels (e.g. 400 kPa), sand particles were less capable of sliding or rolling over each other. The dilation in the sand structure was partially prevented due to compressing and contracting impact of the larger loading conditions applied on the sand specimen. On the contrary, the sand structure dilated which resulted in the development of higher frictional resistances and obtaining greater magnitude of the interface strength values in terms of δ and tan(δ) at lower normal stresses (e.g.. 25 kPa).

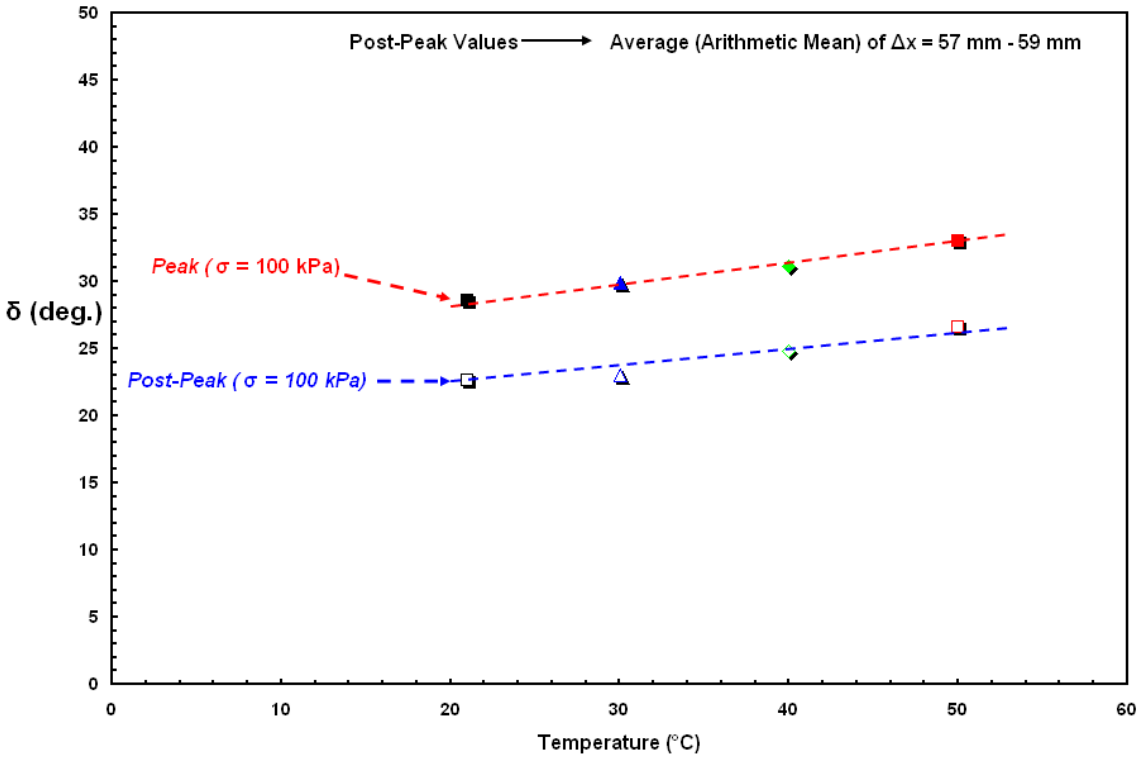

Figure 8.4 The Change in Interface Friction Angle, [δ] with Temperature for Ottawa 20-30 Sand/GSE Smooth HDPE Geomembrane Interface

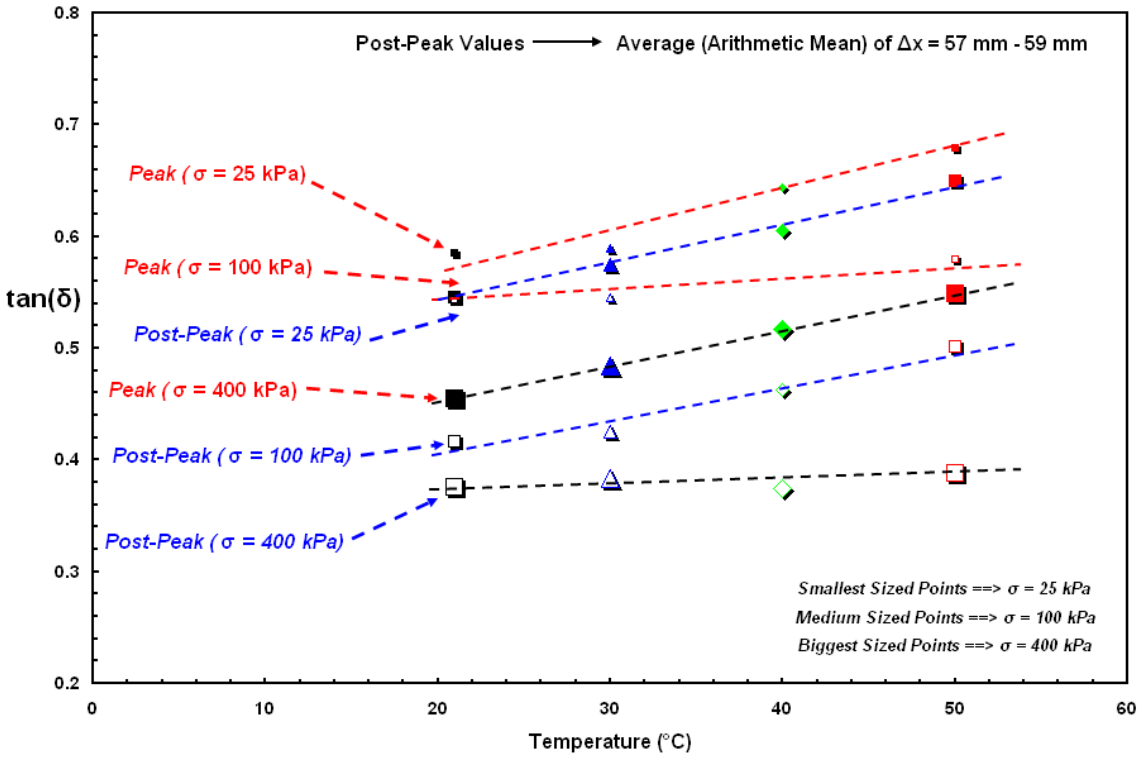

Figure 8.5 The Change in Coefficient of Friction, [tan(δ)] with Temperature at Different Loading Conditions for Ottawa 20-30 Sand/GSE Smooth HDPE Geomembrane Interface

It should also be emphasized that a greater mechanical interaction between individual soil grains at high loading conditions (≥ ~600 kPa) is likely to cause the occurrence of sand particle crushing, or at least the mobilization of fractures and the development of cracks on sand grains which leads to a relative loss of internal frictional strength between the grains in the sand structure. This may result in difference in the interface shear resistance mobilized at the interface between sand and geomembrane.

8.2.2. Failure Envelopes and Comparison of Results at Different Normal Stress Levels

Figure 8.6 presents the Mohr-Coulomb failure envelopes from interface shear test data sets at different loading conditions. The plot demonstrates the changes in the inclination and slope of these envelopes for the interface tests performed at elevated temperatures. Further, the shear strength values were also drawn on log-log scale (Figure 8.7) to illustrate the overall pattern over the entire normal stress range as well as the alternations and transformations at low or high normal stress levels.

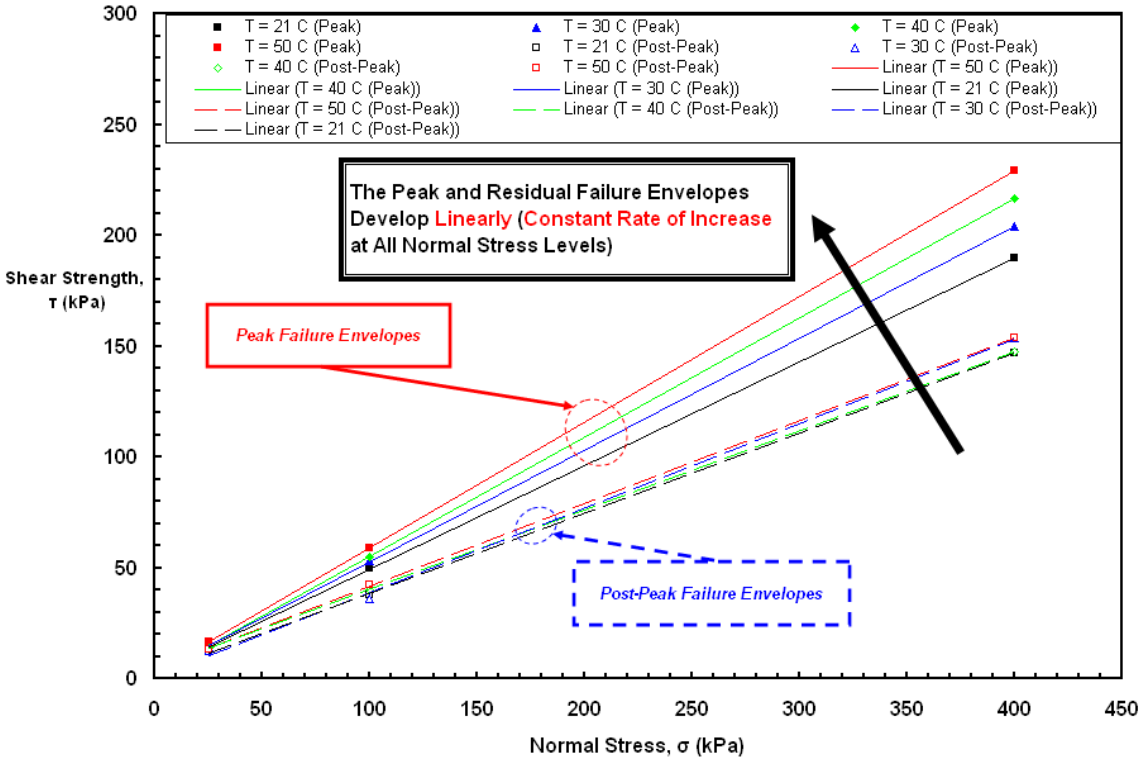

Figure 8.6 The Alteration of Peak and Residual Strength Envelopes with Increasing Temperature for Ottawa 20-30 Sand/GSE Smooth HDPE Geomembrane Interfaces

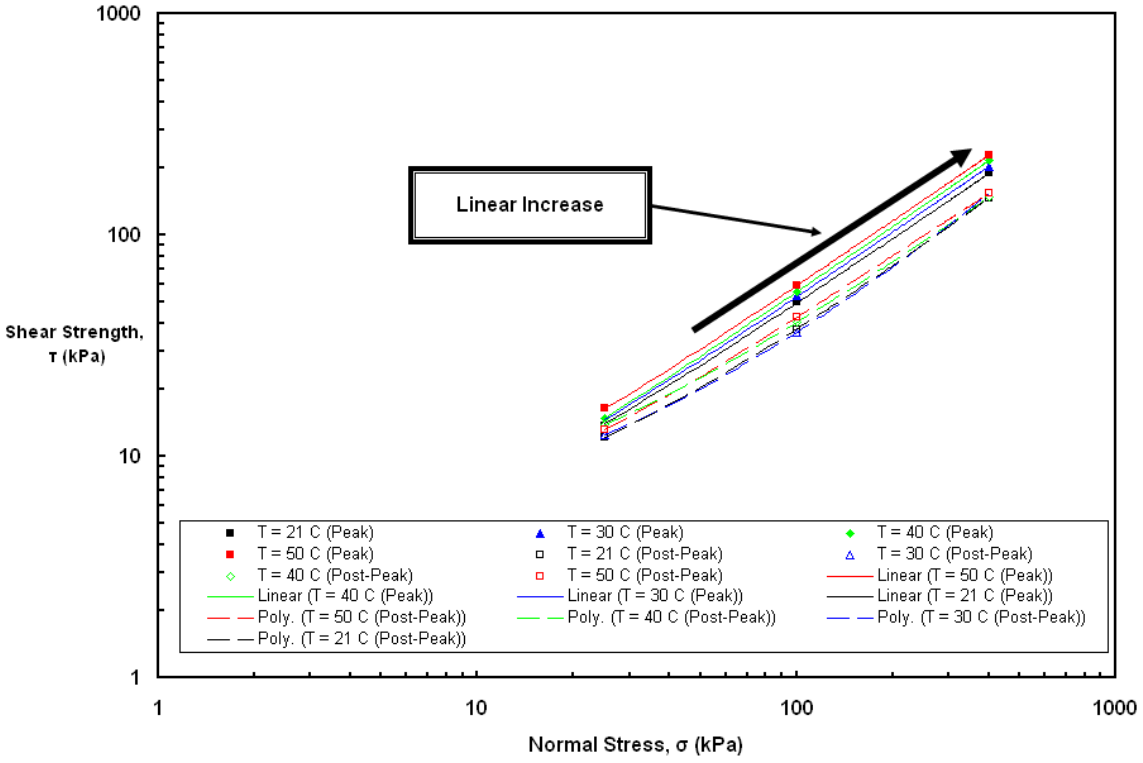

Figure 8.7 The Transformation in Failure Envelopes with Temperature at Different Loading Conditions for Ottawa 20-30 Sand/GSE Smooth HDPE Geomembrane Interface

It is noted that the 25 kPa normal stress level was selected to represent the condition where a 0.5–1.5 m thick layer of sand is placed on landfill liners as a protective cover against construction damage and ultraviolet light. The sliding stability of this soil cover is important in the design and construction of landfill liner systems.

8.3. Temperature Effects on *Angular* Particulate – Smooth *HDPE* Continuum Material Layered Systems

8.3.1. Uniblast Angular Blasting Sand/HDPE Smooth Geomembrane Interfaces

Figure 8.8 shows the shear stress-horizontal displacement behavior of the interface for Uniblast blasting angular sand sheared against smooth HDPE geomembranes over a range of normal loads as well as at different test temperature conditions. For all of the stress-displacement curves, a peak shear stress followed by a reduction to a steady state shear stress, which is a general characteristic of drained tests on dilatant particulate specimens, was observed over the entire test temperature range. The angular blasting sand exhibited higher shear strengths compared to rounded Ottawa 20-30 sand regardless of ambient temperature at which the interface was tested. This is reasonable and anticipated as the angular sand particles were more interlocked; and thus, more resistant to shear than were the rounded particles. Additionally, the angular sand grains were able to indent further and plow deeper into the lining sheet surface at all test temperatures. This was manifested as an increase in frictional resistance at the interface although resulted in more abrasion on the geomembrane liner. Therefore, one can

conclude that based on the experimental results, the shear mechanism for angular granular material versus smooth HDPE geomembrane interfaces over the ambient test temperature ranging from 21 °C up to 50 °C is dominated by plastic plowing with insignificant/very minor elastic sliding. Further, the stress-displacement curves of the different test temperatures for the angular sand versus smooth HDPE geomembrane exhibited a more well-defined peak as compared to the rounded sand case. Additionally, the residual state developed at greater shear displacement.

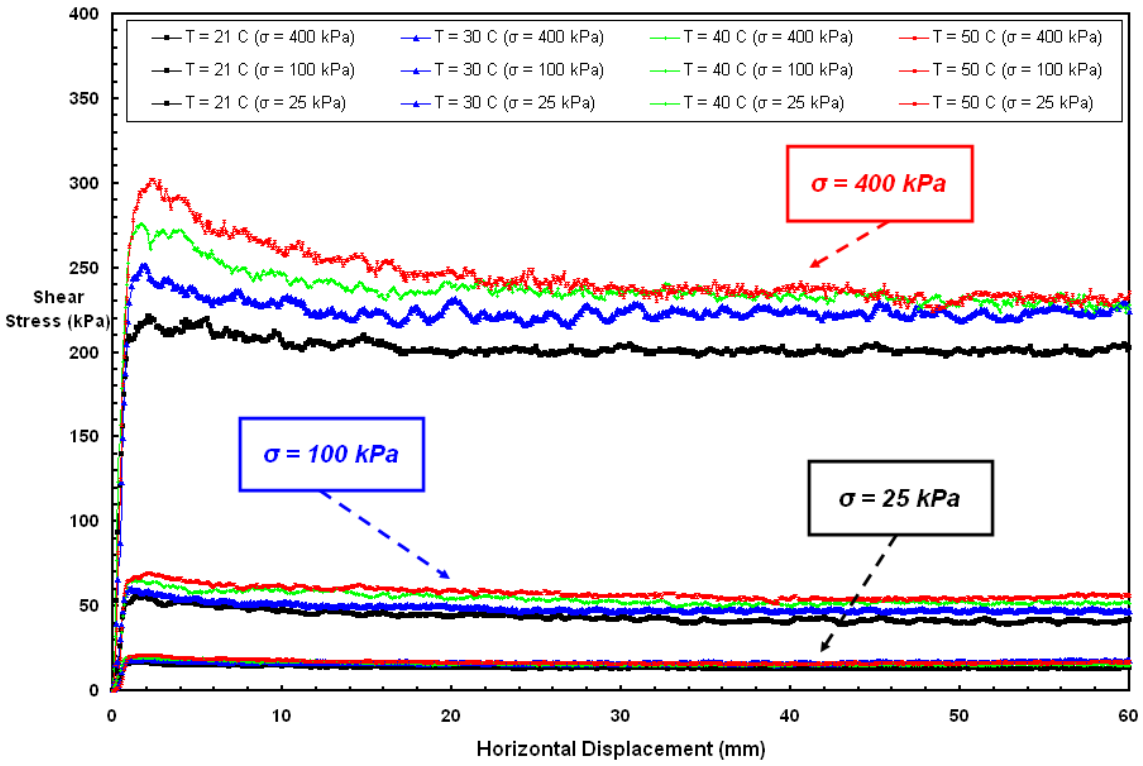

Figure 8.8 Shear Stress–Displacement Curves at Different Loading Conditions; & at Various Test Temperatures for Blasting Sand/GSE Smooth HDPE Geomembrane

The stress versus displacement failure behaviour of the angular blasting sand sheared against smooth HDPE geomembrane liner is similar to that of the textured HDPE geomembrane sheared against NPNW-PP geotextile in terms of having a well-defined

peak strength state. There is a more gradual slight loss in shear strength when the curve passes through the peak stage for the case of angular sand versus smooth liner system. As such the shape of the shear stress versus displacement curve did not follow the same strain softening behavior.

The initial steep rise in shear stress over a small horizontal displacement range of 1-3 mm is followed by a minor decrease to a near constant residual shear stress value at larger displacement for low normal stress level (25 kPa) (Figure 8.9a). However, the degree of post-peak strength loss or the amount of reduction in frictional resistance after peak stage gets larger at higher normal stresses (100 kPa, 400 kPa) (Figures 8.9b and 8.9c, respectively). The mobilized frictional resistance values in terms of the generated shear stresses at pseudo-residual state are similarly equivalent or at least comparable to those developed at peak level; so, after an initial rise in shear stress and the peak strength is mobilized, the value remain approximately constant in an almost perfectly plastic manner particularly for 25 kPa normal stress condition. Therefore, it is indicated that a less pronounced peak strength state were observed at all temperatures tested for the case of low normal stress level (25 kPa) compared to those observed at higher stress conditions (100 and 400 kPa).

It is noted that the angularity/roundedness of soil grains as well as the relative hardness of counterface materials for which the surface hardness of polymeric lining sheets depends are strongly related to the temperature level. Therefore, the use of a more angular soil as an interface material in contact with smooth HDPE geomembranes at elevated temperature field conditions increases the capacity and performance of the lining sheet in terms of the mobilized frictional shear strength.

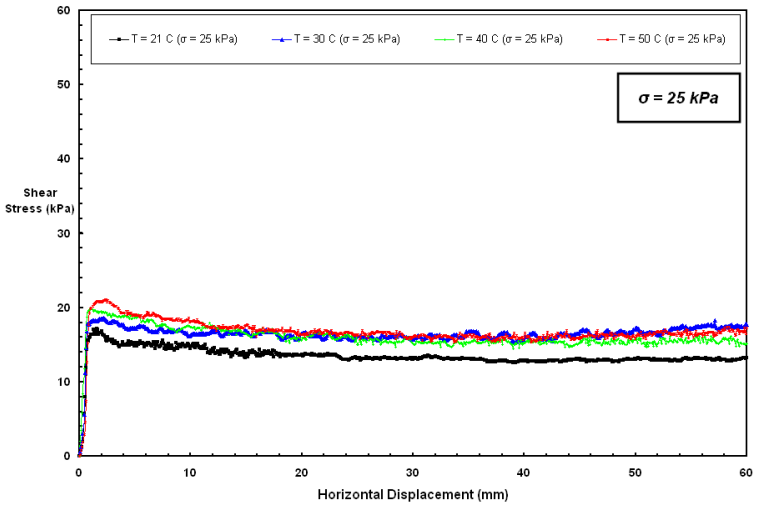

(a)

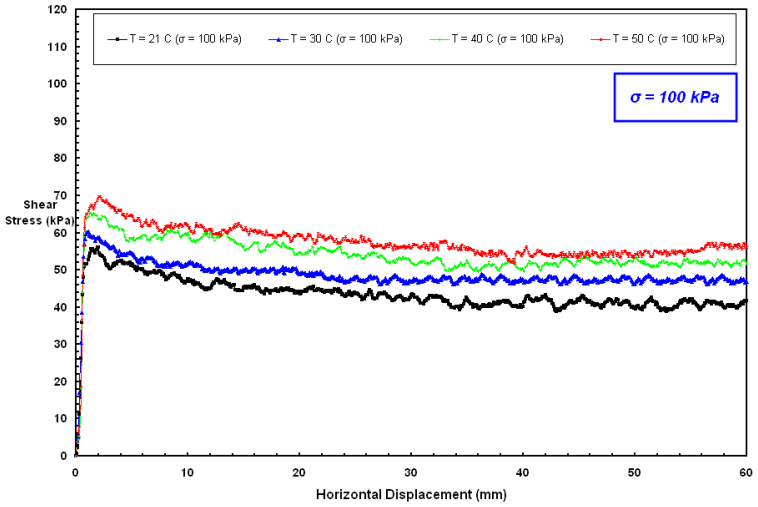

(b)

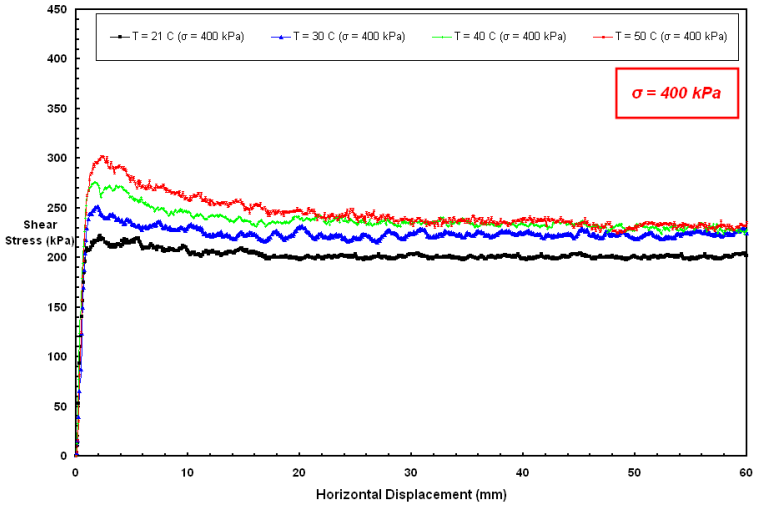

(c)

Figure 8.9 Shear Stress–Displacement Curves at Various Test Temperatures for Blasting Sand/GSE Smooth HDPE Geomembrane: 25, 100 and 400 kPa

The magnitude of the initial peak stresses are higher than the peaks observed in the rounded sands; while, the large strain (i.e. shear displacement) peak values are significantly larger than the case of rounded soil which can favorably contribute to the long term and greater shear resistance as might be appropriate for the case of larger relative displacements and dislocations developed at the interface due to catastrophic events such as earthquakes. Finally, it is noted that residual stresses were achieved for all the interface tests, although at low normal stresses (25 kPa), the decrease in strength from peak to the residual state was often less pronounced than that observed at higher normal stresses (100 and 400 kPa).

The vertical displacement – horizontal displacement behavior of Blasting Sand – smooth HDPE geomembrane interfaces at different temperatures ranging from 21°C to 50°C and tested at normal stress levels of 25, 100 and 400 kPa are shown Figures 8.10a, 8.10b and 8.10c, respectively. It is noted that as the sand grains penetrate deeper into the smooth geomembrane surface, the particles abrade the counterface at a depth beyond the surface owing to the decrease in the hardness of the liner material at elevated temperatures, the shear path for the trailing sand particles following sand grains which has already passed through a given region of the contact surface between sand and smooth HDPE geomembrane become uneven and rougher. This results in the increase of the frictional shear resistance at the contact surface. Since the trailing sand grains that are shearing against the counterface geomembrane after the sand particles (in the leading edge of the shear box) in contact with the geomembrane at the interface encounter higher resistance to plowing at a greater depth which leads to dilation in the sand structure with enables larger internal frictional strength between the particles in the sand specimen.

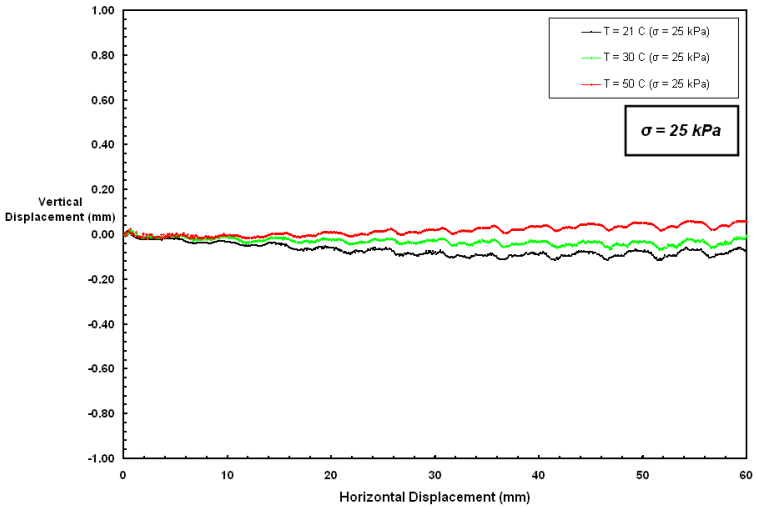

(a)

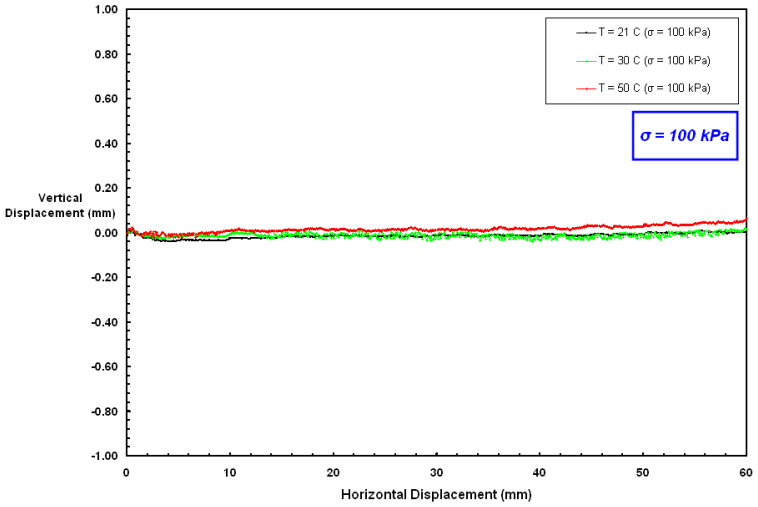

(b)

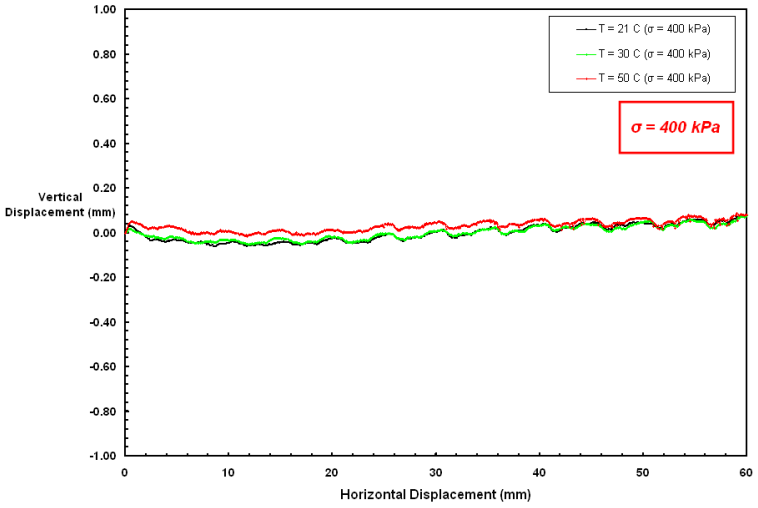

(c)

Figure 8.10 Vertical Displacement – Horizontal Displacement Behavior at Different Temperatures for Blasting Sand/Smooth HDPE Geomembrane: 25, 100 and 400 kPa

It is noted that the dilation initiates from the sand grains existing at the contact surface and adjacent to the interface and progresses through the other sand grains beyond the contact surface and positioned within the volume of the sand sample (Dove, 1996). These particles are realtively free to rearrange their contacts (interlocking between the grains), and thus dilate.

The primary controlling mechanism for angular particulate – smooth geomembrane interfaces was plowing of the soil grains along the surface of the geomembrane over the entire test temperature ranging from 21°C to 50°C. Further, at higher temperatures, as the geomembrane softens, the amount of plowing increased which resulted in a substantially larger increase in interface frictional angle (Figure 8.11), reflecting the additional effort required to penetrate the particles deeper into the geomembrane surface. Therefore, the strength of angular sand-geomembrane interfaces at all temperatures tested is directly related to the ability of soil particles at the interface to plow into the geomembrane surface. As such, the particle must displace the material at the interface to plow into the surface of the geomembrane which requires significant effort. Thus, as temperature increases, increased plowing of angular sand particles during shear depends on the decrease in hardness of the counterface material that is temperature related and correlates directly to increased strength. As shown in Figure 8.12, both peak and post-peak interface shear strength values over the entire range of normal stress levels (25 kPa, 100 kPa, 400 kPa) tested increased with increasing temperature.

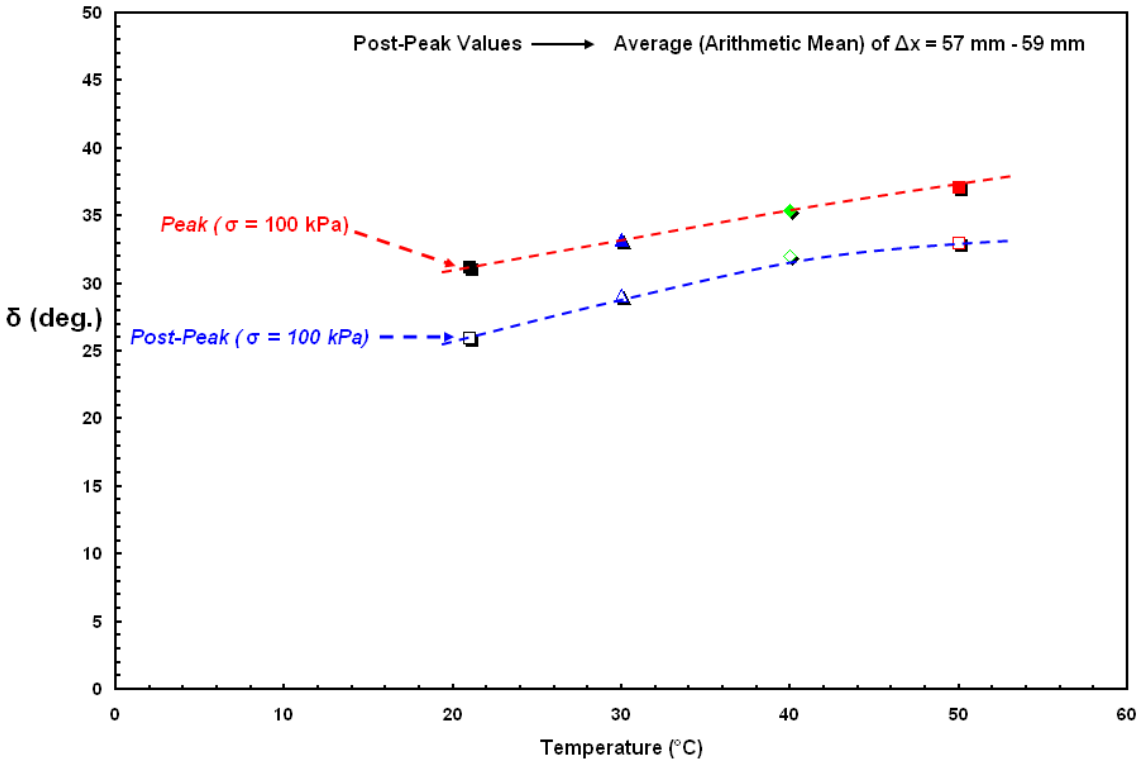

Figure 8.11 The Change in Interface Friction Angle, [δ] with Temperature for Blasting Sand/GSE Smooth HDPE Geomembrane Interface

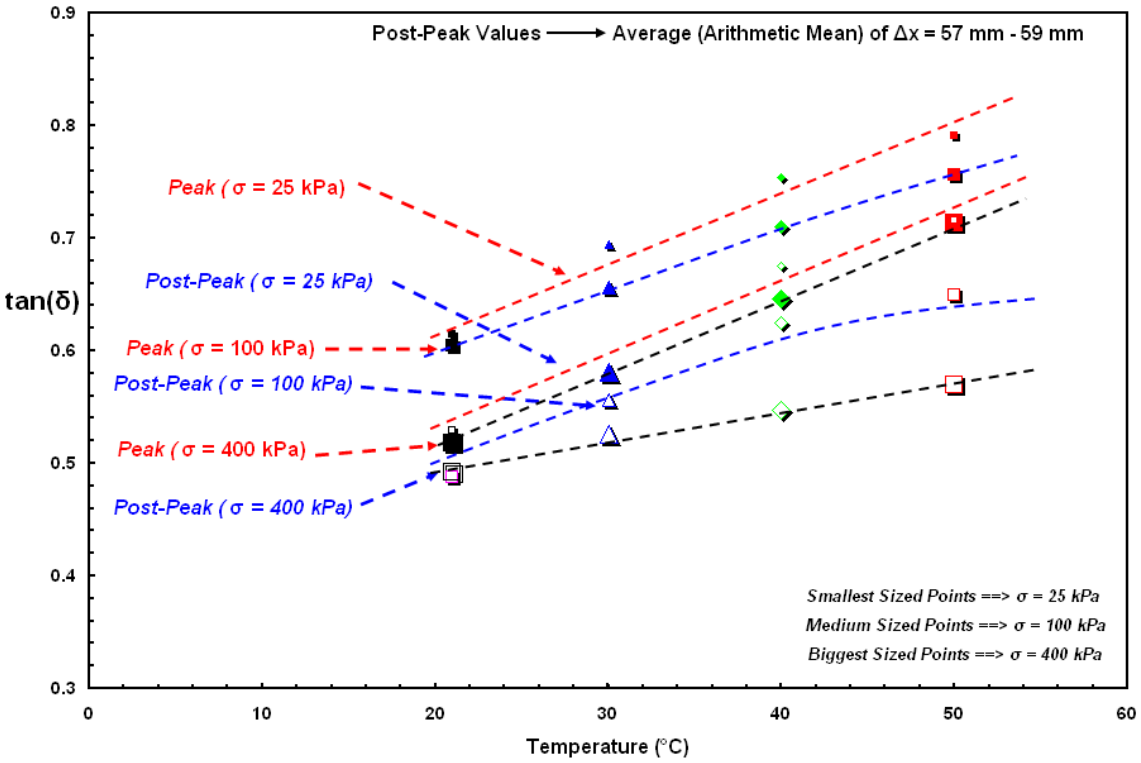

Figure 8.12 The Change in Coefficient of Friction, [tan(δ)] with Temperature at Different Loading Conditions for Blasting Sand/GSE Smooth HDPE Geomembrane Interface

The interface tests performed using angular particulate material resulted in a larger peak and residual (post-peak) shear strengths than those from rounded particulate interfaces. In addition, stress-displacement curves resulting from angular Blasting sand interface tests at all temperatures were located in the upper shear stress-displacement space compared to interface tests from rounded Ottawa 20-30 sand at comparable test temperatures. It is intended to make a comparative analysis for different ambient temperatures by defining a quantative proportionality parameter for peak and post-peak state ($PSR_{Angular/Rounded}$ and $RSR_{Angular/Rounded}$, respectively). In this way, the variations in the behavior as a function of temperature can be relatively evaluated for rounded or angular sand – smooth HDPE geomembrane interfaces. As such, the influence of the particle shape (i.e. roundedness/angularity) on the mobilized peak and residual frictional resistance with temperature change can be represented numerically for objectively assessing the resulted shear response based on a quantitative parameter as follows:

$$PSR_{Angular/Rounded} = \left[\frac{\tau_{P,\,Angular}}{\tau_{P,\,Rounded}} \right] \tag{8.1a}$$

$$RSR_{Angular/Rounded} = \left[\frac{\tau_{R,\,Angular}}{\tau_{R,\,Rounded}} \right] \tag{8.1b}$$

Where;

$PSR_{Angular/Rounded}$: Peak Stress Ratio between Angular and Rounded Particulate Materials

$RSR_{Angular/Rounded}$: Residual Stress Ratio between Angular and Rounded Particulates

$\tau_{P,\ Angular}$: Peak Shear Stress of Angular Sand – Smooth HDPE Geomembrane

$\tau_{P,\ Rounded}$: Peak Shear Stress of Rounded Sand – Smooth HDPE Geomembrane

$\tau_{R,\ Angular}$: Residual Shear Stress of Angular Sand–Smooth HDPE Geomembrane

$\tau_{R,\ Rounded}$: Residual Shear Stress of Rounded Sand–Smooth HDPE Geomembrane

Figures 8.13 and 8.14 show the change in $PSR_{Angular/Rounded}$ and $RSR_{Angular/Rounded}$ for smooth HDPE geomembrane interface as a function of temperature, respectively. The interface tests performed using angular sands in contact with smooth HDPE geomembrane specimens resulted in both higher peak and significantly greater pseudo-residual (post-peak) strengths at all test temperatures. Hence, particle shape and relative hardness of counterface material components have a dominating effect on the observed interface shear behavior at different temperatures. Finally, the results of the direct shear test at different temperatures for a combination of Blasting angular sand and smooth HDPE geomembrane system demonstrated that the angular sand grains have hardness much greater than the counterface material.

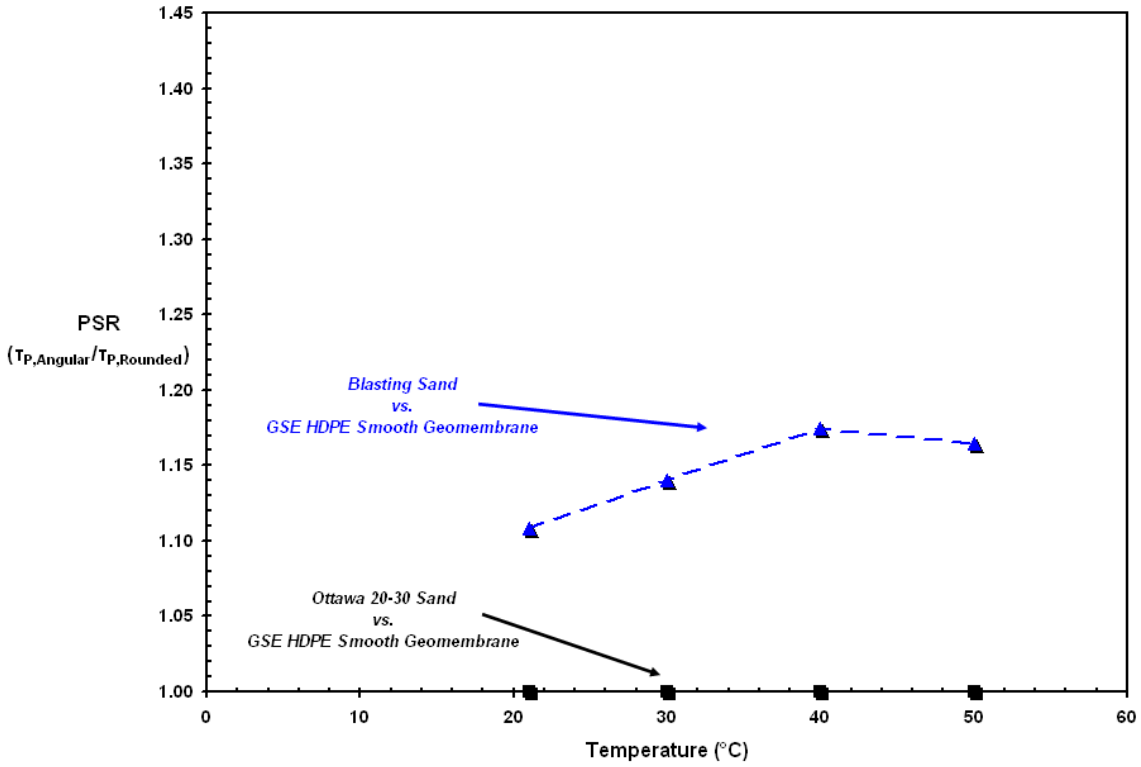

Figure 8.13 Comparative Analyses between Rounded and Angular Material Interfaces to Show the Impact of *Granular Soil Shape* on the Mobilized *Peak Shear Strength*

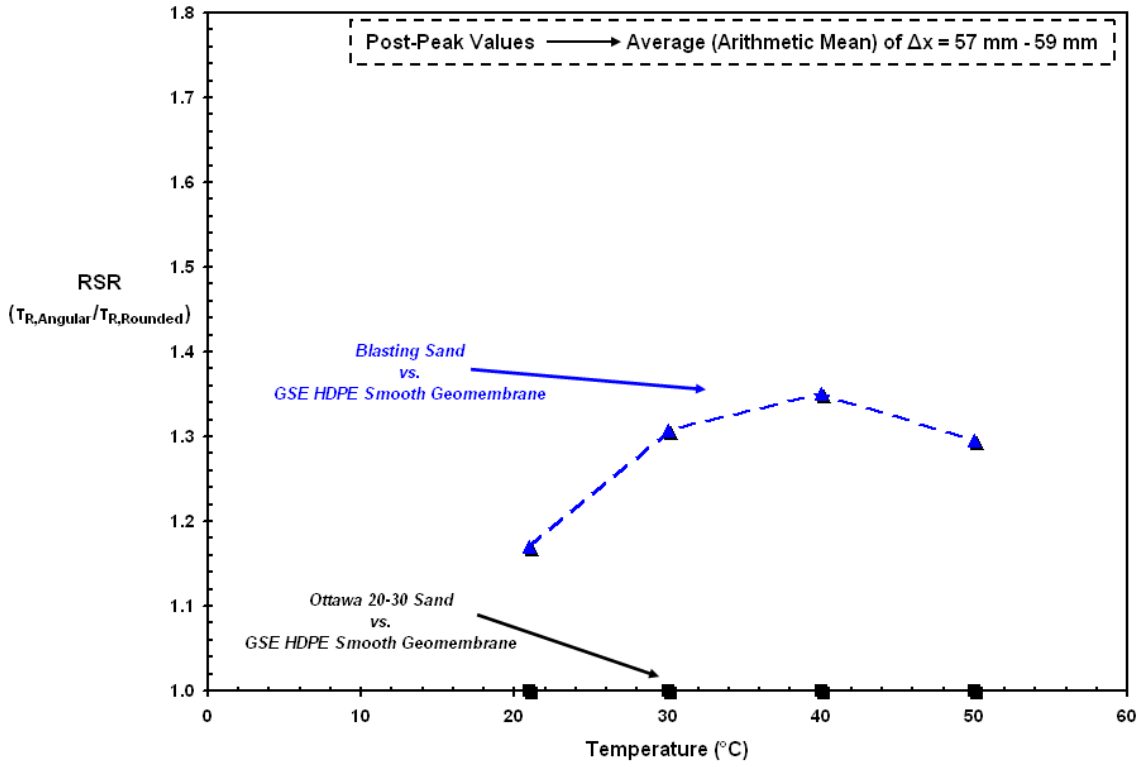

Figure 8.14 Comparative Analyses between Rounded and Angular Material Interfaces to Show the Impact of *Granular Soil Shape* on the Mobilized *Residual Shear Strength*

As seen in the preceding plots, the tendency of the trends for $PSR_{Angular/Rounded}$ and $RSR_{Angular/Rounded}$ exhibits an increase up to the temperature level of 40°C beyond which $PSR_{Angular/Rounded}$ shows a saturation and remains almost at a constant value while $RSR_{Angular/Rounded}$ displays a slight decrease in the value until the highest test temperature level of 50°C. This saturation or marginal decrease in the values can be attributed to the fact that, at higher temperatures ($\sim\geq$ 40°C), the counterface geomembrane softens and its surficial resistance against the indentation (i.e. penetration) tendency of the rounded Ottawa 20-30 sand grains in the interface diminishes. This results in a higher ability of the rounded sand particles to penetrate into surface of the counterface leafing to an increase in shear resistance of the Ottawa 20-30 sand – smooth HDPE geomembrane interface. As a result, the resultant ratio for the mobilized shear strength of the angular Blasting sand interface relative to the interface of the rounded Ottawa 20-30 sand at higher elevated temperatures displayed a slight reduction in the value.

8.3.2. Failure Envelopes and Comparison of Results at Different Normal Stress Levels

The peak and residual shear stresses for Uniblast angular blasting sand versus smooth HDPE interface are shown (linear and logarithmic scales) against the normal stresses in Figures 8.15 and 8.16, repectively. The peak and pseudo-residual (post-peak) strength envelopes developed exponentially in which the rate of increment became larger as the magnitude of normal stress level increased.

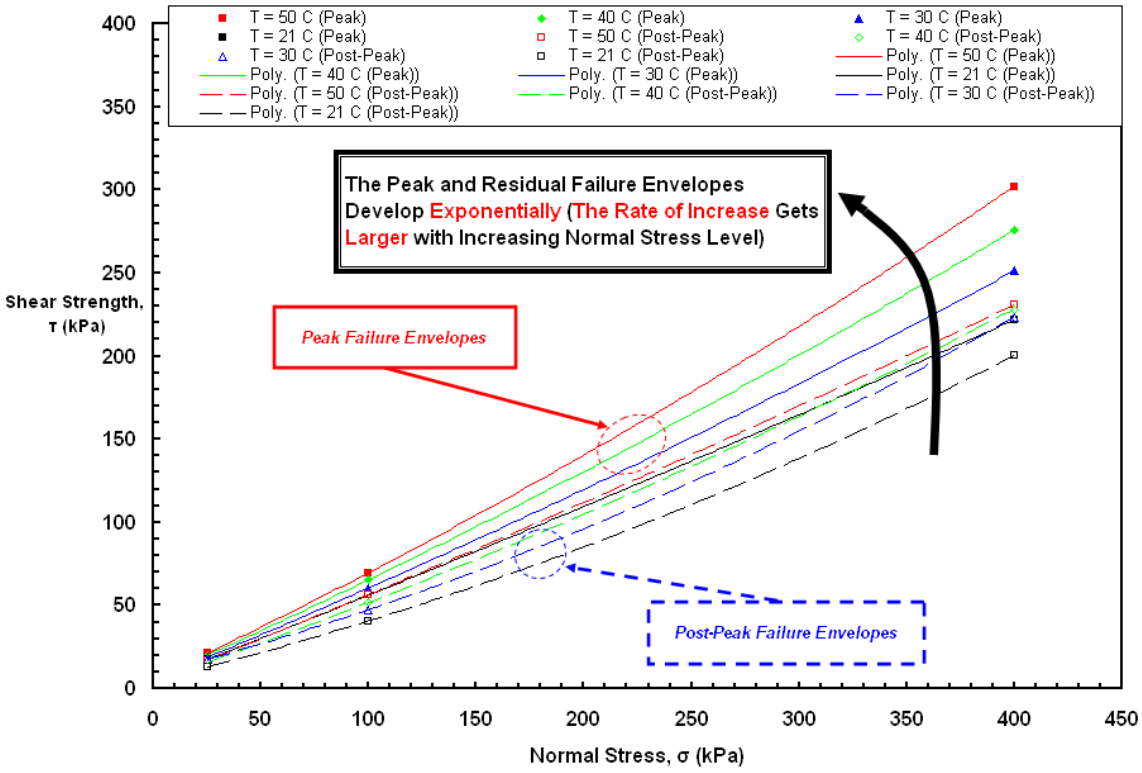

Figure 8.15 The Alteration of Peak and Residual Strength Envelopes with Increasing Temperature for Blasting Sand/GSE Smooth HDPE Geomembrane Interfaces

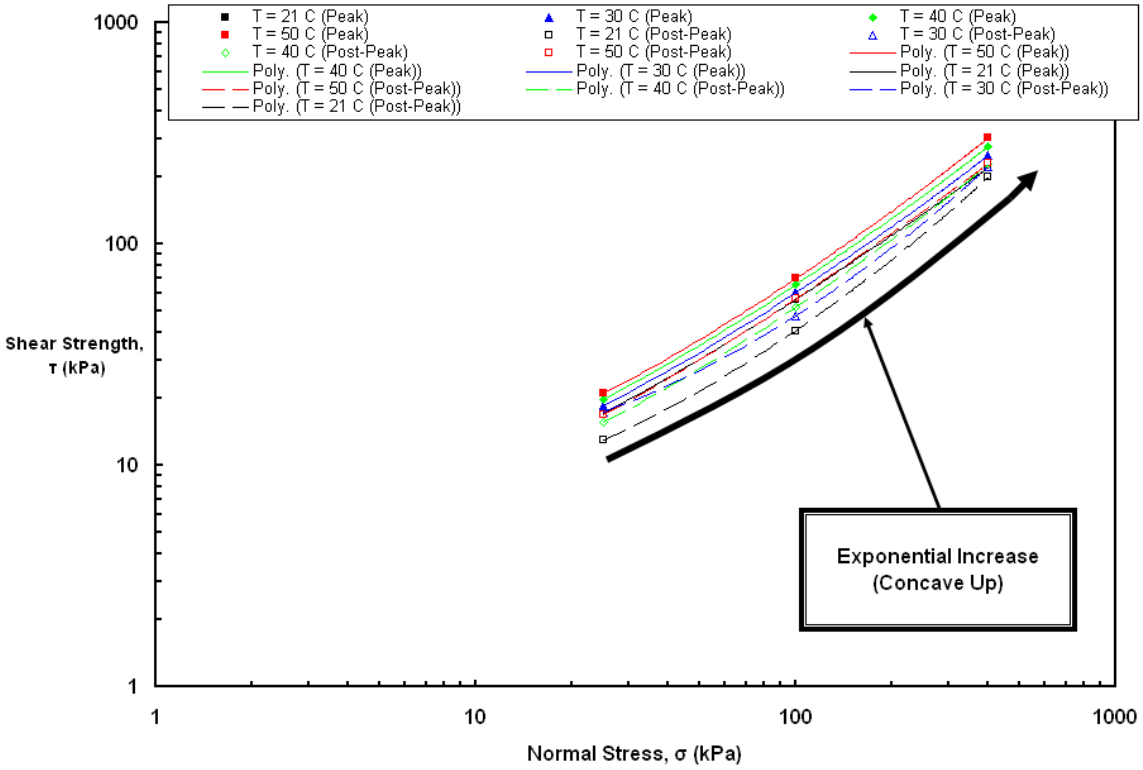

Figure 8.16 The Transformation in Failure Envelopes with Temperature at Different Loading Conditions for Blasting Sand/GSE Smooth HDPE Geomembrane Interface

The failure envelopes became more curved and non-linear with increasing ambient temperature particularly for the test temperatures above 40 °C. This is attributed to deeper indentation and greater plowing of the sand particles under the larger loading conditions as well as due to the reduction and decrease in surface hardness of the counterface geomembrane at elevated temperatures. In order to examine the behavior further and to analyze the attained test results as well as to distinguish and comprehend the alterations in the non-linear shear stress-normal stress relationship at very low loading conditions, the strength envelopes were also replotted on logarithmic scales. The general shape of the failure envelopes for the angular sand versus smooth HDPE geomembrane interface depicted curved shape with concave-up alignment and exponential modal pattern. Besides, the angular shape feature of sand grains resulted in much higher shear strengths and interface resistances mobilized over the specimens entire contact area for granular sand against continuum polymeric liner sheet at all temperatures tested.

8.4. Temperature Effects on *Rounded* Particulate – Smooth *PVC* Continuum Material Layered Systems

8.4.1. Ottawa 20-30 Rounded Sand/PVC Smooth Geomembrane Interfaces

A series of interface shear tests involving Ottawa 20-30 sand and smooth PVC geomembranes were performed at various test temperatures ranging from 21°C to 50°C and at a range of normal stress levels from 25 kPa up to 400 kPa. Stress – displacement curves are presented in Figure 8.17. A rapid increase in shear stress up to peak stage within 1–2 mm of displacement was observed. This was followed by a reduction to some

lower residual shear stress condition with continued loss in frictional resistance as shearing displacement progressed until the termination of the test at 60 mm horizontal displacement. This interface response was observed over the entire range of test temperatures (21 °C – 50 °C) at which the direct shear tests were performed for rounded sand (Ottawa 20-30) and PVC smooth geomembrane interfaces. The increase in normal stress resulted in an increase in the displacement to peak. An increase in the mobilized frictional resistance at sand – smooth PVC geomembrane interfaces with increasing ambient temperature level from 21 °C up to 50 °C was observed although the absolute amount and/or the percentage value of the increase in frictional strength is smaller compared to the results of comparable tests on rounded sand – smooth HDPE geomembrane interfaces over the complete range of elevated temperatures tested.

For the interfaces comprised of rounded particulates in contact with relatively soft polymeric materials at low normal stresses, after small displacements (1-3mm), the rounded sand particles start sliding and a rapid increase to peak stress state occurs. With increased shear displacement, the rounded sand particles at the contact surface (area) exhibit a shear mechanism dominated by rolling on the surface of the relatively soft polymeric counterface material (PVC liner) due to the low confinement of the interface. The transformation of shear mechanism from predominantly sliding to predominantly rolling at the interface results in continuous reduction in the mobilized frictional resistance with increased shear displacement after peak state as shearing progresses futher. Similar observations were previously made by O'Rourke et al. (1990) regarding soft polymeric material interfaces in contact with rounded sand particles.

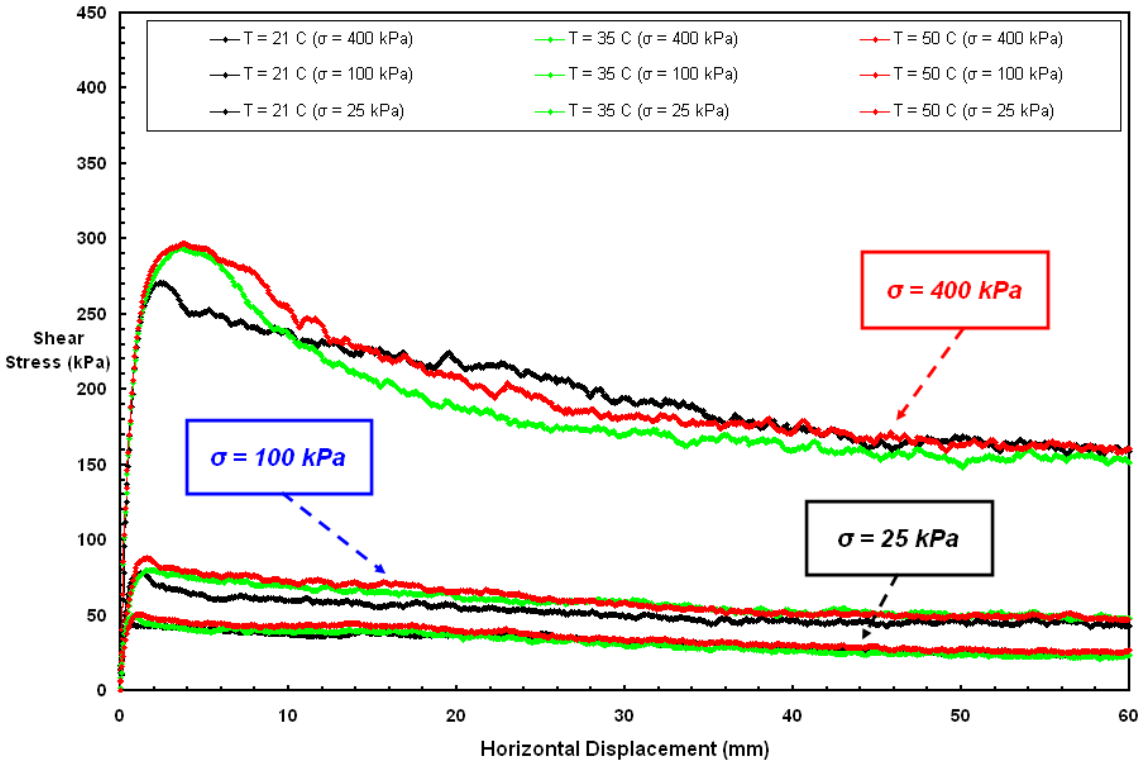

Figure 8.17 Shear Stress–Displacement Curves at Different Loading Conditions; & at Various Test Temperatures for Ottawa 20-30 Sand/EPI Smooth PVC Geomembrane

From the shear test results of Ottawa 20-30 sand versus PVC geomembrane interface presented herein, it can be inferred that the type of base material, from which the geomembrane continuum sheet is produced, plays a significant role in the mobilization of interface shear strength. The interface shear mechanism is dominated by particles rolling on the soft and pliable surface of the PVC liner at lower (cooler) test temperatures whereas, the shear mechanism during the course of shearing displacement is transformed to a plowing mechanism at higher (elevated) test temperature conditions which contributes favorably to an increase in the frictional resistance against shearing as the PVC liner becomes more malleable with increasing temperature. This increase in

interface strength as a function of temperature became more evident as the normal stress was increased from construction level (≤ 25 kPa) to operation level (up to 400 kPa) loading conditions (Figures 8.18a, 8.18b and 8.18c, respectively). This is attributed to the flexible and more plasticized nature of PVC geomembranes compared to the HDPE ones. At low normal stresses, the PVC lining material was able to recover its surface state to some extent and recover some portion of the relative deformation induced changes such as scratches, grooves and striations that were initiated, created and generated, respectively, by the sand grains during shearing displacement so that trailing sand particles following sand grains which has already passed through a given region of the contact surface between sand and smooth PVC liner will encounter a marginally recovered surface. Owing to the pliable and more plasticized nature of PVC geomembranes, the trailing sand particles were given an opportunity, during shear displacement, to enter marginally recovered lining sheet surface which had been scratched already by leading edge sand particles of the specimen box such that the grooves and/or the striations were regained to some extent by the PVC material body due to malleable and ductile nature of the lining sheet surface. In this way, greater frictional resistance/strength at the interface against shear displacement was generated as the sand particles at rear edge sheared against less damaged/scratched planar lining sheet surface compared to the results of the interface tests at corresponding test temperature on HDPE geomembrane specimens.

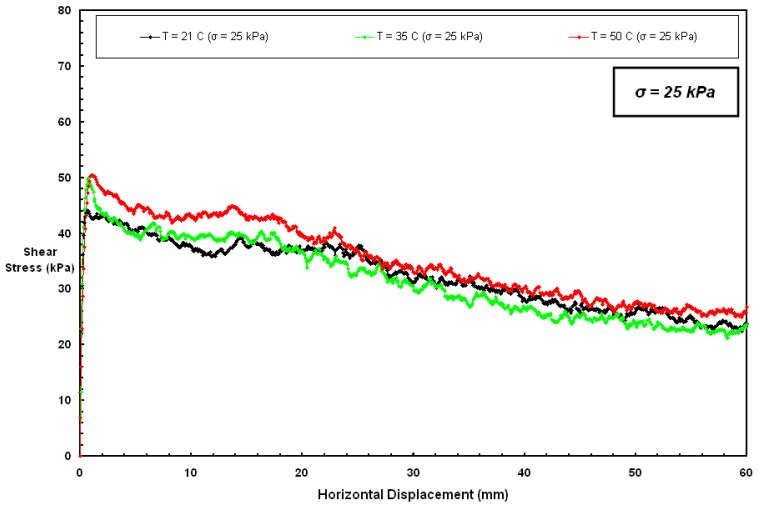

(a)

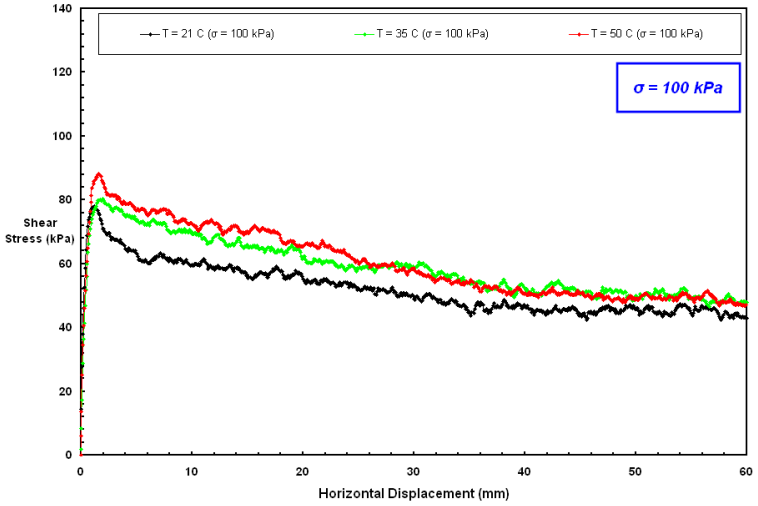

(b)

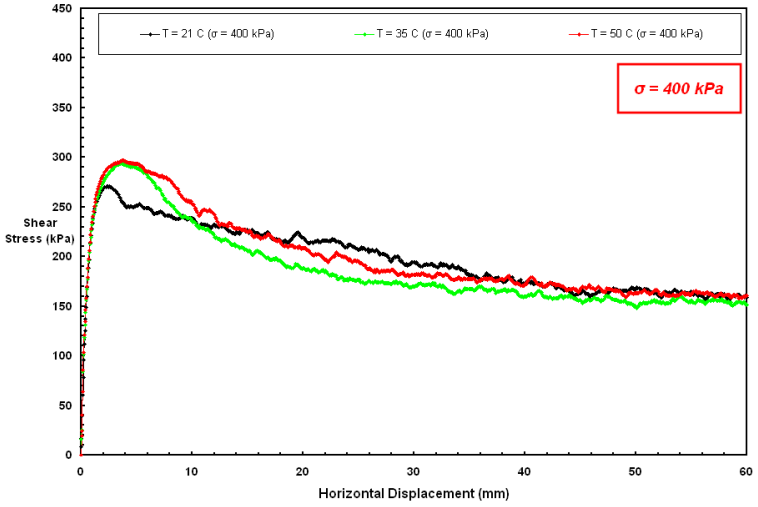

(c)

Figure 8.18 Shear Stress–Displacement Curves at Various Test Temperatures for Ottawa 20-30 Sand/EPI Smooth PVC Geomembrane: 25, 100 and 400 kPa

As ambient test temperature increased, the interface shear failure mechanism changed from rolling/sliding to combination of rolling and plowing with the latter becoming the dominant failure mechanism due to embedment of soil particles into the geomembrane more readily as a result of the decreasing surface hardness. With the additional influence of higher normal stresses (≥ 100 kPa) applied on the interface, the sand grains were able to become further embedded into the geomembrane surface. During the evaluation of this shear mechanism involving further indentation of grains, the interface shear failure no longer developed just at the contact surface with the geomembrane but migrated (transferred) into the soil, resulting in the mobilization of particle-to-particle friction. This resulted in greater frictional strength being generated (Figures 8.17). If the normal stress had been increased even further (>400 kPa), the soil particles would likely have been embedded well into the geomembrane surface depending on the yield strength of the polymeric geomembrane such that the force required for plowing might have exceed the force needed to overcome particle-to-particle friction and the failure surface would have been entirely within the soil mass.

In general, for plowing to take place at the interface in addition to rolling, an increase in the shear strength of the interface for particulate – continuum material combinations occurs. As such the mobilized interface shear strengths at higher elevated temperatures for rounded sand (Ottawa 20-30) versus PVC geomembrane interface system were partly due to sliding and partly due to plowing. However the magnitude of interface shear strength mobilized entirely due to plowing depends on the type of the soil (i.e. rounded versus angular) used in direct shear tests as well as, most importantly, the degree/level of ambient test temperature which should be sufficiently high for all sand

particles at the contact surface to plow along the geomembrane surface in generating a plowing dominated response over the complete extent of the interface. For instance, granular soils consisting of angular particles results in early onset of plowing during the course of shear displacement.

The variation of vertical displacement with horizontal shear displacement and the resulting change in the amount of dilation in the sand mass is presented in Figure 8.19. The dilatancy of the sand mass during shearing resulted from particle rearrangement and overall structural reorganization in the sand mass resulted from the particles penetrating deeper and plowing progressively into the geomembrane as the relatively hard sand particles moved/displaced further on the soft surface of the PVC lining material such that the sand grains at the contact surface over the entire extent of interfacial area encountered greater resistance generated from the counterface material (geomembrane) and resulted in larger dilation. In short, the higher void ratios in the interface zone at higher elevated temperatures were induced by the relatively higher contribution of plowing to shearing mechanism.

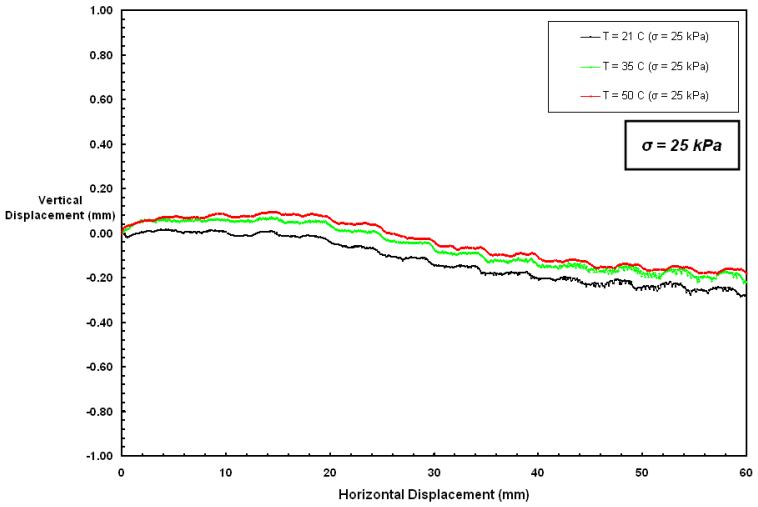

(a)

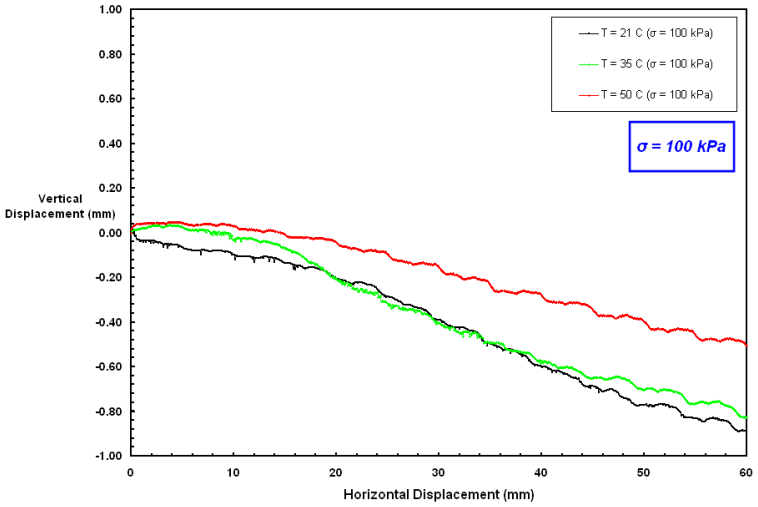

(b)

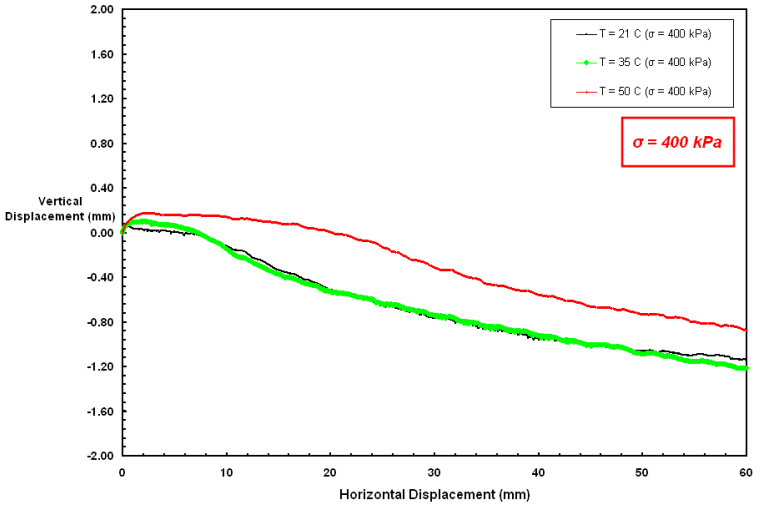

(c)

Figure 8.19 Vertical Displacement – Horizontal Displacement Behavior at Different Temperatures for Ottawa 20-30 Sand/Smooth PVC Geomembrane: 25, 100 and 400 kPa

The dilation response of the smooth PVC geomembrane versus Ottawa 20-30 layered system was different than for the interface tests on smooth HDPE geomembrane versus Ottawa 20-30 sand at all temperatures tested and was attributed to the distinct material properties of PVC geomembranes such as greater pliability and malleability. Further, the vertical versus horizontal displacement behaviors in terms of the shape of the curves at different test temperatures were in such a manner that slight dilation occurred at slower rates of expansion in sand. At larger shear displacements, the rate of the dilation became greater and maintained this pattern until the end of the tests. For relatively lower rate of dilations at smaller displacements, the initial sliding of rounded sand particles induced a marginal contraction in soil structure as opposed to and/or against the tendency of the overall sand mass to expand/dilate so that the void ratio in the interfacial zone did not increase substantially. At the start of the residual state, the soil particles continuously produced deeper scratches; and therefore, yielded larger expansions to be exhibited in sand structure for the interface tests conducted at higher elevated temperature levels than those performed at lower temperatures such as room temperature (21 °C).

The shearing mechanism (i.e. sliding, rolling, and/or interlocking of particles) causing the increase in peak fricition angle and/or friction coefficient is primarily dependent on the surface hardness, particle angularity, operational normal stress, and relative density of the sand. Generally, as particle angularity increases, the destructive impact to the geomembrane surface by sand grains through plowing increases as well as the amount of particle interlocking increases, causing an increase in peak friction coefficient. The increase in the δ and $\tan(\delta)$ with temperature are shown in Figures 8.20 and 8.21, respectively.

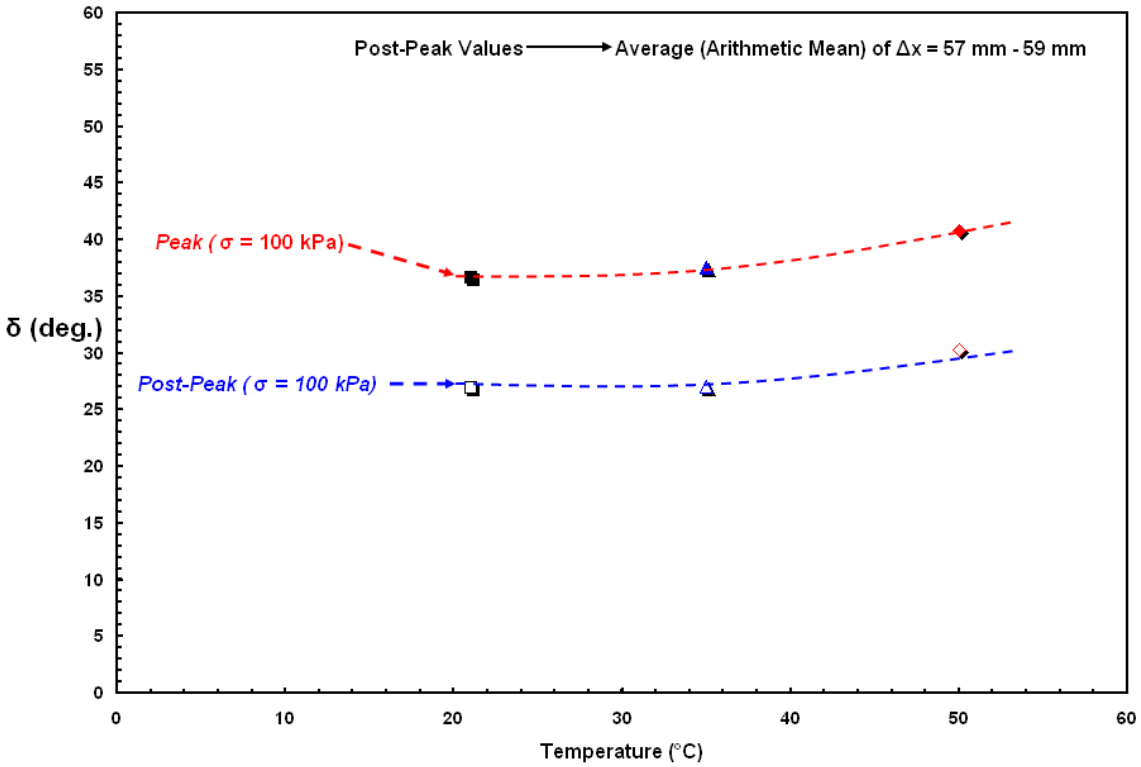

Figure 8.20 The Change in Interface Friction Angle, [δ] with Temperature for Ottawa 20-30 Sand/EPI Smooth PVC Geomembrane Interface

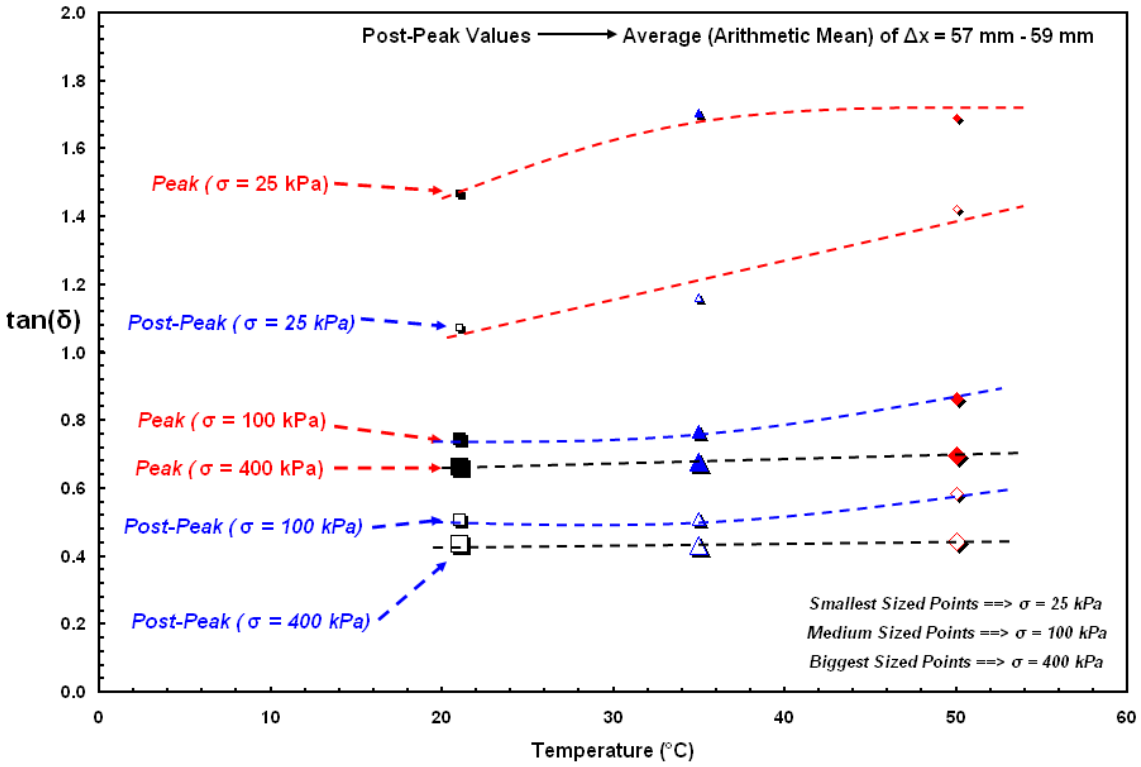

Figure 8.21 The Change in Coefficient of Friction, [tan(δ)] with Temperature at Different Loading Conditions for Ottawa 20-30 Sand/EPI Smooth PVC Geomembrane Interface

The increase in the friction angle and coefficient of friction resulted from the reduction in the surface hardness of the PVC geomembrane liner. Consequently, it is noted that counterface hardness is a major controlling factor in determining contact conditions at particulate-continua interfaces.

For this system of materials, the response is dominated by elastic rolling/sliding up to a higher temperature level (> 35°C). As such, the shear response mainly consists of elastic-plastic contact with a transition to plastic contact at higher elevated temperatures and at higher normal stresses. From the above observations, the following mechanism can be postulated wherein the rounded Ottawa 20-30 sand can induce plowing effects on the smooth pliable/soft nature geomembrane only after certain higher temperatures and larger loading conditions that are sufficient to mobilize this mechanism at the interface in contact with PVC liner. It is likely that penetration of the sand particles into the smooth PVC geomembrane surface induces the occurrence of slightly higher void ratio in the interfacial zone. Beyond the peak stress, the particle movement in the interface zone results in the void ratio decreasing to the average void ratio state by sliding of sand particles. The friction coefficient (both peak and residual), as seen in Figure 8.21, decreased with the normal stress. This non-linearity was, as previously explained by Bishop (1966) and Bolton (1986), due to soil dilatancy. The higher pliability and soft nature of PVC geomembranes resulted in different interface shear behavior observed than with HDPE geomembranes at all temperatures tested. As such, the PVC liners possess higher pliability properties as compared to HDPE geomembranes over the entire test temperature range (21°C – 50°C) and this situation prevents the frictional

strength/resistance of the HDPE geomembrane specimens from reaching that of the PVC liner specimens.

As the frictional shear resistance of geosynthetic interfaces is product dependent and project specific, the discussions on the test results herein are aimed to provide comparative analyses on overall interface shear behavior and relative change (i.e. increment versus decrement) of strength parameters as a function of temperature rather than providing specific shear strength values for use in design applications.

8.4.2. Failure Envelopes and Comparison of Results at Different Normal Stress Levels

Figure 8.22 shows failure envelopes including both peak and residual strength envelopes for Ottawa 20-30 sand versus PVC geomembrane interfaces tested at different temperatures ranging from 21°C to 50°C. The peak and post-peak (residual) failure envelopes exhibited a quadratic functional behavior that reflects an incremental rate of increase over the entire test temperature range with increasing normal stress applied in the direct shear tests. In particular, the rate of this increase became significant at larger stresses (> 100 kPa) and at higher elevated temperatures. As such both the peak and the residual failure envelopes were curved in which there occurred a more significant increase in interface shear strength as the normal stress and ambient test temperature were increased resulting in greater non-linearity in the failure envelopes. At lower normal stresses, the increase in interface shear strength was not as significant as at higher normal stresses. To examine the entire behavior in detail in terms of the occurrence of the developed modal trend with the change in temperature, particularly for low normal stress conditions, the strength envelopes were redrawn on logarithmic scales (Figure 8.23).

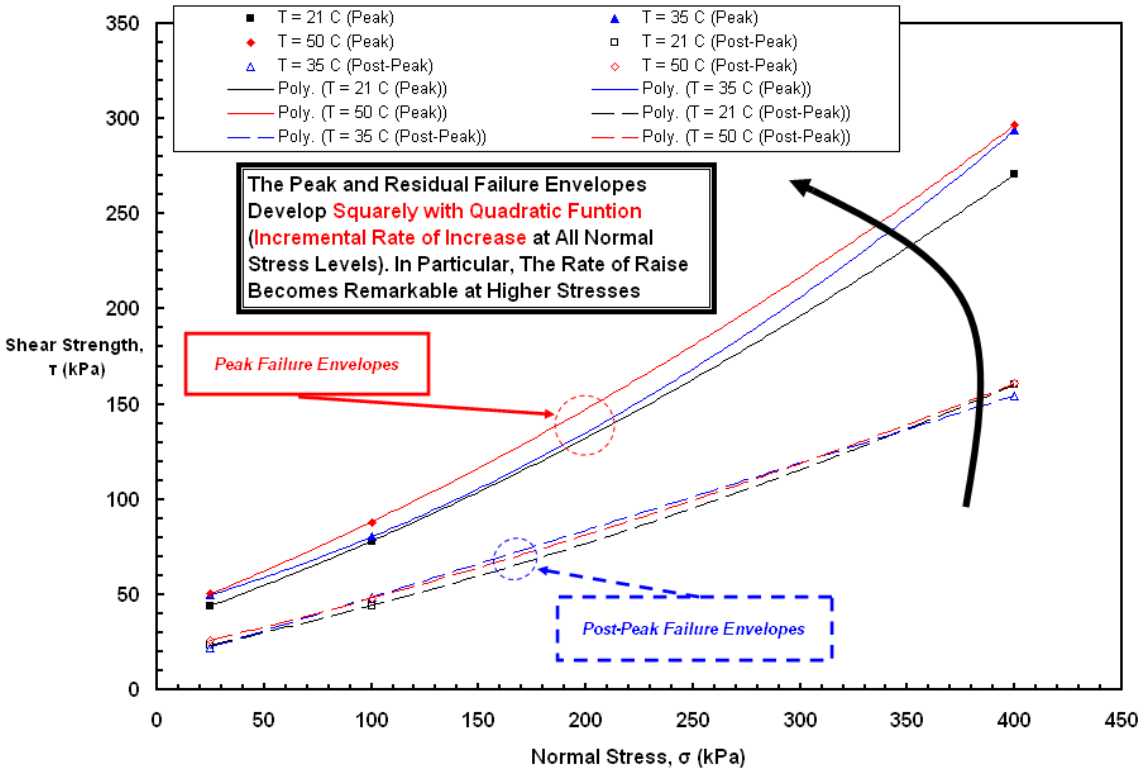

Figure 8.22 The Alteration of Peak and Residual Strength Envelopes with Increasing Temperature for Ottawa 20-30 Sand/EPI Smooth PVC Geomembrane Interfaces

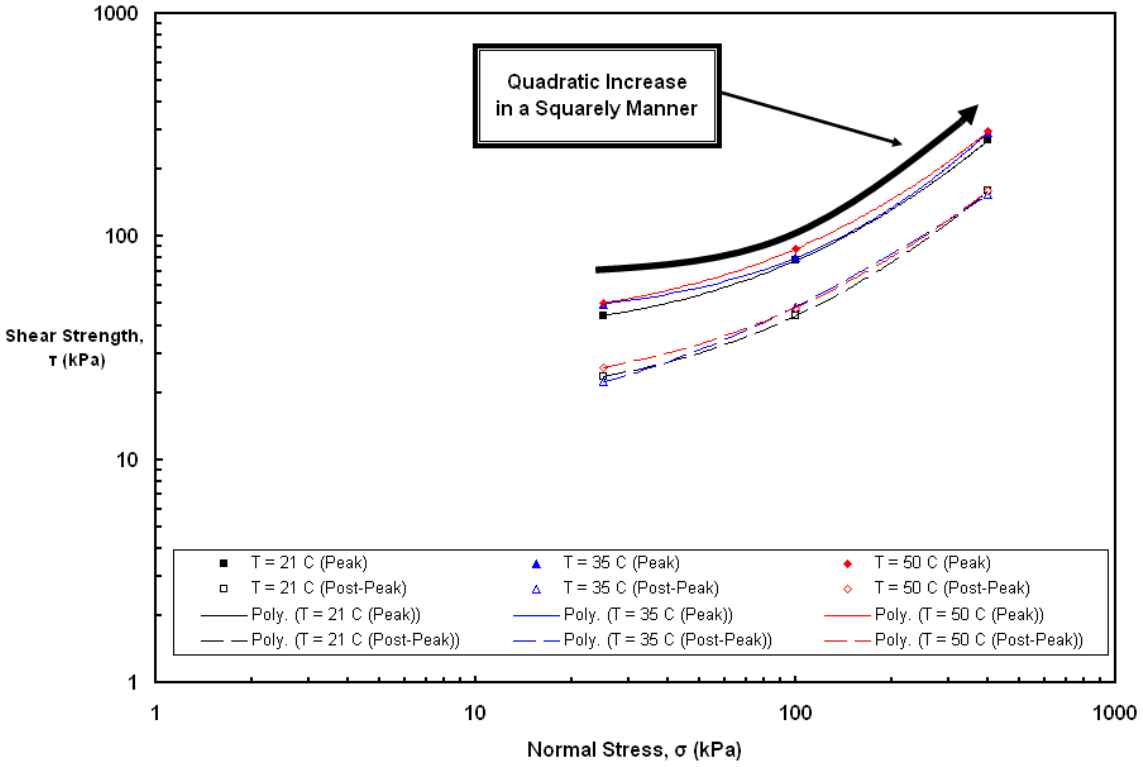

Figure 8.23 The Transformation in Failure Envelopes with Temperature at Different Loading Conditions for Ottawa 20-30 Sand/EPI Smooth PVC Geomembrane Interface

With the current technology and advanced construction techniques as well as with the added requirements for the application of more sophisticated and larger size projects, the range of normal stresses expected in the field has become larger. For this reason, a linear Coulomb-type failure envelope drawn through the data points at low or low-to-medium loading conditions may lead to a loss of accuracy in calculations when designing composite layered systems. Similarly, Giroud et al. (1993) previously proposed a hyperbolic expression in generating shear strength envelopes for soil-geosynthetic interface systems. It was indicated that this type of failure envelopes can be used when test results give a non-linear shear stress versus normal stress relationship.

Conventional interpretation shows that the data appear to fall on a straight line. However, closer examination reveals that the strength envelopes are not linear, but are concave upward. This concavity is due to a combination of flattening of the failure envelopes at lower stresses and an upward curvature at higher normal stresses. For the case of loose sand specimens sheared against smooth geomembranes, the failure envelope would possibly be straight or concave downward with increasing normal stress as dilation is suppressed unless any occurrence of sand particle plowing exists. In contrast, dilation does not contribute significantly to interface shear resistance of dense sand specimens sheared against smooth geomembranes. Additionally, the increased amount of plowing of the sand particles due to reduction in surface hardness of the counterface polymeric geomembrane sheet with increasing ambient temperature and applied normal stress level contributes significantly to the mobilized shear strength that results in the strength envelopes becoming concave upward at higher elevated temperatures as well as at larger loading conditions.

The effect of temperature is evident in both peak and post-peak strength envelopes as presented in Figure 8.22. An increasing trend was observed at all temperatures, particularly for the tests performed at higher elevated temperatures. At each normal stress, the interface strength increased as the temperature increased which is also evident from the differences and/or the divergence in the envelopes generated from the results of different test temperature conditions. This temperature sensitivity is consistent with polymer softening (i.e., reduction in stiffness) as the temperature increases which results in greater penetration of sand particles into the geomembrane surface showing more frictional resistance against shear displacement under a given stress as well as leading an increase in contact area.

8.5. Temperature Effects on *Angular* Particulate – Smooth *PVC* Continuum Material Layered Systems

8.5.1. Uniblast Angular Blasting Sand/PVC Smooth Geomembrane Interfaces

Shear stress-horizontal displacement failure curves at different temperatures for smooth PVC geomembrane sheared against angular Blasting sand under a range of normal stresses from 25 kPa to 400 kPa are presented in Figure 8.24.

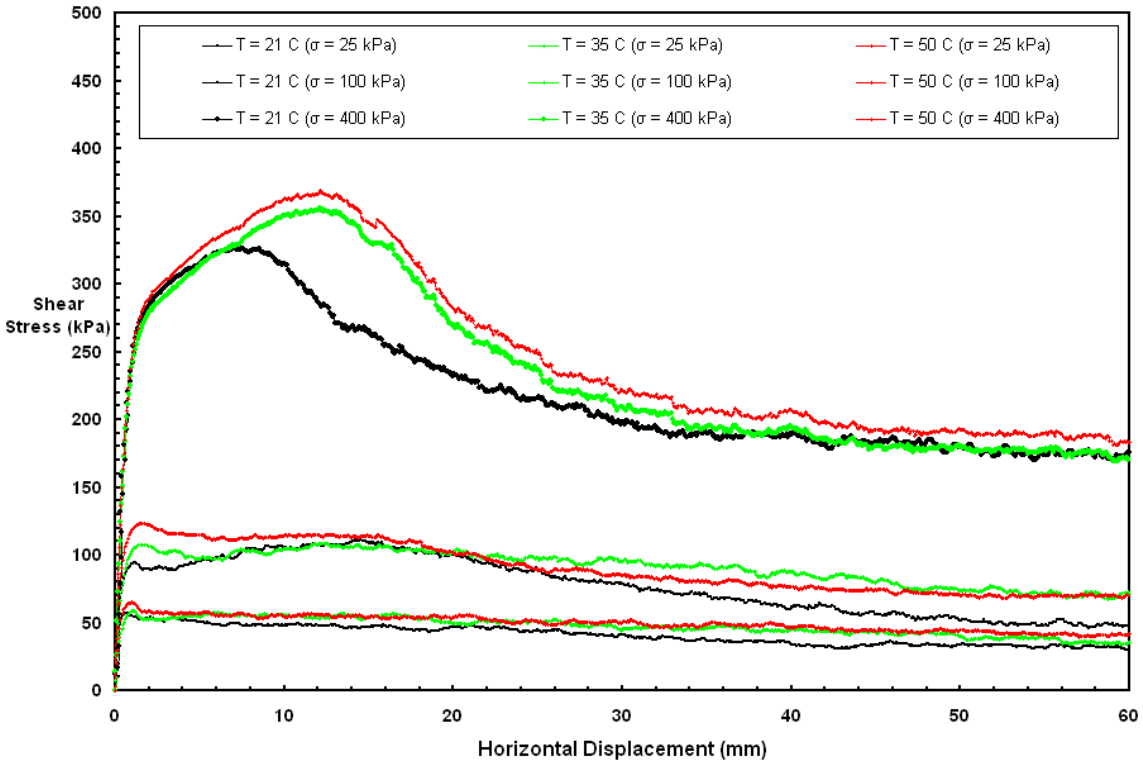

Figure 8.24 Shear Stress–Displacement Curves at Different Loading Conditions; & at Various Test Temperatures for Blasting Sand/EPI Smooth PVC Geomembrane

The interface direct shear tests performed using angular sand resulted in higher peak and residual (post-peak) strengths at all test temperatures as compared to rounded sand. One interesting aspect of the plots is the relative shape of the different curves such that the stress-displacement curves at different temperatures corresponding to the low normal stress condition (25 kPa) (Figure 8.25a) resulted in an initial rise immediately in stress at very small displacements with a slight reduction in frictional resistance after the peak strength state was mobilized. However, as the magnitude of applied normal stress increased to higher stress levels (100 kPa and 400 kPa) (Figures 8.25b and 8.25c, respectively), the stress-displacement curves of the different test temperatures (21°C – 50°C) for the angular sand exhibited well-defined peak state that was followed by a decrease to a residual state. For the highest normal stress (400 kPa), there is a rapid

increase in shear stress within 1 to 2 mm horizontal displacement which is followed by a decrease in the rate of strength gain with displacement to peak level. After a gentle peak stage, a marked reduction in shear stress to an essentially constant large strain condition is seen (Figure 8.25c). These trends of stress-displacement plots were consistent throughout the various test temperatures at which angular sand – smooth PVC geomembrane combinations were tested. This difference in the general characteristic of the stress-displacement failure curves for angular sand systems as compared to rounded sand cases is attributed to the different shear mechanisms developed at the interfaces. For Ottawa 20/30 sand – smooth PVC geomembrane interfaces, the mechanism was predominantly rolling/sliding of the sand grains against the geomembrane; however, the mechanism was primarily plowing of the angular sand particles along the soft smooth geomembrane surface for Blasting sand – smooth PVC liner interfaces. The shear stress versus horiziontal displacement behavior of the angular sand interface is analogous to the textured geomembrane-geotextile interface system. The shape of the stress-displacement failure curves for the particulate versus continuum material interfaces were significantly modified by the use of the angular sand having sharp features on the individual sand grains. The shape of the shear stress curve for Blasting sand interfaces did not show as much strain softening (i.e. strength loss) behavior as those exhibited by the rounded sand interface systems over the entire test temperature range. This resulted from the higher ability of the angular sand particles to indent into and plow along the relatively soft geomembrane surface at all temperatures tested.

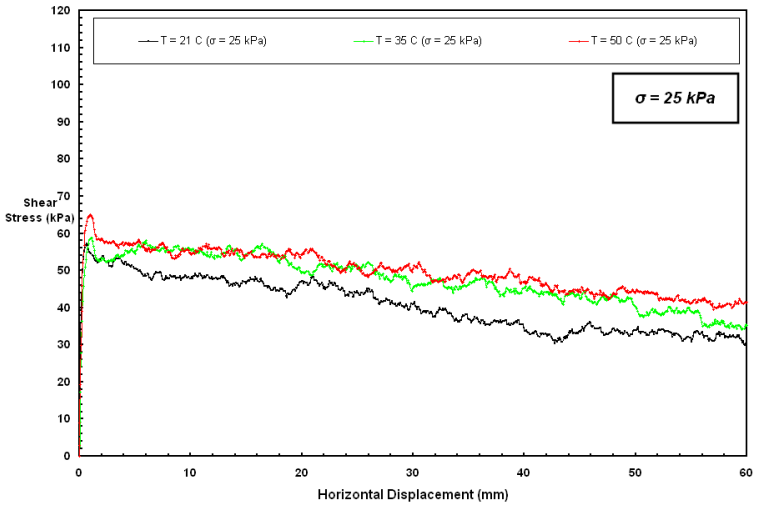

(a)

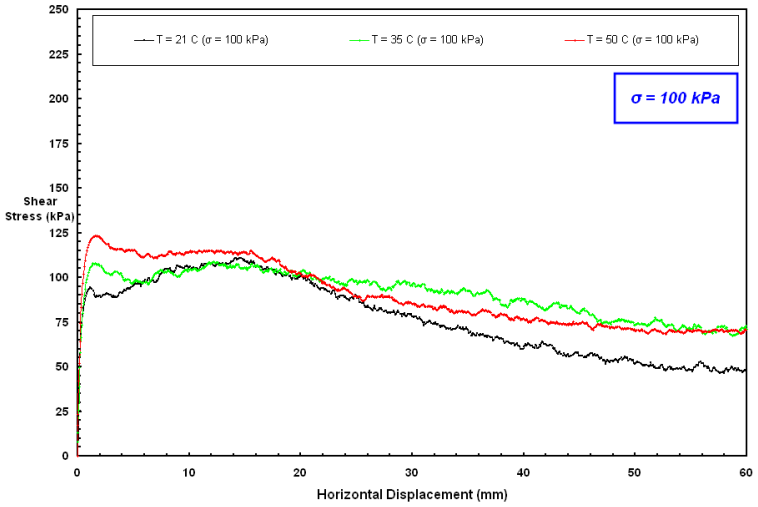

(b)

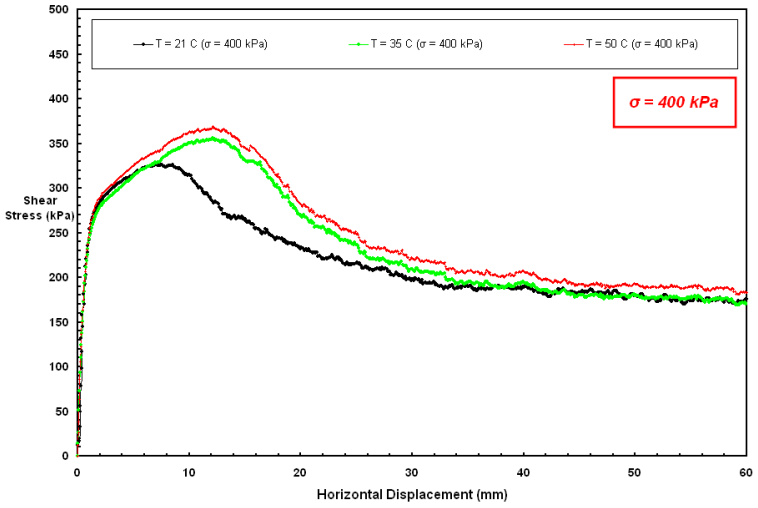

(c)

Figure 8.25 Shear Stress–Displacement Curves at Various Test Temperatures for Blasting Sand/EPI Smooth PVC Geomembrane: 25, 100 and 400 kPa

For PVC geomembrane, the magnitude of the initial peak strengths mobilized in contact with angular sand over the entire test temperature range were significantly higher than the peaks yielded in conjunction with rounded sand; while, the large displacement stress values (i.e. residual state) were also higher. It is noted that the typical shape of shear stress versus displacement curves for the smooth PVC geomembrane systems regardless of test temperature or stress level were inherently different than the HDPE geomembrane interfaces due to the softer and more pliable PVC lining sheet materials. Therefore, the shear mechanism for granular soil and geomembrane interfaces dramatically changes with the geomembrane hardness. The shear strength was developed primarily by rolling/sliding on the lining sheet surface for the case of relatively harder geomembranes at lower temperatures; whereas it is mobilized predominantly by indentation and plowing of sand grains resulting in interlocking and dilation of sand particles during the course of shear displacement against substantially softer geomembranes. Additionally, the angularity of the particles induces higher plowing effects causing greater depth of striations or grooves which directly results in larger residual friction coefficients/angles than rounded sand.

The peak state for sand (i.e. particulate material) in contact with smooth geomembrane interface systems can be considered as indicative of the onset of particle movement as a result of shear displacement leading to shear stresses imposed in interaction zone (i.e. interface) of counterfaces. Once the peak strength has been achieved, the particles either begin to slide along or plow into the geomembrane surface depending on the relative hardness of interface components which is related to ambient temperature. Further, as the normal stress applied on the interface increases, the

displacement required to reach peak and residual strengths increases for all types of particulate materials.

At low normal stresses, the decrease in strength to the residual state was often negligible or not as pronounced as at high normal stresses. As particles began to plow into the geomembrane surface, the initial movements causes wear on the surface. However, as particle displacement continues, particles encountering material previously damaged by the preceding sand particles (i.e. particles in the leading edge of the shear-box) causes little additional damage and no additional strength is required for subsequent displacement. Consequently, in general, the frictional resistance of the interface is strongly correlated to the tendency of the particulate material to plow into the surface of the geomembrane.

The shear stress reduced with displacement beyond the peak stage and reached a constant value. The peak stress is considered as proportional to the dilation of the sand which was reflected in the form of vertical displacement, and in turn which demonstrated the volume of sand involved in the interaction (Figure 8.26). Any difference in residual shear stresses appeared to have been narrowed down if further displacement was allowed in the tests with high normal stresses (> 100 kPa). Blasting sand-PVC geomembrane interfaces did not exhibit a post-peak strength loss at low normal stresses (25 kPa) at all temperatures tested. This behavior has important design implications such that these characteristics of the interface of this material combination suggest that PVC geomembranes are well suited for applications in which low normal stresses are expected such as landfill cover systems, and/or where seismically induced permanent deformations may result in service lifetime.

In summary, stress-displacement failure curves for angular sand systems tested at high normal stresses displayed a distinct peak followed by softening to residual conditions for all temperatures tested. As with the application of lower normal stresses to the interface, residual state was not achieved until near the end of the direct shear test at displacements of the order of 60 mm over the entire test temperature range (21°C – 50°C). It was found that as sand particle angularity and normal load increased; the displacements to reach peak condition increased. Additionally, the stress-displacement failure curves exhibited larger post-peak softening or strength loss as normal stress applied during the operation of direct shear tests increased regardless of test temperature level. This is considered to be due to higher confinement of the interface as a result of the imposed greater normal stress/load during the tests.

The vertical displacement – horizontal displacement plots for angular Blasting sand and smooth PVC geomembrane interface at a range of test temperatures from 21°C to 50°C and for different loading conditions (25, 100 and 400 kPa) are shown in Figures 8.26a, 8.26b and 8.26c, respectively.

The higher contribution of plowing component to the resultant shear mechanism at the interface dominates the mobilized overall frictional strength in the contact surface owing to the sand particle angularity as well as due to a reduction in surface hardness of the geomembrane liner at higher ambient temperatures. This resulted in a greater increase (compared to the other interfaces) for the generated shear strength (peak and post-peak) in the contact surface of this material combination. As such, the relative hardness of sand grains with regard to that of PVC liner material becomes greater with increasing ambient temperature level because of softening of the polymeric geomembrane sheet.

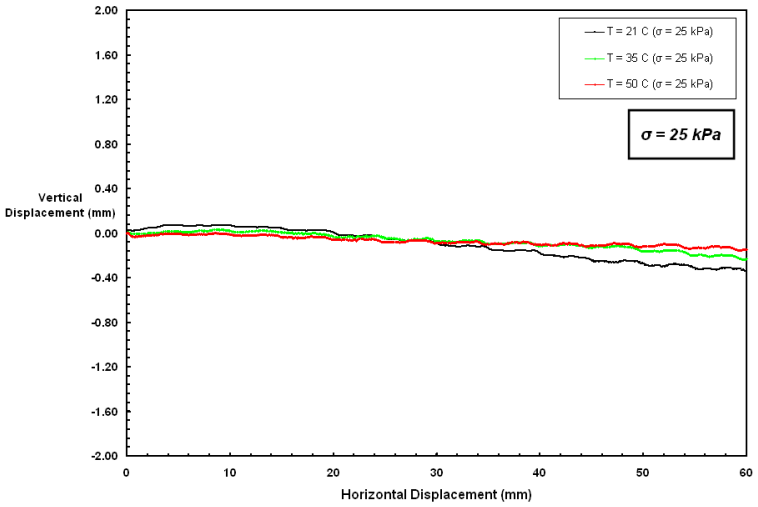

(a)

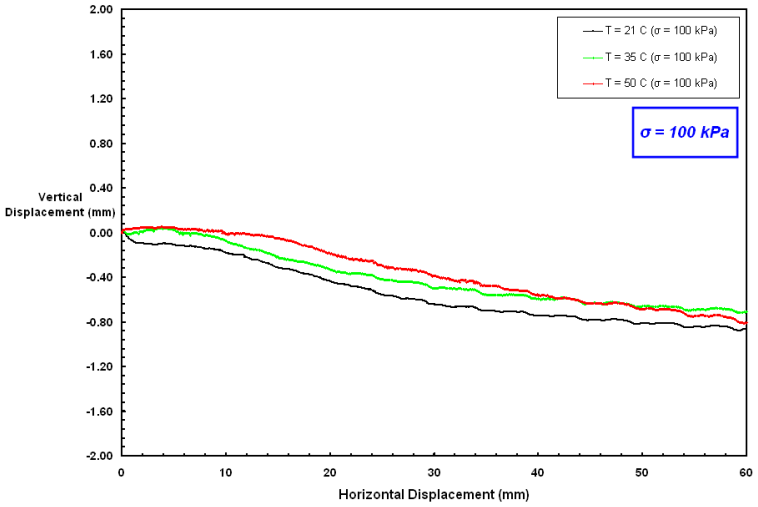

(b)

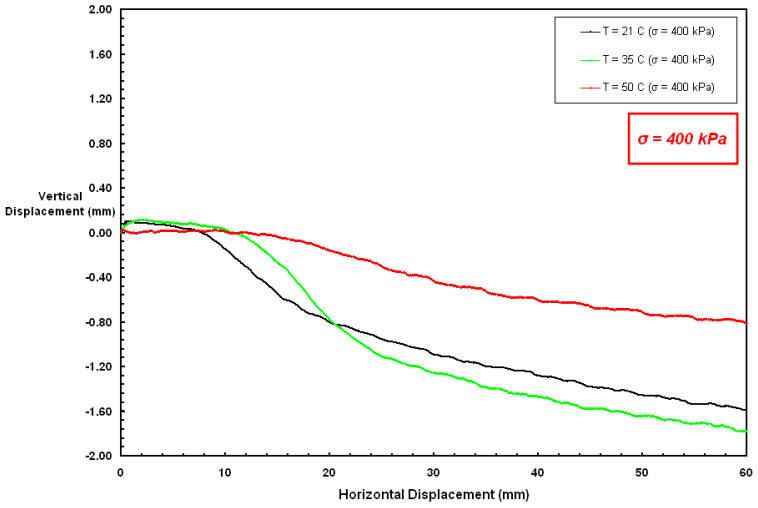

(c)

Figure 8.26 Vertical Displacement – Horizontal Displacement Behavior at Different Temperatures for Blasting Sand/Smooth PVC Geomembrane: 25, 100 and 400 kPa

It was found that the peak interface friction coefficient between angular material and PVC geomembrane decreased with an increase of normal stress (σ) which concurs with the Archard's elastic deformation friction theory. The rate of this reduction depends on the shape (i.e.: angularity) of the sand particles, and most importantly, the hardness of the counterface geomembrane which is strongly influenced by the temperature (Figures 8.27 and 8.28).

The main mechanism for the development of frictional resistance on the contact surface of this material combination is plastic deformation of either one or both of the counterface materials during shearing. Considering the level of normal stresses ($\leq$ 400 kPa) applied throughout the experimental program, the angular sand grains were sufficiently strong and tough to resist plastic deformation. On the other hand, with temperature increase, the geomembrane became softer. Consequently, at higher elevated temperature conditions, the geomembrane deformed plastically more easily against the sand grains due to imposed normal stress on the interface during shearing that resulted in increased penetration and plowing of the sand particles into the surface.

The yielding of one or both of the interface components under the applied loading causing plastic deformations on the materials at the contact surface during the course of shear displacement depends primarily on the *relative hardness* of the counterface materials; and thus, related to the degree of ambient temperature. The plastic deformation component of friction was previously defined by Dove and Frost (1999) such that the geomembrane deforms during grain indentation/penetration into the liner surface. Plastic plowing of the sand grains physically removes the polymer material causing wear on the geomembrane surface. As the temperature and the normal stress applied on the interface

increases, the ability of the soil particles to penetrate into and plow along the geomembrane surface also increases. Therefore, it is considered that both sliding and plowing contribute to the total friction force for angular sand-smooth geomembrane interfaces during shearing at cold temperature conditions due to the harder surface characteristics and stiffness properties of the polymeric lining material. However, it is noted that the magnitude of normal stress on each angular sand particle at the contact surface might be sufficient to exceed the yield strength of the geomembrane; and thereby, the particles would be capable of inducing plastic deformation on hard geomembrane. Therefore, this would add to the total friction force and would result in an increase in the coefficient of friction. For this reason, it should be underlined that the magnitude of normal stress potentially imposed on the layered system during service lifetime is also critical for the mobilization of shear mechanism in addition to the *relative hardness* of the counterface materials. Depending on the hardness of the counterface geomembrane, the coefficient of friction might have continued to decrease due to a decrease in the ambient temperature that would impact the overall design and performance.

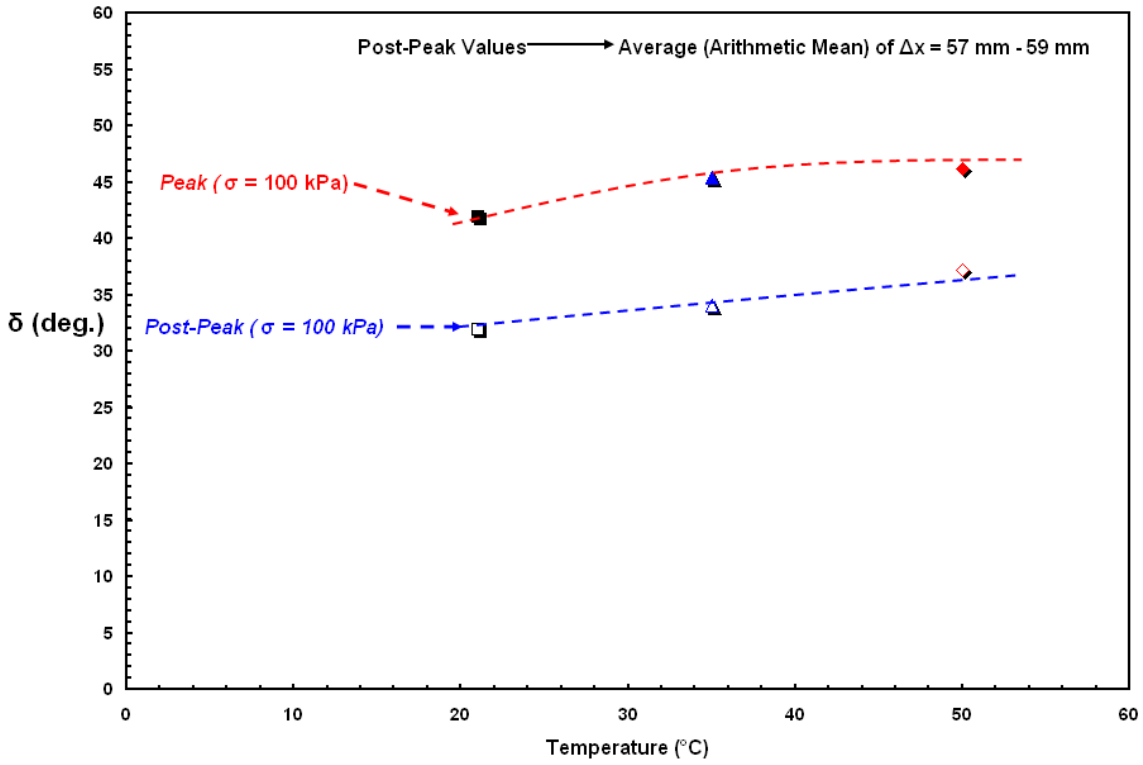

Figure 8.27 The Change in Interface Friction Angle, [δ] with Temperature for Blasting Sand/EPI Smooth PVC Geomembrane Interface

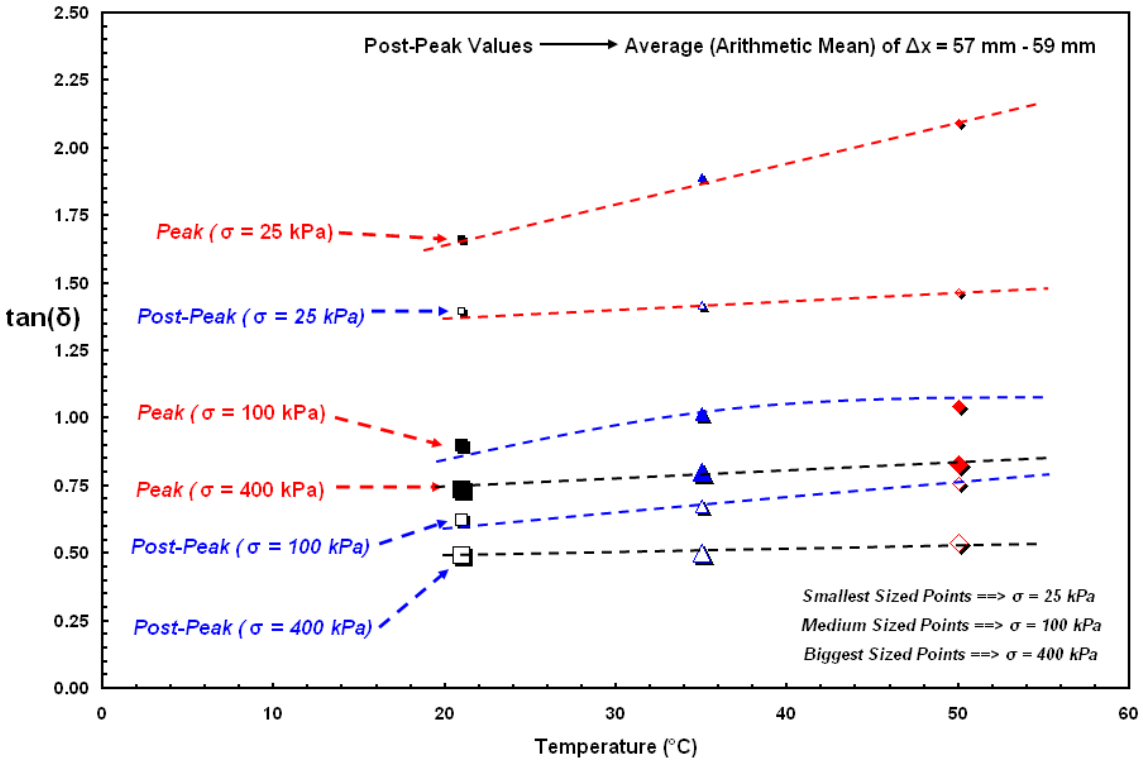

Figure 8.28 The Change in Coefficient of Friction, [tan(δ)] with Temperature at Different Loading Conditions for Blasting Sand/EPI Smooth PVC Geomembrane Interface

The relative contribution of each component of friction depends primarily on the *relative hardness* of the interface components (i.e. strongly temperature dependent for polymeric geomembranes employed in the composite layered system) as well as the level of normal stress and the shape of the sand particles (angular versus rounded). In other words, sand grain shape and geomembrane surface hardness play a significant role in the shear behavior of particulate versus smooth geomembrane interface systems. Similarly, the stress level at the onset of plowing is dependent not only on grain shape but also the relative hardness of the counterfaces.

It is noted that the rounded particulate material system had more brittle interface behavior than the angular blasting material system at all temperatures tested. In contrast to the behavior of angular sand interfaces, strain-softening had been relatively dominant for the shear stress-displacement behavior of the interfaces between rounded particles and particularly relatively hard interface surfaces. However, for both rounded and angular sand interfaces, the ratio of interface shear strength at residual state to that at peak decreased with the increase in the normal stress whereas it increased with increasing temperature. To sum up, as shown in Figures 8.27 and 8.28, the peak and residual strengths increased with the use of angular sand instead of rounded sand all temperatures tested. Additionally, angular sand – smooth PVC geomembrane system mobilized significantly higher peak and substantially larger residual shear strengths than rounded sands with increasing temperature. As such the magnitude of frictional resistance attained at elevated temperatures relative to the shear strength value at room temperature condition was greater for angular sand systems. The experimental data in Figure 8.28 show that both the peak and the post-peak interface friction coefficient (tan(δ)) decreased

with an increase in the normal stress. This relationship concurs with Archard's Theory (Archard, 1957).

Figures 8.29 and 8.30 show the change in $PSR_{Angular/Rounded}$ and $RSR_{Angular/Rounded}$ for smooth PVC geomembrane interface as a function of temperature, respectively. The interface tests performed using angular sands in contact with smooth PVC geomembrane specimens resulted in both higher peak and significantly greater pseudo-residual (post-peak) strengths at all test temperatures. The interface shear behavior observed at different temperatures is predominantly influenced by the particle shape and relative hardness of counterface material components.

Both $PSR_{Angular/Rounded}$ and $RSR_{Angular/Rounded}$ showed an increase up to the elevated temperature level of 35°C beyond which a decrease in the value of the two quantitative parameter until the highest test temperature level (50°C) was observed due to the mobilized ability of the rounded Ottawa 20-30 sand particles at higher elevated temperature conditions to penetrate into and plow along the surface of the softened counterface geomembrane.

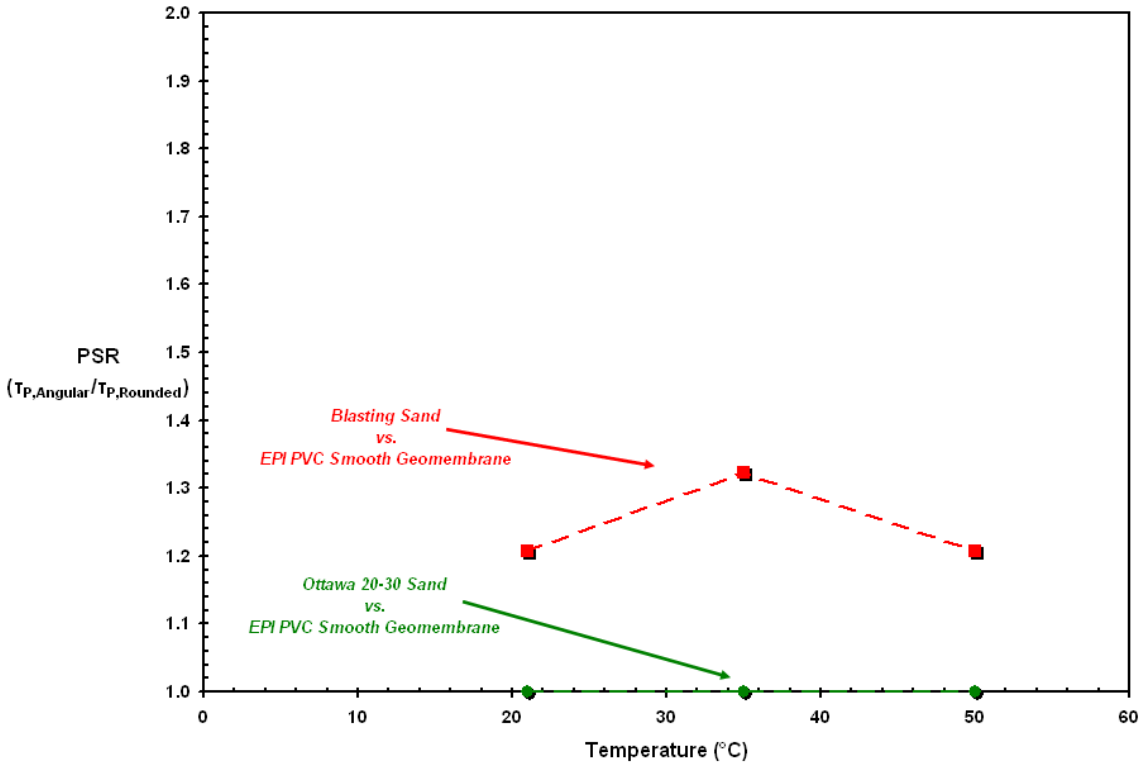

Figure 8.29 Comparative Analysis between Rounded and Angular Material Interfaces for the change in the mobilized Relative *Peak* Shear Strength with Temperature

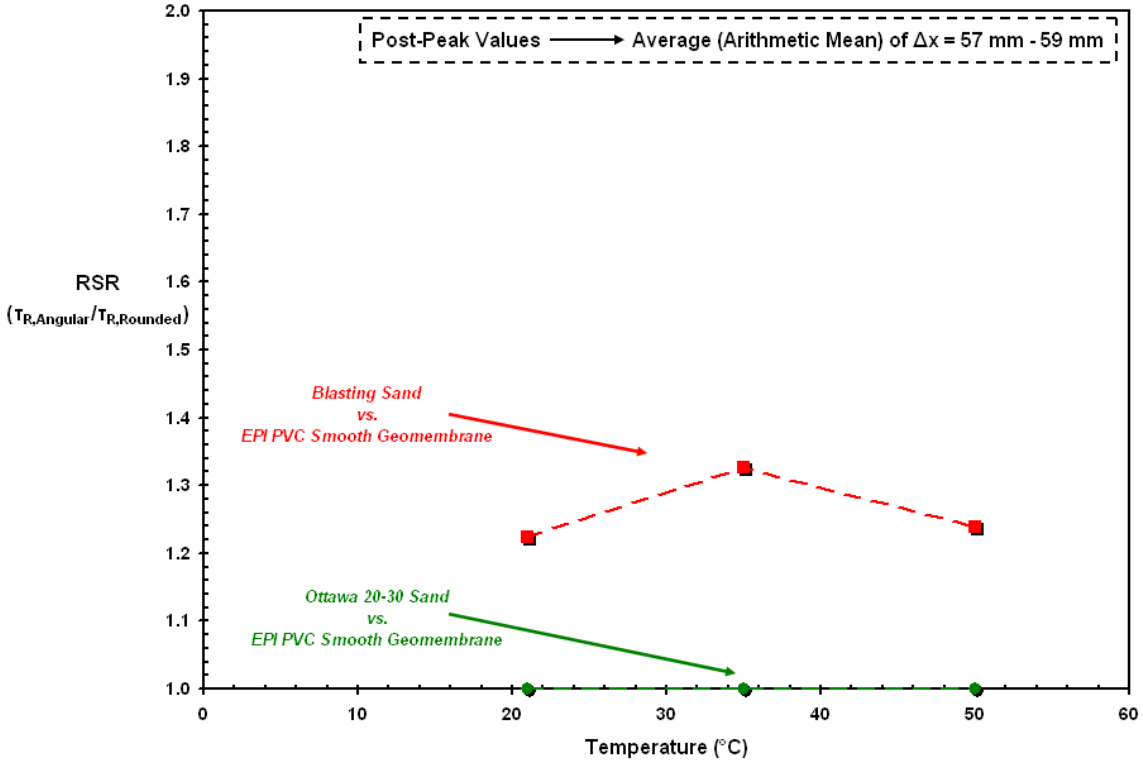

Figure 8.30 Comparative Analysis between Rounded and Angular Material Interfaces for the change in the mobilized Relative *Residual* Shear Strength with Temperature

8.5.2. Failure Envelopes and Comparison of Results at Different Normal Stress Levels

The Mohr-Coulomb failure envelopes mobilized at different temperatures for Blasting angular sand–smooth PVC geomembrane interfaces are plotted and presented in Figure 8.31. There occurs a relatively larger increase in interface shear strength as the temperature is increased with increasing normal stress, resulting in greater non-linearity in the failure envelopes. At lower normal stresses, the increase in interface shear strength is not as pronounced as that at higher normal stresses, and therefore, the non-linearity of failure envelopes reduces at lower normal stresses. This is attributed to the angular sand particles deeper penetration into and/or significant plowing along the geomembrane surface. Moreover, as previously reported by Dove and Frost (1999), particle shape, roughness, normal stress and geomembrane hardness (i.e. strongly temperature dependent and/or varies significantly for geomembrane liners produced from different base polymer resin as HDPE versus PVC) determine which shear mechanism controls the strength behavior of a particulate versus geomembrane combination and directly influences the shape of the stress-displacement failure curve as well as the shape of the conventional strength envelope. As Figure 8.31 shows, both the peak and residual strength envelopes displayed exponential rate of increase. Additionally, the rate of this increase gets higher with increasing normal stress applied on the interface during the tests. Moreover, the strain softening properties of the geosynthetic interfaces means that the determination of the large strain shear strength is of particular importance. Unless rolling/sliding mechanism governs the mobilized frictional resistance, plowing requires additional

energy to move particles through the counterface material; thereby, the peak strength increases at a higher rate than the normal stress. The failure envelopes (peak and residual) were replotted on logarithmic scales as shown in Figure 8.32. The degree of plowing shear mechanism in influencing the mobilized interface strength is directly dependent on two primary factors (sand grain shape and counterface material hardness). Further, the effect of temperature on the mobilized magnitudes of interface shear strength values (both peak and pseudo-residual) attained during the interface tests are consistent with polymer softening at higher temperatures. Sand particles embedded fully into the geomembrane surface and plowed deeper trenches in the surface of the geomembrane during the course of shear displacement at elevated temperatures and the occurrence of this shear mechanism increased under larger loading conditions. As a result, substantially increased/improved frictional resistance was mobilized at the interface in addition to that mobilized at lower temperatures. The onset and the development of plowing mechanism depends upon the temperature, the type of geomembrane, and the type of sand used and therefore, these factors must be incorporated in to the design process. Additionally, this can be considered as further evidence that the design and the interface frictional performance of geosynthetic composite layered systems are project-specific and site-conditions-dependent; therby, project-specific testing on these materials should be carried out for design purposes.

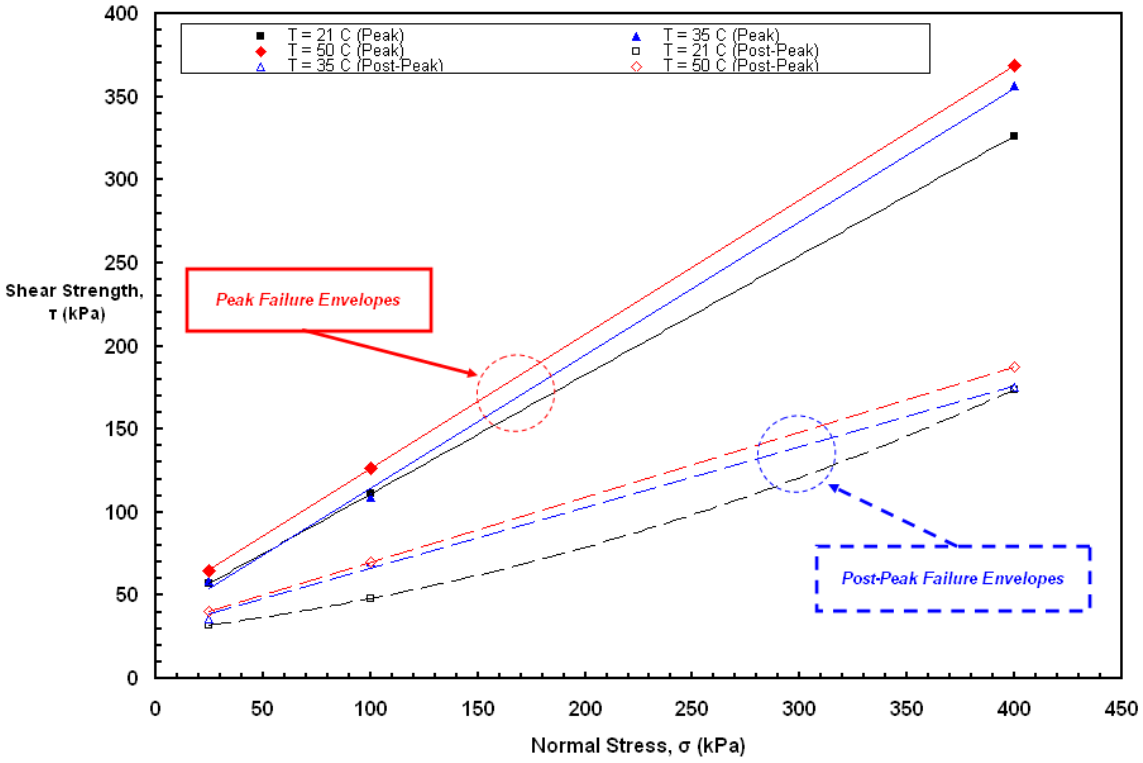

Figure 8.31 The Alteration of Peak and Residual Strength Envelopes with Increasing Temperature for Blasting Sand/EPI Smooth PVC Geomembrane Interfaces

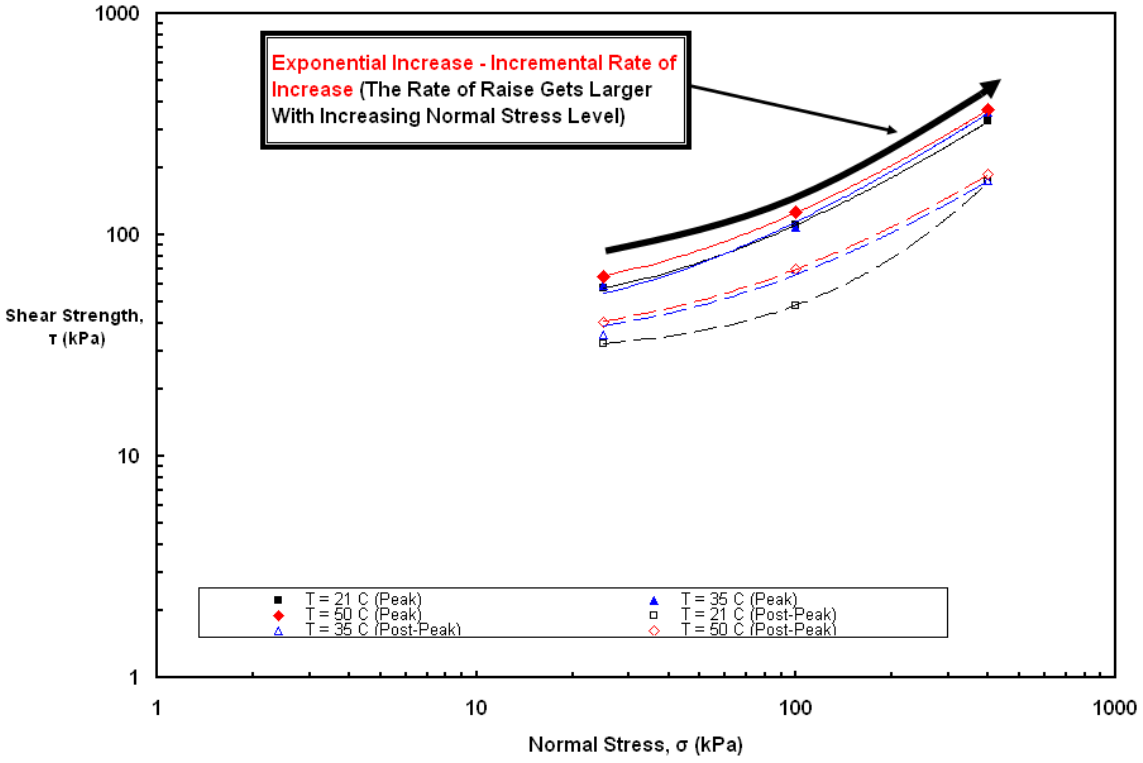

Figure 8.32 The Transformation in Failure Envelopes with Temperature at Different Loading Conditions for Blasting Sand/EPI Smooth PVC Geomembrane Interface

8.6. Comparative Analysis on Relative Contribution of Primary Factors Governing Interface Shear Behavior and the Mobilized Frictional Mechanism

8.6.1. Influence of Angularity of Particles

Figures 8.33 and 8.34 present the comparison of shear stress versus horizontal displacement failure relationships for rounded Ottawa 20-30 and angular Blasting Sands tested at different temperatures ranging from 21°C to 50°C against smooth HDPE or PVC geomembrane, respectively, under 400 kPa normal stress. The failure curves for the rounded sand exhibited an obvious peak; whereas, the failure curves for the angular material did not display such an obvious peak response stage, particularly at lower test temperatures. However as the ambient temperature increased, the appearance of a peak region became more discernible through the shape of the stress-displacement curves at higher elevated temperatures due to softening of the counterface geomembrane and more severe penetration of the angular sand particles into the surface. Compared with Ottawa 20-30, the angular Blasting sand showed substantially higher interface strength characteristics regardless of test temperature level, and required larger horizontal displacements to reach both peak and residual state. Over the entire range of test temperatures, the rounded Ottawa 20-30 sand displayed post-peak strain-softening behavior. In contrast, the angular Blasting sand demonstrated approximately post-peak plastic behavior in terms of the developed shear response in contact with smooth geomembrane liners, particularly at lower temperatures. This phenomenon is principally attributed to the amount of sand particle rearrangement occurring during shearing process as the Blasting sand is an angular material and possesses higher internal friction. As a

result, the particles on the interface surface are less likely to be rearranged during the course of shear displacement unless the applied shear stress on the interface is sufficiently large to overcome the internal friction of the particulate material itself.

In general, the restriction of sand particle rearrangement at and/or beyond the contact surface results in the interface reaching residual strength at low deformations. On the other hand, the rearrangement of the particles near the contact surface occurs with ease as the smoother rounded nature of Ottawa 20-30 sand grains facilitates this mechanism. Additionally, Blasting sand grains possess relatively rough surface characteristics as compared to Ottawa 20-30 grains. As such, particles with smoother surface are more readily able to move relative to each other during shear displacement. This was confirmed and demonstrated through the developed shape of the failure curves that the rounded sand required less horizontal displacement to reach the peak stress than the angular sand at all temperatures tested.

The other important aspect of the generated stress versus displacement curves at different temperatures is that the transition of the curves for the rounded sand from pre-peak to post-peak behavior is brittle as a result of rapid development of slippage for the rounded particulate material. As shown in Figures 8.33 and 8.34, the Blasting sand interface at higher temperatures exhibited more apparent peak state in shear stress-displacement curves than that at low tests temperature levels. This observed behavior resulted from more indentation of sand particles into the surface of the geomembrane specimen which was the primary mechanism that promoted more particle rearrangement at contact surface as well as within the sand structure.

The friction behavior of the rounded Ottawa 20-30 sand differs significantly from the behavior of the angular Blasting sand, particularly at low temperatures (e.g.: 21°C) due to sliding being the predominate mechanism of interface shear. It is expected and very reasonable that an angular material displays higher shear strength properties than a round material as evident that the angular particles are more interlocked and hence, more resistant to shear displacement (Table 8.1). Further, the angular sand particles required longer shearing displacements to rearrange into a residual state than the round particles. The volumetric dilative/contractive behavior of the angular sand is primarily resulting from particle interlocking being present against shear movement. Increased particle embedment into the geomembrane surface with increased normal stress level facilitates the initiation of the transition of the volumetric behavior from dilative to contractive. Volumetric behavior in the dense sand specimen was dilative for the used normal stresses ranging from 25 kPa to 400 kPa. It is deemed, in the condition that normal stresses over 500 – 600 kPa are applied to dense specimens of the used sands composed of strong and durable grains, then the specimen may initially contract and later, will dilate to a net volumetric change resulting in an overall dilative response. The presence of dilation with shearing indicates the presence of some degree of particle indentation, interlocking, and plowing as the dilative behavior requires the rearrangement of the angular particles at and/or beyond the contact surface. The increase in dilation with an increment in ambient test temperature also reflects increased embedment/penetration, interlocking, and thus stronger plowing along the surface of the smooth geomembrane.

Table 8.1 The Peak and Residual Friction Values of Direct Shear Tests on Ottawa 20/30 and Blasting Sands (Iscimen, 2004)

Sand Type	Normal Stress [kPa]	Relative Density [%]	Peak Force		Residual Force		Friction Angle	
			Normal [lb]	Shear [lb]	Normal [lb]	Shear [lb]	Peak (tanδ)	Res. (tanδ)
Ottawa 20/30	80	81.3	57.3	49.1	56.8	32.7	38.9 (0.81)	27.9 (0.53)
	120	73.0	85.5	70.6	85.3	48.3		
	160	77.8	114.2	95.1	113.8	62.8		
Blasting	80	78.0	57.0	89.4	56.9	59.3	43.1 (0.94)	34.6 (0.69)
	120	80.1	85.7	112.1	85.4	79.8		
	160	75.4	114.0	142.7	113.8	98.6		

Moreover, as previously indicated, the angularity of particles influences the behavior of interfaces such that rounded materials yield notably brittle interface behavior as compared to angular materials. This is considered due to the fact that the rounded particle shape of the Ottawa 20-30 sand results in reduced interlocking between particles and the geomembrane compared to the Blasting sand. Further, it is noted that sliding along the geomembrane contact surface is the primary interface shearing mode at lower temperature conditions such as the room temperature. Compared with the results of the angular sand system, the peak shear strength for the rounded systems is mobilized at very small interface displacements (0.5 – 1 mm) after which a considerably greater strain-softening is observed before a stable residual shear strength value is reached.

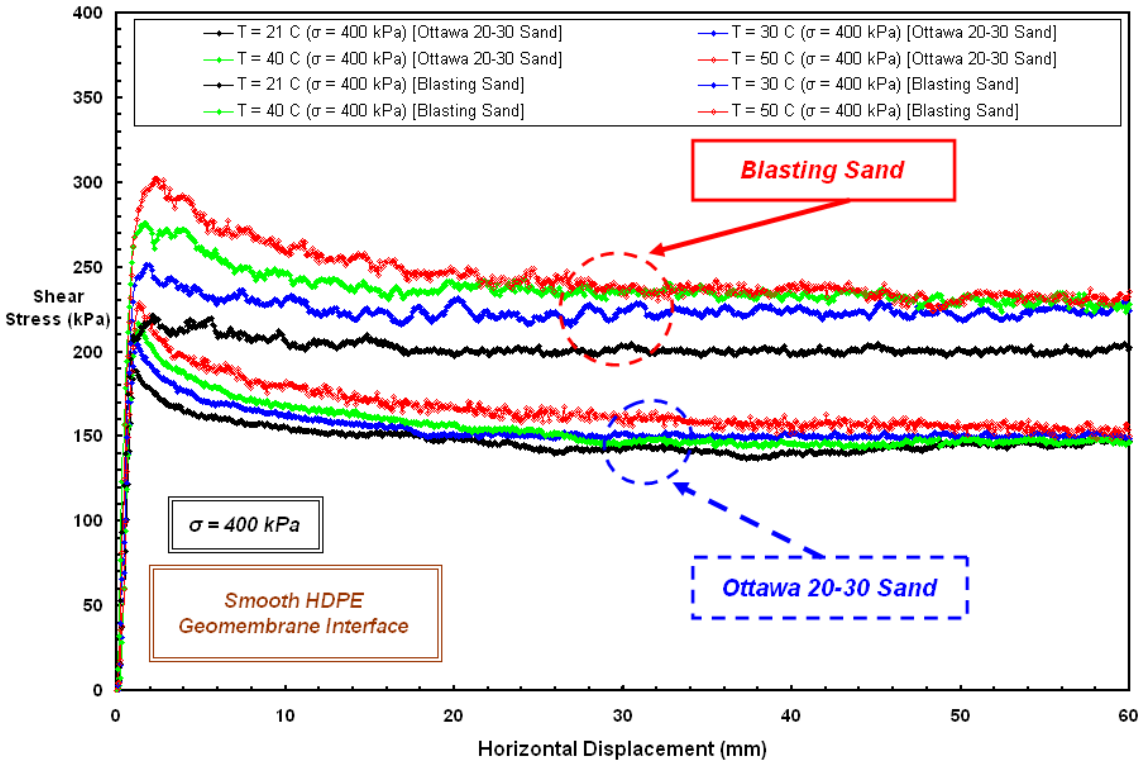

Figure 8.33 Influence of Sand Grain Shape (i.e. Angularity of Particles) on the Resulted Interface Shear Behavior Developed at Different Temperatures: HDPE Geomembrane

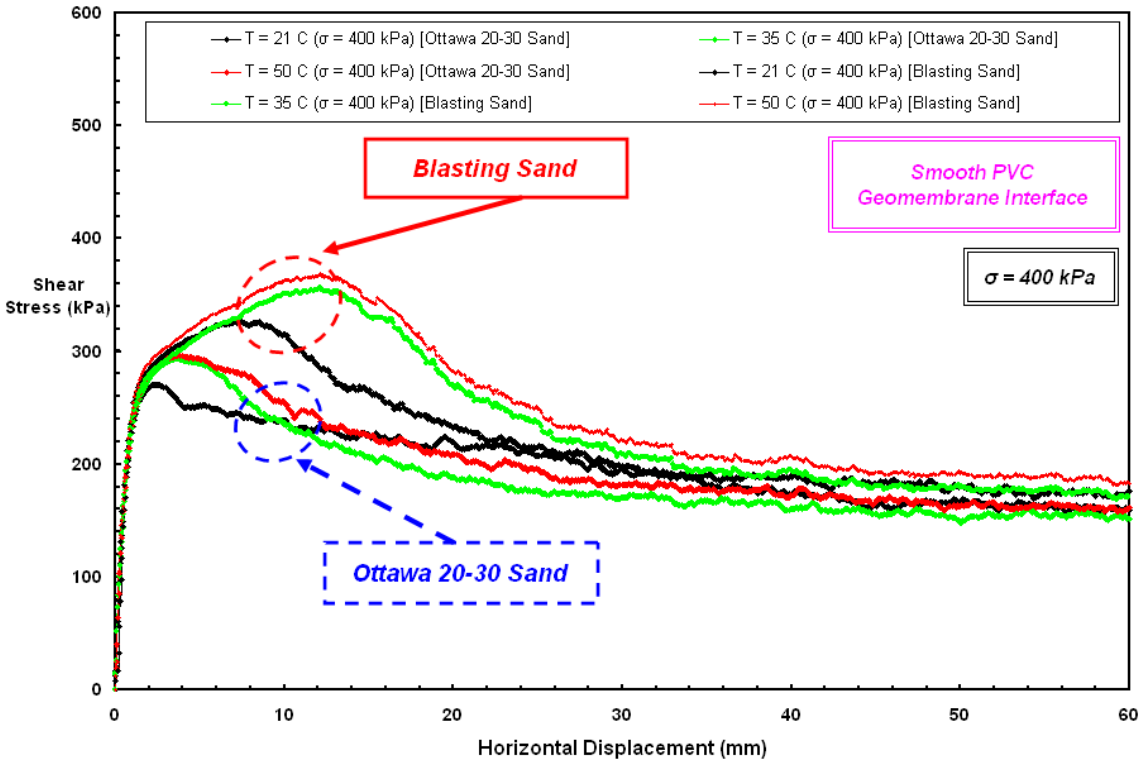

Figure 8.34 Influence of Sand Grain Shape (i.e. Angularity of Particles) on the Resulted Interface Shear Behavior Developed at Different Temperatures: PVC Geomembrane

The difference in the interface shear behavior as seen in the preceding figures is attributed to the difference in particle angularity of these two sand types used in the testing program. These trends of shear stress-displacement curves were consistent throughout the various test temperatures at which sand (rounded, angular) – smooth (HDPE or PVC) geomembrane combinations were tested. They are attributed to the fact that this difference in the general characteristic of the stress-displacement failure curves for rounded and angular sands result from different interface shear mechanisms developed at the interfaces: merely sliding of the particles against the geomembrane at low temperatures, and predominantly sliding along with a marginal contribution of plowing against the geomembrane at high temperatures due to a decrease in surface hardness of the polymeric lining material for Ottawa 20-30 rounded sand versus smooth HDPE or PVC liner interfaces, however, plowing of the sharp angular sand particles against the geomembrane and increased magnitude of this plowing mechanism along with greater indentation as well as a greater amount of plowing of the particles into the surface of the geomembrane for Blasting angular sand versus smooth HDPE or PVC liner interfaces.

The angular shape features of the sand particles promotes the occurrence of higher plowing effects such as plastic deformation and destructive material dislocations on the contact surface of the smooth geomembrane adjacent to the sand specimen along with cooperative contribution of elevated temperatures causing a substantial reduction in surface hardness of the counterface polymeric material. The influence of normal stress was relatively small as compared with other parameters within the ranges examined in this study. Further, it is noted that for the interface between Ottawa 20-30 and smooth

HDPE geomembrane at low temperatures (e.g. 21°C), no significant plowing effect was observed on post-test geomembrane specimens. Therefore, the onset of plowing is primarily a function of particle shape as well as the temperature dependent relative hardness of the counterface materials. As such the angular Blasting sand that has a much lower fullness ratio as compared to that of rounded Ottawa 20-30 sand exhibits plowing regardless of test temperature at all stress levels. Furthermore, since the Ottawa 20-30 sand particles are subrounded to rounded, the contact area between the particles and the geomembrane is relatively constant. On the contrary, for the case of the blasting sand, large contact stresses can develop at particle-geomembrane contacts at a highly angular feature on the particle. Plowing will most likely initiate at the locations of high stress concentrations (Dove, 1996). Therefore, increasing the angularity of the soil particle increased the amount of plowing into the surface of the geomembrane and resulting in higher strength of the interface at each test temperature for Blasting sand compared to Ottawa 20/30. The contact stresses are not large enough to overcome the yield stress of the geomembrane for Ottawa 20/30-geomembrane interfaces at cooler temperatures and the particles primarily slid along the interface, with minimal surficial damage. On the other hand, the particles penetrated more into the geomembrane at even small displacements and continued to do so during shearing to the residual state for Blasting sand-geomembrane interfaces. In summary, the interface direct shear tests results at all test temperatures show that the greatest shear strengths were obtained with the angular blasting sand (Figure 8.35).

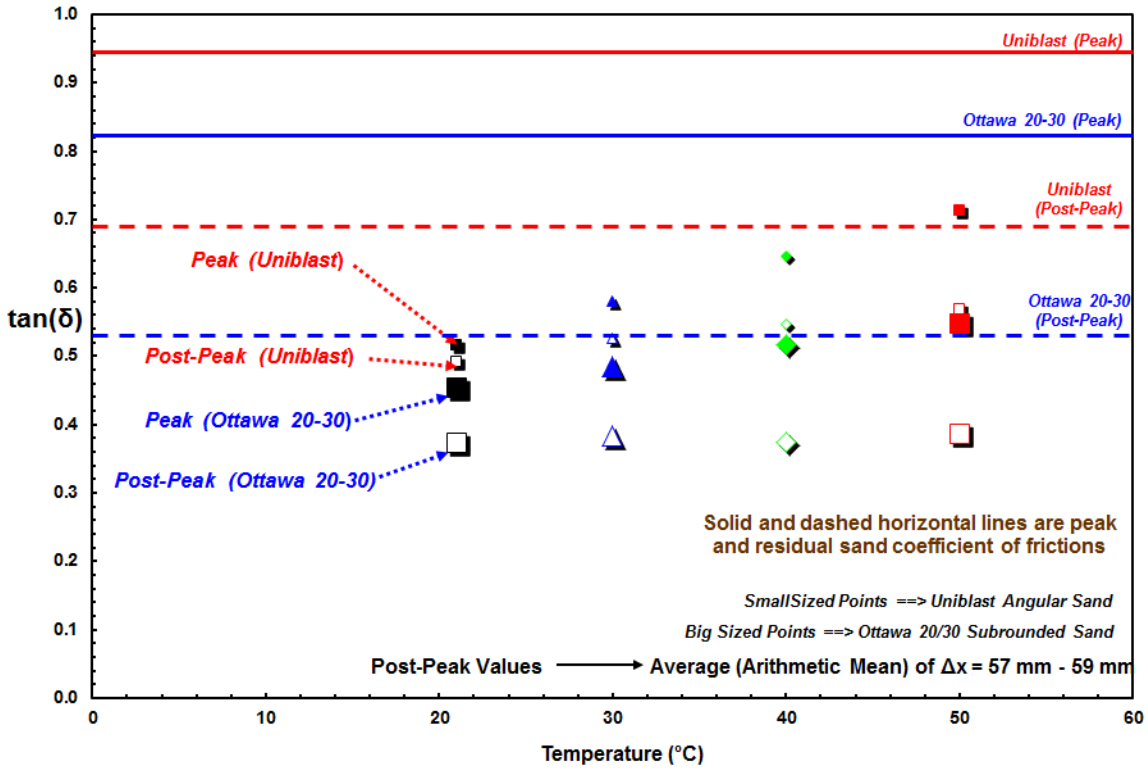

Figure 8.35 Influence of Sand Particle Angularity/Roundedness on Peak and Residual Frictional Shear Strengths Mobilized at Different Temperatures

As Figure 8.35 shows, the resulting peak and post-peak coefficient of friction values of the angular material interface was consistently larger than those of the rounded material interface at all temperatures tested (21°C to 50°C). In addition, with increasing ambient temperature, the angular sand interface exhibited higher increase in the resulting value of peak shear strength ($\tan(\delta_P)$ = ~0.52 to ~0.69 and ~0.45 to ~0.53 for Blasting and Ottawa 20/30 sand interface, respectively) as well as in the magnitude of residual frictional resistance ($\tan(\delta_R)$ = ~0.48 to ~0.55 and ~0.35 to ~0.36 for Blasting and Ottawa 20/30 sand interface, respectively) being generated during shear displacement than the rounded sand interface. This is primarily due to the ability of the angular particles to plow deeper into the geomembrane surface which is also attributed to the large contact stresses

induced by the angular features of the particles at sand-geomembrane interface. An investigation of shear mechanisms by Dove and Frost (1999) mobilized at interfaces between particles and relatively smooth materials using contact mechanics and basic friction theory originally revealed that a combination of sliding and plowing governs dense rounded Ottawa 20-30 sand versus smooth HDPE geomembrane peak interface shear behavior. At higher elevated temperatures, when the onset of plowing of rounded sand grains is mobilized considerably, this results in an increasing peak friction coefficient with increasing normal stress and can produce an upward curvature of the strength/failure envelope above a critical stress level.

In summary, the results presented below in Figure 8.35 indicate that for smooth geomembrane and particulate material interface systems, particle shape is an important governing factor in determining the response of the system. For rounded smooth particles, the measured friction coefficient is relatively low at all temperatures tested and plowing mechanism is not a significant contributor to the developed interface behavior. In contrast, angular and rougher particles display relatively larger coefficients of friction and plowing phenomenon predominates the frictional response at even low temperatures. It is evident that two principle mechanisms are operative in the shearing of the rounded material on the smooth HDPE geomembrane: i) the first is elastic sliding; ii) the second is plastic plowing effect of soil particles into the geomembrane at elevated temperature conditions, and hence the total friction force is the summation of sliding and plowing. The level of ambient test temperature mainly influences the occurrence of these mechanisms and their relative contribution to, or comparative importance in the mobilized frictional resistance.

8.6.2. Influence of Surface Hardness of Continuum Materials

The significant influence of the geomembrane hardness on interface shear behavior including peak and residual states is evident from the results for the rounded and the angular sand interface systems shown in Figures 8.36 and 8.37, respectively. For the softer smooth PVC geomembrane (i.e. possessing lower degree surface hardness), the mobilized peak interface frictional resistance is greater than the harder smooth HDPE geomembrane at corresponding test temperature conditions when sheared against the same particulate materials (either rounded Ottawa 20-30 sand or angular Blasting sand). The average surface roughnesses are in general comparable for both the lining materials but slightly higher for the smooth PVC geomembrane ($R_{a\ PVC}$ = 0.17 μm > $R_{a\ HDPE}$ = 0.13 μm). It is noted that this difference in surface roughnesses would also contribute slightly to the larger frictional resistance of the smooth PVC liner interface. The larger peak shear strengths mobilized, particularly for the angular material interfaces (i.e. 1.8 times) compared to the rounded material interfaces (i.e. 1.4 times) over the entire test temperature ranging from 21°C to 50°C are primarily due to a significant difference in the degree of surface hardness of the continuum materials. For the granular soil and geomembrane layered systems, the lower degree of surface hardness results in deeper penetration of the sand particles into the geomembrane and greater amount of plowing of the geomembrane during shear displacement. Therefore, the interfacial frictional resistance increases as additional force is required to abrade/wear, or damage the geomembrane surface as well as to achieve local material dislocations over the interfacial areal extent of the liner sheet in contact with a granular material.

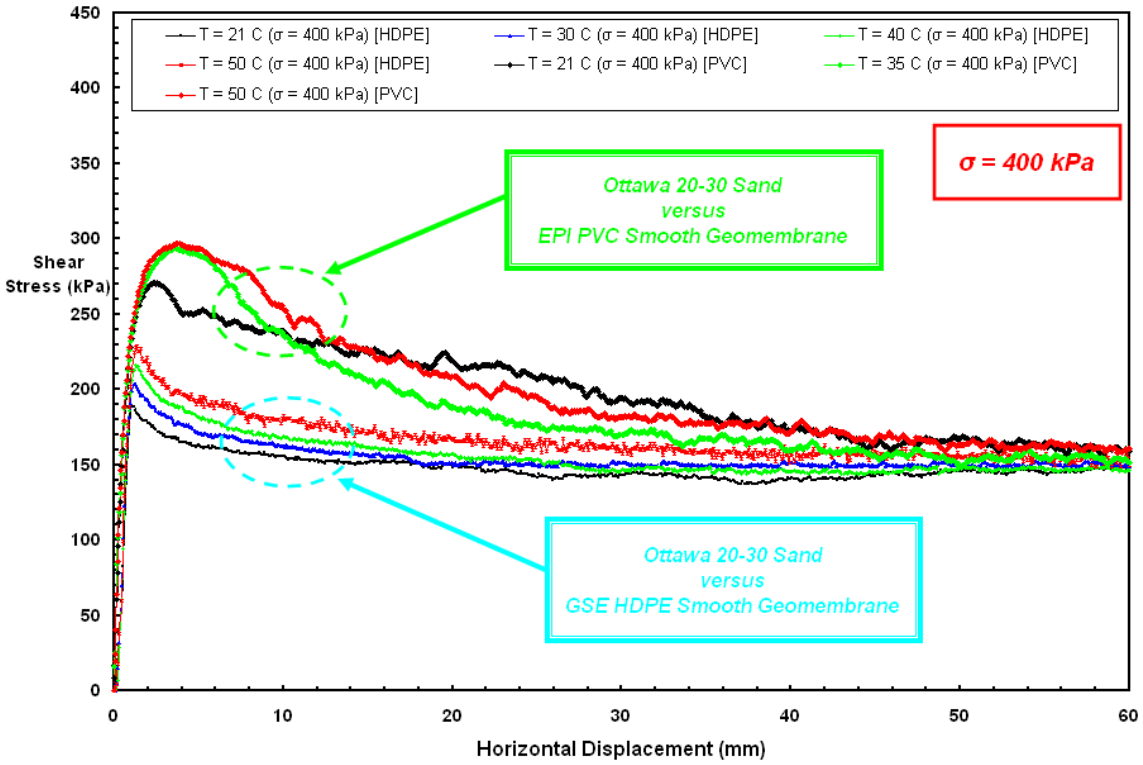

Figure 8.36 Comparison of Shear Stress – Displacement Curves developed at Different Temperatures: Ottawa 20-30 Sand versus Smooth HDPE or PVC Geomembrane Interface

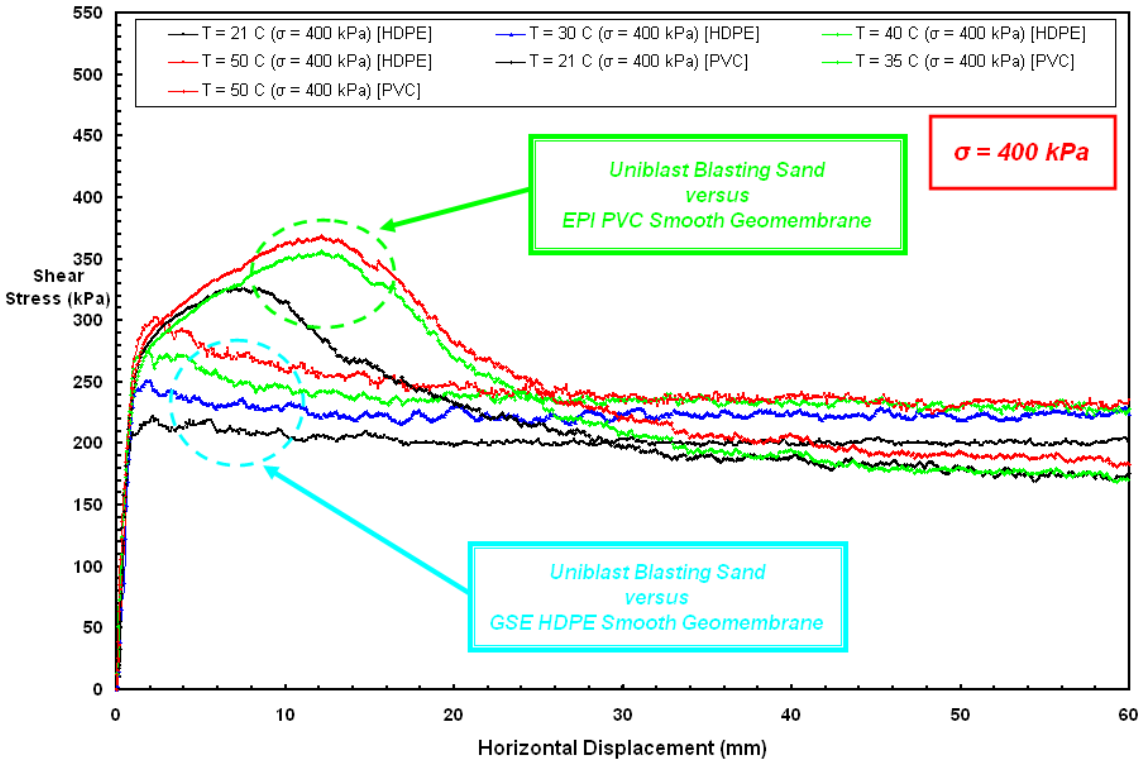

Figure 8.37 Comparison of Shear Stress – Displacement Curves developed at Different Temperatures: Blasting Sand versus Smooth HDPE or PVC Geomembrane Interface

The embedding and onset of particle plowing on the geomembrane surface at low shear displacements such as at pre-peak, peak states results in a relatively large peak strengths. However, this favorable impact of this shear mechanism diminishes once plowing has been initiated for the softer materials such as PVC geomembrane liners as evidently seen through the post-peak stages of the developed stress-displacement curves at different test temperature conditions as shown in Figures 8.36 and 8.37. In particular for the rounded sand systems, in residual shearing, a steady-state shearing condition of particle sliding with a marginally slight contribution of plowing at 100 kPa normal stress exists for both the HDPE and the PVC smooth geomembranes. As such, during the course of residual state, the magnitude of contact point stresses is proportional to the global normal stress provided that it is nearly equivalent and/or slightly greater than the threshold value of the yield strength of the counterface continuum geomembrane. The softer PVC geomembrane interfaces exhibited greater displacement-softening behavior. This shear response observed is attributed to the amount of particle rearrangement that can occur in the course of shearing. Since the frictional resistance of the relatively harder HDPE geomembrane against the shearing of the sand particles is more likely to cause a rearrangement in the sand structure during shear displacement. Further, in particular for the Ottawa 20-30 sand and smooth HDPE geomembrane interface, the transition of the curves from the pre-peak to the post-peak behavior is brittle in nature (i.e. rapid transformation) at all test temperatures. The Blasting sand and smooth PVC geomembrane interface displayed a more obvious peak stress state as being evident through the developed shape of the shear stress-horizontal displacement curves. The greater amount of dilatancy observed in the sand mass at higher test temperatures in the

course of the interface shear tests confirms that the sand specimen was more disturbed as a result of an increase in frictional resistance generated at the interface due to plowing mechanism. This can be considered as analogous to the phenomenon that if the roughness of the interface is increased, then dilatancy of the sand would be expected to occur at greater amounts (Lee, 1998). The difference between the peak stress and the steady-state (i.e. residual) stress is largest for sand alone shear tests (Lehane et al., 1993); and the value of this difference reduces successively to lesser amounts for sand – PVC geomembrane (i.e. lower surface hardness) interface shear tests. It is smallest for sand – HDPE geomembrane (i.e. higher surface hardness) interface shear tests which concurs with the findings of O'Rourke et al. (1990).

8.7. Further Analyses, Discussions and Comparisons on Entire Test Results

The interface shear test results showed that the angular Blasting sand interface exhibited consistently larger peak and residual shear strengths compared to the test results of the rounded Ottawa 20/30 sand at all temperatures ranging from 21°C to 50°C. This is considered to be due to higher angularity of the particles of the Blasting sand. Therefore, the shape of granular soil particles was found to be an important factor on the exhibited larger shear response and the mobilized greater frictional resistance of the angular material interface when sheared against smooth HDPE or PVC geomembrane liner materials. The resultant values of the peak and post-peak friction coefficients mobilized during shear for the tested particulate (angular, rounded) – smooth geomembrane (HDPE, PVC) interfaces as a function of the ambient temperature are shown in Figures 8.38 and 8.39, respectively.

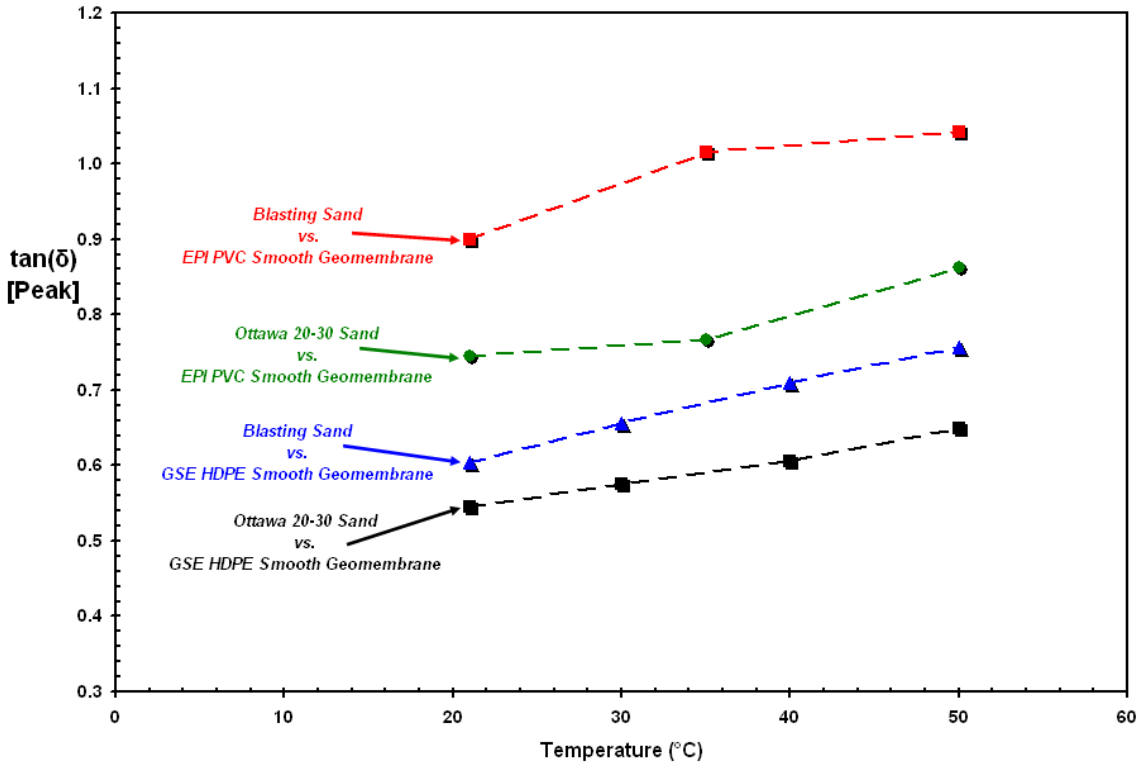

Figure 8.38 Comparison for the Variation of *Peak* Friction Coefficient with Temperature for Sand (Rounded, Angular) – Smooth Geomembrane (HDPE, PVC) Interfaces

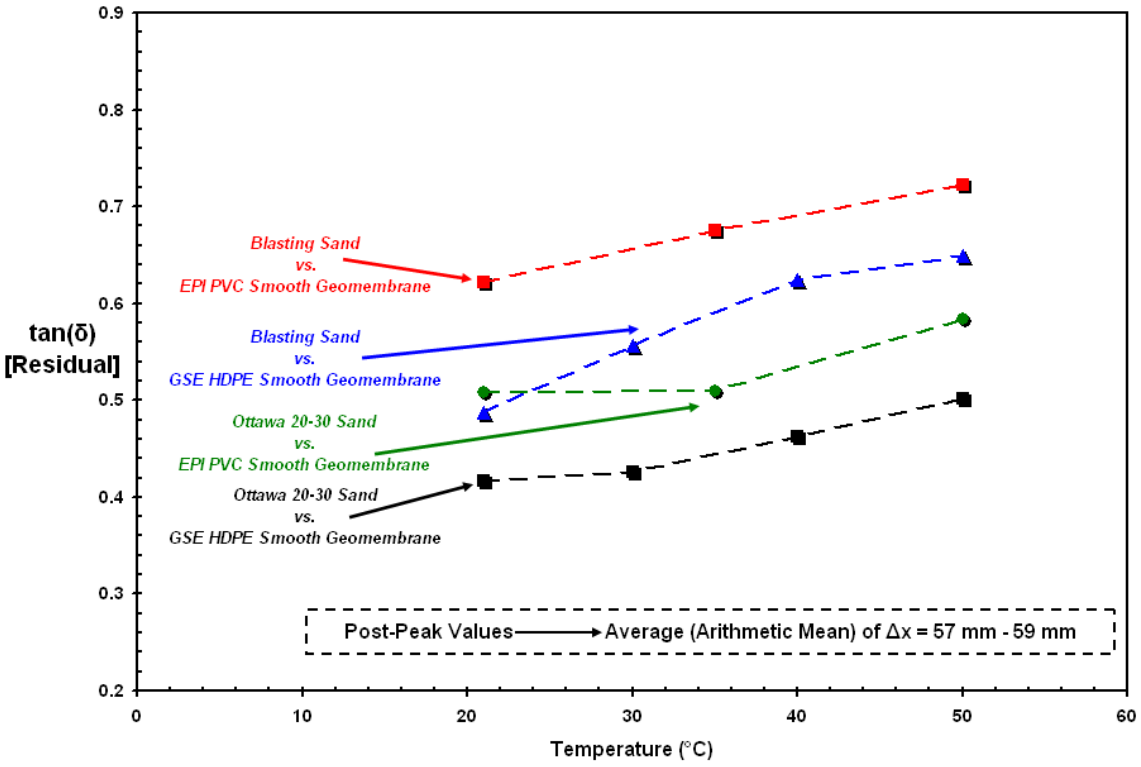

Figure 8.39 Comparison for Variation of *Residual* Friction Coefficient with Temperature for Sand (Rounded, Angular) – Smooth Geomembrane (HDPE, PVC) Interfaces

The angular material sheared against smooth HDPE or PVC geomembranes displayed a higher increase in the value of peak and post-peak strength with temperature compared to that of the rounded material cases. In particular, the Blasting sand showed a larger increase in the magnitude of the mobilized post-peak frictional resistance with increasing test temperature due to the higher contribution of the deeper penetration of the sand grains into the surface of the counterface geomembrane and thus, the frictional behavior during shearing was dominated by the plowing mechanism induced particularly at higher temperatures due to the reduced surface hardness of the counterface geomembrane. Further, the softer smooth PVC liner – rounded or angular particulate layered systems exhibited larger shear resistances compared to the mobilized shear strengths of the relatively harder smooth HDPE geomembrane – rounded or angular particulate interfaces regardless of ambient test temperature.

As discussed previously in this chapter, the stress – displacement curves consistently located at higher shear stress versus horizontal displacement space over the test temperature range. Accordingly, the measured surface reliefs of the geomembrane specimens after the interface shear tests at different temperatures in terms of the created post-test surface roughness of the two geomembranes (HDPE, PVC) demonstrated similar behavior that the increased ambient test temperature level resulted in the larger plowing effect (i.e. peaks and troughs in the post-test roughness profiles) induced during shearing. This is accompanied by greater peak and residual frictional resistances occurring at higher elevated temperatures. The angular sand grains induced deeper grooves on the surface of the counterface geomembrane specimens. This is due to the fact that the relatively sharper angular particles (compared to rounded ones) continuously

abraded/wore the liner surface in the contact area as the shearing reached larger displacements resulting in substantially greater residual frictional resistances mobilized at the interface.

The coefficient of friction (peak and post-peak) versus normal stress plotted on log-log scales are shown in Figures 8.40, 8.41, 8.42 and 8.43 for the lowest (21°C) as well as the highest (50°C) test temperatures for Ottawa 20-30 sand – smooth HDPE geomembrane, Blasting sand – smooth HDPE geomembrane, Ottawa 20-30 sand – smooth PVC geomembrane and Blasting sand – smooth PVC geomembrane interfaces, respectively. The coefficient of friction for the tested sand (rounded, angular) – smooth geomembrane (HDPE, PVC) interfaces decreased with normal stress at low normal stress levels up to ~100 that is consistent with Hertzian contact theory (Johnson 1982). Under higher normal stresses, the coefficient of friction became constant or continued to decrease slightly with normal stress. This is considered to be the influence of the plowing effect that often occurs at a granular material/planar surface interface as previously noted by Dove and Frost (1999).

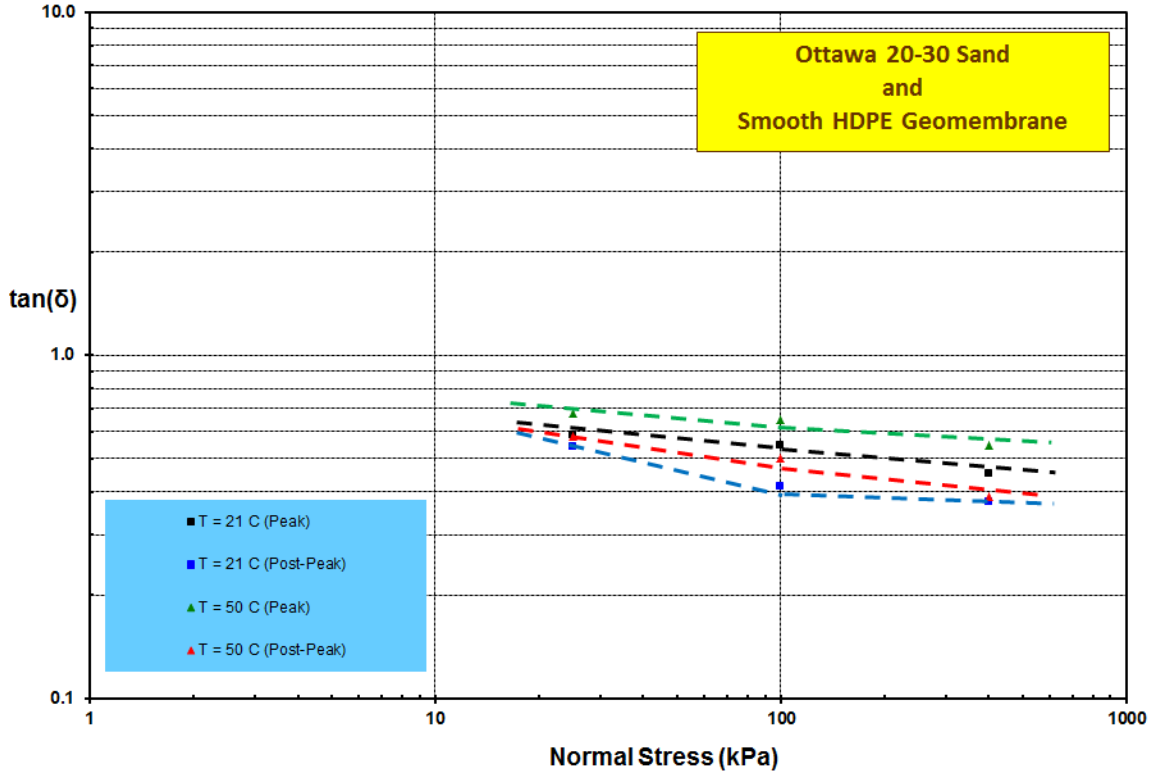

Figure 8.40 Log Coefficient of Friction [tan(δ)] versus Log Normal Stress [σ] Plots for Ottawa 20-30 Sand – Smooth HDPE Geomembrane Interface

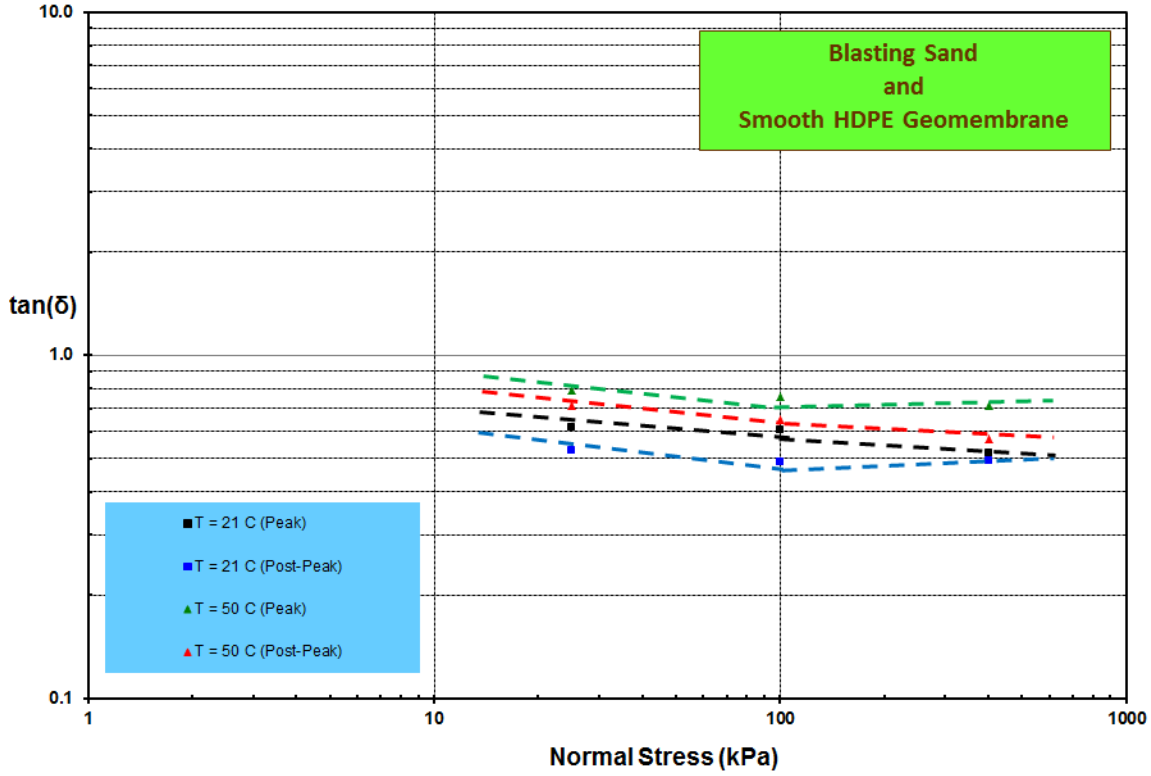

Figure 8.41 Log Coefficient of Friction [tan(δ)] versus Log Normal Stress [σ] Plots for Blasting Sand – Smooth HDPE Geomembrane Interface

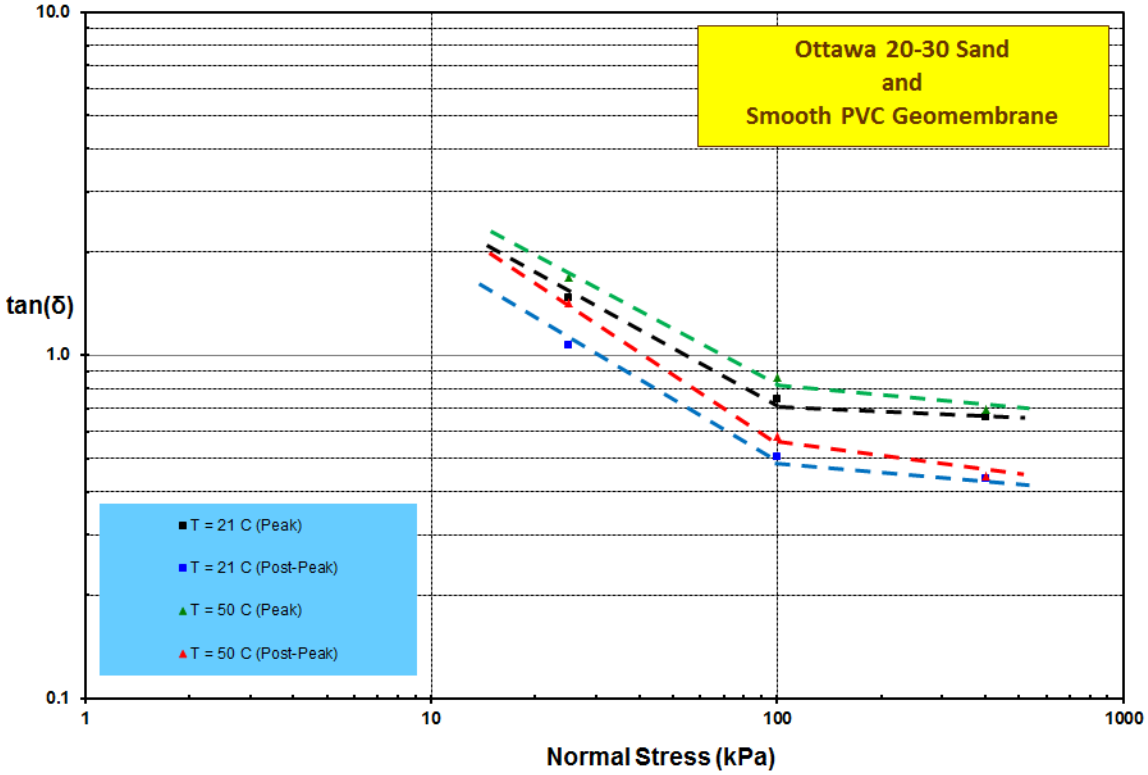

Figure 8.42 Log Coefficient of Friction [tan(δ)] versus Log Normal Stress [σ] Plots for Ottawa 20-30 Sand – Smooth PVC Geomembrane Interface

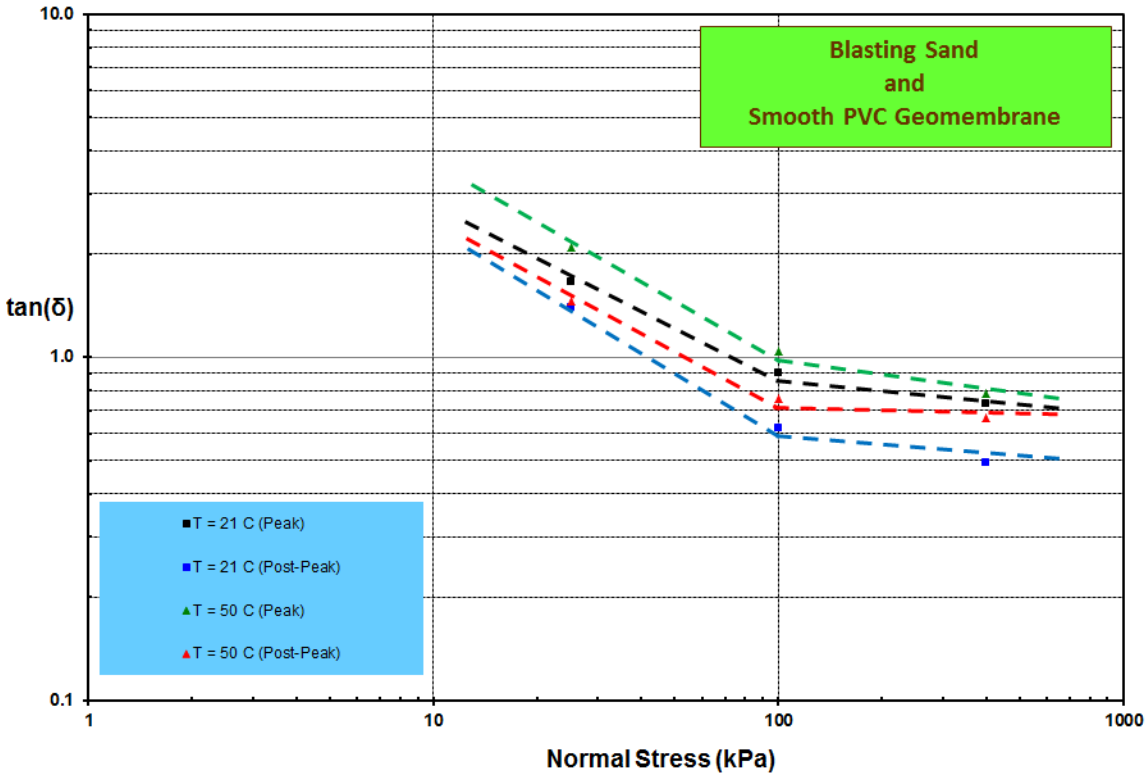

Figure 8.43 Log Coefficient of Friction [tan(δ)] versus Log Normal Stress [σ] Plots for Blasting Sand – Smooth PVC Geomembrane Interface

A useful measure to quantatively show the differences between the peak stress state relative to the residual response of the tested sand – smooth geomembrane interfaces as a function of the temperature is the interface sensitivity, (S_τ) (Equation 8.2):

$$S\tau = \left(\frac{\tau_{Peak}}{\tau_{Residual}} \right) \tag{8.2}$$

Where;

$S\tau$: Interface Sensitivity

τ_{Peak}: Mobilized Peak Shear Strength at the Interface

$\tau_{Residual}$: Developed Residual (Post-Peak) Shear Strength at the Interface

Figure 8.44 shows that smooth HDPE geomembrane interfaces exhibit generally a slight decrease in the sensitivity with temperature. This reduction in the value of the sensitivity is particularly more pronounced for the angular sand and smooth HDPE interfaces than the interfaces of the rounded material. This is attributed to the transition of shear mechanism from sliding to plowing at higher ambient temperatures due to the softening of the polymeric smooth HDPE geomembrane with increased temperature. For the smooth PVC liner (having smaller surface hardness compared to HDPE geomembranes) interface, the sensitivity value displayed similar trend for both rounded and angular material layered systems. The sensitivity showed a marginal increase up to the test temperature level of 35°C beyond which the sensitivity exhibited a slight decrease in the value until the highest test temperature level (35°C). The resultant values

for both rounded and angular sands at 50°C is comparable to those values displayed at lowest test temperature (21°C). This resulted from the enormous ability of the relatively hard sand grains to penetrate deeper into the very soft surface of the PVC liner and thus, plow the counterface severely at larger shear displacements leading to the mobilization of greater residual frictional resistances relative to the shear strength at peak state. Considering the variation in the value of the sensitivity as a function of temperature, the relatively harder surface of the HDPE geomembrane (compared to PVC liner) showed a higher stability and resistance to particle indentation/penetration in the contact area with increasing ambient test temperature particularly for the rounded particulate material interfaces.

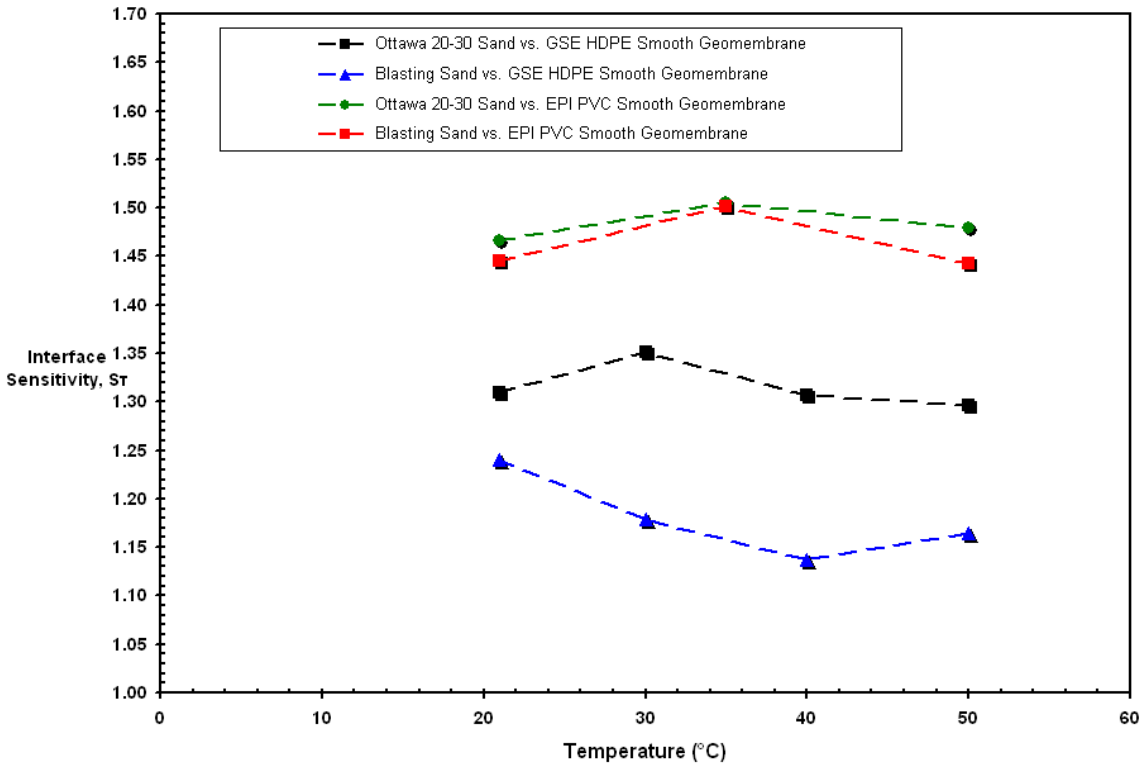

Figure 8.44 The Variation and the Developed Trend for Interface Sensitivity, [Sτ] with Temperature Change for Rounded/Angular Sand – Smooth HDPE/PVC Geomembrane

As seen in Figure 8.44, the resultant values of the sensitivity for Ottawa 20-30 sand interfaces are “notably” and “marginally” higher than that of Blasting sand – smooth HDPE and PVC geomembrane interface, respectively. The post-peak strength loss or reduction in the mobilized peak frictional resistance observed in the shear stress–horizontal displacement failure curves over the entire range of test temperatures results from the following shear mechanism that takes place at *rounded* particulate material versus smooth geomembrane interfaces. As rounded particles begin to predominantly slide along and/or marginally plow into the geomembrane surface, the initial movements cause wear on the surface; thereafter, as particle displacement continues, *rounded* sand particles encounter material previously damaged by preceding particles (i.e. located at front edge of the shear box) resulting in little or no additional strength required for subsequent displacement as rounded shape nature of rounded particles are unable to further penetrate into and plow at relatively greater depth beyond the surface of the lining material due to insufficient magnitude of contact stresses induced by the rounded particles to exceed yield strength of the counterface geomembrane (Dove and Frost, 1999). However, for the case Blasting sand system, the *angular* nature of the sand particles produces greater penetration and plowing to a greater depth during shearing (Frost et al, 1999). High contact stresses can develop at single particle–geomembrane micro-contacts due to existence of smaller contact area under the same loading conditions as well as the angular characteristics of the particles. Consequently plowing will most likely initiate at the locations of these high stress concentrations. As a result of favorable shape features, the blasting sand particles are able to plow the geomembrane surface with a variety of projected geometries and/or *angular* particles are able to plow over a surface

scarred by previous particles; and thus, creating significant wear as shown through post-test profilometer measurements as will be discussed in detail in Section 8.8. For this reason, in contrast to the case of the rounded particle interfaces, the ability of *angular* grains in indenting with an extensive variety of projected geometries is further fortified by the substantially larger residual frictional resistances attained at the Blasting sand systems at all temperatures tested as compared to Ottawa 20-30 sand such that the angular particles travel along a surface damaged by preceding pervious particles, they have a greater tendency to increase the degree of surface damage as a more angular particle may potentially travel along the path of a more-rounded/less-angular particle. As such residual conditions for smooth geomembranes are due to wear process and are essentially achieved only after most sand particles are unable to further plow the counterface material in shallow grooves or striations/scratches formed already in the geomembrane surface by the shear-box front edge particles.

In order to make a comparative analysis in terms of relativeness for the resultant values of the interface sensitivity obtained at elevated temperatures with respect to that at room temperature level for all the tested particulate – geomembrane interfaces, a quantitative proportionality parameter is defined as the normalized sensitivity (Equation 8.3):

$$S_{T°C/21°C} = \left(\frac{S\tau_{@°C}}{S\tau_{@21°C}} \right) \tag{8.3}$$

Where;

$S_{T°C/21°C}$: Normalized Interface Sensitivity w.r.t. Room Temperature (21 °C)

$S\tau_{@°C}$: Interface Sensitivity at T °C

$S\tau_{@21°C}$: Interface Sensitivity at 21 °C

The $S_{T°C/21°C}$ values less than 1.00 indicates that the corresponding stress-displacement curve showed a less strain-softening response (i.e. reduction in peak resistance) at larger shear displacements for the tests at higher temperatures. The trends for $S_{T°C/21°C}$ as function of temperature for all the tested granular soil – geomembrane interfaces are shown in Figure 8.45. The decrease in value of the normalized sensitivity with increasing ambient temperature for particularly angular sand interfaces can be interpreted as greater amount of plowing induced to the counterface geomembranes resulting in facilitating higher sand particle rearrangement during shearing.

For relatively harder surface of smooth HDPE geomembrane particularly at lower test temperatures, the influence of higher surface hardness of the geomembrane liner sheet agrees with the fact that the shear mechanism at the contact surface was constrained to the sliding of sand grains along the geomembrane surface during shearing. This resulted in the lower magnitudes of residual frictional resistance mobilized at larger displacements compared to the interface tests at elevated temperatures for the same material combination tested.

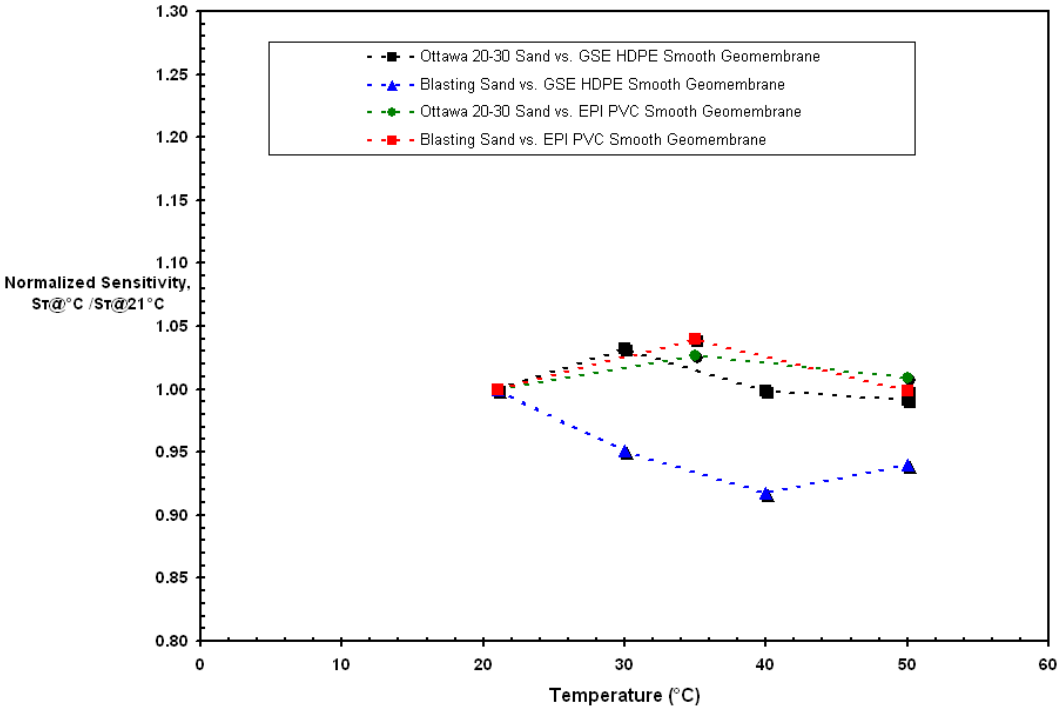

Figure 8.45 The Change in the Normalized Interface Sensitivities displayed at Different Elevated Temperatures relative to Room Temperature Level (21°C)

The influence of sand particle shape (i.e. roundedness, angularity) as well as geomembrane base polymer type (i.e. HDPE, PVC) on the peak and residual shear strengths at different ambient temperatures with respect to the frictional resistance of the rounded sand (Ottawa 20-30) – smooth HDPE geomembrane interface which exhibited the lowest shear resistance at all temperatures tested (21°C to 50°C) is denoted by the ratios (peak stress ratio [PSR] and residual stress ratio [RSR], respectively) to quantitatively evaluate the mobilized shear strength response of the different material combinations tested as a function of temperature. Note that the strength values at temperature level of 35°C for the rounded sand – smooth HDPE geomembrane interface was interpolated from the test results at 40 and 50°C for this material combination which was defined as the basis to calculate the PSR and RSR values at 35°C for the tested rounded or angular sand – smooth PVC liner interfaces.

Figures 8.46 and 8.47 show the change in PSR and RSR with temperature and the resultant trends observed for the different tested particulate – geomembrane interfaces, respectively. The variations in the trend as a function of temperature for Blasting Sand – Smooth HDPE Geomembrane interface displays an increase in the value with rising temperature level up to 40 °C beyond which the PSR and RSR remained approximately constant and displayed a slight decrease in the value until the highest test temperature level of 50 °C. This is attributed to higher ability of the rounded sand grains to plow into the softened surface of the geomembrane. In addition, this minimal decrease in the value can potentially be due to *no* higher ability of the angular sand particles to penetrate more into and to plow the counterface at a further depth. Since the angular sand grains might have already achieved the most potential indentation/penetration depth during shear and thus, the material dislocation that is most possible due to the magnitude of the applied normal stess on the interface.

The tendency of the trends for PSR and RSR as a function of temperature for rounded sand – smooth PVC liner interface is analogous to each other and additionally almost in parallel pattern for the displayed PSR and RSR as a function of temperature ranging from 21°C up to 50°C. As such, for the rounded material interface, the PSR and RSR showed a slight decrease in the value from 21°C to 35°C beyond which they stayed almost constant up to the highest test temperature of 50°C. For angular sand – smooth PVC liner interface, both the PSR and RSR displayed a marginal increase in the value to the temperature of 35°C beyond which they exhibited a slight decrease up to 50°C. This can imply that PVC liners are more susceptible to the change in ambient temperatures than the HDPE geomembranes in terms of the frictional resistance performance in contact with the sands due to different polymeric material properties of the liner sheets.

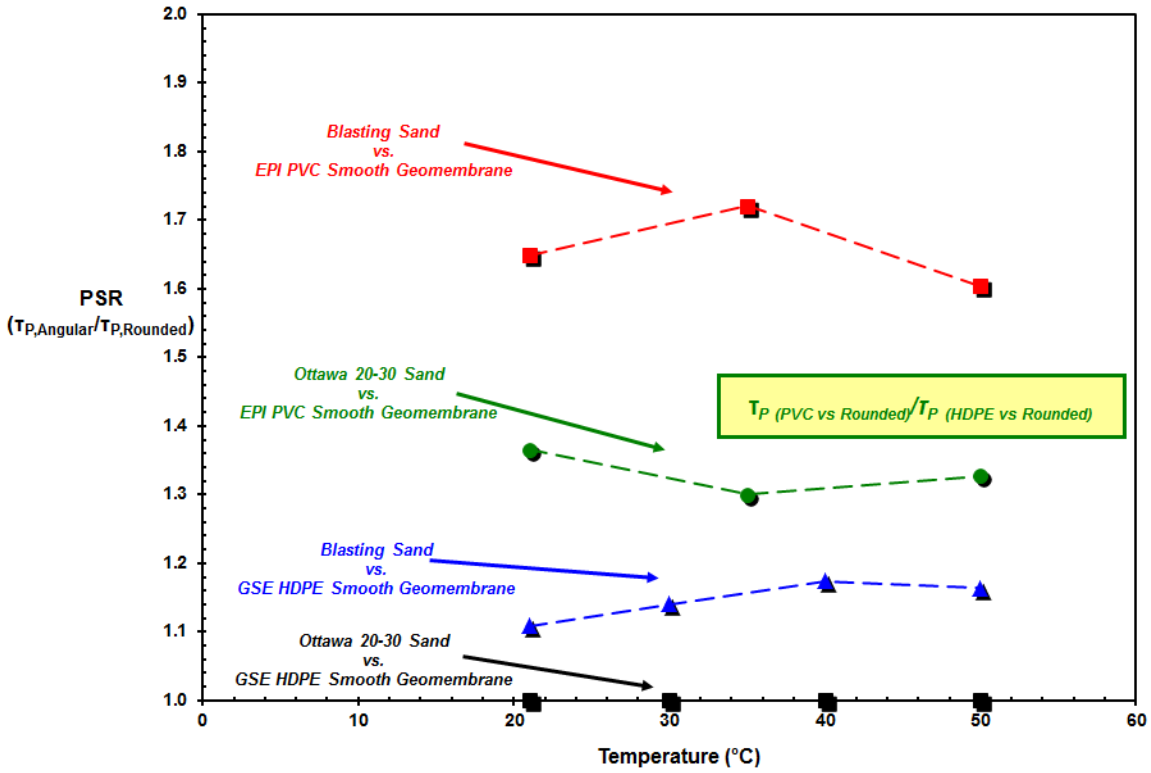

Figure 8.46 Comparative Analyses for the observed Behavior and the developed Trends in the Resultant Values of Relative Peak Shear Strengths with the change in Temperature

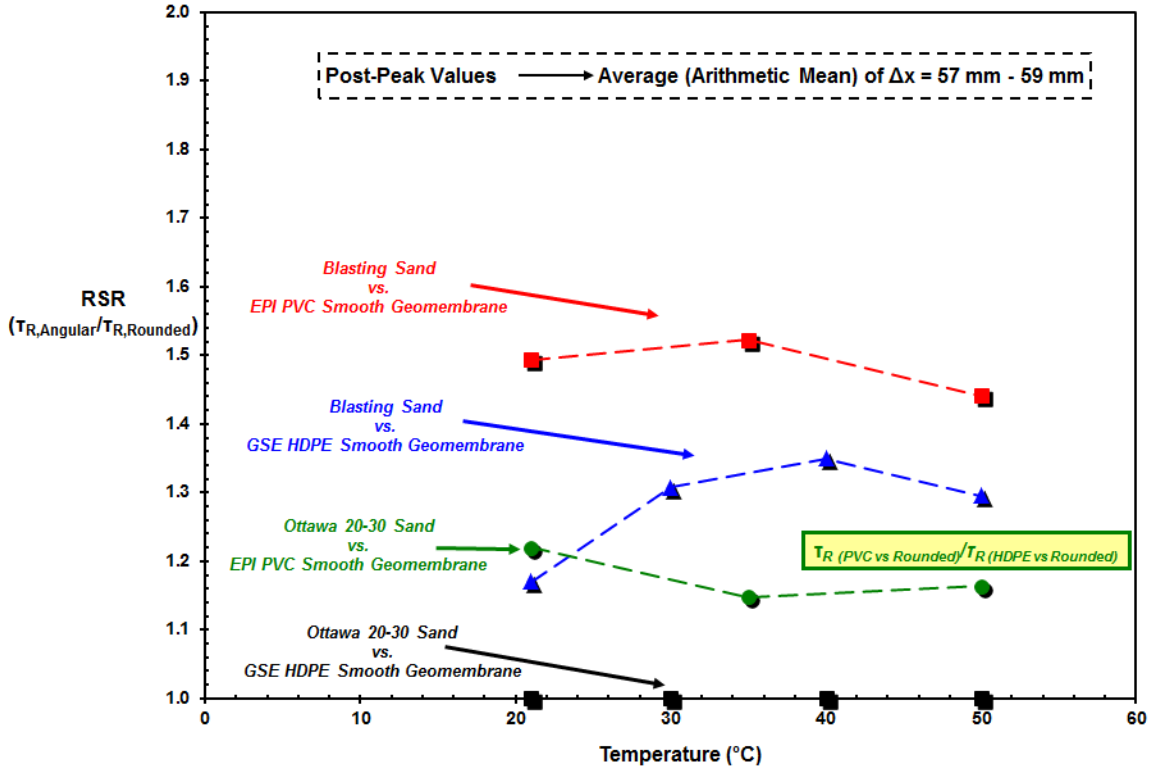

Figure 8.47 Comparative Analyses for the observed Behavior and the developed Trends in Resultant Values of Relative Residual Shear Strengths with the change in Temperature

In summary, the mobilized shear strength of the sand – smooth geomembrane interfaces results from the *relative* contributions of the sand particle shearing mechanisms (i.e. sliding and plowing) along and into, respectively, the counterface geomembrane surface. As such sliding and plowing forces combine together to produce total frictional resistance at the interface against shear displacement. In this perspective, the test results showed that an increase in the contribution of plowing mechanism at higher elevated temperatures is relevant to the increase in interfacial shear strength as more effort and energy was required to plastically deform and dislocate the material on the geomembrane surface during shear displacement. Therefore, the amount of plowing is a function of the state of the interface as well as the relative hardness of the counterface materials. For sand – geomembrane interfaces, this changes with a change in the temperature. Further, the ability of the sand grains to plow deeper into the surface of the counterface geomembrane is dependent on the greater angular features of the particles. As such, the contact area between the rounded sand particles and the geomembrane is relatively larger than the contact area between the angular sand particles and the geomembrane. Hence, the sharper angular sand grains induce larger magnitude of local contact level stress to penetrate into the surface of the counterface polymeric material at lower normal load. By this means, as previously noted by Dove and Frost (1999), plowing is most likely to initiate at locations of these high stress concentrations. The contact stresses for the rounded material interfaces at lower temperatures were not large enough to exceed the yield strength of the counterface geomembrane surface and thus, the sand particles merely slid along the interface with minimal surficial damage incurred by the geomembrane as will be discussed further in Section 8.8.

As a result, it can be concluded that temperature is a significant factor in influencing the resulted peak and post-peak shear strengths mobilized in the sand – smooth geomembrane interfaces along with the other primary governing factors such as particle shape and normal stress level.

8.8. Surface Roughness and Profile Relief Analysis of Post-Test Geomembrane Specimens

8.8.1. Rounded Sand – Smooth HDPE Geomembrane Interface

The shear strength of particulate material versus smooth geomembrane interfaces develops from the contribution of a number of mechanisms occurring at the interface (Frost et al., 1999). The predominant mechanisms are rolling/sliding and/or plowing of the particles against the geomembrane surface (Dove and Frost, 1999). The tendency for particle sliding and/or plowing at the interface is a function of the counterface material properties including surface roughness, material hardness, particle size and angularity as well as the interface conditions including normal stress and sand density. As the material properties or the interface conditions are altered due to the change in ambient temperature, the relative contribution to shear stress from the sliding and plowing components of friction will also be affected. Graphs and quantitative R_a values of pre-shear surface topography for smooth geomembranes were presented in Figure 7.3 and in Section 7.2. Graphs for post-shear surface topography for smooth HDPE geomembrane sheared against Ottawa 20/30 sand are shown in Figures 8.48, 8.49 and 8.50 and for normal stress levels of 10, 100 and 400 kPa, respectively.

Generally for the case of rounded soil particles (e.g. Ottawa 20/30 sand) sheared against smooth continuum lining sheets at low normal stress levels, the soil particles slide and scratch the geomembrane surface during shear whereas at high normal stresses, these particles embed themselves within the geomembrane surface and plow it during shear. In this regard, elevated temperatures facilitate the initiation and the advancement of this mechanism at *lower* normal stress conditions. This contributes to an increase in the frictional shear resistance at the interface due to sand grains further indentation and more deeply abrading through the surface of polymeric counterface material (geomembrane). It was noted that the depth of the trenches being plowed by soil particles depends on the shape and the angularity of soil particles, the density of soil, and the normal stress at the points of contact between soil particles as well as most importantly the softness/hardness of the geomembrane liner surface which is strongly temperature dependent. At higher normal stresses and at higher elevated temperatures, the depth of embedment of soil particles is greater, resulting in deeper trenches being plowed during shear.

From the striations detected on post-test geomembrane specimens, the sliding of the sand particles at lower test temperature and the transformation of the shearing mechanism to plowing at higher normal stresses. This resulted in greater damage to the smooth liner surface due to the harder sand grains was the main interface shearing mechanism mobilized at smooth HDPE geomembrane surfaces. After completion of the interface direct shear testing program, the geomembrane surfaces were profiled to quantify the post-test surficial damage. Results from the profilometer surface measurements demonstrated how surficial scarring of smooth geomemhranes was influenced by ambient temperature condition at which the laboratory tests were

performed as well as the normal stress level, and the particle roundedness/angularity. The particles penetrated further through the intact surface of the membrane at higher temperatures at the initiation of the shear displacement and continued to do so throughout the shearing process. Due to softness and higher pliability of the HDPE lining sheet at elevated test temperatures, particles plowed into the surface of the geomembrane with a variety of projected geometries creating significant wear on the relatively softer continuum material surface. As the soil particles traveled along a surface damaged by previous particles, they had a greater tendency resulted from favorable contribution of ambient temperature level to increase the degree of surface damage as the projected plowing shape varied between contacts. At large displacements, it was detected that the geomembrane surface was no longer smooth, but heavily damaged and particles plowed over a surface scarred by previous particles, resulting in the alteration of an already damaged surface particularly at the highest test temperature (50 °C). Although the spherical particles were primarily sliding along the interface and causing minimal damage to the surface at lowest test temperature (21 °C) even at the large normal stresses. The plot of profile relief versus profile length for post-test geomembrane specimens for Ottawa 20-30 sand and HDPE liner demonstrated that the particles were able to deeply gouge the counterface material surface. This correlated to the profile measurements indicating that the relatively hard sand grains more severely plowed the geomembrane surface with increasing ambient temperature. The profile exhibited minimal relief at the coolest test temperature, which corresponds to the particles principally sliding along the interface that is indication of the dominant interface shearing mechanism being mostly sliding of the particles. It is noted that the relief is related the amount of plowing

occurring; however, the wear patterns produced by Ottawa 20-30 sand grains the spacing (i.e.: distance extent) between the peaks and valleys dependent and being reflective of the particle size.

With respect to the increase in shear strength of the interface, it is directly related to the ability of soil particles at the interface to plow into the geomemhrane surface (Dove and Frost, 1999). As such minimal work is required by the particle to slide along an interface. On the other hand, the particle must displace the material at the contact surface of the interface requiring significant effort, work, and energy to plow into the surface of the geomembrane. Thus, one can correlate and attribute the increased plowing directly to increased frictional strength; and additionally, will result in increased surface topography observed at post-test stage on liner specimens. Further, other geomembrane endurance properties such as durability at long term in the field also influence and regulate the plowing ability of the sand grains. The interface direct shear test results showed that the greatest shear strengths were obtained at the highest test temperatures regardless of normal stresses applied which is attributed to the grater tendency and the ability of the granular material particles to indent into and plow along the geomembrane surface.

Geomembrane post-test specimen surface characterization after which direct shear tested against the particulate material at different temperatures were performed using stylus profilometer to capture an illustrative representation of the cross-shear direction surface profile of the used lining materials at post-test-stage as well as to depict and demonstrate the size, shape, and the interval spacing and separation as well as the resulted generated irregular patterns of the peaks and valleys due to sand particles

abrasion and plowing during test duration in the course of shearing displacement process in intention to gain some comparative information for the purpose of further comprehending the relative size and depth of scours/striations. In this way, post-test surface roughness alterations of geomembrane liners can evidently be utilized and facilitated for visually comparing the degree/amount of plowing which is directly related the resulted frictional resistance attained as well as influence and govern the interface behavior developed and the shear strength mobilized in combination with particulate sands. Surface profiling was carried out over a representative cross-shear distance of 10 mm to be able to distinguish and expose the shape and size of the peaks and valleys as well as to display the post-test geomembrane surface roughness and reveal their modal form. The surface profiling was filtered with Gaussian high-pass and low-pass cutoffs of 8 mm and 8 μm, respectively. The use of Guassian roughness filter in the analyses is to eliminate the waviness component of the roughness. Since the relative scale of the surface features for the smooth geomembrane surfaces are minimal, slight variations in the surface roughness will result in large variation in the resulted damaged profile. All profiles were generated perpendicular to the interface shear direction (Figures 8.48 – 8.50). It is noted that the relief is dependent on ambient temperature level at which the direct shear test was conducted with greater amounts of plowing/scouring occurred at higher elevated temperature conditions. Additionally, the wear patterns are related to the size and gradation of sand particles depending on which the grains created narrow versus wide spacing between the subsequent peaks and valleys. This could be considered as an indicative of the importance of particle size and gradation on particulate–geomembrane interface shear behavior and strength.

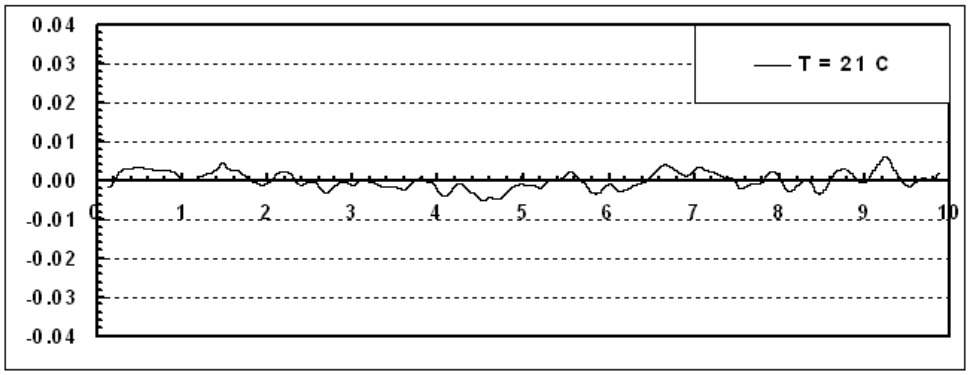

(a)

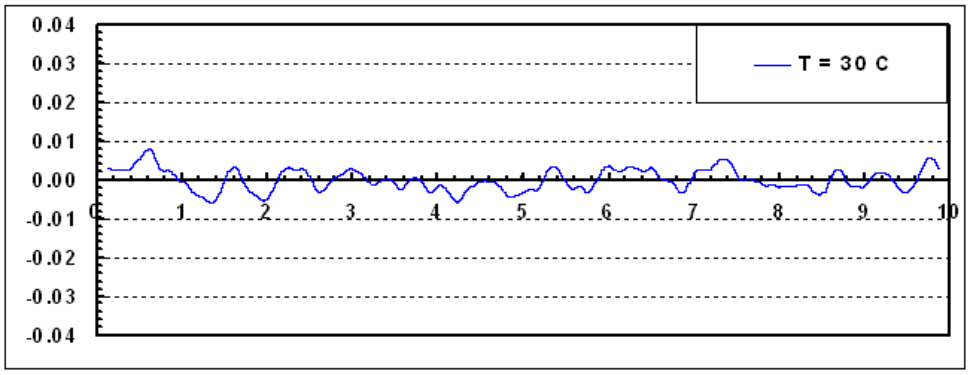

(b)

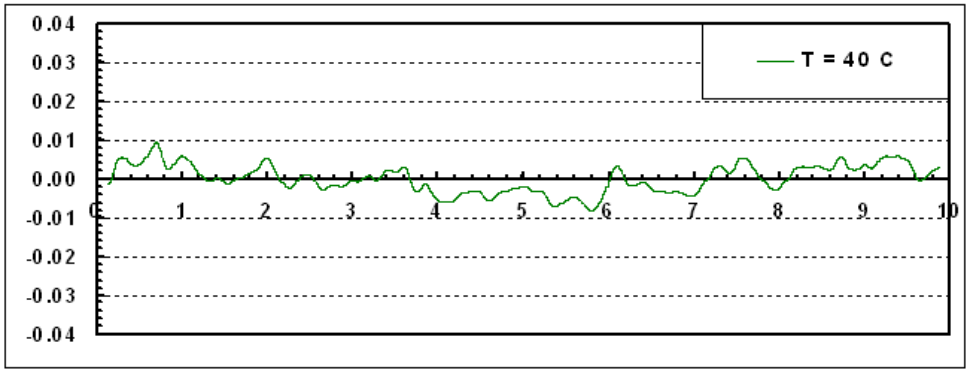

(c)

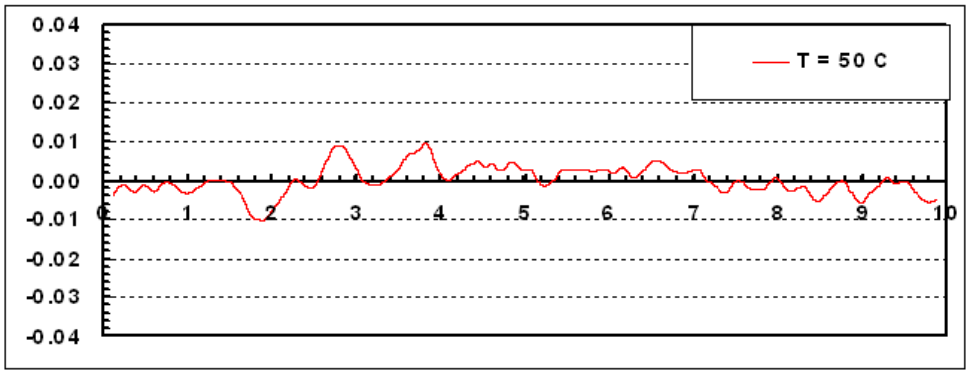

(d)

Figure 8.48 ***GSE Smooth HDPE Geomembrane*** Post-Test Specimen Surface Roughness Profiles Sheared against ***Ottawa 20-30 Sand*** at Different Temperatures **[σ = 25 kPa]**
y: Profile Relief (Vertical Height) [*mm*]; **x:** Projected Profile Segment Length [*mm*]

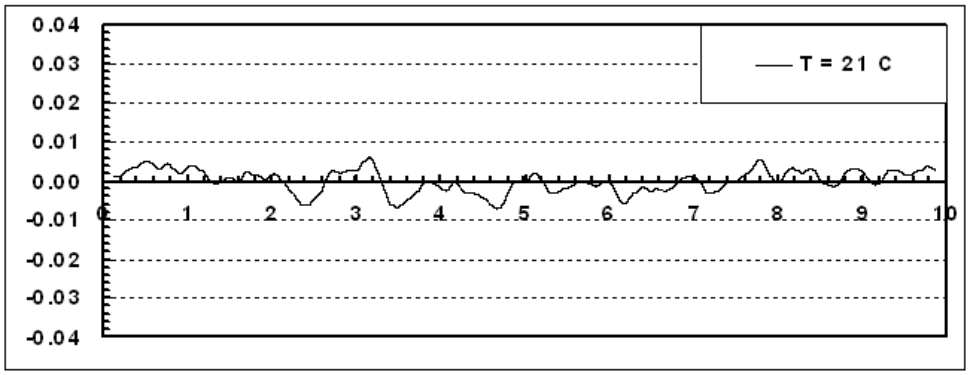

(a)

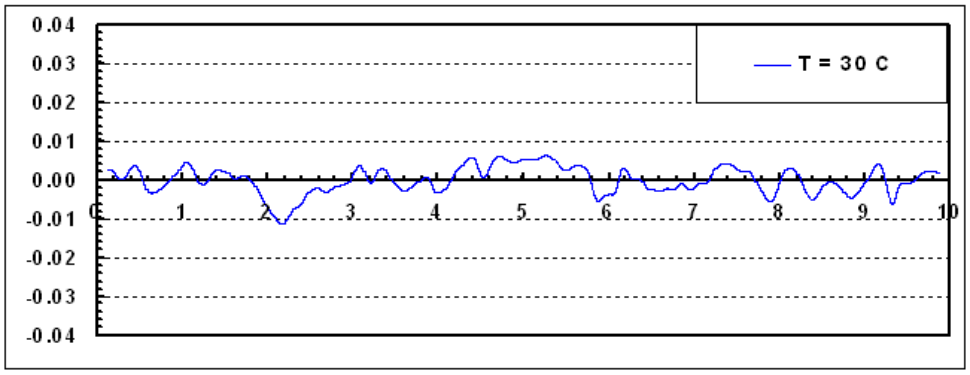

(b)

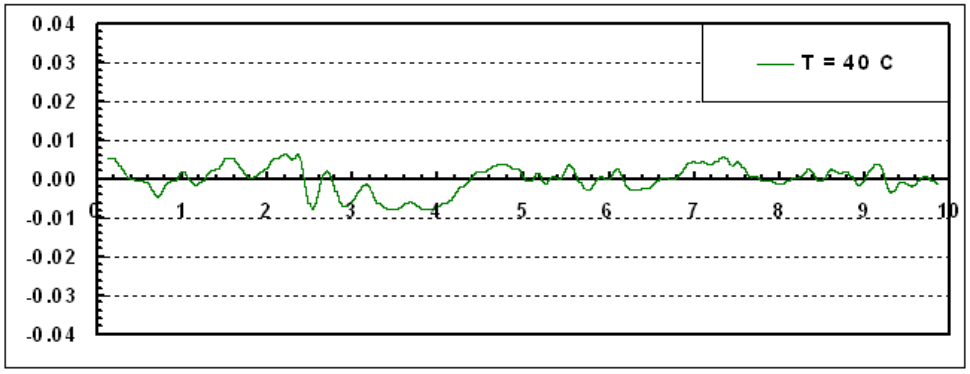

(c)

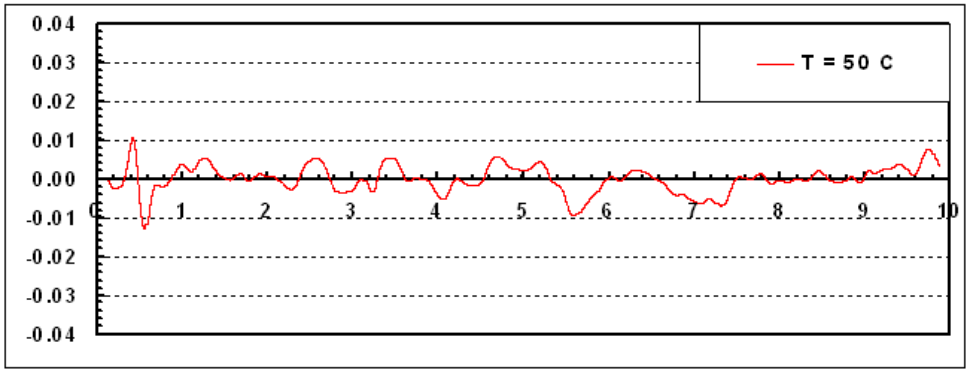

(d)

Figure 8.49 ***GSE Smooth HDPE Geomembrane*** Post-Test Specimen Surface Roughness Profiles Sheared against ***Ottawa 20-30 Sand*** at Different Temperatures **[σ = 100 kPa]**
y: Profile Relief (Vertical Height) [*mm*]; **x:** Projected Profile Segment Length [*mm*]

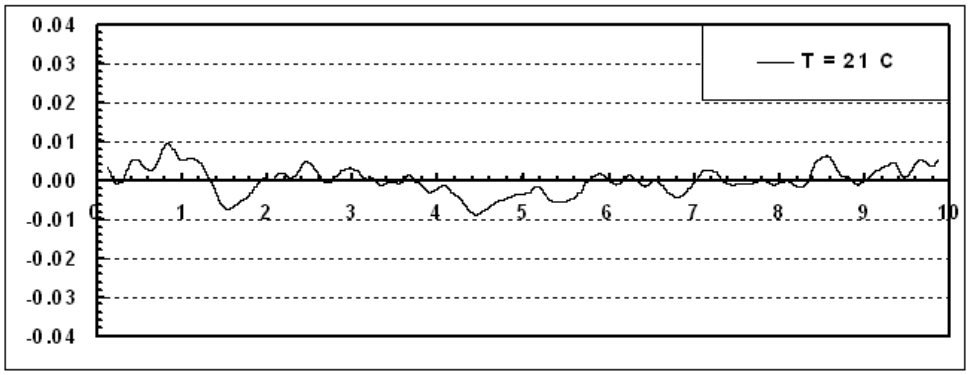

(a)

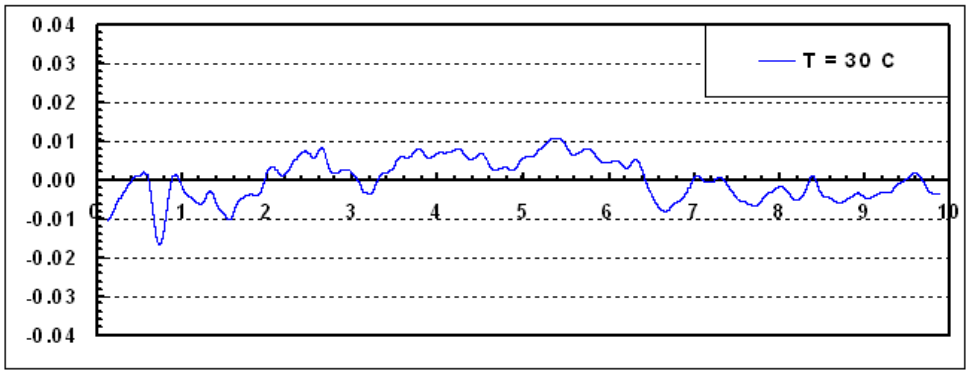

(b)

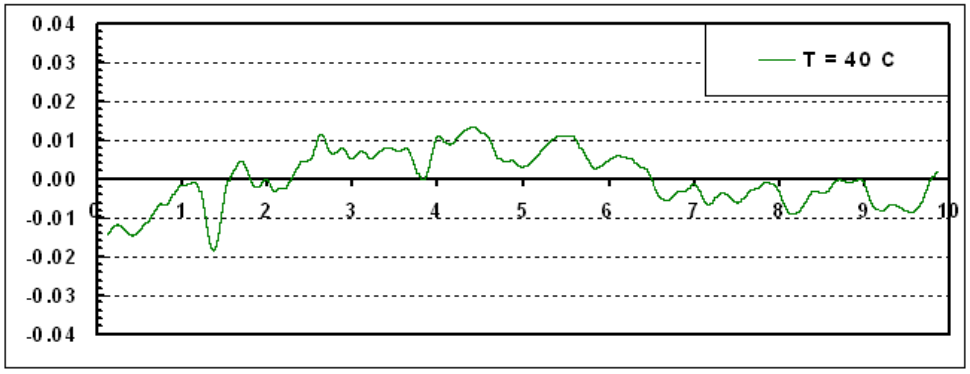

(c)

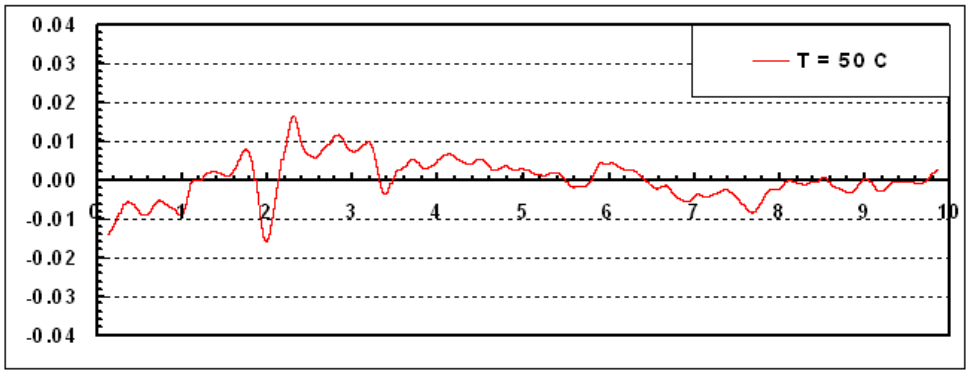

(d)

Figure 8.50 ***GSE Smooth HDPE Geomembrane*** Post-Test Specimen Surface Roughness Profiles Sheared against ***Ottawa 20-30 Sand*** at Different Temperatures **[σ = 400 kPa]**
y: Profile Relief (Vertical Height) [*mm*]; **x:** Projected Profile Segment Length [*mm*]

8.8.2. Angular Sand – Smooth HDPE Geomembrane Interface

It has been observed after the performed interface direct shear tests that the surface topography of smooth HDPE geomembrane was altered significantly, in particular, when sheared against angular particles due to penetrating and plowing of the grains into and along the geomembrane sheet surface, respectively. As such the plowing mechanism resulted in larger amount of wear occurred on the lining material surface area that had been in contact with sand during shearing displacement. Therefore, the amount/degree of surficial damage given to the geomembrane specimen can directly be correlated to the test conditions such as the ambient temperature and the applied load; and hence, governing and determining the resulted frictional strength of the interface based on especially geomembrane hardness. This section will present the results of post-test surface profile measurments using stylus profilometer for illustrative purposes for which geomembrane cross-shear post-test profile was plotted to depict the visual representation and the modal pattern of the altered continuum surface. In this way, both the degree of plowing and the associated change in interface strength was qualitatively and comparably evaluated in terms of relatively comparing the visual form and appearance of the post-test liner surface for different test temperature and loading conditions with respect to the properties of both the particulate material (i.e. grain shape) and the hardness state of smooth HDPE geomembranes dependent on the temperature, as well as the global state of the interface to assess how these factors can alter interface behavior under typical construction and operating conditions. Particulate-continua interfaces and their associated mechanisms have long been identified as being critical to their overall performance in

geotechnical structures. In this way, the factors such as particle shape and liner surface hardness affecting the mobilized interface mechanisms between sand and geomembranes can be focused comparably and qualitatively.

The shear strength values attained over the entire test temperature range (21 °C – 50 °C) for the Uniblast blasting sand were greater than those obtained as a result of direct shear tests performed on the Ottawa 20-30 sand. The plowing effect of the angular sand on the smooth HDPE geomembranes was evident from the variations in surface roughness measured as shown in Figures 8.51 through 8.53. Therefore, it is noted that the post-test profilometer measurements through the evaluation of the cross-shear profile demonstrate this improvement in frictional resistance qualitatively.

Moreover, the angular blasting sand particles were able to plow into the surface of the geomembrane, at lower/cooler ambient test temperatures as well as at normal stresses lower than for the rounded Ottawa 20-30 sand. Comparing the degree of surficial damage given to the geomembrane specimen in the course of interface direct shear tests demonstrates the higher ability of the angular sand grains to indent into and abrade the polymeric lining material substantially as compared to rounded sand circumstances.

The groove depth/width (i.e. size) of plowings, and the frequency of abrasions as well as the gap spacing between striations can be related to the larger shear strengths mobilized by the Uniblast sand at the interface in contact with smooth HDPE geomembrane at all temperatures (21 °C – 50 °C) tested and over wide range of normal stresses (25 kPa – 400 kPa) applied as the degree of post-test surficial damage and the resulted surface roughness relief was extensive. Therefore, the grain shape plays a more significant role in the differing shear mechanisms rather than the size within the general

range of sand particles. Further, the transition from sliding to plowing depends primarily on granular material particle angularity/roundedness as well as on the continuum geomembrane sheet surface hardness. The subsequent plots (Figures 8.51 – 8.53) generated as profile relief (i.e. vertical height] versus projected profile (i.e.: segment) length in sequential arrangement with successively ascending order/series based on ambient test temperature and normal stress level incrementally have qualitatively illustrated that the reduction in geomembrane hardness and the decrease in the lining material pliability with increasing temperature significantly increased the strength/frictional resistance of the blasting sand versus smooth geomembrane interface at elevated temperatures. In the light of this discussion, it is noted that relatively weak interfaces can occur by use of more spherical particles and at cooler ambient temperature conditions in which case the sand particles will primarily slide along the surface of the geomembrane with ease by not encountering any resistance and/or without any confrontation facilitated from the counterface material. This is critical for particulate-geosynthetic layered system designs and constructions in cold climate environment conditions and in the circumstance of the selection and use of the granular soils composed of more spherical/rounded grains. Additionally, aside from the roundedness of the particles, the level of normal stress to which the layered system is subjected or the magnitude of load imposed on the composite system is also critical and important to be considered by engineers in design. For plowing to occur, the normal stress must be sufficiently large such that the yield stress of the geomembrane can be overcome. This discussion has provided qualitative insight in a comparative manner into the mechanisms governing soil-smooth geomembrane interfaces at elevated temperature conditions that

can lead to significant understanding and further comprehension if accounted for in practice. This understanding can ultimately lead to improved insight during practical assessment of potentially mobilized frictional resistance through consideration of current degree of the geomembrane surface hardness as well as back-analysis of failed soil-geomemhrane interfaces and can be used as a basis for evaluating the potential effect of installation ambient temperature on interface strength. In addition, the demonstrated interdependence between hardness and interface strength as will presented in Chapter 9 identifies an alternative factor, in addition to roughness process, which is generally taken into account by geomembrane manufacturers in seeking to optimize soil-geomembrane interfaces. To this end, the interface direct shear test results showed that the greatest shear strengths and the improved interface behavior in terms of the largest stress-displacement failure envelopes, generated during the progression of shearing displacement in interface tests, were obtained at the highest test temperatures (50 °C) regardless of normal stresses applied which is attributed to the greater tendency and the ability of the granular material particles to penetrate into and plow along the geomembrane surface. This was further supported by the transition to plowing for the blasting sand occurring at normal stresses lower than that for the other materials, which is also attributed to the larger contact stresses induced by the angular particles as confirmed and strengthened by the increases in surface roughness, or the degree of post-test surface relief measured and determined on geomembrane specimens. At higher temperatures, even when the normal stress applied on the interface was low, the angular particles were able to abrade the geomembrane surface and thereby, the surface roughness was noticeably affected and altered as the profilometer measurements depict. However, the increase in surface topography was

significant beyond larger loading conditions (≥100 kPa). The shear strengths exhibited by the rounded sand at cooler ambient temperatures tested were the smallest of the overall tested interfaces with the primary mechanism being sliding of the sand grains; while, at high normal stress levels and with increasing temperatures, the behavior was transforming to and indicative of particles plowing along a relatively softer lining sheet surface as the maximum scarring occurred at the 50 °C interface tests.

To sum up, the blasting sand induced larger plowing effects over the entire test temperature range, and continuously made deeper scratches throughout the whole set of direct shear tests at different normal stress levels. The residual strength for angular blasting sand was much higher because it resulted from deeper scratches due to further plowing and penetration of sand particles through the relatively soft surface of the geomembrane. Consequently, it is inferred that Uniblast blasting sand began producing scratches on the geomembrane at early stages of shearing (i.e. the peak stress state); and then, continuously engraved deeper scratches. This plowing effect and the shearing mechanism thus raised/boosted the frictional strengths mobilized at residual states at all test temperatures for angular sand interfaces as compared to that of rounded sand post-peak states, considerably lower than the circumstances of blasting sand tests.

The roughness profile measurments were filtered to remove the influences of any large waviness which could change the appearance of post-test surface profile evidently for the smooth HDPE geomembrane in order to even capture the minimal surface asperities of the smooth geomembrane generated after the interface tests. The waviness component of the surface was basically removed by applying a Gaussian roughness filter to the surface roughness profile with a 2.5 mm cutoff and an 8 μm low-pass cutoff.

Through analyzing profile lengths, it was found that profile lengths of 10 mm provides a better illustration of surface roughness change, the appearance of the peaks (relief) and the valleys (troughs, grooves) and the effect of post-test damage (scarring) created on the planar continuum geomembrane sheet surface.

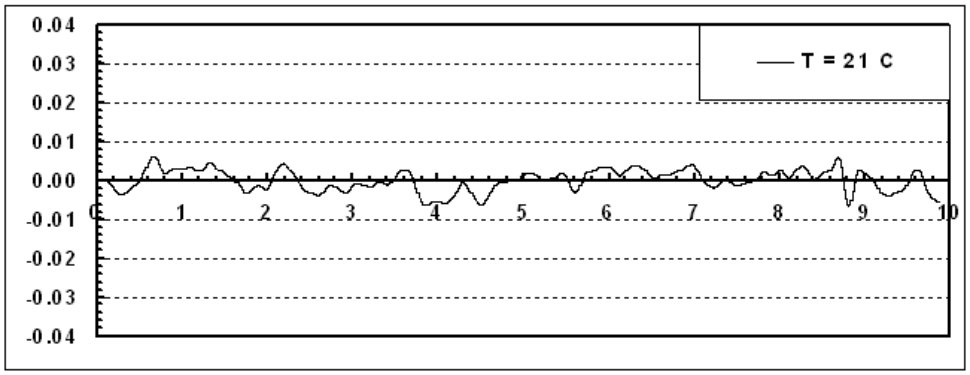

(a)

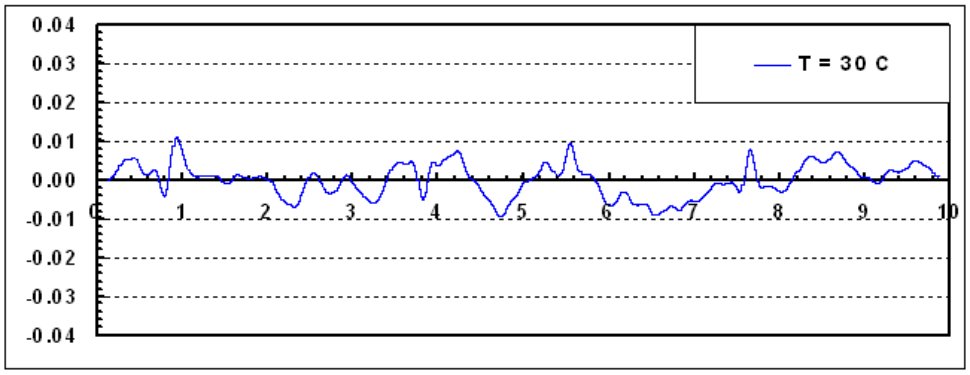

(b)

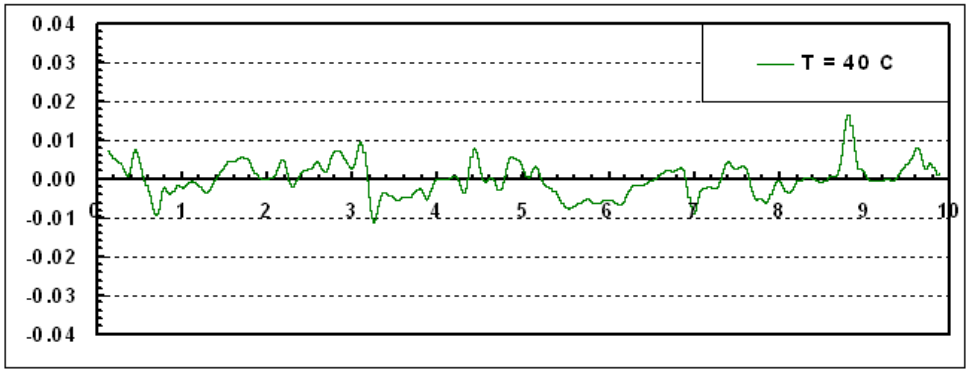

(c)

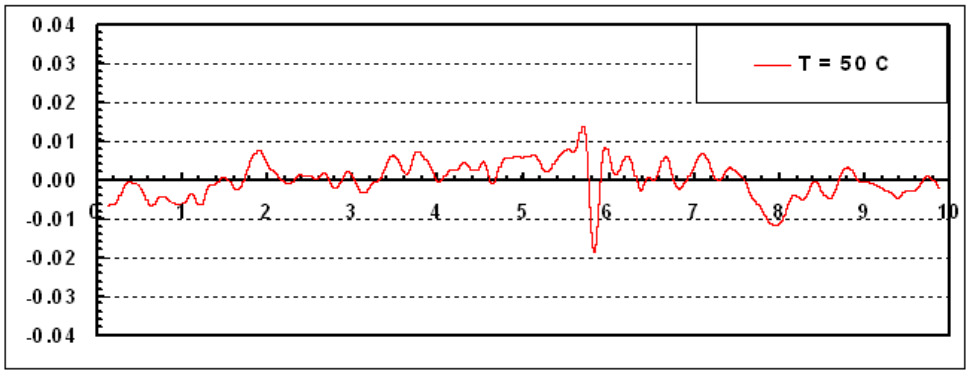

(d)

Figure 8.51 ***GSE Smooth HDPE Geomembrane*** Post-Test Specimen Surface Roughness Profiles Sheared against ***Blasting Sand*** at Different Temperatures **[σ = 25 kPa]**
y: Profile Relief (Vertical Height) [*mm*]; **x:** Projected Profile Segment Length [*mm*]

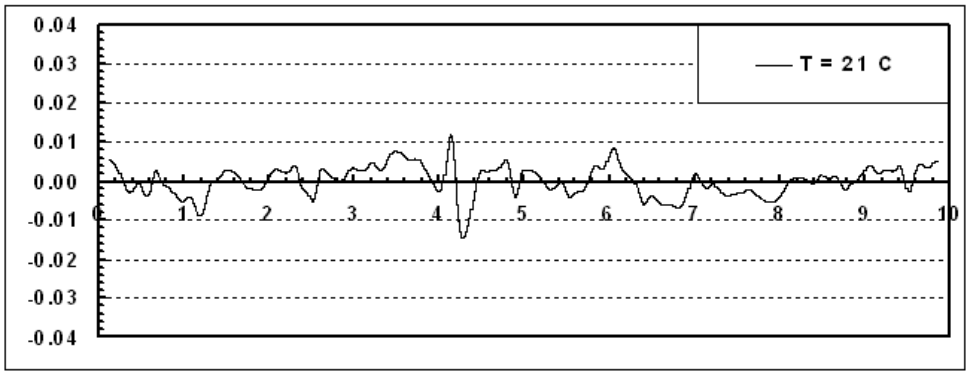

(a)

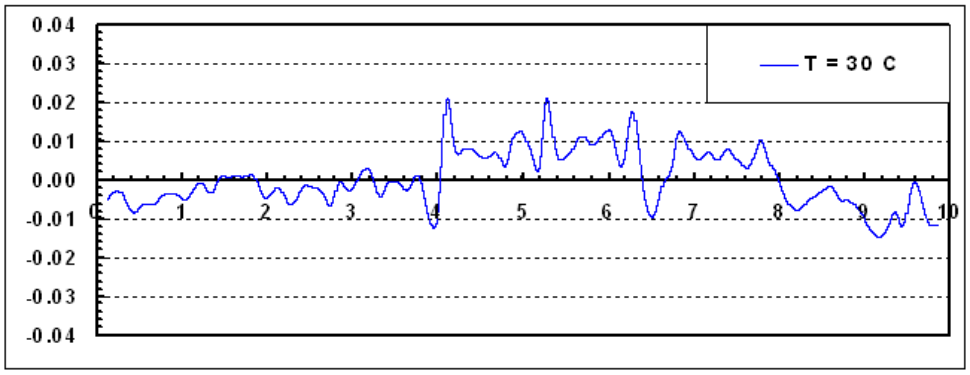

(b)

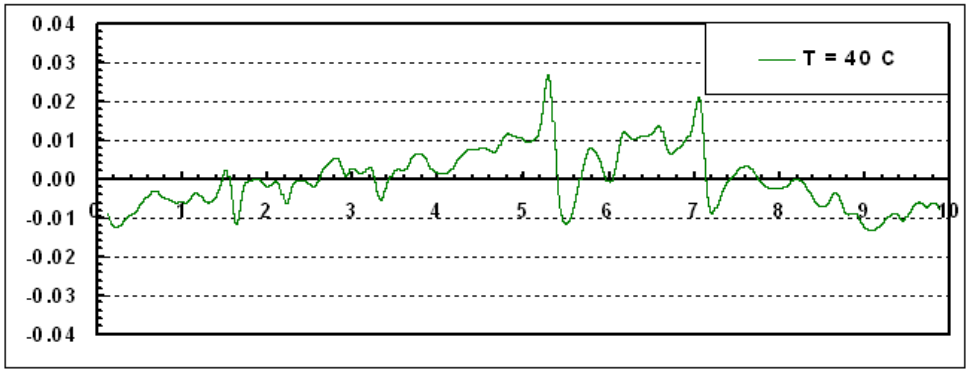

(c)

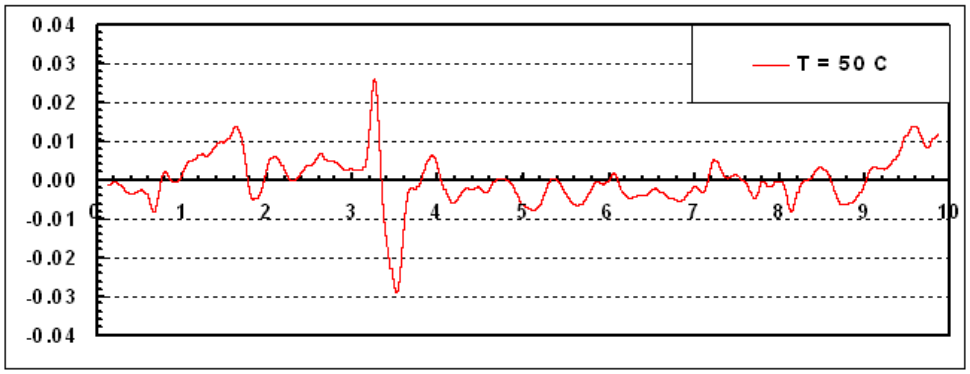

(d)

Figure 8.52 ***GSE Smooth HDPE Geomembrane*** Post-Test Specimen Surface Roughness Profiles Sheared against ***Blasting Sand*** at Different Temperatures **[σ = 100 kPa]**
y: Profile Relief (Vertical Height) [*mm*]; **x:** Projected Profile Segment Length [*mm*]

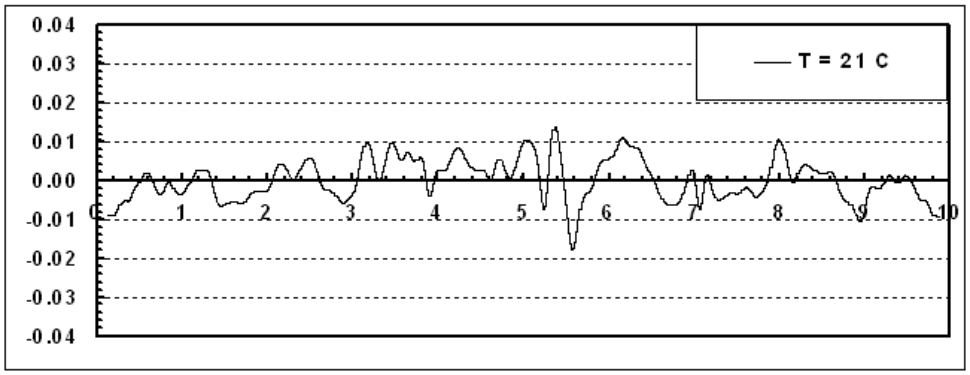

(a)

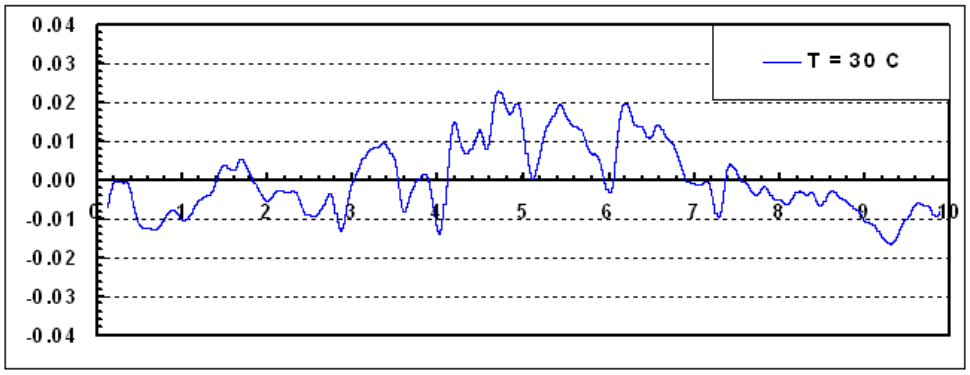

(b)

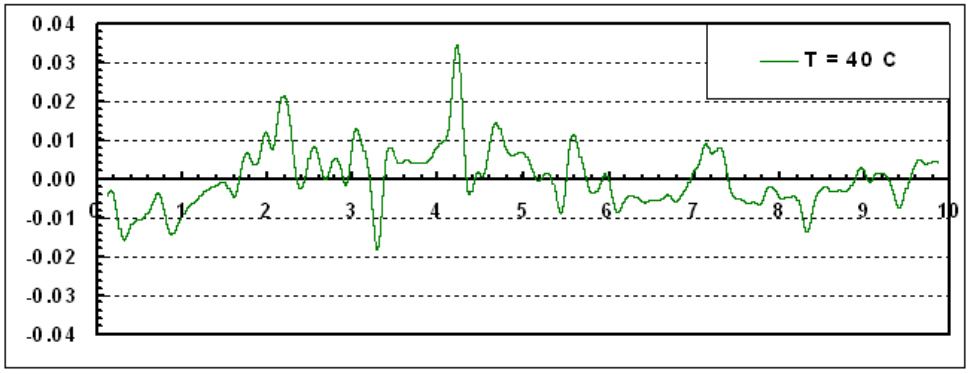

(c)

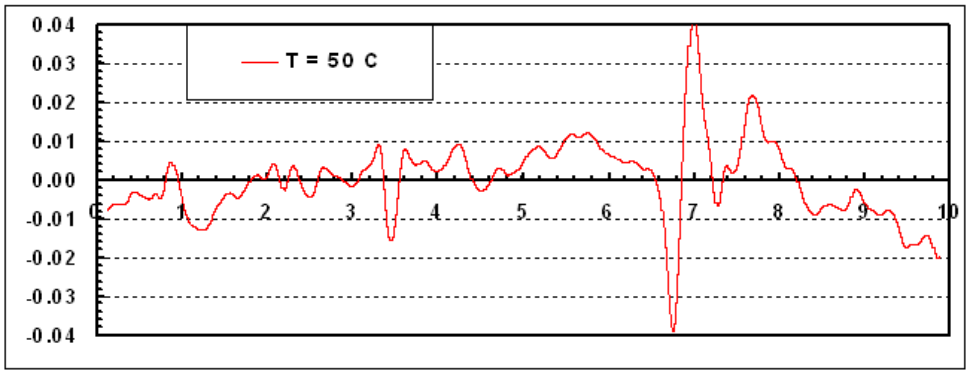

(d)

Figure 8.53 ***GSE Smooth HDPE Geomembrane*** Post-Test Specimen Surface Roughness Profiles Sheared against ***Blasting Sand*** at Different Temperatures **[σ = 400 kPa]**
y: Profile Relief (Vertical Height) [*mm*]; **x:** Projected Profile Segment Length [*mm*]

8.8.3. Rounded Sand – Smooth PVC Geomembrane Interface

The shear strength of rounded particulate material versus smooth PVC geomembrane interfaces results predominantly from rolling/sliding at low temperatures to plowing of the particles at the interface during shear displacement. The relative contribution of particle rolling and/or plowing for a given smooth soft geomembrane surface is principally a function of the relative material hardness (i.e. sand grain with regard to liner sheet), particle shape, and the magnitude of normal stress applied on the interface. When plowing occurs at higher elevated temperatures, the PVC geomembrane surface wears and experience striations and/or deeper grooves depending on the degree of ambient test temperature in addition to the magnitude of loading on the contact surface. This situation results in altered surface roughness that is principally a quantitative measure of surface topography which describes the resulted profile of the continuum sheet surface after the tests. The alteration of surface topography of smooth geomembranes is correlated to the increased interface strength as verified and confirmed through the performed surface roughness analyses or the demonstrated profile relief displays (i.e. graphic representations) on post-test geomembrane specimens sheared against sand at different temperature levels. This section describes the results of the laboratory measurements carried out using a stylus profilometer that portrays/depicts as providing visual illustration for the changes in surface roughness as a function of temperature, normal stress (Figures 8.54 – 8.56) for rounded sand – smooth PVC liner interface at different loading conditions (25, 100 and 400 kPa). Increased temperature and normal stress substantially increased both the geomembrane surface post-test wear and

the resulted interface strength mobilized in the course of direct shear tests. The geomembrane surface topography changes in the early stages of shearing process and additional wear was induced with continued displacement, but not drastically altering the surface rougness further as the latter sand grains slide through the grooves and gave less destruction (i.e. marginally displacing the counterface material as compared to early/initial passes of preceding particles) that had been previously created by the shear box leading edge sand particles.

Damage due to interface shearing may be incurred by both the smooth geomembrane and/or sand particles directly adjacent to contact surface. However, for the Ottawa 20-30 sand versus smooth PVC geomembrane condition, particle breakage was negligible due to high particle strength and softer nature of the PVC liner over the range of normal stresses used (25 kPa – 400 kPa). Further damage to the geomembrane was minimal at low normal stress and lower temperature conditions due to particle rolling/sliding being the primary mode of shearing.

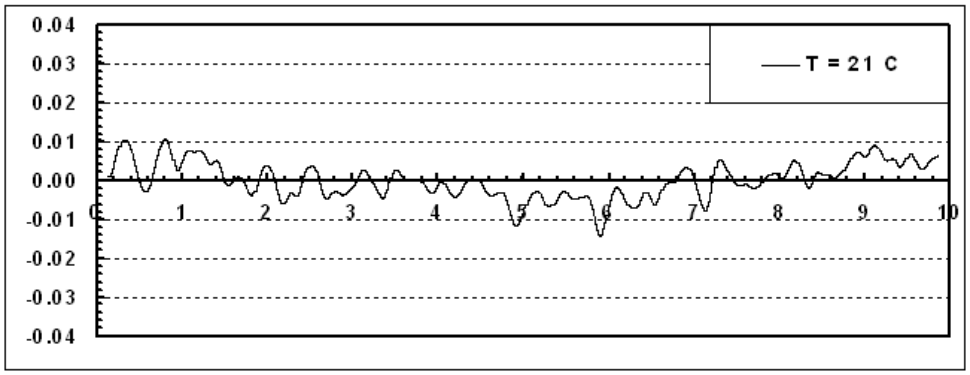

(a)

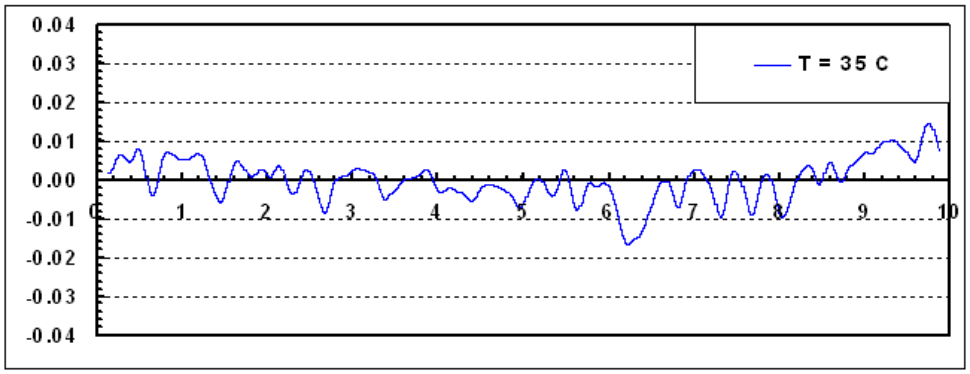

(b)

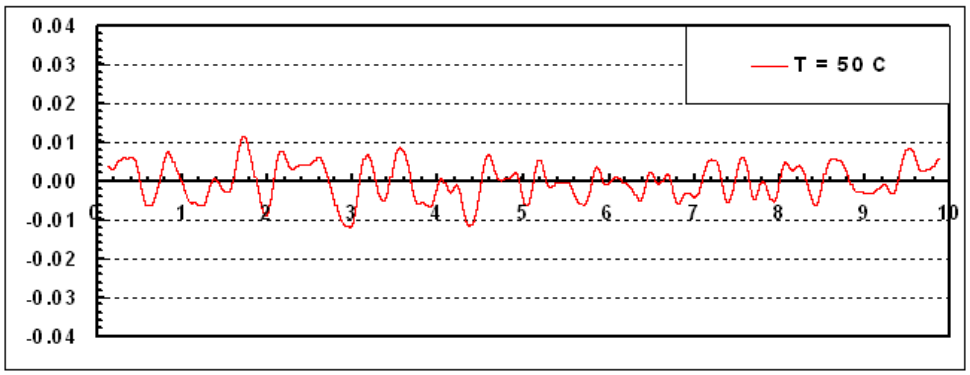

(c)

Figure 8.54 ***EPI Smooth PVC Geomembrane*** Post-Test Specimen Surface Roughness Profiles Sheared against ***Ottawa 20-30 Sand*** at Different Temperatures **[σ = 25 kPa]**
y: Profile Relief (Vertical Height) [*mm*]; **x:** Projected Profile Segment Length [*mm*]

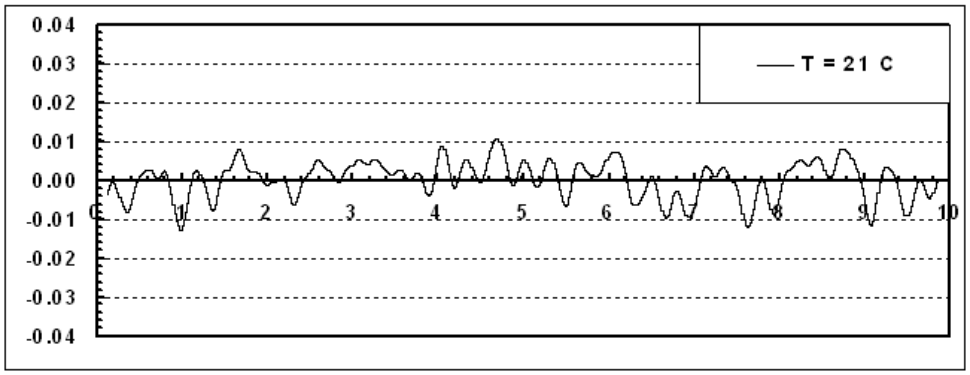

(a)

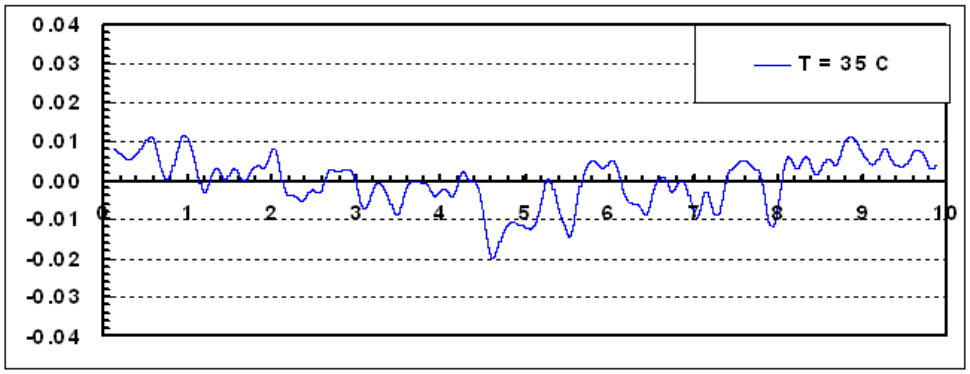

(b)

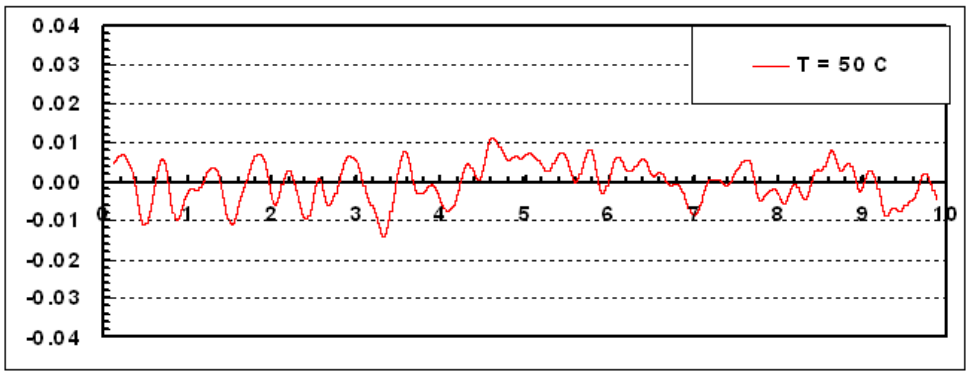

(c)

Figure 8.55 ***EPI Smooth PVC Geomembrane*** Post-Test Specimen Surface Roughness Profiles Sheared against ***Ottawa 20-30 Sand*** at Different Temperatures **[σ = 100 kPa]**
y: Profile Relief (Vertical Height) [*mm*]; **x:** Projected Profile Segment Length [*mm*]

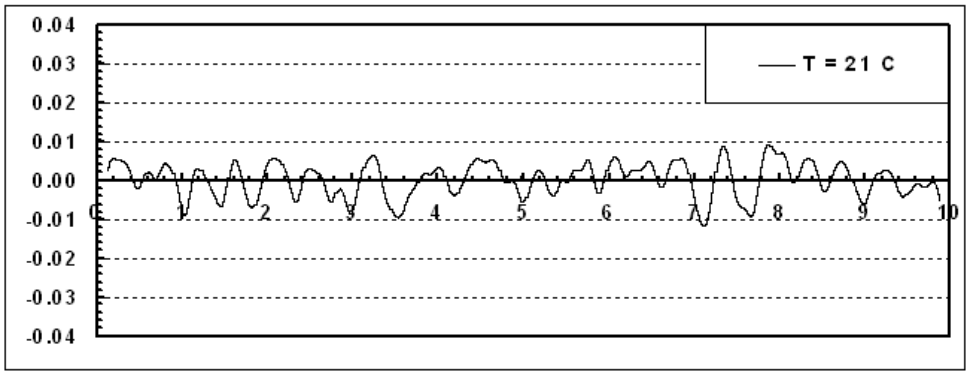

(a)

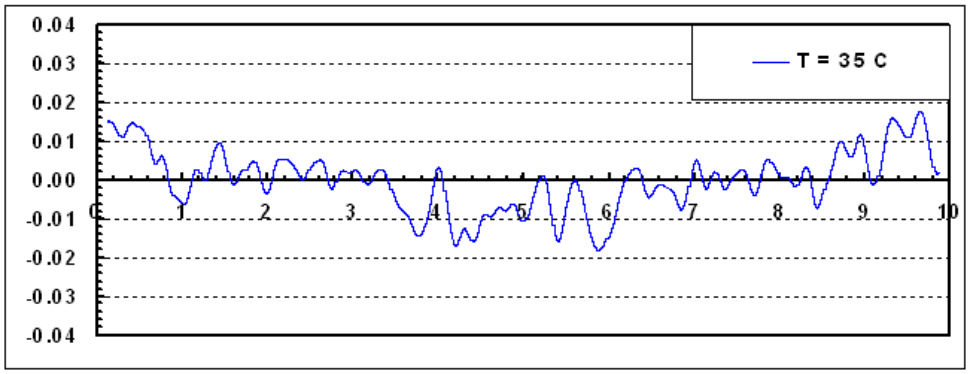

(b)

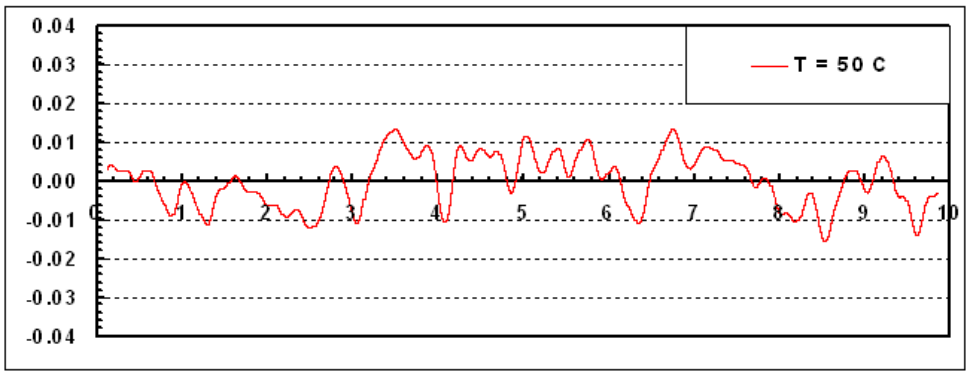

(c)

Figure 8.56 ***EPI Smooth PVC Geomembrane*** Post-Test Specimen Surface Roughness Profiles Sheared against ***Ottawa 20-30 Sand*** at Different Temperatures **[σ = 400 kPa]**
y: Profile Relief (Vertical Height) [*mm*]; **x:** Projected Profile Segment Length [*mm*]

8.8.4. Angular Sand – Smooth PVC Geomembrane Interface

The wear incurred by the geomembrane can be understood through the fundamental mechanisms of friction. Wear given to one of the most common interface component (i.e. geomembrane) of composite layered systems is the inevitable companion to friction. It was originally defined by Williams (1996) as the progressive damage, involving material loss, which occurs on the surface of the interface component as a result of its motion relative to adjacent working parts. During shearing, the surface topography of a smooth geomembrane is potentially damaged due to the plowing of the soil particles, and thereby, the surface will wear. Therefore, the wear can be assessed by examining the change in surface roughness of the geomembrane after the tests and can also be quantified by measuring profilometer relief in the direction perpendicular to shearing direction. As such measuring the created post-test roughness on geomembrane specimens will expand the understanding of the interaction between sand particles and the counterface liner; and thus, enable the quantification of the magnitude (i.e. depth) of sand grain indentation into the geomembrane and the severity (i.e. degree) of plowing mechanism along the surface of the lining material (i.e. dependent on the current yield strength/surface hardness of the geomembrane controlled by ambient temperature) which is directly related to the mobilized frictional resistance during shear displacement. The comparative analysis of incurred wear at different temperature conditions will enable the one with the evaluation of the increased shear strength with temperature as comparing the illustrative visual representation of the post-test surface profile reliefs developed at elevated temperatures with the one generated at lower temperatures. To this end, the resulting surface roughnesses of post-test PVC geomembrane specimens sheared against

the angular sand at different temperatures (21°C – 50°C) and at a range of normal stresses (25 – 400 kPa) were quantified using a stylus profilometer and presented in Figures 8.57 through 8.59 to show a comparative analysis in terms of providing illustrative graphical representations of the induced surface profile roughnesses after the interface tests by demonstrating the severity and the degree of plowing mechanism visually with the generated peaks (i.e. plastic deformation and material dislocation/movement) and troughs (i.e.: striations and grooves) at higher elevated temperatures. Based on surface hardness measurements and visual observations on the specimens in the laboratory, the PVC lining material was always less hard than the HDPE geomembrane over the entire range of test temperatures (21°C – 50°C). Further, the penetration or the indentation of the sand grains was clearly a function of the applied normal stress (Figures 8.57 – 8.59). With the direct shear tests in contact with the Blasting angular sand, the geomembrane underwent material dislocation, wear, and damage with the severity being more dependent on the test temperature and the magnitude of normal stress governing the imposed stresses at particle versus geomembrane contact points. In this perspective, angular sand particles always induce higher contact stresses than that of rounded particles as a result of the decreased interaction/contact area between individual sand grain and planar geomembrane sheet. The wear pattern developed on the geomembrane specimen surface tested at various different temperatures is evident as comparing the resulted graphical images of profile reliefs through the comparison of the created peaks and troughs. The amount and extent of profile relief can provide analogy with the improvement in frictional resistance with an increase in the ambient temperature, or comparatively correlated to the increase in shear strength at elevated temperatures. The plots also show

and confirm that the stylus profilometer was capable of capturing the path of the sand particles. Additionally, these illustrative plot representations of post-test surface profiles for the blasting sand sheared against smooth PVC geomembrane specimen at different temperatures demonstrates that the angular sand grains were able to deeply gouge the softer and more malleable liner surface of the geomembrane at elevated temperature conditions. This correlates to the mobilization of frictional shear mechanism during the process of shear displacement in the course of the interface direct shear tests. The blasting sand particle most severely plowed the surface of the geomembrane at higher elevated temperatures which was associated with the increment in the mobilized shear strength as well as the improvement in the developed overall interface shear behavior including peak and residual states as the shear stress-horizontal displacement failure curves of the interface tests at higher temperatures were located at the upper stress-displacement space of the direct shear tests performed at lower temperatures.

Table 8.2 summarizes the R_a values for the tested sand (rounded, angular) – smooth geomembrane (HDPE, PVC) interfaces at different temperatures ranging from 21°C to 50°C and at a range of normal stresses from 25 kPa up to 400 kPa. In addition, Figures 8.60 and 8.61 show the R_a versus Temperature and R_a versus Shore D hardness (H_D) plots, respectively, for the tested sand (rounded, angular) – smooth geomembrane (HDPE, PVC) interfaces at different normal stresses (25, 100 and 400 kPa). It can be seen that there is a direct correlation between the amount of surface wear which occurs at all normal stresses and at all temperatures. The angular particles cause significantly more wear than the rounded particles for both base polymer types. Further, the relative increase in wear, as quantified by induced roughness, was greater for the angular particles.

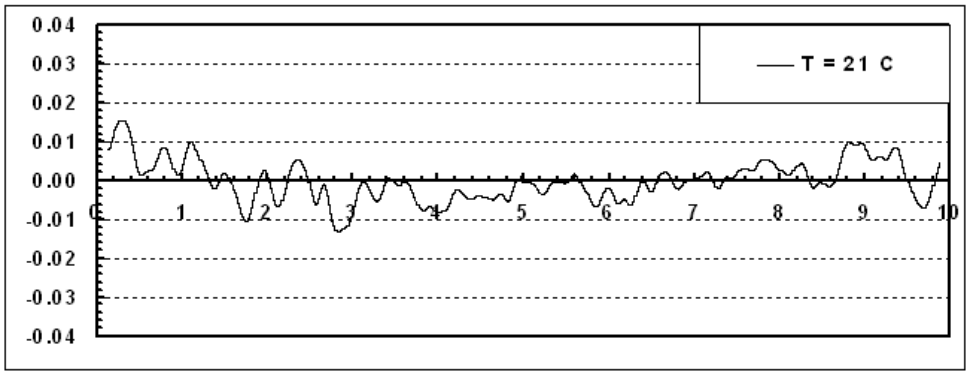

(a)

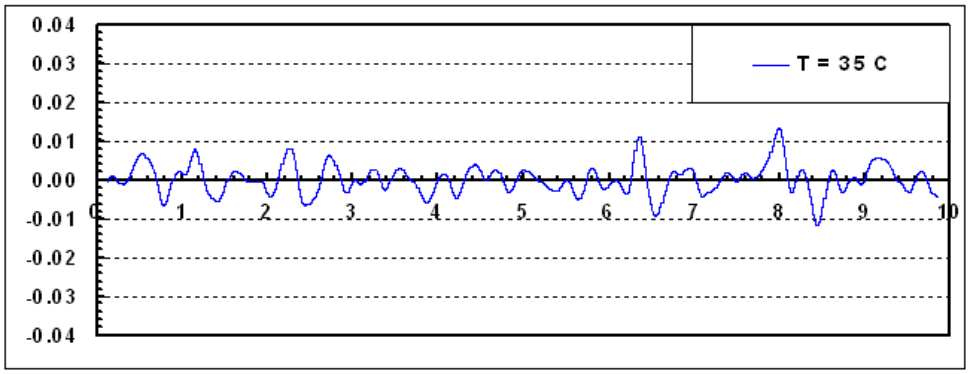

(b)

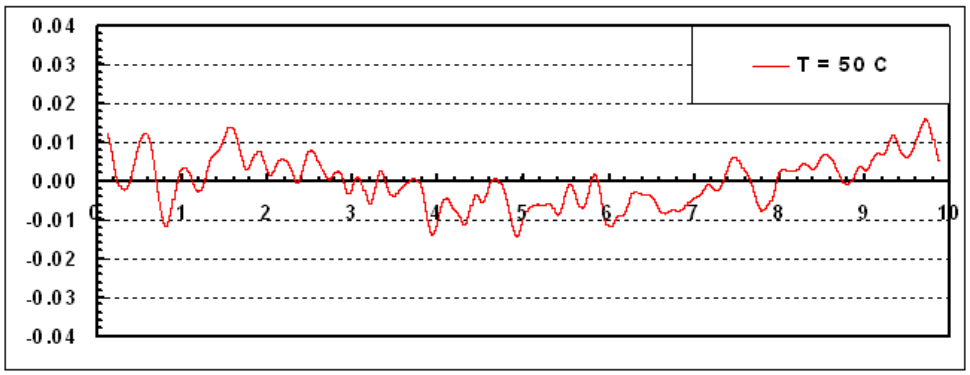

(c)

Figure 8.57 ***EPI Smooth PVC Geomembrane*** Post-Test Specimen Surface Roughness Profiles Sheared against ***Blasting Sand*** at Different Temperatures **[σ = 25 kPa]**
y: Profile Relief (Vertical Height) [*mm*]; **x:** Projected Profile Segment Length [*mm*]

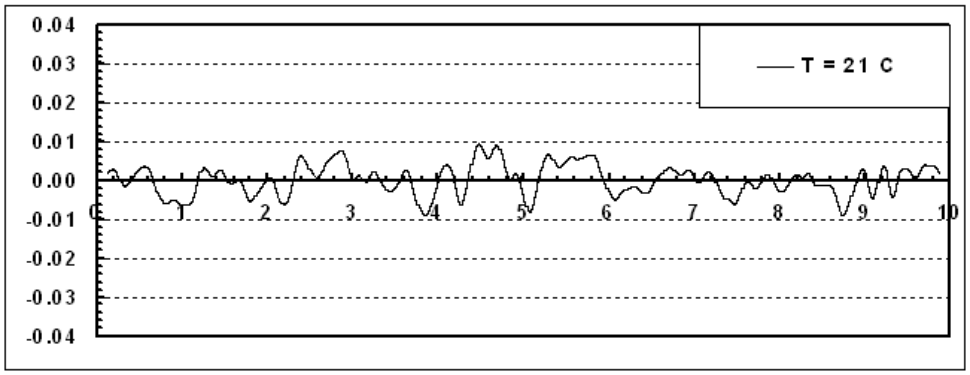

(a)

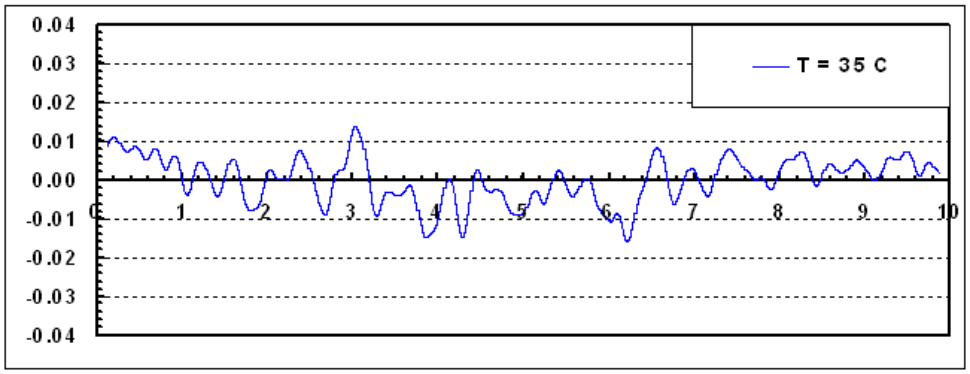

(b)

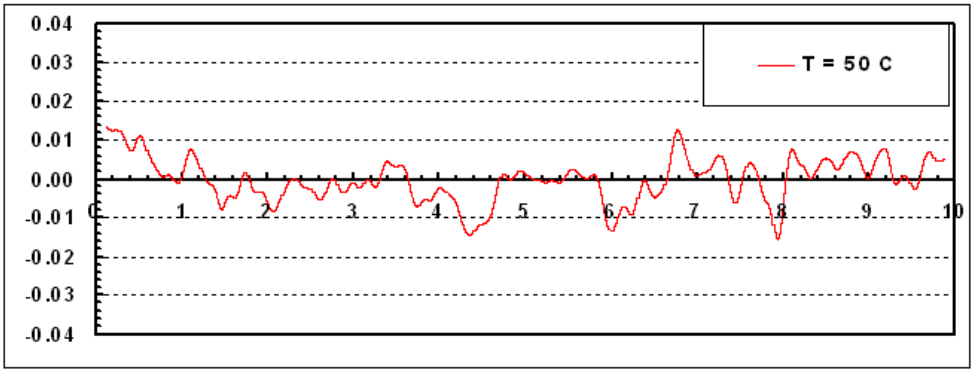

(c)

Figure 8.58 ***EPI Smooth PVC Geomembrane*** Post-Test Specimen Surface Roughness Profiles Sheared against ***Blasting Sand*** at Different Temperatures **[σ = 100 kPa]**
y: Profile Relief (Vertical Height) [*mm*]; **x:** Projected Profile Segment Length [*mm*]

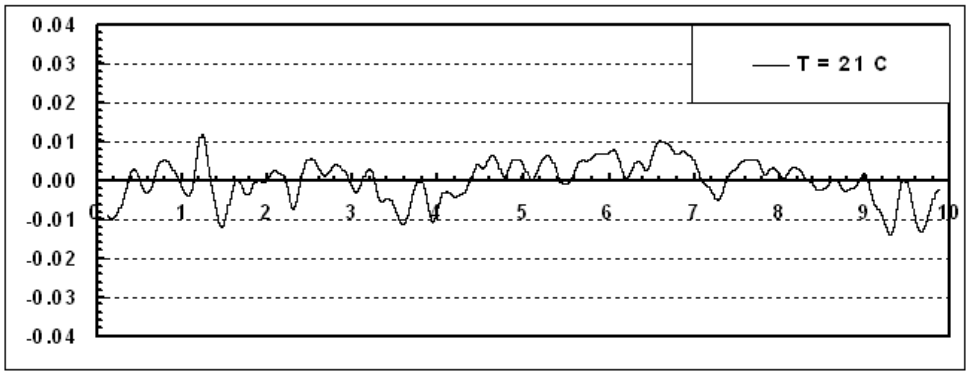

(a)

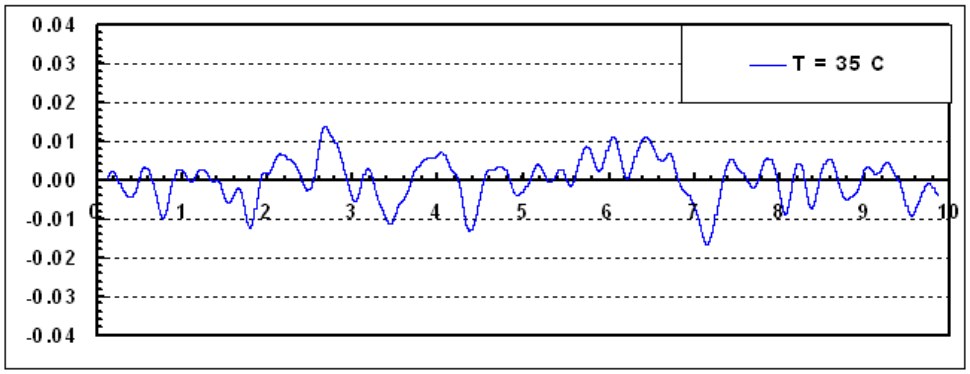

(b)

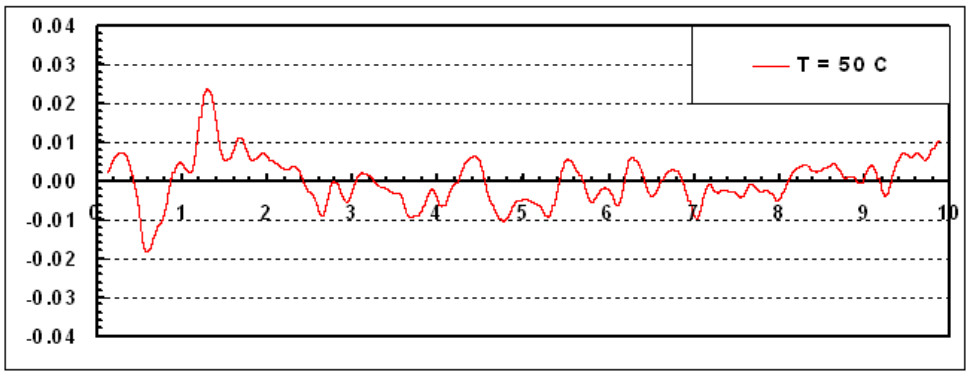

(c)

Figure 8.59 ***EPI Smooth PVC Geomembrane*** Post-Test Specimen Surface Roughness Profiles Sheared against ***Blasting Sand*** at Different Temperatures **[σ = 400 kPa]**
y: Profile Relief (Vertical Height) [*mm*]; **x:** Projected Profile Segment Length [*mm*]

Table 8.2 The R_a Values For The Tested Rounded or Angular Sand – Smooth HDPE or PVC Geomembrane Interfaces at Different Temperatures and Normal Stress Levels

	R_a (μm)					
	σ (kPa)	21 °C	30 °C	35 °C	40 °C	50 °C
Ottawa 20/30 Sand – Smooth HDPE Geomembrane	25	0.15	0.18	–	0.23	0.27
	100	0.38	0.43	–	0.49	0.56
	400	1.13	1.28	–	1.46	1.71
Blasting Sand – Smooth HDPE Geomembrane	25	0.27	0.34	–	0.43	0.55
	100	0.82	1.03	–	1.41	1.76
	400	2.06	2.74	–	3.53	4.89
Ottawa 20/30 Sand – Smooth PVC Geomembrane	25	0.21	–	0.29	–	0.43
	100	0.52	–	0.64	–	0.79
	400	1.54	–	1.79	–	2.35
Blasting Sand – Smooth PVC Geomembrane	25	0.31	–	0.49	–	0.68
	100	0.88	–	1.53	–	2.18
	400	2.24	–	3.59	–	5.12

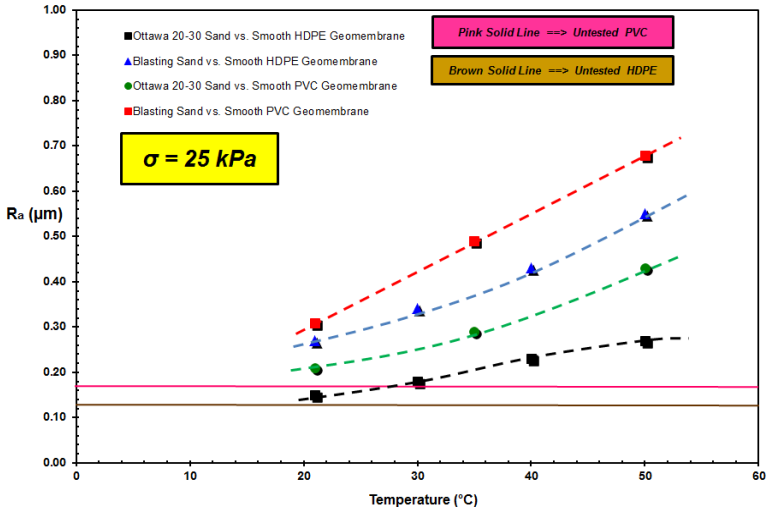

(a)

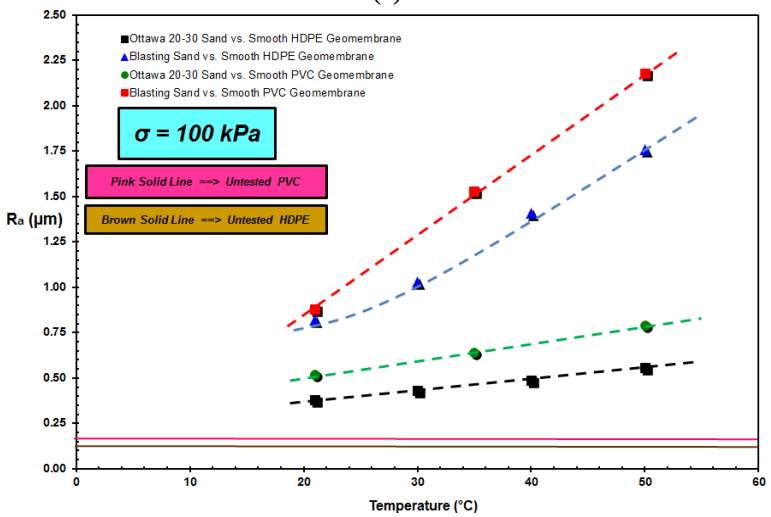

(b)

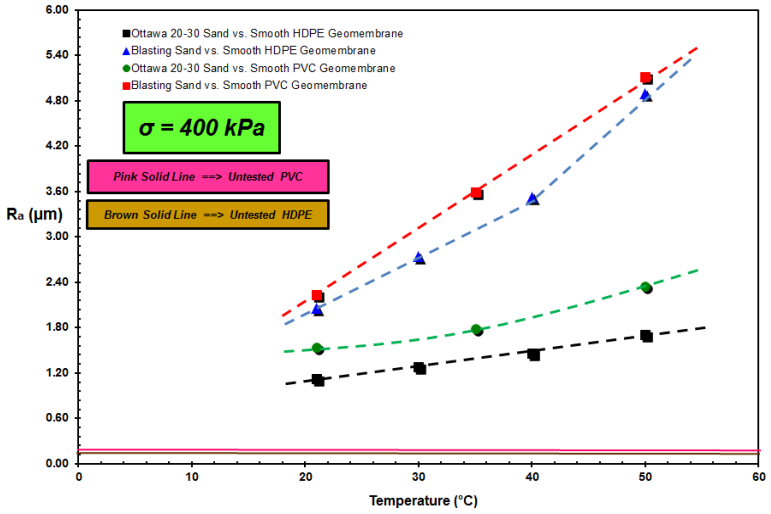

(c)

Figure 8.60 R_a versus Temperature:
(a) σ = 25 kPa; (b) σ = 100 kPa; (c) σ = 400 kPa

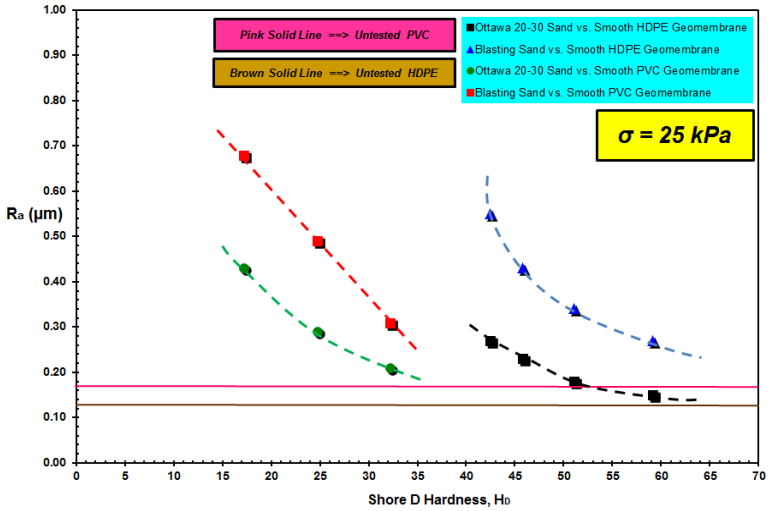

(a)

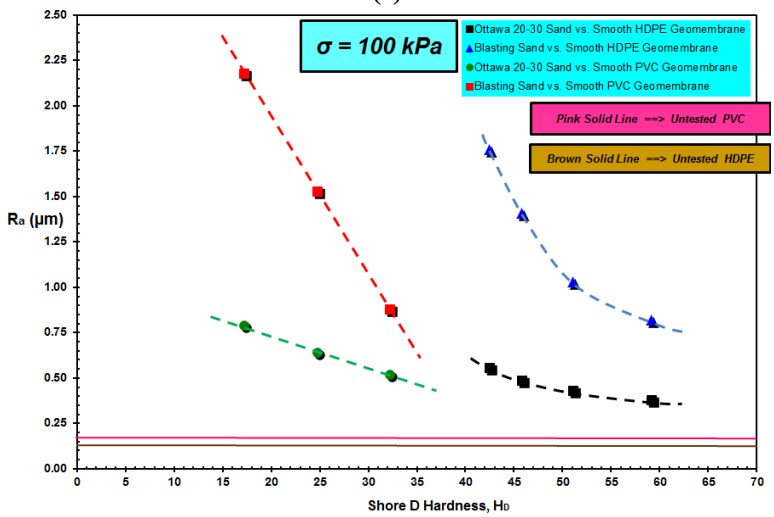

(b)

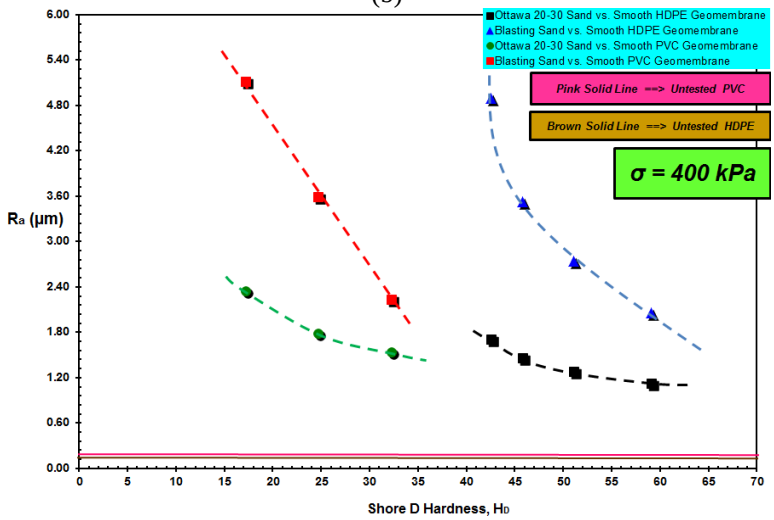

(c)

Figure 8.61 R_a versus Shore D Hardness, H_D:
(a) σ = 25 kPa; (b) σ = 100 kPa; (c) σ = 400 kPa

8.9. Replicate Interface Shear Tests at Various Test Temperatures

In order to confirm the stability of the temperature controlled chamber for heat-up and temperature conservation, and the ability of the TCC to sustain a constant temperature without any significant fluctuatians from the predetermined level, the plots in Figures 8.62 to 8.64 present replicate interface direct shear tests performed at various temperatures for sand – smooth geomembrane tests. Virgin geomembrane specimens were used in each test of the primary testing sequence. The normal stress was applied pneumatically and the same shear displacement rate was used throughout the entire test program. Sand and geomembrane test specimen preparation, placement procedures, as well as conditioning on the test apparatus, and additional force and displacement applications were all consistent. The interface test results demonstrate a high repeatability achieved at different conditions involving various ambient test temperatures and various counterface particulate-continua material combinations.

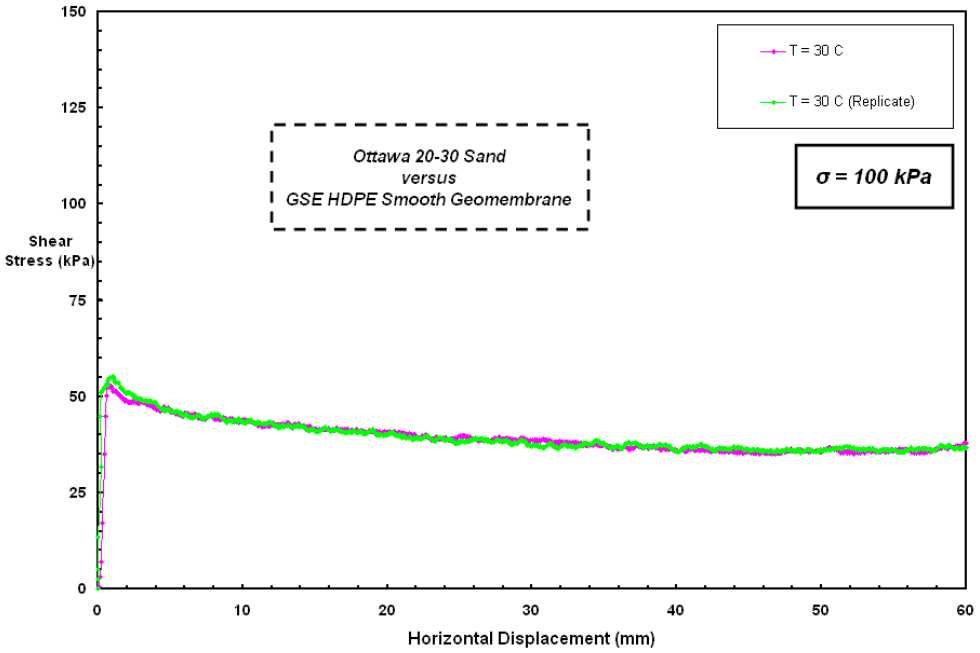

(a)

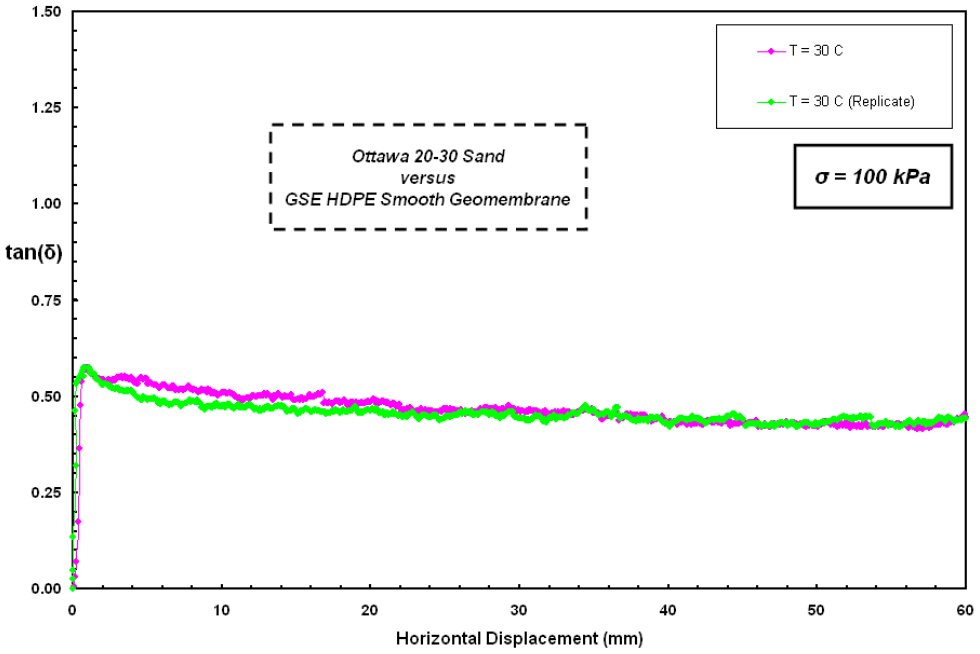

(b)

Figure 8.62 Replicate Interface Shear Tests on Ottawa 20-30 Sand – GSE Smooth HDPE Geomembrane Interface at an Elevated Temperature (T = 30 °C)

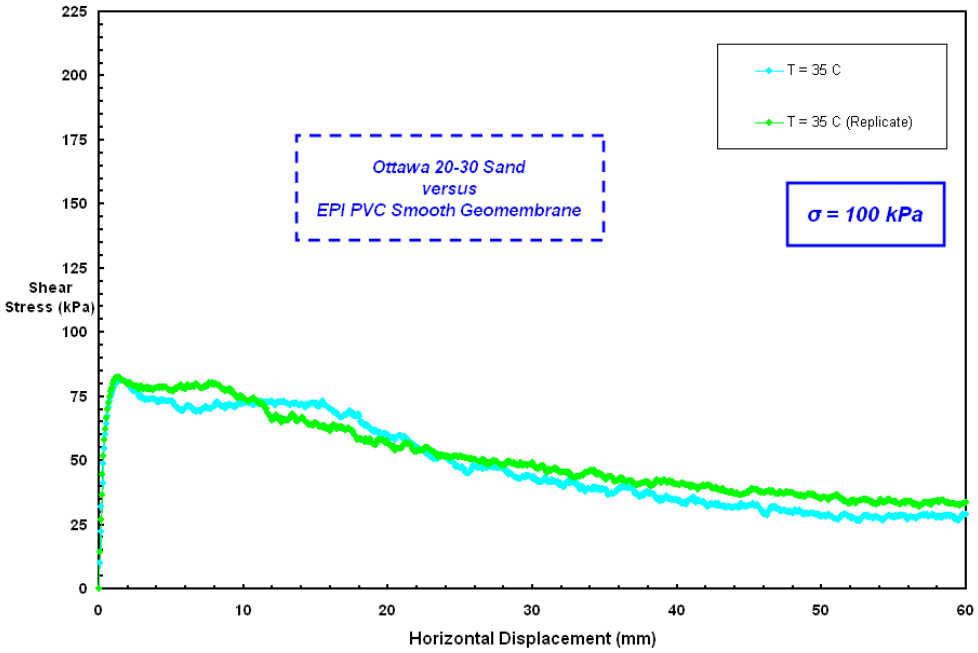

(a)

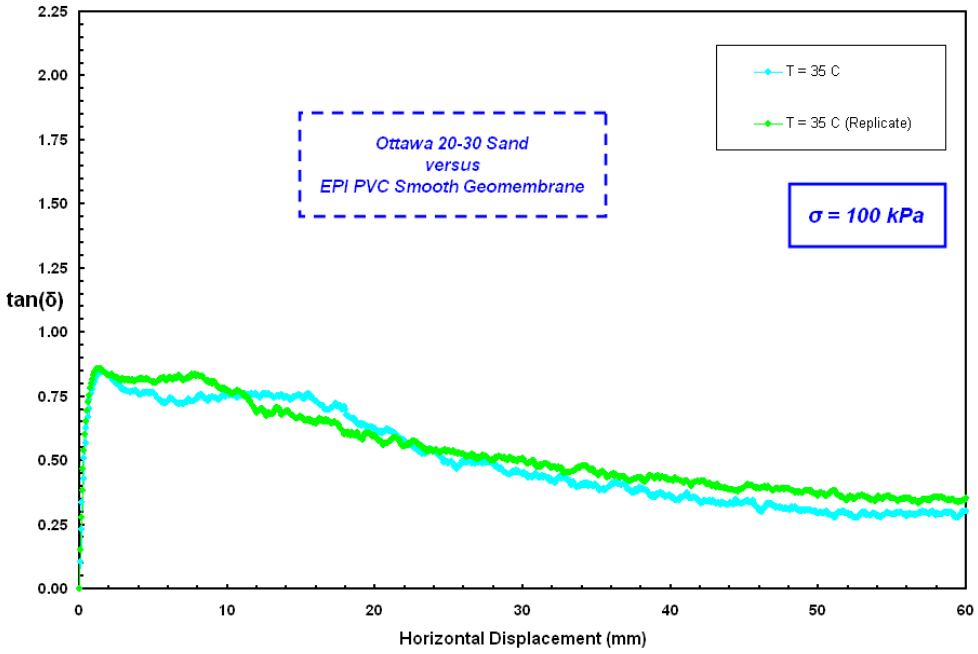

(b)

Figure 8.63 Replicate Interface Shear Tests on Ottawa 20-30 Sand – EPI Smooth PVC Geomembrane Interface at an Elevated Temperature (T = 35 °C)

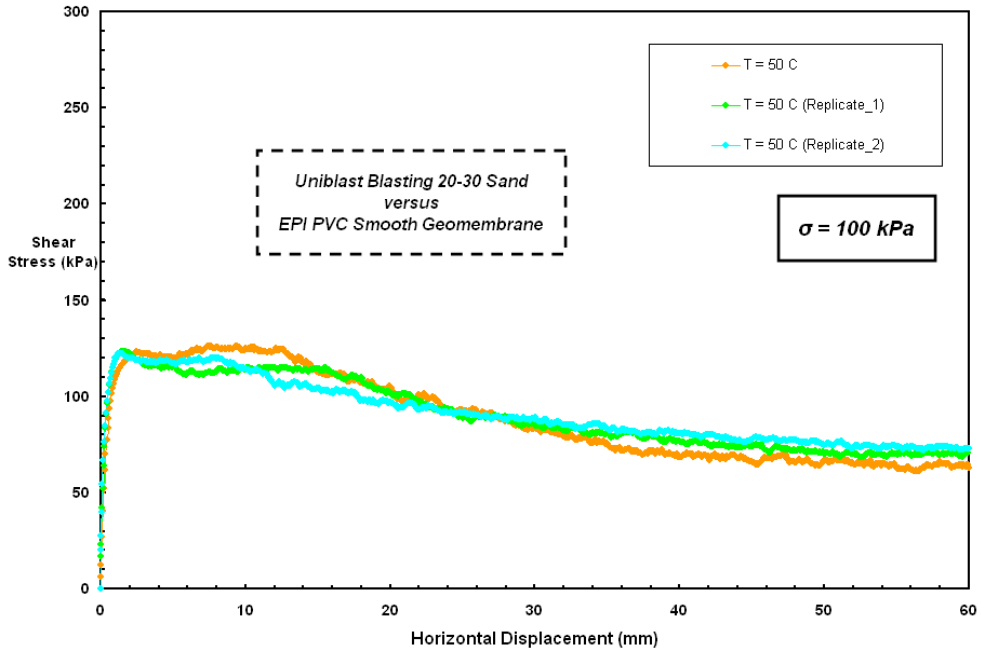

(a)

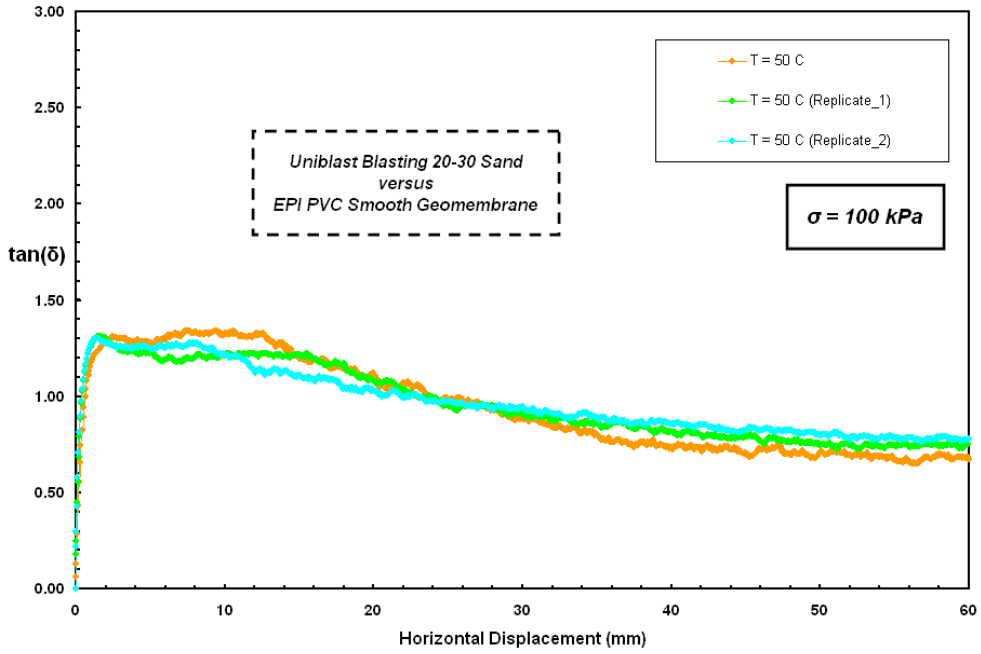

(b)

Figure 8.64 Replicate Interface Shear Tests on Blasting Sand – EPI Smooth PVC Geomembrane Interface at an Elevated Temperature (T = 50 °C)

8.10. Summary and Conclusions

The results and analyses presented herein demonstrate that the shear mechanisms and resulting friction coefficients of particulate – smooth geomembrane interface systems are dependent on a combination of several factors including polymeric material physical/mechanical properties (e.g. hardness), granular soil particle shape (i.e. roundness/angularity) and normal load levels (i.e. low or high). Interface shear tests were performed at a range of test temperatures from 21°C to 50°C and at different normal stresses ranging from 25 to 400 kPa that is consistent with general range of stress levels encountered in the field from construction stage to operation period in geotechnical applications such as landfills. The test results can suggest that if higher shear strength properties are desired for a composite layered system involving smooth HDPE or PVC geomembrane and particulate material interface at different ambient temperatures, then an angular granular soil can provide greater frictional performance in terms of the mobilized shear resistance in contact with smooth geomembrane liners.

The findings of an additional study to expand the understanding regarding the behavior (i.e. surface hardness properties) of the geomembrane liners at elevated temperatures involved in surface hardness measurements of smooth HDPE and PVC geomembranes at different temperatures will be presented in Chapter 9. In addition, pre-test as well as post-test surface profiles of the geomembrane specimens were quantified using a profilometer to observe the influence of temperature and loading conditions on the post-test surficial wear of the geomembrane (compared to pre-test virgin liner specimens) sheared against rounded or angular sands (Section 8.8). This was intended to show how shear induced changes in smooth geomembrane surface topography as a

function of temperature when sheared against a granular soil at elevated temperatures. To this end, the post-test surface wear of the geomembrane specimens after interface shear tests at different temperatures was demonstrated through plotting post-test surface roughness relief over a profile length. The graphical representations visually depict the grooves, scratches (troughs in the plots) and material dislocations (peaks in the plots) with a change in ambient temperature as well as the magnitude of normal stress applied on the interface during shearing. The results show the differences in the resultant surficial wear of the counterface geomembrane due to the shape (rounded/angular) of sand particle in contact with the liner. Accordingly, the results of the interface shear tests at different temperatures can be compared with the post-test surface topography measurements of the smooth HDPE and PVC geomembrane specimens to provide a further understanding for the mechanism (sliding/plowing) mobilized during shearing. As such, the frictional shear resistance of the particulate – continuum material interfaces are also controlled by the ability of granular soil particles to penetrate into the counterface material under load and plow the counterface at a depth in the course of shear displacement. The influence of temperature on the peak and post-peak shear strength of the interfaces were shown through Mohr-Coulomb failure envelopes plotted based on the results of interface shear test at different temperatures for smooth HDPE and PVC geomembrane interfaces in contact with either rounded or angular sand. In summary, this chapter has illustrated the influence of temperature on sand – geomembrane interface shear behavior and frictional strength. The results show that temperature plays a significant role in the mobilized frictional mechanism at the interface during shear displacement (i.e. elastic-plastic sliding or plowing/material dislocation).

CHAPTER IX

9. PRACTICAL IMPLICATIONS AND ASSESSMENT OF TEMPERATURE EFFECTS ON INTERFACE SHEAR STRENGTH

9.1. Introduction and Background

The use of polymeric materials strongly influences geotechnical practice and the interaction between these materials and soil plays a critical role in governing the integrity of numerous critical structures. For example, the stability of modern lining systems for waste containment facilities is controlled by interface shear resistance between multiple geosynthetic components as well as between geosynthetics and the surrounding soil. Numerous research efforts have been undertaken to evaluate the interface shear properties of polymers with the intention of establishing a general range for interface shear characteristics for these materials. The experimental studies of Lupini et al. (1981), Ingold (1982), Martin et al. (1984), Saxena and Wong (1984), Koerner et al. (1986), Williams and Houlihan (1987), O'Rourke and Druschel (1989), Negussey et al. (1989), Mitchell et al. (1990), O'Rourke et al. (1990), Bove (1990), Takasumi et al. (1991), Stark and Poeppel (1994), and Dove and Frost (1999) amongst others, can be considered as important research work on the interface shear resistance of polymeric materials. These experimental studies, in addition to developing a database, also provide designers and engineering agencies with information for estimating the likely range of frictional performance of geosynthetic interfaces in geotechnical applications.

9.2. Concept on Hardness of Materials

Hardness is the measure of how resistant a solid material is to a force application which results in a permanent shape change in the solid material. The complex response behavior of materials under force due to their varied nature resulting from their different physical and chemical properties has led to different measurement modes of hardness to emerge in science: i) scratch hardness; ii) indentation hardness; and iii) rebound hardness. Further, there exists different individual measurement scales defined within each of these modes of hardness measurement. For practical purposes, conversion graphs and tables are used to convert measurement values between one scale and another (e.g. Figure 9.1a – 9.1f). However, the reliability and accuracy of a hardness measurement for a given material will be reduced by converting from one scale to another as the correlations between different scales are often determined through empirical equations based on experimental data. Therefore, the most suitable hardness measurement method, which conforms best to the recommended standards for the technique, should be followed to determine the hardness of the material under consideration. In general, scratch hardness is defined as the measure of resistance of a material to fracture or permanent (plastic) deformation as a result of friction from a sharp object. The most common test is Mohs scale which is generally used in mineralogy (soil and rock geology). Rebound hardness (dynamic hardness) which is related to material elasticity measures the height of the "bounce" of a diamond tipped hammer dropped from a fixed height onto a material. The scales utilized to measure rebound hardness are Leeb rebound hardness test and Bennett hardness scale (Haasen, 1996).

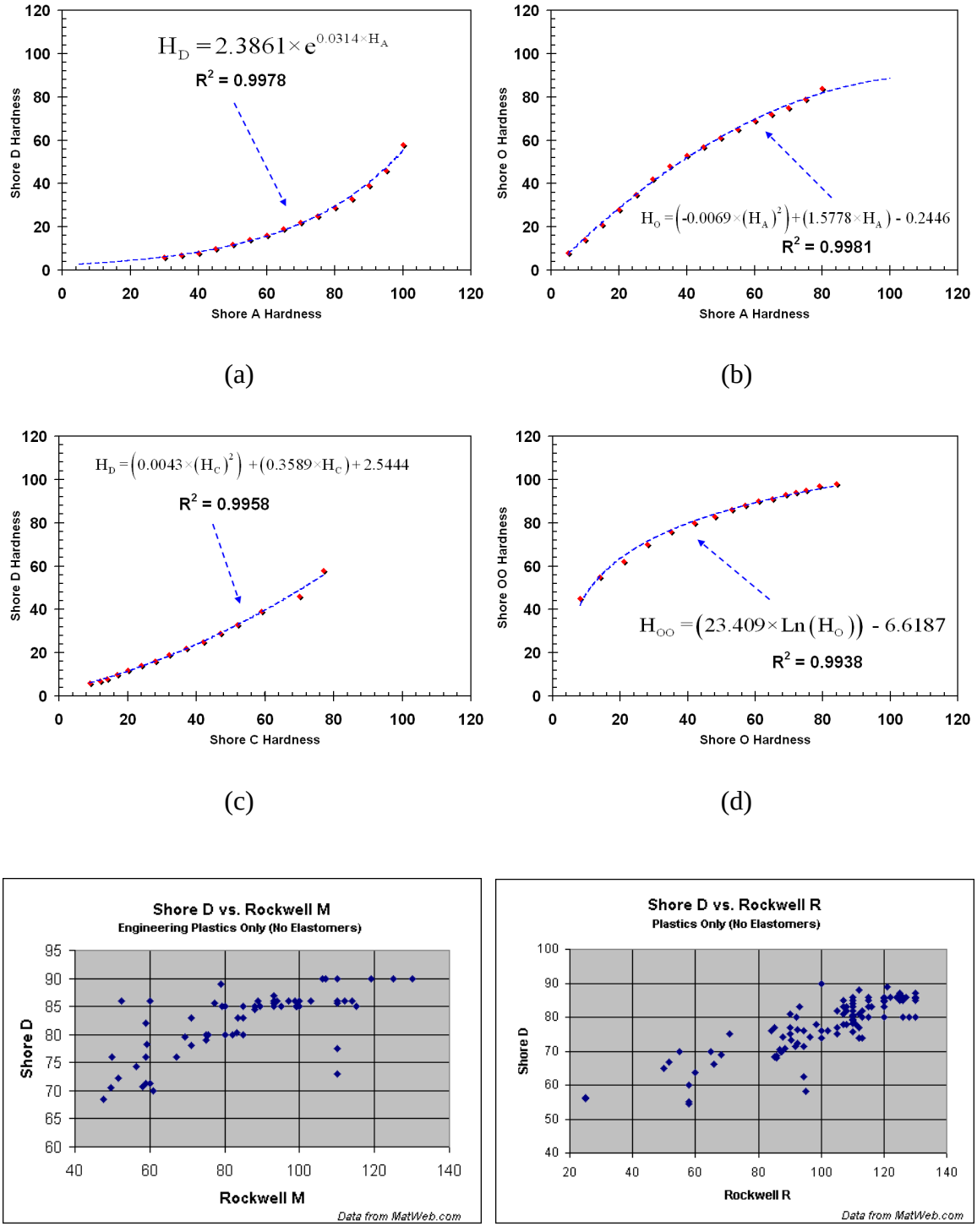

Figure 9.1 Relations and Conversion between Different Hardness Scales:
(a) Shore A versus Shore D; (b) Shore A versus Shore O; (c) Shore C versus Shore D;
(d) Shore O versus Shore OO; (e) Shore D versus Rockwell M;
(f) Shore D versus Rockwell R (Data from MatWeb)

The focus of the current study which is concerned with geomembrane hardness (a plastic material manufactured from polymer) is focused on an indentation hardness measurement approach in which the resistance of a sample is defined and established based on permanent plastic deformation due to a constant compression load from a sharp object. The critical dimensions of an indentation created by a specifically "dimensioned" and "loaded" indenter are measured to find out the indentation hardness in engineering and metallurgy. The most common indentation hardness scales are Rockwell, Vickers, Brinell, and Shore.

The purpose of surface hardness tests on plastics is to measure the "resistance" of these polymeric materials which developed through their physical properties to withstand an indentation force generated by a sharp object attempting to penetrate into their surfaces. Therefore, the indentation hardness is inversely related to the penetration and dependent on elasticity, ductility, plasticity, strain, strength, stiffness, toughness, viscoelasticity, and viscosity properties of the polymeric materials (Haasen, 1996). Among the several hardness scales utilized in engineering and summarized above, Shore Hardness is one of the most common methods of determining surface hardness of rubber and plastic materials (i.e. polymeric materials such as geomembranes). In particular, two types of Shore hardness scales are specifically utilized for polymeric/plastic materials: Shore A (H_A) scale is generally preferred for relatively "softer" plastics; while Shore D (H_D) is used for relatively "harder" plastics (e.g. geosynthetics) to obtain an index value of surface hardness. Additionally, Shore D method is considered to be an appropriate technique for measuring the surface hardness of both smooth HDPE and smooth PVC geomembranes in a consistent manner for the purpose of assessing the hardness of

smooth geomembranes employed in geotechnical applications at varied temperature conditions. Shore D Hardness, (H_D) measurements, which are conducted in accordance with ASTM D 2240-05 (2005), provide an index of the material surface hardness which can then be used in evaluating the interface friction characteristics of geosynthetic materials.

9.3. Influence of Geomembrane Surface Pliability (i.e. Hardness) on the Developed Interface Shear Strength and Behavior

The shear resistance with respect to slope stability along various geosynthetic component interfaces (i.e. sand-geomembrane) is an important design issue for composite liner systems. A number of case histories by Seed et al. 1990, Seed and Boulanger 1991, Byrne et al. 1992, and Stark 1999 revealed that a geomembrane can create a problematic interface due to low frictional resistance between it and soil or another geosynthetic component. The mobilized frictional strength and the developed interface shear behavior at particulate material (sand) – continua (geomembrane) interfaces are influenced by the surface hardness of the geomembrane. Therefore, the measured index value of hardness of the geomembrane based on a particular scale (i.e. Shore D) will provide a useful quantitative value to evaluate the magnitude of shear resistance being generated at the interface between granular soil and geosynthetic. The effect of temperature on sand-geomembrane interface shear behavior results from the temperature dependency of geomembrane properties such as hardness. Consequently, the amount of shear resistance developed at the interface is mainly attributed to geomembrane surface pliability

governed by the material hardness which can vary as a function of the ambient temperature.

In an effort to examine and further investigate the influence of hardness on geomembrane interface shear response, Hillman and Stark (2001) conducted a research study in which the interface shear behavior of polyvinylchloride (PVC) geomembrane (most plasticized, flexible) was compared to that of a high density polyethylene (HDPE) (least plasticized, stiffest) geomembrane and two very flexible polyethylene (VFPE) geomembranes (mid plasticized and softness between the other two). There was a pronounced difference in the shear strength characteristics of the geomembranes, each of which had a different hardness (H_D). These differences and variations observed in interface shear behavior and strength were attributed to the pliability of the PVC geomembrane which is material hardness dependent property and thereby enabled: (i) the PVC geomembrane surface to have greater contact and an integral interface interaction by allowing the counterface material (i.e. geotextile) to settle in completely into its surface; (ii) the counterface components to embed into the geomembrane by forming a more flexible interface interaction as "shearing progresses"; and (iii) being more flexible and therefore less likely to damage the overlying geosynthetic. In order to illustrate the influence of geomembrane surface hardness and pliability on the complete interface shear behavior developed at an interface with another geosynthetic material, Figure 9.2 from Hillman and Stark (2001) presents the shear stress-displacement relationships for three geomembranes produced from different base polymer resins which have dissimilar surface hardness and roughness values. These include a faille PVC, a textured HDPE, and a textured VFPE geomembrane sheared against nonwoven geotextile (540 g/m^2) at a

normal stress of 192 kPa, in a torsional ring shear device. The higher pliability nature of the PVC geomembrane resulted in a different interface shear behavior than PE geomembranes. The VFPE and HDPE geomembrane interfaces reached a peak strength condition after approximately 5 mm of shear displacement and then experienced a substantial post-peak strength loss about 40% to 60%. On the other hand, the faille PVC interface peaked at a shear displacement of approximately 18 mm and lost only 20% to 25% of its peak shear strength.

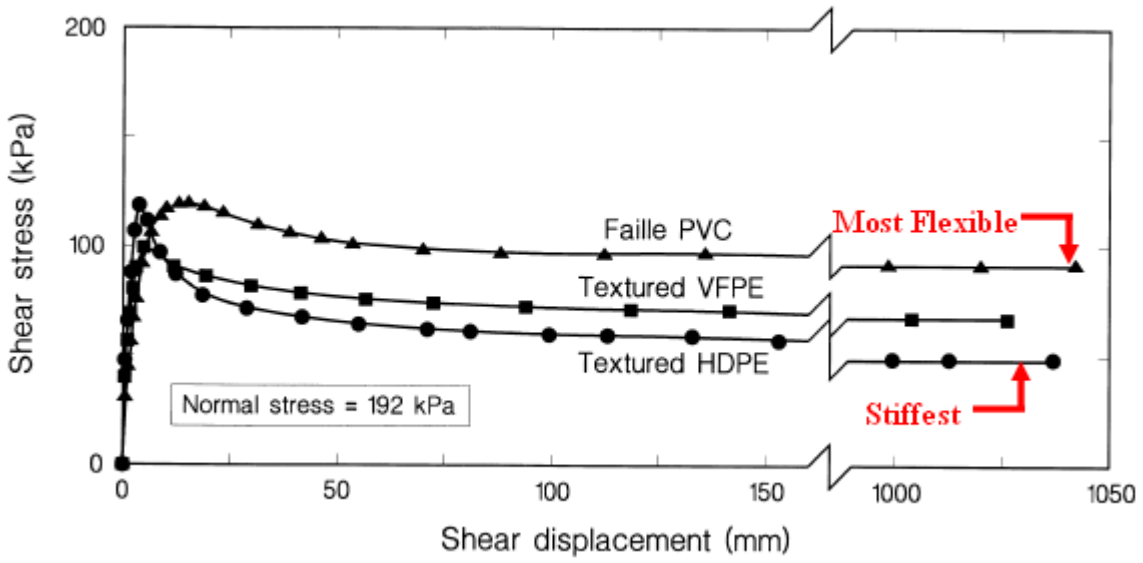

Figure 9.2 Comparisons of Shear Stress-Displacement Relationships for Faille PVC, Textured VFPE, and Textured HDPE Geomembrane versus Nonwoven Geotextile (540 g/m2) (Adapted from Hillman and Stark, 2001)

Note: PVC geomembranes can be manufactured with a smooth side and an embossed side. The surface of the embossed side usually resembles that of a file and is called a "faille-finished" surface. Accordingly, a faille PVC geomembrane interface is one in which the faille-finished surface of a PVC geomembrane is sheared against another geosynthetic component. A smooth PVC geomembrane interface is one in which the smooth surface of a PVC geomembrane is sheared against another geosynthetic component (Hillman and Stark, 2001).

Based on these interface test results, it can be seen that the PVC which contains plasticizers to enhance its flexibility has less hardness and consequently a more pliable geomembrane surface, facilitated and promoted the counterface material to embed into the geomembrane with ease resulting in more extensible interface interaction as the shearing operation progresses. Additionally, the PVC geomembrane is more flexible and thus less likely to pull out and tear geotextile filaments from the fabric during the shearing process. Finally, the softer and more flexible nature of the PVC geomembrane benefited itself to get polished throughout shearing process and lead to a smaller interface sensitivity ($\tau_{Peak}/\tau_{Post\text{-}Peak}$) (Figure 9.3).

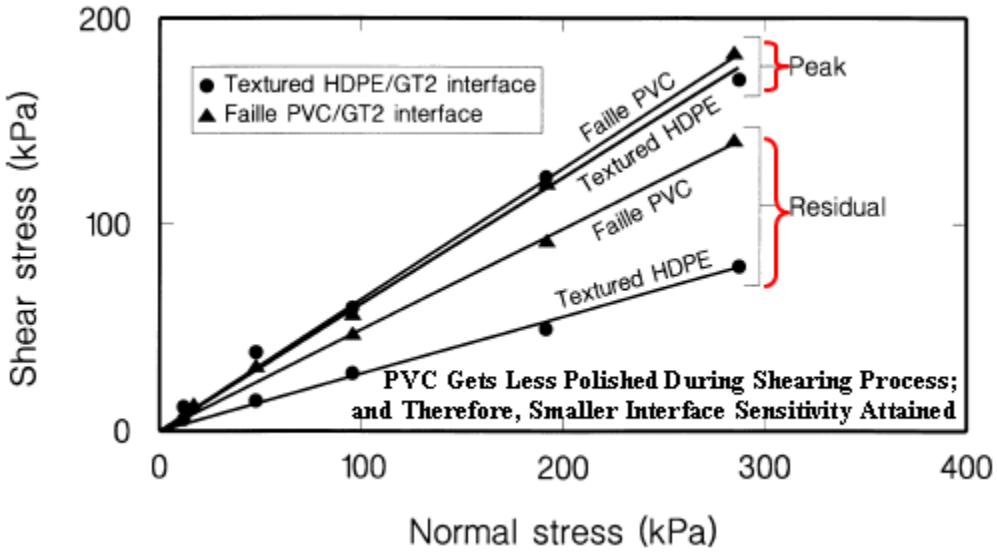

Figure 9.3 Comparison of Failure Envelopes for Faille PVC &Textured HDPE Geomembrane – NW Geotextile (540 g/m2) (Adapted from Hillman and Stark, 2001)

Faille PVC geomembrane-nonwoven geotextile interfaces appeared to yield similar peak shear strengths and considerably higher residual shear strengths as similar textured VFPE geomembrane-nonwoven geotextile interfaces (Figure 9.4). The reason of the "*smooth*" VFPE geomembrane interface for exhibiting both a lower peak and a

residual shear strength than the faille PVC geomembrane interface was attributed by Hillman and Stark (2001) to the difference in surface pliability (i.e. PVC is softer and more pliable than VFPE). It was additionally noted by the authors that even though the VFPE geomembrane is more pliable and flexible than an HDPE geomembrane, it is still less pliable and stiffer than the faille or the smooth PVC geomembrane and, thus, exhibits lower interface strength. However, the role of the dissimilar surface textures between the faille PVC and the smooth VFPE geomembrane resulting in the differences for the displayed frictional resistances and shear responses was not addressed by the authors.

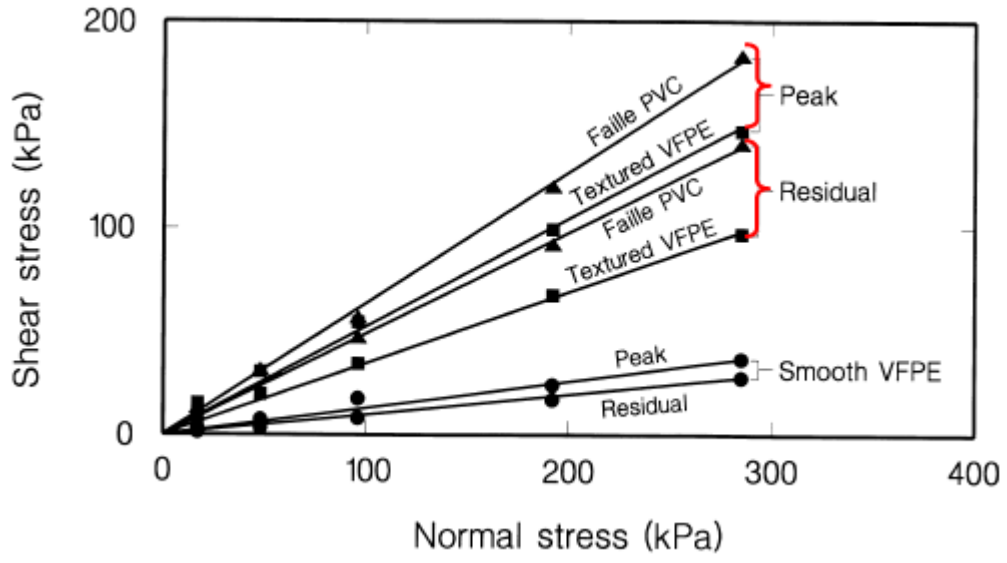

Figure 9.4 Comparison of Failure Envelopes for Faille PVC, Smooth VFPE, and Textured VFPE Geomembrane Versus Nonwoven Geotextile (540 g/m2) (Adapted from Hillman and Stark, 2001)

Figure 9.5 shows the ring shear comparison tests performed by Hillman and Stark (2001) on either the faille PVC or the smooth PVC geomembrane sheared against nonwoven PP geotextile. The smooth PVC geomembrane displayed shear stress versus displacement failure curves located at upper/higher stress space and displayed larger peak

and residual frictional resistances mobilized at the interface in conjunction with the nonwoven geotextile.

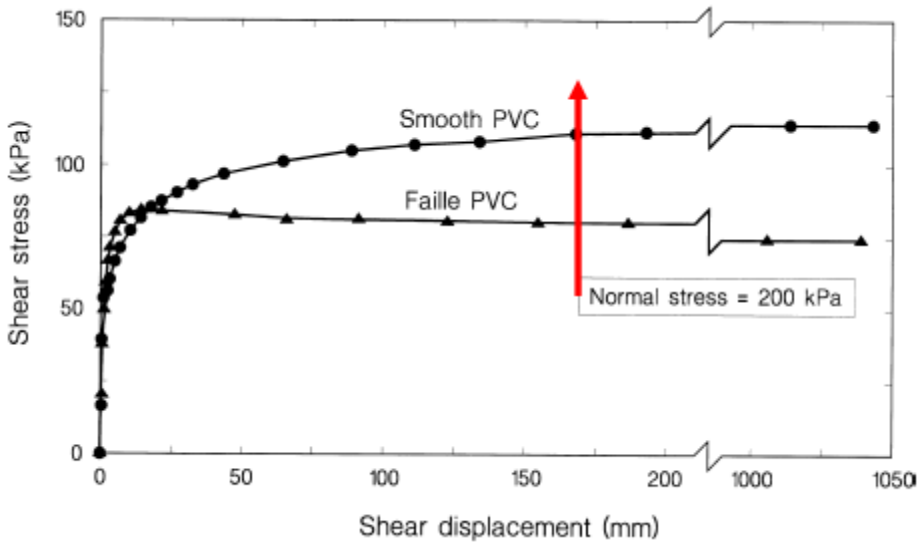

Figure 9.5 Comparison of Shear Displacement Relationships for Smooth and Faille PVC Geomembrane-Nonwoven PP Geotextile (540 g/m^2)
(Adapted from Hillman and Stark, 2001)

The higher frictional strength of the smooth PVC geomembrane was attributed by them to its higher surface pliability as well as establishing greater extent of contact with the counterface material and enabling more extensible emplacement (i.e. further settling down extensively onto the counterface) without having surface deficiencies resulted from the surface depressions of the embossed surface of a faille liner usually resembling that of a file. Additionally, it was indicated that the increased pliability of the PVC liner resulted in a more ductile, malleable, or adaptable surface properties which in return had led to the PVC geomembrane showing higher interface strength and response than that of the "*smooth"* VFPE geomembrane as well as the stress-displacement failure envelopes for the PVC tests are located on the upper space of the failure envelopes from the *"smooth"*

VFPE interface shear tests. The surface hardness of the PVC geomembranes is smaller, and thereby, possesses softer surface nature which can allow for a greater extent of contact at the interface with the counterface material. Additionally, the flexible nature of the PVC liner is less likely to create the surface depressions with the counterface under load such as the case of the stiffer lining materials including the geomembranes made from PE which can result in decrease for the extent of contact between the interface components at the interface (Hillman and Stark, 2001).

As shearing operation progresses, the higher surface pliability and the softer liner surface nature of the PVC allows it to be embedded by the counterface geotextile matrix at global-level and by the fabric filaments at micro-scale, resulting in a larger shear resistance generated with further shear displacement (i.e. based on their results, no post-peak interface strength loss was observed during the course of larger shear displacements in ring shear device). However, the stiffer geomembranes made from PE did not allow the counterface to embed as much as it can on the PVC geomembrane (Hillman and Stark, 2001). This prevented the frictional resistance of the harder PE geomembrane interfaces (i.e. VFPE) from reaching the same values as the PVC. The softer smooth PVC geomembrane seems to have provided an opportunity for this material to exhibit higher shear-displacement failure envelopes during shear without the necessity for extra work performed for texturing process for making geomembrane surface rougher in order to achieve higher interface resistance such as the case of the VFPE geomembrane.

9.4. Hardness and Interface Friction Angle

Based on an experimental program involving over 450 direct shear tests, the work of O'Rourke et al. (1990) revealed an important and principal relation for rapidly and practically evaluating shear strength characteristics of sand-polymer (i.e. geomembrane) interfaces and expressing these characteristics conveniently as the ratio of the interface angle of friction to the direct shear angle of soil friction, (δ/φ'_{ds}). The aim of their research was to investigate and establish a relationship between polymeric material surface hardness and interface friction angle whereby shear resistance could be defined as a function of a general index property which is independent of specific polymer products. A further objective of their research work was to provide an easy and quick means of predicting shear resistance/strength of sand-polymer interfaces from the hardness of the continuum material at the interface. Shore D Hardness measurements are simply performed using a durometer (indentation device) which offers a practical and quick application of the test while allowing for widespread and expedient use in practice. They presented the results of a comprehensive laboratory testing program to determine the direct shear strength and displacement characteristics of granular soils (i.e. sands) in contact with smooth polymeric materials. Surfaces of HDPE, MDPE, PVC, epoxy, and acrylic were studied and SEM (scanning electron microscopy) were utilized to take images of the sheared polymer surfaces against particulate materials having different grain shape. In this way, it was intended to evaluate the roughening and grooving (i.e. plowing effect, scour, and surface damage) occurring on the surface of polymeric materials in contact with harder and stiffer granular soils under typical conditions of construction and service.

The general model developed by O'Rourke et al. (1990) for predicting frictional resistance of granular soil-polymer interfaces is built on a correlation by assessing interface friction angle with the knowledge of soil internal friction angle whereby the ratio of interface angle of shear resistance, (δ) to direct shear angle of soil friction (φ'_{ds}) is related to Shore D Hardness (H_D) index of the polymeric materials. The use of ratio value of (δ/φ'_{ds}) was purposely intended to be applied for both the polymeric material surface properties and granular soil frictional characteristics under consideration. Because the frictional properties of granular soils are less influenced by the change of ambient conditions such as temperature compared with the significant effects of temperature on the physical, and hence, interfacial shear strength characteristics of polymeric materials. Their approach divided the problem logically into two stages by firstly determining the soil property, (φ'_{ds}), and secondly computing the interface property, (δ/φ'_{ds}) which can then be "adjusted" to any value of φ'_{ds}. Moreover, as indicated by the authors, although φ'_{ds} and δ are significantly varied for different sands; the values/proportion of δ/φ'_{ds} display little variation.

The ratios of peak interface friction angle to peak angle of direct shear resistance of the sand, (δ/φ'_{ds}) as a function of the Shore D Hardness, (H_D) for several polymeric/plastic materials including HDPE, MDPE, PVC, epoxy, and acrylic are presented in Figure 9.6. The manufactured geo-products of selected polymeric materials as being lining or pipe have been widely used in geotechnical applications in the field. The changing physical and mechanical properties of these materials are, therefore, appropriate to be examined.

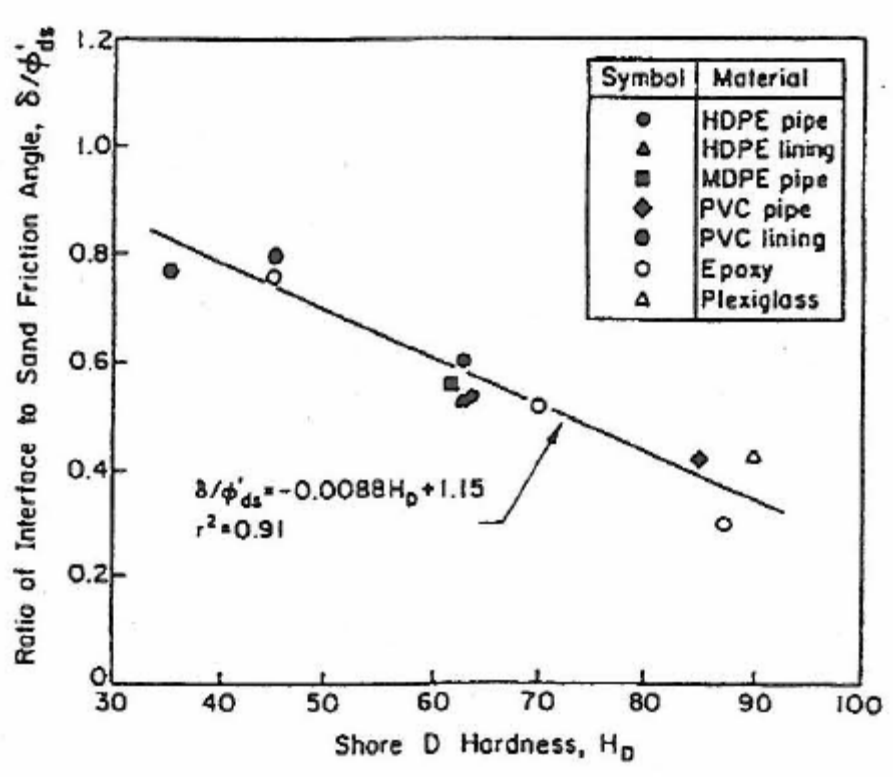

Figure 9.6 Ratio of Peak "Interface" to "Soil" (Direct Shear) Friction Angles, (δ/φ_{ds}) Versus Shore D Hardness, (H_D) (O'Rourke et al., 1990)

As seen on Figure 9.6, the interface property, (δ/φ'_{ds}) decreases with increasing Shore D Hardness, (H_D) for several different sand-polymer interfaces tested. They performed a linear regression on these data, which provided a straight line fit with a high coefficient of determination, (r^2), to show the mathematical correlation (Equation 9.1) relating (δ/φ'_{ds}) to H_D. The closeness of fit ($r^2 = 0.91$) between the regression and test data suggested that Shore D Hardness, (H_D) is a reasonable index for estimating the surface shear strength characteristics, δ/φ'_{ds}, over a broad range of polymers in contact with granular soils (sands).

$$\frac{\delta}{\varphi'_{ds}} = -0.0088 \times H_D + 1.15 \qquad (9.1)$$

Where;

δ: Interface Friction Angle

φ'_{ds}: Soil Direct Shear Friction Angle

H_D: Polymeric Material Shore D Hardness

This model (Equation 9.1) allowed rapid evaluation of interface frictional strength and applies to the composite systems composed of granular materials in contact with plastic/polymeric materials such as smooth geomembranes.

9.5. Hardness and Temperature

9.5.1. Shore D Hardness Measurements at Different Temperatures

A series of measurements were undertaken as part of this research study to investigate the effect of temperature on the hardness of geosynthetic materials as well as to allow for indirect evaluation of temperature effects on the shear strength of granular material-geomembrane interfaces. Shore D Hardness measurements were performed according to ASTM D 2240-05 (2005) at different temperatures to obtain an index value and to investigate the variation of this index value with increasing temperature for surface hardness of smooth HDPE as well as smooth PVC geomembranes using a durometer with constant loader test stand placed in temperature controlled chamber (TCC) (Figure 9.7). The temperature controlled chamber has a size of 1100 mm in length, 760 mm in width

and 510 mm in height. Temperatures above ambient conditions were obtained using heat bulbs as a radiant energy heat source mounted on the walls in the chamber. Fans which have square dimensions of 120 mm by 120 mm and depth of 25 mm and made of steel blade, aluminum frame were selected to be utilized for circulating heated air within the chamber for uniform distribution of temperature inside the TCC. Fans are attached to aluminum handles and located at proximity of the center of the chamber. Hardness tests were performed at temperatures ranging from 21°C to 50°C.

The continuum materials tested including smooth high density polyethylene (HDPE) geomembrane liner as well as smooth polyvinylchloride (PVC) geomembrane liner used throughout this study and were neither corrugated nor textured and had clean smooth surfaces. Both HDPE and PVC geomembrane specimens were composed of plied pieces to obtain the minimum thickness for the purpose of precise hardness determination with the durometer as required by ASTM D 2240-05. The materials to be tested were placed in the temperature controlled chamber (TCC) and kept at constant targeted test temperature (i.e. 30°C, 40°C, 50°C) before the hardness measurements were conducted. It was aimed to ensure that the continuum materials have uniform and stabilized temperatures throughout the entire sample mass at the time of measurements. A surface-mount, fast-response (<0.15 sec.), self adhesive thermocouple (Type T) was attached to the material surface to be tested to be able to measure the exact temperature of the specimen and control the ambient temperature of the TCC environment. Hardness measurements were taken at various locations of each specimen to reduce error in measurements by following a random pattern, to observe the variability in surface

hardness of intact solid continua exposed to elevated temperature conditions, and to investigate the variation in readings across the bulk.

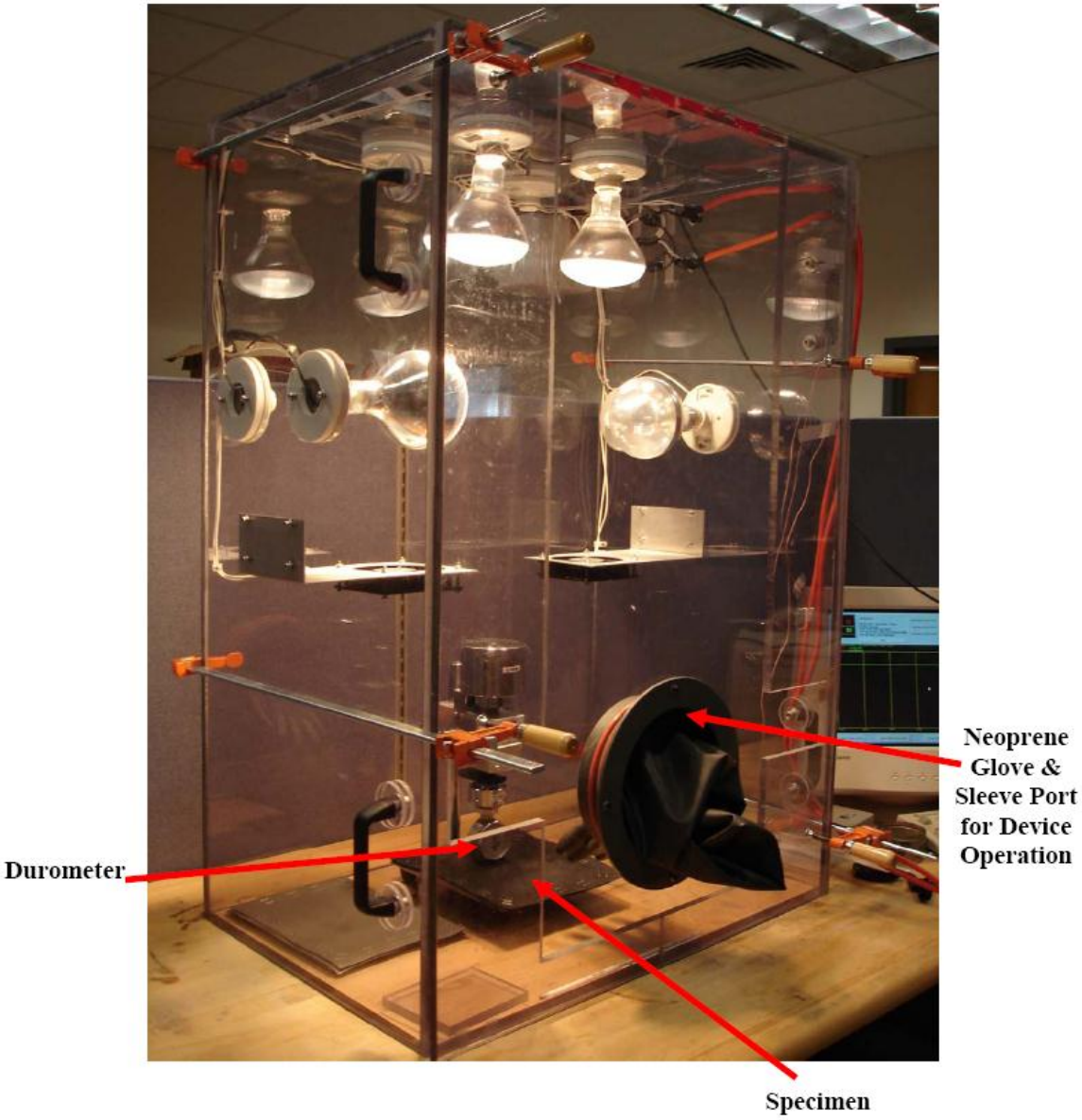

Figure 9.7 Durometer with Constant Loader Test Stand located in the Temperature Controlled Chamber (TCC) for Geomembrane Surface Hardness Measurements

For precise surface hardness measurements of polymeric plastic materials at elevated temperatures, there are two fundamental and important criteria required to be in consideration primarily which are; i) the repeatability/steadiness and consistency of the implementation of durometer measurements, and ii) the stability of the targeted ambient temperature conditions in the measurement environment. A constant loader test stand with an adjustable damping system was used to ensure a constant speed of downward movement of the load shaft provided reliable and dependable results. Additionally, the TCC had precise and stable temperature control for the temperature range (20°C - 50°C) of the experimental program even during very long test durations up to 25 hours (Figure 9.8). The digital temperature (PID) controller was successfully able to keep the constant ambient test temperature within 1 °C of the target preset value. This verifies the overall operational steadiness of the TCC test system enclosing the durometer for hardness measurements at higher temperatures as well as the robust control of the digital temperature (PID) controller in maintaining the chamber environment temperature at constant level without fluctuating significantly from the preset target test value. In addition, the reliable operational performance of the developed heating system consisting of heat bulbs, PID controller, temperature sensor (i.e. thermocouple), SSR, and finned heat sink was validated by successfully maintaining the TCC environment at a constant temperature level for such a long duration (i.e. 25 hours).

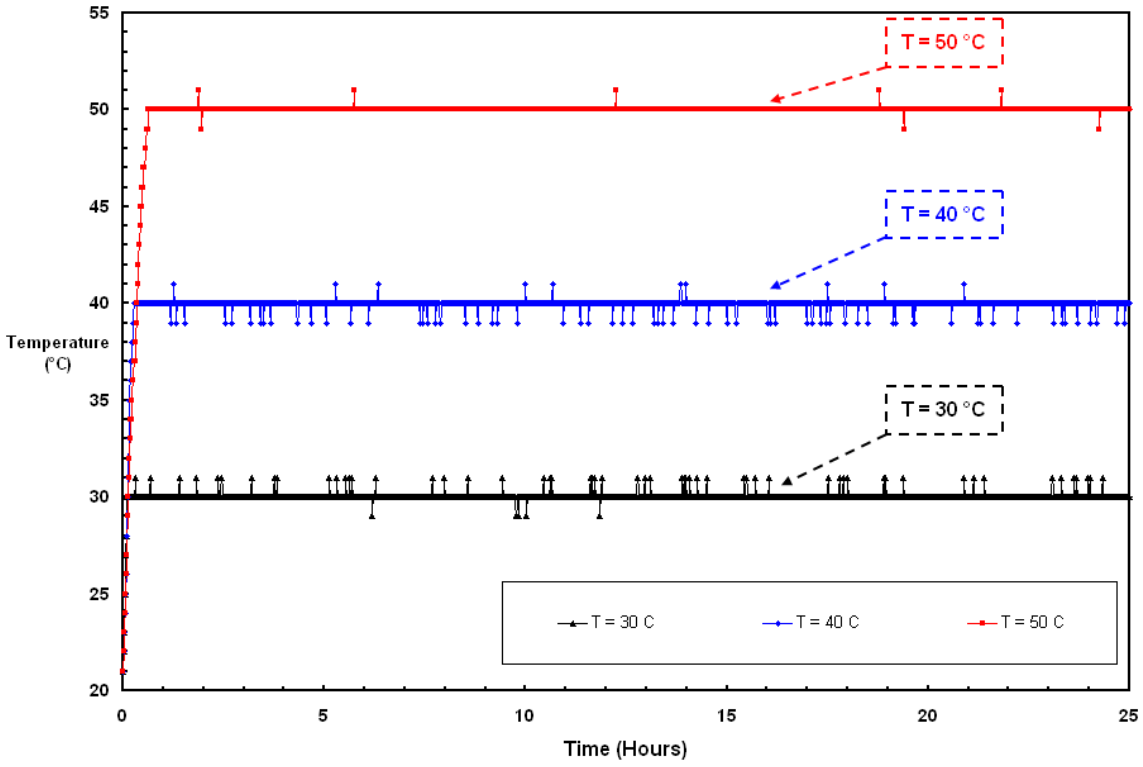

Figure 9.8 Temperature versus Time Data showing Very Minor Fluctuations of the TCC Ambient Temperature for a very Long duration of Test Progress

The geomembrane continuum sheets produced from base polymers such as HDPE and PVC are categorized in the class of relatively hard plastics. Shore D hardness scale, (H_D) ranging from 1 to 100 on Type D durometer gauge was an appropriate scale to attain an index value for surface hardness of these aforementioned geomembranes at different temperatures. Since the magnitude of this hardness value obtained at varied ambient conditions is important in evaluating the interface friction characteristics of sand-geomembrane interfaces at elevated temperature conditions.

A total of 240 measurements were performed on HDPE as well as PVC geomembrane plied samples stacked on top of each other making sure there was no air between the layers. In order to maintain consistency in measurements and to obtain

accurate test results, it is required to conduct all the hardness measurements with the same speed for all the materials tested. A total of 120 measurements were taken on smooth HDPE geomembrane samples. It is recommended as good practice to take several readings and average the results by showing the variability in measurement data. An exactly similar procedure was followed for smooth PVC geomembrane as well in which a total of 120 surface hardness measurements were made on geomembrane samples. The readings, in general, indicated that the variability in measurements was consistent for all the samples tested.

Figure 9.9 presents Shore D, (H_D) surface hardness measurements for both HDPE and PVC geomembranes at temperatures ranging from 20 °C to 50 °C in 10 °C increments based on 30 readings at each test temperature to observe the repeatability of the measured surface hardness variation and material firmness behavior with increasing ambient temperature. The 30 repeat measurements at each test temperature are more than sufficient to constitute a sample population to evaluate the surface hardness change of HDPE and PVC geomembrane liners at each temperature. Geomembranes, which are polymeric continuum sheet materials comprised of a specific polymer resin, are manufactured uniformly to possess homogeneity in terms of physical and mechanical properties as well as a uniform distribution of material characteristics throughout a large lining sheet.

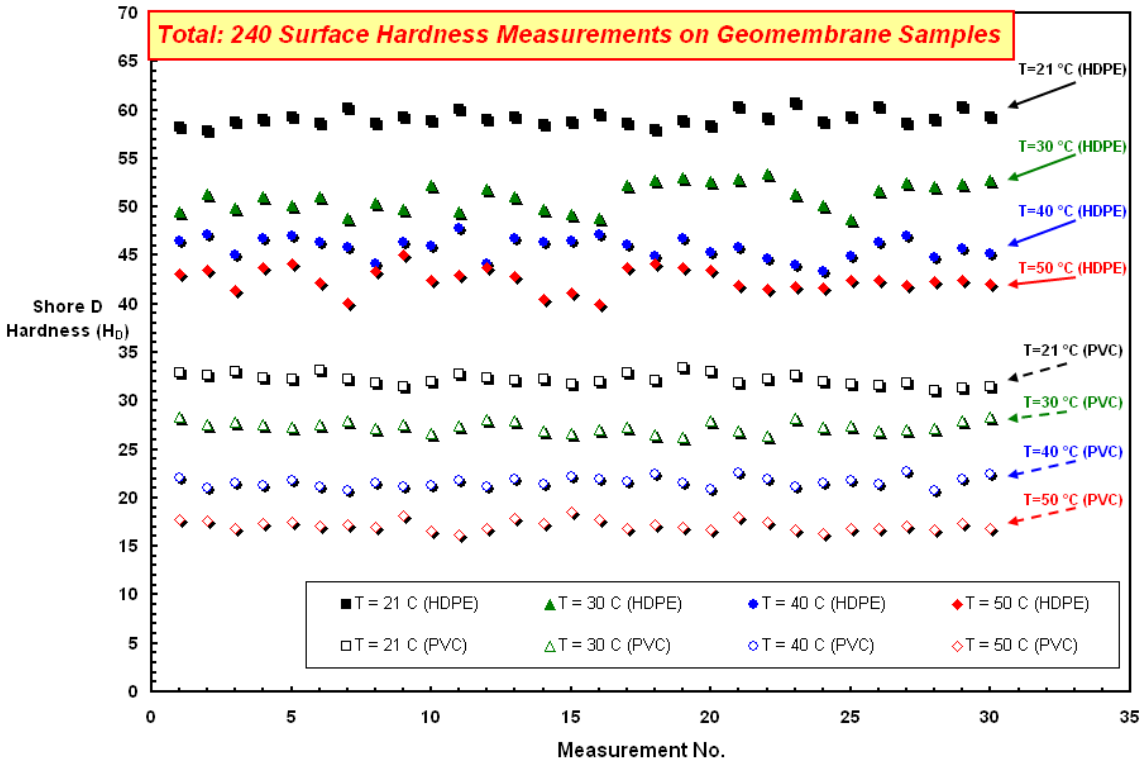

Figure 9.9 The Overall Shore D, (H_D) Hardness Measurements on the Material Surface of HDPE as well as PVC Geomembrane Samples at Different Temperatures

9.5.2. The Variation of HDPE Geomembrane Surface Hardness and the Variability in Measurement Data at Different Temperatures

The overall hardness measurement results for HDPE geomembrane samples (repeated 30 times) at each test temperature distinguished with different colors are presented in Figure 9.10 starting from room temperature of 21 °C up to an elevated temperature of 50 °C. The hardness readings performed on different geomembrane samples at various temperatures were in good agreement amongst the data obtained at each test temperature and indicated that surface hardness of HDPE geomembrane is

clearly dependent on temperature change. The Shore D, (H_D) hardness values decreased from about 60 down to about 40 in the temperature range from 21 °C to 50 °C. It is clearly noticeable in Figure 9.10 that the variation in measured hardness values at room temperature are distinctly located on the plot and separate from the test data at higher temperatures.

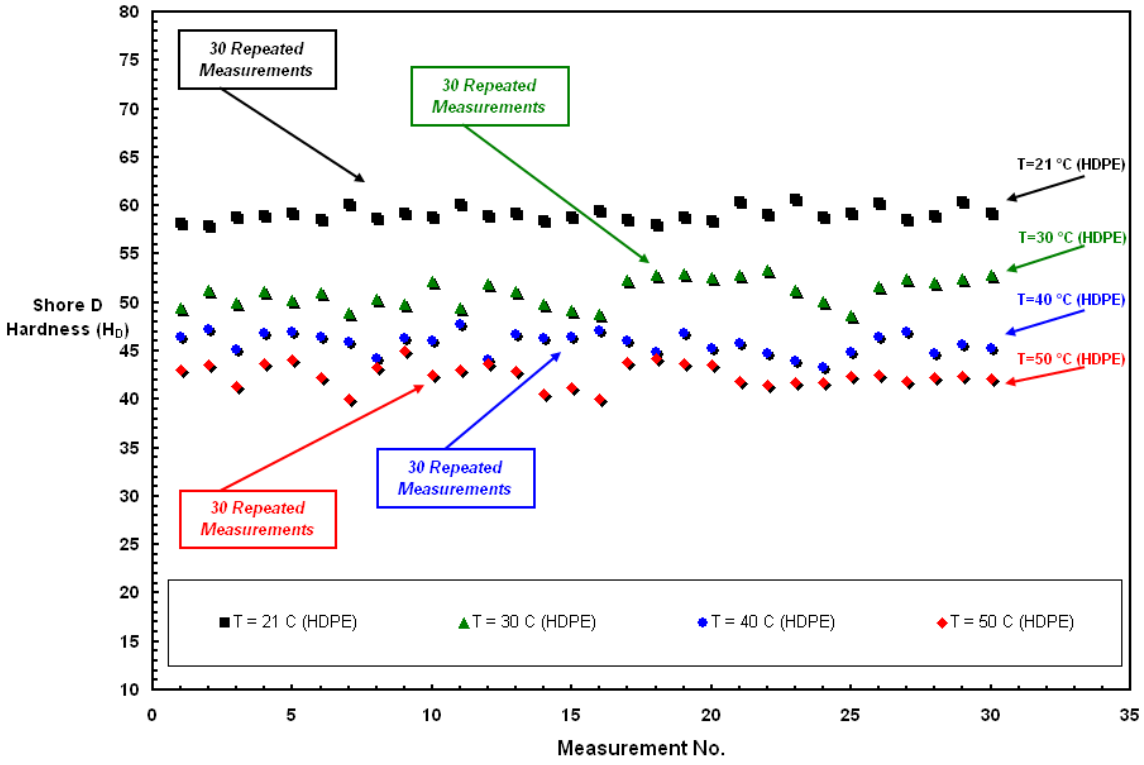

Figure 9.10 Shore D, (H_D) Hardness Measurements on HDPE Geomembrane Samples at Different Temperatures

The measured Shore D, (H_D) values decrease as ambient temperature increases. The rate of the decrease diminishes and becomes slower at higher temperatures for the HDPE geomembrane and additionally, may reach a saturation threshold; a lower

boundary value at further increased temperatures (>60°C). In other words, this observed behavioral trend with temperature change may be an indication for the extreme temperature conditions such that the magnitude of HDPE geomembrane surface hardness may begin to remain almost constant with minor alterations in the measured H_D value. The variability in measurement data gets larger particularly for the highest temperature case as shown on Figure 9.11 in which the error bars at each test temperature are based on 30 repeated readings of every measurement temperature.

The mobilized frictional strength and the developed interface shear behavior at particulate material – continua interfaces are influenced by the surface hardness of geomembrane produced from polymer resins (O'Rourke et al., 1990). Therefore, the measured index value for hardness of the HDPE geomembrane based on a particular Shore D scale will provide a useful quantitative value to evaluate and indirectly gauge the magnitude of shear resistance that will be generated at the interfaces of sands and HDPE geomembranes. The primary influence of temperature on shear behavior of these interfaces results from the temperature dependency of polymeric HDPE geomembrane properties such as hardness. Consequently, the magnitude of shear response developing at the interface is mainly attributed to geomembrane surface pliability governed by the material hardness and dependent on ambient temperature. The vertical line and the symbol at each temperature in Figure 9.11 indicate the range of hardness readings and the average of the readings taken at that temperature, respectively. Additionally, the variability in the measurement data is listed in Table 9.1.

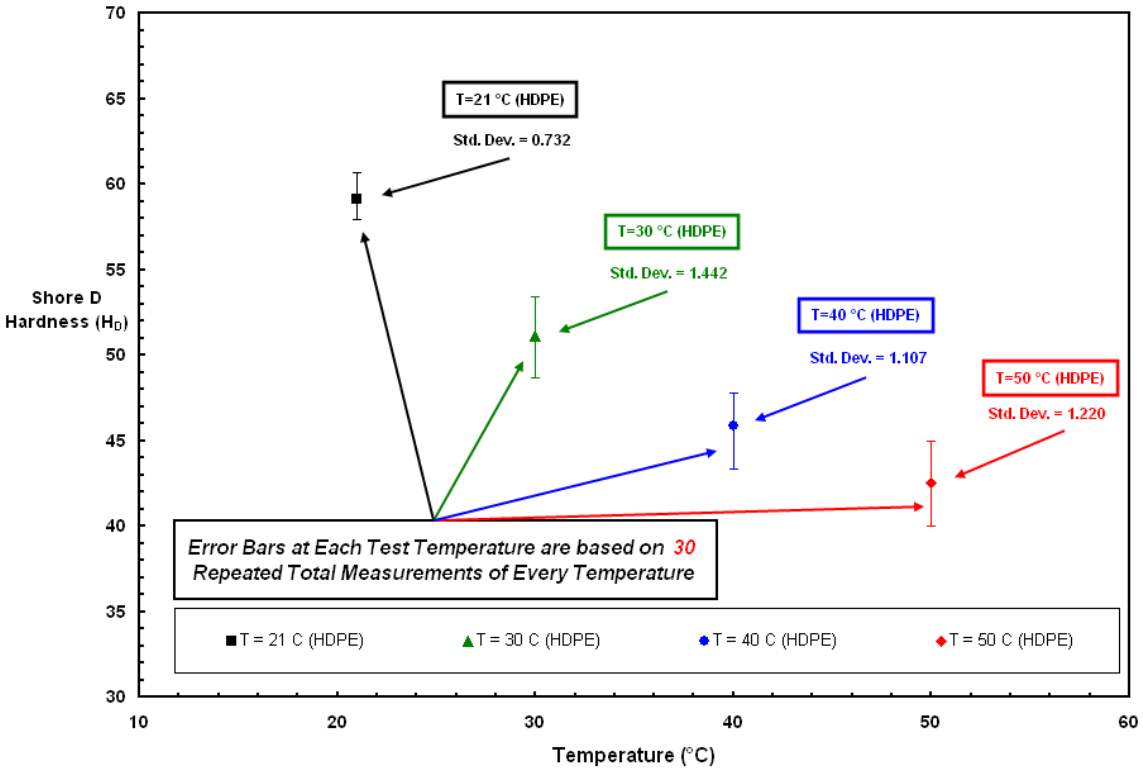

Figure 9.11 Variation of HDPE Geomembrane Surface Hardness and the Variability in Measurement Data at Different Temperatures

Table 9.1 Variability in Measurement Data at Different Temperatures (Smooth HDPE Geomembrane)

Specimen Material	***Temperature (°C)***	***Mean***	***Standard Deviation***	***Range (Max. – Min.)***
HDPE	21	59.1	0.732	2.8
HDPE	30	51.1	1.442	4.7
HDPE	40	45.8	1.107	4.5
HDPE	50	42.5	1.220	5.0

9.5.3. The Mathematical Correlation and Variational Trend between HDPE Geomembrane Hardness and Temperature

Several different types of regression analyses including linear, exponential, polynomial were performed on the overall measurement data of Shore D surface hardness at different temperatures for HDPE geomembrane samples. An exponential regression analysis provided the best correlation between Shore D hardness, (H_D) and temperature (Figure 9.12) such that a good exponential decreasing fit between the intermittent test data and a continuous regression curve with a high coefficient of determination (CoD) of 0.9874 was obtained. For HDPE geomembrane specimens tested at several temperatures, the behavioral trend investigated and the resulting mathematical empirical correlation based on experimental measurement data demonstrating the relation of the variation in surface hardness with respect to the change in temperature, is presented in Figure 9.12.

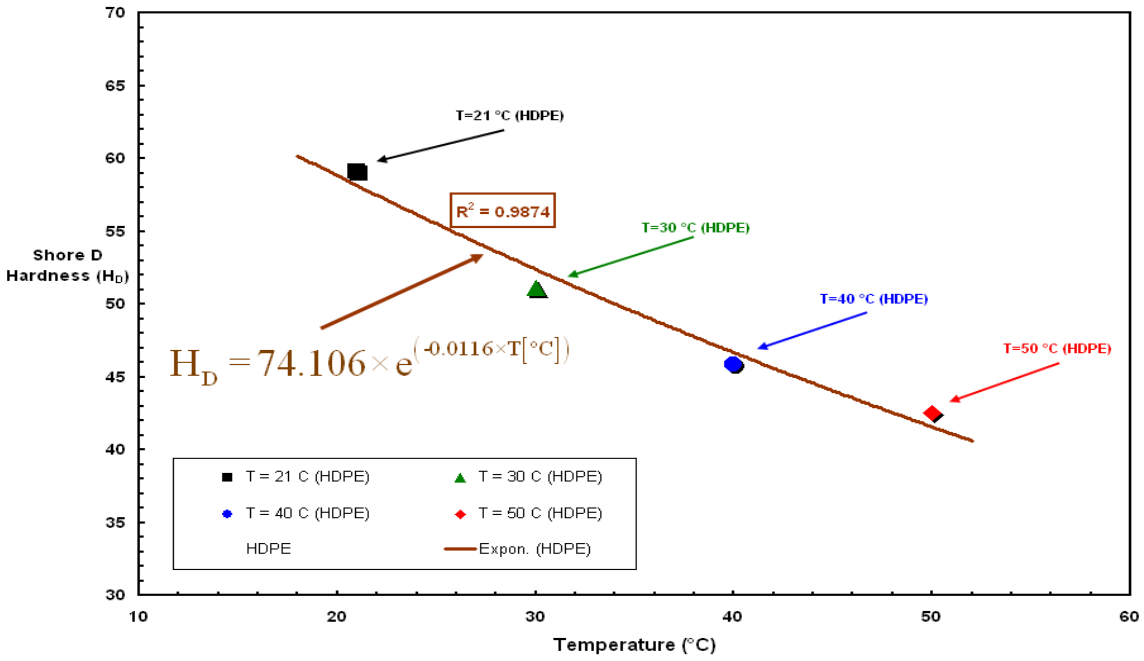

Figure 9.12 Exponential Correlation between HDPE Geomembrane Surface Hardness and Temperature

The exponential correlation developed using the sample population measurement data provides a practical and quick estimate of the geomembrane hardness at different ambient conditions based on the change in temperature. There exists a decrease in the rate of decrease in magnitude of H_D values with increasing temperature, especially at temperatures above 40 °C. A reduction in the rate of decrease indicates that a lower limit boundary (saturation threshold) at further higher temperatures could possibly be expected. For the HDPE geomembrane, the equation relating Shore D Hardness, (H_D) to temperature, (T) is given in Equation 9.2 in which T is in degree Celsius.

$$H_D = 74.106 \times e^{(-0.0116 \times T[°C])} \tag{9.2}$$

Where;

H_D: Shore D Surface Hardness

T: Temperature in Celsius

The preceding empirical relationship (Equation 9.2) between HDPE geomembrane surface hardness and temperature was developed based on the results of durometer measurements at different temperatures and could be utilized as a mathematical co-relational equation to relate the magnitude of Shore D hardness to temperature change in which H_D values follows an exponential decreasing pattern with increasing temperature for the geomembrane liners manufactured from only HDPE base polymer resins. Additionally, the closeness of fit between the regression curve and the discontinuous test data indicates a reliable correlation between a dependent (Shore D

hardness, H_D) and an independent (temperature) variable. For other geomembrane types produced from different resins (i.e. MDPE, LLDPE, VFPE, or PVC), the mathematical relation and variational trend between H_D and T [°C] could be different as will be demonstrated in the following sections for PVC geomembrane case.

9.5.4. The Variation of PVC Geomembrane Surface Hardness and the Variability in Measurement Data at Different Temperatures

The overall hardness measurement results on PVC geomembrane samples (repeated 30 times) at every test temperature distinguished with different colors are presented in Figure 9.13 beginning from room temperature of 21 °C up to an elevated temperature of 50 °C. The hardness readings performed on several geomembrane samples at various temperatures were in closer agreement than those of HDPE geomembrane with very minor variance amongst the data obtained at each test temperature and confirming that surface hardness of PVC geomembranes is manifestly dependent on temperature change. The Shore D, (H_D) hardness values decreased from about 35 down to about 18 in the temperature range from 21 °C up to 50 °C. Figure 9.13 clearly demonstrates that the measurement gap between the different data series for each test temperature are quite similar denoting that a relatively constant reduction in surface hardness of PVC geomembranes occurs as temperature goes up.

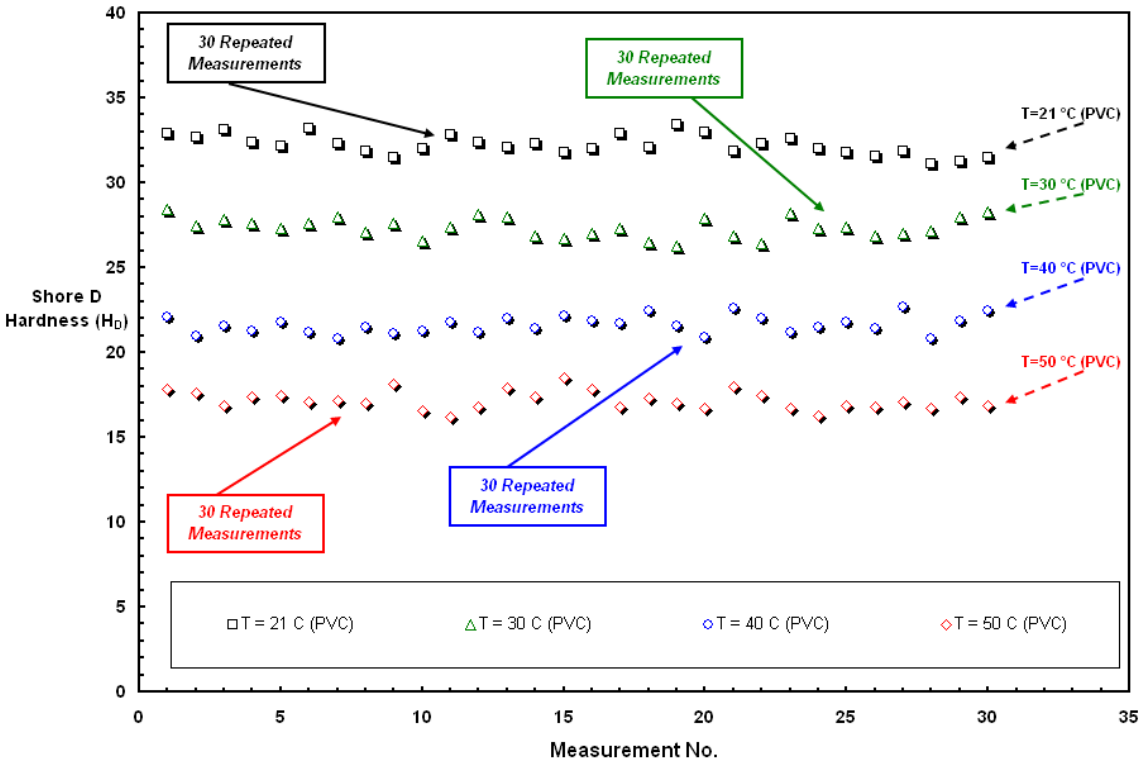

Figure 9.13 Shore D, (H_D) Hardness Measurements on PVC Geomembrane Samples at Different Temperatures

As opposed to the case of HDPE geomembranes, there is no data series of repeatedly measured hardness values at any test temperature which is neither distinctly located on the plot nor isolated from the other test data series of higher temperatures. Therefore, the measurement gap on the chart between the repeated readings series of two consecutive test temperatures are almost equal indicating a first order decrease in surface hardness of the PVC geomembrane.

The Shore D, (H_D) values decreases with increasing ambient temperature for PVC geomembranes as well. The rate of the reduction remains quite constant at the temperature range (21°C - 50°C) over which the hardness measurements were conducted.

Therefore, as opposed to the case of HDPE geomembrane, a saturation threshold in the magnitude of surface hardness of PVC geomembrane may not be expected based on these performed measurements consisting of a very large population of readings at various temperatures; so, it is not feasible to debate a probable existence of a lower boundary value of PVC liner hardness at further excessive temperatures (>60°C). Consequently, this observed reduction with a continuous declination in hardness as temperature rises up may be an indication such that the extreme temperature conditions may be more hazardous and critical for PVC geomembranes employed in civil engineering applications having the possibility of experiencing extreme temperatures during their service life; so, the use of PVC liner may be less safe for the purpose of long-term stable design. On the other hand, the variability in measurement data does neither display any growth nor show an increase in the total variance between the maximum and minimum measured value as seen in Figure 9.14 in which the error bars at each test temperature are based on 30 repeated readings of every measurement temperature that the size and extent of every error bars are pretty much similar. The variability in the measurement data is listed in Table 9.2. This consistency in measurements on relatively soft and flexible geomembranes produced from PVC compared with HDPE liners at higher elevated temperature conditions could be a beneficial advantage of this polymeric material in the field because of it possessing more consistent global material properties in terms of predicting a general index value by performing measurements on a limited portion of the material over a restricted region for estimating the durability properties of this polymeric geomembrane liner employed in situ over a very large area where probable variations in

ambient conditions influencing material endurance characteristics may exist in large areal extent geotechnical projects.

At every temperature tested, the hardness measurements show similar mixture of variation; some readings provide low values, whereas, the others give high values with the majority of data points being close to the mean. The liner materials made from PVC are most plasticized and thus flexible amongst the readily available geomembranes in the market produced from different base polymer resins such as HDPE, MDPE, LLDPE, and VFPE (all having dissimilar surface hardness's). For example, there is a pronounced difference in the magnitude of Shore D hardness, (H_D) values measured at every test temperature between PVC and HDPE geomembrane. The surface hardness of PVC geomembrane is lower than HDPE geomembrane, indicative of relatively softer material.

Shear strength characteristics of the geomembranes, each with substantially different surface hardness values, are strongly dependent on this quantitative property defining the resulted mechanical interaction response of the liner in contact with the other geo-materials. Therefore, the differences and discrepancies observed in interface shear behavior and strength of PVC geomembrane liners compared with those of HPDE liner can be attributed to the surface pliability of the PVC geomembrane which is primarily material hardness dependent and related.

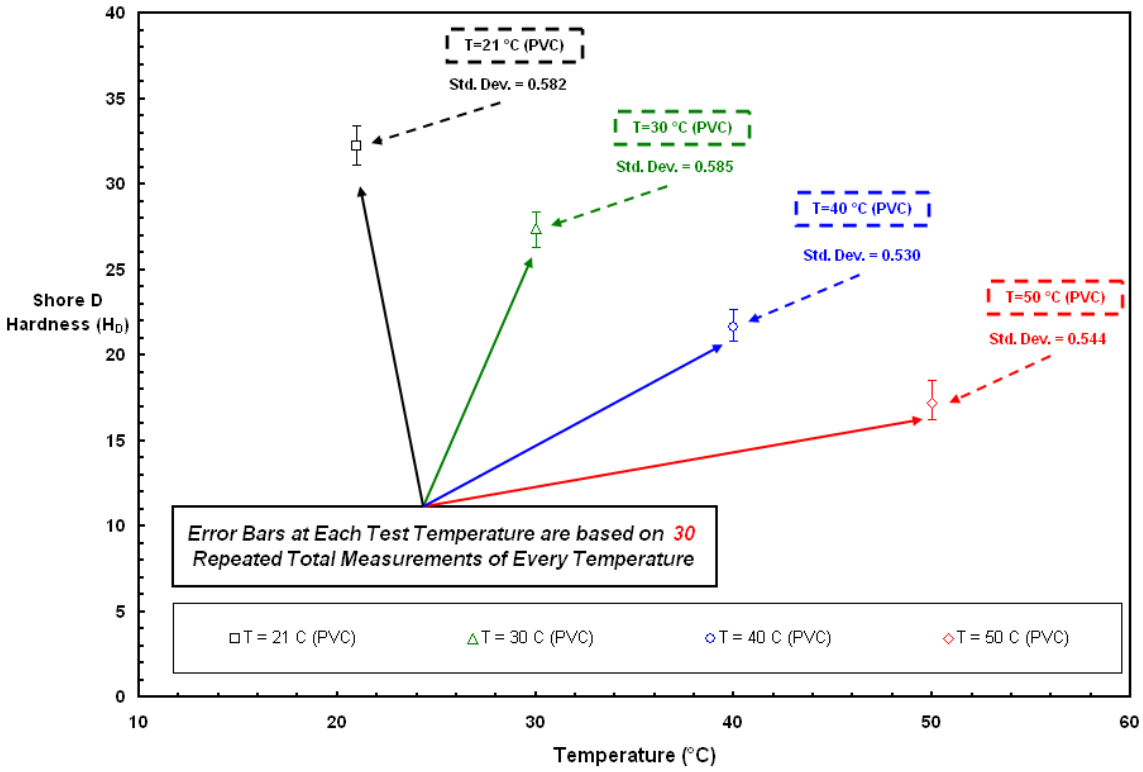

Figure 9.14 Variation of PVC Geomembrane Surface Hardness and the Variability in Measurement Data at Different Temperatures

Table 9.2 Variability in Measurement Data at Different Temperatures (Smooth PVC Geomembrane)

Specimen Material	***Temperature (°C)***	***Mean***	***Standard Deviation***	***Range (Max. – Min.)***
PVC	21	32.2	0.582	2.3
PVC	30	27.4	0.585	2.1
PVC	40	21.6	0.530	1.9
PVC	50	17.2	0.544	2.3

In general, the higher surface pliability of PVC geomembranes results in a different shape shear stress-displacement curve (i.e. elasto-perfectly plastic) and greater interface strength than the other type geomembrane liner materials. The vertical line and the symbol at each temperature in Figure 9.14 indicate the range of hardness readings and the average of the readings taken at that temperature, respectively.

9.5.5. The Mathematical Correlation and Variational Trend between PVC Geomembrane Hardness and Temperature

Among different types of regression analyses, the linear regression process performed on the overall measurement data of Shore D surface hardness at different temperatures for PVC geomembrane samples provided the best correlation, an inversely proportional straight line relation between Shore D hardness, (H_D) and temperature (Figure 9.15) such that a very good linear decrease fit between intermittent test data and continuous regression curve with a high coefficient of determination (CoD) of 0.997 was obtained. The closeness of fit between the regression line and test data indicates that there occurs a proper linear reduction correlation between the temperature and the H_D values measured at various temperatures on the surface of the PVC geomembrane specimens cut from a large rolled sheet of this plastic continuum material. The data indicates that there exists a good and robust correlation between temperature and surface hardness of PVC geomembranes.

For PVC geomembrane specimens tested at several temperatures, the behavioral trend investigated and the resulted mathematical empirical correlation developed based

on experimental measurement data demonstrating the relation of surface hardness change with respect to temperature change is presented in Figure 9.15.

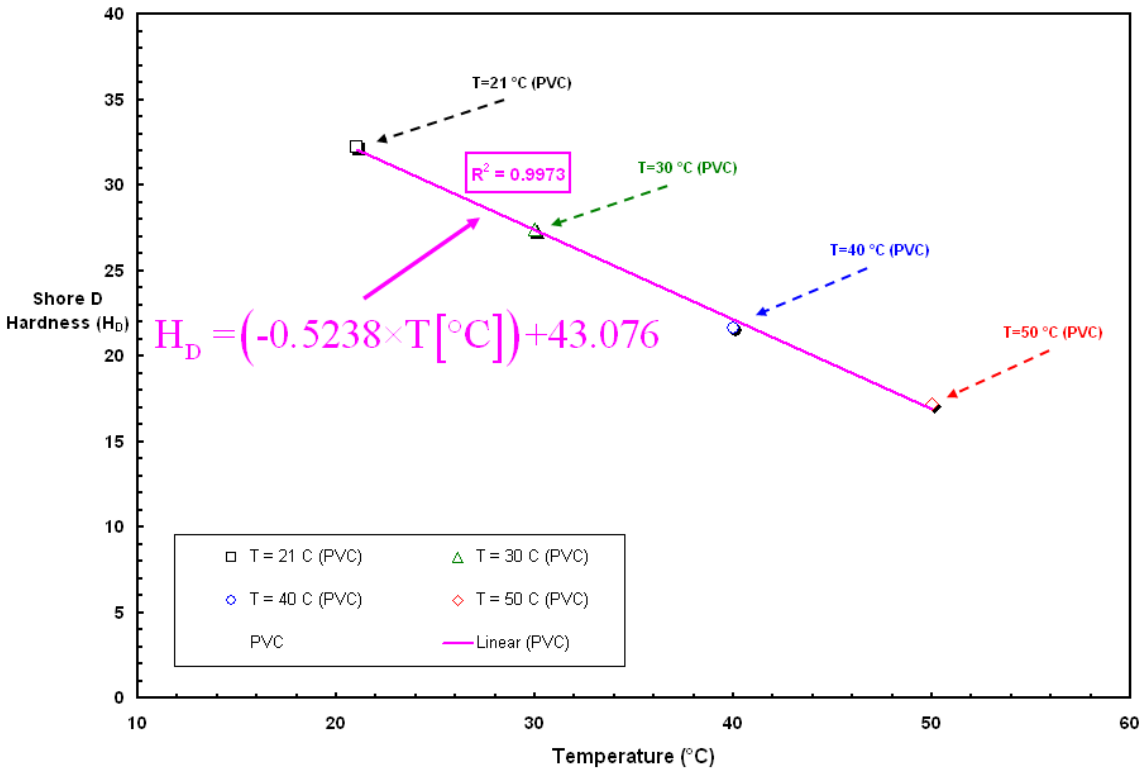

Figure 9.15 Linear Correlation (Inversely Proportional) between PVC Geomembrane Surface Hardness and Temperature

The empirical relationship (Equation 9.3) between PVC geomembrane Shore D hardness and temperature was developed based on the results of durometer measurements at different temperatures and could be utilized as a mathematical co-relational equation to relate the change in the magnitude of Shore D harness, (H_D) to the variation in temperature in which H_D values for PVC liners basically follows an inversely proportional linear pattern with increasing temperature. There is a constant slope decrease in the magnitude of H_D values as temperature increases. Therefore, no reduction in the

rate of this decrease occurs and a lower limit boundary (saturation threshold) at further higher temperatures is not expected. This correlation developed using the experimental data is proposed to show the variation of H_D with temperature in an algebraic form. The use of such mathematical correlations provides the engineer a way of conveniently estimating PVC geomembrane liner hardness. This relationship, obtained through regression analysis of sufficiently large amount of test data, principally describes the variation of H_D with temperature for only a "liner" manufactured from PVC base polymer resin; however for pipes or the other geo-materials made from polyvinylchloride, this empirical relation requires to be revised according to surface hardness measurement on the material at different temperatures. For the PVC geomembrane, the equation relating Shore D Hardness, (H_D) to temperature, (T) is given in Equation 9.3 in which T is in Celsius (°).

$$H_D = \left(-0.5238 \times T[°C]\right) + 43.076 \tag{9.3}$$

Where;

H_D: Shore D Surface Hardness

T: Temperature in Celsius

Moreover, the closeness of fit between the regression curve and the discontinuous test data indicates a reliable correlation between a dependent (Shore D hardness, H_D) and an independent (temperature) variable. For the other geomembrane types produced from different resins (i.e. HDPE, MDPE, LLDPE, or VFPE), the mathematical relation and variational trend between H_D and T [°C] could be different as demonstrated in the preceding section for HDPE geomembrane case.

9.6. Interface Shear Strength and Temperature

Using the general model previously proposed by O'Rourke et al. (1990) for predicting frictional resistance of granular soil-polymeric material interfaces that is based on a correlation by assessing interface peak friction angle with the knowledge of soil internal friction angle whereby the ratio of interface angle of shear resistance, (δ) to direct shear angle of soil friction (φ'_{ds}) was related to Shore D Hardness (H_D) index of the polymeric materials, a new model was developed in this study by substituting the hardness-temperature relationship (Equation 9.2 and 9.3) developed in this study into the interface property (δ/φ'_{ds})-hardness relationship (Equation 9.1) to establish a direct correlation and to investigate the behavioral trend between the interface property, (δ/φ'_{ds}) and the change in temperature, (T) in which T is in the unit of degree Celsius. The interface property, (δ/φ'_{ds}) was, then, plotted with temperature in Figure 9.16 to demonstrate the modal trend between frictional properties of particulates – HDPE, or PVC liners with respect to temperature so that interface shear engineering parameters (δ, tan(δ)) can be interrelated to temperature change for the purpose of indirectly assessing the influence of ambient conditions (e.g. temperature) on interface behavior and strength. The significant effect of temperature on sand-geomembrane interface shear resistance is seen evidently such that there occurs a natural logarithmic increase (i.e. reduction in the rate of increment) and linear increase (i.e. constant rate of increment) relationship for HDPE and PVC geomembrane – granular material interfaces, respectively. The practical significance of this model developed is to provide a rapid and simple means of estimating the interface design parameters with varied temperature simply from measuring Shore D Hardness, H_D of the geosynthetic materials at different temperatures.

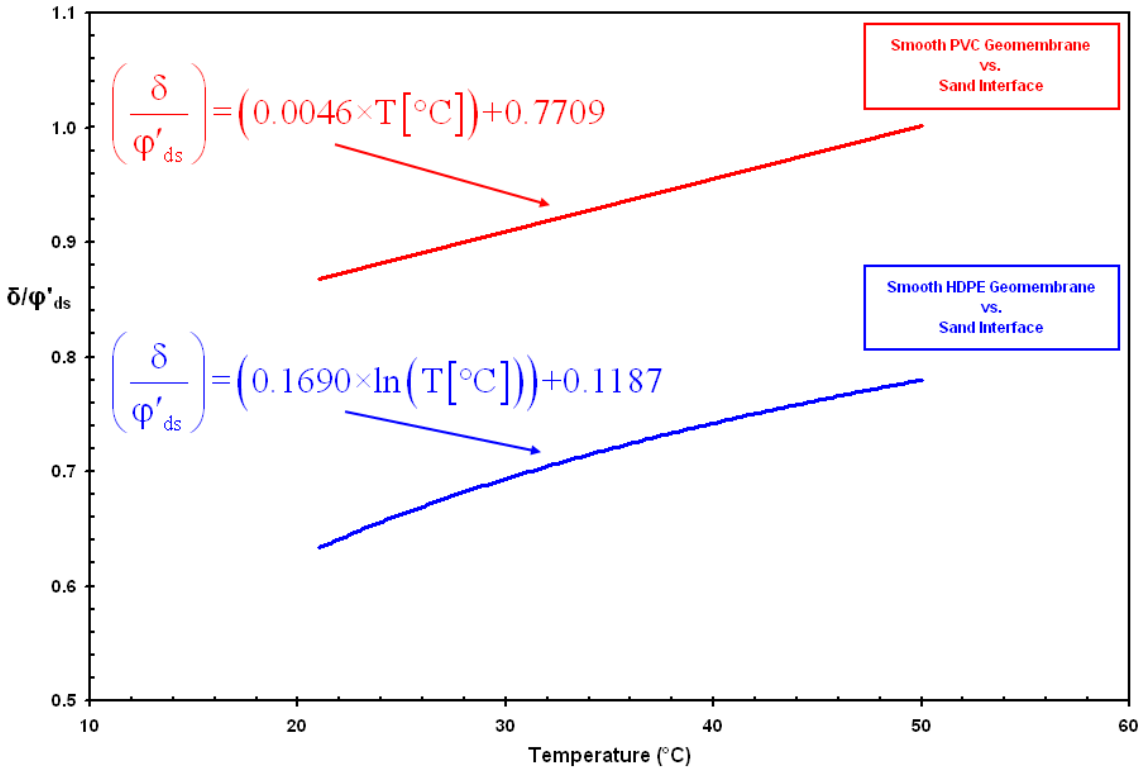

Figure 9.16 Interface Frictional Property versus Temperature for Sand – HDPE or PVC Geomembrane Interfaces

For the HDPE geomembrane, the equation relating the interface friction angle, (δ) normalized with respect to the soil direct shear angle, (φ'_{ds}) to temperature, (T) is given in Equation 9.4 in which T is in degrees Celsius.

$$\left(\frac{\delta}{\varphi'_{ds}}\right)=\left(0.1690\times \ln\left(T[°C]\right)\right)+0.1187 \qquad (9.4)$$

For the PVC geomembrane, the equation relating the interface friction angle, (δ) normalized with respect to the soil direct shear angle, (φ'_{ds}) to temperature, (T) is given in Equation 9.5 in which T is in degrees Celsius.

$$\left(\frac{\delta}{\varphi'_{ds}}\right)=\left(0.0046\times T[^{\circ}C]\right)+0.7709 \tag{9.5}$$

In this way, interface friction angle (i.e. either peak or residual) of sand-geomembrane interfaces can be evaluated with respect to temperature change by knowing the angle of direct shear resistance of the sand itself (φ'_{ds}). These two correlations involving the change in temperature resulted in the high coefficients of determination, (CoD = 0.994, 0.997 for smooth HDPE and smooth PVC interfaces, respectively). Using the developed mathematical models above between the interface property (δ/φ'_{ds}) and temperature, (T [°C]) for geomembranes produced from different polymer resins, an empirical correlation can be established to relate the variation of interface friction angle, (δ) to temperature change for Ottawa 20/30 versus HDPE, or PVC geomembrane as well as for Blasting sand versus HDPE, or PVC geomembrane interfaces. The results of experimental data from laboratory testing programs conducted to explore direct shear angles of Ottawa 20/30 and Blasting sands, as published by Frost et al. (2002), and Iscimen (2004), respectively, were utilized (Table 9.3).

Table 9.3 Peak and Residual Direct Shear Angles for Ottawa 20/30 and Blasting Sands

	φ'_{ds} [Peak]	***φ'_{ds} [Residual]***	
Ottawa 20-30	38.9°	28°	Frost et al. (2002)
Blasting Sand	43.1°	34.6°	Iscimen (2004)

9.6.1. The Variation of Interfacial Frictional Engineering Properties at Sand (Rounded, Angular) – HDPE Geomembrane Interfaces

Figure 9.17 shows the change of interface friction angle, (δ) (i.e. peak and residual) with temperature. For HDPE geomembrane – Ottawa 20/30, or Blasting sand interfaces, a logarithmic increase trend was observed for the relationship between δ [°] and T [°C]. Therefore, the performed natural logarithmic regression analysis provided the best correlation between discontinuous test data and continuous regression curve with a perfectly high coefficient of determination (CoD = 0.994) such that a very good matching logarithmic rise fit with reduction in the magnitude of increment rate was obtained.

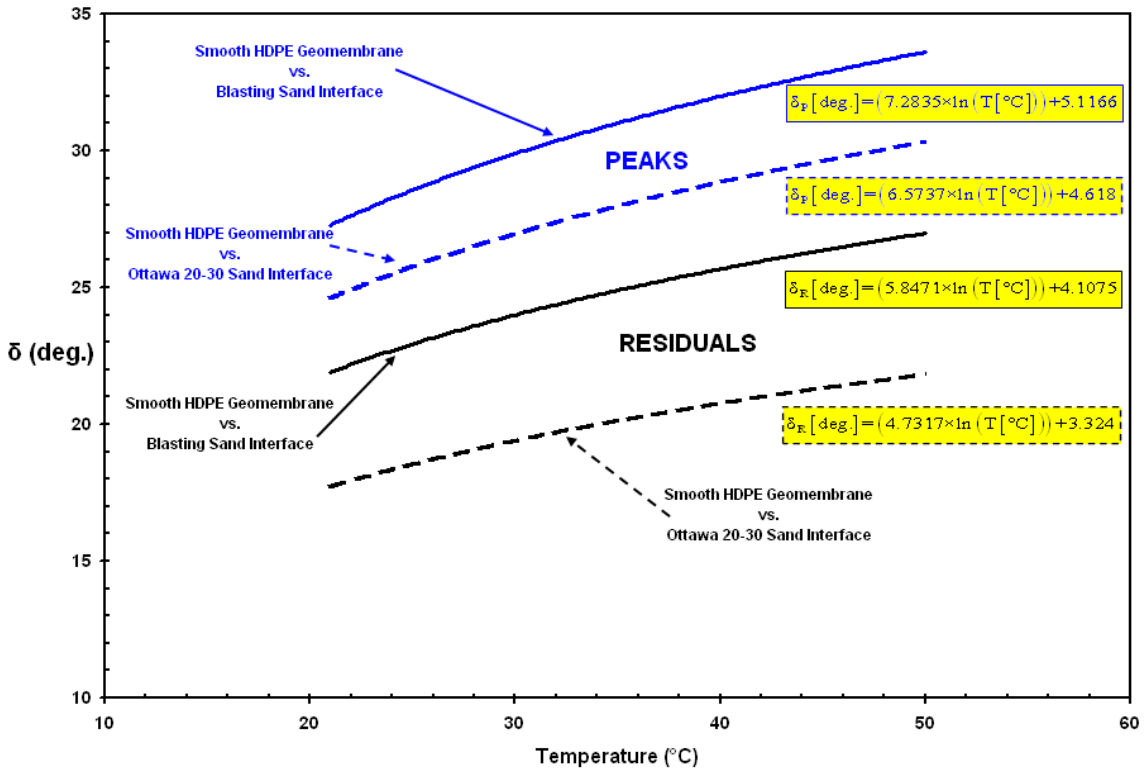

Figure 9.17 Interface Friction Angle with the Change in Temperature for Rounded or Angular Sand – HDPE Geomembrane Interfaces

Direct algebraic equations for peak and residual conditions between the δ for rounded and angular sands and temperature by interrelating through Shore D Hardness, H_D of the smooth HDPE geomembrane measured at various temperatures are given in Equation 9.6 and 9.7, respectively.

Rounded to Subrounded Sand (Ottawa 20-30) – HDPE Interface:

$$\delta_P\left[\text{deg.}\right]=\left(6.5737\times\ln\left(T\left[°C\right]\right)\right)+4.618 \quad (9.6a)$$

$$\delta_R\left[\text{deg.}\right]=\left(4.7317\times\ln\left(T\left[°C\right]\right)\right)+3.324 \quad (9.6b)$$

Angular Sand (Blasting Sand 20-30) – HDPE Interface:

$$\delta_P\left[\text{deg.}\right]=\left(7.2835\times\ln\left(T\left[°C\right]\right)\right)+5.1166 \quad (9.7a)$$

$$\delta_R\left[\text{deg.}\right]=\left(5.8471\times\ln\left(T\left[°C\right]\right)\right)+4.1075 \quad (9.7b)$$

The correlational trend which was obtained by further processing interface friction angle versus temperature relation provided a practical and quick evaluation of coefficient of friction for HDPE geomembrane – Ottawa 20/30, or Blasting sand interfaces at different ambient conditions based fundamentally on the change in temperature in which the relationship principally describes the variation of tan(δ) (peak as well as residual) with temperature (Figure 9.18).

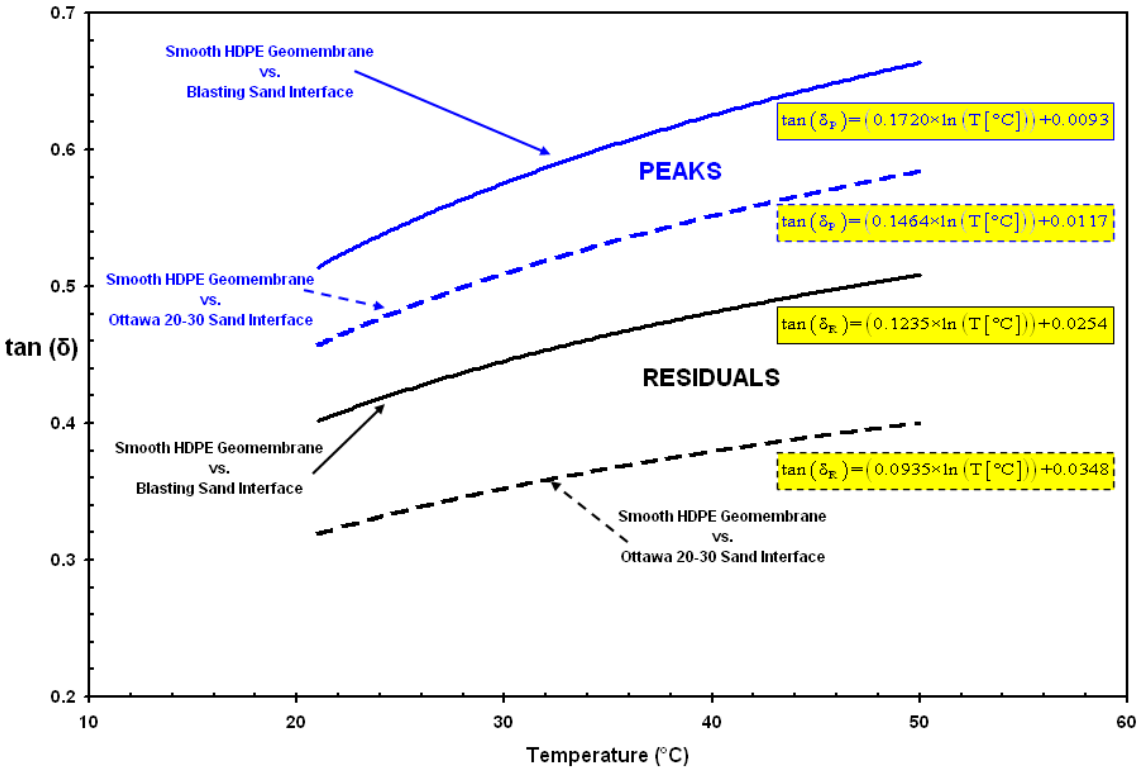

Figure 9.18 Coefficient of Friction with the Change in Temperature for Rounded or Angular Sand – HDPE Geomembrane Interfaces

For the HDPE geomembrane- rounded, or angular sand interfaces, the equation relating tan(δ) to temperature, (T[°C]) is given in Equation 9.8 and 9.9, respectively.

Rounded to Subrounded Sand (Ottawa 20-30) – HDPE Interface:

$$\tan\left(\delta_P\right)=\left(0.1464\times\ln\left(T\left[°C\right]\right)\right)+0.0117 \tag{9.8a}$$

$$\tan\left(\delta_R\right)=\left(0.0935\times\ln\left(T\left[°C\right]\right)\right)+0.0348 \tag{9.8b}$$

Angular Sand (Blasting Sand 20-30) – HDPE Interface:

$$\tan\left(\delta_P\right)=\left(0.1720\times\ln\left(T\left[°C\right]\right)\right)+0.0093 \tag{9.9a}$$

$$\tan\left(\delta_R\right)=\left(0.1235\times\ln\left(T\left[°C\right]\right)\right)+0.0254 \tag{9.9b}$$

The preceding empirical equations between tan(δ) and temperature were developed by interrelating/linking the corresponding frictional resistance parameters for engineering design in the relationships described based on the results of durometer hardness measurements on HDPE geomembrane samples at different temperatures. They could be utilized as a mathematical correlation to rapidly evaluate temperature effects on interface shear strength in which tan(δ) values follows a logarithmic pattern with increasing temperature for only the geomembrane liners manufactured from HDPE base polymer resins. For the other geomembrane types produced from different resins (i.e. MDPE, LLDPE, VFPE, or PVC), the mathematical relation and variational trend between tan(δ) and T [°C] will likely be different as will be demonstrated in the following sections.

9.6.2. The Variation of Interfacial Frictional Engineering Properties at Sand (Rounded, Angular) – PVC Geomembrane Interfaces

For PVC geomembrane – Ottawa 20/30, or Blasting sand interfaces, there exists a linear relationship between interface friction angle, (δ) (i.e. both peak, and residual) and temperature (Figure 9.19). Therefore, linear regression between the intermittent measurement data at different temperatures provided the best correlation between δ, in degrees and temperature, in Celsius (Figure 9.19). A 1^{st} order linear rise fit with a constant slope having a high coefficient of determination (CoD = 0.997) was obtained.

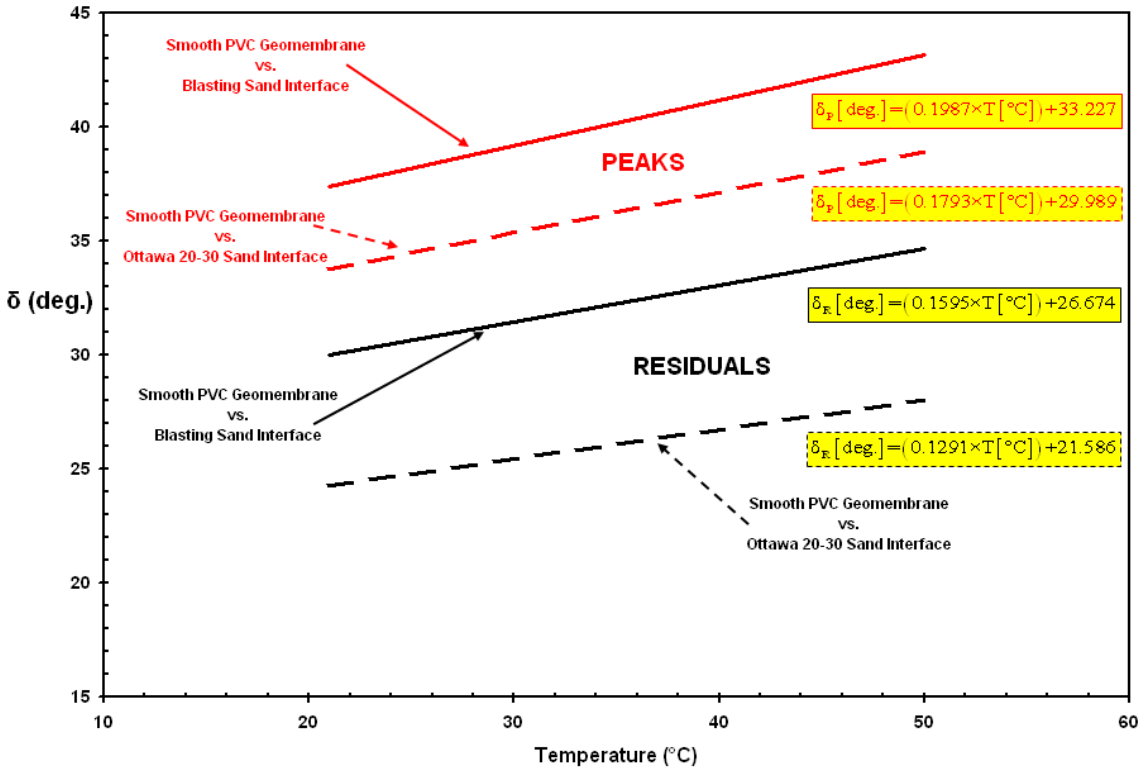

Figure 9.19 Interface Friction Angle with the Change in Temperature for Rounded or Angular Sand – PVC Geomembrane Interfaces

The agreement between the generated regression line and the test data indicates that there exists a robust correlation between interface friction angle, (δ) and temperature. Direct algebraic closed form equations between peak or residual δ [°] and T [°C] for Ottawa 20/30 and Blasting sands by linking through Shore D Hardness of the PVC liner samples measured at various temperatures are presented in Equation 9.10 and 9.11.

Rounded to Subrounded Sand (Ottawa 20-30) – PVC Interface:

$$\delta_P\,[\text{deg.}] = \left(0.1793 \times T[°C]\right) + 29.989 \tag{9.10a}$$

$$\delta_R\,[\text{deg.}] = \left(0.1291 \times T[°C]\right) + 21.586 \tag{9.10b}$$

Angular Sand (Blasting Sand 20-30) – PVC Interface:

$$\delta_P\,[\text{deg.}] = \left(0.1987 \times T[°C]\right) + 33.227 \tag{9.11a}$$

$$\delta_R\,[\text{deg.}] = \left(0.1595 \times T[°C]\right) + 26.674 \tag{9.11b}$$

The results in Figure 9.20 show the relationship between coefficient of friction, (tan(δ)) and temperature for rounded and angular sands in contact with PVC geomembranes only. The correlational trends are presented for different states of interface shear response.

It is necessary to highlight that the empirical equations between tan(δ) and temperature was developed based on the results of durometer measurements on PVC geomembrane specimens at different temperatures. Since a constant rate of increase exists in the magnitude of tan(δ) values per temperature, an upper threshold limit at even higher temperatures can not be predicted from the temperature range (20 °C – 50 °C) hardness measurements that were performed.

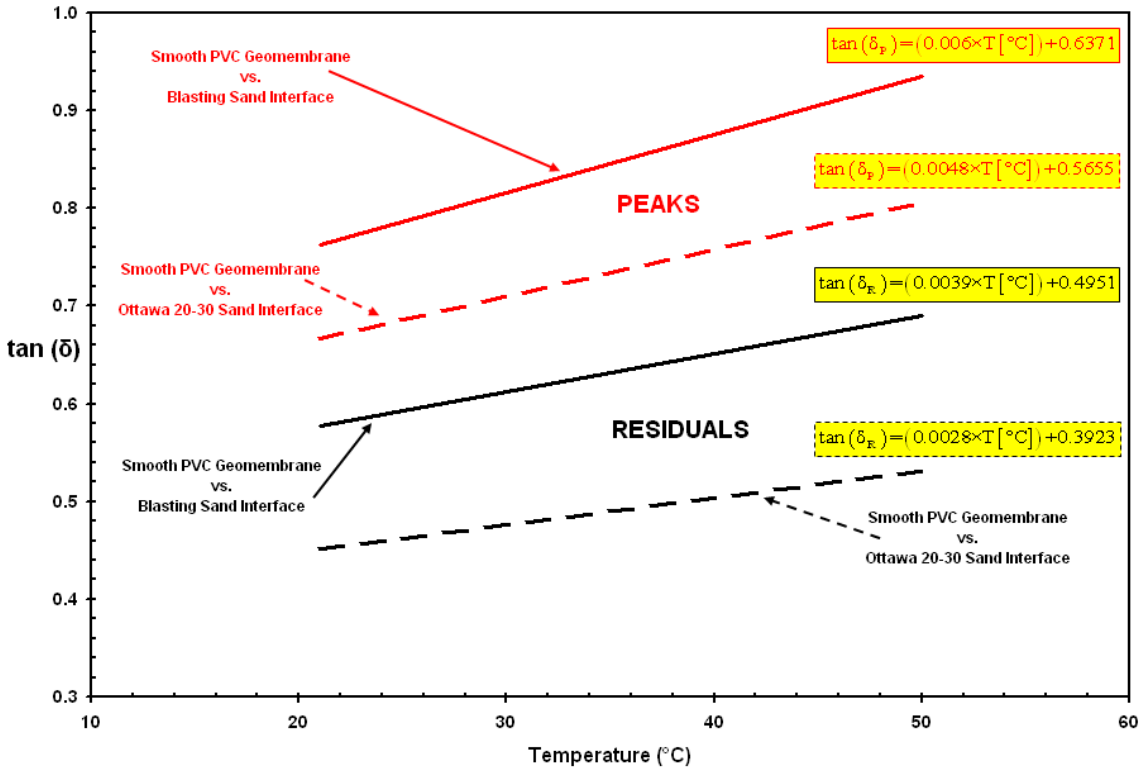

Figure 9.20 Coefficient of Friction with the Change in Temperature for Rounded or Angular Sand – PVC Geomembrane Interfaces

Equation 9.12 and 9.13 presents the change of tan(δ) with temperature for PVC liner in contact with rounded, and angular sands, respectively.

Rounded to Subrounded Sand (Ottawa 20-30) – PVC Interface:

$$\tan\left(\delta_P\right)=\left(0.0048\times T\left[°C\right]\right)+0.5655 \qquad (9.12a)$$

$$\tan\left(\delta_R\right)=\left(0.0028\times T\left[°C\right]\right)+0.3923 \qquad (9.12b)$$

Angular Sand (Blasting Sand 20-30) – PVC Interface:

$$\tan\left(\delta_P\right)=\left(0.006\times T\left[°C\right]\right)+0.6371 \qquad (9.13a)$$

$$\tan\left(\delta_R\right)=\left(0.0039\times T\left[°C\right]\right)+0.4951 \qquad (9.13b)$$

In summary, there are pronounced differences between the interface shear strength properties (δ, and tan(δ)) of HDPE geomembranes and PVC geomembranes. The harder HDPE lining surface resulted in relatively lower values of δ (or tan(δ)) than the softer PVC liner material for the complete temperature range studied. The interface frictional properties of PVC geomembranes are less dependent on temperature (i.e. the rate of change of interface shear parameters is slower than that of HDPE).

9.7. Primary Influence of Continuum Material Hardness on the Shear Mechanisms Mobilizing at Sand-Polymer (Geomembrane) Interfaces

Polymeric material surface hardness plays a significant role in the mechanism of shear transfer such that relatively "hard" polymer surfaces promote sliding of sand particles, whereas relatively "soft" surfaces promote particle rolling. For example, based on scanning electron microscope (SEM) photographs taken of post-test polymer specimen surfaces with H_D = 64 and H_D = 35 (i.e. 1st material surface is harder/stiffer than that of 2nd material), and after making observations on these pictures (i-parallel scratches of several mm long and 10 μm deep on harder polymer surface; whereas, ii-no comparable surface deformation on softer polymer surface), it was pointed out by O'Rourke et al. (1990) that the shear mechanism contributing the striations indicated sand particle movement occurred by sliding along the hard polymer surface. On the other hand, the mechanism of shear transfer between sand-soft polymeric material involved particle rolling which was evidenced by lack of striations on post-test specimen surfaces as shear imposed both a resultant force and overturning moment on the sand grains

adjacent to the interface causing a rolling and recoverable indentation of the relatively soft polymer (Figure 9.21).

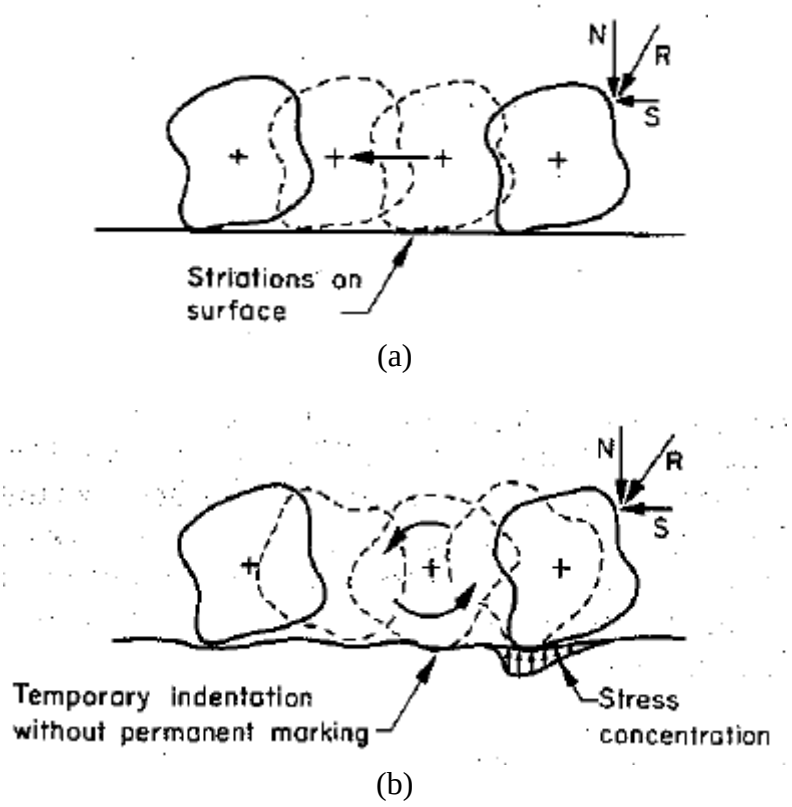

Figure 9.21 Interface Shearing Mechanisms developing at Sand versus: (a) Hard Polymeric Material [Bigger H_D] (Skidding Mechanism); (b) Soft Polymeric Material (Rolling Mechanism) [Smaller H_D] (O'Rourke et al., 1990)

As explained above as well as illustrated in Figure 9.21, these investigations on test results of sand-polymer interface which was developed on SEM photographs of post-test polymer specimen surfaces indicate that the material having less surface hardness, H_D (i.e. PVC geomembrane) yields a higher interface shear resistance (both peak and residual) and response (failure envelope located at upper stress-strain space) than the material having higher surface hardness, H_D (i.e. HDPE geomembrane) due to the larger contact area and higher pliability of the softer surface.

The research work of Dove and Frost (1999) was a complementary advancement to the study of O'Rourke et al. (1990). In addition, they performed further micro-level investigations on the shear mechanisms developing at interfaces between granular (i.e. sand) and relatively smooth planar continuum (i.e. geomembranes) materials based on (micro) contact mechanics and basic friction theory. Their research work revealed that sliding and plowing are the primary mechanisms which govern the sand-geomembrane peak interface shear behavior and shear mechanism controlling the strength resistance that is determined by particulate material shape as well as continuum material hardness and roughness. The first order importance of geomembrane hardness on the developed interface shear behavior and on the mobilized shear strength for the aforementioned interface composed of granular materials in contact and interaction with planar materials was demonstrated and further validated by their study.

9.8. Analysis, Discussion and Comparison of Experimental Measurement Results & Developed Empirical Correlations

The surface hardness of HDPE as well as PVC geomembranes were measured at different temperatures. The change of hardness of these continuum sheet materials with respect to temperature were also examined by developing correlations between Shore D hardness and temperature. Although they depicted different hardness reduction trends (exponential versus linear), the surface hardness for both HDPE and PVC liners were both observed to decrease as temperature increased. This variation in the magnitude of surface hardness of the geomembranes can be attributed to alteration of the stiffness of polymeric materials with temperature since the magnitude of the resistance a polymeric

plastic material surface displays against an outside object indentation is dependent on its elastic modulus and viscoelastic properties. In general, the change in the stiffness of polymeric materials with changing temperature has previously been investigated as presented in Figure 9.22. The stiffness of the materials produced from one or a mixture two different polymer resins decreases as ambient temperature increases. Consequently, this engineering material property is strongly temperature dependent (Figure 9.22). The stiffness of a polymer principally defines its state on the "softness" through "rigidity" scale as well as governs and is related to its surface hardness. As discussed earlier, surface hardness of a plastic material is basically its resistance to an indentation force. The indentation hardness is inversely related to the penetration which means that the deeper/further the sharp indenter penetrates, the lower the surface hardness of the material.

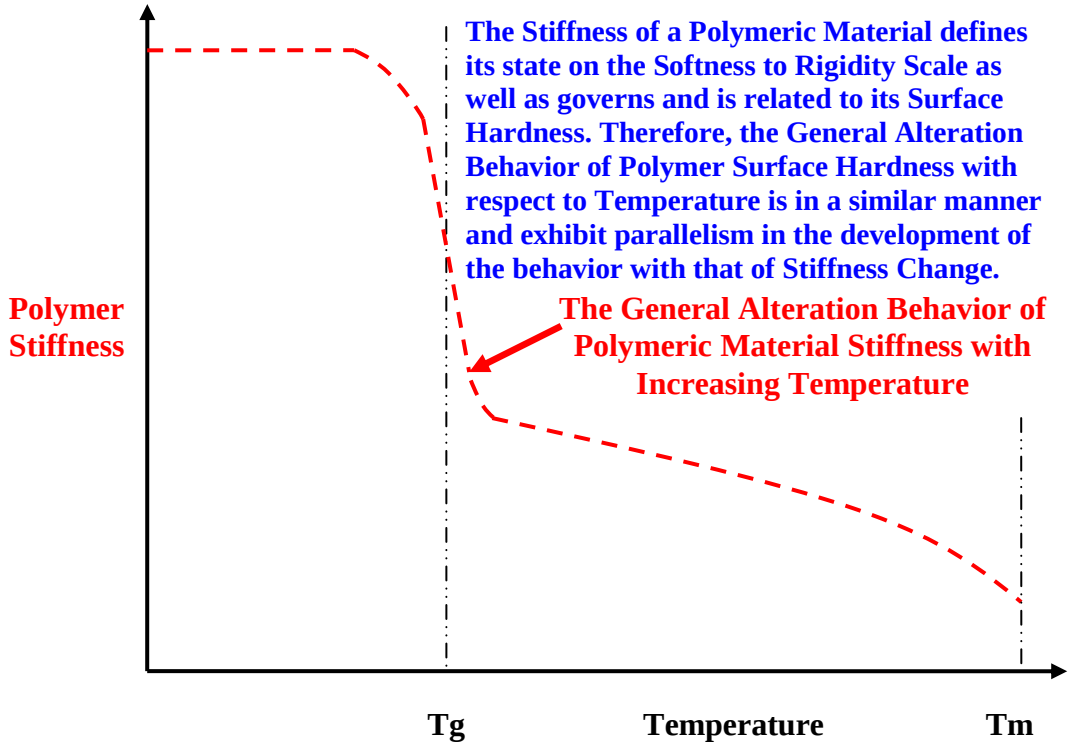

Figure 9.22 The General Alteration Behavior of Polymeric Material Stiffness with respect to Temperature (Adapted from Dowling, 2007)

The differences in the magnitude of surface hardness values measured at different temperatures on the surface of HDPE and PVC liners (Figure 9.23) fundamentally result from the base materials from which the geomembrane continuum sheets were produced as well as are due to the molecular properties of polymer chains in the core material of HDPE and PVC geomembranes (i.e. PVC Liner = Softer Nature versus HDPE Liner = Stiffer Nature) (see Chapter 2).

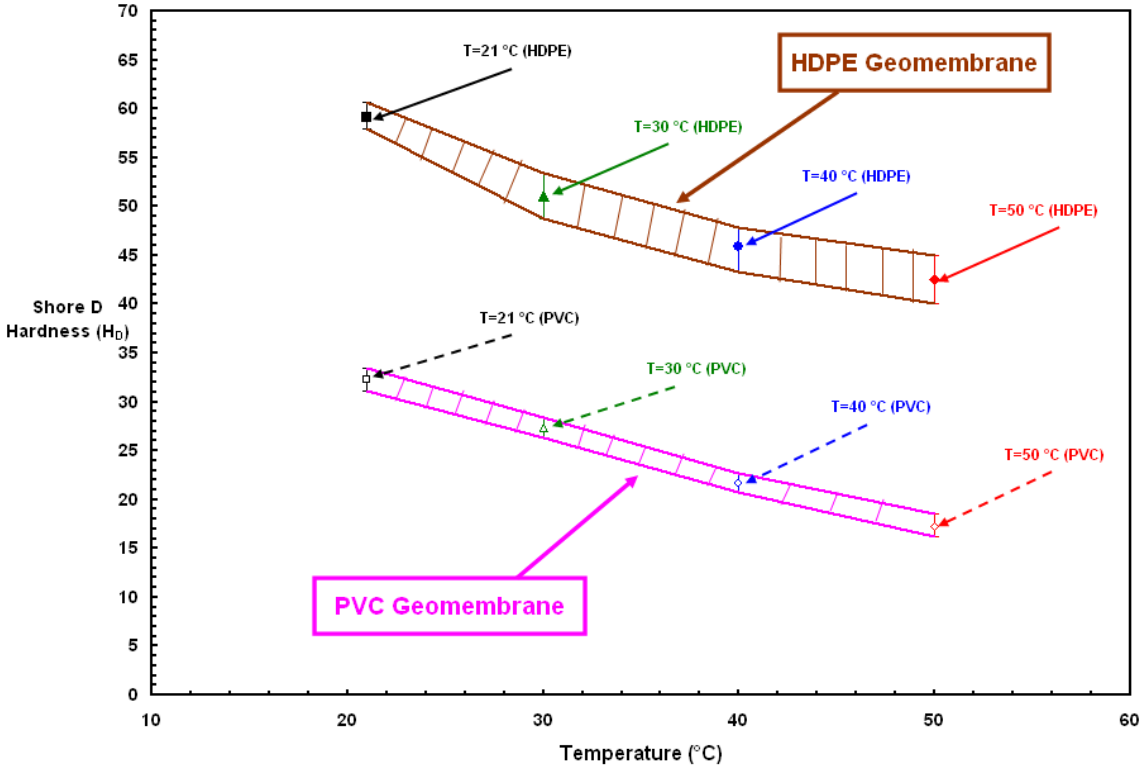

Figure 9.23 Comparison of the Variations in HDPE and PVC Geomembrane Surface Hardness's and the Variability in Measurements at Different Temperatures

As previously determined from the laboratory tests conducted only at room temperature (21°C) by O'Rourke et al. (1990), the shear capacity of particulate-continua interfaces was related to the surface hardness of the polymer. The mobilized frictional strength and the developed interface shear behavior at granular material – geosynthetic interfaces at different temperatures are also fundamentally influenced by surface hardness

of the geomembrane. Therefore, the measured index value of hardness of the geomembrane based on a particular scale (i.e. Shore D) at various temperatures provided a useful quantitative value to evaluate the magnitude of shear resistance being generated at the interface of granular soil-geosynthetic (Figure 9.24). The primary influence of temperature on sand-geomembrane interface shear behavior is essentially caused by temperature dependency of the geomembrane physical properties and not due to the sand. Consequently, it was shown throughout this chapter that the amount of shear response developed at the interface at different ambient temperature conditions can principally be attributed to the surface pliability of the geomembrane continuum sheet which is basically governed by and hence, can be indirectly assessed through surface hardness of the material. The surface hardness of PVC geomembrane is less dependent on temperature in terms of the rate of the change of hardness with temperature (i.e. slower rate) for the temperature range tested.

The reduction in the hardness of the geomembranes with increasing temperature (Figure 9.24) for HDPE and PVC liners further illustrates and validate the differences at elevated temperature conditions observed in the sand-geomembrane interface shear behavior for producing larger stress-displacement envelopes (complete interface response) as well as higher frictional resistances. Additionally, the measured variations in the magnitude of Shore D surface hardness values for HDPE and PVC liners underscore the pronounced difference in the interface shear strength characteristics of these two geomembranes at each test temperature. This results from the dissimilar material nature and physical-mechanical properties of PVC geomembrane which is more plasticized and softer compared with that of HDPE geomembrane which is less plasticized and stiffer.

Further, at higher temperatures, both HDPE and PVC become softer and more malleable as established through the reduction in surface hardness of these materials.

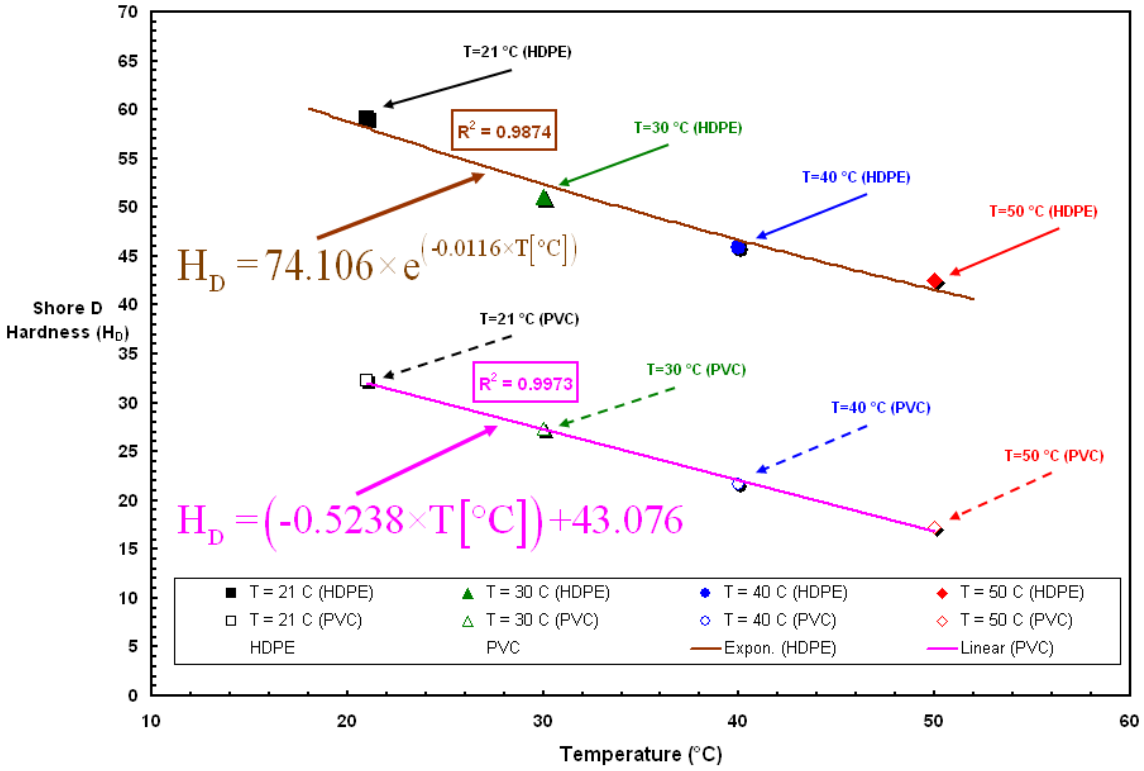

Figure 9.24 Comparison of Correlations and Observed Variational Trends between Surface Hardness and Temperature for HDPE and PVC Geomembranes

The larger interface shear response in terms of failure envelope and greater strength can primarily be attributed to the beneficial influence of the higher surface pliability of the geomembranes at elevated temperature conditions (Figure 9.25, 9.26, 9.27 and 9.28).

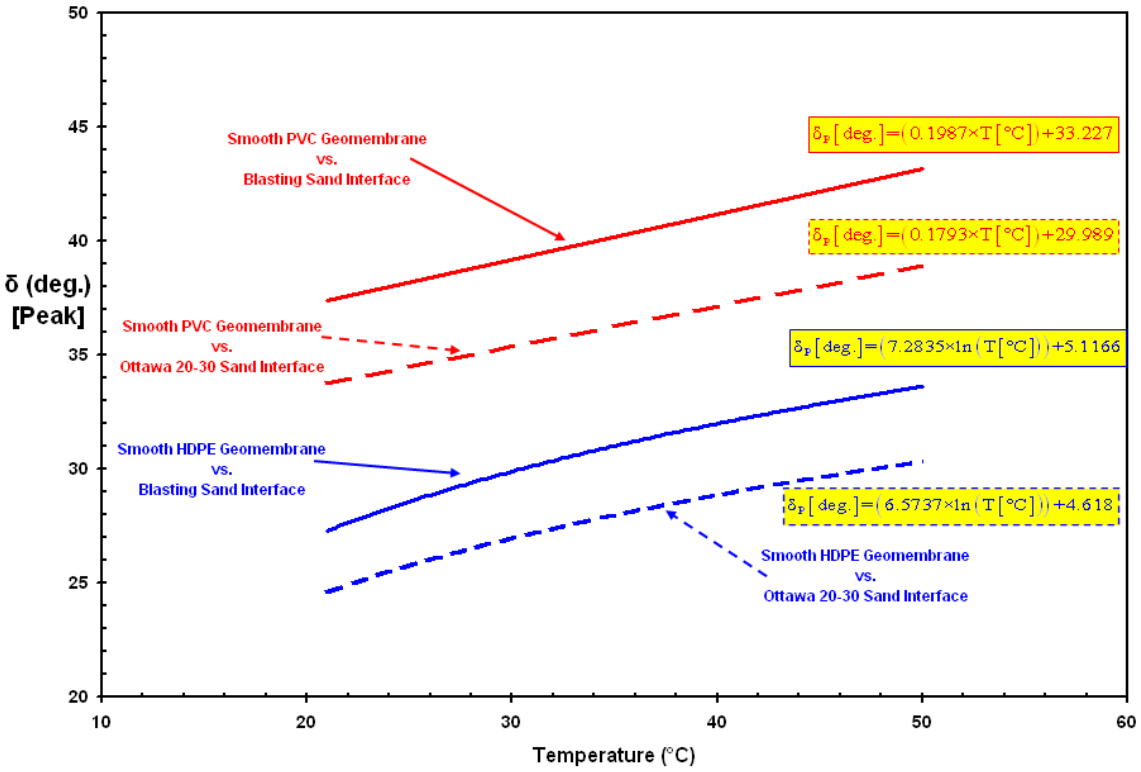

Figure 9.25 Comparison of Peak Interface Friction Angle with Varied Temperature for Rounded or Angular Sand – HDPE or PVC Geomembrane Interfaces

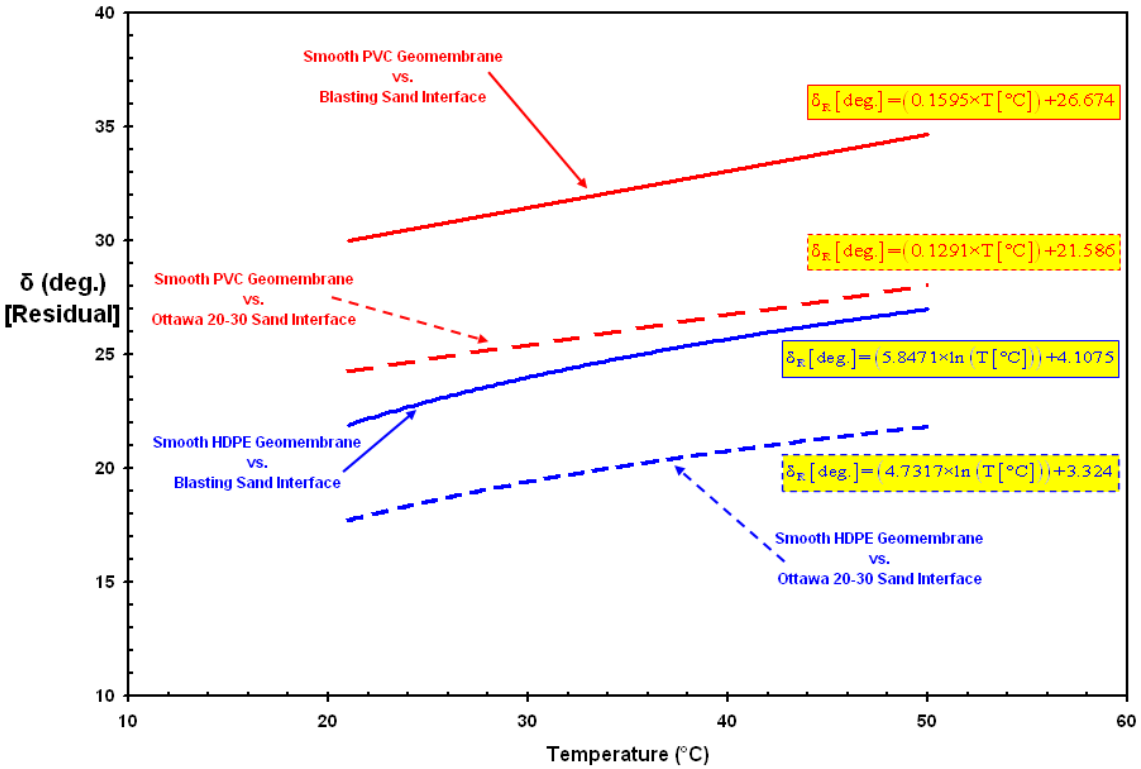

Figure 9.26 Comparison of Residual Interface Friction Angle with Varied Temperature for Rounded or Angular Sand – HDPE or PVC Geomembrane Interfaces

The more plasticized and softer nature of geomembrane liners made from PVC yields advantages for the material in terms of interface shear properties which reflects the importance of material hardness on the mobilized interface shear response and frictional resistance of polymeric geosynthetics utilized in a project. This significant contribution of material hardness properties to the developed interface shear behavior was previously identified by Hillman and Stark (2001) who showed that smooth PVC geomembrane – nonwoven geotextile interfaces yielded similar peak shear strengths and considerably higher residual shear strengths than textured VFPE geomembrane – nonwoven geotextile interfaces.

To sum up, in the light of these analysis developed and the discussions provided, it is vital, in terms of practical perspectives, to consider the significant influence of temperature on interface shear behavior of composite layered systems. The safety factors used in the design will also fluctuate due to the temperature changes influencing the geomembrane hardness. In particular, this change in the magnitude of interface strength mobilizing is critical when short-term conditions are considered during the design. Safety factors are assigned very close to a limit equilibrium state commonly when the temporary conditions are being considered. Therefore, rapid changes in temperature can easily reduce the interface frictional resistance such that safety factor may be reduced substantially in which it will approach the limit equilibrium condition and will potentially be causing failures.

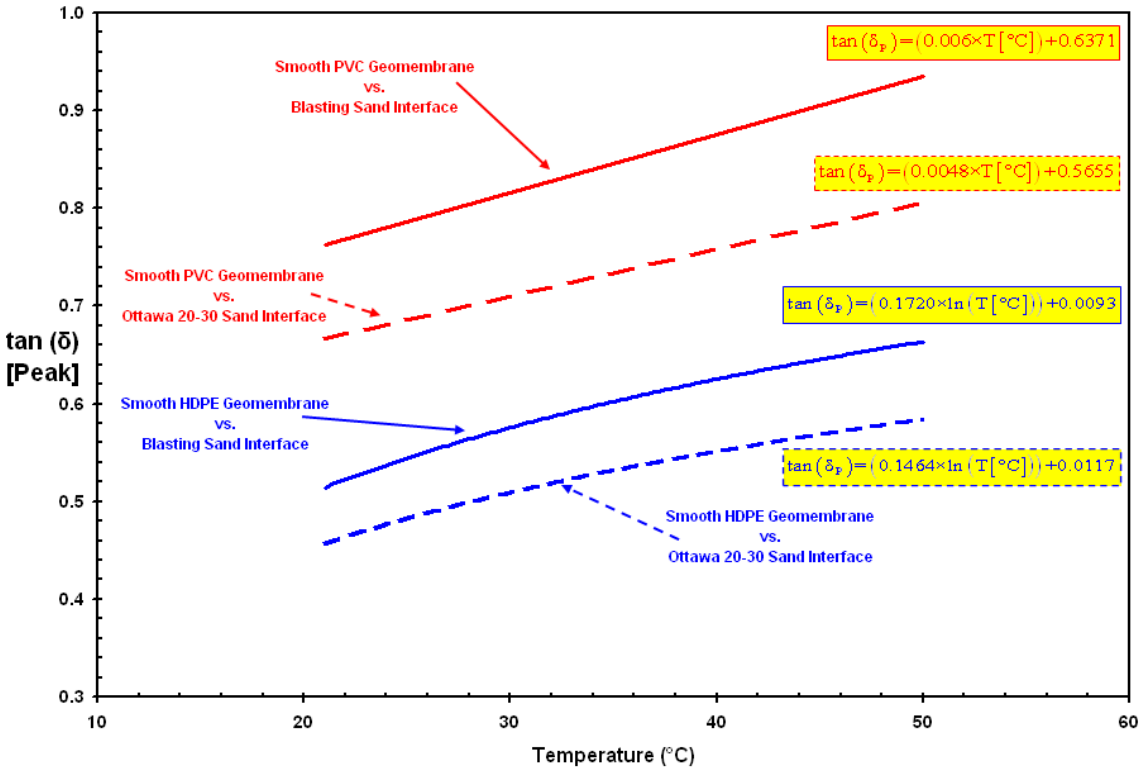

Figure 9.27 Comparison of the Change of Normalized Peak Failure Envelope with Varied Temperature for Rounded or Angular Sand – HDPE or PVC Geomembrane Interfaces

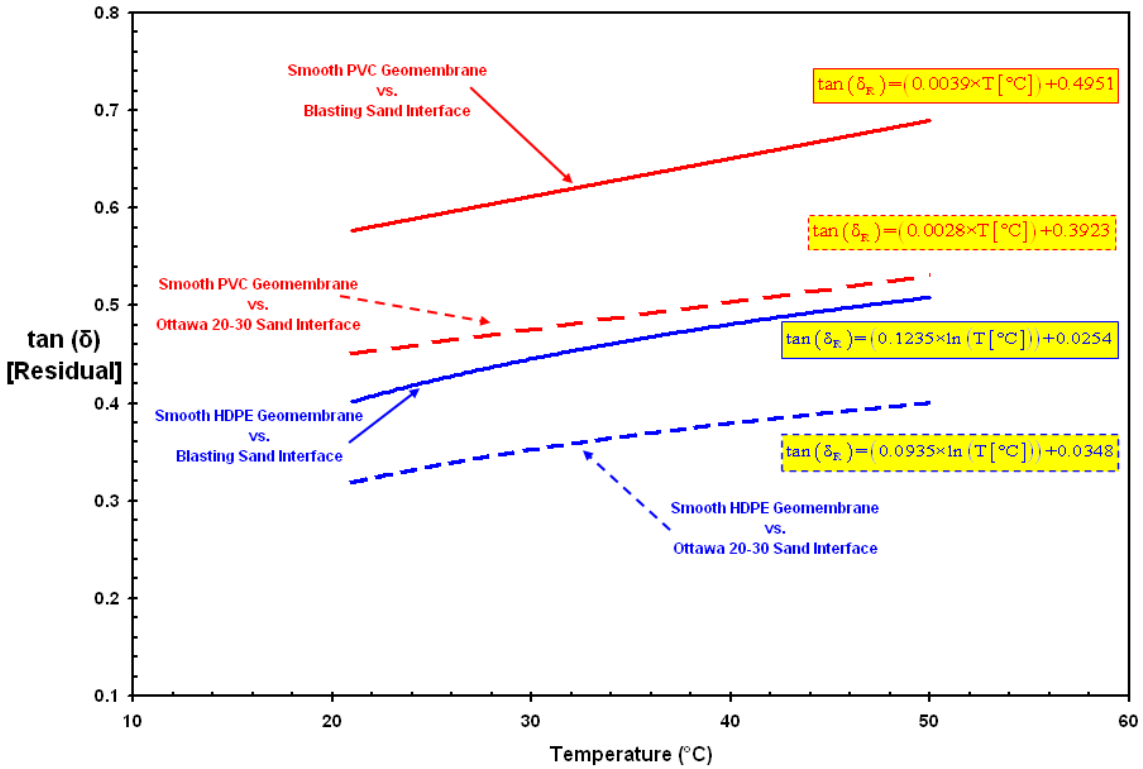

Figure 9.28 Comparison of the Change of Normalized Residual Failure Envelope with Temperature for Rounded or Angular Sand – HDPE or PVC Geomembrane Interfaces

9.9. Comparison of Direct and Indirect Assessments of Temperature Effects on Interface Shear Strength between Sand and Smooth Geomembranes

In general, a reduction in the magnitude of surface hardness of the polymeric geomembrane liner can be associated and linked with the alteration of the polymer material stiffness since the elasticity modulus as well as visco-elastic and plastic properties are strongly temperature dependent. A decrease in hardness is observed with increasing ambient temperature level and hence, a reduction in surface resistance of polymeric lining sheet against indentation as reflected by Shore D hardness index value is seen. Furthermore, the stiffness of a polymer principally defines its state on the "softness" through "rigidity" scale as well as governs and is related to its surface hardness.

Figures 9.29 and 9.30 show coefficient of friction (peak, residual) plotted as a function of temperature for smooth HDPE and PVC geomembrane interfaces, respectively, to make a comparative analysis between direct measurement test results and indirect assessment values analytically calculated using empirical correlations. Similarly, Figures 9.31 and 9.32 show the results of similar comparison between direct and indirect assessment of friction angle (peak, residual) as a function of temperature for smooth HDPE and PVC geomembrane interfaces, respectively.

It is noted that the primary influence of elevated temperature conditions on sand–geomembrane interface shear response and resistance (Figures 9.29 and 9.30) results from the temperature dependency of physical and mechanical properties of the geomembrane liner and are not necessarily due to changes in the sand properties. The

tested HDPE and PVC geomembrane liners softened and the degree of material hardness decreased with an increase in ambient temperature that resulted in the plowing to become governing the shear mechanism predominating at the interface in the course of shear displacement at higher temperatures (Figures 9.31 and 9.32). As it is known that deeper embedding/indentation of the sand particles/grains into the surface of the counterface geomembrane (i.e. increased plowing effect in shear) influences and results in an increase in the frictional shear resistance at elevated temperatures. Since more effort/energy for the particles is required to penetrate into and/or plow at a depth beyond the contact surface of the geomembrane liner. As a result, the friction coefficient or friction angle (Figures 9.29, 9.30 and 9.31, 9.32, respectively) for sand (rounded, angular) – smooth (HDPE, PVC) geomembrane interfaces show an increase in the resultant value or denote an incremental trend in the behavior as a function of temperature.

A decremental increasing trend (i.e. natural logarithmic behavior) for the peak and residual tan(δ) and δ (Figures 9.29 and 9.31, respectively) with temperature change for smooth *HDPE* geomembrane – Ottawa 20/30 or Blasting sand interfaces shows that a reduction in the rate of the increase of these frictional shear strength parameters occurred at higher elevated temperatures which is different than the linearly increasing trend exhibited in smooth *PVC* geomembrane – Ottawa 20/30 or Blasting sand.

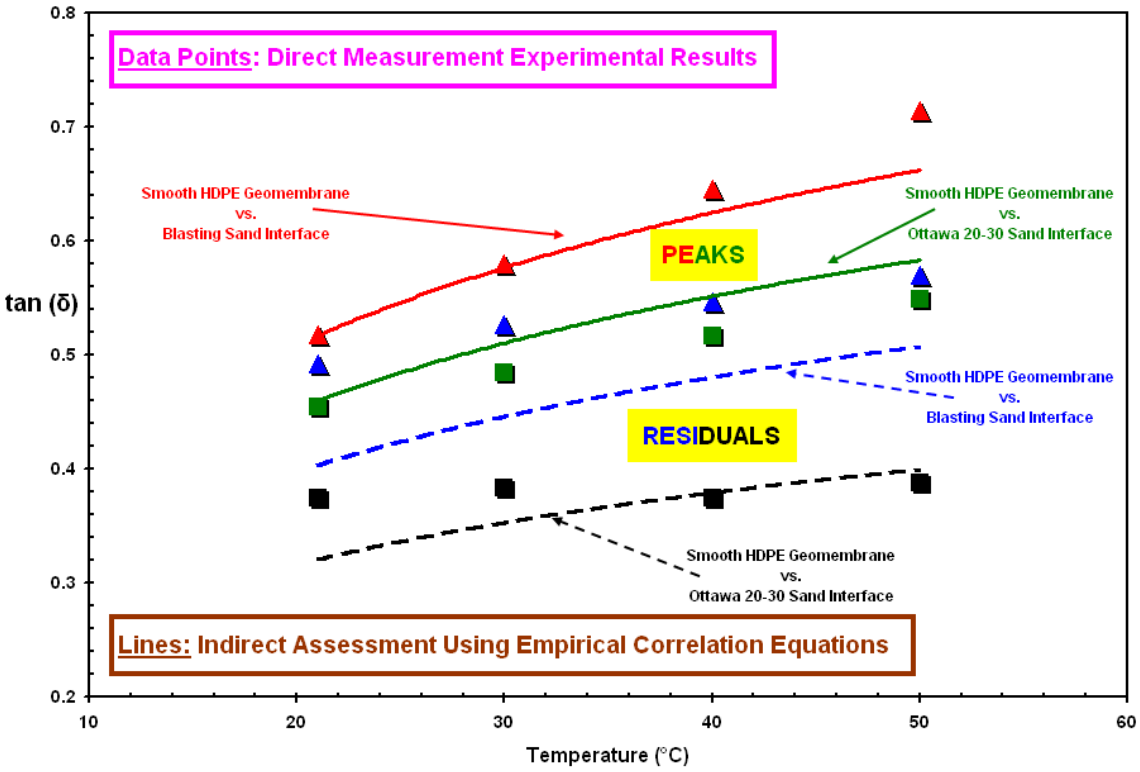

Figure 9.29 Coefficient of Friction (Peak, Residual) versus Temperature: *Comparison between Direct and Indirect Assessments for* ***Smooth HDPE Geomembrane Systems***

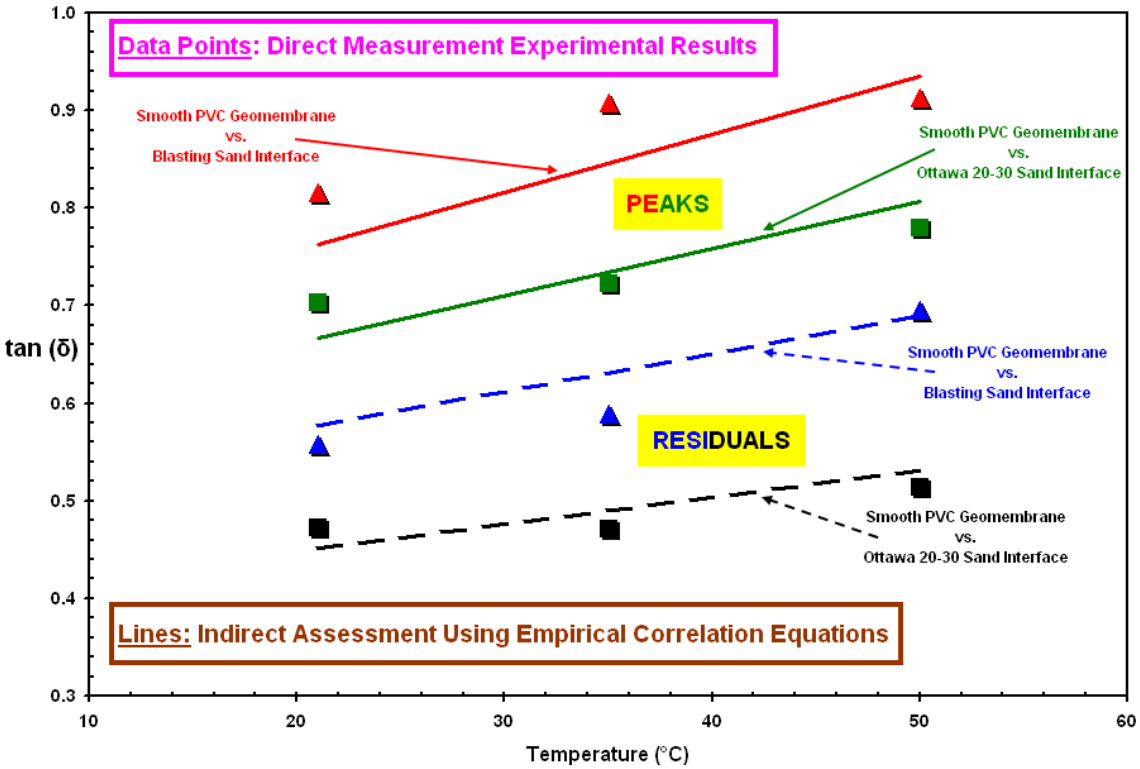

Figure 9.30 Coefficient of Friction (Peak, Residual) versus Temperature: *Comparison between Direct and Indirect Assessments for* ***Smooth PVC Geomembrane Systems***

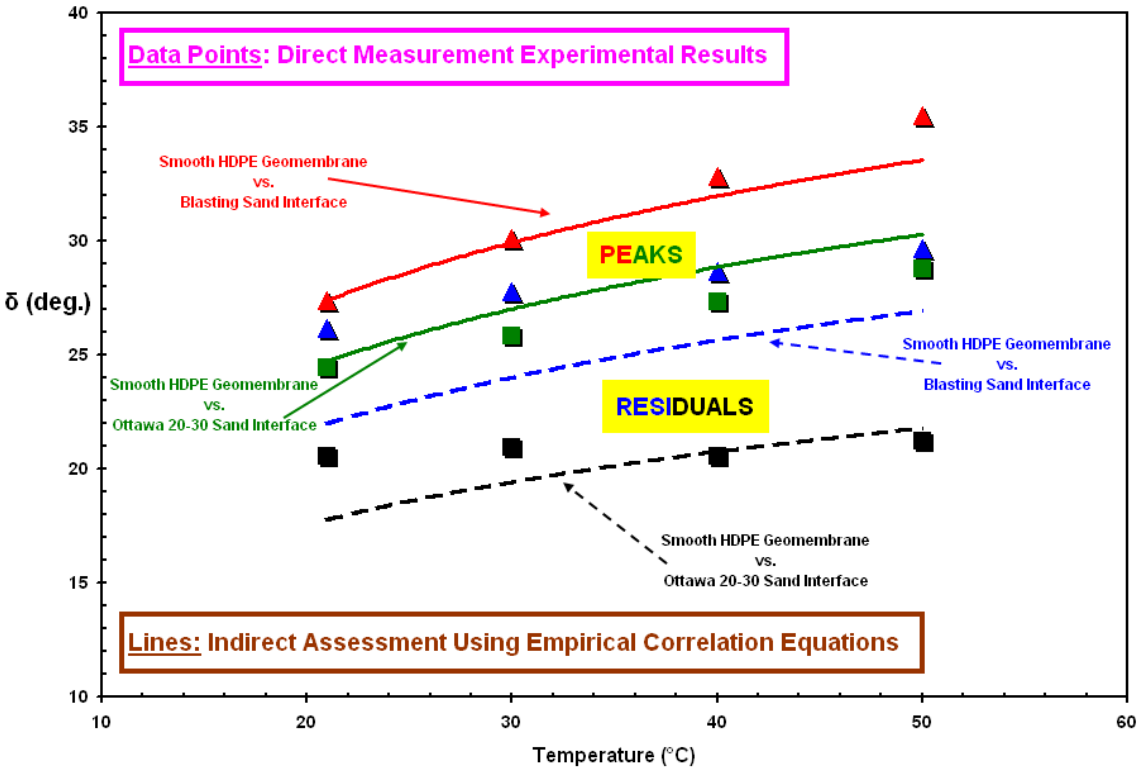

Figure 9.31 Interface Friction Angle (Peak, Residual) versus Temperature: *Comparison between Direct and Indirect Assessments for* ***Smooth HDPE Geomembrane Systems***

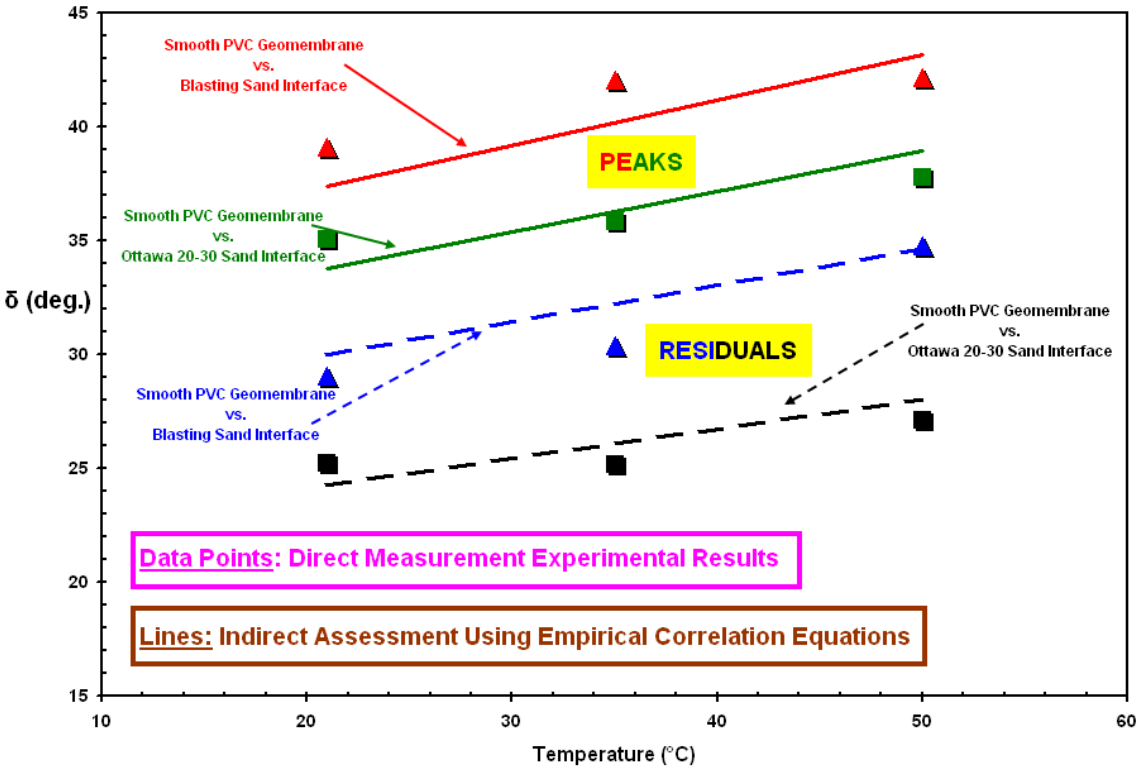

Figure 9.32 Interface Friction Angle (Peak, Residual) versus Temperature: *Comparison between Direct and Indirect Assessments for* ***Smooth PVC Geomembrane Systems***

For the two different geomembrane interfaces (HDPE, PVC), the comparison plots for [$\tan(\delta_{Peak})$] and [$\tan(\delta_{Residual})$] are presented in Figures 9.33 and 9.34, respectively, in which the test results from experimental direct measurements at different test temperatures can be compared to the resultant correlational trends generated through indirect evaluations using the proposed empirical relationships previously presented.

The discontinuous data points from interface shear tests performed at elevated temperatures in the TCC generally concur with the proposed correlation curves. The proposed natural logarithmic and linear behavior trend (HDPE and PVC, respectively) provided the best relationship for the variation of interfacial shear strength properties of the sand (rounded, angular) versus the smooth HDPE or PVC geomembrane interface systems with increasing temperature.

For direct and indirect assessment of the resultant [δ_{Peak}] and [$\delta_{Residual}$] values, the comparison plots are presented in Figures 9.35 and 9.36, respectively. Reasonable similarity between the laboratory test results and the indirect analytical assessment analysis is evident from the proximity of the experimentally measured intermittent values at the predetermined test temperatures (i.e. the discontinuous data points) to the continuous curves/lines that are plotted from the proposed empirical correlation equations presented in detail in Chapter 9. The discontinuous data points of interface shear tests performed at elevated temperatures in the TCC generally concur with the continuous correlation curves with particularly an exception of the angular granular material interfaces which shows a slight difference that will be discussed later in detail in this section.

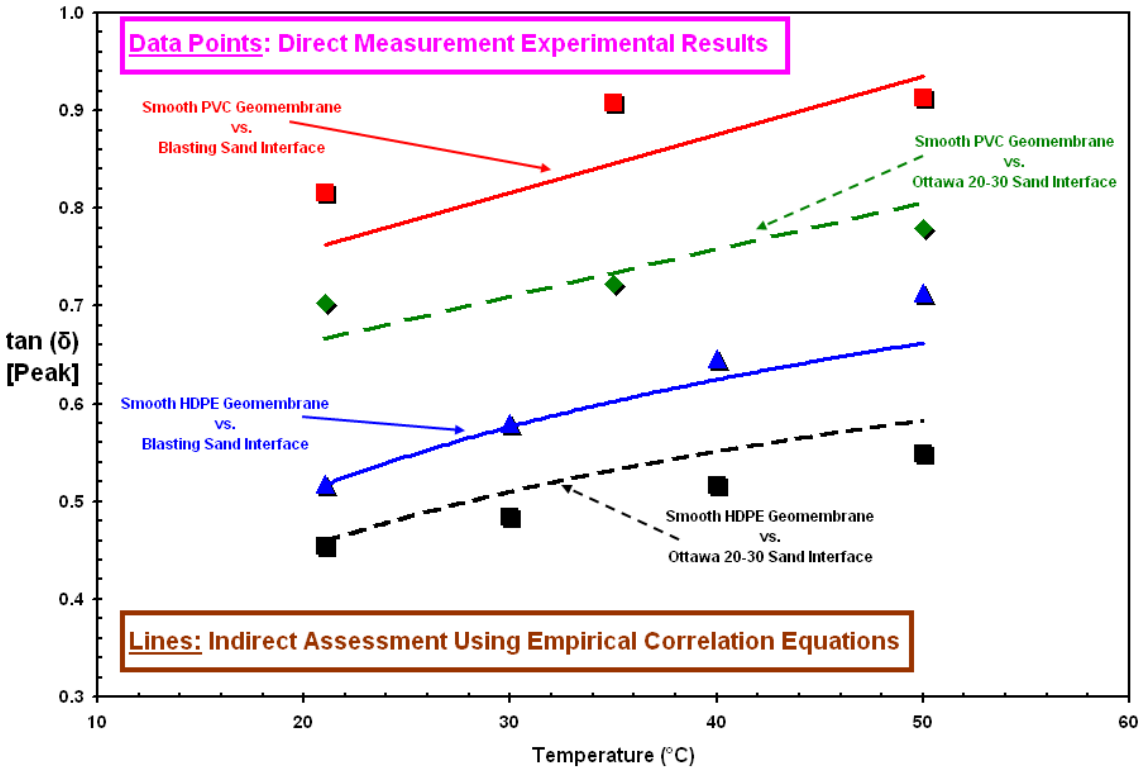

Figure 9.33 **Peak *Coefficient of Friction versus Temperature:*** Comparison between Direct and Indirect Assessments (HDPE Geomembrane ***as compared to*** PVC Liner)

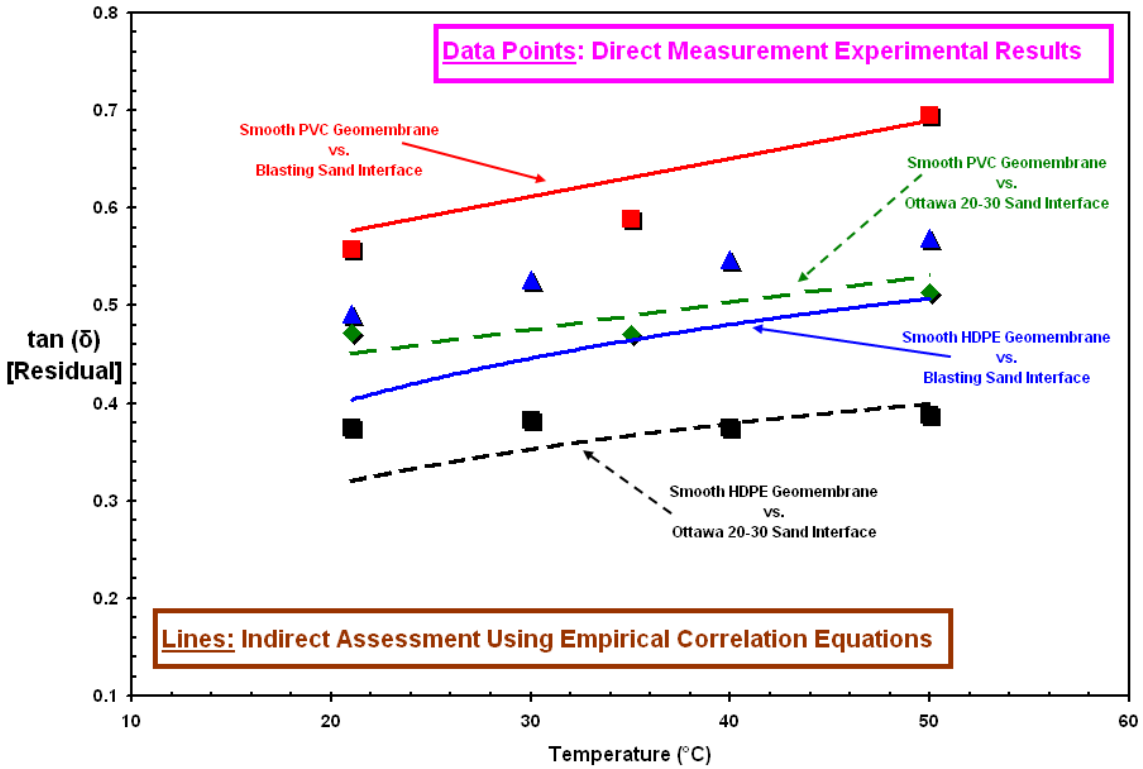

Figure 9.34 **Residual *Coefficient of Friction versus Temperature:*** Comparison between Direct and Indirect Assessments (HDPE Geomembrane ***as compared to*** PVC Liner)

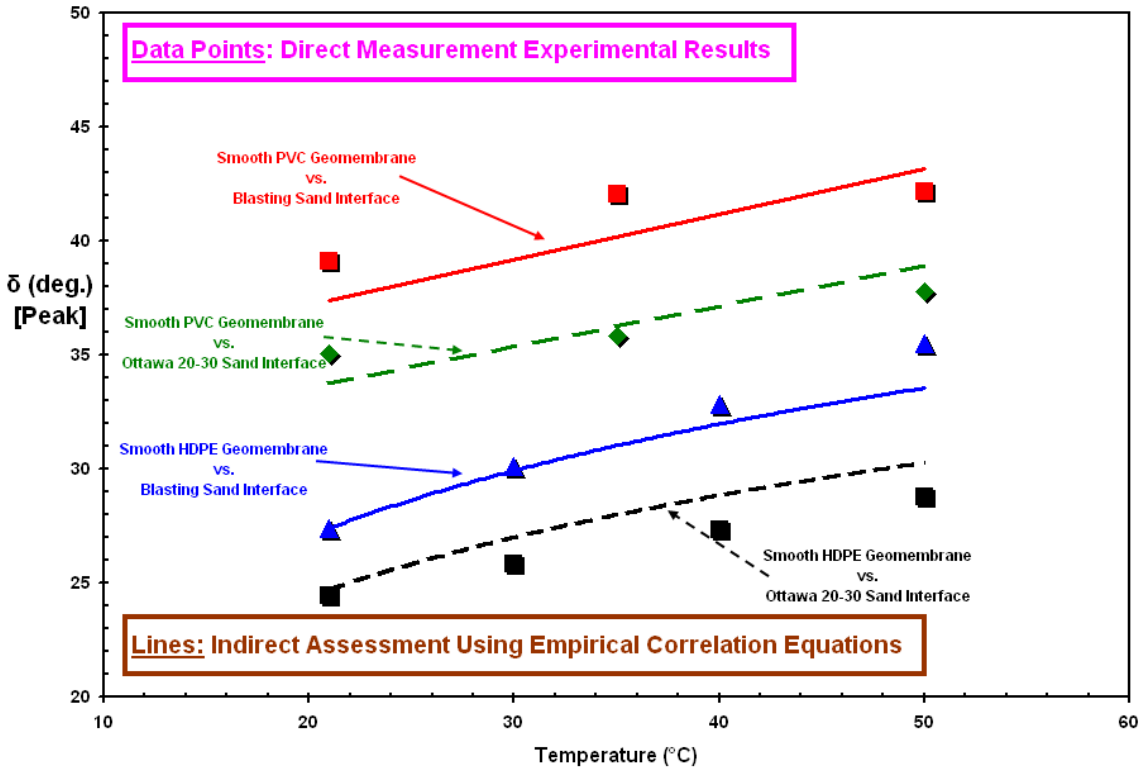

Figure 9.35 **Peak *Interface Friction Angle versus Temperature:*** Comparison between Direct and Indirect Assessments (HDPE Geomembrane ***as compared to*** PVC Liner)

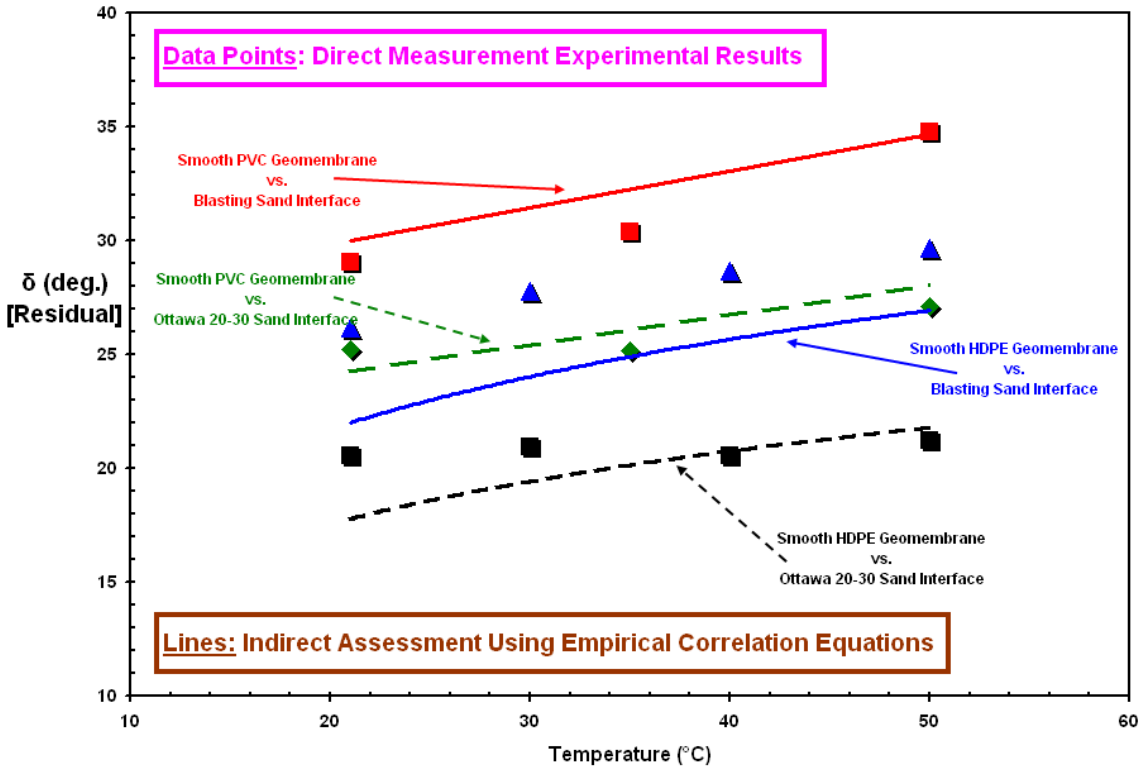

Figure 9.36 **Residual *Friction Angle versus Temperature:*** Comparison between Direct and Indirect Assessments (HDPE Geomembrane ***as compared to*** PVC Liner)

As the preceding figures shows, the geomembrane liners became softer at higher temperatures that resulted in the plowing shear mechanism to become more dominant at contact surface between particulate and continuum material during shearing. The increased plowing of the sand particles into the surface of the counterface geomembrane impacts and correlates directly to the increase of interface shear strength at elevated temperatures as more effort is extended in plowing the particles through the geomembrane surface instead of sliding the particles along the contact surface.

The slight difference observed between the direct and indirect assessments, in particular, for the case of residual state of the angular blasting sand interface system reflects the importance of the shape of soil particles (i.e. rounded versus angular) in contact with a smooth geomembrane material surface. It illustrates the significance of particle shape in governing the resultant frictional strength as well as in defining the relative role of the various interface shearing mechanisms including sliding, rolling and plowing during shear displacement. Based on post-test inspections, it was determined that wear observed in the post-test geomembrane specimens as scarring or striations were greatest for tests involving angular sand grains. The grooves after shearing were deeper for the case of angular sand as compared to that of rounded sand. As shearing progressed at displacements to post-peak residual stage, the magnitude of plowing and scarring along the interface and hence, the depth of indentation and/or penetration of angular sand grains through/into plastic lining sheet surface resulted in larger frictional resistances generated at the interface in comparison to that of indirectly assessed and computed values using empirical correlations. Additional work and energy is required for deeper indentations to scratch the geomembrane surface. Furthermore, as was noted by Dove and Frost (1999),

the main component of the friction force is plowing for interface shear tests performed with angular blasting sand as opposed to rounded Ottawa 20-30 sand. Additionally, they indicated that the increased amount of wear on geomembrane surface after shearing directly corresponds to improved shearing frictional resistance due to plowing; and thereby, the resultant increased value of interface strength properties, [tan(δ) or δ] at the contact surface.

In light of the experimental tests performed and the analyses and discussion presented herein, it is important to consider the significant influence of ambient temperature conditions on the mobilized interface shear strength at sand–geomembrane composite layered systems widely designed and employed in common geotechnical applications. The frictional shear capacity of granular soil and continuum geomembrane sheet interface is dependent strongly on the current degree of surface hardness of the polymeric geosynthetic lining material. Therefore, the measured index value of hardness for the geomembrane samples based on a particular scale at various ambient temperature levels provided a useful quantitative parameter to indirectly assess and gauge the resultant magnitude of interface shear strength.

In summary, the effects of temperature on the friction properties of particulate versus geomembrane interfaces were investigated based on surface hardness measurements at different temperatures. The goal of this experimental work was to examine: i) the change in geomembrane hardness with temperature; and, ii) develop empirical correlations between hardness and temperature; and iii) compare results of empirically predicted interface strength based on temperature measurements with those of direct measurements for sand – geomembrane interfaces obtained through direct interface

shear measurements at different temperatures in the temperature controlled chamber (TCC). The mobilized frictional strength at granular material – geomembrane interfaces at different temperatures is primarily influenced by the surface hardness of the geomembrane. The measured index value of hardness of the geomembrane surface based on a standard scale (i.e. Shore D in this case) at various temperatures provided a useful quantitative value to evaluate and gauge the magnitude of shear resistance generating at the interface of granular soil – geosynthetic material.

The results and analyses presented herein demonstrate that the mobilized shear mechanisms (i.e. sliding and/or plowing) and the resulting frictional resistance (i.e. shear strength behavior) of sand – smooth HDPE geomembrane interface combinations are highly dependent on a combination of temperature, geomembrane physical material properties (i.e. hardness) and particulate shape (i.e. angularity/roundness). Therefore, the degree to which plowing influences and contributes the mobilized interface strength is directly dependent on particulate material grain shape, temperature and continuum material surface hardness properties. The plowing effect is minimal for hard counterface material surfaces that resist indentation of the sand particles where the shear mechanism is dominated by sliding. As temperature increases, the polymeric geomembrane becomes softer and exhibits a reduction in the degree of its surface hardness by showing less surface resistance to the counterface component which results in the increased plowing of the soil particles along the interface into geomembrane sheet surface during the course of shear displacement that correlates directly to the increased interface strength at elevated temperatures as additional work is required to indent and plow the particles through the geomembrane surface at initial shear displacements and to penetrate the sand grains

deeper into the counterface geomembrane with further progression of the shearing process.

9.10. Summary and Conclusions

It is known that the interface friction is temperature dependent. The peak interface strength for sand-geomembrane as well as geotextile-geomembrane interfaces is mainly attributed to the geomembrane micro-texture and depends particularly on the geomembrane properties such as “hardness” and “surface roughness”. In this chapter, the effects of temperature on the interface friction properties of two polymeric geomembrane liners were investigated based on measurement results from surface hardness tests at different temperatures. The aim of this portion experimental work mentioned throughout the chapter was to examine: i) the change in geomembrane hardness with temperature; and then, ii) develop empirical correlational relationships to evaluate shear strength properties of sand – geomembrane interfaces as a function of temperature. Therefore, it was accomplished that the influence of temperature on the mobilized interface shear strength at elevated temperature conditions can indirectly be assessed through the use of the proportional value of δ/φ'_{ds}, proposed by O’Rourke et al. (1990), which applies both for particulate material characteristics and continuum material surface properties. This normalized quantity provides a more comprehensive approach for evaluating shear properties of granular versus polymeric continuum material interfaces. The geomaterials in consideration for this study consisted of HDPE and PVC liners as previously used throughout all interface experimental program in the laboratory.

The empirical relations were developed as follows: the earlier research work of O'Rourke et al. (1990) correlating interface properties to surface hardness were utilized to tie temperature effects to interface friction properties; and then, a new model for interface frictional resistance was developed in which interface friction angle and coefficient of friction was related to temperature of the polymeric geomembrane liners (HDPE, PVC).

The frictional resistance of two geosynthetics liners (HDPE, and PVC) increases pronouncedly within the temperature range from 20°C to 50°C as a result of this analysis developed indirectly by the use of empirical correlations and relating the corresponding engineering parameters interchangeably in between the closed form equations (higher variation in HDPE; lower change in PVC). The temperature conditions ranging from 20°C to 50 °C is the most common elevated temperature range to which most of the geosynthetics infrastructure applications in geotechnical engineering practice are exposed in the field during their service life. This indicates that the safety factors used in the engineering design requires to be revised especially for cooler temperature conditions to sufficiently compensate the reduction in the magnitude of the mobilized shear strength and the diminish in the toughness of the developed shear behavior at the interface of geosynthetic composite systems due to anticipated fluctuations in the ambient environment conditions and the expected variations in temperatures (i.e. seasonal effects, exothermic waste reactions in landfill facilities). Since the magnitude of the change in geosynthetic interface response and resistance is, in particular, critical and important when short-term perspectives of the structure are in consideration during design. For example, the design considerations for landfill side slopes for which interface shear

resistance between geosynthetic components is crucial and designates the performance and stability of the entire infrastructure application. The practical significance of the results of this analysis presented herein provide a rapid and simple means of estimating the interface design engineering parameters with varied temperature simply from measuring Shore D Hardness, H_D of the geosynthetic materials at different temperatures; thus, the indirect assessment of temperature effects on the mobilized frictional resistance and on the developed shear response properties of particulate material – geosynthetic interfaces could be rendered possible quickly in the field in place without laboratory testing by creating the necessary ambience in the lab to imitate elevated temperature conditions; or, through a developed numerical simulation analysis. To sum up, the results of the experimental research study presented throughout this chapter provided a rapid and simple evaluation analysis of temperature effects on interface friction properties, and also showed the importance of ambient temperature on interface shear response of geosynthetics materials. Based on the correlations and experimental data on two different geosynthetic liner materials, the Shore D Hardness, H_D decreases as temperature increases. The test data indicated that the change of surface hardness per temperature change is dependent on the base material from which the geomembrane is produced. Additionally, the surface hardness of PVC liners is less dependent on temperature (i.e. the rate of change of hardness with temperature is slower than that of HDPE).

In particular, the hardness measurement results, the developed empirical relations and analysis, as well as further the provided discussion throughout this chapter will complement, comprehend, and expand the understanding further for the interface shear tests results at different temperatures on sand-geomembrane interfaces. Since, in short,

the mobilized frictional strength and the developed interface shear behavior at particulate material (sand) – continua (geomembrane) interfaces are influenced by surface hardness of geomembrane as being a plastic material and produced from polymer resins and was found to decrease with increasing Shore D Hardness of the polymers.

CHAPTER X

10. CONCLUSIONS AND RECOMMENDATIONS

10.1. Introduction and Content of the Study

The performance of geosynthetic layered systems during service lifetime in terms of interface shear behavior and strength properties is of major importance in selection of geosynthetic materials (i.e. geotextiles, geomembranes) for certain geotechnical applications such as landfills. Interface shear behavior at different ambient temperature conditions is not a single attribute, but a collection of performance attributes of the counterface components which requires a suite of tests to assess the engineering strength properties of the components both independently and collectively.

10.2. Conclusions

An extensive research study was undertaken in an effort to investigate temperature effects on interface shear behavior between (a) NPNW polypropylene geotextiles and both smooth PVC as well as smooth and textured (co-extruded, structured) HDPE geomembranes and (b) sands (rounded, angular) and smooth PVC and HDPE geomembranes. A unique temperature controlled chamber (TCC) was designed and developed to be utilized to simulate the field conditions at elevated temperatures and evaluate shear displacement failure mechanisms at these higher temperatures. The physical laboratory testing program consisted of multiple series of interface shear tests

between material combinations found in landfill applications under a range of normal stress levels from 10 to 400 kPa and at a range of test temperatures from 20 to 50 °C.

Complementary geotextile single filament tensile tests were performed at different temperatures using a dynamic thermo-mechanical analyzer (DMA) to evaluate the thermo-tensile micro-strength properties of single geotextile filaments at elevated temperatures. The single filament studies are important since the interface strength between geotextiles and geomembranes is controlled by the fabric global matrix properties as well as micro-scale characteristics of the geotextile such as filament strength and how it interacts with the geomembrane macro-topography.

The peak interface strength for sand-geomembrane as well as geotextile-geomembrane interfaces is mainly attributed to the geomembrane properties such as hardness and micro surface roughness. To this end, the surface hardness of smooth HDPE and PVC geomembrane samples was measured at different temperatures in the temperature controlled chamber to evaluate how temperature changes and this surface hardness changes, affect the interface shear behavior and strength of geomembranes in combination with granular materials and/or geotextiles. Empirical relationships were developed based on the variation of hardness as a function of temperature to evaluate shear strength properties of sand – geomembrane interfaces and to conduct a comparative analysis between the results of empirically predicted frictional shear strength properties with direct measurements from the interface shear tests performed at different temperatures.

Surface roughness measurements were made on virgin and sheared smooth geomembrane specimens using a stylus profilometer to quantify the extent of wear

resulting from shearing against different counterfaces at different elevated temperatures and different normal stresses.

Further comparative analyses on the experimental test data were used to develop empirical correlations (i.e. analytical closed form solutions) for indirect evaluation of the change in the shear strength with temperature and to make comparisons with the direct measurement test results.

10.2.1. Design and Development of a Unique Temperature Controlled Chamber

As part of this study, a unique temperature controlled chamber was designed and developed to allow interface shear tests to be performed on geosynthetic materials as well as to evaluate shear displacement-failure mechanisms under elevated temperature conditions. The development and validation of the unique temperature controlled chamber test system as well as observations pertaining to system design criteria and the relevance to field conditions was discussed.

Reliable operational performance of the TCC test system has been achieved by appropriate selection of the parts following the main design criteria which were functionality, size, efficiency and long-lasting serviceability. The components employed in the electrical system for controlling temperature were a first order concern to ensure precise and accurate control of the TCC during the laboratory tests.

The designed and developed temperature controlled chamber (TCC) which encloses the large displacement direct interface shear device provided the ability to examine the temperature dependent interface shear behavior of geosynthetic-geosynthetic as well as sand-geosynthetic composite systems.

10.2.2. Geotextile Single Filament

The strength of the NPNW geotextiles is related to the amount of entanglement produced by the needling and the inter-fiber friction. The geotextile samples utilized in the experimental program are produced from polypropylene (PP) fibers that have more frictional surface to facilitate inter-fiber-friction leading to a relatively strong geotextile macro-structural matrix. The tensile response of the fibrous nonwoven geotextile is governed by the micro-scale (filament) and/or global-level (fabric matrix) tensile and elongation properties.

In order to investigate tensile behavior and the developed "micro-scale" stress-strain response of geotextile single filaments at different temperatures, laboratory tests were performed in this study by measuring filament thermo-mechanical properties using DMA. Various test temperatures between 20 °C and 50 °C were chosen to simulate the elevated temperature range expected in the field for geotechnical applications such as landfill liners.

The filaments from GSE NPNW-PP 8 oz/yd^2 geotextile resulted in a similar trend of tensile load-elongation response at all test temperatures such that the tensile force-displacement curve has a nonlinear elasto-perfectly plastic form in terms of stress-strain relationship. The general pattern in force-elongation behavior of polypropylene filaments in tension tests can visually be portrayed in three segments: i) sharp increase to a local maximum; ii) steady rise at a reduced slope; then, iii) leveling off at higher strain levels. The filaments exhibited nearly constant resistances after yielding until they reached rupture at elongations of between 70% and 120%. Before experiencing yield, the elastic portion of the curves develop with a relatively constant rate of change in tensile force

with respect to displacement. The resulting force-displacement curves for lower temperature tests are located on the upper part of the load-extension space compared with force-displacement curves from higher temperature tests. In other words, the tension failure envelopes for the tested filaments diminished as the ambient temperature increased.

The PP single filaments exhibited lower yield strengths and displayed smaller strains (i.e. extensional tensile displacements) prior to yielding at higher temperatures. This is attributed to the loss of the polymer stiffness with increasing temperature. As such the polymeric material becomes softer and its endurance to sustain plastic deformation under tension is diminished. It experiences permanent strains by encountering the yield deformation stage at smaller tensile extensions. As such, the major impacts of temperature on the tensile strength properties of the polymeric filaments were a decrease in ultimate tensile strength and a reduction in stiffness.

With respect to the consequences of the thermo-mechanical tensile strength behavior of single geotextile filaments at different ambient temperatures to the global matrix level response, the total contact area involved during shearing of the geomembranes against geotextiles depends heavily on the development of tension in the fiber and the tendency of the filament to elongate. As such the frictional resistance mobilized at geotextile versus geomembrane interfaces is heavily governed by the magnitude of the interbedding of the surface roughness features into the fabric matrix. This facilitates stronger interlocking between the counterface materials due to the presence of larger contact stresses at contact points at the micro-level due to reduced contact area between the different individual filaments subjected to tensional elongation.

To this end, this study reported on the characterization of the tensile behavior of NPNW-PP single geotextile filaments at the "micro-scale" level to be taken into account in evaluating the interface shear behavior of fabrics (i.e. geotextiles) with continua (i.e. geomembranes) under varied temperatures. At the "micro-scale", the tensile failure takes place due to breakage of filaments whereas at the global scale, the slippage between filaments and the structural deformation due to inherent internal geotextile void space that is governed by fabric manufacturing and fiber processing type, dominates.

As a result, globally full mobilization of tensile capacity of geotextile fabric is associated with full mobilization of filament tensile strength at micro-scale. Consequently, the development of force-elongation response of a fibrous material (i.e. geotextile) based on its characteristic tensile stress-strength-strain behavior is a multi-scale phenomenon and this is very important to be considered in design and analysis of geosynthetic composite layered systems incorporating geotextiles. As pointed out by Mitchell and Seed (1990), sliding failure mobilized at geotextile-geomembrane interfaces is known to accompany the tension of geotextiles.

10.2.3. Geomembrane Surface Hardness

The findings of additional supplemental research which involved the measurement of geomembrane surface hardness at different temperatures are summarized below. The focus of this portion of the experimental work was to examine:

i) The change in geomembrane hardness with temperature.

ii) Develop empirical relationships to predict shear strength properties of sand – geomembrane interfaces as a function of temperature.

iii) Compare the results of empirically predicted frictional shear strength properties with the results of direct measurements from the interface shear tests performed at different elevated temperatures.

The effects of temperature on the friction properties of particulate versus geomembrane interfaces were examined based on surface hardness measurements at different temperatures and showed that the mobilized frictional strength at granular material – geomembrane interfaces at different temperatures is primarily influenced by the surface hardness of the geomembrane. In this context, the measured index value of hardness of the geomembrane surface based on a standard scale (i.e. Shore D in this case) at various temperatures provided a useful quantitative value to evaluate and gauge the magnitude of shear resistance being generated at the interface of granular soil – geosynthetic material.

10.2.4. Smooth Geomembrane – Geotextile Interface

To examine the influence of temperature on interface shear strength and response, multiple series of interface direct shear tests were performed on smooth geomembrane (HDPE, PVC) – NPNW geotextile interfaces at the different ambient temperatures ranging from 20°C up to 50°C as well as at normal stress levels ranging from 10 to 400 kPa. The interface frictional resistance of both smooth HDPE or PVC geomembranes and NPNW geotextile interfaces increased with increasing ambient temperature owing to a decrease in material hardness, and hence, an increase in surface pliability of the geomembranes. It is considered that the acceleration of the polymer relaxation at elevated temperatures resulted in quick dispersion of the concentrated stresses over the interface

contact area after the application of load leading to more uniform stress distribution over the entire contact surface at the interface during shear displacement.

Due to the differences in surface hardnesses of HDPE and PVC geomembranes, the smooth PVC exhibited higher shear stress – displacement curves than those of the smooth HDPE at all temperatures tested although both lining sheet material posssess similar and analogous surface roughness characteristics. In this context, the interface tests carried out at elevated temperatures conditions for PVC liner showed similar responses in which shear displacement hardening behavior occurred after yielding in contrast to the behavior observed with smooth HDPE geomembranes where a post-peak strain softening response developed. The tendency of PVC smooth geomembrane – geotextile interfaces to behave in this fashion was completely dependent on the differing material properties compared with HDPE liners. Additionally, the hardness reduction contributed to some very minor increase in strength with increasing temperature level compared to HDPE. However, the smooth HDPE geomembrane showed a higher increase in strength with temperature for same normal stress level tested.

The higher surface pliability of the PVC lining materials compared to that of the HDPE geomembranes at all temperatures tested, allows it to get worn by being embedded by the counterface geotextile and resulting in a larger shear resistance. The stiffer and harder nature of HDPE liners does not facilitate the counterface filament embedment into the geomembrane surface as much as the softer PVC liner. This also prevents the frictional resistance of the smooth HDPE from reaching that of the smooth PVC. In short, the higher surface pliability of the smooth PVC enables the strength-increasing mechanisms discussed above to develop more readily than for the smooth HDPE which

accounts for the larger shear strength attained by the smooth PVC under the same normal stress level at all test temperatures ranging from 21 °C to 50 °C.

The strain-softening/strain-hardening behavior of the interfaces at different ambient temperatures was quantified by a ratio between peak and residual strengths. The interfaces with a relatively stiff HDPE geomembrane compared to those with a pliable PVC liner resulted in higher sensitivity values observed over the entire range of normal stresses and temperatures tested. It is noted that the higher malleability and more plasticized nature of the PVC can also account for the marginal post-peak strength-gain (i.e. displacement-hardening behavior) observed with the counterface geotextile over the entire test temperatures ranging from 21 °C up to 50 °C. The counterface geotextile was able to embed into the softer surface of the smooth PVC geomembrane.

10.2.5. Textured Geomembrane – Geotextile Interface

For geotextile – textured geomembrane interfaces, the prevailing mechanism controlling the shear behavior were the interbedded interactions between the fabric matrix and the continua textural features due to load application as well as temperature increase that induced larger contact area at the contact surface of the materials as a result of relaxation at higher temperatures. The combination of surface texture and normal stress were sufficient to create larger interactions between the counterfaces particularly at higher loading conditions (≥ 100 kPa). The combination of sufficient amount of textures (roughness features: micro, meso and macro texture elements) to engage the geotextile fabric globally at matrix level instead of at individual filaments and the application of normal stress to allow the geotextile fabric to further penetrate into the geomembrane

texture allows a higher global strength of the NPNW geotextile to be realized for a particular normal stress level. In addition, the relaxation of the counterface materials at higher temperatures resulting in more effective placement, better deployment, and larger interaction (contact area) of the interface components which leads to the larger frictional response and resistance being realized at elevated temperature conditions compared to cooler ambient temperatures.

The stress-displacement curves of the tested textured geomembranes showed greater post-peak strength loss/reduction throughout the test temperature range compared to smooth geomembranes. This significant post-peak softening at all test temperatures for the tested textured (coextruded, structured) geomembrane (GSE, PloyFlex and Agru) – geotextile interfaces represented a transition dominant mechanism in interface shear behavior at all temperatures tested. Additional shear displacement resulted in removing microtextural features from the geomembrane core. Therefore, the failure occurring at peak shear displacement can be considered to primarily be initiated by a decrease in the micro-scale interlocking between continua micro-texture features and geotextile filaments due to geomembrane surface degradation at microscopic level because of shearing force and displacement. Such a failure mechanism results in a smooth peak and gradual transition of the stress-displacement curves. Increased normal stress level makes the geotextile filaments denser adjacent to the surface of the geomembrane which result in deeper penetration of the geomembrane texture elements into the geotextile. This leads to higher resistance at the interface due to stronger opposition of the texture elements against shear motion through firmer interlocking of these two materials during compression and subsequently during shearing compared to smooth counterparts.

Further, it is noted that larger shear displacements/deformations are necessary to attain peak and pseudo-residual states for textured liner – fabric interface system compared to smooth liners.

The displacements to peak for PolyFlex textured geomembrane interface tests were slightly smaller than for the GSE textured geomembrane at the same test temperatures. This difference is attributed to the effect of the slight differences in the stiffness of the sheet materials along with adhered textural properties from the different manufacturers. Based on laboratory inspections, the GSE coextruded-textured geomembrane liner is stiffer than the PolyFlex coextruded-textured liner which is a more ductile geomembrane liner sheet having more flexibility and less Velcro type behavior (i.e. hook and loop). The interface shear test results showed that, as the core material of the continuum sheet becomes less ductile or less flexible, a more sharply peaked stress displacement curve is likely to be observed.

The resulting shear-displacement curves from the tested textured (coextruded, structured) geomembranes consisted of multiple distinct stages including: i) initially, a sharp rise; ii) a reduction in the rate of this increase up to the peak point; iii) a decrease in resistance; and iv) finally, an interface response (i.e. remains essentially constant) which progresses in almost a fully plastic manner.

A detailed examination of the full shear stress-displacement behavior exhibited at different temperatures of the individual selected normal stress levels depicts an increase in displacement to peak stress with increasing ambient test temperature (from 21 °C up to 50 °C) which is indicative of greater geotextile filament engagement with the stronger rounded spikes as the surface pliability and the interaction capability of the continuum

geomembrane liner increases. Consequently, the frictional interactions occur at greater depths into the geotextile matrix beyond the interface contact surfaces with higher stiffness than the surficial shallow hook and loop interactions. Moreover, the favorable contributing influence of higher temperature conditions, in terms of increased surface pliability as well as greater relaxation and flexibilty of the polymeric counterface geosynthetics, promotes an improved and complete settlement of one geosynthetic material into the other resulting in greater interaction and interlocking between interface components. This results in the interface exhibiting larger shear responses at elevated temperature conditons for the same normal stress level.

Nonwoven geotextile – *structured* geomembrane (Agru) interfaces reached both peak and post-peak conditions at greater shear displacements than nonwoven geotextile – *coextruded* geomembrane interfaces (both GSE and PolyFlex) at the same test temperatures. The larger displacement required with the interface involving the microspiked liner was attributed to the fact that as the liner sheet surface roughness increases, the displacement to reach peak state increases. Subsequent to this, the shear stress – displacement curve progresses more or less constant with repeated peaks and troughs like a sinusoidal periodic motion. As opposed to the coextrusion process which generates random textures over a broad size range of features, structuring typically produces more uniform surface textures consisting of macro-spike configuration organized in multiple sequential arrays of spikes recurring at distinct intervals with micro and meso texture existing on the base substrate only. Further, the structured geomembrane sheet can be visibly seen to be composed of two distinct surface textural schemes in terms of roughness properties such that the micro and meso texture region is

seen as an elemental part of the liner sheet whereas, the microspikes appear as more external features. After the normal stress is applied but before the shearing process is initiated, the geotextile becomes compressed and progressively interbedded between the macrotextural features (spikes) of the contacting structured geomembrane resulting in matrix level frictional interactions and interlockings. At the same time, the micro and meso texture of the base substrate become involved in supplemental interlocking interactions. Once the shearing is initiated, the micro and mesotexture present on the base of the tested geomembranes result in a counterface that provides for the supplemental interactions and interlocking in mobilizing higher peak strength gains and attaining the larger frictional resistance of peak level which is similar with that of the coextruded liners in terms of the shape of the curve. Further, even though no fluctuations were observed during pre-peak and peak stages of shear response for the structured geomembrane – geotextile interfaces, the development of oscillating post-peak interface behavior is attributed to the repetitive surface texture configuration of consecutive series of the spikes. As a result, the governing components of the evolution of the pseudo-residual shear behavior for geotextile and textured geomembrane interfaces are macro-texture isotropy, uniformity, and recurrence properties. The isotropical/ anisotropical configuration of macro-texture asperities influences the interface fricitional characteristics of the corresponding geosynthetic lining material in terms of exhibited interface shear response, in particular, during the residual state of the stress-displacement failure curves.

To quantify the post-peak strength loss exhibited by relatively stiff HDPE textured (coextruded, structured) geomembrane – NPNW geotextile interfaces as well as

to highlight the differences in the peak and psuedo-residual responses at different test temperatures, a useful quantitative parameter (interface sensitivity, $S\tau$) was utilized. The results showed that the sensitivity increased minimally as ambient temperature increased from 21 °C and 50 °C. The PolyFlex HDPE coextruded textured geomembrane interface showed slightly higher interface sensitivity values than those from the interfaces of GSE coextruded and Agru structured textured geomembrane at all test temperatures ranging from 21°C to 50°C for normal stress levels (10, 100 kPa). However, at higher normal stress level (400 kPa), all the textured interfaces displayed negligible (for the coextruded systems) or marginal increase (for the structured system) in the value with an increase in the temperature. This invariability in the resulting values of the sensitivity at 400 kPa normal stress level can be attributed to the higher confinement of the counterface materials due to greater magnitude of normal load applied on the interface during shear.

The magnitude of the increase in the sensitivity was smaller throughout the test temperature range from 21°C to 50°C for the smooth geomembrane – NPNW geotextile interfaces compared to that of the textured counterparts. This is considered to be the influence of the different shearing mechanisms mobilized at the interface during shear displacement. As such, the lesser increase in the magnitude of the interface sensitivity for the smooth counterface systems (GSE HDPE Smooth and EPI PVC Smooth) is due to the fact that the main frictional strength generating mechanism is sliding arising at the contact surface of the smooth liner – fibrous geotextile interface. Further, the global interaction mechanisms of the two distinct systems (smooth versus textured) displayed diverse interface shear behaviors (e.g. shape and progression of the stress-displacement

curve) as a result of the distinctive characteristics and differences in the surface roughness properties.

In order to compare the frictional performance of the interfaces and additionally, the interface strength loss occurring at different test temperature levels, a normalized quantitative parameter ($S_{[T°C/21°C]}$ = the normalized interface sensitivity) was defined that is the ratio of peak shear stress (τ_{Peak}) to pseudo-residual stress ($\tau_{Residual}$) at an elevated temperature (26 °C – 50°C) relative to that at room temperature (21 °C). At low normal stress level (10 kPa), the resulting values at same ambient test temperatures were comparable and the variational trend was similar for both PolyFlex coextruded and Agru structured textured geomembrane interfaces. In the case of 100 kPa normal stress level, all the textured systems exhibited an increase in the normalized sensitivity. It is notable that PolyFlex coextruded and Agru microspiked geomembrane interfaces showed a linear increase in the value for the normalized sensitivity up to the elevated temperature of 40°C whereas these values stayed constant beyond 40°C until the highest test temperature level (50°C). On the other hand, GSE textured system displayed the least variation in the normalized values of the sensitivity and depicted a consistent linear increasing trend from room temperature (21°C) up to the highest elevated temperature level (50°C). For all the textured interfaces, similar normalized sensitivity trends were observed for high normal stress level of 400 kPa and the normalized sensitivity stayed almost constant in the temperature range from 21°C to 50°C with an exception that only Agru structured geomembrane showed a marginal change (slight increase) in the normalized value. Consequently, it is noted that at high normal stress level (400 kPa), all the textured geomembranes irrespective of texturing method (coextruded or structured) displayed

similar degrees of change with elevated temperatures (≤ 50°C) in the magnitude of the sensitivity as normalized with respect to room temperature (21°C).

10.2.6. Smooth Geomembrane – Sand Interface

For smooth geomembrane (HDPE, PVC) – sand (rounded, angular) interfaces, the resulting stress-displacement curves followed a reduction to a steady state shear stress after a peak shear stress was observed over the entire test temperature range. This is a general characteristic of drained tests on dilatant particulate specimens. The angular blasting sand exhibited higher shear strengths compared to rounded Ottawa 20-30 sand regardless of ambient temperature for the interface tests when sheared against smooth HDPE or PVC geomembranes. This is reasonable and anticipated as the angular sand particles were more interlocked and thus, more resistant to shear than were the rounded particles. Additionally, the angular sand grains were able to indent further and plow deeper into the lining sheet surface at all test temperatures. This was manifested as an increase in frictional resistance at the interface although it resulted in more abrasion on the geomembrane liner.

The difference in the general characteristics of the stress-displacement failure curves for rounded and angular sands result from different shear mechanisms developed at the interfaces: sliding of the particles against the geomembrane at low temperatures; and predominantly sliding along with a marginal contribution of plowing against the geomembrane at high temperatures due to a decrease in surface hardness of the polymeric lining material for Ottawa 20-30 rounded sand versus smooth HDPE or PVC liner interfaces. Plowing of the angular sand particles against the geomembrane and an

increased amount of plowing along with greater indentation of the particles into the surface of the geomembrane were observed for Blasting angular sand versus smooth HDPE or PVC liner interfaces.

The mobilized shear strength of the sand – smooth geomembrane interfaces results from the *relative* contributions of the sand particle shearing mechanisms (i.e. sliding and plowing) along and into, respectively, the counterface geomembrane surface. The sliding and plowing forces combine together to produce total frictional resistance at the interface against shear displacement. The frictional resistance (δ, tan(δ)) (peak, post-peak) increased with temperature from 21 °C to 50 °C at which the interface direct shear tests were performed. The polymeric geomembrane liner sheet became softer and showed less surface resistance. This resulted in the sand grains penetrating into and plowing along the geomembrane surface during the course of shearing displacement with less energy than at cooler temperature conditions. It is noted that the relative hardness of counterface materials for which the surface hardness of polymeric lining sheets depends are strongly related to the temperature level. The use of a more angular soil as an interface material in contact with smooth geomembranes at elevated temperature field conditions increases the capacity and performance of the lining sheet in terms of the mobilized frictional shear strength.

The presence of dilation with shearing particularly for the angular material interfaces indicated the presence of some degree of particle indentation, interlocking, and plowing as the dilative behavior requires the rearrangement of the angular particles at and/or beyond the contact surface. The increase in dilation with an increment in ambient test temperature also reflects increased embedment/penetration, interlocking, and thus

stronger plowing along the surface of the smooth geomembrane. At higher normal stress levels (e.g. 400 kPa), sand particles were less capable of sliding or rolling over each other. The dilation in the sand structure was partially prevented due to the increased confinement conditions applied on the sand specimen. On the contrary, the sand structure dilated which resulted in the development of higher frictional resistances and a greater magnitude of the interface strength values in terms of δ and $\tan(\delta)$ being achieved at lower normal stresses (e.g. 25 kPa).

The interface shear mechanism was dominated by particles sliding on the relatively stiff surface of the HDPE geomembrane at lower (cooler) test temperatures whereas, the shear mechanism during the course of shearing displacement is transformed to a plowing mechanism at higher (elevated) test temperature conditions which contributes favorably to an increase in the frictional resistance against shearing as the HDPE geomembrane becomes softer with increasing temperature. For Blasting sand – smooth HDPE geomembrane interfaces, the primary controlling mechanism for angular particulate – smooth geomembrane interfaces was plowing of the soil grains along the surface of the geomembrane over the entire test temperature ranging from 21°C to 50°C. As such, the angular shape features of the sand particles promotes the occurrence of higher plowing effects such as plastic deformation and destructive material dislocations on the contact surface of the smooth geomembrane adjacent to the sand specimen along with cooperative contribution of elevated temperatures causing a substantial reduction in surface hardness of the counterface polymeric material.

For Ottawa 20/30 sand – smooth PVC geomembrane interfaces, the mechanism was predominantly rolling/sliding of the sand grains against the geomembrane. However,

the mechanism was primarily plowing of the angular sand particles along the soft smooth geomembrane surface for Blasting sand – smooth PVC liner interfaces. Further, at higher temperatures, as the geomembrane softens, the amount of plowing increased which resulted in a substantially larger increase in interface frictional angle reflecting the additional effort required to penetrate the particles deeper into the geomembrane surface. Therefore, the strength of angular sand-geomembrane interfaces at all temperatures tested is directly related to the ability of soil particles at the interface to plow into the geomembrane surface. As such, the particles must displace the material at the interface to plow into the surface of the geomembrane which requires significant effort. Thus, as temperature increases, increased plowing of angular sand particles during shear depends on the decrease in hardness of the counterface material.

At low normal stresses, the PVC lining material was able to recover its surface state to some extent and recover some portion of the relative deformation induced during shearing changes such as scratches, grooves and striations that were initiated, created and generated, respectively, by the sand grains during shearing displacement so that trailing sand particles following sand grains which has already passed through a given region of the contact surface between sand and smooth PVC liner will encounter a marginally recovered surface. Owing to the pliable and more plasticized nature of PVC geomembranes, the trailing sand particles were given an opportunity, during shear displacement, to enter marginally recovered lining sheet surface which had been scratched already by the leading edge sand particles of the specimen box such that the grooves and/or the striations were regained to some extent by the PVC material body due to malleable and ductile nature of the lining sheet surface. In this way, greater frictional

resistance/strength at the interface against shear displacement was generated as the sand particles at rear edge sheared against less damaged/scratched planar lining sheet surface compared to the results of the interface tests at corresponding test temperature on HDPE geomembrane specimens.

Considering the highest level of normal stresses ($\leq$ 400 kPa) applied throughout the experimental program, the angular sand grains were sufficiently strong and tough to resist plastic deformation themselves. On the other hand, with temperature increase, the geomembrane became softer. Consequently, at higher elevated temperature conditions, the geomembrane deformed plastically more easily against the sand grains due to imposed normal stress on the interface during shearing that resulted in increased penetration and plowing of the sand particles into the surface. As such, the yielding of one or both of the interface components under the applied loading causing plastic deformations on the materials at the contact surface during the course of shear displacement depends primarily on the *relative hardness* of the counterface materials; and thus, is related to the degree of ambient temperature. The plastic deformation component of friction was previously defined by Dove and Frost (1999) such that the geomembrane deforms during grain indentation/penetration into the liner surface. Plastic plowing of the sand grains physically removes the polymer material causing wear on the geomembrane surface. As the temperature and the normal stress applied on the interface increases, the ability of the soil particles to penetrate into and plow along the geomembrane surface also increases.

Smooth HDPE geomembrane interfaces exhibited generally a slight decrease in the sensitivity with temperature. This reduction in the value of the sensitivity is

particularly more pronounced for the angular sand and smooth HDPE interfaces than the interfaces of the rounded material. This is attributed to the transition of shear mechanism from sliding to plowing at higher ambient temperatures due to the softening of the polymeric smooth HDPE geomembrane with increased temperature. For the smooth PVC liner (having smaller surface hardness compared to HDPE geomembranes) interface, the sensitivity value displayed similar trends for both rounded and angular material layered systems. The sensitivity showed a marginal increase up to the test temperature level of 35°C beyond which the sensitivity exhibited a slight decrease in the value until the highest test temperature level (50°C). The resultant values for both rounded and angular sands at 50°C is comparable to those values displayed at lowest test temperature (21°C). This resulted from the ability of the relatively hard sand grains to penetrate deeper into the very soft surface of the PVC liner and thus, plow the counterface severely at larger shear displacements leading to the mobilization of greater residual frictional resistances relative to the shear strength at peak state. Considering the variation in the value of the sensitivity as a function of temperature, the relatively harder surface of the HDPE geomembrane (compared to PVC liner) showed a higher stability and resistance to particle indentation/penetration in the contact area with increasing ambient test temperature particularly for the rounded particulate material interfaces.

The resulting values of the normalized sensitivity ($S_{T°C/21°C}$) less than 1.00 indicated that the corresponding stress-displacement curve showed a less strain-softening response (i.e. reduction in peak resistance) at larger shear displacements for the tests at higher temperatures. For relatively harder surface of smooth HDPE geomembrane particularly at lower test temperatures, the influence of higher surface hardness of the

geomembrane liner sheet agrees with the fact that the shear mechanism at the contact surface was constrained to the sliding of sand grains along the geomembrane surface during shearing. This resulted in the lower magnitudes of residual frictional resistance mobilized at larger displacements compared to the interface tests at elevated temperatures for the same material combination tested. However, the decrease in value of the normalized sensitivity with increasing ambient temperature for particularly angular sand interfaces can be interpreted as a greater amount of plowing induced to the counterface geomembranes resulting in greater sand particle rearrangement during shearing.

To quantitatively evaluate the mobilized shear strength response of the different material combinations tested as a function of temperature, a comparative analysis was performed for the tests at different ambient temperatures by defining a quantative proportionality parameter for peak and post-peak state ($PSR_{Angular/Rounded}$ and $RSR_{Angular/Rounded}$, respectively). In this way, the variations in the behavior as a function of temperature was relatively evaluated for rounded or angular sand – smooth HDPE or PVC geomembrane interfaces. The influence of the particle shape (i.e. roundedness/angularity) as well as the hardness of liner base material (HDPE, PVC) was found to be predominant factors on the mobilized peak and residual frictional resistance and shear response with temperature change for the tested sand – smooth geomembrane interfaces.

10.2.7. Geomembrane Pre-test and Post-test Surface Roughness

Pre-test as well as post-test surface profiles of the geomembrane specimens were quantified using a profilometer to observe the influence of temperature and loading conditions on the post-test surficial wear of the geomembrane (compared to pre-test virgin liner specimens) sheared against rounded or angular sands. This was intended to show shear induced changes in smooth geomembrane surface topography as a function of temperature when sheared against a granular soil at elevated temperatures. To this end, the post-test surface wear of the geomembrane specimens after interface shear tests at different temperatures was demonstrated through plotting post-test surface roughness relief over a profile length. The graphical representations visually depicted the grooves, scratches (troughs in the plots) and material dislocations (peaks in the plots) with a change in ambient temperature as well as the magnitude of normal stress applied on the interface during shearing. The results show noticeable differences in the resulting surficial wear of the counterface geomembrane due to the shape (rounded/angular) of the sand particles in contact with the liner. Accordingly, the results of the interface shear tests at different temperatures can be compared with the post-test surface topography measurements of the smooth HDPE and PVC geomembrane specimens to provide a further understanding for the mechanism (sliding/plowing) mobilized during shearing. As such, the frictional shear resistance of the particulate – continuum material interfaces are also controlled by the ability of granular soil particles to penetrate into the counterface material under load and plow the counterface at a depth in the course of shear displacement. In this context, the test results showed that an increase in the contribution of plowing mechanism at higher elevated temperatures is relevant to the increase in

interfacial shear strength as more effort and energy was required to plastically deform and dislocate the material on the geomembrane surface during shear displacement. Therefore, the amount of plowing is a function of the state of the interface as well as the relative hardness of the counterface materials. For sand – geomembrane interfaces, this changes with a change in the temperature. Further, the ability of the sand grains to plow deeper into the surface of the counterface geomembrane is dependent on the greater angular features of the particles. As such, the contact area between the rounded sand particles and the geomembrane is relatively larger than the contact area between the angular sand particles and the geomembrane. Hence, the sharper angular sand grains induce larger magnitude of local contact level stress to penetrate into the surface of the counterface polymeric material at lower normal load. It was noted that the depth of the trenches being plowed by soil particles depends on the shape and the angularity of soil particles, the density of soil, and the normal stress at the points of contact between soil particles as well as most importantly the softness/hardness of the geomembrane liner surface which is strongly temperature dependent. At higher normal stresses and at higher elevated temperatures, the depth of embedment of soil particles is greater, resulting in deeper trenches being plowed during shear.

In summary, the results from the profilometer surface measurements demonstrated how surficial scarring of smooth geomemhranes was influenced by ambient temperature condition at which the laboratory tests were performed as well as the normal stress level, and the particle roundedness/angularity. The particles penetrated further through the intact surface of the membrane at higher temperatures at the initiation of the shear displacement and continued to do so throughout the shearing process. Due to

softness and higher pliability of the polymeric geomembrane liner at elevated test temperatures, particles plowed into the surface of the geomembrane with a variety of projected geometries creating significant wear on the relatively softer continuum material surface. Therefore, the amount/degree of surficial damage given to the geomembrane specimen can directly be correlated to the test conditions such as the ambient temperature and the applied load; and hence, governing and determining the resulted frictional strength of the interface based on especially geomembrane hardness.

10.2.8. Comparative Analysis on Direct/Indirect Assessment of Interface Shear Strength at Different Temperatures

As previously determined from the laboratory tests conducted only at room temperature (21°C) by O'Rourke et al. (1990), the shear capacity of particulate-continua interfaces was related to the surface hardness of the polymer. The mobilized frictional strength and the developed interface shear behavior at granular material – geosynthetic interfaces at different temperatures are also fundamentally influenced by the surface hardness of the geomembrane. To this end, a series of measurements were undertaken as part of this research study to investigate the effect of temperature on the hardness of geosynthetic materials as well as to allow for indirect evaluation of temperature effects on the shear strength of granular material – geomembrane interfaces. Shore D Hardness measurements were performed at different temperatures to obtain an index value and to investigate the variation of this index value with increasing temperature for surface hardness of smooth HDPE as well as smooth PVC geomembranes using a durometer with constant loader test stand placed in temperature controlled chamber (TCC).

The reduction in the hardness of the geomembranes with increasing temperature for HDPE (exponential decrease) and PVC (linear decrease) geomembrane liners was observed. The surface hardness of PVC geomembrane was less dependent on temperature in terms of the rate of the change of hardness with temperature (i.e. slower rate) for the temperature range tested. Further, the measured differences in the magnitude of Shore D surface hardness values for HDPE and PVC liners at the same ambient temperatures underscore the pronounced difference observed in the interface shear strength characteristics of these two geomembranes for the same temperature conditions. This results from the dissimilar material nature and physical-mechanical properties of PVC geomembrane which is more plasticized and softer compared with that of HDPE geomembrane which is less plasticized and stiffer. Further, at higher temperatures, both HDPE and PVC become softer and more malleable as established through the reduction in surface hardness of these materials. This variation in the magnitude of surface hardness of the geomembranes can be attributed to alteration of the stiffness of polymeric materials with temperature. Since the stiffness of a polymer principally defines its state on the "softness" through "rigidity" scale as well as governs and is related to its surface hardness. The stiffness of the materials produced from one or a mixture two different polymer resins decreases as ambient temperature increases.

For practical assessment as well as indirect evaluation of frictional shear strength properties of sand – geomembrane interface, the empirical relations were developed by utilizing an empirical equation proposed earlier by O'Rourke et al. (1990) correlating interface properties to surface hardness in order to relate temperature effects to interface friction properties. In this way, a new model for interface frictional resistance was

developed in which interface friction angle and coefficient of friction was related to temperature of the polymeric geomembrane liners (HDPE, PVC). It was found that the frictional resistance of two geosynthetics liners (HDPE and PVC) increases pronouncedly within the temperature range from 20°C to 50°C as a result of this analysis developed indirectly by the use of empirical correlations and relating the corresponding engineering parameters interchangeably in between the closed form equations (higher variation in HDPE; lower change in PVC).

As a result, the measured index value of hardness of the geomembrane based on a particular scale (i.e. Shore D) at various temperatures provided a useful quantitative value to evaluate the magnitude of shear resistance being generated at the interface of granular soil-geosynthetic. The primary influence of temperature on sand-geomembrane interface shear behavior is essentially caused by temperature dependency of the geomembrane physical properties and not due to the sand and hence, can be indirectly assessed through surface hardness of the material.

10.3. Concluding Remarks

In conclusion, for the multiple test series presented in the thesis, a general summary table is presented in Table 10.1 to qualitatively estimate the influence of temperature on the tested different interfaces comprised of various material combinations as well as on the performed geotextile single filament thermo-micro-tensile strength tests and geomembrane surface hardness measurements at different temperatures. Additionally, the ratio of peak and post-peak (pseudo-residual) friction coefficients mobilized at the highest elevated test temperature (50 °C) for the tested different

geosynthetic material combinations relative to the friction coefficients observed at the lowest (standard) test temperature level (21 °C) for NPNW geotextile – smooth HDPE and PVC or textured HDPE geomembranes as well as sand (rounded, angular) – smooth HDPE or PVC geomembrane interfaces are presented in Figure 10.1 and 10.2, respectively. This is intended to provide a concise summary for comparison purposes to quantitatively demonstrate the influence of elevated temperature as well as to quantitatively evaluate the degree of this influence of elevated temperatures on the different geosynthetic material combinations. It can be seen from the figures that an increase in temperature from the standard laboratory test temperature of 21 °C to an equivalent in-situ temperature of 50 °C increase the peak and residual interface friction values by a minimum of 15%. For selected combinations of materials, the amount of increase can be in excess of 20% and as high as 35%.

Table 10.1 Qualitative Estimate of Effect for the Tested Different Interfaces Comprised of Various Material Combinations as well as for the Performed Single Filament Thermo-Micro-Tensile Strength Tests and Geomembrane Surface Hardness Measurements at Different Temperatures

INTERFACE	**EFFECT OF NORMAL STRESS**	**EFFECT OF ELEVATED TEMPERATURE (PEAK/RESIDUAL)[1]**
Smooth HDPE Geomembrane – NPNW Geotextile	Medium to High	High/High
Smooth PVC Geomembrane – NPNW Geotextile	Medium	Low/Low to Medium
Coextruded Textured HDPE Geomembrane – NPNW Geotextile	High	Medium to High/Medium to High
Structured Textured HDPE Geomembrane – NPNW Geotextile	Medium to High	Medium to High/Medium
Smooth HDPE Geomembrane – Rounded Sand	Medium to High	Medium to High/Medium
Smooth PVC Geomembrane – Rounded Sand	High to Very High	Medium/Low to Medium
Smooth HDPE Geomembrane – Angular Sand	High to Very High	High to Very High/Very High
Smooth PVC Geomembrane – Angular Sand	Very High	High/Medium to High
Filament Strength	–	Medium to High
Surface Hardness	–	Very High

[1] For strain-hardening stress-displacement response, peak is defined as the value at a particular displacement.

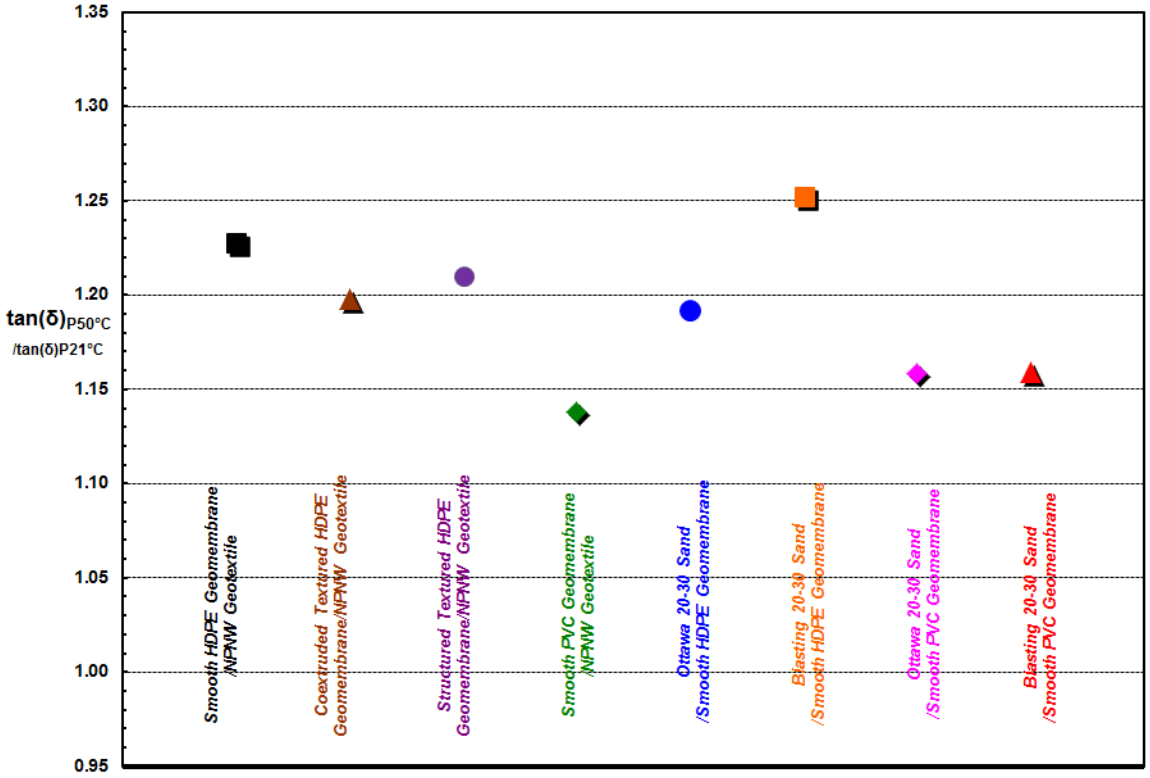

Figure 10.1 Broad-Spectrum Quantitative Comparison of the Mobilized ***Peak*** Interface Strengths at 50 °C relative to those at 21 °C for Several Distinct Composite Systems

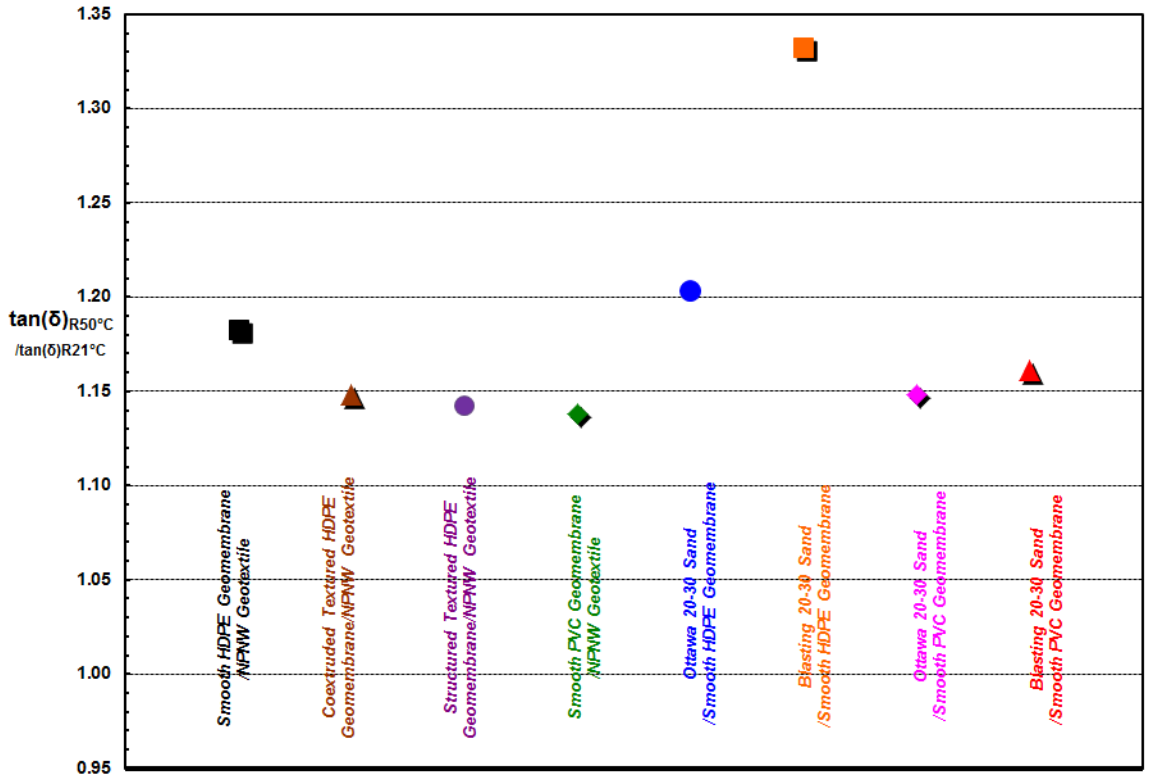

Figure 10.2 Concise Quantitative Summary & Analysis of the Mobilized ***Residual*** Shear Strengths at 50 °C relative to those at 21 °C for Several Distinct Composite Systems

10.4. Recommendations

It is important to highlight that the frictional resistance of geosynthetic interface layered systems is project-specific and product-dependent (Koerner, 1998). The presentation and discussion of the experimental results in this thesis have concentrated on the shear behavior and the changes in shear response due to change in temperature rather than providing specific shear-strength values for use in design applications. This experimental database can provide invaluable insight into understanding the frictional shear performance of certain geosynthetic interfaces at elevated temperatures, as well as can provide guidance for selecting appropriate geomembrane liner materials required for the design of composite layered systems comprising geotextiles in conjunction with geomembranes to maximize the shear resistance mobilized at the interface in harsh environmental conditions at elevated temperatures. Additionally, it is noted that site-specific interface testing should be required for the design of particular geotechnical applications exposed to varied temperature conditions.

Moreover, in order to expand the understanding from the influence of temperature on interface shear strength and behavior of geotextile – geomembrane and sand – geomembrane interfaces, numerical simulations to complement the experimental studies presented herein can be performed. Additionally, these numerical analyses can be extended to the other composite geosynthetic layered systems in terms of further illuminating the influence of ambient conditions (i.e. temperature) on these polymeric materials.

Furthermore, for expanding understanding to include combined leachate-temperature effects, the interface shear response between geotextile-geomembrane as

well as sand-geomembrane interfaces can be examined by performing the direct shear tests at different ambient temperature conditions at which the interface is submerged in leachate intending to observe ageing effect including chemical reactivity on the resulting frictional response.

Finally, as known, the creep effect is the accumulation of several factors including the permanent load effect, the accelerating influence of temperature and most importantly the augmentative impact of time duration for the stress or constant strain induced on a polymeric geosynthetic layered system. In field applications, the composite geosynthetic systems are anticipated to remain under load for long durations (i.e. > months/years). The laboratory experimental assessments for the evaluation of strength and deformation properties of the geosynthetic layered systems are generally performed in a relatively short time durations compared to field conditions. In this perspective, the performance of the geosynthetic layered systems to maintain its strength and durability properties for long durations should be evaluated in terms of the consequences of the creep impact in the field.

REFERENCES

Amonton, G. (1699). Histoire de l'Acade´mie Royale des Sciences avec les Me´moires de Mathe´matique et de Physique, page 206.

Andersland, O. B., and Al-Moussawi, H. M. (1987). "Crack Formation in Soil Landfill Covers due to Thermal Contraction." Waste Management & Research, 5(4), 445-452.

Andrawes, K.Z., McGown, A. and Kabir, Md. H. (1984).Uniaxial Strength Testing of Woven and Nonwoven Geotextiles" Geotextiles and Geomembranes, Vol. 1(1), 41-56

Archard, J. F., (1957), "Elastic Deformation And The Laws Of Friction", Proceedings of the Royal Society of London, Series A, Mathematical and Physical Sciences, Vol. 243, Issue 1233, pp. 190-205.

ASTM D1004. Standard Test Method for Initial Tear Resistance of Plastic Film and Sheeting. ASTM International, West Conshohocken, PA, USA.

ASTM D1505. Standard Test Method for Density of Plastics by the Density-Gradient Technique. ASTM International, West Conshohocken, PA, USA.

ASTM D1603. Standard Test Method for Carbon Black in Olefin Plastics. ASTM International, West Conshohocken, PA, USA.

ASTM D2240-05 (2005) Standard Test Method for Rubber Property - Durometer Hardness ASTM International, West Conshohocken, PA, USA.

ASTM D3379 (1970; Reapproved 1989) "Standard Test Method for Tensile Strength and Young's Modulus for High-Modulus Single-Filament Materials," West Conshohocken, PA.

ASTM D3822, (2001) "Standard Test Method for Tensile Properties of Single Textile Fibers," West Conshohocken, PA.

ASTM D4254, "Standard Test Methods for Minimum Index Density and Unit Weight of Soils and Calculation of Relative Density." ASTM, West Conshohocken, PA

ASTM D4439, "Standard Terminology for Geosynthetics," ASTM International, West Conshohocken, PA, USA

ASTM D4491. Standard Test Methods for Water Permeability ofGeotextiles by Permittivity. ASTM International, West Conshohocken, PA, USA.

ASTM D4632. Standard Test Method for Grab Breaking Load and Elongation of Geotextiles. ASTM International, West Conshohocken, PA, USA.

ASTM D4633. Standard Test Method for Energy Measurement for Dynamic Penetrometers. ASTM International, West Conshohocken, PA, USA.

ASTM D4751 (1999a; Reapproved 2004) "Standard Test Method for Determining Apparent Opening Size of a Geotextile," West Conshohocken, PA.

ASTM D4833. Standard Test Method for Index Puncture Resistance of Geotextiles, Geomembranes and Related Products. ASTM International, West Conshohocken, PA, USA.

ASTM D5199. Standard Test Method for Measuring the Nominal Thickness of Geosynthetics. ASTM International, West Conshohocken, PA, USA.

ASTM D5261. Standard Test Method for Measuring Mass per Unit Area of Geotextiles. ASTM International, West Conshohocken, PA, USA.

ASTM D5321, "Standard Test Method for Determining the Coefficient of Soil and Geosynthetic or Geosynthetic and Geosynthetic Friction by the Direct Shear Method," West Conshohocken, PA.

ASTM D6693. Standard Test Method for Determining Tensile Properties of Nonreinforced Polyethylene and Nonreinforced Flexible Polypropylene Geomembranes. ASTM International, West Conshohocken, PA, USA.

ASTM D7176. Standart Test Method for measuring Functional Requirements for a Liner Material. ASTM International, West Conshohocken, PA, USA.

Bacas, B.M., Konietzky, H., Berini, J. C. Sagaseta, C. 2011. “A new constitutive model for textured geomembrane/geotextile interfaces” Geotextiles and Geomembranes Vol. 29 (2), pp. 137-148

Bandis, S., Lumsden, A.C., Barton, N., 1983. Fundamentals of rock joint deformation. Int. J. Rock Mech. Min. Sci. Geomech. Abstr. 20, 249e268.

Barone, F. S., Costa, J. M. A., and Ciardullo, L. (2000). “Temperatures at the base of a municipal solid waste landfill.” Proc., 6th Environmental Engineering Specialty Conf. of the CSCE, London, Ontario, Canada, 41–48

Barton, N., 1973. Review of a new shear strength criterion for rock joints. Eng. Geol. 7, 287-332. Elsevier.

Barton, N., Choubey, V., 1977. The shear strength of rock joints in theory and practice. Rock Mech. 10, 1-54.

Barton, N., Bandis, S., Bakhtar, K., 1985. Strength, deformation and conductivity coupling of rock joints. Int. J. Rock Mech. Min. Sci & Geomech.Abstr 22 (No 3), 121-140.

Bely, V., Sviridenok, A., Petrokovets, M., Savkin, V., 1982. In: Jackson, G. (Ed.), Friction and Wear in Polymer-Based Materials. Pergamon Press, NewYork.

Bhushan, B. (1999) Principles and Applications of Tribology, John Wiley & Sons, 1020p.

Bilgin O, and Stewart, H.E., (2006). "Effect of temperature on surface hardness and soil interface shear resistance of geosynthetics.", Proc., 8ICG 8th International Geosynthetics Conference, Millpress Science Publishers, Yokohama, Japan.

Bishop, A.W. (1966) "The Strength of Soils as Engineering Materials," Geotechnique, 16(2), pp. 89-130.

Bleiker, D.E., Farquhar, G., and McBean, E. (1995). "Landfill Settlement and the Impact on Site Capacity and Refuse Hydraulic Conductivity." *Waste Management and Research,* 13 (6): 533-554.

Bove, J.A. (1990) "Direct Shear Friction Testing for Geosynthetics in Waste Containment", Geosynthetic Testing for Waste Containment Applications, ASTM STP 1081, pp. 241-256.

Bowden, F. P., Tabor, D., (1939), "The Area Of Contact Between Stationary and Between Moving Surfaces", Proceedings of the Royal Society of London, Series A, Mathematical and Physical Sciences, Vol. 169, Issue 938, pp. 391-413.

Bowden, F. P., Tabor, D., (1956), Friction And Lubrication, John Wiley & Sons Inc, New York, 150 pp.

Bowden, F.P. and Tabor, D. (1954) Friction and Lubrication, London: Methuen and Company LTD.

Brandl, H., 1992. "Mineral liners for hazardous waste containment." Geotechnique, 42, 57-65.

Briscoe, B. J. (1992). ''Friction of organic polymers.'' Fundamentals of friction: Macroscopic and microscopic processes, I. L. Singler and H. M. Pollock, eds., Kluwer, Dordrecht, The Netherlands, 167–182.

Broms, B.B. (1977). “Triaxial Tests with Fabric-Reinforced Soil,” C.R Coll. Inst. Soils Text. Paris, Vol. 3, pp. 129-133.

Budiman, J., 1994. Effects of temperature on physical behavior of geomembrane, Proceedings of the Fifth International Conference on Geotextiles, Geomembranes, and Related Products. International Geosynthetics Society, Easley, SC, USA, pp. 1093–1096.

Byrne, R., Kendall, J., and Brown, S. (1992), “Cause and Mechanism of Failure, Kettleman Hills Facility, Kettleman City, California”, Report Prepared for Chemical Waste Management, Inc. by Geosyntec Consultants, Atlanta, Georgia.

Collins. H., 1993. Impact of the Temperature Inside the Landfill on the Behaviour of Barrier Systems. In: Proceedings of Sardinia '93, 4th International Landfill Symposium. S, Marghertita di Pula, Cagliari, Italy. CISA, Environmental Sanitary Engineering Center, Cagliari, pp. 417 432.

Corser, P., and Cranston, M. (1991). "Observations on Long-Term Performance of Composite Clay Liners and Covers." *Proceedings of the Conference on Geosynthetic Design and Performance*, Vancouver Geotechnical Society, Vancouver, British Colombia, pp. 1–15.

Coulomb, C.A. (1776) "Essai sur une application des regles de Maximus et Minimis a quelques Problemes de Statique, relatifs a l'Architecture", Memoires de Mathematique et de Physique, Presentes a l' Academie Royale des Sciences, par divers Savans, et lus dans ses Assemblees, Paris, Vol. 7, (volume for 1773 Published in 1776).

Ctori, P., 1989. The effects of temperature on the physical properties of cohesive soils. Ground Engineering 22 (5), 26-27.

Daniels, C., 1989. Polymers: Structure and Properties. Technomic Publishing Company, Inc., Lancaster, PA, USA

De Meulemeester, D., and Nicoloff, I. (1936) "Stress-Extension Recording Dynamometer for Textile Fibres," Textile Institute Journal, Vol. 27(3), pp. 84-87.

Den Hoedt, G. (1986), Creep and relaxation of geotextile fabrics, Geotextiles and Geomembranes, 4(2), 83-92.

Donaldson, J. J. (1995) "Texturing Techniques," Proceedings of a Seminar Held at the Geosynthetic Research Institute, Drexel University, Philadelphia, PA, pp.113-122.

Dove, J.E. (1996) "Particle-Geomembrane Interface Strength Behavior as Influenced by Surface Topography", Ph.D. Dissertation, School of Civil and Environmental Engineering, Georgia Institute of Technology, 323 pp.

Dove, J. E., and Frost, J.D. (1996) "A Method for Measuring Geomembrane Roughness," Geosynthetics International, Vol. 3 (3), pp. 369-392.

Dove, J. E., Frost, J. D., Han, J., and Bachus, R. C. (1997). ‘‘The influence of geomembrane surface roughness on interface strength.’’ Proc., Geosynthetics ’97, 2, Industrial Fabrics Association International, Roseville, Minn., 863–876.

Dove, J. E., and Frost, J.D. (1999) "Peak Friction Behavior of Smooth Geomembrane-Particle Interfaces," Journal of Geotechnical and Geoenvironmental Engineering, ASCE, Vol. 125 (7), pp. 544-555.

Dove, J.E. and Harpring, J.C. (1999) “Geometric and Spatial Parameters for Analysis of Geomembrane/Soil Interface Behavior”, Proceedings of Geosynthetics ’99, Boston, MA, Vol. 1, pp. 575-588.

Dowling, N.E. (2007). Mechanical behavior of materials, 3rd edition, Pearson Prentice Hall, Upper Saddle River, NJ, p912.

Eppersonwaste Company Inc. Website (2011) (www.eppersonwaste.com)

Findley, W.N. (1960). Mechanism and mechanics of creep of plastics, Society of plastics engineers (SPE) journal, 16(1), 57-65.

Fleming IR, Sharma JS, Jogi MB (2006). “Shear strength of geomembrane-soil interface under unsaturated conditions.” GEOTEXTILES AND GEOMEMBRANES 24(5), 274 - 284.

Fox, P.J., Rowland, M.G., Scheithe, J.R., 1998. Internal shear strength of three geosynthetic clay liners. Journal of Geotechnical and Geoenvironmental, ASCE 124 (10), 933–944.

Frobel, R. K. (1988). Geosynthetics in the NATM tunnel design. Geosynthetics for Soil Improvement, Geotechnical Special Publication 18, Holtz, R. D., Editor, ASCE, Reston, VA, pp. 51–67.

Frost, J.D. (1989) "Studies on the Monotonic and Cyclic Behavior of Sands", Ph.D. Dissertation, School of Civil Engineering, Purdue University, 333 pp.

Frost, J.D., and Han, J. (1999) "Behavior of Interfaces between Fiber-Reinforced Polymers and Sands", ASCE Journal of Geotechnical and Geoenvironmental Engineering, Vol. 125 (8), pp. 633-640.

Frost, J.D., Lee, S.W., and Cargill, P.E. (1999) "The Evolution of Sand Structure Adjacent to Geomembranes," Proceedings of Geosynthetics '99, Boston, MA, Vol. 1, pp. 559-573.

Frost, J. D., and Lee, S.W. (2001) "Microscale Study of Geomembrane-Geotextile Interactions," Geosynthetics International, Vol. 8 (6), pp. 577-597.

Frost, J. D., DeJong, J. T., Recalde, M., (2002), "Shear Failure Behavior Of Granular-Continuum Interfaces", Engineering Fracture Mechanics, Vol. 69, No. 17, pp. 2029-2048.

Frost, J. D., Evans, T.M., Heberler, G.L., and Giroud, J.P. (2002) "Influence of Wear Mechanisms on Geosynthetic Interface Strengths," Proceedings of the Seventh International Conference on Geosynthetics, Nice, France, vol. 4, pp.1325-1328.

Gilbert, R., Liu, C., Wright, S., and Trautwein, S., 1995. "A double interface test method for measuring interface strength." Proceedings of the Conference on Geosynthetics '95. Industrial Fabrics Association International, St. Paul, MN, USA, pp. 1017–1029.

Gilbert, R.B, Liu, C.N. (2006). "Graphical solutions for estimating geosynthetic loads in geosynthetic-soil layered systems on slopes - Discussion and response." GEOSYNTHETICS INTERNATIONAL, 13(4), 171-172.

Girard, H., Fischer, S., and Alonso, E. (1990) "Problems of Friction Posed by the Use of Geomembranes on Dam Slopes. Examples and Measurements," Geotextiles and Geomembranes, Vol. 9(2), pp. 129-143.

Giroud, J. P. (1984) "Geotextiles and Geomembranes," Geotextile and Geomembranes, Vol. 1(1), pp. 3-40.

Giroud, J.P. (2005). Mercer Lecture at 8ICG 8th International Geosynthetics Conference, Millpress Science Publishers, Yokohama, Japan.

Gokhale, A. M., and Drury, W.J. (1990) "General Method for Estimation of Fracture Surface Roughness. Part II. Practical Considerations," Journal of Metallurgical Transactions, Vol. 21A(5), pp. 1201-1207.

Gokhale, A. M., and Drury, W.J. (1994) "Efficient Measurement of Microstructural Surface Area Using Trisector," Metallurgical and Materials Transactions A, Vol. 25A, pp. 919-928.

Gonsalves, V. E. (1947) "Determination of Denier and Strength of Single Filaments by Vibroscope and Heim Tensile Tester," Textile Research Journal, Vol. 17(7), pp. 369-375.

Haasen, P. (1996) “Physical Metallurgy”, 3rd Edition, Cambridge University Press, Cambridge, 420p.

Han, J. (1997). ‘‘Mechanical behavior of fiber reinforced polymeric piles in sand,’’ PhD dissertation, School of Civil and Environmental Engineering, Georgia Institute of Technology, Atlanta.

Hearle, J. W. S., and Stevenson, P.J. (1963) "Nonwoven Fabric Studies, Part III: The Anisotropy of Nonwoven Fabrics," Textile Research Journal, Vol. 33(11), pp. 877-888.

Hearle, J. W. S., and Stevenson, P.J. (1964) "Studies in Nonwoven Fabrics, Part IV: Prediction of Tensile Properties," Textile Research Journal, Vol. 34(3), pp. 181-191.

Hebeler, G. L. (2005) Multi-Scale Behavior at Geomaterial Interfaces, Ph.D. Thesis, School of Civil and Environmental Engineering, Georgia Institute of Technology, Atlanta, 772p.

Hebeler, G. H., Frost, J.D., and Myers, A.T. (2005) "Quantifying Hook and Loop Interaction in Textured Geomembrane-Geotextile Systems," Geotextiles and Geomembranes, Vol. 23(1), pp. 77-105.

Hillman, R. P., and Stark, T.D. (2001) "Shear Strength Characteristics of PVC Geomembranes-Geosythetics Interfaces," Geosynthetics International, Vol. 8(2), pp. 135-162.

Hindman, H. (1948) "Instron Tensile Tester," American Society of Mechanical Engineers - Advanced Papers, Vol. 48-A68, pp. 3.

Hsuan, Y. G., and Koerner, R. M. (1998). “Antioxidant depletion lifetime in high density polyethylene geomembranes.” J. Geotech. Geoenviron. Eng., 124(6), 532–541.

Iscimen, M. (2004) Shearing Behavior of Curved Interfaces, M.S. Thesis, School of Civil and Environmental Engineering, Georgia Institute of Technology, Atlanta 130p.

Jefferson, I., and Rogers, R. C. D. (1998). “Liquid limit and the temperature sensitivity of clays.” Engineering Geology, 49(2), 95-109.

Johnson, K. L. (1982). One hundred years of hertz contact. Proceedings of the Institution of Mechanical Engineers, 196, pp. 363–378

Johnson, K. L. (1985) Contact Mechanics, Cambridge University Press, Cambridge, UK., 452p.

Jones, D. (2000) "Wide-width geotextile testing with video extensometry," ASTM Special Technical Publication, Vol. (1379), pp. 83-87.

Jones, D.R.V., Dixon, N., 1998. Shear strength properties of geomembrane/geotextile interfaces. Geotextiles and Geomembranes 16(4), 45–71.

Khire, M., Benson, C., and Bosscher, P. (1997). "Water Balance Modeling of Earthen Landfill Covers." *Journal of Geotechnical and Geoenvironmental Engineering*, ASCE 123 (8), 744–754.

Kim, D. (2006) Multi-Scale Assessment of Geotextile – Geomembrane Interaction, Ph.D. Thesis, School of Civil and Environmental Engineering, Georgia Institute of Technology, Atlanta, 250p.

Kingcounty Website (2011) (www.kingcounty.gov)

Koerner, R.M., Martin, J.P., and Koerner, G.R. (1986), "Shear Strength Parameters between Geomembranes and Cohesive Soils", Geotextiles and Geomembranes, 4(1), 21-30.

Koerner, R.M., Hsuan, Y.G., and Lord, A.E., Jr., 1993. "Remaining Technical Barriers to Obtain General Acceptance of Geosynthetics", The 1992 Mercer Lecture, Geotextiles and Geomembranes, 12 (1), pp. 1-52

Koerner, G.R., and Koerner, R.M. (1995). "Temperature behavior of field deployed HDPE geomembranes." Proc., Geosynthetics'95, IFAI, St. Paul, Minn., 921-937.

Koerner, R.M., 1998. Designing with Geosynthetics, 4th ed. Prentice- Hall, Upper Saddle River, NJ, USA, 761p.

Koerner, G. R. (2000) "Wide-width geomembrane testing," ASTM Special Technical Publication, Vol. (1379), pp. 18-27.

Koerner, R.M. (2005). Designing with Geosynthetics, 5th ed. Prentice Hall, Englewood Cliffs, NJ. p796.

Koerner, G.R., and Koerner, R.M. (2006). "Long-Term Temperature Monitoring of Geomembranes at Dry and Wet Landfills." Geotextiles and Geomembranes, Vol. 24 (1), 72-77.

Koerner, R.M., and Koerner, G.R., 2007. "Interpretation(s) of Laboratory Generated Interface Shear Strength Data for Geosynthetic Materials with Emphasis on the Adhesion Value," GRI White Paper # 11, Geosynthetic Institute, Folsom, PA, USA.

Krais, P. (1928) "The Tensile Testing of Single Fibres," Textile Institute Journal, Vol. 19(1), pp. 32-36.

Laguros, J.G., 1969. Effect of temperature on some engineering properties of clay soils. In: Mitchell, J,K. (Ed.), Proceedings of the International Conference on Effects of Temperature and Heat on the Engineering Behaviour of Soils, Special Report 103. Highway Research Board, Washington DC, pp. 186-193.

Lawson, C.R. (1986). Geosynthetics in soil reinforcement, Proceedings of symposium on geotextiles in civil engineering, Institution of engineers Australia, Newcastle, 1-35.

Lehane, B.M., Jardine, R.J., Bond, A.J., and Frank, R. (1993) "Mechanisms of Shaft Friction in Sand from Instrumented Pile Tests" Journal of Geotechnical Engineering, ASCE, Vol. 119(1), 19-35.

Lee, S.W. (1998) "Influence of Surface Topography on Interface Strength and Counterface Soil Structure", Ph.D. Dissertation, School of Civil and Environmental Engineering, Georgia Institute of Technology, 336 pp.

Lee, S.W., Frost, J.D., and Righter, G.K. (1998) "The Influence of Geomembrane Surface Roughness on Geomembrane-Geotextile Interface Strength", Proceedings of Geosynthetics '98, Atlanta, GA, Vol. 1, pp. 433-438.

Li, M. and Gilbert, R.B. (1999) "Shear Strength of Textured Geomembranes and Nonwoven Geotextile Interfaces", Proceedings of Geosynthetics '99, Boston, MA, Vol. 1, pp. 505-516.

Li, M.-H. & Gilbert, R. B. (2006). Mechanism of post-peak strength reduction for textured geomembrane-nonwoven geotextile interface. Geosynthetics International, 13, No. 5, 206–209.

Li, R. (2000). Time-temperature superposition method for glass transition temperature of plastic materials, Material science and engineering A, Vol. 278, 36-45

Lim, J.Y., Donahue, H.J., and Kim, S.Y. (2003). Strain rate, temperature, and microstructure-dependent yield stress of poly(ethylene terephthalate), Macromolecular chemistry and physics, 204(4), 653-660.

Lord, A., Soong, T., Koerner, R., 1995. Relaxation behavior of thermally induced stress in HDPE geomembranes. Geosynthetics International 2 (3), 626–634.

Lord, E. (1955) "Air Flow through Plugs of Textile Fibres," Textile Institute Journal, Vol. 46(3), pp. 191-213.

Lunenschloss, J., and Albrecht, W. (1985) Non-Woven Bonded Fabrics,J. Translation editor: Hock, Ellis Horwood, 549p.

McGillivray, C. B. (2009) Lubrication Mechanisms and Their Influence on Interface Friction During Installation of Subsurface Pipes, Ph.D. Thesis, School of Civil and Environmental Engineering, Georgia Institute of Technology, Atlanta, 254p.

Martin, J.P., Koerner, R.M., Whitty, J.E., 1984. Experimental friction evaluation of slippage between geomembranes, geotextiles and soils. In: Proceedings of International conference on Geomembranes, IFAI, Denver, CO, June 20-23, pp. 191–196.

McCrum, N.G., Buckley, C.P., and Bucknall, C.B. (1997). Principles of polymer engineering, 2nd edition, Oxford University Press, p447.

McGown, A., Andrawes, K.Z., and Kabir, M.H. (1982) "Load-Extension Testing of Geotextiles Confined in Soil," Proceeding of 2nd International Conference on Geotextiles, IFAI, pp. 793-796.

McGown, A., Yogarajah, I., Andrawes, K.Z., and Saad, M.A. (1995), Strain behavior of polymeric geogrids subjected to sustained and repeated loading in air and in soil, *Geosynthetic international*, 2(1), 341-355.

Mitchell, J.K., 1969. Temperature effects on the engineering properties and behaviour of soils. In: Mitchell, J.K. (Ed.), Proceedings of the International Conference on Effects of Temperature and Heat on the Engineering Behaviour of Soils, Special Report 103. Highway Research Board, Washington DC, 9-28.

Mitchell, J. K., Seed, R.B., and Seed, H.B. (1990) "Kettleman Hills Waste Landfill Slope Failure. I: Liner System Properties," Journal of Geotechnical Engineering, Vol. 116(4), pp. 647-668.

Montgomery, R., and Parsons, L. (1990). "The Omega hills cover test plot study: fourth year data summary." Proceedings of the 22nd Mid-Atlantic Industrial Waste Conference, Technomic Publishing Company, Inc., Lancaster, PA, USA, pp. 1–12.

Morton, W. E., and Hearle, J.S.W. (1962) Physical Properties of Textile Fibres, 1st Edition, Manchester & London, The Textile Institute, Butterworths, 608p.

Morton, W. E., and Hearle, J.S.W. (1993) Physical Properties of Textile Fibres, 3rd Edition, Manchester & London, The Textile Institute, Butterworths, 725p.

Mueller-Rochholz, J. and C. Recker (2000) "Tensile strength and clamping of geogrids," ASTM Special Technical Publication, Vol. (1379), pp. 28-36.

Negussey, D., Wijewickreme, W.K.D., and Vaid, Y.P. 1989. “Geomembrane interface Friction” Canadian Geotechnical Journal, 26(1), 165-169.

Nielsen, L.E. (1974), Mechanical properties of polymers and composites, Vol. 1, 2, Marcel Dekker Inc., NY.

Nielsen, L.E. and Landel, R.F. (1994), Mechanical Properties of Polymers and Composites, Marcel Dekker, Inc., New York, N.Y.

O’Rourke, T. D., Druschel, S. J., and Netravali, A. N. (1990). ‘‘Shear strength characteristics of sand-polymer interfaces.’’ J. Geotech. Engrg., ASCE, 116(3), 451–469.

Osswald, T., Menges, G., 1995. Material Science of Polymers for Engineers. Hanser/Gardner Publications, Cincinnati, Ohio, USA.

Oweis, J.S., Smith, D.A., Ellwood, R.B., and Green, D.S. (1990). "Hydraulic Characteristics of Municipal Refuse." *Journal of Geotechnical Engineering*, 116 (4): 539-553.

Painter, P.C. and Coleman. M.M. (1997), Fundamentals of polymer science, 2nd Ed., CRC press, Boca Raton, FL.

Pasqualini, E., Sand, D., and Roccato, M. (1993), “Factors Influence Geomembrane Interface Friction,” Waste Disposal by Landfill Green’93, R.W. Sarsby ed., Bolton Institute of Higher Education, United Kingdom, pp. 349-356.

Poulos, H. G. (1971), “Behavior of Laterally Loaded Piles: I-Single Piles” Journal of Soil Mechanics and Foundations Division,ASCE, Vol. (97) No. SM 5, pp. 711-731.

Rowe, P. W. (1961). “The Stress-Dilatancy Relation for Static Equilibrium of an Assembly of Particles in Contact” Proceeding of Loyal Society, London, No: 269, pp. 500-527.

Rowe, R. K., Fleming, I. R., Armstrong, M. D., Cooke, A. J., Cullimore, R. D., Rittmann, B. E., Bennett, P., and Longstaffe, F. J. (1997). “Recent advances in understanding the clogging of leachate collection systems.” Proc., 6th Int. Landfill Symp., Vol. 3, S. Margherita di Pula-Cagliari, Italy, 383–392.

Rowe, R. K. (1998). “Geosynthetics and the minimization of contaminant migration through barrier systems beneath solid waste.” Keynote Lecture, Proc., 6th Int. Conf. on Geosynthetics, Atlanta, 27–103.

Rowe, R. Kerry. 2006. "Some factors affecting geosynthetics used for GeoEnvironmental applications Source: 5th ICEG Environmental Geotechnics: Opportunities, Challenges and Responsibilities for Environmental Geotechnics - Proceedings of the ISSMGE 5th Int. Congress, v I, 5th ICEG Environmental Geotechnics: Opportunities, Challenges and Responsibilities for Environmental Geotechnics - Proceedings of the ISSMGE 5th Int. Congress, p 43-69.

Roylance, D. (2001), Modulus in mechanics of materials, Massachusetts institute of technology, Cambridge, MA. (http://web.mit.edu)

Runco Environmental, Inc. Website (2011) (www.runcoenviromental.com)

Sangam, H. P., and Rowe, R. K. (2002). "Effects of exposure conditions on the depletion of antioxidants from HDPE geomembranes." Can. Geotech. J., 39(6), 1221–1230.

Santamarina, J. C., Klein, K. A. and Fam, M. A. (2001), *Soils and Waves*, Chichester, England ; J. Wiley & Sons.

Saxena, S.K., Wong, Y.T., 1984. Friction characteristics of a geomembrane. In: Proceedings of International Conference on Geomembranes, Denver, CO, pp. 187–190.

Scheirs, J. (2009) "A Guide to Polymeric Geomembranes: A Practical Approach", John Wiley & Sons Ltd., West Sussex, UK, 499 p.

Seed, R. B., Mitchell, J.K., and Seed, H.B. (1990) "Kettleman Hills Waste Ladnfill Slope Failure. II: Stability Analysis," Journal of Geotechnical Engineering, Vol. 116(4), pp. 669-690.

Seed, R.B., Boulanger, R.W., 1991. Smooth HDPE-clay liner interface shear strengths:compaction effects. Journal of Geotechnical Engineering 117 (4), 686–693.

Shooter K. V. (1951). ''Frictional properties of plastics.'' Proc., Royal Soc. of London, Ser. A, 212, Royal Society of London, 488-491.

Shooter, K. V., and Tabor, D. (1952). ''The frictional properties of plastics.'' Proc., Phys. Soc., Ser. B, 65, 661–671.

Sinclair, J.E. and Edgemond, J.W. (1969). Investigation of creep phenomena in polyethylene and polypropylene, Journal of applied polymer science, 13, 999-1012.

Smeets, P., Jacobs, M., Mertens, M. (2001). Creep as a design toll for HMPE ropes in long term marine and offshore applications, Oceans MTS/IEEE conference, Honolulu, HI. 685-690.

Soong, T.Y. 1995. “Effects of Four Experimental Variables on the Stress Relaxation Behavior of HPDE Geomembranes”, Proceedings of Geosynthetics’ 95, IFAI, Vol.3, Nashville, TN, USA, February 1995, 1139-1147.

Southen, J.M., Rowe, R.K., and von Maubeuge, K. (2002). “Thermally-Induced Moisture Movement Beneath Geosynthetic Clay Liners.” 7th International Conference on Geosynthetics, Nice, France, 2, 577-580.

Southen, Jonathan M. , and Kerry Rowe, R. (2004). “Investigation of the behavior of geosynthetic clay liners subjected to thermal gradients in basal liner applications.” ASTM Special Technical Publication, n 1456, Advances in Geosynthetic Clay Liner Technology: 2nd Symposium, 121-133.

Southen, J. M., and Rowe, R. K. (2005). “Laboratory Investigation of Geosynthetic Clay Liner Desiccation in a Composite Liner Subjected to Thermal Gradients.”, Journal of Geotechnical and Geoenvironmental Engineering, ASCE 131(7), 925-935.

Stark, T., Williamson, T., Eid, H., 1996. HDPE geomembrane/geotextile interface shear strength. Journal of Geotechnical Engineering, ASCE 122 (3), 197–203.

Stein, R. S. and Powers, J. (2006). “Topis in Polymer Physics” Imperial College Press, London, 414 pp.

Stoewahse, C., Dixon, N., Jones, D.R.V., Blumel, W., Kamugisha, P. (2002). “Geosynthetic interface shear behavior: Part 1 test methods.” Ground Engineering, 35(2), 35-41.

TA Instruments DMA Technical Specifications (Product Technical Specifications Manual) (2011) 9www.tainstruments.com

Tabor, D. (1955) "The Mechanism of Rolling Friction. II. The Elastic Range," Proceedings of the Royal Society of London, Series A, Mathematical and Physical Sciences, Vol. 229(1177), pp. 198-220.

Takasumi, D.L., Green, K.R., and Holtz, R.D. 1991. “Soil-Geosynthetic Interface Strength Characteristics: A Review of State-of-the-Art Testing Procedures”, Proceedings of Geosynthetics’91, IFAI, Vol.1, Atlanta, Georgia, USA, February 1991, 87-100.

Task Force #27. (1991). Guidelines for the design of mechanically stabilized earth walls, AASHTO-AGC-ARTBA Joint committee, Washington, DC.

Terzaghi, K. (1952). Permafrost. Journal of the Boston Society of Civil Engineers, Boston, MA.

Tidfors, M., Sallfors, G., 1989. Temperature effect on preconsolidation pressure. Geotechnical Testing Journal 12, 93-97.

Tisinger, L. G., Peggs, I. D., Dudzik, B. E., Winfree, J. P., and Carraher, Jr., C. E., (1990). "Microstructural Analysis of a Polypropylene Geotextile After Long-Term Outdoor Exposure", Geosynthetic Testing for Waste Containment Applications, ASTM STP 1081, Robert M. Koerner, ed., American Society for Testing and Materials, Philadelphia, pp. 335-351.

Triplett EJ, Fox PJ. (2001). "Shear strength of HDPE geomembrane/geosynthetic clay liner interfaces." Journal of Geotechnical and Geoenvironmental Engineering, 127 (6), 543-552.

Uesugi, M., and Kishida, H. (1986) "Frictional Resistance at Yield between Dry Sand and Mild Steel," Soils and Foundations, Japanese Society of Soil Mechanics and Foundation Engineering, Vol. 26(4), pp. 139-149.

Underwood, E.E. (1969) "Stereology, or the Quantitative Evaluation of Microstructure," Journal of Microscopy, Vol. 89, Pt 2, pp. 161-180.

Underwood, E.E. (1970) Quantitative Stereology, Addison-Wesley Publishing Company, Inc., 274p.

Vaid, Y. P., Chung, E. K. F., and Kuerbis, R. H. (1990). ''Stress path and steady state.'' *Can. Geotech. J*., Ottawa, 27(1), 1–7.

Vaid, Y.P. and Rinne, N. (1995) "Geomembrane Coefficients of Interface Friction", Geosynthetics International, Vol. 2, No. 1, pp. 309-325.

Ward, H. C. (1982) Profile Characterization, Chapter 4. In: Rough Surfaces, Longman, London, 261p.

Williams, J.A. (1996) *Engineering Tribology*, New York: Oxford University Press, 488

Williams, N. D., and Houlihan, M. (1986) "Evaluation of Friction Coefficients between Geomembranes, Geotextiles, and Related Products," Third International Conference on Geotextiles, Viena, Austria, pp.891-896.

Williams, N.D., and Houlihan, M.F. 1987. "Evaluation of Interface Friction Properties Between Geosynthetics and Soils", Proceedings of Geosynthetics'87, IFAI, Vol.2, New Orleans, Louisiana, USA, February 1987, 616-627.

Yeh, W.-Y. and Young, R.J. (1998). Deformation processes in poly(ethylene terephthalate) fibers, Journal of macromolecular science-Physics, B37(1), 83-118.

Yoshida, H., Tanaka, N., and Hozumi, H. (1997). "Theoretical Study on Heat Transport Phenomena in a Sanitary Landfill." *Proceedings of Sardinia: Sixth International Landfill Symposium*, Cagliari, Italy.

Yoshida, H., Tanaka, N., Hozumi, H., (1999). Theoretical study on temperature distribution in landfills by three-dimensional heat transport model. Second International Congress on Environmental Geotechnics, vol. 1. Osaka, pp. 323–328.

Yoshida, H., and Rowe, R. K. (2003). "Consideration of landfill liner temperature." Proc., 9th Int. Waste Management and Landfill Symp., S. Margherita di Pula-Cagliari, Sardinia, Italy.

Yoshida, H., Rowe, R.K., 2003. Consideration of landfill liner temperature. Proceedings of Eighth International Waste Management and Landfill Symposium, S. Margherita di Pula, Cagliari, Sardinia, Italy, October, CD-ROM, 9p.

Yoshimi, Y. and Kishida, T. (1982). "A Ring Torsion Apparatus for Evaluating Friction between Soil and Metal Surfaces" Geotechnical Testing Journal, Vol. 4(4), pp. 145-152.

Youssef, M.S., Sabry, A., Ramli, A.H.EI., 1961. "Temperature changes and their effects on some physical properties of soils." In: Proceedings of the 5th International Conference on Soil Mechanics and Foundation Engineering, Paris, Vol. 1, 419-421

Zettler, T. E., Frost, J.D., and DeJong, J. T. (2000) "Shear-Induced Changes in Smooth HDPE Geomembrane Surface Topography," Geosynthetics International, Vol. 7(3), pp. 243-267.